fib
CEB - FIP

Structural Concrete

Textbook on Behaviour, Design and Performance
Updated knowledge of the CEB/FIP Model Code 1990

Volume 2

Structural Concrete

Textbook on Behaviour, Design and Performance

Updated knowledge of the CEB/FIP Model Code 1990

Volume 2

Basis of design

July 1999

Structural Concrete, the Textbook on Behaviour, Design and Performance, is published in 3 volumes (*fib* Bulletins 1, 2, 3):

Volume 1   Chapter 1: Introduction
Chapter 2: Design process
Chapter 3: Materials

Volume 2   Chapter 4: Basis of design

Volume 3   Chapter 5: Durability
Chapter 6: Design for fire resistance
Chapter 7: Members design
Chapter 8: Assessment, maintenance and repair
Chapter 9: Practical aspects

Coverphoto : Bridge over the Salginatobel (Robert Maillart, 1930), photo courtesy institute MCS, EPFL

Contents

4.3 Serviceability limit states (Principles)

4.4   Ultimate limit state (Principles)

4.5   Anchorage and detailing principles

Contents Volume 1

Contents Volume 3

4 Basis of design

4.1 Structural analysis

by Josef Eibl

4.1.1 Introduction

The aim of structural analysis is to quantify the consequence of external or internal actions on structural members or systems. This is done by mapping real structures onto idealised mechanical models (see e.g. chapter 4.1.4), which are then analysed using the tools of mechanics and mathematics.

The mechanical basis for the analysis of statically loaded structural systems is the theory of continuum mechanics predominantly with

Equilibrium conditions,
Kinematic relations - compatibility equations - and
Constitutive laws.

While the first two sets of equations are out of discussion, the appropriate description of the complex material behaviour of reinforced concrete is the most difficult problem, as it controls the numerical approximation of the real physical structures' behaviour to a high extent and therefore may be rather complicated.

In the following mainly the behaviour of beam structures is treated because an exhaustive instruction on the structural analysis in general would exceed the frame of this chapter.

4.1.2 Elastic analysis of linear members

(1) Basis of the theory

In case of the theory of elasticity one may start with the **equilibrium conditions**

$$\frac{dM}{dx} = V, \qquad -\frac{d^2M}{dx^2} = -\frac{dV}{dx} = q_V \qquad \frac{dN}{dx} = -q_H \qquad (4.1-1)$$

where

q_H local horizontal force and
q_V local vertical force,

and the **kinematic relations** (see Fig. 4.1-1)

$$u = u_0(x) + z\theta = u_0(x) - z \cdot \frac{dw}{dx} \qquad (4.1\text{-}2)$$

$$\varepsilon(x) = \frac{du}{dx} = \frac{du_0}{dx} - z \cdot \frac{d^2w}{dx^2} = \varepsilon_o + z \cdot 1/r \qquad (4.1\text{-}3)$$

where u and w are displacement components of a point,

$$\varepsilon(x,z) = \begin{bmatrix} 1 & 0 \\ 0 & z \end{bmatrix} \cdot \begin{Bmatrix} \varepsilon_0 \\ 1/r \end{Bmatrix} = \begin{Bmatrix} \dfrac{du_0}{dx} \\ -z\dfrac{d^2w}{dx^2} \end{Bmatrix} \qquad (4.1\text{-}4)$$

which are the result of the Bernoulli-Navier assumption, postulating a linear strain distribution over the cross-section (see Fig. 4.1-1).

$$\varepsilon_0 = \frac{du}{dx}, \quad \theta = -\frac{dw}{dx}, \quad \frac{1}{r} = \frac{d\theta}{dx} = -\frac{d^2w}{dx^2}$$
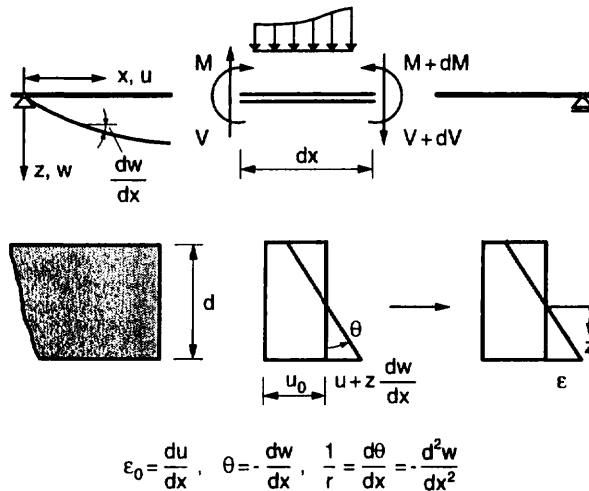
Fig. 4.1-1: Definitions

The basis for the theory of elasticity is a very simple **linear constitutive law**, which has nothing in common with the real behaviour of steel and concrete in the cracked state (Fig. 4.1-2)

$$\sigma = E \cdot \varepsilon . \qquad (4.1\text{-}5)$$

This is explained by the historical development of mechanics where one started with the most simple assumption to describe material behaviour. Otherwise the resulting analytical problems could not have been overcome.

With the equivalence relations

$$\begin{Bmatrix} N_i \\ M_i \end{Bmatrix} = \int_A \begin{Bmatrix} \sigma \; dA \\ \sigma{\cdot}z \; dA \end{Bmatrix} , \qquad (4.1\text{-}6)$$

regarding eqs. (4.1-3) and (4.1-4) one finds

$$\begin{Bmatrix} N_i \\ M_i \end{Bmatrix} = E \cdot \begin{Bmatrix} A \dfrac{du_0}{dx} \\[2mm] -I \dfrac{d^2w}{dx^2} \end{Bmatrix} ,$$

(4.1-7)

where

A   area of cross section
I   moment of inertia of cross section.
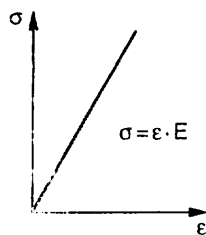
Fig. 4.1-2. Ideal-elastic constitutive law
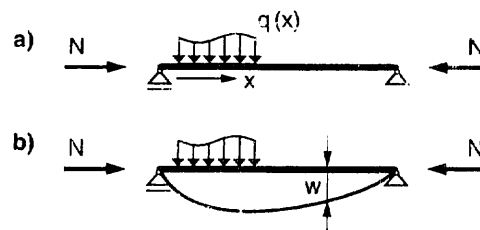
Fig. 4.1-3: System – II. Order theory

This equation may be written in an alternative form if one considers the last expression in eqs. (4.1-1)

$$\begin{Bmatrix} q_H \\ q_V \end{Bmatrix} = E \cdot \begin{Bmatrix} -A \dfrac{du_0}{dx} \\[2mm] \dfrac{d^2}{dx^2}\left(I \dfrac{d^2w}{dx^2} \right) \end{Bmatrix} .$$

(4.1-8)

The eqs. (4.1-7) and (4.1-8) are the classical differential equations (DE) of the elastic beam and the basis of all the well known formulas of structural beam analysis. Due to eqs. (4.1-3), (4.1-5) and (4.1-6) the normal force N = f (u$_0$) and the moment M = g(w") are decoupled. Therefore in the case of Fig. 4.1-3 a we have the following moment equilibrium condition for the **undeformed** bar with EI = const.

$$\begin{array}{ll} EIw'' & = -M_q(x) \\ \text{internal} & \text{external} \end{array} \qquad \text{I. Order Theory} \qquad (4.1\text{-}9\ a)$$

Here M$_q$ characterizes the external moment at the undeformed bar. However, taking the physically existent deformations exactly into account and writing the equilibrium condition for the **deformed** system according to Fig. 4.1-3 b we find

$$\begin{array}{ll} EIw'' & = -(M_q + N \cdot w) \\ \text{internal} & \text{external} \end{array} \qquad \text{II. Order Theory}$$

In this case vertical loading of the beam at constant normal force leads to an over-proportional displacement with regard to the load. This behaviour different from (4.1-9 a) is called **geometrically nonlinear** – equilibrium at the deformed system – and is indicated by a basically different type of differential equation (DE)

$$EIw'' + N \cdot w = -M_q(x) \qquad II.\ Order\ Theory \qquad (4.1-9\ b)$$

where superposition does not hold except in case of N/EI = constant. In case of big displacements as relevant e.g. when buckling occurs, one always has to use (4.1-9 b).

However in many cases one may omit the term $N \cdot w$ when either N or w is negligible small. If this approximation is allowed and $q_V(x)$ and $q_H(x)$ are known, the linear DE (4.1-9 a) can easily be integrated to get e.g. the flexibility coefficients at the supports of continuous girders e.g. for the different statically determined spans (see Fig.4.1-4) which are then used to form a solution system – superposition holds – of the following form

$$\begin{bmatrix} \delta_{11} & \cdots & \delta_{1n} \\ \vdots & \ddots & \vdots \\ \delta_{n1} & \cdots & \delta_{nn} \end{bmatrix} \cdot \begin{bmatrix} X_1 \\ \vdots \\ X_n \end{bmatrix} + \begin{bmatrix} \delta_{10} \\ \vdots \\ \delta_{n0} \end{bmatrix} = 0 \ , \qquad (4.1-10)$$

where the δ_{ik} are the displacements at the nodes under unit forces and moments and the δ_{i0} are the displacements at the statical determined subsystems under loads.
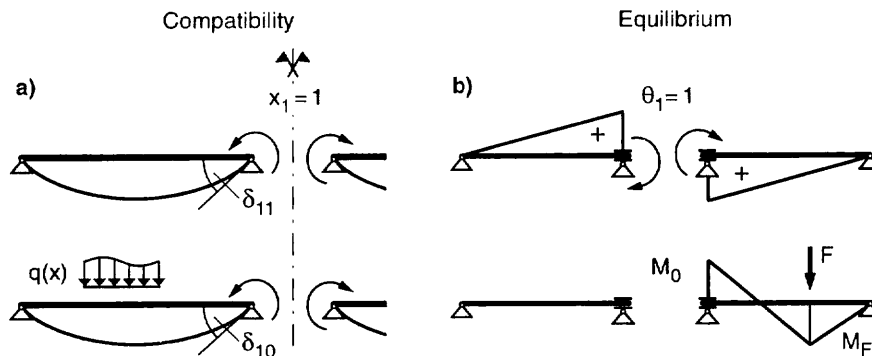
Fig. 4.1-4: Compatibility – equilibrium method

These **compatibility** equations may also be written in an alternative form

$$\Delta \cdot X + \delta_0 = 0 \quad or\ in\ indices\ notation \quad \delta_{ki} \cdot X_i + \delta_{k0} = 0 \ . \qquad (4.1-11)$$

In a similar manner **equilibrium** conditions may be derived for every support (see also Fig. 4.1-4 b).

$$K \cdot u = f \qquad resp. \qquad K_{ik} \cdot u_k = f_i \ , \qquad (4.1-12)$$

where **K** is the stiffness matrix and **u** resp. **f** are the displacement vector resp. the vector of external forces.

This theory of elasticity was the first consistent theory to analyse structures in its extended forms in one, two and three dimensions. Due to the linear constitutive law many civil engineering problems could finally be brought to linear differential equations, which had to be solved by analytical procedures.

For the serviceability state the gained results are sufficiently realistic for practical designing in spite of the underlying very simple constitutive law. Even nowadays the theory of elasticity is a useful tool to investigate RC-structures keeping in mind its restrictions for the ultimate state of loading.

(2)   Time-dependent behaviour

(2.1)   Creep at unbonded cables

For posttensioned reinforced concrete (RC) beams one has to regard the losses of prestress due to creep and shrinkage.

Starting with a simple creep law of the form

$$\varepsilon_{c.c}(t) = \frac{\sigma_c}{E_c} \cdot \phi(t)$$
(4.1-13)

the whole time-dependent deformation of concrete [see eq. (4.1-14)] consisting of an elastic and a creep part is

$$\bar{\delta}_{c1.i}(t) = [1 + \phi(t)] \cdot \delta_{c1.i} \,,$$
(4.1-14)

while in case of a steel member with no time-dependence

$$\delta_{p1.i}(t) = \delta_{p1.i} \,.$$
(4.1-15)
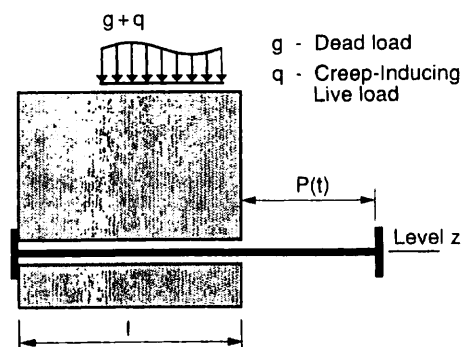
Fig. 4.1-5: Unbonded cable

Shrinkage is assumed to occur in time affinity to creep

$$\varepsilon_{c,s}(t) = \phi(t) \cdot \frac{\varepsilon_{c,s\infty}}{\phi_\infty} \,.$$
(4.1-16)

Exchanging X with P(t) in the compatibility eq. (4.1-10) for the case of an **unbonded** cable according to Fig. 4.1-5 then reads at any time increment

$$\frac{d}{dt}[(\bar{\delta}_{c1,1} + \delta_{p1,1}) \cdot P(t)] + \frac{d}{dt}[\bar{\delta}_{c1,o}(t)] + \frac{d}{dt}\left[-\frac{\varepsilon_{c,s\infty}}{\phi_\infty} \cdot \phi(t) \cdot l\right] = 0 \ . \tag{4.1-17}$$

Neglecting the creep of dP/dt one finds by differentiation

$$\frac{dP}{dt} \cdot \left(\delta_{c1,1} + \delta_{p1,1}\right) + P \cdot \delta_{c1,1} \cdot \frac{d\phi}{dt} +$$

$$+ \delta_{c1,0} \cdot \frac{d\phi}{dt} - \frac{\varepsilon_{c,s\infty}}{\phi_\infty} \cdot \frac{d\phi}{dt} \cdot l = 0 \qquad \left| \ \frac{dt}{d\phi} \cdot \frac{1}{\delta_{11}} \right. \tag{4.1-18}$$

or

$$\frac{dP}{d\phi} + P \cdot \frac{\delta_{c1,1}}{\delta_{11}} + \frac{\delta_{c1,0}}{\delta_{11}} - \frac{\varepsilon_{c,s\infty}}{\phi_\infty} \cdot \frac{l}{\delta_{11}} = 0 \ . \tag{4.1-19}$$

With

$$\frac{\delta_{c1,1}}{\delta_{c1,1} + \delta_{p1,1}} = \alpha \tag{4.1-20}$$

and

$$\frac{\delta_{c1,0}}{\delta_{11}} = -P_{(g+q)} \quad ; \quad \frac{\varepsilon_{c,s\infty}}{\phi_\infty} \cdot \frac{l}{\delta_{11}} = -\frac{\delta_{c,s\infty}}{\phi_\infty \cdot \delta_{11}} = \frac{P_{c,s\infty}}{\phi_\infty} \tag{4.1-21}$$

eq. (4.1-19) becomes

$$\frac{dP}{d\phi} + P \cdot \alpha - P_{(g+q)} - \frac{P_{c,s\infty}}{\phi_\infty} = 0 \ . \tag{4.1-22}$$

The solution of this Euler-equation is

$$P(\phi) = A \cdot e^{-\alpha\phi} + \frac{P_{(g+q)}}{\alpha} + \frac{P_{c,s\infty}}{\alpha \cdot \phi_\infty} \ . \tag{4.1-23}$$

With the initial condition:

$$\text{for} \quad t = 0 \quad \text{i.e.} \quad \phi = 0 \quad \rightarrow \quad P(\phi=0) = P_{(g+q)} + P_p \tag{4.1-24}$$

the undetermined value A becomes

$$A = P_{(g+q)} \cdot \left(1 - \frac{1}{\alpha}\right) + P_0 - \frac{P_{c,s\infty}}{\alpha \cdot \phi_\infty} \qquad (4.1\text{-}25)$$

and

$$P(\phi) = e^{-\alpha \cdot \phi} \cdot \left[P_{(g+q)} \cdot \left(\frac{\alpha - 1}{\alpha}\right) + P_0 - \frac{P_{c,s\infty}}{\alpha \cdot \phi_\infty}\right] + \frac{P_{(g+q)}}{\alpha} + \frac{P_{c,s\infty}}{\alpha \cdot \phi_\infty} . \qquad (4.1\text{-}26)$$

Then the decay of the prestressing force due to creep and shrinkage is

$$\Delta P(t) = P(\phi) - P_{(g+q)} - P_0 \qquad (4.1\text{-}27)$$

$$\Delta P(t) = -(1 - e^{-\alpha \cdot \phi}) \cdot \left[P_0 - \left(\frac{1-\alpha}{\alpha}\right) \cdot P_{(g+q)} - \frac{1}{\alpha \cdot \phi_\infty} \cdot P_{c,s\infty}\right] . \qquad (4.1\text{-}28)$$

Regarding eq. (4.1-16)

$$\frac{1}{\alpha \cdot \phi_\infty} \cdot P_{c,s\infty} = \frac{1}{\alpha \cdot \phi_\infty} \cdot \frac{P_{c,s}(t)}{\phi(t)} \cdot \phi_\infty = \frac{1}{\alpha \cdot \phi(t)} \cdot P_{c,s}(t) \qquad (4.1\text{-}29)$$

one finds the following loss of force in an **unbonded** prestressing cable

$$\Delta P(t) = -\left(1 - e^{-\alpha \cdot \phi(t)}\right) \cdot \left[P_0 - \left(\frac{1-\alpha}{\alpha}\right) \cdot P_{(g+q)} - \frac{1}{\alpha \cdot \phi(t)} \cdot P_{c,s}(t)\right] . \qquad (4.1\text{-}30)$$

(2.2) Creep after grouting

Following the derivations for the case of an unbonded cable according to section (2.1) it may easily be shown, that in case of a **bonded** cable one just has to substitute the global compatibility condition between steel and concrete by a local compatibility condition at every location x along the beam. One just has to replace $\delta_{c,i}$, $\delta_{p,i}$ by $\varepsilon_{c,i}$ and $\varepsilon_{p,i}$. From there it follows that the loss of stress in the cable at x is

$$\sigma_{p,s+c}(t) = -(1 - e^{-\alpha\phi(t)}) \left[\sigma_{p,o} - \frac{1-\alpha}{\alpha}\sigma_{p,(g+q)} - \frac{1}{\alpha\phi}\sigma_{p,s}\right] , \qquad (4.1\text{-}31)$$

where

$\sigma_{p,s+c}$ cable stress decay at level z due to shrinkage (S) and creep (C)
$\sigma_{p,o}$ cable stress at level z due to initial prestressing
$\sigma_{p,(g+q)}$ cable stress at level z due to creep initiating load
$\sigma_{p,s}$ cable stress at level z due to concrete shrinking.

However with a simplification proposed by Kupfer [see e.g. Rüsch/Kupfer (1975)] the problem may be linearized as follows (see Fig. 4.1-6)

Starting with the compatibility equation

$$\varepsilon_{cz,s+c} = \varepsilon_{p,s+c} \quad , \tag{4.1-32}$$

where $\varepsilon_{cz,s+c}$ means the **concrete strain** at steel **level z** due to creep and shrinkage, one has

$$\varepsilon_{c,s} + \varepsilon_{c,p(g+q)} \cdot \phi + \varepsilon_{c,s+c} = \varepsilon_{p,s+c} \quad . \tag{4.1-33}$$

With the linearization (see Fig. 4.1-6)

$$\sigma_{cz}{}^m = \sigma_{c,p(g+q)} + \frac{\sigma_{c,s+c}}{2} \tag{4.1-34}$$

eq. (4.1-33) becomes

$$\varepsilon_{c,s} + \left[\sigma_{c,p(g+q)} + \frac{\sigma_{c,s+c}}{2} \right] \cdot \frac{\phi}{E_c} + \frac{\sigma_{c,s+c}}{E_c} = \frac{\sigma_{p,s+c}}{E_p}$$

$$-\frac{\sigma_{p,s+c}}{E_p} + \frac{\sigma_{c,s+c}}{E_c} \cdot \frac{\phi}{2} + \frac{\sigma_{c,s+c}}{E_c} = -\varepsilon_{c,s} - \frac{\sigma_{c,p(g+q)}}{E_c} \cdot \phi \quad . \tag{4.1-35}$$

Regarding that

$$\sigma_{c,s+c} = \sigma_{p,s+c} \cdot \frac{\sigma_{c,p}}{\sigma_{p,p}} \tag{4.1-36}$$

where

$\sigma_{c,p}$ concrete stress due to prestressing
$\sigma_{p,p}$ cable stress due to prestressing

one finds with $\alpha_e = E_p/E_c$

$$\sigma_{p,s+c} \left[1 - \alpha_e \frac{\sigma_{c,p}}{\sigma_{p,p}} \left(\frac{\phi}{2} + 1 \right) \right] = \varepsilon_{c,s} \cdot E_p + \alpha_e \phi \sigma_{c,p(g+q)} \tag{4.1-37}$$

or finally the prestress loss in the cable due to shrinkage and creep

$$\sigma_{p,s+c} = \frac{\varepsilon_{c,s} \cdot E_p + \alpha_e \phi \sigma_{c,p(g+q)}}{1 - \alpha_e \frac{\sigma_{c,p}}{\sigma_{p,p}} \left(1 + \frac{\phi}{2} \right)} \quad . \tag{4.1-38}$$
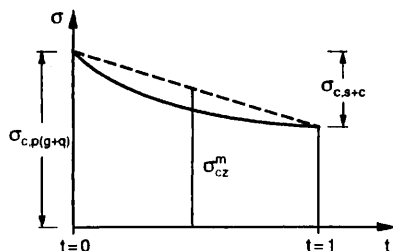
Fig. 4.1-6: Time dependent concrete stress at level z
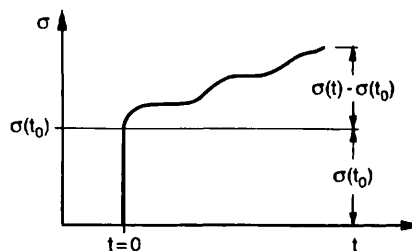
Fig. 4.1-7: Time dependent stress

The approach in CEB resp. EC 2 is slightly different, as it uses instead of eq. (4.1-13) the following creep formulation based on the so called superposition principle,

$$\varepsilon_{c,c}(t) = \sigma(t_0) \cdot J(t, t_0) + \int_{\tau = t_0}^{\tau = t} \left[J(t, \tau) \frac{\partial \sigma(\tau)}{\partial \tau} \right] d\tau \tag{4.1-39}$$

different from Dischinger's approach [see Dischinger (1939)], and where $\varepsilon_{c,c}$ is the concrete strain due to creep.

Instead of evaluation the integral exactly with regard to the load history changing in time, EC2 allows an approximation derived from a more or less mean constant load over the time under consideration (see factor 0.8 in eq. (4.1-40) and Fig. 4.1-7) to find for the whole strain including also the elastic one

$$\varepsilon(t) = \varepsilon_{c,s}(t) + \sigma(t_0) \cdot \frac{\phi(t, t_0)}{E_c(t_0)} + \left[\sigma(t) - \sigma(t_0) \right] \left[\frac{1}{E_c(t_0)} + 0.8 \frac{\phi(t, t_0)}{E_{c,28}} \right]. \tag{4.1-40}$$

Regarding that

$$\varepsilon_{c,s+c} = \frac{1}{E_c} \cdot \sigma_{p,s+c} \cdot A_p \cdot \left[\frac{1}{A_c} + \frac{1}{I_c} \cdot e^2 \right] \tag{4.1-41}$$

where e is the distance between cable fibre and the axis of gravity, the compatibility equation (4.1-33) leads to the following expression

$$\varepsilon_{c,s} + \frac{\varepsilon_{c,p(g+q)} \cdot \phi(t, t_0)}{E_c} + \sigma_{p,s+c} \cdot \frac{A_p}{E_c} \left[\frac{1}{A_c} + \frac{1}{I_c} \cdot e^2 \right] \cdot [1 + 0.8\phi(t, t_0)] = \frac{\sigma_{p,s+c}}{E_p} \tag{4.1-42}$$

and isolating $\sigma_{p,s+c}$ to

$$\sigma_{p,s+c} = \frac{E_p \cdot \varepsilon_{c,s} - \alpha_e \, \sigma_{c,p(g+q)} \cdot \phi}{1 + \alpha_e \cdot \frac{A_p}{A_c} \left[1 + \frac{A_c}{I_c} \cdot e^2 \right] \cdot [1 + 0.8 \, \phi]}. \tag{4.1-43}$$

(2.3)   Creep of systems

In several cases also the creep of systems, prestressed or not, is of interest. This means the change of internal forces in a RC-beam which deforms due to creep while connected to a steel girder which does not deform, or the change of internal forces when the static system of RC-structures is changed during the erection process. E.g. quite often simple supported prefabricated girders are first put on their supports and afterwards connected to one continuous girder (see Fig. 4.1-8).

Starting with the approach by Trost [see e.g. Trost (1973)] or *EC 2* to describe creep deformations and neglecting shrinkage we split up the internal moment resp. force in $X_k = X_{k,o} + X_{k,\phi}$ corresponding to $\sigma(t_0)$ rsp. $\sigma(t) - \sigma(t_0)$ (eq. (4.1 - 40)), to write

$$\bar{\delta}_{i,k}(t) = \delta_{i,k}[1 + \phi(t)] \cdot X_{k,0} + \delta_{i,k}[1 + \rho\phi(t)] \cdot X_{k,\phi}(t) \ . \tag{4.1-44}$$

So we have for a multiple indeterminate system

$$(1 + \phi) \cdot \boldsymbol{F} X_0 + (1 + \rho\phi) \cdot \boldsymbol{F} X_\phi(t) = -\delta_0(t) \tag{4.1-45}$$

where $\boldsymbol{F}$ is the usual flexibility matrix of the δ_{ik}'s, while X_0, $X_\phi(t)$ and $\delta_0(t)$ are the vectors of the X_k's at $t = 0$ and $t = t_\phi$ and the δ_{ko}'s. If one also has to consider structural members which do not creep like e.g. steel beams, one has to enlarge the equation to

$$[(1 + \phi) \cdot \boldsymbol{F}_c + \boldsymbol{F}_s] X_0 + [(1 + \rho\phi) \cdot \boldsymbol{F}_c + \boldsymbol{F}_s] X_\phi(t) = -[\delta_{0,c}(t) + \delta_{0,s}(t)] \tag{4.1-46}$$

where the subscripts c and s stand for concrete and steel.

In case of a monolithically built continuous system without steel elements we have

$$\bar{\delta}_{o,c} = (1 + \phi)\delta_{o,c} \tag{4.1-47}$$

or according to eq. (4.1-46)

$$(1 + \phi) \cdot [\boldsymbol{F}_c] X_0 + (1 + \rho\phi) [\boldsymbol{F}_c] X_\phi(t) = -(1 + \phi)\delta_{o,c} \ . \tag{4.1-48}$$

As

$$[\boldsymbol{F}_c] X_0 = -\delta_{o,c} \tag{4.1-49}$$

we find

$$(1 + \rho\phi) \cdot [\boldsymbol{F}_c] X_\phi(t) = 0 \quad or \quad X_\phi = 0 \ . \tag{4.1-50}$$

This confirms that a **monolithically** built continuous system without structural steel members – not reinforced – deforms but does not change its internal moments resp. force distribution.

Let us now discuss the example of a two-span girder which is erected so that two single supported prefabricated beams are put in position and then monolithically connected by concrete

over the internal support, disregarding the short age effects of the two different concretes (Fig. 4.1-8)
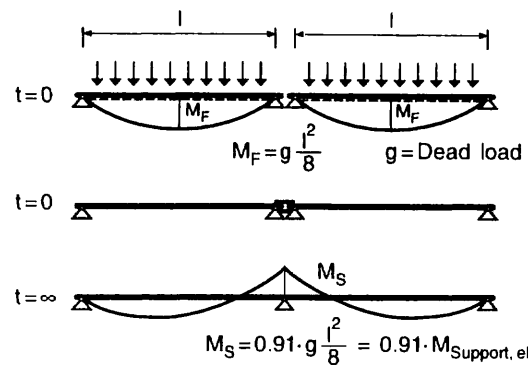
Fig. 4.1-8: Single span beams - converted to a continuous girder

At time t = 0 we have $X_{1,0} = 0$ and $\bar{\delta}_{10,c}(t) = \phi(t) \cdot \delta_{10,c}$, as there is no $\delta_{10,c}$ due to the closing process and therefore (see eq. 4.1-48)

$$(1 + \rho\phi)\,\delta_{11,c}\,X_\phi = -\phi\delta_{10,c}$$

(4.1-51)

so that

$$X_\phi = \frac{-\phi}{(1+\rho\phi)} \cdot \frac{\delta_{10,c}}{\delta_{11,c}} = M_{Support,el} \cdot \frac{\phi}{(1+\rho\phi)}$$

(4.1-52)

$$X_{t=\infty} = X_0 + X_\phi = \frac{\phi}{1+\rho\phi} \cdot M_{support,el}$$

As $M_{support,el}$ is the full elastic support moment for a continuous girder, we find for e.g. values of $\phi_\infty = 2.5$ and $\rho = 0.7$

$$X_{t=\infty} = X_0 + X_\phi = 0.91 \cdot M_{Support,el}$$

(4.1-53)

This result shows that 90 % of the elastic support moment enters by creep into the support location, when the two beams are monolithically connected at t = 0 with a support moment M_S equal 0 at that time.
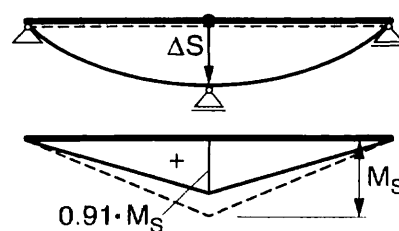
Fig. 4.1-9: Differential settlement of a two-span girder

In a similar manner one finds for a **sudden settlement** of a two span girder (Fig. 4.1-9) with

$$X_0 = M; \quad \delta_{10,c}(t) = \delta_{10,c} = const.$$

according to (4.1-48)

$$(1 + \phi) \cdot \delta_{11} \cdot M + (1 + \rho\phi)\, \delta_{11} \cdot X_\phi = -\, \delta_{10}$$

$$M + \phi M + (1 + \rho\phi)\, X_\phi = -\, \frac{\delta_{10}}{\delta_{11}} \tag{4.1-54}$$

$$X_\phi = M \cdot \frac{-\phi}{1 + \rho\phi}$$

or finally

$$X(t) = \left[1 - \frac{\phi}{1 + \rho\phi} \right] \cdot M . \tag{4.1-55}$$

With the parameters $\phi_\infty = 2.5 \quad \varrho = 0.7$ e.g. one finds

$$X_\infty = 0.091 \cdot M . \tag{4.1-56}$$

For a **slow settlement** affine to the creep-function where

$$X_0 = 0 \quad and \quad \delta_{10}(t) = \phi(t)\, \frac{\delta_{10}}{\phi_\infty}$$

we start again using eq. (4.1-48) to find

$$(1 + \phi)\, \delta_{11} \cdot 0 + (1 + \varrho\phi)\, \delta_{11}\, X_\phi = -\, \frac{\phi}{\phi_\infty}\, \delta_{10} \tag{4.1-57}$$

$$X_\phi = \frac{-\phi}{\phi_\infty} \cdot \frac{\delta_{10}}{\delta_{11}} \cdot \frac{1}{(1 + \varrho\phi)} \tag{4.1-58}$$

$$X_\phi = M \cdot \frac{\phi}{\phi_\infty(1 + \varrho\phi)} \tag{4.1-59}$$

$$X(t) = 0 + \frac{\phi}{\phi_\infty(1 + \varrho\phi)} \cdot M \tag{4.1-60}$$

and again with $\phi_\infty = 2.5 \quad \varrho = 0.7$

$$X_\infty = 0.364 \cdot M . \tag{4.1-61}$$

The difference between eqs. (4.1-56) and (4.1-61) is due to the fact, that in the first case the "driving creep force", which reduces the moment due to the settlement is higher than in the second case.

4.1.3   Elasto-plastic analysis of linear members

Already about a hundred years ago several experimentalists demonstrated that the theory of elasticity is a poor tool to describe realistically the behaviour of RC-structures in their **ultimate limit state**, what does not mean that the application of the theory of elasticity combined with an appropriate design format could not lead to a safe structure.
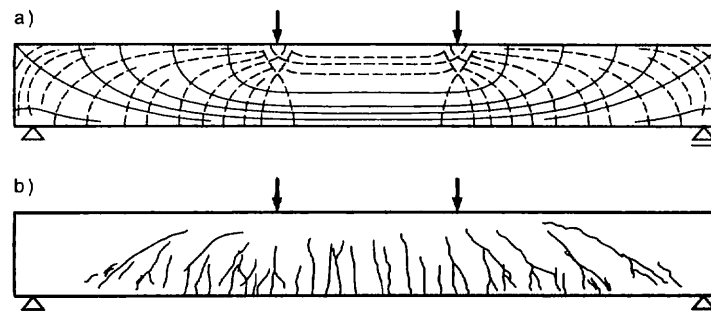
Fig. 4.1-10: a) Trajectories of an elastic beam; b) Cracked state of a realistic RC-beam

Nowadays we know, that due to the nonlinear behaviour of steel and concrete real structures show a nonlinear load deformation relation. Crack formation and the bearing capacity at the ultimate state can only be analysed taking this behaviour into account.

Probably the first authors who developed methods to analyse RC-structures in the ultimate limit state more precisely were Ingerslev (1921) and Johansen (1943), later on among others followed by Hillerborg (1975) with the so called **strip-method** named after him. These procedures are orientated and meanwhile more consistently developed on the basis of the theory of plasticity. The latter is also the basis of the so called strut and tie method, which is a well known engineering tool to treat RC-structures at the ultimate limit state.

It was the experimentalists' finding, that with incrementally loaded RC-structures like beams or plates cracks concentrate more and more at the locations of maximum moments within short locations or bands which might be called hinges.
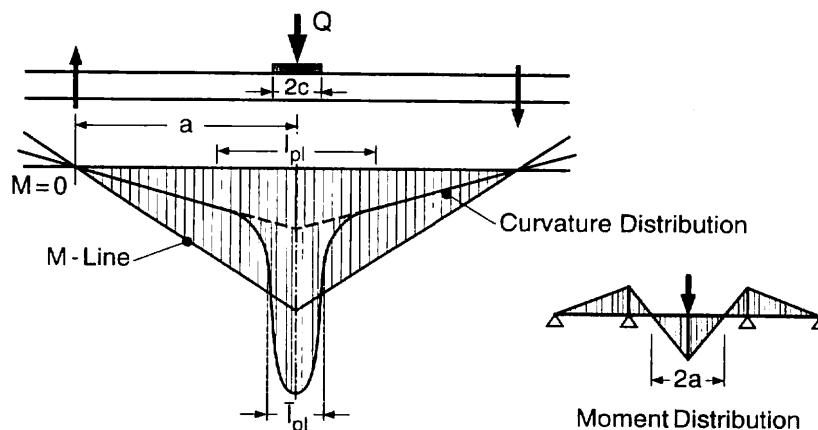
Fig. 4.1-11: Plastified length l_{pl} resp. $\bar{l}_{pl}$ of a three span girder under load [according to Dilger (1966)]
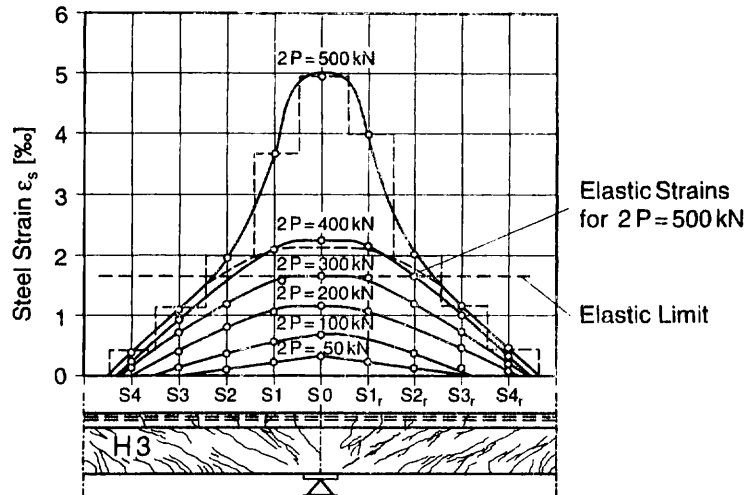
Fig. 4.1-12: Steel stresses over the middle support of a two span girder at different load stages [according to Dilger (1966)]

From there it seemed reasonable to base a more realistic analysis on the behaviour of such hinges and their moment-rotation relations (Fig. 4.1-13 a). The latter may be derived from more complex **constitutive laws**, as shown e.g. in Fig. 4.1-13 b to find the relevant **moment-rotation relations** as shown in Fig. 4.1-13 d for an elastic σ-ε behaviour, in Fig. 4.1-13 e for an elasto-plastic behaviour and in Fig. 4.1-13 f for an idealized rigid-plastic behaviour.

For reasons of simplicity it seems appropriate to work with a bilinear constitutive law – explicitly recommended in EC 2 – representing an ideal elasto-plastic behaviour as given in Fig. 4.1-13 b (2). However, as the first elastic part is of less influence, some principal considerations may also be derived from a so called rigid plastic behaviour (Fig. 4.1-13 b (1) resp. Fig. 4.1-13 f) as treated in the meanwhile classical theory of plasticity [see e.g. Szilard (1974), Thürlimann et al. (1983) or Thürlimann (1985)].
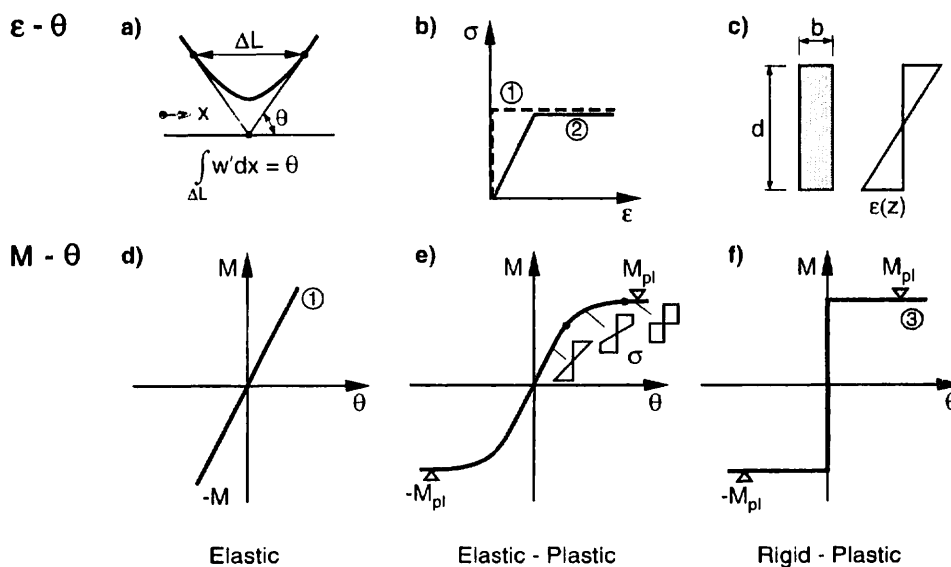
Fig. 4.1-13: Moment-rotation relations

The static limit theorem of this theory states that a system of loads acting on a structure in an allowed stress state which does not violate the yield-conditions, is always a lower bound for the sustainable loads. By definition this allowed stress state has to fulfill the equilibrium and static boundary conditions.

(In engineering terms: A system of loads in equilibrium under static boundary conditions and in agreement with the yield conditions fails only if one further weakens the structure or the static boundary conditions. This means that the calculated capacity is always smaller – at least equal – than the endurable one).

The kinematic limit theorem states that a system of loads being in equilibrium condition at an allowed kinematic state of deformation is always an upper bound for the endurable load. By definition this kinematic allowed state of deformation is one which is in accordance with the yield conditions and the geometric boundary conditions.

(In engineering terms: A n-times indeterminate beam needs n+1 plastic hinges to become a mechanism. Reaching the yield moments at these hinges at equilibrium, there might be always points within the structure where the available yield moments are surpassed, what means that not enough yield lines have been assumed. Only strengthening at those points would keep the structure safe. Therefore the calculated capacity is always higher – at least equal – than the real bearing capacity).

Let us now start to investigate the continuous RC-beam, one time undetermined, as given in Fig. 4.1-15. The plastic Moments $+M_{pl}$ and $-M_{pl}$ are easily determined according to Fig. 4.1-14.

By means of the equilibrium condition

$$f_y A_s = f_c \cdot \alpha d b \tag{4.1-62}$$

where f_y resp. f_c are yield stress of steel resp. concrete strength and A_s is the steel area,

and the definition of the mechanical reinforcement ratio

$$\omega = \frac{A_s}{bd} \cdot \frac{f_y}{f_c} \tag{4.1-63}$$

it follows immediately that $\alpha = \omega$, so that the yield moment is determined by

$$M_y = f_y \cdot A_s \cdot d \left(1 - \frac{\omega}{2}\right) . \tag{4.1-64}$$
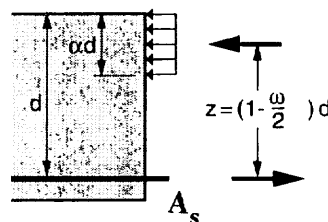
Fig. 4.1-14: Plastic moment
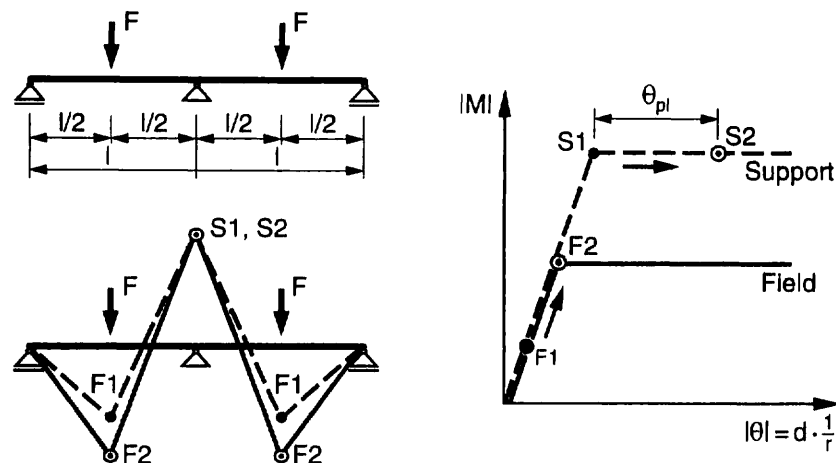
Fig. 4.1-15: Elasto-plastic beam (absolute values of M and θ)

To study the elasto-plastic behaviour of the structure in Fig. 4.1-15 in agreement with the general solution strategy for nonlinear equations we start increasing the load in Fig. 4.1-15 incrementally in several steps from zero to the ultimate load capacity.

In the first step we load until the yield moment at the internal support is reached – the yield moments at design being chosen as such. Now a hinge forms at the support. We are at points F1 and S1 in the moment-rotation diagram. In a second step we increase the load further. While the field moment rises to the plastic moment at F2, the support moment remains constant, rotating just along θ_{pl} to reach finally S2.

Now we have reached the ultimate bearing capacity of the system as a mechanism is formed and the load can no more be augmented.

However, to reach this state it is required that the necessary plastic rotation θ_{pl} is available at the hinge from S_1 to S_2 according to Fig. 4.1-15. Otherwise a premature failure could occur.

From these considerations a very simple design procedure results: Just choose arbitrarily the yield moments at the supports and the yield moments in the fields according to equilibrium, so that

$$\frac{M_{S,y}}{2} + M_{F,y} = \frac{Fl}{4} \qquad (4.1-65)$$

and design the hinges using the yield strength of steel. This is a safe state as long as the necessary rotation capacity θ_{pl} is available at the relevant hinges. From these considerations another interpretation of the static limit theorem is possible:

Every equilibrium state is a safe one as long as all necessary rotations – deformations – are available by sufficient ductility of the structure.

As will be demonstrated however the question whether the necessary rotation capacity is available plays an important role within such a plastic design. For different types of detailing at the locations of plastic hinges special diagrams have to be developed.

Tests at the authors institute for different designs of frame corners (Fig. 4.1-16) which were carried out to find the relevant moment-rotation diagrams have shown [see Eibl/Akkermann (1997)] that several conventionally used structures are by far not a priori good-natured. Bad detailing with regard to ductility may not allow a big plastic rotation at the frame corner. So in many cases, where not enough practical experience exists, a check of the type

$$\text{rotation}_{\text{calc}} \leq \text{rotation}_{\text{available}}$$

might be necessary .
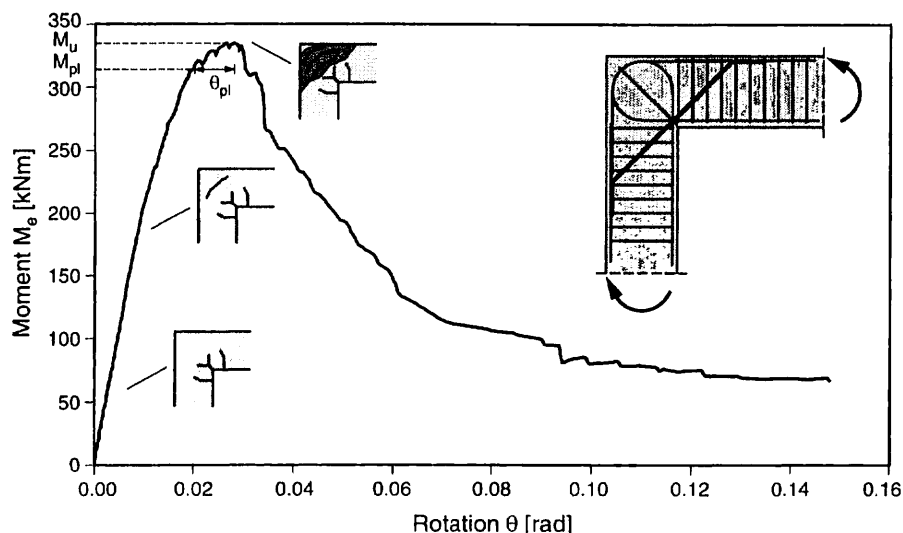
Fig. 4.1-16: Moment-rotation relation for a frame corner

Starting from Fig. 4.1-15 the principal method to do such a comparison may be sketched as follows:

One starts with a more or less arbitarily chosen system of plastic hinges, determined by their yield moments which fulfill the statical boundary conditions and the equlibrium condition. Then the curvatures along the different beam sections between the hinges have to be integrated using material mean values and assuming cracked cross sections in moment curvature diagrams. The so gained resulting rotations can now be compared with the endurable ones at the hinges.

Codes like EC 2 striving for simplification of course provide special boundary conditions at which internal forces and moments calculated according to the theory of elasticity may be "redistributed" **without** any check of allowed rotation. This means that the relevant moments at the supports and fields may be changed pragmatically within certain limits fulfilling just the equilibrium conditions.

(1) Remarks on the strut-and-tie method

The strut-and-tie method (ST-method) is a useful tool to describe approximately the ultimate state behaviour of a RC-structure if some boundary conditions of the method are observed. Usually it is not applicable to determine the serviceability state.

This method is based on the theory of plasticity, mainly on its static limit theorem. The designer chooses a ST-model which is in static determinate equilibrium and fulfills the static boundary conditions. The selection of this equilibrium model may be supported by an elastic investigation indicating the "flow of forces" which fulfill also the elastic compatibility conditions.
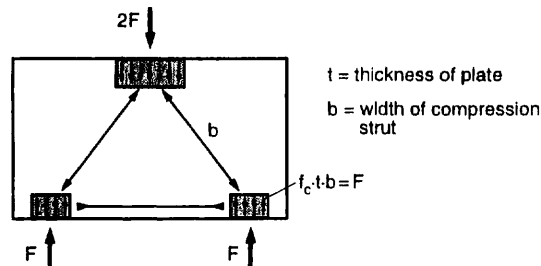
Fig. 4.1-17: Strut-and-tie model

Fig. 4.1-17 shows the typical example of an inplane loaded RC-plate under single forces. In such a static determinate equilibrium system the compression diagonals and the tension chords may easily be determined. The width of the compression "strut" can be very roughly approximated as long as sufficient space is available for the compression stresses to spread out. If one small portion of the strut is overstressed the force spreads according to the curved stress-strain relation of concrete in compression.

At critical points the effective width may be determined by equilibrium conditions, e.g. at the locations of the outer forces by means of $F = f_c \cdot t \cdot b$. Hints to choose b_{effect} in other cases are given in chapter 4.4.
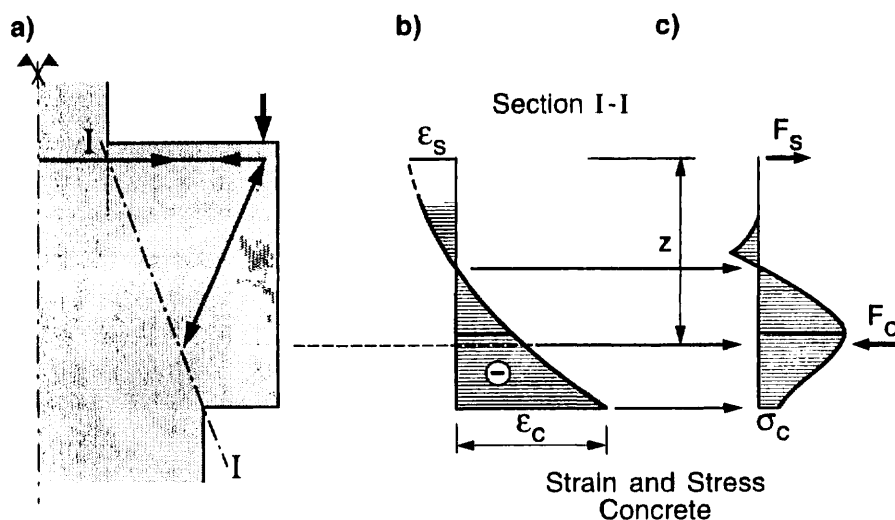
Fig. 4.1-18: Stress-concentration in the reentrant corner of a corbel

However in situations with a highly nonlinear strain distribution one has to be cautious. In experiments with corbels the author and Zeller (1991) found highly nonlinear strain distributions (see Fig. 4.1-18) in the reentrant corner, where the peak strain was far beyond the value belonging to the endurable peak stress of concrete (Fig. 4.1-18 b and 4.1-18 c). The bearing capacity

of the corbel was only 2/3 of the calculated value. The reason is that the concrete at the corner due to extreme strain values will be crushed at the reentrant corner loosing its strenght. Now an unstable situation arises when with a further increment of loading a shortening of the internal lever arm occurs, which again leads to a further increase of strain.

There is a slight deficiency within the ST-method, as it does not include compatibility conditions to find the only one compatible equilibrium system. A further imperfection is, that it is based on a moment rotation behaviour as shown in Fig. 4.1-19 a, while in reality, depending on the constitutive behaviour of concrete and also reinforcement detailing, curves similar to Fig 4.1-19 b are relevant.
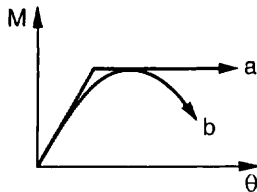
Fig. 4.1-19:   a) ideal elasto-plastic,   *Fig. 4.1-20:*   Equilibrium system, alternative to Fig. 4.1-17
              b) realistic moment-rotation-curve

From a theoretical point of view there is a general infinity of allowed equilibrium systems, wich are all safe if the required ductility is available. However, there is no consistent method within the frame of the strut and tie method alone to find out which one will show up in reality.

As an example in Fig. 4.1-20 a second equilibrium system for the same load configuration as in Fig. 4.1-17 is sketched, of course leading to a different stress distribution. Only compatibility could decide which is the realistic one in an experiment.

However this deficiency can be healed if the equilibrium system to be chosen is orientated at the results of an investigation based on the theory of elasticity. According to the latest code developments, it is necessary to check the serviceability state anyhow.

In such a case one starts carrying out an elastic calculation by means of a computercode, which is able to plot the main stresses also with regard to direction and stress intensity. Now one takes a pencil and draws a "similar" simplified equilibrium system over this plot based on the knowledge of a reasonable reinforcement layout. Then this equilibrium system may be used to design for the ultimate limit state. So usually one has now ductility problems or is alarmed at least if the stress plot shows extreme compression concentrations, which cannot spread out to the surrounding neighbourhood.

(2)   Slabs

(2.1)   Lower bound – static method

This method is based on the theory of plasticity as e.g. is shown in a very consistent form by the Zürich-School in Thürlimann/Marti/Pralong/Rotz/Zimmerli (1983). To demonstrate its principal use we discuss an example of this publication as shown in Fig. 4.1-21 with reinforcement at the bottom of the slab able to endure a plastic moment

$$m_{x,R} = m_{y,R} = m_R .$$ (4.1-67)

We assume a parabolic moment distribution of the type

$$m_x = m_{xo} (1 - A \cdot x^2)$$
$$m_y = m_{yo} (1 - B \cdot y^2)$$ (4.1-68)

which fulfills the static boundary conditions $m_x = 0$ and $m_y = 0$ with

$$x = \pm a/2; \qquad y = \pm b/2$$
$$A = 4/a^2 \quad \text{and} \quad B = 4/b^2.$$

so that

$$m_x = m_{xo}(1 - 4\frac{x^2}{a^2}) ; \qquad m_y = m_{yo}(1 - 4\frac{y^2}{b^2}) .$$ (4.1-69)
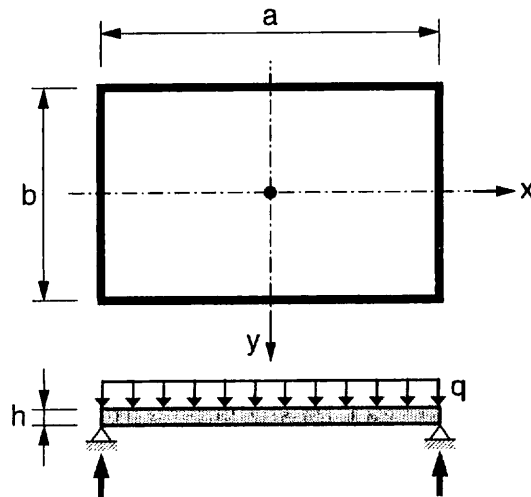
Fig. 4.1-21: Rectangular slab supported at four hinges

From vertical equilibrium conditions (see Fig. 4.1-22)

$$\frac{\partial^2 m_x}{\partial x^2} + 2\frac{\partial^2 m_{xy}}{\partial x \partial y} + \frac{\partial^2 m_y}{\partial y^2} + q = 0$$ (4.1-70)

we find easily

$$q = 8 m_{xo} \frac{1}{a^2} + 8 m_{yo} \frac{1}{b^2}$$ (4.1-71)

and by use of the yield conditions

$$m_R - m_{xo} \geq 0 \quad \text{and} \quad m_R - m_{yo} \geq 0$$ (4.1-72)

we get finally the bearing capacity

$$q_{max} = \frac{8 m_R}{b^2} (1 + \frac{b^2}{a^2}) \ .$$ (4.1-73)

By means of the moment-equilibrium conditions around the axis x resp. y

$$\frac{\partial m_x}{\partial x} + \frac{\partial m_{yx}}{\partial y} - v_x = 0, \qquad \frac{\partial m_y}{\partial y} + \frac{\partial m_{xy}}{\partial x} - v_y = 0$$ (4.1-74)

we can also derive the shear forces V_x and V_y by differentiation to find

$$v_x = - 8 m_R \frac{x}{a^2} \ , \qquad v_y = - 8 m_R \frac{y}{b^2} \ .$$ (4.1-75)
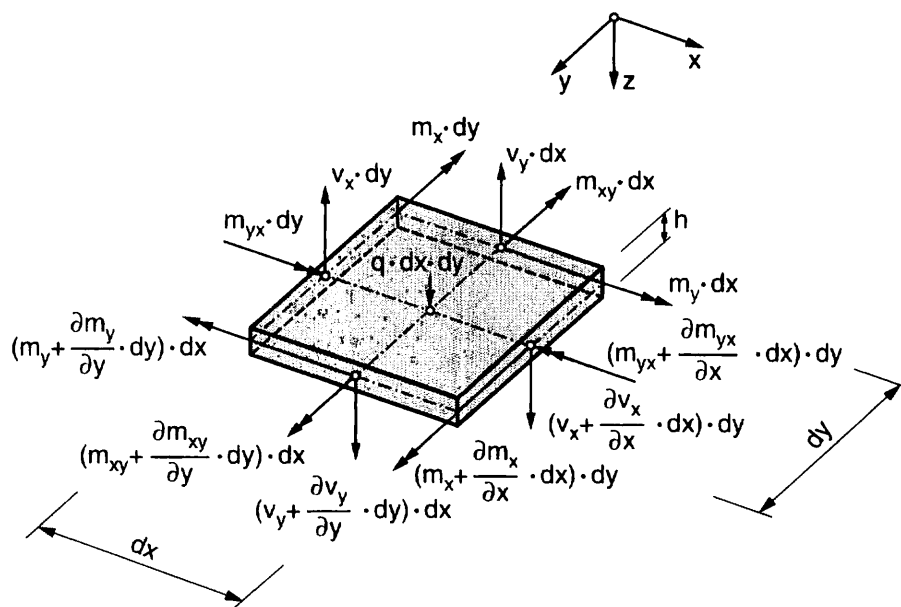
Fig. 4.1-22: Plate element [Scilard (1974)]

(2.2)   Strip-method according to Hillerborg/Marcus

This method has been proposed already by Markus (1924) in connection with the theory of elasticity at that time. In the meantime it is known as the Hillerborg-strip-method as Hillerborg (1975) developed it to the nowadays applicated form. Theoretically it is also based on the lower bound theorem of the theory of plasticity.

One just chooses a system of strips – beams – which are in equilibrium with the whole external loads of the slab. The internal forces and moments of each individual beam may then be calculated due to the theory of elasticity or again just by fulfilling equlilibrium conditions. Finally a cross section design is carried out for each beam [according to Fig. 4.1-23 and Kordina et al. (1992)]. Compatibility of deformations is in most cases not controlled.
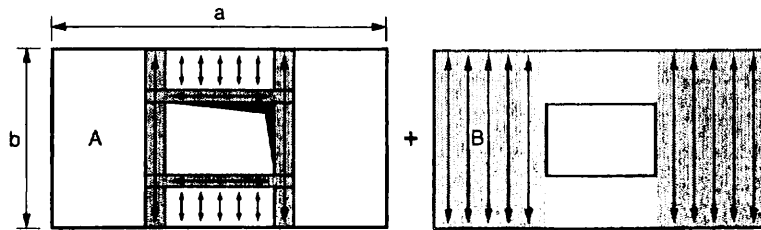
Fig. 4.1-23: Equilibrium system of strips

The result of such a design however is – as already mentioned – only safe, if sufficient ductility is guaranteed by a reasonable steel behaviour and if, as EC 2 demands, a separate serviceability state control is carried out.

(2.3)   Yield-line method

According to the kinematic theorem of the theory of plasticity one starts from a state of deformation characterized by rigid parts between hinges – yield line pattern – which is in accordance with the yield conditions and the geometric boundary conditions and then formulates the virtual work equation i.e. the equilibrium conditions [see e.g. Szilard (1974)]

$$W_e - W_i = 0 .$$ (4.1-76)

Diagram of a Plate Segment "j"
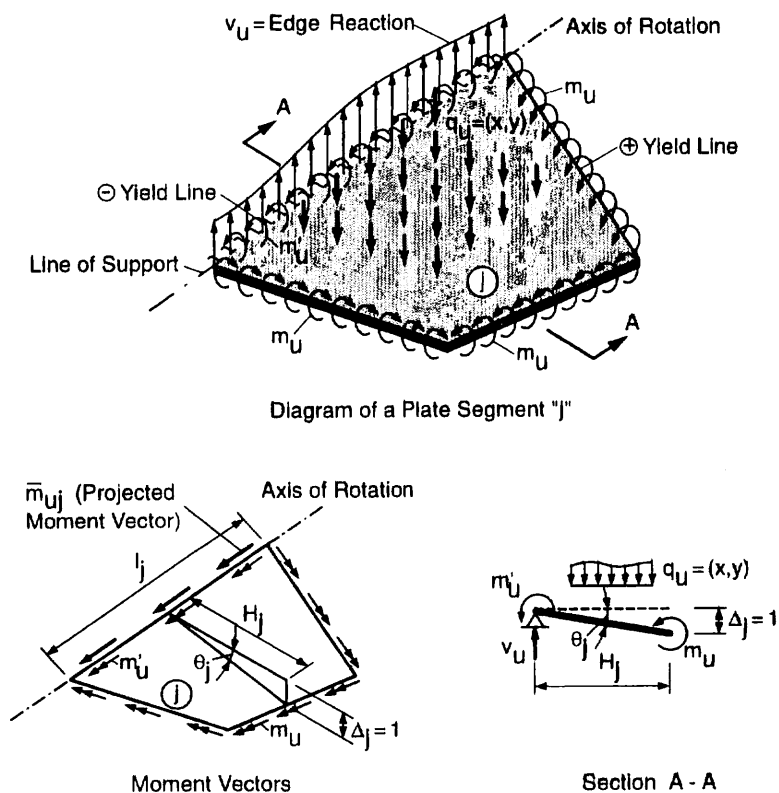
Fig. 4.1-24: Plate segments [taken from Szilard (1974)]

The work of the external loads due to a virtual displacement $\delta(x,y)$ is

$$W_e = \sum_n \left(\iint_A q(x,y) \cdot \delta(x,y) \, dA + \int_l Q(s) \cdot \delta(s) \, ds + \sum_i Q_i \cdot \delta_i \right) \qquad (4.1\text{-}77)$$

where

$Q(s)$ external line loads,
Q_i single loads and
$q(x,y)$ distributed loads.

The internal virtual work is

$$W_i = \sum_j (\theta_j \, m_j \, l_j) \qquad (4.1\text{-}78)$$

where

θ_j Δ_j / H_j = "normal" rotation of the plate segments,
m_j yield moment projected to the hinge line (see Fig.4.1-24) and
l_j length measured along the yield line.

To find yield line patterns, the following general hints may be helpful

– Yield lines are usually straight lines,
– Yield lines with negative moments develop, along fixed boundaries
– Yield lines pass through the intersections of the axis of rotation of adjacent slab elements.

A collection of sampled yield line patterns for the most relevant boundaries are also given in Szilard (1974) (see e.g. Fig. 4.1-25).
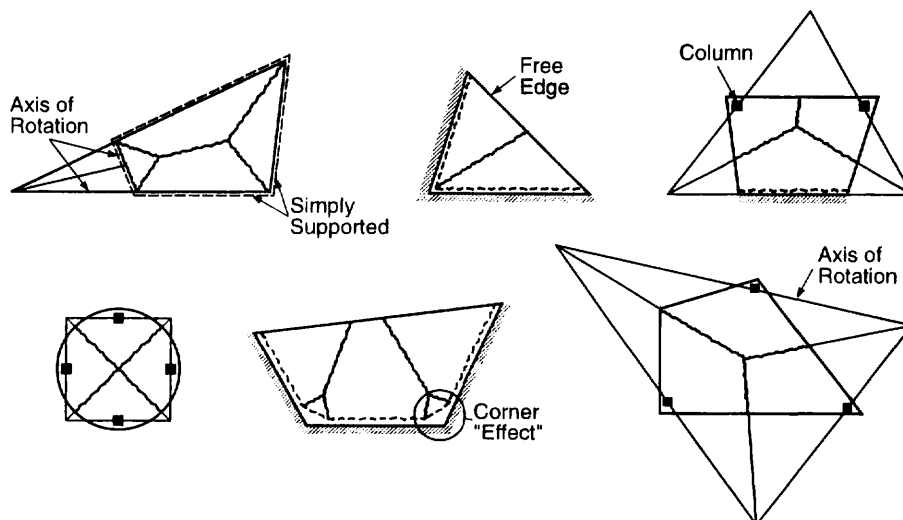
Fig. 4.1-25: Possible yield-line pattern [Szilard (1974)]

Now a typical example, where the positive yield moment is $m_R = 0.8\,M$ and the negative $m'_R = 1.6\,M$ may demonstrate the method [see Fig. 4.1-26 and Kordina et al. (1992)].

The external work done by the distributed loads is

$$W_e = q\,(V_{1a} + V_{1b} + V_2)\tag{4.1-79}$$

where V represents the "volume of the pyramid" produced by the virtual displacement, so that

$$W_e = q \cdot \Delta \left[(a - x) \cdot \frac{b}{2} + \frac{xb}{2} \cdot \frac{1}{3} + \frac{xb}{2} \cdot \frac{1}{3} \right].\tag{4.1-80}$$

With $\theta_1 = \dfrac{\Delta}{b}$ and $\theta_2 = \dfrac{\Delta}{x}$ the internal virtual work is

$$W_i = M \left[(1.6\frac{\Delta}{x} \cdot b + 0.8\frac{\Delta}{x} \cdot b) + (1.6\frac{\Delta}{b} \cdot a + 0.8\frac{\Delta}{b} \cdot x) \right].\tag{4.1-81}$$

Equating (4.1-80) and (4.1-81) one finds a function

$$q = f(M, a, b, x)\tag{4.1-82}$$

which may be minimized with regard to x from

$$\frac{df}{dx} = 0\,.\tag{4.1-83}$$
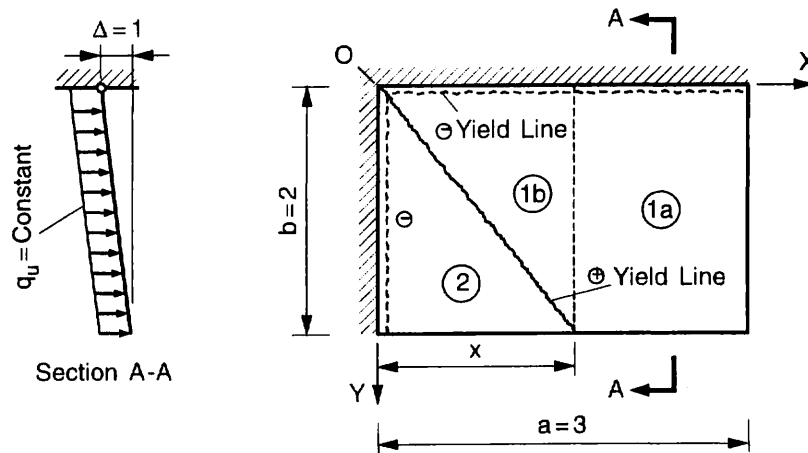
Fig. 4.1-26: Uniformly loaded plate with free and clamped edges

Remember however that this calculated bearing capacity may not be a safe one per se according to the kinematic limit theorem of the theory of plasticity.

4.1.4 Nonlinear analysis

(1) Basic equations - linear members

Of course a nonlinear analysis has to fulfill the equilibrium conditions as already given in chapter 4.1.2

$$\frac{d^2M}{dx^2} = -q_V$$

$$\frac{dN}{dx} = -q_H$$

(4.1-84)

as well as the kinematic relation

$$\varepsilon = \varepsilon_0 + z \cdot 1/r .$$

(4.1-85)

Also the equivalence relations (4.1-7)

$$\left\{ \begin{array}{c} N_i \\ M_i \end{array} \right\} = \int_A \left\{ \begin{array}{cc} \sigma(\varepsilon) & dA \\ \sigma(\varepsilon) \cdot z & dA \end{array} \right\}$$

(4.1-86)

must hold.
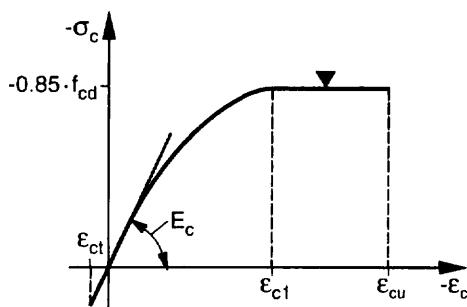
Fig. 4.1-27: Stress-strain relation for concrete according to CEB Model Code (MC 90)

Nonlinearity is introduced with the constitutive law for concrete according to CEB MC 90 (Fig. 4.1-27)

$$\sigma_{cd} = 0.85 f_{cd} \cdot \left[2 \left(\frac{\varepsilon_c}{\varepsilon_{cl}} \right) - \left(\frac{\varepsilon_c}{\varepsilon_{cl}} \right)^2 \right] \qquad for \quad \varepsilon_c < \varepsilon_{cl}$$

$$\sigma_{cd} = 0.85 f_{cd} \qquad for \quad \varepsilon_{cl} \le \varepsilon_c \le \varepsilon_{cu}$$

(4.1-87)

and also a modified stress-strain relation for steel (see Fig. 4.1-30).

With this set of

2 equilibrium equations	(4.1-84)
1 kinematic equation	(4.1-85)
2 equivalence equations	(4.1-86)
2 constitutive equations	(4.1-87), (Fig. 4.1-30)

the 7 unknowns – q_V, q_H being known – M, N, ε, u, w and σ_c, σ_s can be determined.

However the determination of forces and moments in a statically indeterminate beam considering material nonlinearity by these equations is only possible by a numerical solution technique. There are of course several such methods (see e.g. also the Finite Difference Method). It is even possible to treat them as an initial boundary value problem by means of the so called dynamic relaxation method. In doing so one starts with a dynamic equilibrium equation which includes mass terms, chooses a reasonable high artificial damping to find finally the static solution as the final state of the dynamic problem [see e.g. Kesting (1979), Eibl (1981) or Eibl & Häußler (1996)].

However according to the current state of the art it is advisable to discuss the specific problems of reinforced concrete within the usual Finite Element Method (FEM).

Following Eibl/Häußler/Retzepis (1990) we start with the principle of virtual displacement – equilibrium conditions

$$\int_V (\delta \varepsilon^T \cdot \sigma) dV = \int_l (\delta u^T \cdot f) dx + \sum_i (\delta u^{iT} \cdot F^i) \tag{4.1-88}$$

where the stresses, strains resp. curvatures and the forces and moments are given as follows (see also chapter 4.1.2 equation (4.1-4) to (4.1-7))

$$f = \begin{pmatrix} f_x \\ f_z \\ m_y \end{pmatrix} \qquad F = \begin{pmatrix} F_x \\ F_z \\ M_y \end{pmatrix} \tag{4.1-89}$$

$$\varepsilon = \begin{pmatrix} \varepsilon_0 \\ 1/r \end{pmatrix} = B \cdot u \tag{4.1-90}$$

$$\sigma = \begin{Bmatrix} N \\ M \end{Bmatrix} = \int_A \begin{Bmatrix} \sigma(\varepsilon) \, dA \\ \sigma(\varepsilon) \cdot z \, dA \end{Bmatrix} = C \cdot \begin{pmatrix} \varepsilon_0 \\ 1/r \end{pmatrix} = C \cdot B \cdot u \ . \tag{4.1-91}$$

The matrix C includes the constitutive laws.

As it is well known, the equilibrium conditions for the element then are

$$k \cdot u = r \tag{4.1-92}$$

with the element stiffness matrix **k** and the load vector **r**

$$k = \int_0^l B^T \cdot C \cdot B \, dx \, , \qquad r = \int_0^l H^T \cdot f \, dx + F \, . \tag{4.1-93}$$

H^T is the element-shape function, for which one may choose a three node isoparametric element with the node-deformations $u(x)$, $w(x)$ and the rotation $\theta(x)$ (see Fig. 4.1-28)

$$u = \begin{pmatrix} u(x) \\ w(x) \\ \theta(x) \end{pmatrix} = \begin{bmatrix} H_1 & 0 & 0 \\ 0 & H_2 & 0 \\ 0 & 0 & H_3 \end{bmatrix} \cdot \begin{pmatrix} u_1 \\ w_1 \\ \theta_1 \\ \vdots \\ u_3 \\ w_3 \\ \theta_3 \end{pmatrix} = H \cdot u^e \, . \tag{4.1-94}$$
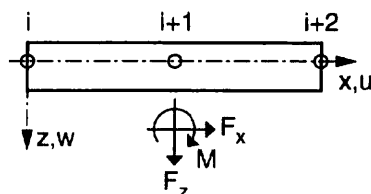
Fig. 4.1-28: Element and notations

The elements of the matrix $H = (H_1, H_2, H_3)$ are a second order Hermite polynom for $N_u(x)$, a fifth order Hermite polynom for $N_w(x)$ and and derivations from them

$$H_i = \begin{pmatrix} N_u(x) & 0 & 0 \\ 0 & N_w(x) & N_\theta(x) \\ 0 & \dfrac{-dN_w}{dx} & \dfrac{-dN_\theta}{dx} \end{pmatrix} \, . \tag{4.1-95}$$

By means of these shape functions

$$\varepsilon = \begin{bmatrix} \dfrac{d}{dx} & 0 & 0 \\ 0 & -z\dfrac{d^2}{dx^2} & 0 \end{bmatrix} \cdot u = B \cdot u \tag{4.1-96}$$

and the constitutive laws for concrete and steel also the matrix C

$$\sigma = \begin{pmatrix} N \\ M \end{pmatrix} = \int_A \begin{pmatrix} \sigma(\varepsilon) \ dA \\ \sigma(\varepsilon) \cdot z \ dA \end{pmatrix} = \frac{0.85 f_{cd}}{\varepsilon_{cl}} \cdot \begin{pmatrix} C_{11} & C_{12} \\ C_{21} & C_{22} \end{pmatrix} \cdot \begin{pmatrix} \varepsilon_0 \\ 1/r \end{pmatrix} \tag{4.1-97}$$

can be determined. The resulting elements of C as developed by Eibl/Häußler/Retzepis (1990) are

$$C_{11} = \left(\frac{\varepsilon_0}{\varepsilon_{cl}} - 2 \right) S_0, \tag{4.1-98}$$

$$C_{12} = 2 \left(\frac{\varepsilon_0}{\varepsilon_{cl}} - 1 \right) S_1 + \frac{1/r}{\varepsilon_{cl}} S_2, \tag{4.1-99}$$

$$C_{21} = \left(2 - \frac{\varepsilon_0}{\varepsilon_{cl}} \right) S_1, \tag{4.1-100}$$

$$C_{22} = -2 \left(\frac{\varepsilon_0}{\varepsilon_{cl}} - 1 \right) S_2 + \frac{1/r}{\varepsilon_{cl}} S_3, \tag{4.1-101}$$

where the area moments S_k are defined as $\int_A z^k \, dA$ (see Fig. 4.1-29)

$$S_k = \int_A z^k \, dA = \frac{1}{k+1} \cdot \sum_i^m b_i \cdot (z^{k+1}_{i_{up}} - z^{k+1}_{i_{down}}). \tag{4.1-102}$$

For a better understanding of the evaluation of the C_{ij}'s the terms C_{11} and C_{12} are determined as follows. Let us start with $N = N(\varepsilon_0, 1/r)$ or $N = \int_A \sigma(\varepsilon) dA$.
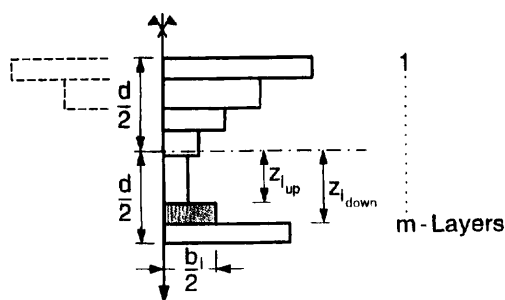
Fig. 4.1-29: Discretization of beam cross section

Regarding that [see (4.1-87)]

$$\varepsilon = \varepsilon_0 + z \cdot 1/r, \qquad \sigma_c = -0.85 f_{cd} \left[2 \left(\frac{\varepsilon_c}{\varepsilon_{cl}} \right) - \left(\frac{\varepsilon_c}{\varepsilon_{cl}} \right)^2 \right] \tag{4.1-103}$$

and that σ is negative in compression, we find [see also eq. (4.1-102)] for $N = \int_A \sigma(\varepsilon) da$ according to

$$N = \begin{vmatrix} C_{11} & \vert & C_{12} \\ \hline & \cdots\cdots\cdots\cdots\cdots\cdots\cdots\cdots\cdots\cdots & \end{vmatrix} \cdot \begin{Bmatrix} \varepsilon \\ 1/r \end{Bmatrix} \qquad (4.1\text{-}104)$$

$$N = \begin{vmatrix} \left(\dfrac{\varepsilon_0}{\varepsilon_{cl}} S_0 - 2S_0 \right) & \vert & \left(2\dfrac{\varepsilon_0}{\varepsilon_{cl}} S_1 - 2S_1 + \dfrac{1/r}{\varepsilon_{cl}} S_2 \right) \\ \hline & \cdots\cdots\cdots\cdots\cdots\cdots\cdots\cdots\cdots\cdots & \end{vmatrix} \cdot \begin{Bmatrix} \varepsilon \\ 1/r \end{Bmatrix} \qquad (4.1\text{-}105)$$

As long as no more exact modelling e.g. including a bond law is applied, the reduced steel strain due to the surrounding concrete may be taken into account using a stress-strain relation for steel σ-ε_R as given in Fig 4.1-30 with f_{yk} resp. f_{tk} for the characteristic yield strength of steel resp. the characteristic strength of steel at rupture (see chapter 3.2).

The steel stress σ_{sr} at cracking is derived with $\alpha_e = E_s/E_c$ from the condition

$$E_s \varepsilon_c A_s + E_c \varepsilon_c A_c = A_s \sigma_{sr}$$

$$E_s \varepsilon_c \left[1 + \frac{1}{\alpha_e \mu} \right] = \sigma_{sr} . \qquad (4.1\text{-}106)$$

Fig. 4.1-30: Stress-strain relation for embedded steel (tension stiffening) according to MC 90

(2)   Constitutive laws for plane biaxial RC-structures within a FE-code

(2.1)   Concrete

To treat biaxial structures by means of the FE-method one needs again elements and shape functions to start with an assumption for the displacement field $u = f(x,y)$, $v = g(x,y)$. This problem is not RC-specific and can be taken from any text book on Finite Elements. Its main steps are just repeated as follows:

Starting with generalized deformations, where the u^e are the element-node-displacements

$$u = \begin{vmatrix} u \\ v \end{vmatrix} = |\phi| \cdot u^e \qquad (4.1\text{-}107)$$

we find strains, curvature etc. by a differential operation in the usual form

$$\varepsilon = Lu = B \cdot u^e . \qquad (4.1\text{-}108)$$

Adding a constitutive law

$$\sigma = D \cdot \varepsilon \qquad (4.1\text{-}109)$$

and using the virtual work equation – equilibrium – one finally finds the governing displacement equation

$$K(u) \cdot u = F \qquad (4.1\text{-}110)$$

with the relevant element values of **K** and **F**

$$k = \int_A B^T DB \cdot dA$$

$$f_q = \int_A \phi^T q \cdot dA \qquad . \qquad (4.1\text{-}111)$$

$$f_Q = \int_S \phi^T Q \cdot dS$$

where Q resp. q are line resp. area loads.

Regarding reinforced concrete the main problem within this process is to find an appropriate formulation for the constitutive law for concrete [see. eq. (4.1-109)].

To demonstrate the **principal** approach for plane two-dimensional structures just one approach for concrete is explained, which may be used in a layered concept [see chapter 2 of Stempniewski/Eibl (1992) or e.g. Darwin/Pecknold (1974), Chen/Saleeb (1982)].

For this purpose we start from the well-known orthotropic elastic relation

$$
\begin{Bmatrix} d\sigma_{11} \\ d\sigma_{22} \\ d\tau_{12} \end{Bmatrix} = \frac{1}{1 - \nu_1 \cdot \nu_2} \cdot \begin{bmatrix} E_1 & \nu_2\sqrt{E_1 E_2} & 0 \\ \nu_1\sqrt{E_1 E_2} & E_2 & 0 \\ 0 & 0 & G(E_1,E_2) \end{bmatrix} \cdot \begin{Bmatrix} d\varepsilon_{11} \\ d\varepsilon_{22} \\ d\gamma_{12} \end{Bmatrix}
\qquad (4.1\text{-}112)
$$

with $\nu = \sqrt{\nu_1 \cdot \nu_2}$ and the shear term

$$
G(E_1,E_2) = \frac{1}{4} \cdot \left[E_1 + E_2 - 2 \cdot \nu\sqrt{|E_1 \cdot E_2|} \right] .
\qquad (4.1\text{-}113)
$$

Bringing eq. (4.1-112) into the following form

$$
\begin{Bmatrix} d\sigma_{11} \\ d\sigma_{22} \\ d\tau_{12} \end{Bmatrix} = D \cdot \begin{bmatrix} E_1 \cdot \tilde{C}_{11} & E_1 \cdot \tilde{C}_{12} & 0 \\ E_2 \cdot \tilde{C}_{21} & E_2 \cdot \tilde{C}_{22} & 0 \\ 0 & 0 & G(E_1,E_2) \end{bmatrix} \cdot \begin{Bmatrix} d\varepsilon_{11} \\ d\varepsilon_{22} \\ d\gamma_{12} \end{Bmatrix}
\qquad (4.1\text{-}114)
$$

one may write

$$
\begin{aligned}
d\sigma_{11} &= E_1 \cdot \left(\tilde{C}_{11} \cdot d\varepsilon_{11} + \tilde{C}_{12} \cdot d\varepsilon_{22} \right) = E_1 \cdot d\varepsilon_{1u} \\
d\sigma_{22} &= E_2 \cdot \left(\tilde{C}_{21} \cdot d\varepsilon_{11} + \tilde{C}_{22} \cdot d\varepsilon_{22} \right) = E_2 \cdot d\varepsilon_{2u} .
\end{aligned}
\qquad (4.1\text{-}115)
$$

With

$$
d\varepsilon_{iu} = \frac{d\sigma_i}{E_i} \qquad (i = 1,2)
\qquad (4.1\text{-}116)
$$

$$
\varepsilon_{iu} = \sum_k \Delta\varepsilon_{iu} \qquad (k = 1,...,increments)
\qquad (4.1\text{-}117)
$$

the so called equivalent uniaxial strains ε_{iu} are defined (4.1-115). $E_1(\varepsilon_{iu})$, $E_2(\varepsilon_{iu})$ and $G(E_1, E_2)$ are to remain constant also under a coordinate transformation.

$$
\begin{Bmatrix} d\sigma_{11} \\ d\sigma_{22} \\ d\tau_{12} \end{Bmatrix} = D \cdot \begin{bmatrix} E_1(\varepsilon_{1u}) & 0 & 0 \\ 0 & E_2(\varepsilon_{2u}) & 0 \\ 0 & 0 & G(E_1,E_2) \end{bmatrix} \cdot \begin{Bmatrix} d\varepsilon_{1u} \\ d\varepsilon_{2u} \\ d\gamma_{12} \end{Bmatrix} .
\qquad (4.1\text{-}118)
$$

It is now assumed that for the two principal stress directions 1, 2 in a biaxially loaded concrete independent modified monoaxial stress strain curves can be used (see Fig. 4.1-31).

Based on the the Saenz equation the ascending part is formulated as given in eq. (4.1-119) [see also Eibl/Stempniewski (1992)]. The descending branch is assumed as linear.
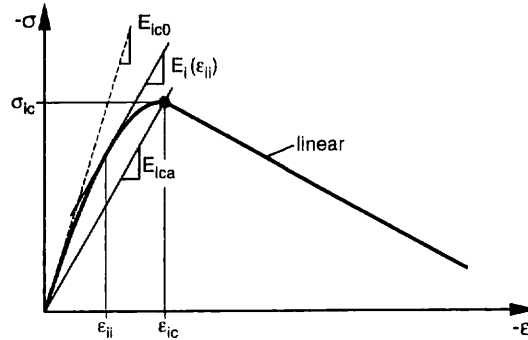
Fig. 4.1-31: Stress strain relations σ_i - ε_i

By these means the $E_1(\varepsilon_{1u})$ and $E_2(\varepsilon_{2u})$ in the eq. (4.1-119) may be determined taking E_{ico} from mono-axial tests and using σ_{ic}-values from the bi-axial failure surface in Fig. 4.1-32 according to the the actual stress situation $\sigma_1/\sigma_2 = a$.

$$\sigma_i = \frac{E_{ico} \cdot \varepsilon_{iu}}{1 + \left(\dfrac{E_{ico}}{E_{ica}} - 2\right) \cdot \dfrac{\varepsilon_{iu}}{\varepsilon_{ic}} + \left(\dfrac{\varepsilon_{iu}}{\varepsilon_{ic}}\right)^2} \tag{4.1-119}$$

$$\varepsilon_{ic} = \begin{cases} \varepsilon_c \cdot \left[-1.60 \cdot b^3 + 2.25 \cdot b^2 + 0.35 \cdot b\right] & \wedge \quad \sigma_{ic} \geq f_{cm} \\[2mm] \varepsilon_c \cdot \left[3 \cdot b - 2\right] & \wedge \quad \sigma_{ic} < f_{cm} \end{cases} \tag{4.1-120}$$

$$b = \frac{\sigma_{ic}}{f_{cm}}$$

For the **compression-compression** region this related "failure" surface for $\sigma_1 \leq 0 \wedge \sigma_2 \leq 0$ (see Fig. 4.1-32) is given by

$$\sigma_{2c} = \frac{1 + 3{,}65\,a}{(1 + a)^2} \cdot f_{cm} \tag{4.1-121}$$

$$\sigma_{1c} = a \cdot \sigma_{2c} \qquad a = \sigma_1/\sigma_2 \,.$$

Having determined σ_t and ε_t at stage t of a Newton/Raphson process within a FE-approach one starts the iteration cycle for the next stress increment with the tangent modulus of the updated strain according to the new uni-axial stress strain curve at t+Δt which belongs to the updated σ_1/σ_2 relation according to Kompfner (1983), (see also Fig. 4.1-33).
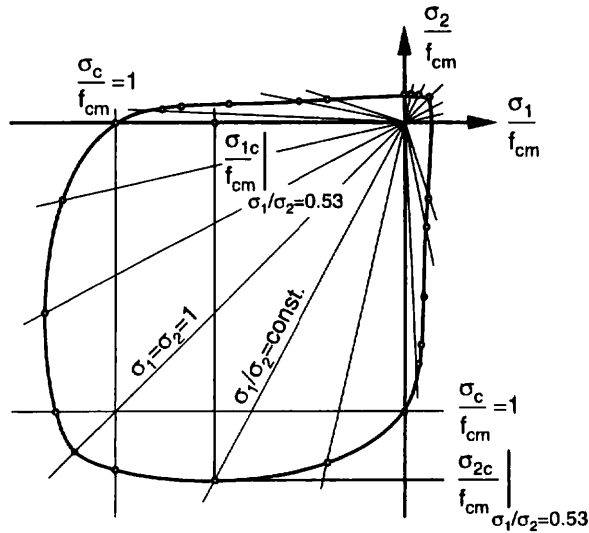
Fig. 4.1-32: Biaxial failure surface
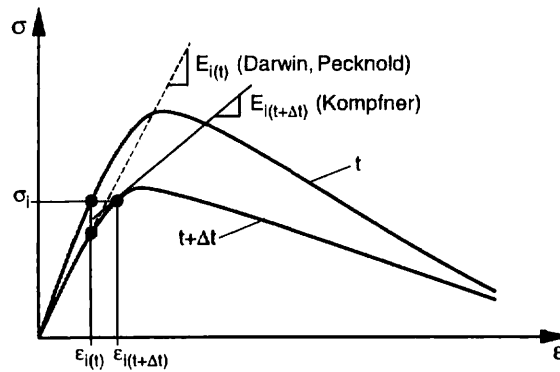
Fig. 4.1-33: Modification of stiffness

Thus solving eq. (4.1-119) for ε_{iu} leads to

$$\varepsilon_{iu}^* = \frac{E_{ico} - \dfrac{\sigma_i \cdot R}{\varepsilon_{ic}} - \sqrt{\left(\dfrac{\sigma_i \cdot R}{\varepsilon_{ic}} - E_{ico}\right)^2 - \left(2\dfrac{\sigma_i}{\varepsilon_{ic}}\right)^2}}{2 \cdot \dfrac{\sigma_i}{\varepsilon_{ic}^2}} \qquad (4.1\text{-}122)$$

and with

$$R = \frac{E_{ico}}{E_{ica}} - 2 \qquad (4.1\text{-}123)$$

to the new tangent modulus

$$E_{c,T} = E_{ico} \cdot \left[\frac{1 - \left(\dfrac{\varepsilon_{iu}}{\varepsilon_{ic}}\right)^2}{\left(1 + R \cdot \left(\dfrac{\varepsilon_{iu}}{\varepsilon_{ic}}\right) + \left(\dfrac{\varepsilon_{iu}}{\varepsilon_{ic}}\right)^2\right)^2} \right] \cdot \qquad (4.1\text{-}124)$$

For the Poisson's number

$$\nu_t = \begin{cases} \nu_0 & \text{in the compression -compression and tension -tension region} \\ \nu_0 + 0.6 \cdot \left(\dfrac{\sigma_2}{f_{cm}}\right)^4 + 0.4 \cdot \left(\dfrac{\sigma_1}{f_{ctm}}\right)^4 & yet \leq 0.99 \end{cases} \qquad (4.1\text{-}125)$$

is taken.

For the failure surface in the **compression-tension** region $\sigma_1 > 0 \wedge \sigma_2 \leq 0$, we use with $a = \sigma_1/\sigma_2$ [see Stempniewski/Eibl (1992)]

$$\sigma_{2c} = \frac{1 + 3.28\,a}{(1 + a)^2} \cdot f_{cm} \qquad \geq 0.65 f_{cm} \qquad (4.1\text{-}126)$$

$$\sigma_{1t} = \sigma_t$$

and a bilinear σ-ε relation for the **tension-tension** region $\sigma_{1t} = \sigma_{2t} = f_{ctm}$ (see Fig. 4.1-32).

In case of tension the falling branch may be approximated by a fictitious continuous strain

$$\varepsilon_{fi} = \frac{\delta}{l_{ch}} = \frac{2 G_F}{f_{ctm}\, l_{ch}} \qquad (4.1\text{-}127)$$

according to Fig. 4.1-34 using discrete crack opening δ, the fracture energy of concrete G_F and defining a characteristic length l_{ch}. The latter may be given following Brameshuber (1988)

$$l_{ch} = G_F \cdot \frac{E_c}{f_{ctm}^2} \cdot \qquad (4.1\text{-}128)$$

Then in case of a FE-calculation, where the crack occurs in an element (e) with a characteristic length l_{ch}^e, one gets the continuous element strain ε^e by means of

$$\varepsilon^e = \frac{\varepsilon_{fi} \cdot l_{ch}}{l_{ch}^e} \qquad (4.1\text{-}129)$$

For more refinement concerning "nonlocal" cracking see e.g. Ozbolt (1995)
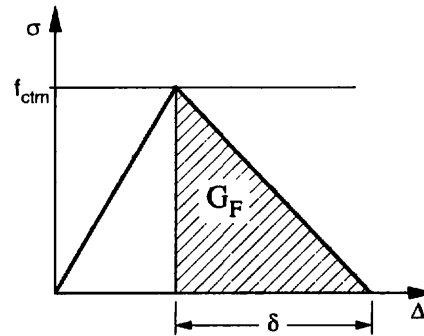
Fig. 4.1-34: Crack width and fracture energy

(2.2)   Steel

Reinforcing steel may be considered by a modified concrete tensile resistance or better by coupling of steel elements with a modified steel stress-strain relation according to Fig. 4.1-30 which is derived in chapter 3.4.2. This means that just additional element stiffness has to be considered at the nodes of the concrete elements.

(2.3)   Crack formation

The first cracks may form at relevant principal tensile stresses which also control the crack orientation.

At an opened crack the incremental change of the "equivalent maximal strain" is

$$\Delta^t \varepsilon_{ju} = \frac{\Delta^t \sigma_j}{E_j} \qquad\qquad\qquad\qquad (4.1\text{-}130)$$

parallel to the crack and the change of the crack width perpenticular to the crack is

$$\Delta^t c_i = \Delta^t \varepsilon_i + v \cdot \Delta^t \varepsilon_{ju} \qquad \left(i,j \ for \ \begin{array}{l} the \ main \ stresses \\ resp. \ strains \end{array} \right) . \qquad (4.1\text{-}131)$$

Therefore the whole "crack strain" is

$$c_i = \frac{\sigma_t}{E_{co}} + \sum_t \Delta^t c_i . \qquad\qquad\qquad (4.1\text{-}132)$$

The corresponding non-equilibrated stresses at crack formation which have to be considered in the next iteration step of a Newton/Raphson process are found as follows:

According to Fig. 4.1-35 the stress **after** cracking is

$$\vec{\sigma}_{xy}^{\,t+\Delta t} = |\Phi| \cdot \vec{\sigma}_{rs}^{\,t+\Delta t}$$

$$\vec{\sigma}_{xy} = \left| \vec{\theta} \ \vec{*} \ \vec{*} \ \right| \cdot \begin{Bmatrix} \sigma_r \\ 0 \\ 0 \end{Bmatrix}$$

$$\vec{\sigma}_{xy}^{\,t+\Delta t} = \vec{\theta} \cdot \sigma_r^{\,t+\Delta t}$$

(4.1-133)

where $\vec{\theta}$ is a column vector of the stress-transformation matrix $|\Phi|$.
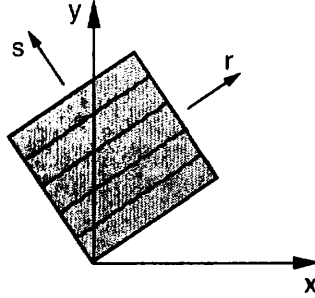
Fig. 4.1-35: Cracked concrete, local - global coordinate system

According to eq. (4.1-133) then

$$\sigma_{rs} = |\Phi|^{-1} \cdot \sigma_{xy}$$

$$\begin{Bmatrix} \sigma_r \\ * \\ * \end{Bmatrix} = \left| \begin{matrix} \vec{\theta}^{\,T} \\ * \\ * \end{matrix} \right| \cdot \begin{Bmatrix} \sigma_x \\ \sigma_y \\ \tau_{xy} \end{Bmatrix}$$

(4.1-134)

$$\sigma_r^{\,t+\Delta t} = \vec{\theta}^{\,T} \cdot \begin{Bmatrix} \sigma_x \\ \sigma_y \\ \tau_{xy} \end{Bmatrix}^{t+\Delta t}$$

The stress state $\vec{\sigma}_{xy}^{\,t}$ before cracking is changed by $\Delta\vec{\sigma}_{xy}$ due to cracking. This part is

$$\Delta\vec{\sigma}_{xy} = \vec{\sigma}_{xy}^{\,t} - \vec{\sigma}_{xy}^{\,t+\Delta t}$$

(4.1-135)

or

$$\Delta\vec{\sigma}_{xy} = [I] \cdot \begin{Bmatrix} \sigma_x \\ \sigma_y \\ \tau_{xy} \end{Bmatrix}^{t+\Delta t} - \vec{\theta} \cdot \vec{\theta}^{\,T} \cdot \begin{Bmatrix} \sigma_x \\ \sigma_y \\ \tau_{xy} \end{Bmatrix}^{t+\Delta t} .$$

(4.1-136)

and has to be distributed to the remaining system.

(2.4)   Remarks to the safety format in nonlinear calculations

Any nonlinear investigation, if numerically treated, needs an incremental solution algorithm in any case. With the FE-method we get the complete deformation history under an increasing load, which ends up with the maximum endurable load defined by the failure strains of steel or concrete. The corresponding load capacity can be compared with the acting load directly using different safety factors depending on the governing parameters of failure, steel or concerte.

This safety check at the load levels substitutes the usual cross-section design at the ultimate limit state (ULS) which does not even distinguish between statically determinate and undeterminate structures and the possibilities of redistribution in the latter case.

A special serviceability check is not necessary as the state of the system may be followed at every loading stage.

From these considerations the following design procedure is reasonable e.g. in the case of a multispan girder:

Choose more or less reasonable support moments for the intended load pattern and determine the aequivalent moments in the span due to equilibrium conditions.Then calculate the necessary reinforcement by means of the inner lever arm z and the yield strength of the selected steel. With this starting values a nonlinear design is done as a final check giving also informations on the different phases of the serviceability state.

4.1.5   Selected comments

(1)   Variable inclination of compression diagonals in shear design

Many engineers are astonished that the inclination of compression diagonals is to some extend variable in MC 90. One may ask wether this is possible, as physical problems of such a type usually have an unique solution. The answer is Yes.

First, the theorem of plasticity states that every equilibrium system which is possible is a safe one, as long as some ductility requirements are considered. So several solutions are possible on principle. Second, different assumed angles of the compression struts lead to a different amount of reinforcement and therefore also to different stiffness conditions. Therefore any different design will lead to a differing result in a nonlinear calculation for the same outer load conditions.

(2)   Linear elastic computer codes for two-dimensional reinforced concrete members

In several cases slabs show singular moments, where the local moment tends to infinity. This is usually a consequence of the application of the Love/Kirchhoff-theory for slabs, a simplified plate theory, which in many cases is not able to describe the behaviour of slabs at such singular points realistically. As a FE-code strives to approximate the value "infinite", different discretizations give completely different results for the "maximum moment". E.g. this is the case, if one tries to model flat slabs. A better and more realistic solution can only be gained by a better

elastic theory as e.g. by the so called Mindlin/Reißner-theory or by a simplified three-dimensional treatment.

But even these results are not very realistic in case of a reinforced concrete slab. Locally overloaded concrete will crack in areas of excessive moments and therefore changes its stiffness. The moments spread to less cracked areas. A realistic result to compare with tests e.g. is only possible, if a two-dimensional nonlinear code is used, or if necessary, even a three-dimensional one.

Local stress concentrations in a plate due to bending are in most cases not very significant in practical design as long as an overall equilibrium is possible. Only cracks may occur. However dangerous may be a high local stress concentration due to shear, as a redistribution of shear is hardly possible.

(3)   Evaluation of the prestressing state in T-beams

The effective width of a T-beam changes not only with geometry and support conditions but also with the load distribution. Therefore different values of these parameters lead to a different effective width and also to different locations of the centre of gravity along the beam's length. Calculating the prestressing stresses one usually starts with normal forces and moments induced by the prestressing cables. These moments however depend on the cable forces exerted relative to the centres of gravity, which themselves are also influenced by the cable forces. Therefore calculation difficulties arise, when one tries to proceed in such a manner. A thorough analysis however is necessary as the final stress state of a the structure is the result of the superposition of such substates and very sensitive to calculation errors.

If there are any doubts one should load the T-beam by the cable forces exerted to the structure by the cables' curvature relative to a line connecting both anchorage points and then use an elastic FE-code to compute the stresses at critical points.

(4)   Nonlinear stress ranges within in plane loaded plates

An unsolved question is how to judge only roughly calculated compressive stresses in areas of nonlinear strain concentrations – so called D-regions – when only a more or less arbitrarily defined effective strut width is available.

The answer is, that whenever concrete space is available beside the assumed effective width overloading is practically impossible due to the plastic plateau of the concrete stress-strain law. The system is only endangered if stresses cannot spread out due to lacking concrete space or if a widening of the effective width itself would increase the total force in the strut as shown e.g. in Fig. 4.1-18.

(5)   Rough estimation of creep

In spite of available algorithms to describe the creep behaviour of structures realistically it is often sufficient to do an elastic calculation using $E/(1+\phi)$ instead of E as a reasonable boundary for the structures behaviour in creep.

(6)   **Torsional stiffness of statically indeterminate structures**

Whenever torsional stiffness is included in the analysis of a statically indeterminate system, one has to consider that this stiffness usually drops extremely at a certain level of the applied torsional moment. Fig. 4.1-36 shows the degradation of the real torsional stiffness related to the ideal elastic torsional stiffness with increasing torsion according to Leonhardt (1973).
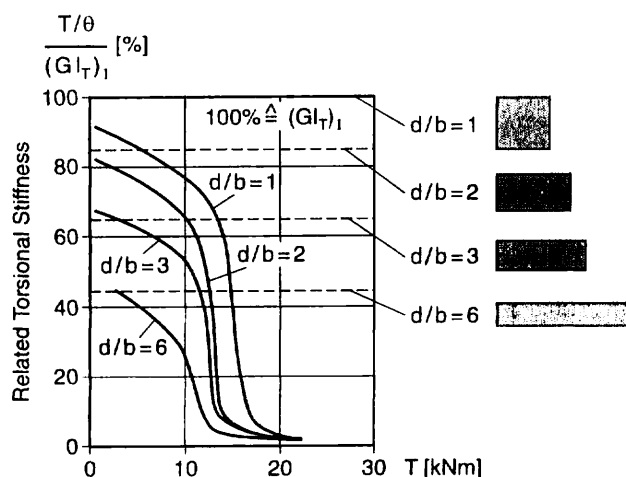
Fig. 4.1-36: Degradation of torsional stiffness [Leonhardt (1973)]

Therefore if a combination of torsional stiffness and bending stiffness is of decisive influence one should do a two-step analysis. For the serviceability state one should include torsional stiffness of the uncracked cross section in order to calculate sufficient reinforcement to reduce cracks width. However for the analysis of the bearing capacity it is proposed to neglect the torsional stiffness setting it to zero in order to get a safe solution.

(7)   **Modelling of reinforced concrete for a nonlinear calculation**

In many cases with a reasonable amount of reinforcement where yielding of steel initiates failure an exact modelling of the compression range is not necessary. This may simplify FE-calculations especially in cases of bi- or three-dimensional compression. Also an exact bond modelling is not always important. A modified stress-strain law for steel as shown in chapter 4.1.4 is sufficient for practical design purposes. Of course if discrete cracks as e.g. in case of a frame corner are decisive for failure a rather realistic modelling of crack formation and bond is mandatory.

References

Brameshuber, W. (1988): Bruchmechanische Eigenschaften von jungem Beton. Dissertation und Heft 5 der Schriftenreihe des Instituts für Massivbau und Baustofftechnologie der Universität Karlsruhe

Chen, W.F., Saleeb, A.F. (1982): Constitutive Equations for Engineering Material, Volume 1: Elasticity and Modelling. J. Wiley & Sons Toronto

Darwin, D., Pecknold, D. (1974): Inelastic Model for Cyclic Biaxial Loading of Reinforced Concrete. Civil Engineering Studies, Struct, Research Series No. 409, University of Illinois at Urbana-Champaign

Dilger, W. (1966): Veränderlichkeit der Biege- und Schubsteifigkeit bei Stahlbetontragwerken und ihr Einfluß auf Schnittkraftverteilung und Traglast bei statisch unbestimmter Lagerung. DafStb-Heft 179, Verlag Ernst & Sohn Berlin

Dischinger, F. (1939): Elastische und plastische Verformungen der Eisenbetontragwerke und insbesondere der Bogenbrücken. Der Bauingenieur, 1939, Heft 5/6

Eibl, J. (1981): Nonlinear Analysis versus Linear and Plastic Analysis. CEB-Course: Nonlinear Analysis and Design of Reinforced Concrete and Prestressed Structures. Pavia, Sept. 1981

Eibl J., Akkermann, J. (1997): Rotationsfähigkeit von Rahmenecken. Forschungsbericht, Institut für Massivbau und Baustofftechnologie, Universität Karlsruhe

Eibl J., Häußler U. (1996): Baudynamik. Betonkalender 1997, Teil II, Verlag Ernst & Sohn Berlin, S. 755 - 861

Eibl J., Häußler U., Rezepis I. (1990): Zur Ermittlung der Spanngliedkräfte bei Vorspannung ohne Verbund. Der Bauingenieur 65(1990), 227 - 233

Eibl J., Schmidt-Hurtienne, B. (1996): Nichtlineare Traglastermittlung von Stahlbetonstrukturen nach Eurocode 2 - Stochastische Finite Elemente. Baustatik - Baupraxis 6, 7./8. März 1996, Hochschule für Architektur und Bauwesen Weimar, Eigenverlag, 2.1-2.15

Eibl J., Zeller W. (1991): Untersuchungen zur Traglast der Druckdiagonalen in Konsolen. Bericht, Institut für Massivbau und Baustofftechnologie, Universität Karlsruhe

Hillerborg, A. (1975): Design of reinforced Concrete Slabs according to the Strip Method. Cement and Concrete Association, London

IABSE-COLLOQUIUM (1979): Plasticity in Concrete. Introductory Report, Intern. Association for Bridge and Structural Engineering, Zürich

Ingerslev, A. (1921). Om en elementaer Beregningsmetode of krydsarmerede Plader. Ingeniøren 30, No. 69(1921), pp. 507

Johansen, K.W. (1943): Brudlinieteorier. J. Gjelerup Copenhagen

Kesting, K. (1979): Berechnung von Stahlbetonwänden und Platten unter Berücksichtigung geometrischer und physikalischer Nichtlinearität. Dissertation Universität Dortmund

Kompfner, T.A. (1983): Ein finites Elementmodell für die geometrisch und physikalisch nichtlineare Berechnung von Stahlbetonschalen. Dissertation Universität Stuttgart

Kordina, K. et al. (1992): Bemessungshilfsmittel zu Eurocode 2 Teil 1, Planung von Stahlbeton- und Spannbetontragwerken. DAfStb-Heft 425, Beuth-Verlag Berlin

Leonhardt, F. (1973): Vorlesungen über Massivbau. Teil 1, Grundlagen zur Bemessung im Stahlbetonbau. 2. Auflage, Springer-Verlag Berlin, Heidelberg, New York

Leonhardt, F. (1978): Vorlesungen über Massivbau. Teil 4, Nachweis der Gebrauchsfähigkeit. 2. Auflage, Springer-Verlag Berlin, Heidelberg, New York

Marcus, H. (1924): Die vereinfachte Berechnung biegsamer Platten. Der Bauingenieur, Band 5, Springer Verlag Berlin

Ožbolt, J. (1995): Maßstabseffekt und Duktilität von Beton- und Stahlbetonkonstruktionen. Mitteilungen, Institut für Werkstoffe im Bauwesen, Universität Stuttgart

Rüsch, H., Kupfer, H. (1975): Bemessung von Spannbetonbauteilen. Betonkalender 1976, Teil I, Verlag Ernst &. Sohn Berlin

Saenz, L.P.(1964): Equation for the Stress-Strain of Concrete, ACI Vol. 61, pp. 1227-1239

Stempniewski, L., Eibl, J. (1992): Finite Elemente im Stahlbeton. Betonkalender 1993 Teil 2, Verlag Ernst & Sohn Berlin, S. 249-312

Szilard R. (1974): Theory and Analysis of Plates. Prentice-Hall, Inc. Englewood Cliffs New Jersey

Thürlimann, B. (1985): Plastizitätstheorie im Stahlbetonbau. Vorlesungen des Instituts für Massivbau der Universität Stuttgart

Thürlimann B., Marti P., Pralong J., Ritz P., Zimmerli B. (1983): Anwendung der Plastizitätstheorie auf Stahlbeton. Institut für Baustatik und Konstruktion, Eidgenösssische Technische Hochschule Zürich

Trost, H. (1973): Zeitabhängiges Verformungsverhalten von Stahl und Beton bei Spannbetonbauteilen. 7. Informationstag "Spannbeton- und Stahlleichtbeton" des Innenministeriums Nordrhein-Westfalen

Zienkiewicz, O.C., Taylor, R.L. (1998): The Finite Element Method. 4. Edition Vol. 1 & 2, McGraw-Hill Book Comp. New York

4.2 Design Format

by Gert König, Nguyen Tue, Dmitri Soukhov, Carsten Ahner

4.2.1 Definitions of limit states

For the user, a building is in a critical condition if either normal use of the building is no longer possible or if there is an immediate danger for the structural stability. This generally means that if one of these states occurs the requirements of the structure can no longer be satisfied. For the design of the structure these critical states are defined as limit states. Depending on whether the calculated stability or the qualities of use are concerned the two different limit states should be considered:

- ultimate limit state;
- serviceability limit state.

Achieving the ultimate limit states results in the calculated failure. This can be caused by loss of global equilibrium, by reaching critical strain conditions at the most stressed cross sections, by failure of stability as well as fatigue of the materials used. For the design of reinforced concrete and prestressed concrete structures the calculated structural failure is described by calculation models taking into account the different effects due to action (internal forces) on the bearing behaviour of the structure. These are in detail:

- ultimate limit states for bending and longitudinal force;
- ultimate limit states for shear force;
- ultimate limit states for torsion;
- ultimate limit states for punching;
- ultimate limit state as a result of structure deformation;
- ultimate limit states as a result of material fatigue.

It should be noticed that the design of a structure, as a rule, does not have to include the verification of all limit states as mentioned above. Only such proofs must be delivered which are decisive for the design of the concerning structure. For example the ultimate limit states as a result of material fatigue is not usually decisive for general buildings.

The limit states of serviceability characterise a structure condition in which, if it is achieved, the agreed requirements of use can not longer be satisfied. For reinforced concrete and prestressed concrete structures this can be caused by cracking, deformation or sensitivity to vibration. Therefore the calculation models are developed for:

- limit states of cracking,
- limit state of deformation and
- vibration behaviour.

Apart from the mentioned limit states the stresses in concrete, reinforcing and prestressing steel should be limited under service load, because exceeding the permissible stresses may cause an impairment of the qualities of use of the buildings. For example a concrete stress exceeding $0.4 \cdot f_{ck}$ may cause increased microcracking and therefore plastic deformations influencing the deformations of the buildings negatively.

As the material properties and therefore the design resistance as well as the actions are statistical values a complete exclusion of achieving the limit states is not possible theoretically (residual risk). Every building, however, shall be designed not to achieve the limit states with an acceptable probability during the service life. The probability to achieve the limit states is called failure probability. The determination of the failure probability is the function of the reliability theory. The reliability analysis provides for the civil engineering design practical aids as safety factors, allowing the observance of the required building reliability. The following section includes at first the basis of the safety procedure in the civil engineering design as a summary. Afterwards the verification procedure derived from this for both limit states will be described.

4.2.2   Safety concept

(1)   Theoretical connections

(1.1)   Distribution, frequency and probability

If the experimentally reached cylinder compressive strengths of a particular concrete strength class in a concrete plant for an extended period are outlined arranged to classes then a histogram is created (Fig. 4.2- 1).
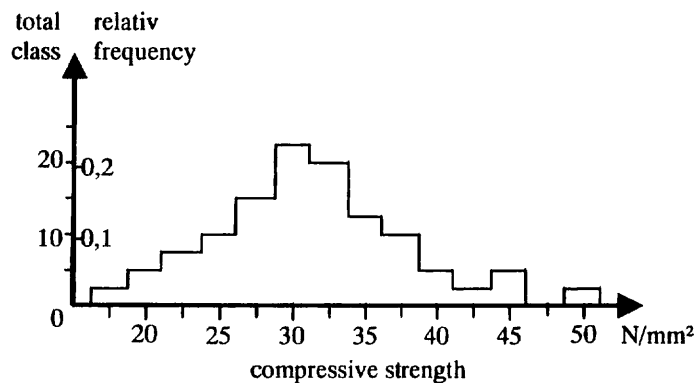
Fig. 4.2- 1 : Histogram of cylinder compressive strength

The cumulative frequency according to Fig. 4.2- 2 is obtained, if the number of events is outlined, which does not exceed the upper interval limit of the concerning class. To get comparable results the relative frequency is used, enabling a percentage statement.
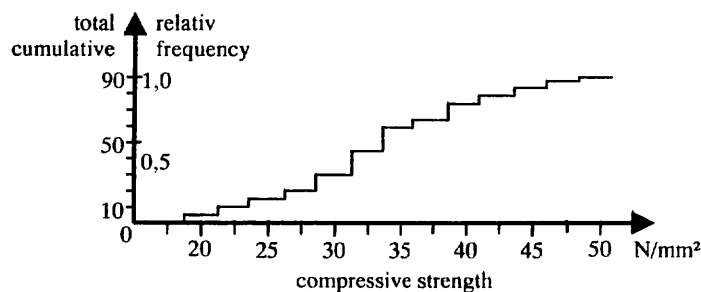
Fig. 4.2- 2 : Cumulative frequency of cylinder compressive strength of concrete

If class amplitude tends to zero and number of experiments to infinity then the random sample becomes population and the histograms change to curves that can be described by functions. The function arisen from the histogram is called probability density or density $f_X(x)$ and the function arisen from the cumulative frequency is called probability distribution function or short distribution $F_X(x)$ (Fig. 4.2- 3). The connection between probability density function $f_X(x)$ and probability distribution function $F_X(x)$ can be indicated as follows:

$$F_X(x) = \int_{-\infty}^{x} f_X(x)dx \qquad \text{or} \qquad \frac{dF_X(x)}{dx} = f_X(x) \qquad (4.2\text{-}1)$$

The function value $F_X(x_1)$ is also called probability p_1 of an event. It means which part of the event is smaller or at most equal x_1. It is:

$$p_1 = F_X(x_1) = \int_{-\infty}^{x_1} f_X(x)dx \qquad (4.2\text{-}2)$$
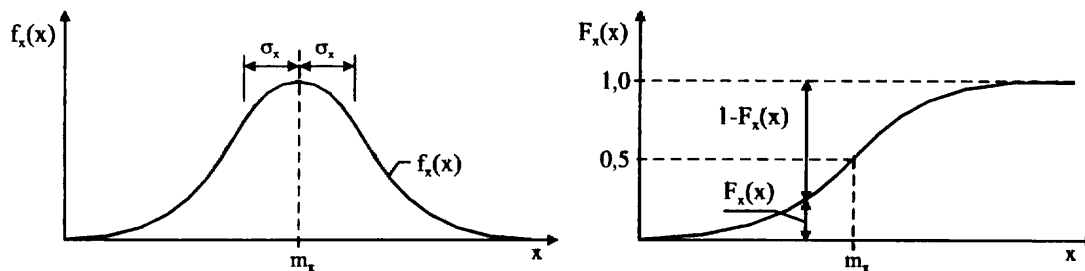
Fig. 4.2- 3 : Symmetrical probability distribution function $F_X(x)$ and probability density function $f_X(x)$ (the graphical example based on the Normal distribution)

(1.2)   Parameters of distributions and densities

Density and distribution are described, as a rule, by the following parameters:

median $\breve{x}$: It is exceeded or not reached with the same probability. The performance of many random experiments will therefore lead to the same number of results above and below this value:

$$F_X(\breve{x}) = 0,5 \qquad (4.2\text{-}3)$$

modal value $\hat{x}$: It indicates the maximum value of density and can be find from the equation:

$$\frac{d(f_X(x))}{dx} = 0 \qquad (4.2\text{-}4)$$

mean $\bar{x}$ **or** m_X : It can be described graphically as gravity centre of the area under the density function:

$$\bar{x} = \int_{-\infty}^{+\infty} x \cdot f_X(x)dx \qquad (4.2\text{-}5)$$

If a random sample of the size n (number of the samples) is available, the arithmetical mean is the best assessed value for $\bar{x}$:

$$\bar{x} = \frac{1}{n} \sum_{i=1}^{n} x_i \qquad (4.2\text{-}6)$$

The parameters mean, median and modal value are equal for symmetric distribution functions.

Scattering or variance (Dispersion) σ_x^2 : It can be interpreted as second moment of area under the density function (about the centre of gravity $\bar{x}$):

$$\sigma_x^2 = \int_{-\infty}^{+\infty} (x - \bar{x})^2 \cdot f_x(x) dx \qquad (4.2\text{-}7)$$

For a sample of size n the scattering can be calculated by approximation as follows:

$$\sigma_x^2 = \frac{1}{(n-1)} \sum_{i=1}^{n} (x_i - \bar{x})^2 \qquad (4.2\text{-}8)$$

standard deviation σ_x : It is the square root of the dispersion:

$$\sigma_x = \sqrt{\sigma_x^2} \qquad (4.2\text{-}9)$$

coefficient of variation V_x : The coefficient of variation is introduced for the non-dimensional notation:

$$V_x = \frac{\sigma_x}{\bar{x}} \qquad (4.2\text{-}10)$$

p-%-fractile x_p : A value not, or at most reached, with p-% probability is called p-%-fractile x_p. For Normal distribution is:

$$x_p = \bar{x} \pm k \cdot \sigma_x \qquad (4.2\text{-}11)$$

In the above equation k is the fractile factor (see section (2.1)), the positive sign is used for fractiles over 50% and the negative sign for fractiles under 50%.

(2)   Frequently used distribution functions in civil engineering

(2.1)   Gaussian normal distribution

The equations of the normal distribution are:

$$f_x(x) = \frac{1}{\sigma_x \cdot \sqrt{2 \cdot \pi}} \cdot \exp\left[-\frac{1}{2} \cdot \left(\frac{x - m_x}{\sigma_x} \right)^2 \right] \qquad (4.2\text{-}12)$$

$$F_x(x) = \frac{1}{\sigma_x \cdot \sqrt{2\pi}} \cdot \int_{-\infty}^{x} \exp\left[-\frac{1}{2} \cdot \left(\frac{x - m_x}{\sigma_x} \right)^2 \right] dx \tag{4.2-13}$$

Introducing the standardised normal random variable z

$$z = \frac{x - m_x}{\sigma_x} \tag{4.2-14}$$

results in the standardised normal density function as well as in the standardised normal distribution function:

$$\varphi(z) = \frac{1}{\sqrt{2 \cdot \pi}} \cdot \exp\left[-\frac{1}{2} z^2 \right]$$

$$\Phi(z) = \Phi\left(\frac{x - m_x}{\sigma_x} \right) = \frac{1}{\sqrt{2\pi}} \cdot \int_{0}^{z} \exp\left(-\frac{1}{2} t^2 \right) dt \tag{4.2-15}$$

For the fractile x_p is:

$$x_p = m_x \pm z \cdot \sigma_x \tag{4.2-16}$$

The connections for the Gaussian normal distribution are shown in Fig. 4.2-4.

density function   standardised density function   standardised distribution function
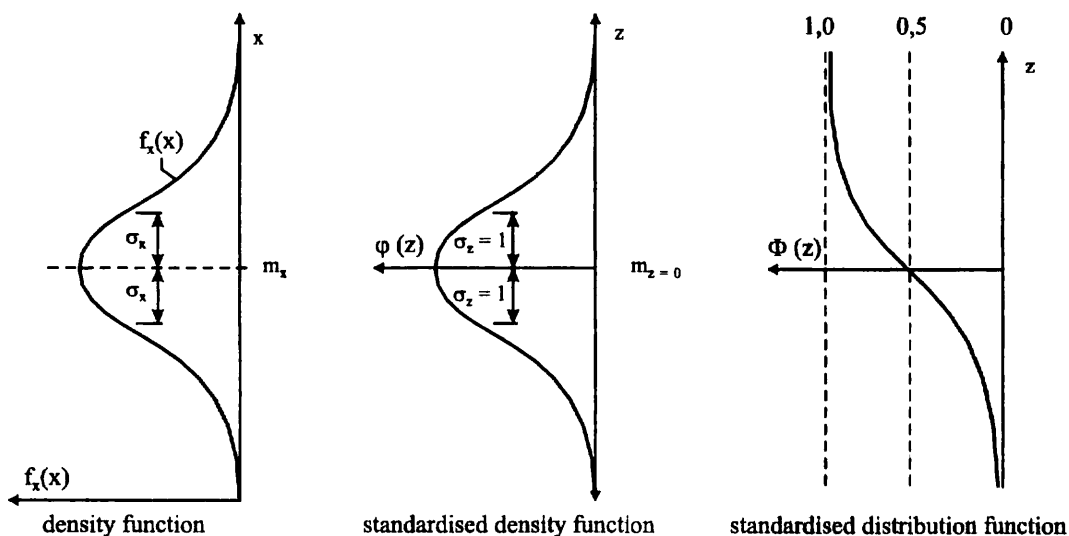
Fig. 4.2- 4 : Connections of the Gaussian normal distribution

The function values $\Phi(z)$ cannot be integrated in a closed form. In table 4.2-1 some values of z for the relevant fractiles x_p (expressed by p-%) are indicated.

p-%	50	20	10	5	2,5	2,275	1,0	0,135	0,0032
z	0	0,842	1,282	1,645	1,960	2,000	2,326	3,000	4,000

Table 4.2-1 : Connection between probability and fractiles (standardised normal distributed variable)

Therefore the 5%-fractile is: mean minus 1.645 times the standard deviation.

$$x_{5\%} = m_x - 1{,}645 \cdot \sigma_x = m_x \cdot (1 - 1{,}645 \cdot V_x) \qquad (4.2\text{-}17)$$

For many practical problems the Gaussian normal distribution is very useful because of the property that each linear combination of independent normally distributed values is normally distributed again. A great disadvantage is, however, the indefinite ends. This means that also negative values (e.g. of strength) occur - even though with a low probability. Of course this is physically of no sense. For this reason the log-normal distribution is generally used for such random values.

(2.2)   The log-normal distribution

Characteristic for this distribution is that the logarithms of the random values are normally distributed. Each occurring value r_i owns a value x_i with $x_i = \ln r_i$.

Corresponding to the Gaussian normal distribution the probability density and the probability distribution function of the log-normal distribution are defined as follows:

$$f_r(r) = \frac{1}{\sigma_X \cdot \sqrt{2 \cdot \pi}} \cdot \frac{1}{r} \exp\!\left(-\frac{(\ln r - m_x)^2}{2 \cdot \sigma_X^2} \right) \qquad (4.2\text{-}18)$$

$$F_r(r) = \frac{1}{\sigma_X \cdot \sqrt{2\pi}} \cdot \int_{-\infty}^{r} \exp\!\left(\frac{(\ln t - m_x)^2}{2\sigma_x^2} \right) dt \qquad (4.2\text{-}19)$$

The relation between the means of r and x can be written as follows:

$$m_R = \exp\!\left(m_X + \frac{\sigma_X^2}{2} \right) \qquad (4.2\text{-}20a)$$

$$m_X = \ln m_R - \frac{\sigma_X^2}{2} \qquad (4.2\text{-}20b)$$

With the approximation $\sigma_x \approx V_R$ (valid for $V_R < 0.3$) the fractile can be indicated as follows:

$$r_p = m_R \cdot \exp(-0{,}5 \cdot V_R^2 \pm k \cdot V_R) \qquad (4.2\text{-}21)$$

According to Table 2.1 the 5%-fractile can be written:

$$r_{5\%} = m_R \cdot \exp\!\left(-1{,}645 \cdot V_R - 0{,}5 \cdot V_R^2 \right) \qquad (4.2\text{-}22)$$

The connections for the log-normal distribution are shown in Fig. 4.2- 5.
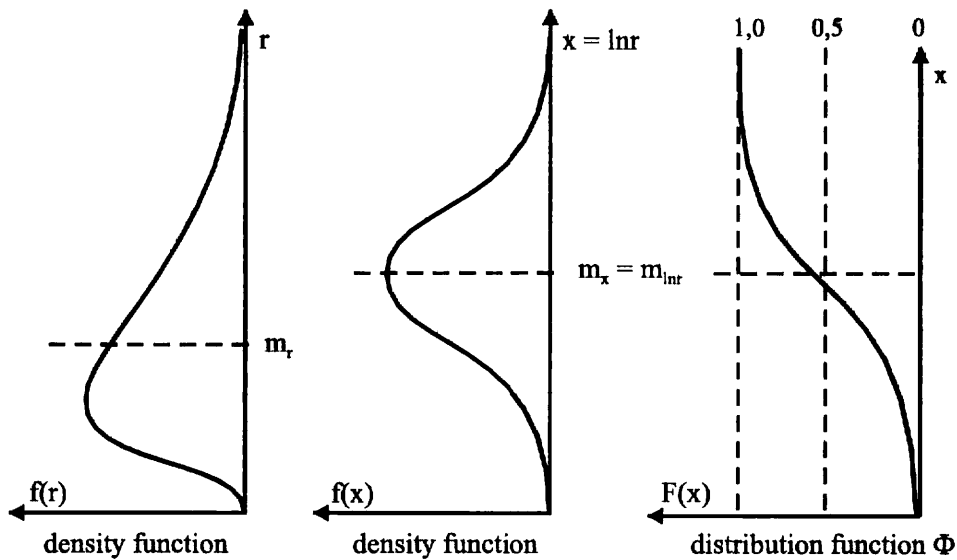
Fig. 4.2- 5 : Connections of the log-normal distribution

(3) Failure probability and reliability index

The limit state of the structure or of the part of it being considered generally is assumed to be reached, if its resistance R is equal to the actions S applied to it. Here S, as a rule, is a combination of different actions applied simultaneously to the structure concerned. The design equation for each limit state can therefore be formulated as follows:

$$R = S \qquad\qquad\qquad\qquad (4.2\text{-}23)$$

In reality for buildings neither R nor S can be determined directly. Because of the dispersion of the material properties, of the actions and other influences, e.g. those of the construction, R and S are generally random variables. They can be compared and described by their probability density functions $f_R(r)$ and $f_S(s)$ (Fig. 4.2- 6).
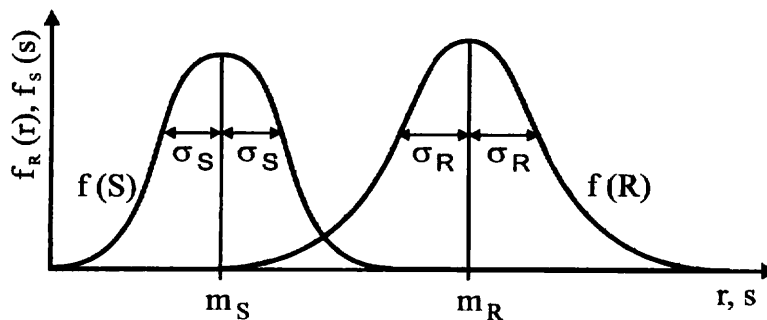
Fig. 4.2- 6 : Probability density functions of R and S

The density functions of r and s overlap. Thus cases are imaginable, in which a random resistance r is smaller than the simultaneously occurred action s. This case is mentioned as failure of structure. From Fig. 4.2- 6 it is possible to identify that the failure probability is mainly dependent on the scattering. If scatter of $f(S)$ or $f(R)$ increases then the probability of failure increases also.

Mathematically probability of failure can be found using the probability density of action s and probability distribution function of resistance r (explanation can be found in Fig. 4.2-7). For small interval ds it can be written:

$$P(s < S \le s + ds) = f_S(s)\,ds \tag{4.2-24}$$

According to the definition of probability distribution function:

$$P(R \le s) = F_R(s) \tag{4.2-25}$$

Using the intersection of these two events the following probability can be calculated:

$$P\{(s < S \le s + ds) \cap (R \le s)\} = F_R(s)\,f_S(s)\,ds \tag{4.2-26}$$

The failure occurs if the left part of this equation is realised, i. e. if action s is in interval $(s;\ s+ds)$ and simultaneously resistance r is less or equal s. Therefore this is conditional probability. To obtain unconditional probability of failure it is necessary to integrate the equation (4.2-26) within all possible values of s:

$$P_f = \int_{-\infty}^{+\infty} F_R(s)\,f_S(s)\,ds \tag{4.2-27}$$
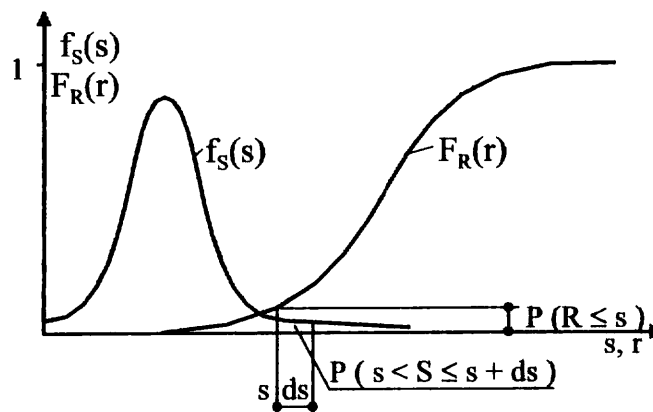
Fig. 4.2- 7 : Interpretation of the failure probability

The difference

$$Z = R - S \tag{4.2-28}$$

is denoted as a safety zone. In Fig. 4.2- 8 the connection between safety zone and failure probability is illustrated. The greater the safety zone, the smaller is the failure probability. Two safety zones can be used. The central safety zone is the distance between mean value of resistance m_R and mean value of action m_S . Instead of mean values the upper fractile S_q of action and the lower fractile R_p of resistance can be considered, where q is the probability that the value S_q is exceeded and p is the probability that the value R_p is not exceeded during some reference period. Then the nominal safety zone is the difference between the values R_p and S_q .
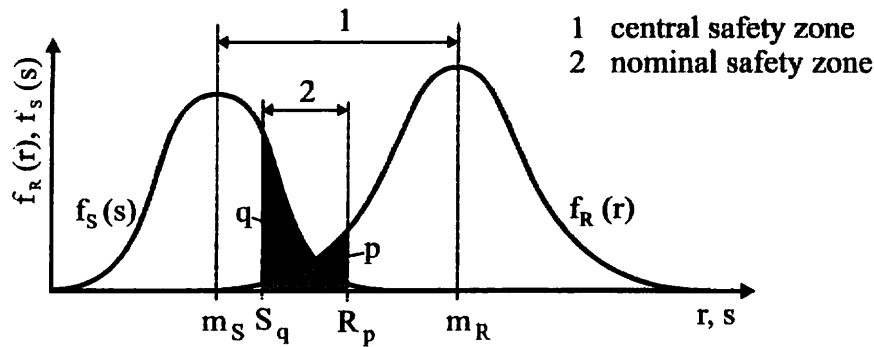
Fig. 4.2- 8 : Connection between safety zone and failure probability

If S and R are independent from each other and normally distributed then Z is normally distributed as well. Mean, standard deviation and coefficient of variation of Z follow from the law of error propagation:

$$m_Z = m_R - m_S \tag{4.2-29}$$

$$\sigma_Z = \sqrt{\left(\sigma_R^2 + \sigma_S^2\right)} \tag{4.2-30}$$

$$V_Z = \frac{\sigma_Z}{m_Z} \tag{4.2-31}$$

If the mean m_Z is defined as β-times standard deviation σ_Z

$$m_Z = \beta \cdot \sigma_Z \tag{4.2-32}$$

the failure probability can be indicated as follows:

$$p_f = \int_{-\infty}^{0} f_Z(z)dz = F_Z(z=0) = \Phi\left(-\frac{m_Z}{\sigma_z}\right) = \Phi(-\beta) \tag{4.2-33}$$
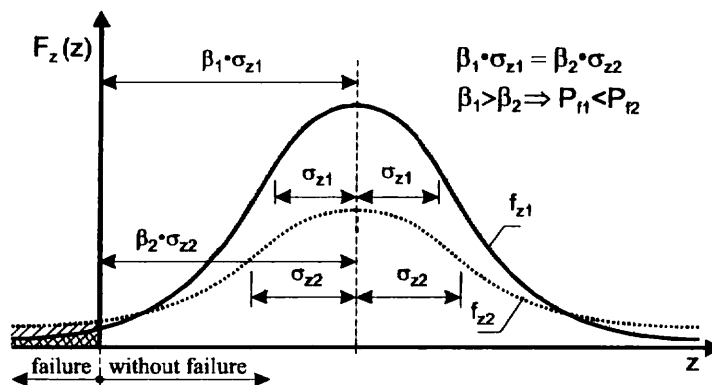
Fig. 4.2- 9 : Geometric interpretation of the reliability index

I.e. same values β result in same reliabilities. Rising β increases the reliability. This is the reason to call β "reliability index". In other words: for the design m_R must be always set according to the actual σ_Z in order to get the same reliability for different dispersions. The geo-

metrical interpretation of the reliability index β is shown in Fig. 4.2- 9 for two different dispersions σ_Z.

The connection between the failure probability p_f and the reliability index β_I (reference period is equal to 1 year) can be seen from the Table 4.2-2. For the reference period R (year) other than 1 year reliability index can be recalculated by the following formula:

$$\beta_R = \Phi^{-1}\left\{\left[\Phi(\beta_1)\right]^R\right\}$$

(4.2-34)

The reliability index β_{50} (reference period is equal to 50 years) can be also seen from the Table 4.2-2

Failure probability p_f	10^{-1}	10^{-2}	10^{-3}	10^{-4}	10^{-5}	10^{-6}	10^{-7}
Reliability index β_I (reference period 1year)	1,3	2,3	3,1	3,7	4,2	4,7	5,2
Reliability index β_{50} (reference period 50year)		0,21	1,67	2,55	3,21	3,83	4,41

Table 4.2-2: Failure probability p_f and reliability index β for reference periods of 1 year and 50 years

The structures should be designed with appropriate degrees of reliability. This degree of reliability should be adopted taking account of:

- the possible consequences of failure in terms of risk to life, injury, potential economic losses and the level of social inconvenience;
- the expense, level of effort and procedures necessary to reduce the risk of failure;
- the social and environmental conditions in a particular location.

Structural reliability is important first and foremost if people may be killed or injured as a result of collapse. An acceptance maximum value for the failure probability in those cases might be found from a comparison with risk resulting from other activities: a value of 10^{-6} per year seems reasonable to use. From an economical point of view, the target level of reliability should depend on a balance between the consequences of failure and the costs of safety measures.

The [ENV-1991, Part 1 "Basis of Design", 1994] gives values of reliability index β equals 4,7 for Ultimate Limit State and 3,0 for Serviceability Limit State (the values are referred to one year). The corresponding values of p_f from Table 4.2-2 are the target values for probability of failure. These values should be considered as reasonable minimum requirements, following from calibration to existing praxis, assuming that existing practice is optimal. Existing practice is partly established in codes and standards. Thus, calibration should be based on existing codes (more can be seen for example by [Schneider, 1997]).

The safety concept performed in this section can be also applied for the durability problems by taking into consideration the aspects of time (by actions and resistance).

(4)   Relation between reliability index and safety factors

By usual design a high action fractile is compared with a low resistance fractile (Fig. 4.2- 10).
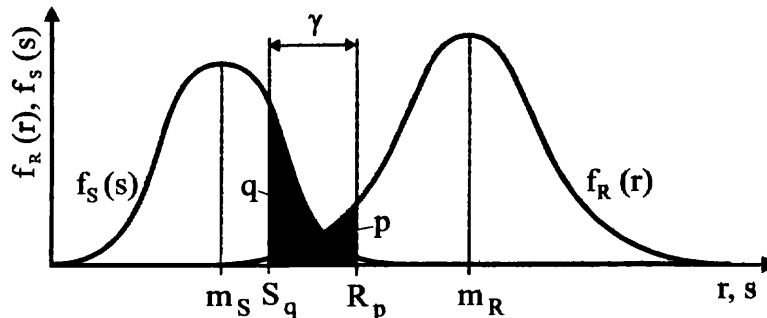
Fig. 4.2- 10 : Nominal safety factor

With the nominal safety factor γ the general design equation can be indicated as follows:

$$R_p \geq \gamma \cdot S_q \tag{4.2-35}$$

The fractiles of actions and of resistance are defined as follows:

$$R_p = m_R - k_R \cdot \sigma_R \tag{4.2-36}$$

$$S_q = m_S + k_S \cdot \sigma_S \tag{4.2-37}$$

In the above equation k_R and k_S are the corresponding fractile factors (see Table 4.2-1) for the actions and the resistance. The connection between safety factor γ and reliability index β results after some transformations as follows:

$$\gamma = \frac{m_R \cdot (1 - k_R \cdot V_R)}{m_S \cdot (1 + k_S \cdot V_S)} \tag{4.2-38}$$

$$\gamma = \left(\frac{1 + \beta \cdot \sqrt{V_R^2 + V_S^2 - \beta^2 \cdot V_R^2 \cdot V_S^2}}{1 - \beta^2 \cdot V_R^2} \right) \cdot \left(\frac{1 - k_R \cdot V_R}{1 + k_S \cdot V_S} \right) \tag{4.2-39}$$

The evaluation of equation (4.2-39) is shown in Fig. 4.2- 11. It is visible that the reliability depends on the dispersion of the resistance R and of the actions S. It is possible to make the γ-factors to a great extent independent on V_S by the indication of different fractiles for the actions S. This would come close to the aim to work with one safety factor for the same reliability.
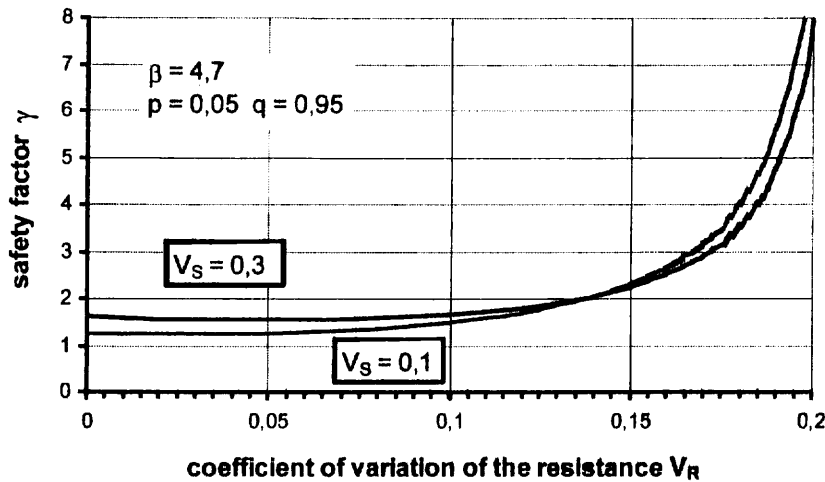
Fig. 4.2-11 : Safety factors as function of V_R *and* V_S

Another procedure can be achieved by the following linearization:

$$\sqrt{\sigma_S^2 + \sigma_R^2} = \alpha_R \cdot \sigma_R + \alpha_S \cdot \sigma_S \tag{4.2-40}$$

This results in the following relations:

$$m_R - m_S = \beta \cdot (\alpha_R \cdot \sigma_R + \alpha_S \cdot \sigma_S) \tag{4.2-41}$$

$$m_R - \beta \cdot \alpha_R \cdot \sigma_R = m_S + \beta \cdot \alpha_S \cdot \sigma_S \tag{4.2-42}$$

If the partial safety factors

$$\gamma_{R_0} = \frac{1}{1 - \beta \cdot \alpha_R \cdot V_R} \tag{4.2-43}$$

$$\gamma_{S_0} = 1 + \beta \cdot \alpha_S \cdot V_S \tag{4.2-44}$$

are introduced, the conditional equation for the design with the partial safety factors can be indicated as follows:

$$\frac{m_R}{\gamma_{R_0}} = \gamma_{S_0} \cdot m_S \tag{4.2-45}$$

By the fixing of the constant sensitivity factors α a decoupling of partial safety factors is possible. The price for this simple procedure is that no equal reliability for the different design situations can be reached. In order to decrease the difference in reliability of structures the ratio σ_R/σ_S must be considered for the choice of the sensitivity factors. For the determination of the partial safety factors these sensitivity factors are set in [ENV 1991, Part 1 "Basis of Design", 1994] with the following values:

$$\tilde{\alpha}_R = 0,8 \tag{4.2-46}$$

$$\tilde{\alpha}_S = 0,7 \tag{4.2-47}$$

Only small deviations from the intended safety level in the whole design will result.

(5) To the determination of the failure probability

The level of the structural reliability is expressed by an operative failure probability. Assuming action and resistance are independent from each other the failure probability p_f can be determined according to the law of error propagation as follows:

$$p_f = \int\limits_{-\infty-\infty}^{\infty\, r=s} \int f_R(r) \cdot f_S(s)\, dr\, ds \qquad (4.2\text{-}48)$$

Geometrically the separation between the failure area and the survival area can occur by the limit state straight line (Fig. 4.2- 12):

$$r = s \qquad (4.2\text{-}49)$$

The volume of the probability density

$$f_{R,S} = f_R(r) \cdot f_S(s) \qquad (4.2\text{-}50)$$

below this straight line corresponds to the failure probability (Fig. 4.2- 12).
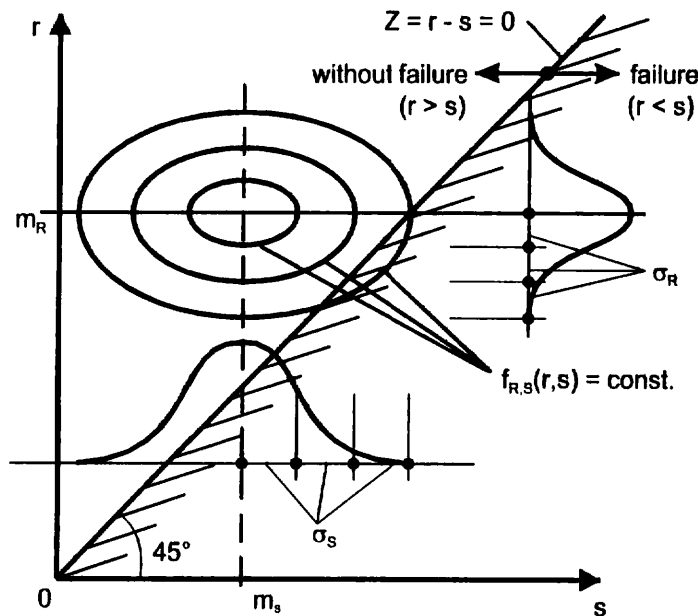
Fig. 4.2- 12 : Geometric interpretation of the failure probability

With the transformation of r and s into new variables

$$x = \frac{r - m_R}{\sigma_R} \qquad\qquad y = \frac{s - m_S}{\sigma_S} \qquad (4.2\text{-}51)$$

the limit state function can be described in the new system of co-ordinates as:

$$y \cdot \sigma_S + m_S = x \cdot \sigma_R + m_R \qquad\qquad (4.2\text{-}52)$$

The closer the limit state function to the origin the greater is the failure probability p_f of the concerning structure or a part of it. By the transformation of (4.2-52) to the standard form of Hesse:

$$x \cdot \frac{-\sigma_R}{\sqrt{\sigma_R^2 + \sigma_S^2}} + y \cdot \frac{\sigma_S}{\sqrt{\sigma_R^2 + \sigma_S^2}} = \frac{m_R - m_S}{\sqrt{\sigma_R^2 + \sigma_S^2}} \qquad (4.2\text{-}53)$$

the distance between the limit state function and the origin can be read off. It corresponds to the reliability index β:

$$\beta = \frac{m_R - m_S}{\sqrt{\sigma_R^2 + \sigma_S^2}} = \frac{m_Z}{\sigma_Z} \qquad\qquad (4.2\text{-}54)$$

Within the transformed system of co-ordinates the reliability index β, therefore, corresponds to the shortest distance between limit state function line and origin (Fig. 4.2- 13).
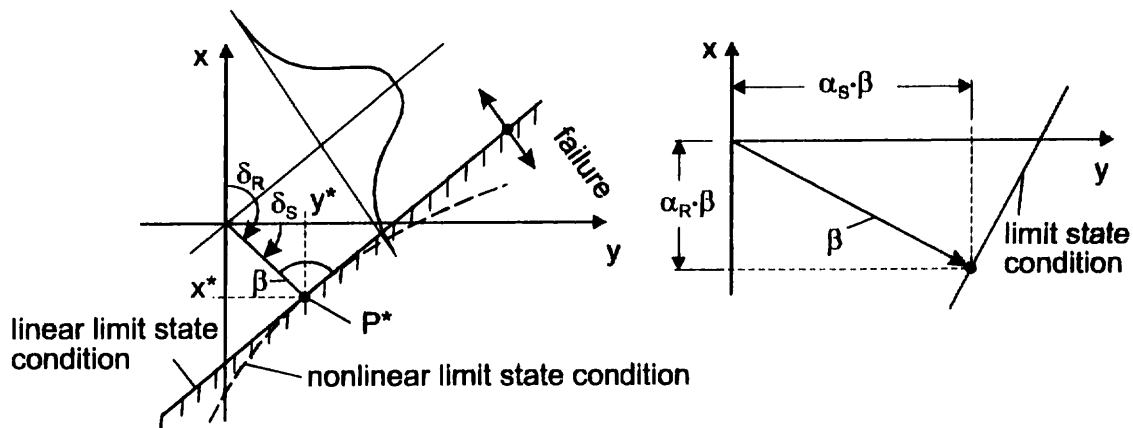
Fig. 4.2- 13 : Geometric interpretation of the safety index

For the reliability index β the following relation can be indicated using δ_R and δ_S in Fig. 4.2- 13:

$$\beta = y \cdot \cos \, \delta_S + x \cdot \cos \, \delta_R \qquad\qquad (4.2\text{-}55)$$

The co-ordinates y^* and x^* in Fig. 4.2- 13 can be determined with the following relations:

$$y^* = \beta \cdot \cos \, \delta_S = \beta \cdot \frac{\sigma_S}{\sqrt{\sigma_S^2 + \sigma_R^2}} \qquad\qquad (4.2\text{-}56)$$

$$x^* = \beta \cdot \cos \, \delta_R = \beta \cdot \frac{-\sigma_R}{\sqrt{\sigma_S^2 + \sigma_R^2}} \qquad\qquad (4.2\text{-}57)$$

With the sensitivity factors α_R and α_S

$$\alpha_R = \frac{\sigma_R}{\sqrt{\sigma_R^2 + \sigma_S^2}}$$

(4.2-58)

$$\alpha_S = \frac{\sigma_S}{\sqrt{\sigma_R^2 + \sigma_S^2}}$$

(4.2-59)

corresponding to eq. (4.2-56/57) they can now be written as:

$$y^* = \beta \cdot \alpha_S$$

(4.2-60)

$$x^* = \beta \cdot (-\alpha_R)$$

(4.2-61)

It can be stated that the failure probability has a maximum at the point with the co-ordinates (y^*, x^*). This means for the design that it is sufficient to check the reliability of the concerning structural part as indicated by the smallest reliability index β at this selected point. This point P^* with the co-ordinates (y^*, x^*) is, therefore, called the design point. The co-ordinates of the design point P^* within the original r-s-system can be indicated as follows:

$$y^* = \frac{s^* - m_S}{\sigma_S} = \beta \cdot \alpha_S \qquad \rightarrow \qquad s^* = m_S + \beta \cdot \alpha_S \cdot \sigma_S$$

(4.2-62)

$$x^* = \frac{r^* - m_R}{\sigma_R} = \beta \cdot (-\alpha_S) \qquad \rightarrow \qquad r^* = m_R - \beta \cdot \alpha_R \cdot \sigma_R$$

(4.2-63)

The general design equation is now:

$$r^* = s^*$$

$$m_R - \beta \cdot \alpha_R \cdot \sigma_R = m_S + \beta \cdot \alpha_S \cdot \sigma_S$$

(4.2-64)

(6)   Determination of the partial safety factors

(6.1)   General

The partial safety factor for the action should take of:

- unfavourable deviations of the action
- uncertainties in the action model
- uncertainties in the action effect model

The partial safety factor for the material property should cover:

- unfavourable deviations from the characteristic values
- uncertainties in the resistance model
- variation of geometrical properties
- conversion factor (e.g. for concrete)

The safety factors can be obtained taking into account the target probability of failure (see Table 4.2-2 above) by means of different methods of reliability theory. The target probability of failure and, therefore, the safety factors do not cover the gross human errors. Effect of these errors should by taken into account be means of appropriate strategy "Quality Assurance" (more about this problem can be found by [Schneider, 1997]).

Each verification must show that the investigated limit state is not reached with pre-set reliability. For random variables with coefficient of variation V_x depending on the mean m_x the design values r_i^* and s_i^* as a product of partial safety factors γ_{fi}, γ_{mi} and characteristic values r_{ki}, s_{ki} (fractiles) can be indicated as follows:

$$r_i^* = \frac{r_{ki}}{\gamma_{mi}} \qquad\qquad (4.2\text{-}65)$$

$$s_i^* = \gamma_{fi} \cdot s_{ki} \qquad\qquad (4.2\text{-}66)$$

In above the equations the subindex f for action (force) and the subindex m for resistance (material) is introduced.

For random variables the mean of which being zero (e.g. imperfections, deflections of the plumb bob line of columns, internal forces and moments in the moment or shear force zero point) additive safety elements δ_i are introduced appropriately. It is:

$$r_i^* = r_{ki} - \delta_{mi} \qquad \text{for resistance} \qquad\qquad (4.2\text{-}67)$$

$$s_i^* = s_{ki} + \delta_{fi} \qquad \text{for action} \qquad\qquad (4.2\text{-}68)$$

The design equation can now generally be indicated as follows:

$$\gamma_f \cdot s_k + \delta_f \leq \frac{r_k}{\gamma_m} - \delta_m \qquad\qquad (4.2\text{-}69)$$

(6.2)   Partial safety factors γ_m for resistance R

If the log-normal distribution is the basis for the resistance then the design value of resistance can be obtained as follows:

$$r_i^* = m_{R_i} \cdot \exp\left(-\tilde{\alpha}_R \cdot \alpha_{R_i} \cdot \beta \cdot V_{R_i} - 0{,}5 \cdot V_{R_i}^2\right) \qquad\qquad (4.2\text{-}70)$$

If the 5%-fractile is set for the characteristic value r_k the partial safety factors can be determined generally as follows:

$$\gamma_{mi} = \frac{r_{ki}}{r_i^*} = \frac{m_{R_i} \cdot \exp(-1{,}645 \cdot V_{R_i} - 0{,}5 \cdot V_{R_i}^2)}{m_{R_i} \cdot \exp(-\tilde{\alpha}_R \cdot \alpha_{R_i} \cdot \beta \cdot V_{R_i} - 0{,}5 \cdot V_{R_i}^2)}$$

$$= \exp\left[\left(\tilde{\alpha}_R \cdot \alpha_{R_i} \cdot \beta - 1{,}645\right) \cdot V_{R_i}\right] \qquad\qquad (4.2\text{-}71)$$

The evaluation of equation (4.2-71) for $\tilde{\alpha}_R = 0.8$ is shown in Fig. 4.2-14.
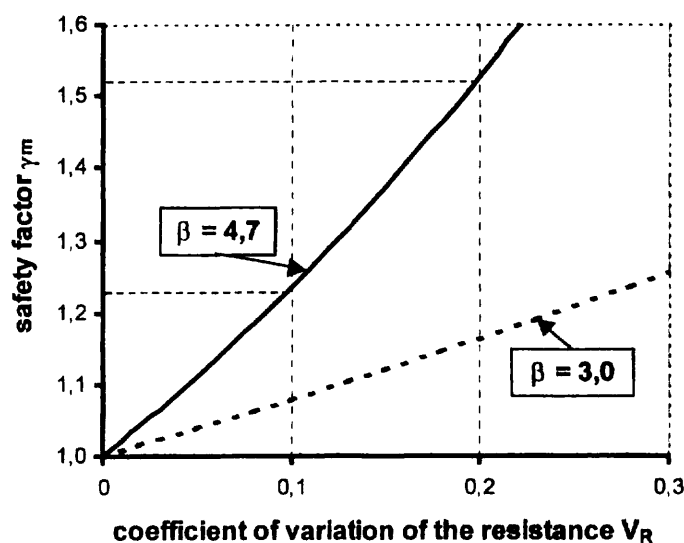
Fig. 4.2-14 : Partial safety factor for resistance as function of V_R

(6.3)   Partial safety factors γ_C for concrete

In the concept of Eurocodes a partial safety factor for concrete γ_C is defined as a value of 1.5. This safety factor consists of two parts:

The first part is the factor $\gamma_M = 1.30$, which considers unfavourable deviation of concrete strength from its characteristic value f_{ck}, model uncertainties, variation of geometrical properties, and the safety level. It is calculated by following formula [ENV 1991, Background Documentation, 1996], based on log-normal distribution:

$$\gamma_M = \exp[\alpha_R \cdot \beta \cdot V_R - 1{,}645 \cdot V_R]$$ (4.2-72)

with

- α_R = 0.8   - sensitivity factor for resistance
- β = 3.8   - reliability index
- V_R = $\sqrt{(V_m^2 + V_G^2 + V_f^2)}$
- V_f = 0.15   - coefficient of variation of material properties
- V_m = 0.05   - coefficient of variation for model uncertainties
- V_G = 0.05   - coefficient of variation of geometrical properties

Consequently the part of γ_M, which represents the variability of material properties is:

$$\gamma_{M1} = \exp[\alpha_R \cdot \beta \cdot V_f - 1{,}645 \cdot V_f] = 1{,}23$$ (4.2-73)

The remaining part represents the variation of geometrical properties and model uncertainties:

$$\gamma_{M2} = \frac{\gamma_M}{\gamma_{M1}} = \frac{1{,}30}{1{,}23} = 1{,}05$$ (4.2-74)

The second part is a conversion factor $\gamma_{conv.} = 1.15$, which takes into account the decrease of in-place strength versus the characteristic strength f_{ck}. In the research literature the inverse value of 0.85 often is used. The investigation of this value was recently undertook [König, Jungwirth, Soukhov, 1997] taking into account the work of [MacGregor, 1996]. The ratio f_s / f_{ck} (f_s - in-place strength of concrete) was considered as a random variable (log-normally distributed). The investigation shows that mean values of concrete compressive strength controlled at plant and the mean value of in-situ concrete compressive strength are approximately of the same magnitude for the age of concrete at 28 days. But due to different effects (such as transportation, temperature changes, placing, compaction, curing) the variation of in-situ concrete strength is essentially larger (coefficient of variation is about 0,23) as the variation of ready-mixed concrete at plant (coefficient of variation is about 0,13). Therefore, the safety factor $\gamma_M = 1,3$ is not be able to cover this increase of variation and additional factor should be used (γ_{conv}) as a value multiplied by γ_M. To find this additional factor the in-situ strength, or a ratio f_s / f_{ck}, was evaluated. Based on the German and Canadian data the 5% fractile of this ratio was found as a value of 0,90 for columns and walls and as a value of 0,83 for slabs and beams. These results correspond to the factor 0,85 currently used in the Eurocode.

4.2.3   Design format

(1)   General

As already mentioned in the last section the general design equation for all limit states is

$$S \le R \tag{4.2-75}$$

As a rule, for the calculated check of the design equation for the ultimate limit states the effect of the actions S is determined by a global examination (determination of internal forces and moments). On the other hand R is the resistance of a cross section, so being a local value. For the determination of the internal forces and moments it is, in addition to the structural system, necessary to consider all actions applied to the structure (see section by Prof. Eibl).

Dependent on their properties the actions are classified as:

- load actions always producing internal forces and moments,
- deformation actions leading to internal forces and moments only by restriction of these

Concerning the frequency of occurrence they are classified as:

- permanent actions G, the time rate of change of which being small and rare or monotonic,
- variable actions Q, the time rate of change of which being frequent and not monotonic,
- accidental actions A, characterised by a long return period.

A further differentiation is made in static and dynamic actions. Static actions do not activate the forces of gravity. Dynamic actions excite vibrations of the structures and, therefore, forces of gravity are activated.

According to design formats of Eurocodes some representative values are defined for variable actions. The main representative value is the characteristic one. This value has normally the return period of 50 years.

In common case some variable actions can occur together. But the probability that these actions occur simultaneously with their maximum values is very small. This is taken into account by means of combination value. Other representative values are frequent and quasi permanent ones. Corresponding to the frequency of their occurrence the representative values are classified as:

- characteristic value Q_k
- combination value $\psi_0 \cdot Q_k$
- frequent value $\psi_1 \cdot Q_k$
- quasi-permanent value $\psi_2 \cdot Q_k$

According to [ENV 1991, Part 1 "Basis of Design", 1994] such a value is defined as being frequent, which occurs during 5% within a chosen period of time or 300 times per year. A quasi-permanent value is assumed, if it occurs longer or equal than the half of the chosen period of time.

Furthermore, for the structural design it must be considered that the actions as mentioned above can influence the resistance of the structures either positively or negatively. For example the self-weight is a positive factor for securing a building against buoyancy. On the other hand it is a negative factor for limiting the soil pressure. As the serviceability and stability of buildings must be ensured even under most unfavourable conditions, for the permanent actions with positive influence the lower limit values are used in determining the action combination. Variable actions with positive influence are here, usually, not considered.

(2)   Design format for the ultimate limit state

For the calculated investigations of the ultimate limit states two different situations are defined:

- usual design situation
- accidental design situation (e.g. vehicle impact, earthquake)

Background for this differentiation are economic considerations taking into account the low frequency of occurrence of accidental actions. It is the general opinion in this case that it is defensible if the structural reliability for the accidental design situation is smaller than this for the usual service condition.

According to eq. (4.2-75) the design equation for the ultimate limit state is as follows:

$$S_d \leq R_d \tag{4.2-76}$$

In the above equation R_d is the structure resistance to be determined. For calculated investigations it is, generally, for simplification, equated with the resistance of the so-called decisive cross section, which is determined with the design values of the material properties under consideration of the cross-sectional dimensions. The design values of the material properties of steel and concrete can be determined from the characteristic values f_{yk} and f_{ck} (see section by Prof. Hilsdorf) under consideration of the partial safety factors γ_s and γ_c. It is:

$$f_{cd} = \frac{f_{ck}}{\gamma_c} \tag{4.2-77}$$

$$f_{yd} = \frac{f_{yk}}{\gamma_s}$$

(4.2-78)

Corresponding to the design situations the partial safety factors for steel and concrete can be taken from Table 4.2-3 (based on ENV 1992 "Design of Concrete Structures", Part 1 "General Rules and Rules for Buildings", 1992).

type of combination	building materials	
	concrete γ_c	steel γ_s
basic combination	1.5	1.15
accidental combination	1.3	1.0

Table 4.2-3: Partial safety factors for building materials for both design situations, acc. to ENV-1992

Corresponding to the simplification for the determination of the structural resistance (structural resistance = resistance of cross section) S_d represents in equation (4.2-76) the inner forces in the considered cross section caused by the decisive combination of actions. The decisive combination of actions can be put together according to the design situation by means of the equations (4.2-79) or (4.2-80) (based on ENV 1991 "Basis of Design and Actions on Structures", Part 1 "Basis of Design", 1994).

- usual design situation

$$\left[\sum \gamma_{G,i} \cdot G_{k,i} + \gamma_p \cdot P_k + \gamma_{Q,1} \cdot Q_{k,1} + \sum_{i>1} (\gamma_{Q,i} \cdot \psi_{0,i} \cdot Q_{k,i}) \right]$$

(4.2-79)

- accidental design situation

$$\left[\sum \gamma_{GA,i} \cdot G_{k,i} + \gamma_p \cdot P_k + A_d + \psi_{1,1} \cdot Q_{k,1} + \sum_{i>1} (\psi_{2,i} \cdot Q_{k,i}) \right]$$

(4.2-80)

where:

- $G_{k,i}$ characteristic values of the permanent actions (taken out from valid standards)
- $Q_{k,1}$ characteristic value of a leading variable action (taken out from valid standards)
- $Q_{k,i}$ characteristic values of further variable actions (taken out from valid standards)
- A_d design value of accidental actions(taken out from valid standards)
- P_k characteristic value of prestressing action
- γ_{GA} partial safety factor of permanent actions for accidental design situation
- γ_G partial safety factor of permanent actions for the basic combination
- γ_Q partial safety factor of variable actions
- γ_p partial safety factor of prestressing actions

- $\psi_{0,i}$ coefficient for combination value for the variable actions i
- $\psi_{1,i}$ coefficient for frequent value for the variable actions i
- $\psi_{2,i}$ coefficient for quasi-permanent value for the variable actions i

The partial safety factors for the actions and the ψ coefficients can be taken from Table 4.2-4 (based on ENV 1991 "Basis of Design and Actions on Structures", Part 1 "Basis of Design", 1994) and Table 4.2-5.

type of design situation	actions		
	permanent	variable	
		dominant	others
usual	$\gamma_G = 1.35$	1.5	1.5
accidental	$\gamma_{GA} = 1.0$	1.0	1.0

Table 4.2-4: Partial safety factors for actions for both design situations

For general buildings the combination values were fixed in [German NAD for EC1, Part1, 1991]. Here also the probability of occurrence of both design situations is considered (Table 4.2-5).

action	combination value		
	ψ_0	ψ_1	ψ_2
live load on floors			
- residence; office; sales areas up to 50 m²; corridors; balconies; rooms in hospitals	0.7	0.5	0.3
- assembly rooms; garages and car parks; gymnasiums; stands; corridors in teaching buildings; libraries; archives	0.8	0.8	0.5
- exhibition and sales rooms; office buildings and department stores	0.8	0.8	0.8
wind loads	0.6	0.5	0
snow loads	0.7	0.2	0
other actions	0.8	0.7	0.5

Table 4.2-5 : Combination values for the variable actions

(3) Design format for the limit state of serviceability

According to eq. (4.2-75) the design equation for verification of the limit states of serviceability can be indicated as follows:

$$S_d \leq C_d \tag{4.2-81}$$

In eq. (4.2-81) C_d is the nominal value of a particular structure or structural part property. Examples for C_d are permissible deformations, maximum permissible crack width or permissible steel or concrete stress. The permissible values of the different structural properties are in most cases empirical values (e.g. deformations) or values derived from experiments (e.g. crack width).

S_d is the core value (crack width, deformations, etc.) occurring at the structure or structural part as a result of the decisive action combination. These core values should be determined using the characteristic values of the material properties considering the effect of long-term loading (e.g. creep and shrinkage of concrete). These decisive action combinations are classified as follows (based on ENV 1991 "Basis of Design and Actions on Structures", Part 1 "Basis of Design", 1994):

- rare combination

$$E_d = E_d\left[\sum G_{k,i} + P_k + Q_{k,1} + \sum_{i>1}(\psi_{0,i} \cdot Q_{k,i})\right] \tag{4.2-82}$$

- frequent combination

$$E_d = E_d\left[\sum G_{k,i} + P_k + \psi_{1,1} \cdot Q_{k,1} + \sum_{i>1}(\psi_{2,i} \cdot Q_{k,i})\right] \tag{4.2-83}$$

- quasi-permanent combination

$$E_d = E_d\left[\sum G_{k,i} + P_k + \sum_{i\geq1}(\psi_{2,i} \cdot Q_{k,i})\right] \tag{4.2-84}$$

This classification of the different action combinations for the limit state of serviceability shall express the significance of the individual verifications for the use. For example the proof of the limitation of crack width is very important for the basement waterproofing of reinforced concrete without seal. Therefore, this proof of crack width must be performed with the actions of the rare combination. On the other hand the proof of crack width for an office building is, usually, not so important. It can, therefore, be performed with the quasi-permanent combination.

References

Augusti. G., Baratta A., Casciati F.,1984, "Probabilistic Methods in Structural Engineering", London, New York, Chapman and Hall

Benjamin J.R., Cornell A., 1970, "Probability, Statistics, and Decision for Civil Engineers", McGraw-Hill Book Company

Bolotin V.V., 1969, "Statistical Methods in Structural Mechanics", Holden Day, San Francisco

CIRIA, 1977, "Rationalisation of Safety and Serviceability Factors in Structural Codes", Report 63, CIRIA, London

ENV 1991 "Basis of Design and Actions on Structures", Part 1:"Basis of Design", August 1994

ENV 1992 "Design of Concrete Structures", Part 1-1:"General Rules and Rules for Buildings", December 1991

ENV 1991 "Basis of Design and Actions on Structures", Part 1:"Basis of Design", Background Documentation, March 1996

Ferry-Borges. J., Castaneta M., 1971, "Structural Safety", LNEC, Lisbon

"Grundlagen zur Festlegung von Sicherheitsanforderungen für bauliche Anlagen", Berlin: Normenausschuß Bauwesen im DIN. Beuth 1981

Hanisch J., Struck W., 1985, "Charakteristischer Wert einer Boden- oder Materialeigenschaft aus Stichprobenergebnissen und zusätzlicher Information", Bautechnik 10/1985

Hasofer A.M., Lind N.C., 1974, "Exact and Invariant Second-Moment Code Format", Proceedings ASCE

International Standard Organisation (ISO), 1998, "General Principles on Reliability for Structures", ISO/FDIS 2394

Joint Committee on Structural Safety, 1976, "Common Unified Rules for Different Types of Constructions and Materials", CEB Bull. d'Info., 116-E

König G., Hosser D., 1982, "Praktische Beispiele und Hinweise zur Festlegung von Sicherheitsanforderungen für bauliche Anlagen nach den Empfehlungen des NABau", Bauingenieur 57, 1982

König G., Hosser D., Schobbe W., 1982, "Sicherheitsanforderungen für die Bemessung von bauliche Anlagen nach den Empfehlungen des NABau - eine Erläuterung", Bauingenieur 57, 1982

König G., Soukhov D., Jungwirth F., 1997, "Conformity and Safety of Concrete according to prEN 206 and Eurocodes", Leipzig Annual Civil Engineering Report (LACER) No. 2, Leipzig, 1997

MacGregor J. G., Bartlett F. M., 1996, "Statistical Analysis of the Compressive Strength of Concrete in Structures", ACI Materials Journal, March - April 1996

NAD for ENV 1992 "Design of Concrete Structures", Part 1-1:"General Rules and Rules for Buildings", "DAfStb-Richtlinie zur Anwendung von Eurocode 2, Fassung Nov. 1991

Rackwitz. R., 1976, "Practical Probabilistic Approach to Design", CEB Bull. d'Info., 112

Rackwitz R., 1981, "Zur Statistik von Eignungs- und Zulassungsversuchen für Bauteile", Bauingenieur 56, 1981

Schneider J., 1997, „Introduction to Safety and Reliability of Structures", IABSE, Structural, Engineering Documents, Volume 5.

4.3   Serviceability Limit States (Principles)

4.3.1   General
by Andrew W. Beeby

It will already be clear that there are two basic aspects of behaviour which must be dealt with in design: issues related to the load carrying capacity of the members or structure considered and issues related to the performance of the members or structure under service loads. Seviceability limit states are concerned with the second of these aspects. Though other serviceability limit states can be critical in particular cases, there are two which are the most generally important and which Codes tend to deal with at some length. These are: deflections and cracking. This chapter will mainly be concerned with these two subjects. Other limits are to stress levels in tension and compression and vibration. Very little guidance is given in CEB MC90 on the control of vibrations and it will not be considered further in this chapter.

CEB MC90 sets out the design principle for the Serviceability Limit States in Clause 1.6.6.2 as follows:

(a) Limit state of cracking and excessive compression:

It should be verified that in any cross section:

$\sigma(F_d) < \alpha f_d$ for crack formation and excessive creep

$w(\sigma_f, f) < w_{lim}$ for maximum crack width

$\sigma(F_d) \leq 0$ for crack re-opening.

Where:
σ is a defined stress
σ_f is a tensile, shear or compressive design strength
w_{lim} is a defined crack width.

(b) Limit state of deformations

It should be verified that:

$a(F_d, \sigma_f) \leq a_{lim}$

where a is a defined deformation (generally a deflection) and a_{lim} is a limiting deformation.

(c) Limitation of vibrations.

In most common cases the limitation is ensured by indirect measures, such as limiting

the deformations or the period of vibration of the structure in order to avoid risk of resonance. In other cases a dynamic analysis is necessary.

Before considering deflections or cracking in detail, however, some general issues about serviceability will be discussed.

A critical point to note is that, while the Ultimate Limit States are mainly concerned with the strength of materials and sections, Serviceability Limit States are mainly concerned with the deformations of members or sections and hence are concerned dominantly with stiffness. This statement is, of course, a generalisation; for example, failure of members due to classical buckling is related to stiffness rather than material strength, but it remains a useful general distinction. Deflection is clearly related directly to member stiffness. Crack widths are related to the tensile strains that develop in a member and how these strains are accommodated when the tensile strain capacity of the concrete is exceeded. Thus, whether or not cracking occurs will depend on the tensile strength of the concrete but the widths of the resulting cracks will depend on the stiffness of the system. It is generally the second of these issues which is the more important. Bearing in mind this importance of stiffness, developments in the basic materials used in structural concrete over the years are significant. Figure 4.3-1 (taken from (Beeby (1999)) shows how the stresses under service loads in reinforcement have changed over the past 80 years where designs have been carried out to UK codes. While this figure relates to UK practice, it is likely that practice in other countries has followed the same general trend. It will be seen that service stresses have increased at every amendment to the regulations and that the allowable stresses, ignoring redistribution, have increased by a factor of 3 over the period considered while, if redistribution is taken into account, the increase rises to a factor of 4.5. These increases result from a number of causes:

Figure 4.3-1 variation in permitted service stresses with time (UK values)
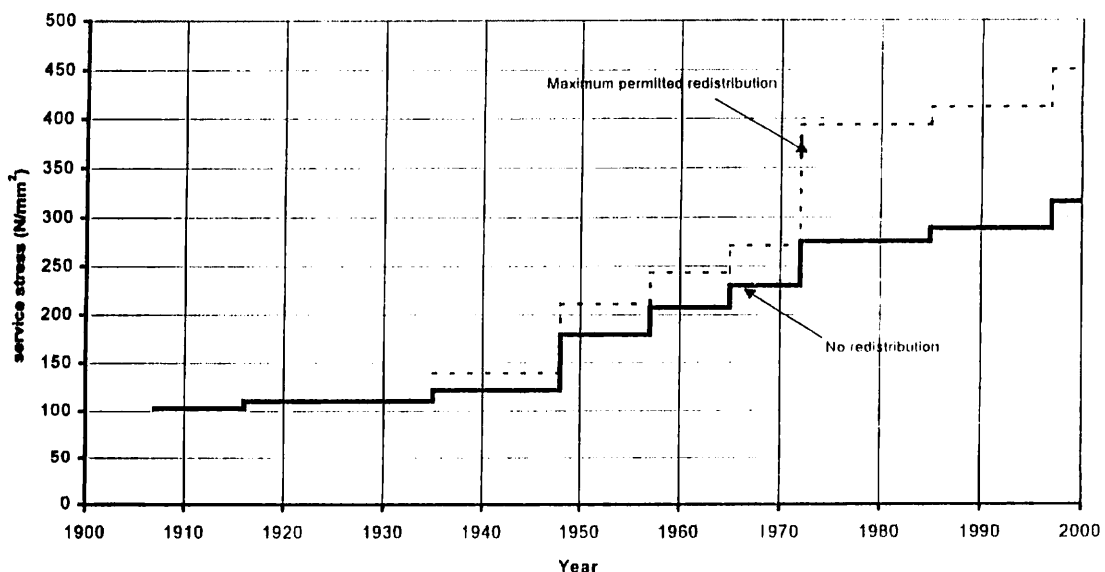
Figure 4.3-1 increase in service stresses in reinforcement over time (UK experience)

- Increase in the strength of reinforcement
- Reduction in safety factors
- The introduction of redistribution and the increase in the allowable redistribution
- The change from elastic methods of section analysis to ultimate load methods.

Not indicated here is a general increase due to the refinements in analytical techniques permitted by the use of computers and economic pressures to minimise the use of materials. The importance of the changes shown in Figure 4.3.1 for serviceability is that the modulus of elasticity of reinforcement does not change with increase in strength and thus the increase in stress leads to a more or less directly proportional increase in deflections and crack widths.

A similar increase has occurred in the service compressive stress levels in concrete over the years. Figure 4.3-2 (taken from (Beeby and Hawes (1986)) is an attempt to illustrate this for UK practice up to 1985 for a particular mix. The changes result from three main causes:

- Increasing strength of Portland Cement
- Reduced safety factors
- Changes from elastic to semi-plastic methods for the analysis of sections.

Not considered here is the general move towards the use of higher strength concretes to meet durability requirements and to speed up the construction process. Unlike steel, there is an increase in elastic modulus of concrete with increase in strength, but not a proportional increase; a doubling in concrete compressive strength from 20 N/mm^2 to 40 N/mm^2 only results in a 20% increase in elastic modulus. Thus, again, this increase in general stress level will have resulted in a general increase in deformations.
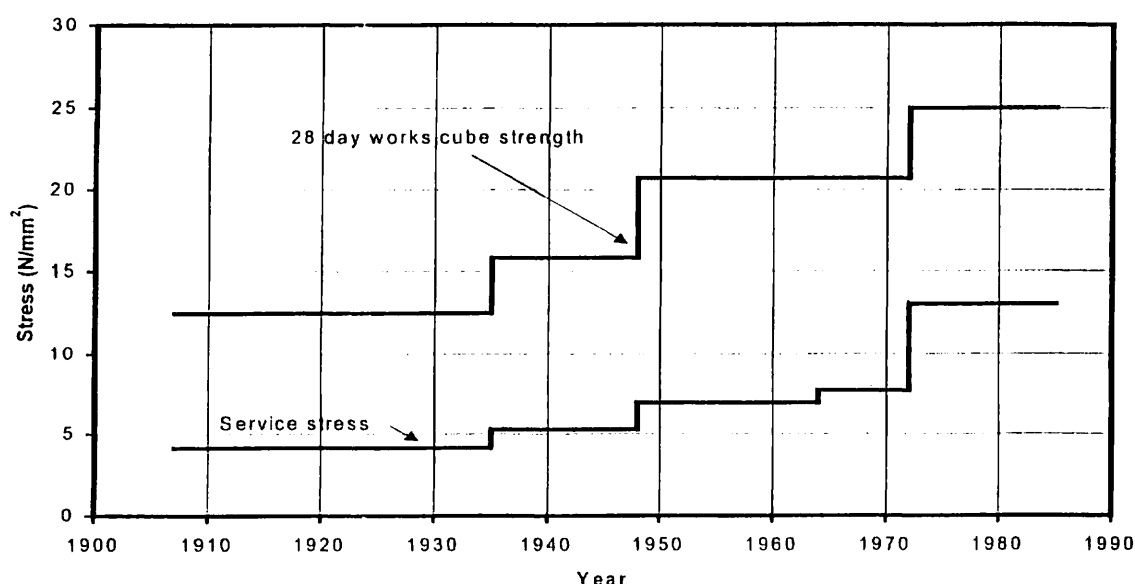
Figure 4.3-2 Increase in cube strength and service stress for a 1:2:4 concrete (from Beeby & Hawes 1986)

The result of these changes in practice is that the importance of serviceability in design has increased over the years. In the first half of this century, It was hardly necessary to take any measures in design to ensure adequate service performance; if a structure was strong enough then it was also almost certain to be stiff enough. This is no longer true and the attention given to design for serviceability has increased in all codes of practice over recent years. Indeed, it can be argued that the situation is approaching where, if a structure has been properly designed for service conditions, it can be assumed without more than a simple check that it will also be strong enough (Beeby and Fathibitaraf (1996)).

The importance in design for serviceability is thus increasing and should now probably have an importance in the design process equal to that of the Ultimate Limit States. That most codes still treat it as a secondary issue is probably mainly due to history and has the disadvantage of obscuring the true situation. For example, one of the fundamental economic decisions in the design of a multi-storey building is the thickness of the slabs. This has a major influence on the dead weight of the structure and can significantly affect the storey height and hence the number of floors that can be included. Choice of a suitable thickness is governed almost entirely by considerations of deflection control yet most current design rules deal with this in the crudest possible way by the use of very unsophisticated span/depth ratio limits.

It has to be said that there are real difficulties in the formulation of truly rational design methods for the Serviceability Limit States, both at a philosophical and a practical level. At the practical level, the prediction of service behaviour is both more complex and inherently less accurate than predictions of ultimate behaviour. These points will be appreciated more fully when the following sections are studied. The philosophical issues may usefully be considered slightly further here.

When carrying out a detailed design for any limit state, the following four essentials are required:

- Criteria defining the limits to acceptable behaviour
- The definition of the design loading conditions under which the criteria should be checked
- The definition of design material properties for use in carrying out any checks
- A behavioural model which can use the design loads and material properties to predict behaviour and hence permit the predicted behaviour to be compared with the criteria.

In simplified design methods, such as the use of span/depth ratios for deflection control or bar size and spacing rules for crack control, these four essential pieces of information may not be explicitly required but assumptions about them are implicit in the particular methods.

For the Ultimate Limit States, there is a clear single criterion; that the design strength of the structure should not be less than the design load. Strength is an unambiguous

quantity: it is the maximum load that the structure will support without failing. If the load is below this, the structure remains standing; if an attempt is made to apply a higher load, the structure collapses.

No such clear cut situation exists for serviceability criteria. It cannot, for example, be said that a structure which deflects marginally less than the limiting value is totally satisfactory while one where the deflection marginally exceeds the limit is totally unsatisfactory. In practice, it would be impossible to differentiate between the performance of the two members. The same may be said for crack widths or vibrations. Furthermore, the criteria are not universal; a deflection which will be acceptable in one circumstance will be unacceptable in others. There are a great variety of reasons why deflections should be limited and the following is not a complete list, merely a selection. Deflections may be limited in order:

- To avoid visual sag which would upset the occupants
- To avoid damage to partitions built on the slab
- To avoid upsetting the alignment and functioning of delicate apparatus or machinery supported by the member
- To avoid doors jamming or the glass in windows being broken
- Etc.

Whether a particular reason is an issue or not will depend on the particular member considered and its function. It is, in principle, not possible to set down a complete set of deflection limits in a standard. It must be the duty of a designer to establish what the functional requirements are for the particular structure considered and select suitable limits accordingly. It is unfortunate that neither the writers of standards nor designers find this concept easy to accept. Designers would like to have clearly defined rules which they have to obey and which, provided they have obeyed them, will relieve them from responsibility if the structure does not behave adequately. The writers of codes and standards are put under very strong pressure to provide such rules with the result that they frequently do so. The drafters increasingly write qualifying clauses into codes pointing out that the limits given are only for general guidance and that the designer should ensure that the limits are appropriate for the particular structure considered. In practice these carry little weight with designers or with those who have the duty of approving calculations; both groups will require the code limits to be obeyed slavishly however irrelevant they may be for the particular structure considered.

The definition of a limiting crack width is almost equally difficult. There are three common reasons given for the control of crack widths. These are:

- To reduce the risk of corrosion of the reinforcement (or prestresssing tendons)
- To avoid leakage through cracks
- To avoid unsightly appearance.

The first of these reasons has been the subject of research over many years but, so far, no clear relationship between crack width and corrosion has been established and

certainly no specific crack width limit has been established which will avoid corrosion. Many research projects show little difference between the corrosion found on cracked concrete and uncracked concrete.

Clearly there will be an increase in leakage with wider cracks (where other factors remain unchanged) but research has yet to arrive at a generally acceptable design relationship between crack width, hydraulic head, wall thickness, some measure of crack roughness and flow through the cracks. Furthermore, a fundamental issue related to volume of leakage through a wall or slab is the number of cracks and the length of the cracks. This is information which current crack formulae do not provide.

Appearance is now generally accepted as generally the most important reason for controlling crack widths and some research suggests that cracks with widths below 0.3 mm are unlikely to cause complaint. However, the width of crack which will be acceptable will clearly depend on the distance from which the crack can be observed and the surface finish on the concrete.

Clearly, the definition of a crack width limit is at least as complex and uncertain as the definition of an appropriate deflection limit.

The remaining area where codes define criteria is limitations to service stresses. The compressive stress in concrete under the service load is commonly limited to some fraction of the compressive strength. Two reasons are given for doing this: firstly to limit the possibility of the formation of microcracks which might impair durability and secondly to avoid excessive creep deformations if stresses beyond the limit for linear creep are to be sustained for an extended time. As far as can be established, no properly documented case exists of a situation where durability has been impaired due to excessive compressive stress and the cases where excessive creep might be a problem are rare. In CEB MC90, a limit of $0.6f_{ck}$ is suggested to avoid microcracking or longitudinal cracking. This should generally not cause problems since the calculations for the Ultimate Limit State should ensure that this limit is not seriously exceeded. MC90 does not provide a specific limit (as does Eurocode 2, which limits stresses under quasi-permanent loads to $0.45f_{ck}$) to avoid excessive creep; it merely correctly points out that, at high levels of stress, the assumption of linear creep will become invalid and alternative calculation models may be more appropriate.

The remaining stress limit is a limit under service loads to the stress level in reinforcement to, generally, 80% of the yield strength or 0.2% proof stress under loading or f_{yk} where the stresses are due to imposed deformations. There is a clear logic for this limit since, once non-linearity occurs in the reinforcement, large local strains tend to develop. This will result in excessive crack widths which will not close on removal of the load. Deviation from the linear will start to occur significantly below the 0.2% proof stress in cold worked steels so a limitation to 80% of the proof stress is logical.

In defining suitable loads for checking serviceability conditions, it is clear that a

variety of possible conditions may need to be considered depending on circumstances.

Clearly, in order to be able to calculate the effects of creep, it is necessary to have a definition of those loads which are likely to be applied to the structure more-or-less continuously. This is dealt with in Eurocode 2 and MC90 by defining a 'quasi-permanent' combination of loads. This is taken as the dead weight of the structure plus a fraction of the imposed loads; this fraction depending on the nature of the imposed load.

When checking the maximum value of deflection or crack width, it is necessary to give more thought to the level of loading considered. Decisions have to be taken on how significant an occasional exceedance of the criterion considered may be. For example, if a limit to overall sag of a member is being considered from the point of view of visibility, will it matter if, occasionally, the sag exceeds the specified limit provided that the deflection will reduce to within the limit when the load is removed? If it is concluded that occasional exceedance is not important then clearly a load with a significant chance of being exceeded during the expected life of the structure may be selected. If exceedance of the limit is likely to cause more trouble, for example, if exceedance of a deflection or crack width limit is likely to cause significant damage to cladding or to partitions supported by the member, a load with a considerably lower probability of being exceeded may be appropriate. To provide scope for this, both Eurocode 2 and MC90 define two load combinations: the 'frequent combination' and the 'rare combination'. These differ in the proportion of the variable loads included. It may be noted that these combinations may not necessarily be appropriate for all service checks and the designer should be satisfied that they are appropriate for the particular circumstance considered. As a possible example, in the design of some types of industrial installation, it may be more appropriate to define an 'operating load combination', corresponding to the client's specification of the loading which he expects to occur in operation of the plant. Some safety factor should then be applied to ensure that, considering the uncertainties in the materials and the calculation models, the plant can be guaranteed to behave satisfactorily when subjected to the operating conditions.

It is normally satisfactory to consider the material properties to be the mean values corresponding to the characteristic strength of the material. There may, however, be situations where this is not entirely appropriate. An example here is the provision of minimum reinforcement for crack control. The provision of less reinforcement than the minimum can lead to local yield and consequent uncontrolled cracks. The amount of reinforcement required is proportional to the tensile strength of the concrete and thus it would seem appropriate to use a high estimate of this rather that an estimate of the mean tensile strength assuming that the concrete is at it's characteristic strength. It should be noted that there is a high probability that the concrete strength will be above characteristic. A practical problem with this line of reasoning is that it tends to suggest a requirement for substantially greater areas of reinforcement than have commonly been used in practice and so many codes have been forced to compromise on this issue. It may also be noted that probably the main cause of uncertainty in the prediction of deflections, and possibly also in the prediction of crack widths due to imposed deformations, is uncertainty about the tensile strength of the concrete. If, for example, it is required to

gain some idea of the actual expected deflection rather than the design value, it may be appropriate to try to put bounds on the deflection by considering a range of *tensile strengths* rather than accepting a single value.

In summary, it will be seen that the Serviceability Limit States are fundamentally different to the Ultimate Limit States. The criterion for the Ultimate Limit States is clear and universal. Furthermore, there is a public interest in safety since people who are not the owners of structures can be put at risk by unsafe structures. Levels of safety may therefore reasonably be specified by legal authorities in the country concerned and may be stated as absolute requirements in codes and standards. Serviceability Limit States, on the other hand, are concerned with ensuring that the structure will serve the function that the client has specified. The criteria for serviceability are primarily a matter between the client and the designer and should be chosen to ensure that the structure performs as required by the client. Codes and standards can only advise on these matters and there is no public interest unless the public is the client. The designer has a duty to ensure that the criteria he chooses will satisfy the client's requirements. He cannot hide behind the recommendations of a code.

References.

Beeby, A. W.(1999)   Keynote paper on innovation in the construction industry. To be published in proceedings of an International Congress on Creating with Concrete. September 1999.

Beeby, A. W. and Hawes, F.(1986), Action and reaction in concrete design, 1935 – 1985. Cement and Concrete Association Reprint 3/86.

Beeby, A. W. and Fathibitaraf, F.(1996), The design of framed structures; a proposal for change. Concrete in the service of mankind: Appropriate concrete technology (Ed Dhir and McCarthy) E & FN Spon, 1996.

4.3.2   Crack control

by György L. Balázs

Cracks are unavoidable in concrete structures. Cracks may be classified as cracks already formed in the fresh concrete (early cracking) or in the hardened concrete. Cracks may be induced by loads or by imposed deformations.

We may otherwise distinguish between cracks that are formed within the concrete body and cracks that appear on the surface. Cracks which are developed only around the reinforcing bars but not appearing on the concrete surface are often called ***micro-cracks***. Their existence was experimentally shown by Broms (1965a) and Goto and Otsuka (1971) (Fig. 4.3-1.a), respectively. Size and orientation of micro-cracks depend on the load level, rib pattern of reinforcing bar and produced slip. (See more details in Chapter 3.1).

Cracks appearing on the concrete surface are generally simply referred to as ***cracks*** and should be controlled by reinforcement. Shape and width of cracks is influenced by the reinforcement: width of cracks is slightly smaller at the level of reinforcing bars than below or above (Fig. 4.3-3 b). It is an evidence of the effect of bond (or tension stiffening).

Cracks may be formed ***transverse or parallel*** to the main reinforcement. Cracks transverse to the main reinforcement are our main concern herein. Cracks parallel to the axis of the reinforcing bar are called ***splitting cracks*** (Fig. 4.3-3 m) caused by the radial component of the bond stresses leading to splitting of the concrete cover. These cracks should be controlled by stirrups. Corrosion of reinforcement may produce cracks parallel to the reinforcement owing to the volumetric increase of the corrosion products. ***Too small concrete cover*** may also initiate cracks clearly indicating the position of the reinforcement (generally that of stirrups).

A surface crack is a visible and measurable discontinuity of the concrete matrix. ***Crack control means to keep crack widths below acceptable limits.*** In this chapter a description of the cracking phenomenon is given together with possibilities to crack control basically for cracks transverse to the main reinforcement and induced by loads. Early cracks and cracks induced by imposed deformations are not dealt with here.

(1)   Causes and types of cracks

(1.1)   Early cracks and cracks induced by imposed deformations

Cracks may already form soon after casting, due to settlement of plastic concrete. During hardening, ***hydration heat*** produces temperature differences between internal and external portions and is likely to cause cracking in thick elements. Rapid evaporation can also lead to ***plastic shrinkage*** (Figs. 4.3-3 c) [Leonhardt (1976a/b, 1985, 1988)]. Cracking due to plastic shrinkage of concrete can be reduced by applying ***plastic fibers*** [Balaguru and Shah (1992)]. ***Concrete technology and curing*** can also have a considerable influence on cracking. Important is to avoid high temperature gradients caused by the hydration heat by reducing heat transfer on the surface.

After hardening, besides the dead load and the live load, ***restraint forces*** in statically indeterminate structures produced by differential settlement of foundations or by different
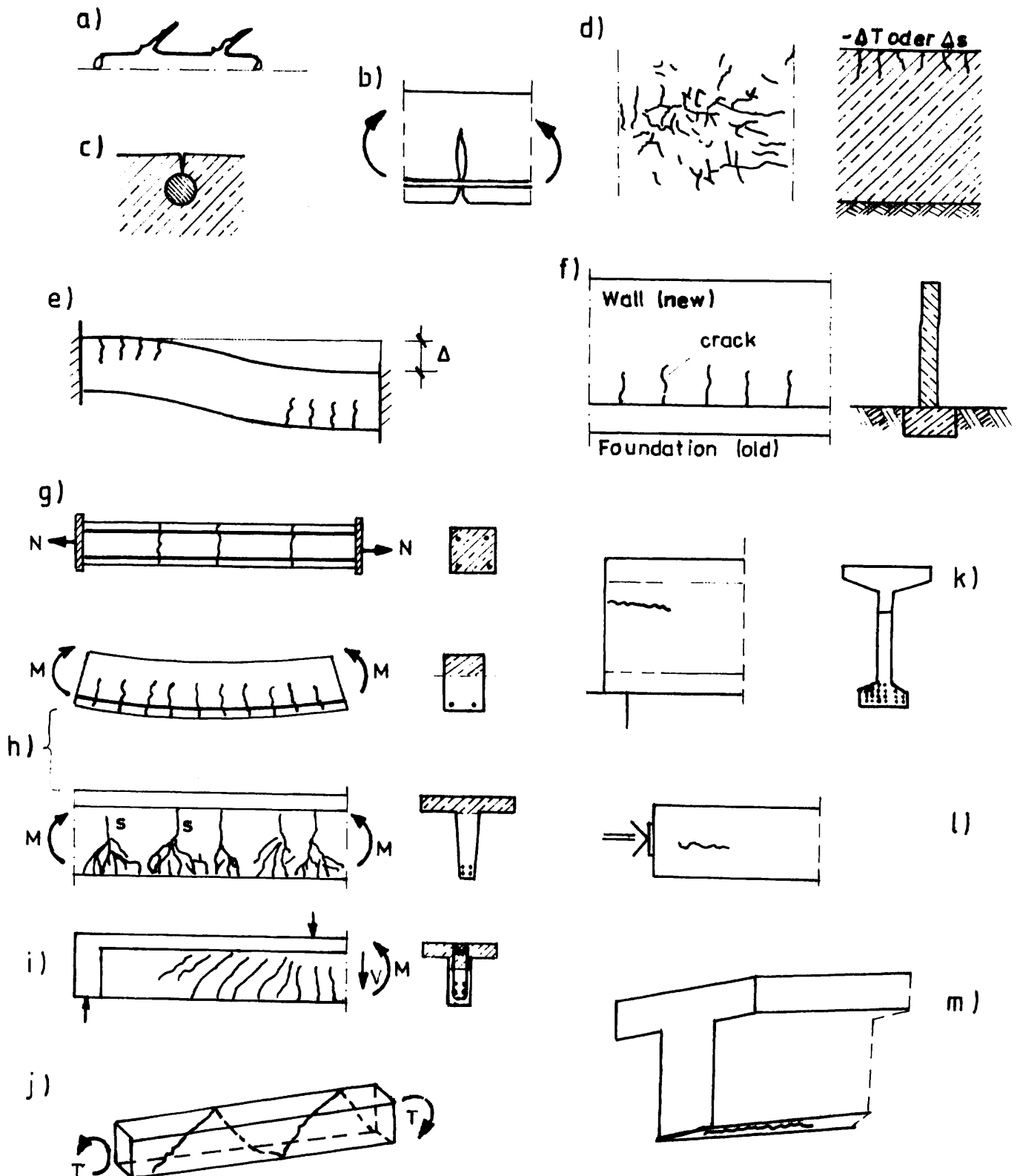
Fig. 4.3-3 Types of cracks in concrete structures [partly by Leonhardt (1976a)]

a) micro-cracks
c) settlement of plastic concrete
e) cracks due to diff. settlements
g) tensile cracks
i) shear cracks
k) spalling crack
m) splitting crack in the anchorage zone

b) shape of crack
d) hydration heat or shrinkage cracks
f) shrinkage cracks in connected members
h) bending cracks
j) torsional cracks
l) bursting crack

temperatures of the top and bottom faces of the element may cause cracking (Figs. 4.3-3 d and e). *Shrinkage* often leads to cracks between connected members of significantly different sizes or ages (Fig. 4.3-3 f) [Leonhardt (1976a)]. *Construction joints* are anyway important to concentrate concrete shrinkage strains in order to avoid irregular cracking of the member.

(1.2)   Cracks induced by loads

Pure tension produces cracks with almost parallel sides over the whole section (Fig. 4.3-3 g). *Flexural cracks* start at the tension face and stop before reaching the neutral axis (Fig. 4.3-3 h). If a high amount of reinforcement is placed into the tensile flange, the cracks may be more distributed in the flange than in the web. *Shear cracks* follow the inclined trajectories in the zone of high shear forces (Fig. 4.3-3 i). Torque produces *helical cracks* (Fig. 4.3-3 j).

Introduction of prestressing force may cause cracks almost parallel to the axis of the member. They are known as *horizontal cracks* [CEB (1987)] and are classified as *spalling cracks* (Fig. 4.3-3 k) if caused by spalling stresses in the web or as *bursting cracks* (Fig. 4.3-3 ℓ) if caused by bursting stresses in the axis of the prestressing tendon or concentrated load.

(2)   Reasons for crack control, limits for crack widths

Crack control is required:

a) First of all for *aesthetic reasons*. Limits are needed so that the structure' s appearance is not impaired nor is public alarm created. A crack width of more than 0.25 mm is likely to create concern [Beeby (1978b)];

b) On the other hand *to insure water- or gas-tightness*, and *to limit the risk of corrosion of reinforcement*. However, research results [Schießl (1975), Beeby (1978a/b)] indicated that no direct relationship between corrosion and crack width exist: crack widths up to 0.4 mm do not significantly reduce the corrosion protection of the non-prestressed reinforcement in concrete provided the concrete cover is sufficiently thick and dense and chloride attack is excluded.

Limit values of crack width (different for reinforced and for prestressed members) are often expressed as a function of the exposure condition of the element. The more severe is the exposure condition, the lower the crack width limit. A detailed list of the exposure classes is given in Chapter 5 on Durability. Maximum value of crack width limit in case of indoor conditions is generally 0.4 mm for reinforced members and 0.2 mm for prestressed members.

According to MC90 *for reinforced concrete members* $w_{lim}=0.3$ mm may be assumed for exposure classes 2 to 4 under the quasi permanent combination of actions with respect to both appearance and durability if watertightness is not required. For exposure class1, this limit may be relaxed provided that it is not necessary for reasons other than durability. *For prestressed members* crack width limits given in Table 4.3-1 are provided. Owing to the highly probabilistic nature of cracking, such nominal values for crack width limits may only serve as

means to apply the design criterion of Section (7) of this Chapter and can in no case be compared to actual crack widths measured in situ.

There are two reasons to provide *a minimum amount of reinforcement* in concrete members (hints for minimum reinforcement are included in Chapter 4.5 on Detailing):

1) *To ensure enough **ductility*** for avoiding brittle failure of the member by the appearance of the first crack. (In prestressed members or reinforced members subject to compressive normal force, the minimum amount of reinforcement may be reduced below that necessary for ordinary reinforced concrete members.) Cracking is a sudden energy release when the crack quickly runs up almost to the neutral axis where the concrete tensile strength is reached.

2) *To ensure enough **durability*** by distributing possible cracks from effects that were not considered by the analysis (such effects can be: different temperatures, shrinkage of concrete or different settlements, etc.)

Exposure class	Post-tensioned	Pretensioned
1	0.20	0.20
2	0.20	No tension within the section is allowed
3 and 4	(a) No tension is allowed within the section, or (b) if it is accepted, impermeable ducts or coating of the tendons should be applied; in this case $w_{lim}=0.2$ mm	

Table 4.3-1   Crack width limits (in mm) for prestressed members under the frequent load combination according to MC90

Unfortunately, surface cracks often become accentuated by streaks of dirt and material leached from the crack. The possibility of leakage of liquid or gas from the structure depends on the pressure, the thickness of concrete, and the nature of the crack (i.e., whether it penetrates the whole section).

(3)   Definition of crack width

Cracks occur whenever the *principle tensile strain* from loads or restraint forces would exceed the ultimate tensile strain of concrete. Due to the formation of cracks, *the compatibility of deformations between steel and concrete is not maintained*. The accumulation of strain differences produces relative displacement (slip). The width of a crack at the steel is provided by the sum of the two slip values reaching the crack from either sides. Nevertheless, a rigorous formulation of the crack width (w) is to be based on the integration of the actual steel (ε_{sx}) and

concrete (ε_{cx}) strain differences over the crack spacing (s_r) to obtain the two slips values (s_1 and s_2):

$$w = \int_{(s_r)} (\varepsilon_{sx} - \varepsilon_{cx})dx = s_1 + s_2 \tag{4.3-1}$$

In absence of bond stresses (otherwise if they are neglected), the crack widths could be simply determined by the integral of constant steel strains between cracks:

$$w = s_r \sigma_s / E_s$$

Eq. (4.3-1) indicates that crack width is calculated at the *level of the reinforcement* and it should be compared to measurements at the same level. Test results with Moiré photo-optic method demonstrated that widths of a crack below or above the reinforcement are higher owing to the bond stresses reducing concrete deformations (Fig. 4.3-3 b).

(4) Phases of crack formation

Two phases of crack formation are generally distinguished as: crack formation and stabilized cracking phases. Fig. 4.3 4 indicates force, stress, strain, slip, first derivative of slip and bond stress distributions for both for crack formation (Fig. 4.3-4 a) and for stabilized cracking phases (Fig. 4.3-4 b), respectively. Descriptions of the diagrams are given in the following sections.

Actually, the crack pattern in members subject to cyclic or long term loads never can be considered completely stabilized owing to the redistribution of bond stresses. Above distinction between crack formation and stabilized cracking phases is, however, helpful for the discussions.

(4.1) Crack formation phase

Initial cracks form when the tensile strength of concrete is exceeded at *weak sections*, which are distributed randomly. At the cracks the concrete is free from stress, and the reinforcement carries the tensile load. However, tensile stress is present in the concrete between the cracks because tension is transmitted from the steel to the concrete by bond. The magnitude and distribution of bond stresses between cracks determine the distribution of tensile stresses in the steel and the concrete. Slip occurs between the steel and the concrete and reaches its maximum at the cracks.

At the *crack formation phase* (Fig. 4.3-4 a), a portion of the element between cracks exists over which steel and concrete strains are equal, i.e., slips and bond stresses are not produced. Where the bond stress starts to develop (this section is considered to be the origin of the local co-ordinate system x=0), *both the slip (s_0) and its first derivative (s_0') are equal to zero* (Fig.4.3-4 a (F) and (G)):

$$s_0 = 0 \tag{4.3-2 a}$$

$$s'_0 = \varepsilon_{s0} - \varepsilon_{c0} = 0 \qquad\qquad (4.3\text{-}2\ b)$$

In the crack formation phase, the crack spacing is greater than twice the transmission length (ℓ_t) that is required to transmit the tensile force from the steel to the concrete. The crack affects the stresses only within a distance of ($\pm\ell_t$) measured from the crack. The minimum distance to the next crack is ℓ_t (since the crack has reduced the concrete stress below its tensile strength within a distance of $\pm\ell_t$). The next crack forms outside this region. If cracks are produced at a distance greater than $2\ell_t$, another crack may form in an intermediate section.

Fig. 4.3-4   Investigated member (A), force (B), stress (C-D), strain (E), slip (F-G) and bond stress (H) distributions between two cracks [Balázs (1993)]
a) Crack formation phase   b) Stabilized cracking phase

(4.2)   Stabilized cracking phase

The crack pattern is theoretically fully developed if all the crack spacings vary between ℓ_t and $2\ell_t$ (Fig. 4.3-4 b). This phase is referred to as *stabilized cracking phase*.

The steel stress reaches its minimum where the slip is zero and the bond stress changes its sign. This point is approximately half-way between the cracks, but it may be shifted if a new crack forms close to ℓ_t, measured from the previous crack [Windisch (1982)]. Even if *the slip is equal to zero at the point of minimum steel stress, the first derivative of slip* (i.e., the difference in steel and concrete strains) will not remain zero (Fig. 4.3-4 b (F) and (G)):

$$s_0 = 0 \tag{4.3-3 a}$$

$$s_0' = \varepsilon_{s0} - \varepsilon_{c0} > 0 \tag{4.3-3 b}$$

Eq. (4.3-3 b) results in a slope of the bond stress distribution which is different from zero at the section of zero slip (Fig. 4.3-4 b (E)).

(5)   **Contribution of tensioned concrete between cracks**

In a cracked concrete cross section, all tensile forces are resisted by the steel. Between adjacent cracks, however, tensile forces are transmitted from the steel to the surrounding concrete by bond stresses. Watstein and Mathey (1959) have already noted in 1959 that concrete between cracks contributes to carrying tensile loads. The contribution of concrete between cracks may be considered to increase the stiffness of the tensile reinforcement. Therefore, this effect is known as **tension stiffening** effect. Tension stiffening is, however, a direct result of bond between tensioned steel bar and tensioned concrete, nevertheless, it is automatically considered in our models if a realistic bond-slip law is used. Otherwise, the application of a tension stiffening relationship helps to indirectly consider the bond behaviour and is needed if our model does not go back to the bond slip law. Further details on tension stiffening are given in Chapter 3.3.3.

The reinforcement controls crack widths only within a small area around the bars. This area is defined as the *effective concrete area in tension*, $A_{c,ef}$. In flexural members, a general approach is to take an area of concrete surrounding the main steel and having the same centroid as the steel as $A_{c,ef}$. The steel ratio becomes 2.5 to 4 times greater than the tensioned steel ratio by relating the tensioned steel area to the effective concrete are in tension ($\rho_{s,ef} = A_s / A_{c,ef}$), where $A_{c,ef} = b \cdot h_{ef}$ with $h_{ef} = 2.5$ (h-d)) [Noakowski (1985)]. MC90 limits h_{ef} to (h-x_2)/3.

(6)   **Definition of crack spacing**

Crack spacing means the distance of adjecent cracks in the investigated region. The minimum and maximum crack spacings are considered to be:

$$s_{r,min} = \ell_t \qquad \text{and} \qquad s_{r,max} = 2\ell_t$$

respectively (see Sections (4.1) and (4.2) above). Since ℓ_t means the length that is required to transmit the tensile force from the steel to the concrete (fulfilled by an equilibrium equation), ℓ_t hence s_r in general is a function of the concrete tensile strength, bond stress distribution, bar diameter, steel cross section and effective concrete area in tension (or directly the steel ratio: $\rho_{s,ef} = A_s / A_{c,ef}$. (Further details are given in Section (7.1) of this Chapter).

(7) Approaches to crack control

Crack control in concrete members can be reached either by applying calculation procedures (see Chapters (7.1) and (7.2) here), or by fulfilling appropriate practical rules (see Chapter (7.4) here). Calculation procedures are always required if serviceability limit states provide the governing design conditions, however, in some cases practical rules are satisfactory for a fast verification of crack control.

(7.1) Analytical procedures for crack control in reinforced concrete members

Crack control is reached by using mechanical models for predicting the characteristic crack width (w_k) and comparing it to the crack width limit (w_{lim}) taking into consideration the exposure conditions (w_{lim} is indicated in Section (2) of this Chapter):

$$w_k \leq w_{lim} \tag{4.3-4}$$

Crack width calculations were always a matter of interest. There are almost 60 formulas developed all over the world. The following small list of references intends to give guidance for those who wish to study cracking in more details: Saliger (1936), Rüsch and Rehm (1957a, b), Watstein and Mathey (1959), Kaar and Mattock (1963), Kaar and Hognestad (1965), Broms (1965), Broms and Lutz (1965), Base, Read, Beeby and Taylor (1966), Ferry-Borges (1966), Gergely and Lutz (1968), Rehm and Martin (1968), Holmberg (1970, 1973), Guschcha (1971), Edwards and Picard (1972), Venkateswarlu and Gesund (1972), MC78, Beeby (1979), Martin, Schießl, and Schwarzkopf (1980), CEB (1981), Windisch (1982), CEB (1984), Krips (1985), Noakowski (1985), ACI Com 224 (1986, 1989), Janovic (1986), Schießl and Wölfel (1986), Oh and Kang (1987), Schießl (1989), Yannopoulos (1989), MC90, Balázs (1993), Wicke (1993) and König and Tue (1996).

Semi analytical approaches to determine w_k are based on the *mathematical model of force transfer* (from steel bar to concrete) and apply measured or supposed bond stress - slip (τ_b-s) relationships. The analysis is generally carried out on a concentrically loaded tensile specimen to simulate conditions in the constant moment region of a beam between tensile cracks. In this way the curvatures of the element are neglected and a constant tensile stress distribution is assumed, having a resultant at the centroid of steel bars. If a beam is sufficiently deep, conditions near the bottom of the tension zone approach pure tension.

(7.1.1)   Assumptions

The following assumptions are considered in developing the mathematical model:

1. Except at cracks, concrete participates in resisting the load (i.e., bond stresses are produced);

2. Slips arise due to the strain differences of steel and concrete. Slips produce bond stresses. The bond stress - slip relationship is an interface property that is supposed to be valid along the bar (i.e., $\tau_{bx}(s)=\tau_b(s)$);

3. Bond stress reaches zero where $\varepsilon_s=\varepsilon_c$ (for initial crack formation phase), or halfway between cracks (for stabilized cracking phase);

4. The width at the surface of reinforcement is equal to the difference between the elongation of steel and that of concrete (i.e., the sum of slips from either sides);

5. Micro-cracking and micro-crushing may develop in front of the bar lugs in the concrete. (This produces nonlinearity of the bond stress - slip relationship.);

6. There is no splitting crack along the bars.

7. The resultant of the steel stresses and that of the concrete tensile stresses coincide.

(7.1.2)   Physical laws

Steel and concrete follow Hooke' s law (Fig.4.3-5).

A separate physical law is applied not only for the materials but also for their interaction (see Fig.4.3-5). Even if linear elastic physical laws are considered both for steel and concrete, the mathematical model becomes nonlinear if a nonlinear bond stress - slip relationship is used. *Bond stress - slip relationships* (called bond stress - slip laws if used for modelling) are discussed in Chapter 3.3.2. Here we give only details that are necessary to understand cracking.
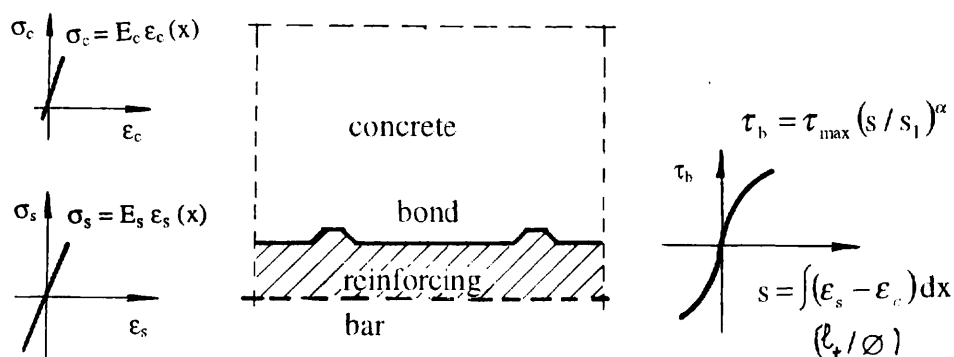
Fig. 4.3-5 Physical laws and bond - slip law considered in the model

It has been experimentally shown [Rehm (1961)] that the bond stress (τ_b) is a basic function of the relative displacement (s) of steel to concrete: $(\tau_b=f(s))$. Although there were attempts to develop it theoretically, the available τ_b-s relationships are obtained from pull-out tests or beam tests showing a nonlinear behaviour for deformed bars.

The τ_b-s relationship has a very important role in analysing cracking (as well as anchorage and transmission lengths). The type of the differential equation (used as mathematical model – see eq. (4.3-11) below) is governed by the τ_b-s relationship providing linearity or nonlinearity, homogeneity or inhomogeneity, etc. of the equation. Therefore, different approaches of the τ_b-s relationship are available: *constant* [König and Fehling (1988)], *linear* [Lutz and Gergely (1967), Ngo and Scordelis (1967), Edwards and Picard (1972), Tepfers (1973)], *bilinear* [Giuriani (1982)] or various *nonlinear* [Nilson (1968), Noakowski (1985), Krips (1985), Ciampi, Eligehausen, Bertero and Popov (1982), Balázs (1987)]. Most of the codes use the simplest constant approach giving a τ_b value independently on the slip which is often expressed as a function of the concrete tensile strength:

$$\tau_b = k \ f_{ctm} \qquad \text{where} \qquad 1 \le k \le 2 \qquad (4.3\text{-}5)$$

This approach was earlier reasonable for plain reinforcing bars but is rather inaccurate for deformed bars. MC90 adopted a nonlinear approach which was first proposed by Ciampi, Eligehausen, Bertero and Popov (1982) as a power function (Fig. 4.3-5):

$$\tau_b = \tau_{max} \left(\frac{s}{s_1} \right)^\alpha \qquad (4.3\text{-}6)$$

where τ_{max} is the bond strength (equal to $2.5\sqrt{f_{ck}}$ or $2.0\sqrt{f_{ck}}$ N/mm² for confined or for unconfined concrete), s_1 is the slip corresponding to the bond strength (equal to 1.0 or 0.6 mm for confined or for unconfined concrete) and $0 \le \alpha \le 1$ being generally 0.4.

(7.1.3)   Equilibrium conditions
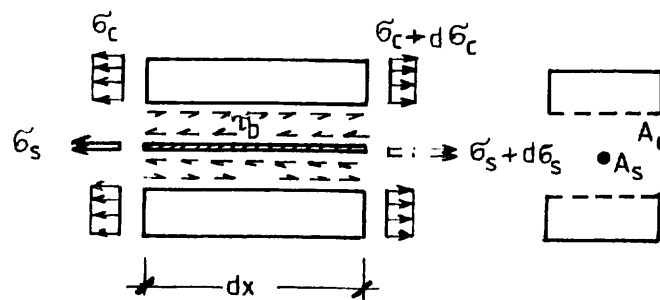
Fig. 4.3-6 Local equilibrium of a short element

Local equilibrium means that the force transmitted over a dx-element is equal to the change of the force in the steel or in the concrete (Fig. 4.3-6):

$$\tau_{bx}\varnothing\pi dx = d\sigma_{sx}A_s \qquad \text{or} \qquad \tau_{bx}\varnothing\pi dx = d\sigma_{cx}A_c \qquad (4.3\text{-}7)$$

Global equilibrium requires that (see Fig. 4.3-4 (B)):

$$F_{sx} + F_{cx} = F_{s2} \qquad (4.3\text{-}8)$$

(7.1.4)   Compatibility conditions

Due to the relative displacements between steel and concrete sections, compatibility means that the local change of slip is equal to the difference in strains (see Fig. 4.3-4 (F)):

$$s_x' = \varepsilon_{sx} - \varepsilon_{cx}$$ (4.3-9)

Slip is obtained by taking its integral and meaning the difference between the absolute displacements of the steel and concrete sections (see Fig. 4.3-4 (G)):

$$s_x = u_{sx} - u_{cx}$$ (4.3-10)

The differential equation of the slipping contact is obtained by combining the compatibility and equilibrium equations, concerning the physical laws and substituting the bond stress - slip law (in this case) in form of eq. (4.3-6):

$$s_x'' - \frac{4(1+\alpha_e \rho_{s.ef})}{\varnothing E_s} \frac{\tau_{max}}{s_1^\alpha} s_x^\alpha = 0$$ (4.3-11)

This is a second-order ordinary differential equation. The advantage of a bond stress - slip law like eq. (4.3-6) that it has an infinite tangent at the origin of the τ_b-s co-ordinate system which provides the possibility to solve the mathematical model in closed form (at least for the crack formation phase).

(7.1.5)   Solutions for the crack formation phase

Considering homogeneous initial values given by eq. (4.3-2), eq. (4.3-11) can be solved by multiplying both sides by 2s', then separating the variables. Following two integrations, the *slip distribution* is (Fig. 4.3-4 a (G):

$$s_x = \left(\frac{2(1-\alpha)^2 (1+\alpha_e \rho_{s.ef})\tau_{max}}{(1+\alpha)E_s} \frac{x^2}{s_1^\alpha \varnothing} \right)^{\frac{1}{1-\alpha}}$$ (4.3-12)

The bond stress distribution can be obtained by substituting eq. (4.3-12) into eq. (4.3-6) (Fig. 4.3-4 a (H)).

$$\tau_b(x) = \tau_{max}\left(\frac{s(x)}{s_1} \right)^\alpha$$

This bond stress distribution gives its maximum value at the cracked section which is a consequence of the *second assumption* considered to develop the model (see above) and that of the bond stress - slip relationship (eq. (4.3-6)) which has an increasing tendency up to s_1. In many interpretations $\tau_b(x)$ is defined to have a zero value at the cracked section (see Fig. 4.3-4 (H)) and reaches its maximum in the close vicinity of the crack.

The steel stress distribution is be obtained from the equilibrium equation (see Fig. 4.3-4 a (C)):

$$\sigma_{sx} = \sigma_{sl} + K\left(\frac{x^{(1+\alpha)}}{s_1^\alpha \varnothing}\right)^{\frac{1}{1-\alpha}}, \quad K = \tau_{max}\frac{4(1-\alpha)}{1+\alpha}\left[\frac{2(1-\alpha)^2(1+\alpha_e\rho_{s,ef})\tau_{max}}{(1+\alpha)E_s}\right]^{\frac{\alpha}{1-\alpha}} \quad (4.3\text{-}13)$$

where σ_{sl} is the steel stress over the portion where $\varepsilon_s = \varepsilon_c$. The inverse of eq. (4.3.13) gives *the length over which the steel stress σ_{s2} can be transferred to the concrete* (see Fig. 4.3-4 a (A)):

$$\ell_t = \left[\frac{(s_1^\alpha \varnothing)^{1/(1-\alpha)}}{1+\alpha_e\rho_{s,ef}}\frac{\sigma_{s2}}{K}\right]^{\frac{1-\alpha}{1+\alpha}} \quad \text{[mm]} \quad (4.3\text{-}14)$$

The crack width at the bar surface for initial crack formation is obtained by substituting eq. (4.3-13) into eq. (4.3-12) when $x=\ell_t$, hence $\sigma_{sx}=\sigma_{s2}$ (see Fig. 4.3-4 a (G)):

$$w = 2\left[\frac{(1+\alpha)s_1^\alpha\varnothing}{8(1+\alpha_e\rho_{s,ef})}\frac{\sigma_{s2}^2}{\tau_{max}E_s}\right]^{\frac{1}{1+\alpha}} \quad \text{[mm]} \quad (4.3\text{-}15)$$

The parameters indicate that the crack width is a function of the steel stress at the crack, the bar diameter, the bond properties (τ_{max}, s_1, α), the moduli of elasticity and the effective steel ratio. Steel stress has a major importance owing to its highest power. Substituting $\alpha = 0.4$, the power of the steel stress in eq. (4.3-15) is $2/(1+\alpha) = 1.43$.

(7.1.6)   Examples for the crack formation phase

The obtained formulas are suitable for:

- cracking analysis of a single crack or some distant crack that do not interact (e.g. cracks of a reinforced concrete member subject to low load, analysis of a spalling crack in the web of a prestressed concrete member or opening of a preformed crack transverse to the reinforcement), and
- anchorage analysis of reinforcing bars having zero slip at the unloaded end of the anchorage length or transmission analysis of pretensioned tendons.

Examples for crack widths and development lengths using eqs. (4.3-15) and (4.3-14) are presented in Fig.4.3-7 a as a function of the steel stress and concrete grade and in Fig. 4.3-7 b as a function of the steel stress and the bar diameter.

(7.1.7)   Solutions for stabilized cracking phase

The number of cracks is stabilized if the distance between cracks is too close to develop the tensile strength of concrete again. As indicated in Fig. 4.3-4 b (E) to (G) the slip remains equal

to zero, however, the first derivative of slip becomes different from zero at the point of minimum steel stress providing initital values to the differential equation. From mathematical point of view, the modification of boundary conditions makes it impossible to solve the differential equation in a closed form; otherwise various numerical methods are available for the solution.

$$\tau_b = 2.5\sqrt{f_{ck}}\,(s/s_1)^\alpha \qquad s_1 = 1.0\ \text{mm} \ ; \ \alpha = 0.4$$
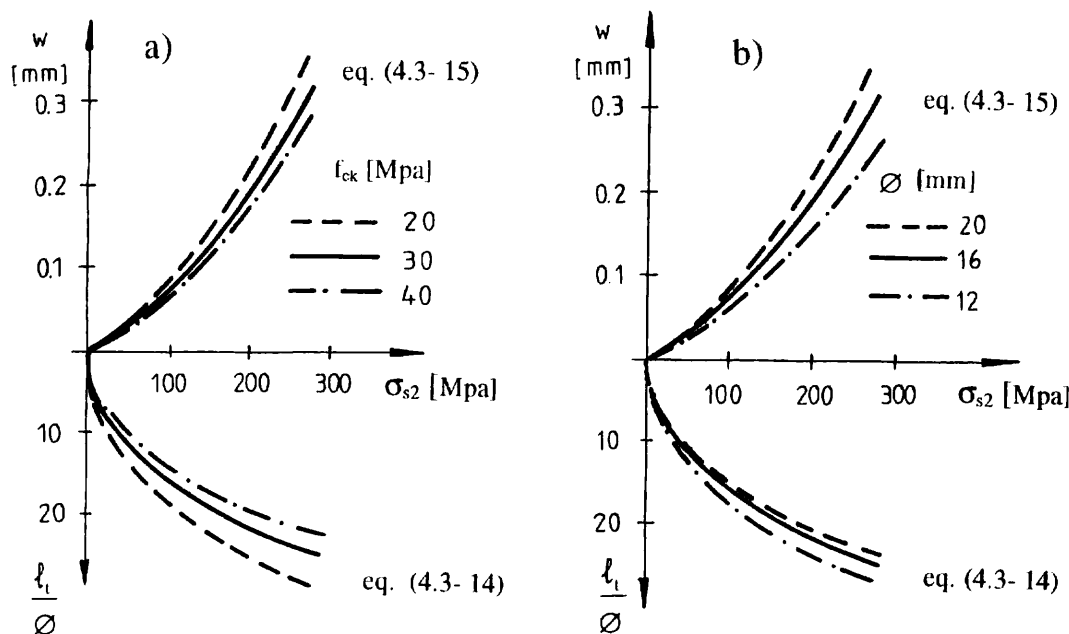
Fig. 4.3-7 Crack widths and development lengths in the phase of crack formation [Balázs (1993)]

  a) as a function of the steel stress and the concrete grade
  b) as a function of the steel stress and the bar diameter

(7.1.8)   Examples for stabilized cracking phase

Crack width as function of steel stress at crack, crack spacing and concrete grade is presented in Fig. 4.3-8 using the fourth order Runge-Kutta method to solve the mathematical model. Calculated results indicate an almost linear relationship over the 150 to 350 N/mm^2 steel stress range. (The same conclusion was experimentally obtained by Yannopoulos (1989)). Fig. 4.3-8 indicates that the smaller the crack spacing and the higher the concrete grade, the smaller the crack width.

The influence of bond capacity on the crack width is indicated in Fig. 4.3-9. Assuming $\tau_{max} = 3.5\sqrt{f_{ck}}$ improved bond strength rather than $\tau_{max} = 2.5\sqrt{f_{ck}}$ a quicker increase of steel stress is induced toward the cracks.

(7.1.9)   MC90 approach

MC90 cracking philosophy is to predict the **characteristic crack width** both for crack formation and stabilized cracking phases as a multiple of the maximum length over which slip

Bond stress- slip relationship:

$$\tau_b = 2.5\sqrt{f_{ck}(\frac{s}{s_1})^\alpha}$$

$s_1 = 1.0 \, mm$ $\alpha = 0.4$

Fig. 4.3-8   *Calculated crack widths in stabilized cracking phase as a function of the steel stress, the crack spacing and the concrete grade [Balázs (1993)]*

$$\tau_b = 2.5\sqrt{f_{ck}}(s/s_1)^\alpha \qquad \alpha = 0.4$$
$$\tau_b = 3.5\sqrt{f_{ck}}(s/s_1)^\alpha \qquad s_1 = 1.0 \, mm$$

Fig. 4.3-9   *Effect of bond strength (τ_{max}) on force transfer between adjecent cracks [Balázs (1993)]*
(Applied parameters: $f_{ck}=20 \, N/mm^2$, $s_r=10\emptyset$, $s_0=0$, $s'_0=0.01$)
     a) Bond stress distribution   *b) steel stress distribution*

occurs to one crack ($\ell_{s,max}$) (see Fig. 4.3-10) and the average steel strain (ε_{sm}) reduced by the average concrete tensile strain (ε_{cm}) and the concrete shrinkage strain (ε_{cs}):

$$w_k = \ell_{s,max} (\varepsilon_{sm} - \varepsilon_{cm} - \varepsilon_{cs})$$ (4.3-16)

Eq. (4.3-17) assumes evenly distributed bond stresses between two cracks. Maximum crack spacing in eq. (4.3-16) is expressed by MC90 as:

$$\ell_{s,max} = 2 \frac{\sigma_{s2} - \sigma_{sE}}{4\tau_{bk}} \oslash$$ (4.3-17)

which can be considered as:

$$\ell_{s,max} = \frac{\sigma_{s2}}{2\tau_{bk}} \oslash \frac{1}{(1 + \alpha_e \rho_{s,ef})}$$ for crack formation phase and (4.3-17 a)

$$= \frac{\oslash}{3.6\rho_{s,ef}}$$ for stabilized cracking phase (4.3-17 b)

where

σ_{s2} is the steel stress at crack

σ_{sE} is the steel stress at the point of zero slip

α_e $= E_s / E_c$ is the modular ratio

$\rho_{s,ef}$ $= A_s / A_{c,ef}$ is the effective reinforcement ratio and

τ_{bk} is the lower fractile of the average bond stress that can be assumed for high bond bars according to Table 4.3-2

$\oslash$ is the nominal diameter of the reinforcing bar or the equivalent diameter of the bundled bars.

Type of loading	Single crack formation		Stabilized crack formation	
	β	τ_{bk}	β	τ_{bk}
Short term loading	0.6	$1.8 f_{ctm}(t)$	0.6	$1.8 f_{ctm}(t)$
Long term or re-peateded loading	0.6	$1.35 f_{ctm}(t)$	0.38	$1.8 f_{ctm}(t)$

Table 4.3-2 τ_{bk} and β values to determine the maximum crack spacing (MC90)
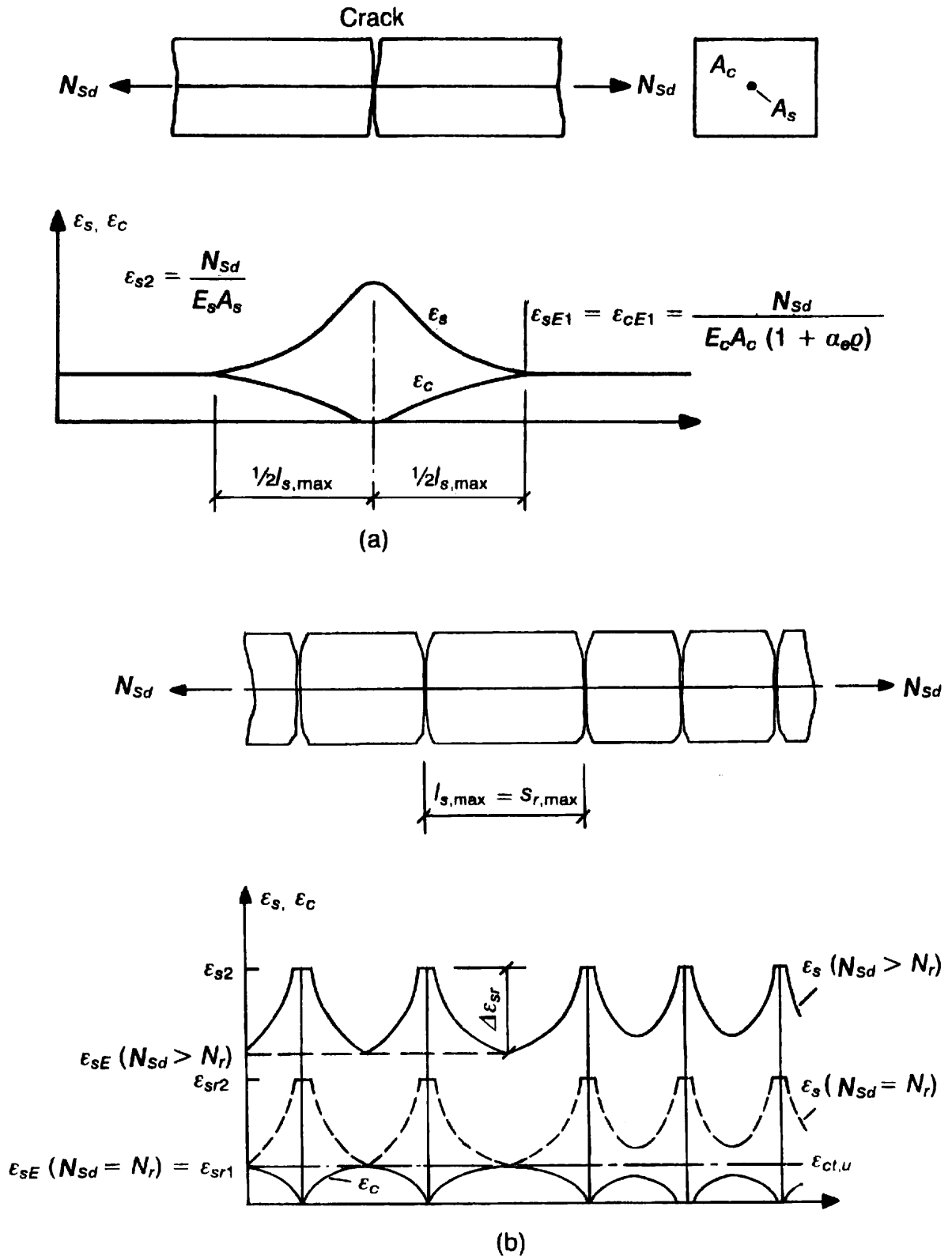
Fig. 4.3-10 Strain distributions to calculate the crack spacing and the average strains according to MC90
     a) Crack formation phase   *b) Stabilized cracking phase*

As indicated in Fig. 4.3-10, $\ell_{s,max}$ is the overall slip length where steel and concrete strains contribute to the width of a crack from either side of the crack. For stabilized cracking $\ell_{s,max} = s_{r,max}$. For stabilized cracking the average crack width may be estimated on the basis of an average crack spacing: $s_{rm} \approx \dfrac{2}{3}\ell_{s,max}$.

The difference of the average steel and concrete strains can be expressed as (Fig. 4.3-10):

$$\varepsilon_{sm} - \varepsilon_{cm} = (\varepsilon_{s2} - \beta\Delta\varepsilon_{sr}) - \beta\varepsilon_{sr1} = (\varepsilon_{s2} - \beta(\varepsilon_{sr2} - \varepsilon_{sr1})) - \beta\varepsilon_{sr1} = \varepsilon_{s2} - \beta\varepsilon_{sr2} \qquad (4.3\text{-}18)$$

where

$$\varepsilon_{sr2} = \frac{f_{ctm}(t)}{\rho_{s,ef}E_s}(1 + \alpha_e\rho_{s,ef})$$

$$\Delta\varepsilon_{sr} = \varepsilon_{sr2} - \varepsilon_{sr1}$$

ε_{s2}	is the steel strain at the crack
ε_{sr2}	is the steel strain at the crack, under forces causing $f_{ctm}(t)$ within $A_{c,ef}$
ε_{sr1}	is the steel strain at the point of zero slip under cracking forces reaching $f_{ctm}(t)$
$f_{ctm}(t)$	is the mean value of the concrete tensile strength at the time t when the crack appeared
β	is an integration factor for the strain distribution (see Table 4.3-2)

The cross-section of tensile reinforcement required for crack control can be calculated by:

$$A_s = \sqrt{\frac{\varnothing F_{cr}(F_s - \beta F_{cr})}{2E_s w_k \tau_{bk}(1 + \alpha_e\rho_{s,ef})}} \qquad (4.3\text{-}19)$$

where

F_s	is the force in the concrete transmitted by the reinforcement
F_{cr}	indicates the force to be introduced into concrete by bond
$F_{cr} = F_s$	for crack formation phase
$F_{cr} = (1 + \alpha_e\rho_{s,ef})A_{c,ef}f_{ctm}$	for stabilized cracking phase.

In contrary to MC90, *the philosophy of EC2* for crack widths (which was adopted from MC78) is to calculate first the average crack width (w_m) as a product of the average crack spacing (s_{rm}) and the average steel strain (ε_{sm}) and multiplying it by a factor of 1.7 (which intends to take into account the stochastic character of the crack width) to get the characteristic value of crack width.

(7.2) Cracking in two dimensional reinforced concrete members

When in an orthogonally reinforced two dimensional member cracks are expected to form inclined to the reinforcement, the following expression may be used to calculate crack spacing:

$$\ell_{s,max} = \left(\frac{\cos\theta}{\ell_{sx,max}} + \frac{\sin\theta}{\ell_{sy,max}} \right)$$

(7.3)   Analytical procedures for crack control in prestressed concrete members

Calculation of crack widths in prestressed pretensioned concrete members generally follows the procedure given in Section (7.1) of this Chapter. In case of full prestressing $\Delta\sigma_p$ (tendon stress above decompression) has to be considered as steel stress.

When prestressed and non-prestressed reinforcements are simultaneously used in a member (partially prestressed members) both equilibrium and compatibility conditions are to be considered. The total tensile force above decompression is:

$$\Delta F_{s+p} = A_s \sigma_{s2} + A_p \Delta\sigma_p \qquad\qquad (4.3\text{-}20)$$

Compatibility requires

$$w_{sk} = w_{pk}$$

hence

$$0.5\ell_{s,max}\sigma_{s2} = 0.5\ell_{p,max}\Delta\sigma_p \qquad\qquad (4.3\text{-}21)$$

For single crack formation different transmission lengths for reinforcing (ℓ_s) and for prestressing (ℓ_p) steels are obtained from eqs. (4.3-17 a and b) considering $1 + \alpha_e \rho_{s,ef} \approx 1$:

$$\ell_{s,max} = \frac{\varnothing}{2\tau_{bs,k}}\sigma_{s2} \qquad\text{and}\qquad \ell_{p,max} = \frac{\varnothing_p}{2\tau_{bp,k}}\Delta\sigma_p$$

Substituting these equations into eq. (4.3-21):

$$\Delta\sigma_p = \sqrt{\frac{\tau_{bp,k}\varnothing}{\tau_{bs,k}\varnothing_p}}\sigma_{s2} = \sqrt{\xi_1}\,\sigma_{s2} \qquad\text{where}\qquad \xi_1 = \frac{\tau_{bp,k}\varnothing}{\tau_{bs,k}\varnothing_p}$$

and

$\tau_{bp,k} / \tau_{bs,k}$	$= 0.20$	for prestressing wires
	$= 0.40$	for indented wires and strands
	$= 0.60$	for ribbed prestressing bars

By substituting $\Delta\sigma_p$ into the equilibrium condition (4.3-20) and expressing σ_{s2}, the equivalent steel stress in the reinforcing steel at the crack, calculated on the basis of different bond characteristics for reinforcing bars and prestressing tendons:

$$\sigma_{s2} = \frac{\Delta F_{s+p}}{A_s + \sqrt{\xi_1} A_p}$$

(7.4) Practical rules for crack control

By applying practical rules, crack control is indirectly reached by controlling parameters other than crack width. *Crack widths are not calculated in these cases.*

(7.4.1) Limits for concrete tensile stresses

Crack control is reached by controlling concrete tensile stresses (σ_{ct}) which is calculated considering *all actions, loads and imposed or restrained deformations*:

a) $\sigma_{ct} \le 0$ - the whole section is compressed (e.g. prestressed) or at least

b) $\sigma_{ct} \le f_{ctk,min}$

Point b) is not considered to be a good measure for crack control owing to the uncertainties both in σ_{ct} and in $f_{ctk,min}$.

(7.4.2) Limits for reinforcing bar diameter or bar spacing

Crack control may be reached by choosing bar diameters ($\varnothing_{max}$) or bar spacings (s_{max}) not greater than the following limiting values:

a) $\varnothing_{max} = f(\sigma_{s2})$ - $\varnothing_{max}$ values are given in Table 4.3.3

b) $s_{max} = f(\sigma_{s2})$ - s_{max} values are given in Table 4.3.3

Steel stresses (σ_{s2}) in Table 4.3-3 are calculated under quasi-permanent loads (for reinforced members) or under frequent loads and characteristic value of prestress (for prestressed members).

$\varnothing_{max}$ and s_{max} values are calculated considering typical bond conditions for deformed bars in addition to:

0.3 mm   crack widths for reinforced members and
0.2 mm   crack widths for prestressed members, respectively.

Maximum bar diameters as well as maximum bar spacings according to MC90 are given in Table 4.3-3.

(8)   Long term and cycles dependent cracking

Repeated and long term loads may produce a significant increase of crack widths owing to an increase in concrete deformations, decrease in tension stiffening and increase in slip along the reinforcing bar resulting in a drop of neutral axis and, consequently, an increase of steel

Steel stress, σ_{s2} [N/mm^2]	For reinforced concrete sections		For prestressed concrete sections	
	$\varnothing_{max}$	s_{max}	$\varnothing_{max}$	s_{max}
160	32	300	25	200
200	25	250	16	150
240	20	200	12	100
280	14	150	8	50
320	10	100	6	-
360	8	60	5	-
400	6	-	4	-
450	5	-	-	-

Table 4.3-3　Maximum bar diameters ($\varnothing_{max}$) and maximum bar spacings s_{max} (both given in mm) for which no calculation of crack width is required according to MC90

stress in the cracks and an increase in curvature [CEB (1997)]. Typical examples by Lovegrove and Din (1982) for the development of the maximum crack width in a beam subjected to repeated loading are presented in Fig. 4.3-11 a. Measurements on strain redistribution under long term loading by test results of Stevens (1972) are shown in Fig. 4.3-11 b which also indicates the drop of neutral axis and increase of steel strain.

Crack widths increase with the number of load cycles or the time elapsed under long term loads and may even exceed the double of the initial value of the crack width. Crack widths at unloading have also an increasing tendency. Several parameters have an influence on the increase of crack widths such as: *load history, load level, steel ratio, rib pattern and size of reinforcing bars, concrete strength and state of cracking by applying the repeated or long term loads, etc.* Repeated loads produce a faster increase in crack widths compared to long term loads on the same level and time interval.

With increasing number of load cycles or increasing time under long term loads tension stiffening decreases and yields to an increase in the average steel strain and increase of crack widths together with a decrease in the overall stiffness. The smaller the relative rib area of the reinforcing bar, the faster the increase of the average steel strain. Influence of repeated load on the average steel strain decreases with increasing steel ratio.

The ratio of the characteristic crack width after long term or repeated loading ($w_{k,n,t}$) to its initial value (w_k) according to MC90 is:

$$\frac{w_{k,n,t}}{w_k} = \frac{\varepsilon_{s2} - 0.38\varepsilon_{sr2} - \varepsilon_{cs}}{\varepsilon_{s2} - 0.60\varepsilon_{sr2} - \varepsilon_{cs}}$$

The $w_{k,n,t}$ to w_k ratio according to EC2 and MC78 for high bond bars is:

$$\frac{W_{k,n,t}}{W_k} = \frac{1 - 0.5\left(\dfrac{\sigma_{sr}}{\sigma_{s2}}\right)^2}{1 - \left(\dfrac{\sigma_{sr}}{\sigma_{s2}}\right)^2}$$

Cyclic creep strain of concrete is not accounted for in these equations. The crack spacing is assumed to be constant independently on the duration of load or the number of load

Maximum crack width [mm]
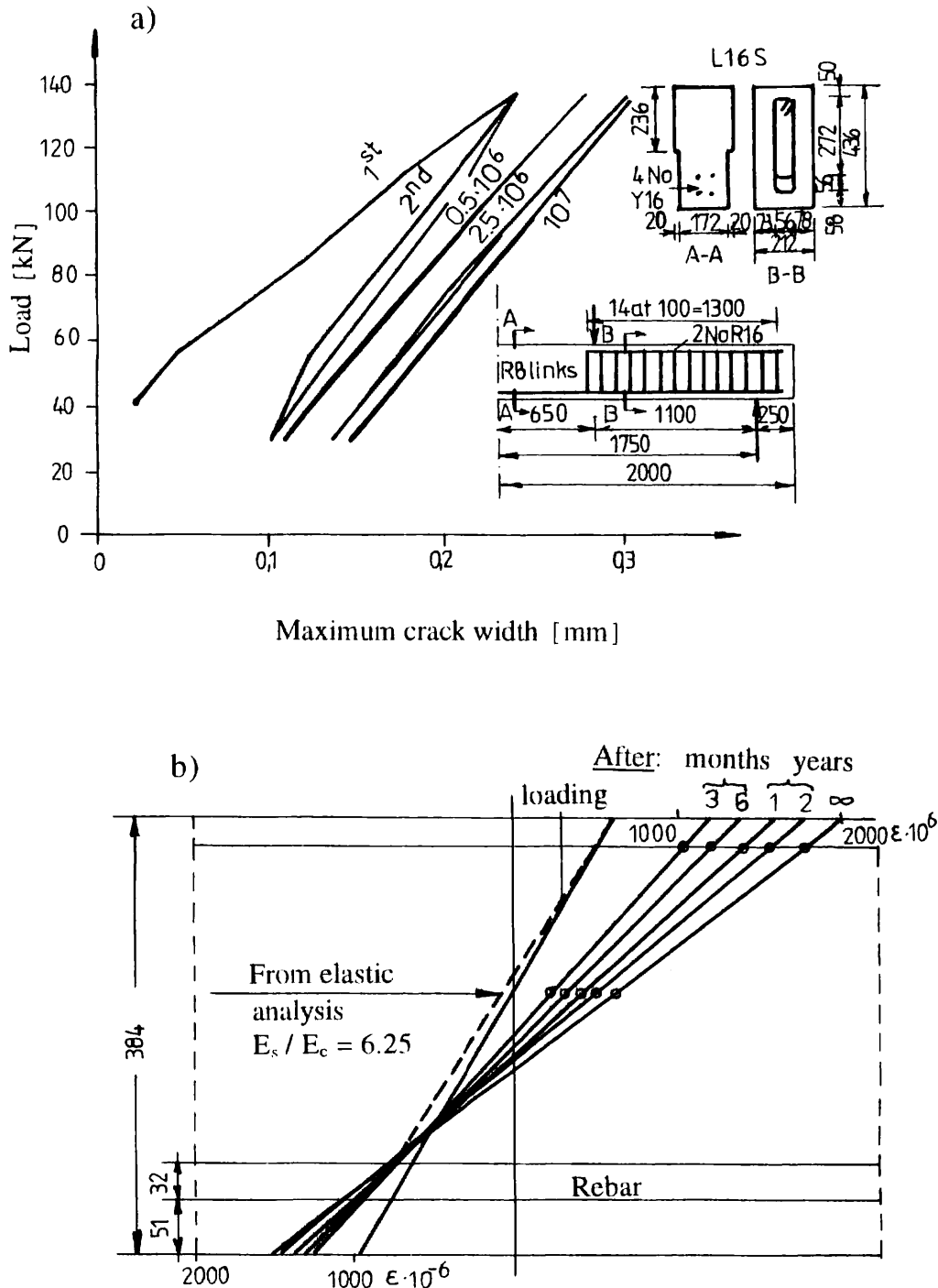
Fig. 4.3-11 Influence of repeated and long term loads on cracking

      a) Increase of max. crack width under repeated loading, Lovegrove and Din (1982)

      b) Modification of strain distribution under long term loads, Stevens (1972)

(9) Further examples

The following examples indicate the use of the MC90 procedure first for direct **(a)** and then for indirect **(b)** crak control. Material properties are considered according to MC90. The applied formulae are discussed above.

$$d = 600 \text{ mm} \qquad h = 650 \text{ mm}$$

2⌀14

4⌀22 $A_s = 1520.5 \text{ mm}^2$

$$b = 300 \text{ mm}$$

M_{Sd}
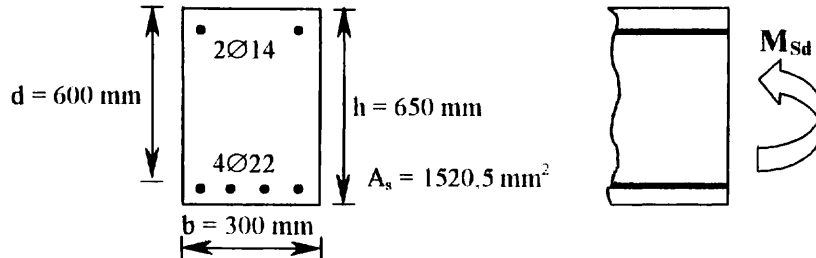
<u>Materials:</u>

● Steel: Grade 500

E_s $= 200000 \text{ N/mm}^2$ MC90 clause 2.2.4.3

● Concrete: C 30   MC90 clause 2.1.1.2

f_{ctm} $= 2,91 \text{ N/mm}^2$ MC90 eq. (2.1-4)

E_{ci} $= 33550 \text{ N/mm}^2$ MC90 eq. (2.1-15)

$E_{c,ef}(t,t_0) = E_{ci}/(1+\phi\,(t,t_0)) = 9261 \text{ N/mm}^2$ MC90 eq. (5.8-4)

$\phi(t,t_0)$ $= 2,54$ creep coefficient, interpolated from Table 2.1.10. of MC90 (considering $t_0 = 28$ days, $t = 70$ years, indoor conditions with

notional size $\dfrac{2A_c}{U} = 205,3 \text{ mm}$)

<u>Load:</u> M_{Sd} $= 160 \text{ kNm}$ (short term as well as long term)

(a) Calculation of crack widths

<u>Cross-sectional data:</u>

short term load:	**long term load:**
● Modular ratio: $\alpha_e = \dfrac{E_s}{E_{ci}} = \dfrac{200000}{33550} = 5,96$	$\alpha_e = \dfrac{E_s}{E_{c,ef}(t,t_0)} = \dfrac{200000}{9261} = 21,60$

● Uncracked section:

	short term	long term
Neutral axis:	$x_1 = 333,1 \text{ mm}$	$x_1 = 354,5 \text{ mm}$
Moment of inertia:	$I_2 = 2,18 \cdot 10^9 \text{ mm}^4$	$I_1 = 9,51 \cdot 10^9 \text{ mm}^4$

● Cracked section:

	short term	long term
Neutral axis:	$x_2 = 159,7 \text{ mm}$	$x_2 = 257,4 \text{ mm}$
Moment of inertia:	$I_1 = 7,54 \cdot 10^9 \text{ mm}^4$	$I_2 = 5,83 \cdot 10^9 \text{ mm}^4$

● Cracking moment: $M_r = 69,27 \text{ kNm}$ $M_r = 93,73 \text{ kNm}$

<u>Steel stress</u>

short term load:	**long term load:**
$\sigma_{s2} = \alpha_e \dfrac{M_{Sd}}{I_2}(d - x_2) = 192,41 \text{ N/mm}^2$	$= 202,99 \text{ N/mm}^2$

Effective tension area: $h_{ef} = 2,5(h-d) = 125$ mm $<$ $(h-x_2)/3 = 163,4$ mm

$$A_{c,ef} = 2,5(h-d) \, b = 37500 \text{ mm}^2$$

Cracking condition:

	short term load:	**long term load:**
$\rho_{s,ef} = \dfrac{A_s}{A_{c,ef}}$	$= \dfrac{1520,5}{37500} = 0,0405$	$= \dfrac{1520,5}{37500} = 0,0405$
$\alpha_e \cdot \rho_{s,ef}$	$= 5,96 \cdot 0,0405 = 0,242$	$= 21,60 \cdot 0,0405 = 0,876$
$1 + \alpha_e \cdot \rho_{s,ef}$	$= 1,242$	$= 1,876$
$\rho_{s,ef} \cdot \sigma_{s2}$	$= 0,0405 \cdot 192,41 =$	$= 0,0405 \cdot 202,99 =$
	$= 7,80 \text{ N / mm}^2$	$= 8,23 \text{ N / mm}^2$
$f_{ctm} \cdot (1 + \alpha_e \cdot \rho_{s,ef})$	$= 2,91 \cdot 1,242 =$	$= 2,91 \cdot 1,876 =$
	$= 3,62 \text{ N / mm}^2$	$= 5,46 \text{ N / mm}^2$
$\rho_{s,ef} \cdot \sigma_{s2} > f_{ctm} \cdot (1 + \alpha_e \cdot \rho_{s,ef})$	$\rightarrow$ ***stabilized cracking***	$\rightarrow$ ***stabilized cracking***

Calculation of crack width:

$$\bullet \, \ell_{s,max} = \frac{\varnothing}{3,6 \cdot \rho_{s,ef}} = \frac{22}{3,6 \cdot 0,0405} = 150,72 \text{ mm}$$

$$\bullet \, w_k = \ell_{s,max} \cdot (\varepsilon_{sm} - \varepsilon_{cm} - \varepsilon_{cs})$$

where:

$$\varepsilon_{sm} - \varepsilon_{cm} = \varepsilon_{s2} - \beta \cdot \varepsilon_{sr2}$$

	short term load:	**long term load:**
$\varepsilon_{s2} = \dfrac{\sigma_{s2}}{E_s}$	$= \dfrac{192,41}{200000} = 0,96 \cdot 10^{-3}$	$= \dfrac{202,99}{200000} = 1,01 \cdot 10^{-3}$
β	$= 0,6$	$= 0,38$
$\varepsilon_{sr2} = \dfrac{f_{ctm} \cdot (1 + \alpha_e \cdot \rho_{s,ef})}{\rho_{s,ef} \cdot E_s}$	$= \dfrac{2,91 \cdot 1,242}{0,0405 \cdot 200000} =$	$= \dfrac{2,91 \cdot 1,876}{0,0405 \cdot 200000} =$
	$= 0,45 \cdot 10^{-3}$	$= 0,67 \cdot 10^{-3}$
$\dfrac{2A_c}{U} = 205,3 \Rightarrow$	$\varepsilon_{cs} = -0,55 \cdot 10^{-3}$	$\varepsilon_{cs} = -0,55 \cdot 10^{-3}$
$(\varepsilon_{sm} - \varepsilon_{cm} - \varepsilon_{cs})$	$= 1,24 \cdot 10^{-3}$	$= 1,31 \cdot 10^{-3}$

$$w_k \quad = 150{,}72 \cdot 1{,}24 \cdot 10^{-3} = \qquad = 150{,}72 \cdot 1{,}31 \cdot 10^{-3} =$$
$$= \underline{0{,}19 \text{ mm}} \qquad\qquad = \underline{0{,}20 \text{ mm}}$$

$$w_k < w_{lim} = 0{,}3 \text{ mm} \qquad \text{O.K.}$$

The next diagram indicates characteristic crack width vs. bending moment relationships both for short term and long term loads. In stabilized cracking phase the crack width is higher for long term loads than for short term loads. The observed difference is often exceeded in the reality. The considerable difference between the two diagrams in the 70 to 120 kNm moment region is caused by the different crack phases (crack formation or stabilized cracking phases).

Bending moment, M_{Sd} [kNm]
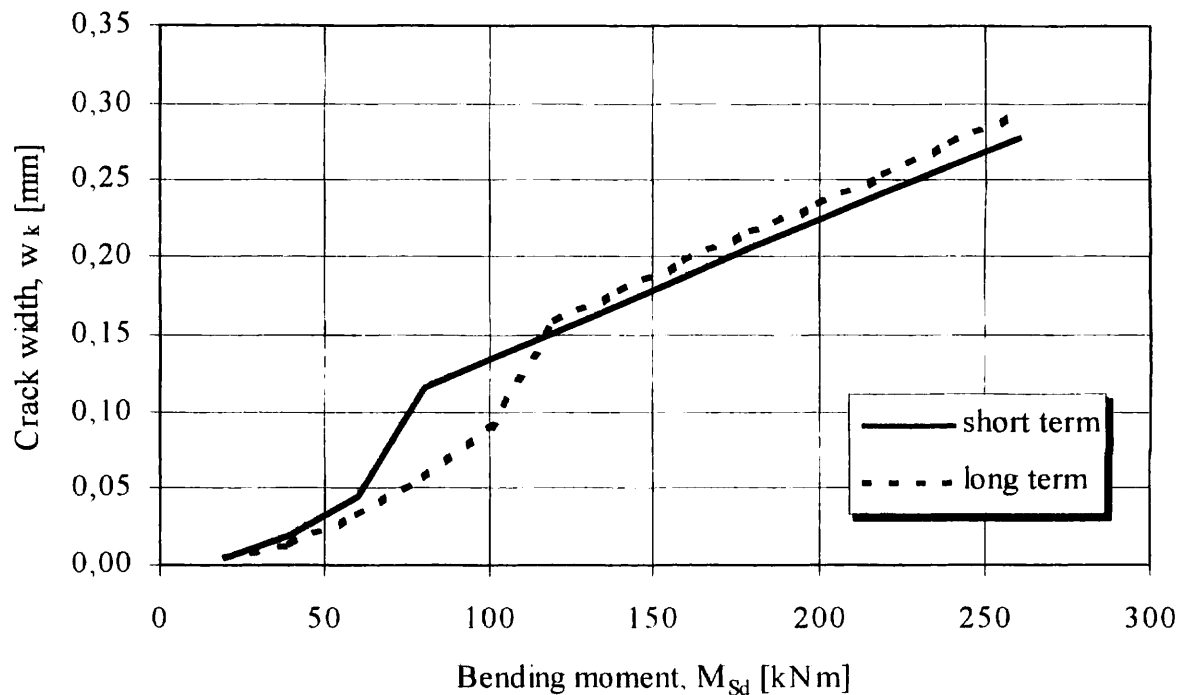
(b) Indirect crack control

$$A_{s,min} = \sqrt{\frac{\varnothing \cdot F_{cr} \cdot (F_s - \beta \cdot F_{cr})}{2 \cdot E_s \cdot w_k \cdot \tau_{bk} \cdot (1 + \alpha_e \cdot \rho_{s,ef})}}$$

	short term load:	long term load:
$F_{cr} = A_{c,ef} \cdot f_{ctm} \cdot (1 + \alpha_e \cdot \rho_{s,ef})$	= 135,6 kN	= 204,8 kN
$F_s = A_s \cdot \sigma_{s2}$	= 1520,5·192,41·10⁻³ =	= 1520,5 · 202,99·10⁻³ =
	= 292,5 kN	= 308,6 kN
β	= 0,6	= 0,38
w_k	= 0,3 mm	= 0,3 mm
$\tau_{bk} = 1{,}8 \cdot f_{ctm}$	= 1,8·2,91 = 5,24 N/mm²	= 1,8·2,91 = 5,24 N/mm²
$A_{s,min}$	= $\underline{898{,}1 \text{ mm}^2}$	= $\underline{938{,}9 \text{ mm}^2}$

$$A_{s,min} < A_s = 1520{,}5 \text{ mm}^2 \qquad \text{O.K.}$$

The next diagram indicates characteristic crack widths vs. bending moment relationships both for short term and long term loads.
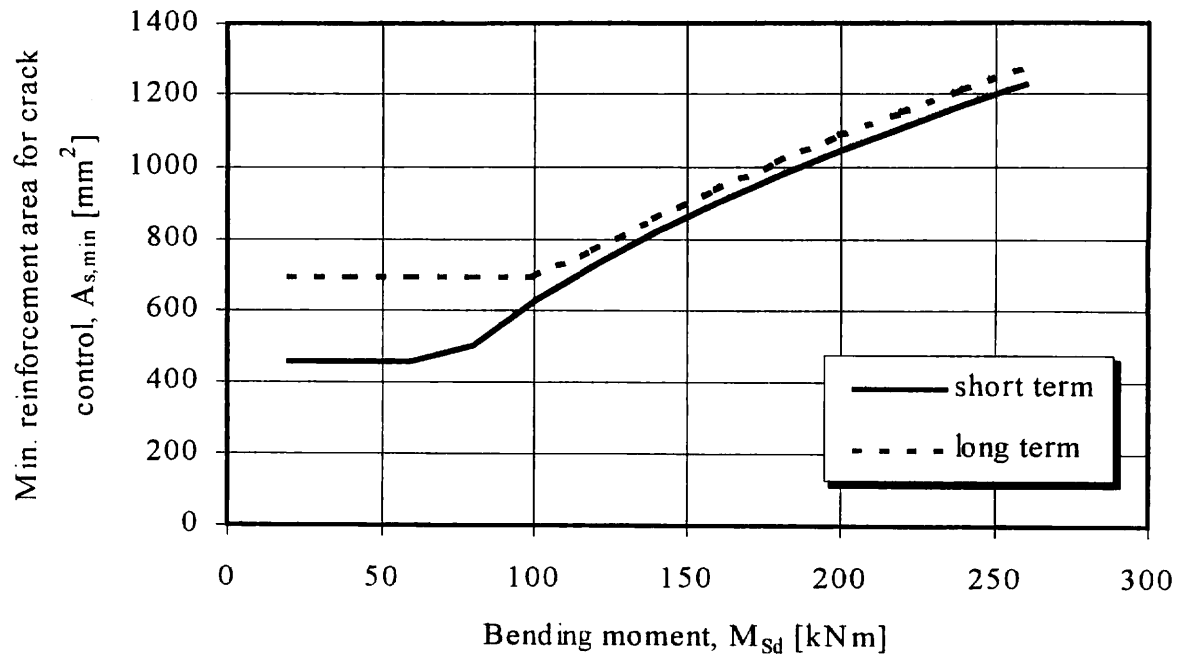
References

ACI (1986). Cracking of Concrete Members in Direct Tension, ACI Committee 224, ACI Journal January-February 1986, 3-13.

ACI (1989). Control of Cracking in Concrete Structures, ACI 224R-80 (rev. 1984), ACI Manual of Concrete Practice 1989, Part 3, 1-41.

Balaguru, P.N., Shah, S.P. (1992). Fiber-Reinforced Cement Composites, McGraw-Hill, Inc. 1992

Balázs G.L.(1987). Bond Model with Non-linear Bond-Slip Law, Studi e Ricerche, Politecnico di Milano, Italia, Vol.9, 1987, 157-180.

Balázs G.L.(1989). Analysis of Slipping Contact, Zeitschrift für angewandte Mathematik und Mechanik, Vol.69/5. 1989, 496-497.

Balázs G.L.(1993). Cracking Analysis Based on Slips and Bond Stresses, ACI Materials Journal, Vol.90, No.4, July-August 1993, 340-348.

Base, G.D., Read, J.B., Beeby, A.W., Taylor, H.P.J. (1966). An investigation of the crack control characteristics of various types of bar in reinforced concrete beams, Research Report 18, Part1, 44p.

Beeby, A.W. (1978a). Corrosion of reinforcing steel in concrete and its relation to cracking, The Structural Engineer, March /No.3. 1978, Vol.56A, 77-81.

Beeby, A.W. (1978b). Cracking: what are crack width limits for?, Concrete, July 1978, 31-33.

Beeby, A.W. (1979). The prediction of crack width in hardened concrete, The Structural Engineer, Vol.57A, No.1, January, pp.9-17.

Broms, B.B. (1965). Technique for Investigation of Internal Cracks in Reinforced Concrete Members, ACI Journal, Vol.62, No.1, Jan. 1965, 35-43.

Broms, B.B., Lutz, L.A. (1965). Effects of Arrangement of Reinforcement on Crack Width and Spacing of Reinforced Concrete Members, ACI Journal, Proceedings V. 62, No. 11, Nov. 1965, pp. 1395-1410.

CEB (1981). Cracking and Deformation, CEB Bulletin d'Information No.143, 1981

CEB (1984). CEB Design Manual Cracking and Deformations, CEB Bulletin d'Information No.158, 1958

CEB (1987). Anchorage Zones of Prestressed Concrete Members, CEB Bulletin d'Information No.181, 1987

CEB (1997). Behaviour and modelling in serviceability limit states including repeated and sustained loads, CEB Bulletin d'Information No.235, 1997

CEB-FIP (1993). CEB-FIP Model Code 1990 - Design Code, Comité Euro-International du Béton, Thomas Telford, London, 1993

Ciampi,V., Eligehausen,R., Bertero,V.V., Popov,E.P. (1982). Analytical Model for Concrete Anchorages of Reinforcing Bars Under Generalized Excitations, Report No. EERC82-83, Earthquake Engineering Research Center, University of Califonia, Berkeley, California, Dec. 1982, 111 pp.

Edwards,A.D., Picard,A. (1972). Theory of Cracking in Concrete Beams, Proc. ASCE Journal of Structural Division, V:98; ST12, Dec. 1972, 2687-2700.

Ferry-Borges, J. (1966). Cracking and deformability of Reinforced Cocrete Beams, IABSE Publication, Zürich, Vol.26, pp.75-79.

Gergely, P., Lutz, L.A. (1968). Maximum Crack Width In Reinforced Flexural Members, Causes, Mechanism and Control of Cracking in Concrete, ACI SP-20, 87-117.

Gambarova, P., Giuriani, E. (1985). Fracture Mechanics of Bond in Reinforced Concrete, Discussion, Journal of Structural Engineering, ASCE, V.III, No. 5, May 1985, pp. 1161-1164.

Giuriani, E. (1982), On the effective stiffness of a bar in cracked Concrete, Bond in Concrete, Proceedings, Applied Science Publishers London 1982, 107-126.

Goto, Y., Otsuka, K. (1971). Studies on Internal Cracks Formed in Concrete Around Deformed Tension Bars, ACI Journal, Vol.68. No.4, April 1971, 244-251.

Holmberg, Ã. (1973). Crack Width, Prediction and Minimum Reinforcement for Crack Control, Bygningsstatiske Meddelser, Vol. 44, Copenhagen 1973

Holmberg, Ã., Lindgren, S. (1970). Crack Spacing and Crack Widths due to Normal Force or Bending Moment, National Swedish Building Research, Document 2: 1970

Janovic, K. (1986). Zur Rißbildung im Stahlbeton- und Spannbetonbau", Beton+Fertigteil-Technik Heft 12, pp.161-169.

Kaar, P.H., Mattoch, A.H. (1963). High strength bars as concrete reinforcement, Part 4 Control of cracking, Journal of the Portland Cement Association Research and Development Laboratories, Vol.5, No. 1, pp. 15-38.

Kaar, P. H., Hognestad, E. (1965). High strength bars as concrete reinforcement, Part 7 Control of cracking in T-beam flanges, Journal of the Portland Cement Association Research and Development Laboratories, Vol.7, No. 1, pp. 42-53.

König, G., Fehling, E. (1988). Zur Rißbreitenbeschränkung im Stahlbetonbau", Beton-und Stahlbetonbau No.6/1988, 161-167. + No.7/1988, 199-204.

König, G., Tue, N. V. (1996). Grundlagen und Bemessungshilfen für die Rißbreitenbeschränkung im Stahlbeton und Spannbeton sowie Kommentare, Hintergrundinformationen und Anwendungsbeispiele zu den Regelungen nach DIN 1045, EC2 und Model Code 90, Deutscher Ausschuss für Stahlbeton Heft. 466, 55 pp.

Krips, M. (1985). Rißbreitenbeschränkung im Stahlbeton und Spannbeton, Verlag für Architektur und Technische Wissenschaft, Berlin, Ernst und Sohn, Heft 33, 108 pp.

Leonhardt, F. (1976a). Vorlesungen über Massivbau, 4. Teil, Springer Verlag

Leonhardt, F. (1976b). Rissebeschränkung", Beton- und Stahlbetonbau, No.7/1976, 14-20.

Leonhardt, F. (1985). Zur Behandlung von Rissen im Beton in dem deutschen Vorschriften, Beton und Stahlbetonbau, 1985, No.7, pp.179-184. + No.8, pp.209-215.

Leonhardt, F. (1988). Cracks and Crack Control in Concrete Structures, PCI Journal, July-August 1988, 124-145.

Lovegrove, J.M. and Din, S.E. (1982). Deflection and Cracking of Reinforced Concrete Concrete Under Repeated Loading and Fatigue, ACI SP-75: Fatigue of Concrete Structures (ed. Shah), 133-150.

Lutz, L.A., Gergely,P. (1967). Mechanics of Bond and Slip of Deformed Bars in Concrete, ACI Journal, 64(11) 1967, 711-721.

Martin, H, Schießl, P., Schwarzkopf, M. (1980). Ableitung eines allgemeingültiges Berechnungsverfahren für Rißbreiten aus Lastbeanspruchung auf den Grundlage von theoretischen Erkenntnissen und Versuchsergebnissen, Forschung Straßenbau und Straßenverkehstechnik, Heft 309, Köln, 33-66.

Ngo, D., Scordelis, A.C. (1967). Finite Element Analysis of Reinforced Concrete Beams, ACI Journal, Vol.64, No.3, March 1967, 153-163.

Nilson, A.H. (1968) Nonlinear Analysis of Reinforced Concrete by the Finite Element Method, ACI Journal, Sept.1968, 757-766.

Noakowski, P. (1985), Verbundorientierte, kontinuierliche Theorie zur Ermittlung der Rissbreite, Beton- und Stahlbetonbau No.7/1985, 185-190. und No.8/1985, 215-221.

Oh, B.H., Kang,Y.H. (1987). New Formulas for Maximum Crack Width and Crack Spacing in Reinforced Concrete Flexural Member, ACI Structural Journal March-April, pp.103-112.

Rehm, G. (1961). Über die Grundlagen des Verbundes zwischen Stahl und Beton (On the Basic Principles of Bond Between Steel and Concrete)", German Institute for Reinforced Concrete (DAfStb), Heft 138, 1961, Berlin, 59 pp.

Rehm, G., Martin, H. (1986). Zur Frage der Rißbegrenzung im Stahlbetonbau, Beton- und Stahlbetonbau No.8, pp.175-182.

Rüsch, H., Rehm, G. (1957a). Notes on Relation between Crack spacing and crack width in Members Subjected to Bending, *Proceedings*, RILEM Symposium on Bond and Crack Formation in Reinforced Concrete Stckholm,Vol.2, pp.507-511.

Rüsch, H., Rehm, G. (1957b). Notes on Crack spacing in Members Subjected to Bending", *Proceedings*, RILEM Symposium on Bond and Crack Formation in Reinforced Concrete Stckholm Vol.2, pp.525-532.

Saliger, R. (1936), High-Grade steel in Reinforced Concrete, Proceedings, Second Congress of the International Association for Bridge and Structural Engineering, Berlin-München (cited according to Ref. Beeby (1979))

Schießl, P. (1976). Zur Frage der zulässigen Rißbreite und der erforderlichen Betondeckung im Stahlbetonbau unter besonderer Berücksichtigung der Karbonatisierungstiefe des Betons, Deutscher Ausschuss für Stahlbeton, Heft 255

Schießl, P. (1989). Grundlagen der Neuregelung zur Beschränkung der Rißbreite, Deutscher Ausschuß für Stahlbeton, Heft 400, pp.158-175.

Schießl, P., Wölfel, E. (1986). Konstruktionsregeln zur Beschränkung der Rißbreite -- Grundlage zur Neufassung DIN 1045, Beton- und Stahlbetonbau, No.12, pp.230-236.

Stevens, R.F. (1972). Deflection of reinforced concrete beams, Proceedings, Institution of Civil Engineers (London), Part 2, Research and Theory, Sept., 207-224.

Tepfers, R. (1979). Cracking of concrete cover along anchored deformed reinforcing bars, Magazine of Concrete Research, Vol.31, No.106, March 1979, 3-11.

Venkateswarlu, B., Gesund, H. (1972),"Cracking and Bond-Slip in Concrete", ASCE Proceedings, V.98. ST12, Dec., pp.2663-2685.

Watstein, D., Mathey, R.G. (1959). Width of Cracks in Concrete at the Surface of Reinforcing Steel Evaluated by Means of Tensile Bond Specimens, ACI Journal, July, pp.47-56.

Wicke, M. (1993). CEB-FIP Model Code 1990 Serviceability Limit States, CEB Bulletin d' Information No.217 on Selected Justification Notes

Windisch, A. (1982). Probabilistic Aspects of Bond-Governed Problems Based on Local Bond Force-Slip Diagrams Determined by a New Method, Proceedings, Int. Symp. on Bond in Concrete, Applied Science Publishers London, 458-466.

Yannopoulos, P.J. (1989). Variation of concrete crack width through the concrete cover to reinforcement, Magazine of Concrete Research, June 1989, 63-68.

4.3.3   Deformation
by Andrew W Beeby

(1)   Introduction

The major area where deformations need to be calculated in the design of concrete structures is in the estimation of the deflection of members. This is often a critical factor in design; indeed, the thickness of slabs is commonly governed by considerations of deflection control rather than by considerations of strength. Over the years, deflection control has become increasingly important. This is because, in reinforced concrete members, the deflection is roughly proportional to the stress in the reinforcement and the levels of stress used in reinforcement has steadily increased. This has occurred firstly due to changes in the strength of reinforcing steels and secondly due to reductions in the overall safety factors as our confidence in the material has increased. A lower overall safety factor or use of a higher strength steel automatically means a higher level of stress under service loads. In addition to this, modern buildings tend to require longer spans than those designed 30 to 50 years ago and there has been constant pressure to economise by using less materials. Though it is not possible to draw definite conclusions, it could well be argued that structures designed today may be four or more times more flexible than those designed 50 years ago. This trend towards higher stresses, lighter structures and longer spans seems likely to continue and, indeed, the time may arrive when ultimate strength ceases to be the critical limit state for design generally and design has to be realigned to give the dominant role to serviceability.

In this chapter, attention will be given to those factors which govern the criteria for deflection control and to the means of calculating deflections for relatively simple situations. More complex and rigorous methods exist for the calculation of deformations and there are now many Finite Element systems available which will take account of the non-linear properties of the materials and can model the effects of tension stiffening and creep (e.g. ABAQUS, DIANA, ANSYS, etc.). This type of approach will not be considered in this chapter.

Examples will be given in the chapter, many of them carried out using spreadsheets. It is assumed that the reader will be familiar with spreadsheets. The spreadsheet program used is Microsoft EXCEL5 but no operations will be carried out which should not be available on any reasonably modern spreadsheet program.

(2)   Criteria for deflection control

(2.1)   Limits to deflections

Limits are set to deflections for various reasons. These can be summarised as follows:

- To avoid visual sag which may upset users or occupants of a structure.
- To avoid impairment of the proper functioning of the structure.
- To avoid damage to brittle partitions or finishes.
- As an indirect means of avoiding problems from vibrations.

A few words may be said about each of these reasons.

(2.2)   Visible sag

Visible sag tends to reduce confidence in the safety of the structure in the eyes of non-technical observers, even where there is, in fact, no impairment of safety. It is therefore prudent to try to design visible members so that any deflection is not apparent to the naked eye. There is a general consensus that a sag of less than about span/250 will not be noticeable. A survey of German experience reported by Meyer and Rusch (1967) produced about 50 cases where visual sag had been the cause of complaint. No case was reported where the sag was less than span/300 and only 2 where the sag was less than span/250. This suggests that the generally accepted limit is reasonable. When considering visible sag, it should be noted that the deflection considered here must be the total final deflection below a line joining the supports. It will be seen that complaint will arise whether the sag is the result of deflection under load or deflection of the formwork during concreting. It should also be clear that, if a deflection greater than span/250 is expected, then some of this may be offset by precambering the element in question. The limit may obviously be relaxed if there is no possibility of the soffit of the member being able to be observed relative to its supports. This has relevance to situations where, for example, there is a false ceiling. It may also have relevance to the case of a flat slab, where it is far from clear how the limit should be interpreted. In this case it might be suggested that the deflection at the centre of a panel should be considered relative to the deflection at points on the line of the columns but mid-way between the columns while others have suggested that the span should be taken as the length of the diagonal of the panel.

One cannot sensibly discuss deflection limits in isolation from the loads under which they should be checked. In this case, an occasional exceedance of the limit under a high level of load cannot be serious provided the deflection decreases to below the limit after the action causing the deflection has reduced. A relatively low estimate of the imposed loading, having a significant probability of exceedance thus seems appropriate. Indeed, since a major proportion of the loading of concrete structures tends to be dead weight and a major part of the deflection will be the creep deflection under this load, it may well often be satisfactory to check against this limit considering only the quasi-permanent loads.

(2.3)   Impairment of function

The deflection may impair the proper functioning of a structure in a variety of ways, though problems are generally limited to certain types of structure. A hypothetical example of the type of problem considered could be the deflection of a beam across the front of an aircraft hangar which supported sliding doors. Excessive deflection of the beam could result in the doors being unable to operate. A more common problem is the deflection of crane rails. Here, deflections may be substantial because of the very large imposed loads applied to the crane rail supporting beams by the fully loaded crane. Excessive deflection can lead to overloading of the motors propelling the crane due to the gradient of the rails or to difficulties in controlling the speed of traversing when passing over the supports where there may be a sudden change in gradient. It is possible to think of many other cases where deflections could upset the alignment or functioning of precision apparatus.

The fundamental factor here is that the limits to the allowable deflection will depend on the particular function of the member or structure. The designer will have to obtain information from the manufacturers or specifiers of the apparatus or machinery which will be

accommodated in the structure relating to the tolerances of deflection or deformation which are acceptable. Standards or Codes of practice cannot provide information on suitable limits. Similarly, the function will define the loading appropriate to checking the particular limit.

It should also be noted that the limiting condition may not necessarily be to the deflection but could be to the gradient of the member or the local change in gradient. The nature of the deformation may also be a function of usage; for example, the limitation may be on the variation in deflection under the action of frequent loads rather than changes in total, or long term deformation.

(2.4)   Damage to partitions or finishes

This is probably the commonest form of problem and the possible examples of how this may occur are too numerous to fully cover. What follows is thus only intended to illustrate the general problem. Figure 4.3-12 shows a section through a small office building. The partitions between offices was provided by concrete blockwork walls with a glass window across the top. The floor supporting the wall was a fairly flexible waffle slab. In the course of a few months after completion, cracks started to develop in the blockwork as shown in the figure. With time these cracks increased in width till they were in the region of 8mm wide. There was no safety risk here; indeed no visible cracks formed in the floor slab, but the cracks in the walls were very unsightly and, not surprisingly, led to complaint. The reason for the cracking is not hard to see. With the passage of time, creep caused the floor to deflect. The wall, however, did not follow the floor but became self-supporting as a deep beam or, since there was no reinforcement in the wall, it might be more accurate to consider the wall as acting as an arch. If the wall acts as an arch, then the concrete blockwork near the centre and at the bottom is redundant. In this case, some of this redundant masonry has followed the floor while the 'arch' of compressed masonry has remained self-supporting. The result is that almost the full increment in deflection of the floor occurring after construction of the wall appeared in the crack. Measurements of deflection showed that the crack width was indeed much the same as the central deflection of the floor. The deflection of the floors of 8 to 10 mm was structurally insignificant but was nevertheless sufficient to cause major damage to the partitions. In addition to the damage shown to the blockwork partition, deflection of the floors cracked the glass panels on the top of the walls.

The cracking shown in Figure 4.3-12 is far from the only form of cracking that may occur in partitions. Figures 4.3-13(a) to (e) show some of the other forms of cracking that may occur. Figure (a) shows the form of diagonal cracking which may occur if the edges of the walls are fixed to the surrounding frame by wall ties. Figures (c) and (d) are basically the same as that shown in Figure 4.3-12. Figure (e) shows what may happen where a partition wall is built across a support. The width of the crack at the top is not a function of the deflection but of the change in slope of the supporting beam or slab over the support and the height of the wall (the author has seen a crack 30mm wide at the top of a high blockwork wall produced by this mechanism).

Waffle slab
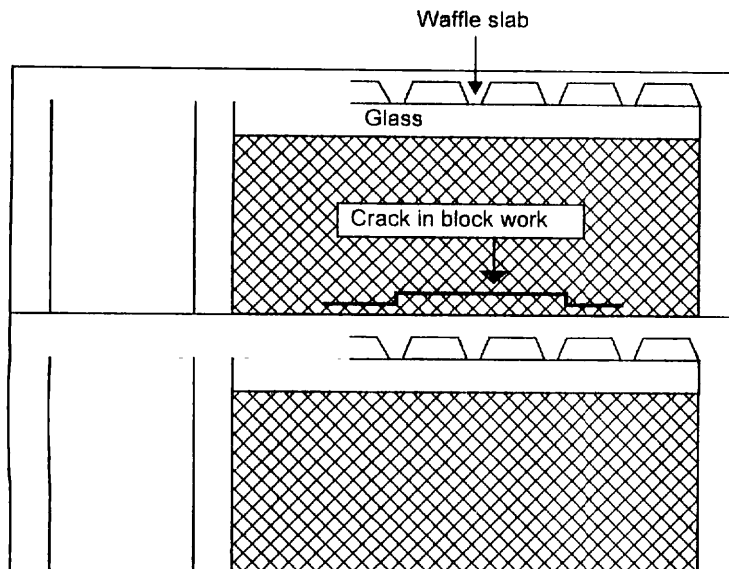
Fig 4.3-12: Damage to masonry partition wall due to deflection

The deformation which will cause disruption of partitions or finishes is difficult to define with exactitude since it clearly depends on the nature of the partition, however, attempts have been made to establish limits from practice. As early as 1820, Treadgold had proposed a limit of span/480 for timber structures as necessary to avoid the cracking of plaster. By 1885, the rather greater deflection of span/360 was proposed by Kidder (1984) and this value seems to have become generally accepted until relatively recently.. Mayer and Rusch (1967) reported numerous examples of damage to partition walls from the deflection of reinforced concrete supporting beams or slabs. Figure 4.3-14 shows a histogram of values of span/deflection taken from .Mayer and Rusch (1967) which led to complaints. Though there are cases where the deflection was assessed to be less than span/1000, it will be seen that the percentage of cases with span/deflection greater than 350 is small. The limits given in modern codes and standards are usually in the range span/300 to span/500, which will be seen to be consistent with Mayer and Rusch's findings.

It should be pointed out that, while data such as that reported by Mayer and Rusch is very useful, one should be careful not to read too much into it. In particular, it is not known what proportion of all members built have problems and what proportion of these is represented by the published data. The data are therefore unable to tell us anything reliable about the probability of problems related to deflection occurring if a particular deflection limit is specified.

The deflection considered in the case of damage to partitions and finishes is clearly only that part of the deflection that occurs after the partitions have been installed. This is likely to be the creep under the quasi-permanent loads plus any short term increase in deflection on occasions when the load increases above the quasi-permanent value.

(2.5)　　Control of vibrations

Vibrations can cause problems in structures either by causing discomfort to occupants or users, or by upsetting sensitive apparatus. For some structures, such as footbridges, regulations apply limits, however, more generally it is assumed that the control of deflections will ensure that vibrations are not a problem. Much work has been carried out into the

definition of criteria for vibration but, in simplified terms, provided the deflection is limited so that:

$$a < \beta/f$$

where:
a = the deflection
β = a constant
f = natural frequency of the member or structure

then vibration will not be a problem. The coefficient β will depend on the nature of the structure and the material. Since $1/f$ is proportional to $\sqrt{a}$, it can be seen that controlling the deflection will automatically provide a limit to vibrations. It can normally be assumed that satisfying the deflection limits specified for visual sag or damage to finishes will automatically ensure that vibrations are not a problem.
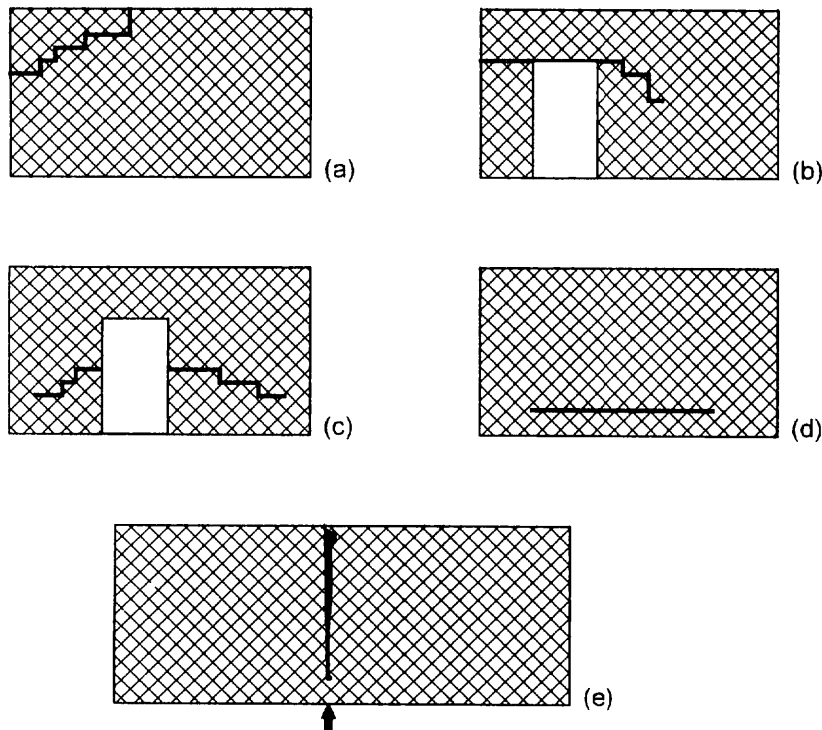
Fig. 4.3-13: Various forms of cracking in partitions due to deflections

(3)   Basic equations for the calculation of deflections

The calculation of the deformations of reinforced or prestressed concrete structures or members subject to bending depends on being able to predict the moment-curvature response of the sections. This is covered in Chapters 3.3.3 and 3.3.2, though the equations may be restated here for convenience and clarity, their derivation will not be discussed further.

Number of cases

Ratio span/deflection
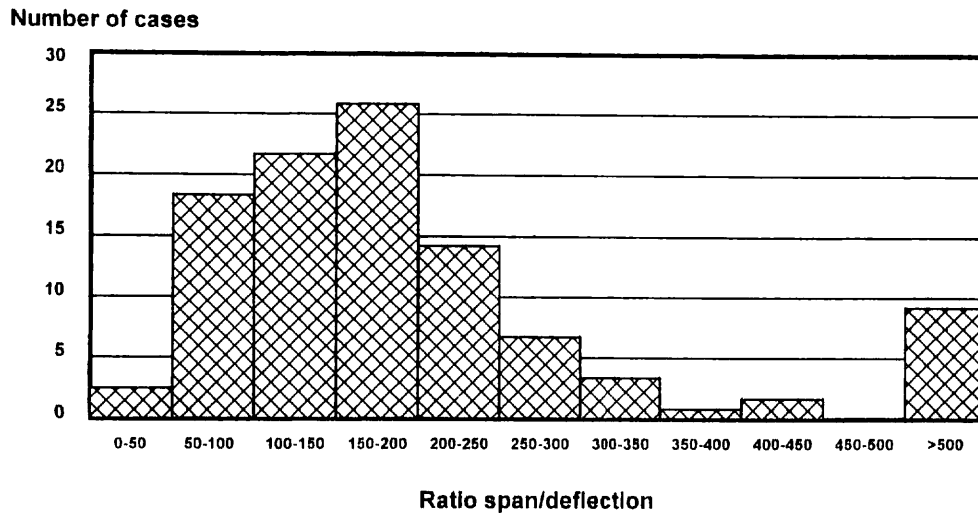
Fig. 4.3-14: Data from Mayer and Rusch

In order to ensure that the procedures which will be developed in this section are clear, it may help to summarise the basic theory of the calculation of deflections. The starting point is to define the term 'curvature'. The curvature of a section is the angle change in radians between the ends of a unit length of the member. It is equal to 1/(the radius of curvature of the section), (1/r), and is clearly a function of the moment to which the section is subjected.

If the distribution of the strains in a member is known then there are a variety of ways in which the curvature may be expressed, any of which may be used in calculations. The possibilities may be written as:

$$1/r = \varepsilon_c/x = \varepsilon_t/(d - x) = (\varepsilon_c + \varepsilon_t)/d \tag{4.3-22}$$

where :

ε_c strain at the compression face
ε_t strain in the tension zone at a depth d from the compression face
x   depth from the compression face to the neutral axis

Furthermore, it must be clear that the total angle change between any two points on a member will be given by the integral of the curvature between these points, hence:

$$\theta = \int(1/r)dx$$

Figure 4.3-15 shows a longer section of a member divided into segments. It will be seen that the deflection at the end of the section relative to the beginning is given by:

$$a = \theta_1\delta x + \theta_2\delta x + \theta_3\delta x + \theta_4\delta x$$
$$= \Sigma\theta_i\delta x$$
or, as δx approaches zero:6
$$a = \int\theta dx$$
and hence, substituting for θ:

$$a = \iint(1/r)dx \tag{4.3-23}$$

This is a completely general equation based on geometry. The only assumption made is that plane sections remain plane.

If the further assumption is made that the beam is made from an elastic material, then the curvature is given by the well known relation:

$1/r = M/EI$

where M is the applied moment at the section considered
   E is the modulus of elasticity of the material
   I is the second moment of area of the section

This then leads to the classical equation for deflection:

$a = \iint (M/EI)dx$ (4.3-24)
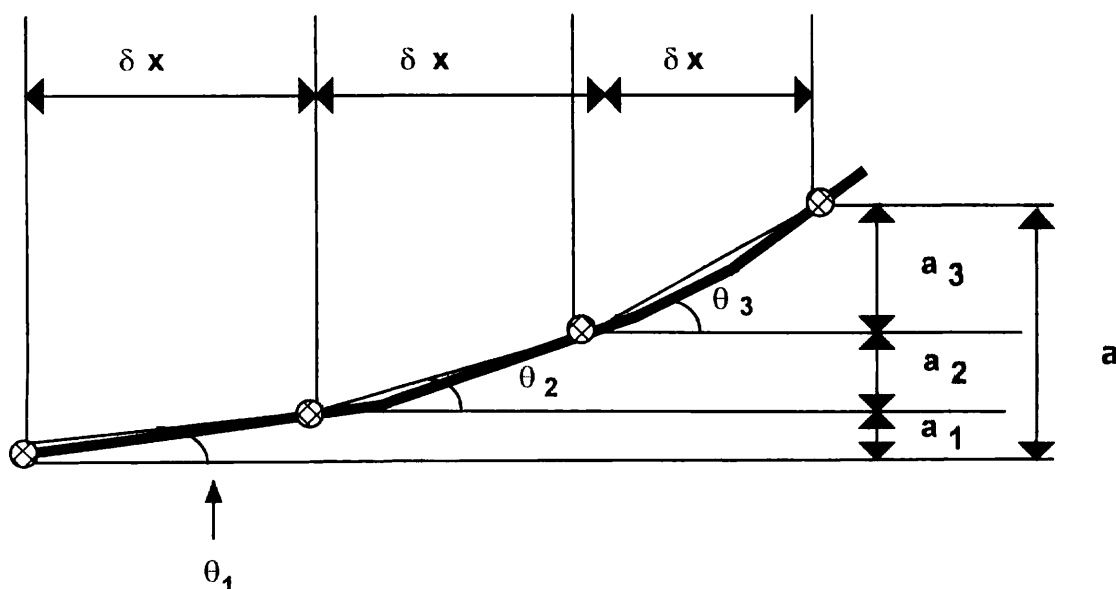
Fig. 4.3-15: Calculation of deflection of a beam from rotations at defined intervals.

For classical elastic beams, where an equation can easily be derived for the variation of the bending moment over the length of a beam, the above equation may be used directly to calculate the deflected shape of the beam. Though this will have been covered fully in other parts of an undergraduate course, an example of this procedure will be given as it will provide some useful information.

(3.1)   Example

Derive an equation for the deflected shape of a uniformly loaded simply supported beam of uniform section made from an elastic material.

The moment at any distance x from the right-hand support of the beam is given by the relation:

$M_x = qLx/2 - qx^2/2$

where:
Mx   the moment at a section a distance x from the right-hand support

q   the load per unit length of the beam
L   the span of the beam

hence:

a = ∫∫(qLx/2 - qx²/2)/EI dx

integrating twice gives:
a = q/2EI(Lx³/6 - x⁴/12) +Ax + B

Since the deflection must be zero at both supports, a = 0 when x = 0 and x = L
From this it can be found that B = 0 and A = ql³/24EI.

Substituting for A and B and rearranging slightly gives:

a = q/24EI{2Lx³ - x⁴ - L³x}

This equation gives the deflection at any point x along the beam. At the centre, x = L/2 and substituting for this gives the central deflection as:

$$a_{max} = \frac{5qL^4}{384EI}$$

Since the maximum moment is given by:

$$M_{max} = \frac{qL^2}{8}$$

this may be rewritten as:

$$a_{max} = \frac{5M_{max}L^2}{48EI}$$

The format of the above equations is quite general. The maximum deflection of any beam may be expressed in the form:

$$a_{max} = \frac{\eta_w wL^4}{EI} \qquad\qquad a_{max} = \frac{\eta_w M_{max}L^2}{EI} \qquad\qquad (4.3\text{-}25)$$

Many design handbooks give values of η_w for various forms of loading and support conditions. For reinforced concrete design using simplified approaches to deflection calculation, it is more useful to have values of η_m. Table 4.3-4, taken from Rowe et al (1972) gives values of η_m for calculation of the mid-span deflection for a variety of common forms of bending moment diagram.

A fundamental problem with reinforced concrete, once it has cracked, is that it is not elastic and so Equation 4.3-24 is not strictly applicable and so, for a rigorous calculation of the deflection, Equation 4.3-23 must be used. Since it is not usually practical to give a simple
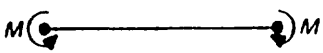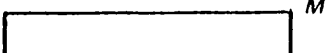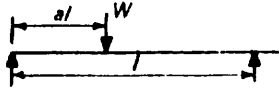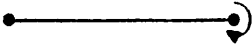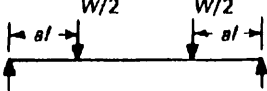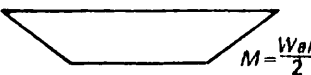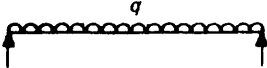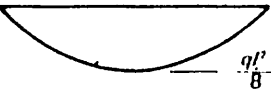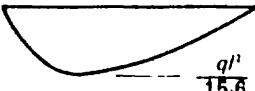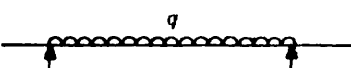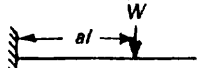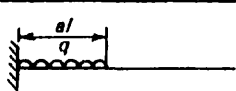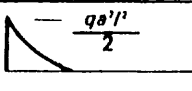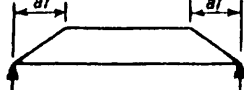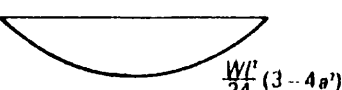
Loading	Bending Moment Diagram	η
M ◯——————◯ M	M	0·125
$\overset{a l}{\longmapsto}\overset{W}{\downarrow}$	$M = Wa\,(1-a)l$	$\dfrac{4a^2-8a+1}{48a}$ if $a=\frac{1}{2}$ $\eta=\frac{1}{12}$
•——————◯	M	0·0625
$\overset{W/2}{\underset{a l}{\downarrow}}\quad\overset{W/2}{\underset{a l}{\downarrow}}$	$M=\dfrac{Wal}{2}$	$0\cdot125-\dfrac{a^2}{6}$
q (uniform)	$\dfrac{ql^2}{8}$	0·104
q (triangular)	$\dfrac{ql^2}{15\cdot6}$	0·102
q (uniform)	M_A M_B M_c	$\eta=0\cdot104\left(1-\dfrac{\beta}{10}\right)$ $\beta=\dfrac{M_A+M_B}{M_c}$
$\overset{al}{\longmapsto}\overset{W}{\downarrow}$ (cantilever)	$-Wal$	end deflection $=\dfrac{a\,(3-a)}{6}\eta$ load at end $\eta=0\cdot333$
$\overset{al}{\underset{q}{\longmapsto}}$ (cantilever)	$-\dfrac{qa^2l^2}{2}$	$\dfrac{a(4-a)}{12}$ if $a=1$ $\eta=0\cdot25$
↓ (central point)	M_A M_B M_c	$\eta=0\cdot083\left(1-\dfrac{\beta}{4}\right)$ $\beta=\dfrac{M_A+M_B}{M_c}$
$\overset{al}{\longmapsto}\quad\overset{al}{\longmapsto}$	$\dfrac{Wl^2}{24}(3-4a^2)$	$\dfrac{1}{80}\,\dfrac{(5-4a^2)^2}{3-4a^2}$

Table 4.3 – 4   Values of η for various shapes of bending moment diagram.

equation for the distribution of curvature along a beam, it is necessary to use numerical integration techniques. These are considered in the next section.

(4)   Calculation of deflections by numerical integration

The procedure for calculating the deflection of simple beams by numerical integration is not difficult, though it is tedious if done by hand. It will be illustrated here by an example and, to develop a more generally useful tool, the example will be carried out by developing a spreadsheet using Microsoft Excel. Having developed the basic spreadsheet, it can be used for parameter studies and easily be developed to handle more complex problems. As will be seen, the spreadsheet is written in general terms but, in order to explain the development clearly, a specific example will be used. The short term deflection will be calculated of a rectangular sectioned beam supporting a uniformly distributed load of 12.4 kN/m over a span of 8 m. The section is 300 mm wide by 500 mm deep. 500 mm^2 of compression reinforcement is provided at a depth from the compression face of 50 mm and 200mm^2 of tension reinforcement is provided at a depth of 450 mm from the compression face. The concrete strength f_{ck} is 30 N/mm^2.

The spreadsheet is shown in Figure 4.3-16(a). The grey box at the top contains all the basic information for the calculation as given in the paragraph above. The figures in the remainder of the sheet are calculated from these data. Details of the calculations are explained below.

The Elastic modulus of the concrete and the tensile strength are calculated from the compressive strength by the formulae given in Chapter 2 of the Model Code. The modular ratio α_e is then given as $200/E_c$. Having obtained these basic materials data, it is necessary to calculate the neutral axis depth and the second moment of area of the uncracked and the cracked section.

For the uncracked section, it may well be sufficiently accurate to ignore the reinforcement and just calculate the second moment of area on the basis of the concrete section alone. Here, however, the reinforcement has been taken into account. By taking moments about the top of the section and using the transformed areas of the reinforcement ($\alpha_e A_s$ and $\alpha_e A'_s$), the neutral axis depth, x_1, can be shown to be given by:

$$x_1 = \frac{bh^2 + \alpha_e\left(A'_s + A_s d\right)}{bh + \alpha_e\left(A'_s + A_s\right)}$$ (4.3-26)

and hence the second moment of area, $I1$, is given by:

$$I_1 = bh^3/12 + bh(h/2 - x_1)^2 + \alpha(A_s(d - x_1)^2 + A'_s(x_1 - d')^2)$$ (4.3-27)

The neutral axis depth for the fully cracked section is obtained by the same approach as:

$$x_2 = \left[\frac{\left(\alpha_e A'_s + \alpha_e A_s\right)}{b^2} + \frac{2\left(\alpha_e A'_s d' + \alpha_e A_s d\right)}{b}\right]^{0.5} - \frac{\alpha_e A'_s + \alpha_e A_s}{b}$$ (4.3-28)

and hence the second moment of area is given by:

$$I_2 = \frac{bx_2^3}{3} + \alpha_e A_s (d - x_2)^2 + \alpha_e A_s' (x_2 - d)^2 \tag{4.3-29}$$

The cracking moment may now be calculated as:

$$M_r = f_{ctm} I_1 / (h - x_1) \tag{4.3-30}$$

The beam is now divided into sections and the moment and curvature calculated at each section. In Figure 4.3-16(a), the beam has been divided into 20 equal segments, giving 21 sections. As numerical integration is an approximate process, the accuracy will be increased by using more segments but 10 is normally adequate. In the example given here, the reduction in accuracy achieved by using 10 segments rather than 20 is found to be about 1.2%. By using the method to calculate the deflection of an uncracked beam it is possible to obtain an absolute value for the error when using 20 segments. This turns out to be 0.4%. Column 1 in the table gives the distance from the left-hand support of each section. The moment at each section may now be calculated from the relation:

$$M_x = qLx/2 - qx^2/2$$

where M_x is the moment at a distance x from the left-hand support.

Columns 3 and 4 give, respectively, the curvatures calculated on the basis of an uncracked and a fully cracked section using the relation: $(1/r) = M/EI$

Column 5 gives the values of $(1/r)_{ts}$, the tension stiffening correction, which is given in MC90 by the equation:

$$(1/r)_{ts} = \{(1/r)_{1r} + (1/r)_{2r}\} \beta (M_r/M)$$

where:

$(1/r)_{1r}$	curvature in state 1 (uncracked) under the cracking moment
$(1/r)_{2r}$	curvature in state 2 (fully cracked) under the cracking moment
β	coefficient taking account of the effects of bond and duration of loading (taken as 0.8 for high bond bars and short term loading)
M_r	the cracking moment

Column 6 gives the calculated curvature which is obtained as the greater of the uncracked curvature $(1/r)_1$ or the cracked curvature minus the tension stiffening correction $(1/r)_2 - (1/r)_{ts}$.

We now come to the integration. Each figure in column 7 of the table is the integral of the curvature up to the section considered calculated using the trapezoidal rule. By this rule, the integral between the (i-1)th and the ith section is given by:

$$A_{(i-1 \text{ to } i)} = \delta((1/r)_{(i-1)} + (1/r)_i)/2$$

span of beam (m)	=	8				
overall section depth (mm)	=	500				
effective depth (mm)	=	450				
section breadth (mm)	=	300	load	=		12.4
depth to top steel (mm)	=	50	concrete grade	=		30
area of bottom steel (mm^2)	=	2000				
area of top steel (mm^2)	=	500				

modular ratio, α =	5.961154		elastic modulus (kN/mm^2) =	33.55055
			tensile strength (N/mm^2) =	2.896468
			cracking moment (kNm) =	44.83247
cracked n. axis dpth =	148.3848			
cracked I x 10^{-6} =	1440.158		At cracking moment:	
uncracked n depth =	260.8448		$1/r_{2r}$ =	0.927861
uncracked I x 10^{-6} =	3701.721		$1/r_{1r}$ =	0.360985

1	2	3	4	5	6	7	8	9
distance from support (mm)	moment (kNm)	$(1/r)_1$ x 10^6	$(1/r)_2$ x 10^6	$(1/r)_{ts}$ x 10^6	$(1/r)$ x 10^6	first integral x 10^3	second integral	deflection (mm)
0	0.00	0.00	0.00	0.00	0.00	0	0.00	0.00
400	18.85	0.15	0.39	1.08	0.15	0.03	0.01	-1.75
800	35.71	0.29	0.74	0.57	0.29	0.12	0.04	-3.48
1200	50.59	0.41	1.05	0.40	0.65	0.30	0.12	-5.15
1600	63.49	0.51	1.31	0.32	0.99	0.63	0.31	-6.72
2000	74.40	0.60	1.54	0.27	1.27	1.08	0.65	-8.13
2400	83.33	0.67	1.72	0.24	1.48	1.63	1.19	-9.34
2800	90.27	0.73	1.87	0.23	1.64	2.26	1.97	-10.32
3200	95.23	0.77	1.97	0.21	1.76	2.94	3.01	-11.04
3600	98.21	0.79	2.03	0.21	1.83	3.66	4.33	-11.47
4000	99.20	0.80	2.05	0.20	1.85	4.39	5.94	-11.62
4400	98.21	0.79	2.03	0.21	1.83	5.12	7.84	-11.47
4800	95.23	0.77	1.97	0.21	1.76	5.84	10.04	-11.04
5200	90.27	0.73	1.87	0.23	1.64	6.52	12.51	-10.32
5600	83.33	0.67	1.72	0.24	1.48	7.15	15.24	-9.34
6000	74.40	0.60	1.54	0.27	1.27	7.70	18.21	-8.13
6400	63.49	0.51	1.31	0.32	0.99	8.15	21.38	-6.72
6800	50.59	0.41	1.05	0.40	0.65	8.48	24.71	-5.15
7200	35.71	0.29	0.74	0.57	0.29	8.66	28.13	-3.48
7600	18.85	0.15	0.39	1.08	0.15	8.75	31.62	-1.75
8000	0.00	0.00	0.00	0.00	0.00	8.78	35.12	0.00
						maximum deflection (mm) =		11.62

Fig. 4.3-16(a): Calculation of the short term deflection of a simply supported beam using the curvature calculation given in CEB MC90 clause 3.6.

where δ is the distance between the two sections. Since it is the cumulative integral that is used in the table, this is given by:

$$A_{(0 \text{ to } i)} = A_{(0 \text{ to } i-1)} + \delta((1/r)_{(i-1)} + (1/r)_i)/2$$

As an example, the value in column 7 for a distance of 3200 mm from the support will be given by the value in Column 7 at the previous section, = 2.12 plus 400 x (1.59 + 1.70)/2000 = 2.78 (division by 1000 is necessary as curvatures are multiplied by 10^6 but the values in Column 7 are only multiplied by 1000).

The values in Column 8 for the second integral are obtained in exactly the same way as those in Column 7 but operating on the values in Column 7 rather than the curvatures. The values in Column 8 are the deflections of the beam at each section relative to the tangent at the left-hand support. Since this tangent is not horizontal, a correction has to be made to the values in Column 8 to produce the deflections relative to the line joining the supports. This may be done by recognizing that the deflection at the right-hand support must be zero. It is therefore necessary to rotate the deflected shape in a clockwise direction until this is achieved. Mathematically, this requires a linear transformation to be carried out on the values in Column 8 such that each value in Column 8 is reduced by $a_L x/L$ where x is the distance from the left-hand support to the section considered and a_L is the calculated deflection in Column 8 at the right-hand support (i.e. when x = L). These corrected values are given in Column 9 and these are the calculated deflections at each section. For convenient reference, the maximum deflection is determined and printed underneath the table.

Having produced the spreadsheet, deflections for other uniformly loaded rectangular beams and other loadings may easily be calculated simply by changing the values in the shaded box at the top.

Having calculated the deflection using the curvature calculation method given in MC90, it may be of interest to calculate the deflection using the method of calculating the curvature given in Appendix A to Eurocode 2. To do this, it is merely necessary to modify columns 5 and 6 in the spreadsheet. This is done in Figure 4.3-16(b). The alternative values in Columns 5 and 6 are explained below.

Column 5 gives the distribution coefficient, ζ. Since a short term deflection is being calculated and it is assumed that ribbed bars are being used, β_1 and β_2 are both taken as 1.0. Also, for bending without axial load, σ_{sr}/σ_s is identical to M_r/M. Thus, the simplified formula given below is used in this case for ζ.

$$\zeta = 1 - (M_r/M)^2$$

The curvature is now calculated in column 6 from the relation:

$$(1/r) = \zeta(1/r)_2 + (1 - \zeta)(1/r)_1$$

A comparison of the two approaches may be seen from Figure 4.3-17 which shows load - maximum deflection curves for a beam with the same overall dimensions as that considered in Figures 4.3-16(a) and 4.3-16(b) but with 1000 mm^2 of tension reinforcement and no compression reinforcement calculated according to MC90 and EC2. These were obtained by changing the reinforcement areas in the appropriate spreadsheet and then changing the loading in steps. It will be seen that the results obtained by the two methods are almost indistinguishable in this case.

In fact, the two methods can easily be shown to be identical except that, in CEB MC90, the coefficient β is taken as 0.8 for short term loads whereas in Eurocode 2, it is taken as 1.0. The identity of the two methods may be proved as follows:

Substitution for ζ in the Eurocode equation for curvature gives:

$$(1/r) = (1 - \beta(M_r/M)^2)(1/r)_2 + \beta(M_r/M)^2 \, (1/r)_1$$

multiplying out the above expression gives:

$$(1/r) = (1/r)_2 - \beta(M_r/M)^2(1/r)_2 + \beta(M_r/M)^2 \, (1/r)_1$$

However, $(1/r)_1$ is equal to $(M/M_r)(1/r)_{1r}$ and $(1/r)_2$ is equal to $(M/M_r)(1/r)_{2r}$. Substituting for these in the second two terms of the right-hand side of the equation gives:

$$(1/r) = (1/r)_2 - ((1/r)_{2r} - (1/r)_{1r}) \, \beta(M_r/M)$$
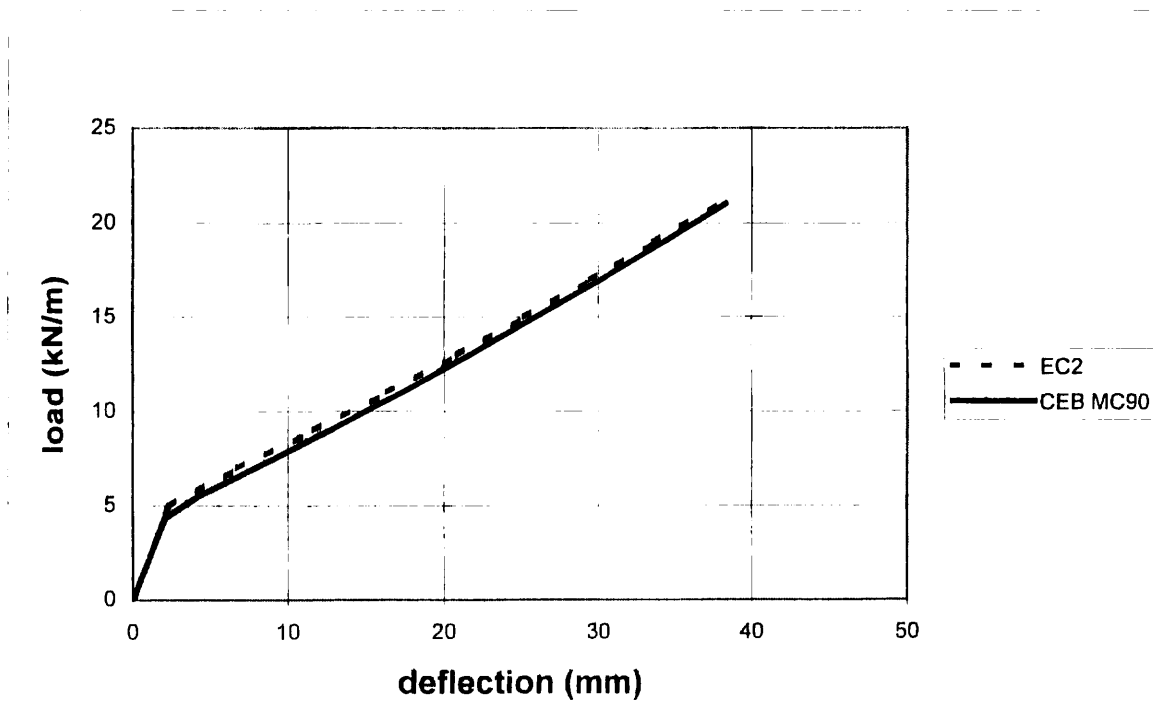
Fig. 4.3-17: Calculated load-deflection response

This is the CEB MC90 equation. It has to be said that, while the MC90 formulation may be slightly easier to use, the Eurocode 2 formulation provides a clearer conceptual model.

Though the spreadsheets have been developed for the simple case of a beam with uniform reinforcement over the whole span and constant cross-section, the basic approach is applicable to more complex situations such as varying reinforcement and varying cross-section or the addition of prestress; the spreadsheet would simply be rather more complex with the requirement to calculate the section properties at each section rather than just once for the whole beam.

(5)   **Calculation of the deflection of indeterminate beams by numerical integration**

The application to indeterminate structures is less simple, though still possible. There are two reasons for this. The first, and most obvious, is that where the moments may be either hogging or sagging, it is necessary to establish whether the top or bottom steel is the tension steel and calculate the section properties accordingly. The second is more fundamental and may be illustrated by an example. The calculation of the deflected shape of the beam shown in Figure 4.3-18 will be considered. The deflections have been calculated using a modified version of Figure 4.3-16(a) which permits the full bending moment diagram shown in Figure 4.3-18 to be input and the curvatures at each section to be calculated correctly depending on whether the moment is hogging or sagging. It also handles different amounts of top and bottom reinforcement at each section. The bending moment diagram given in Figure 4.3-18 has been calculated by normal elastic analysis assuming a constant second moment of area over all spans of the beam.
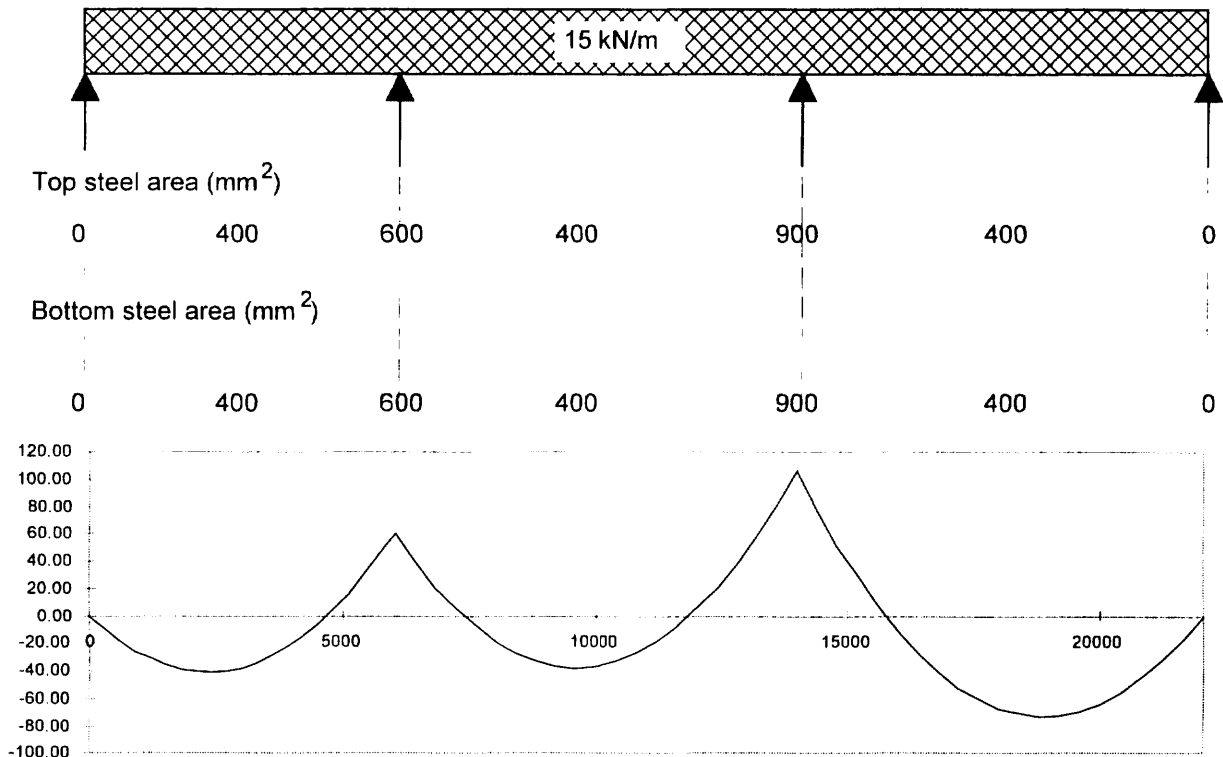
Fig. 4.3-18: Continuous beam example.
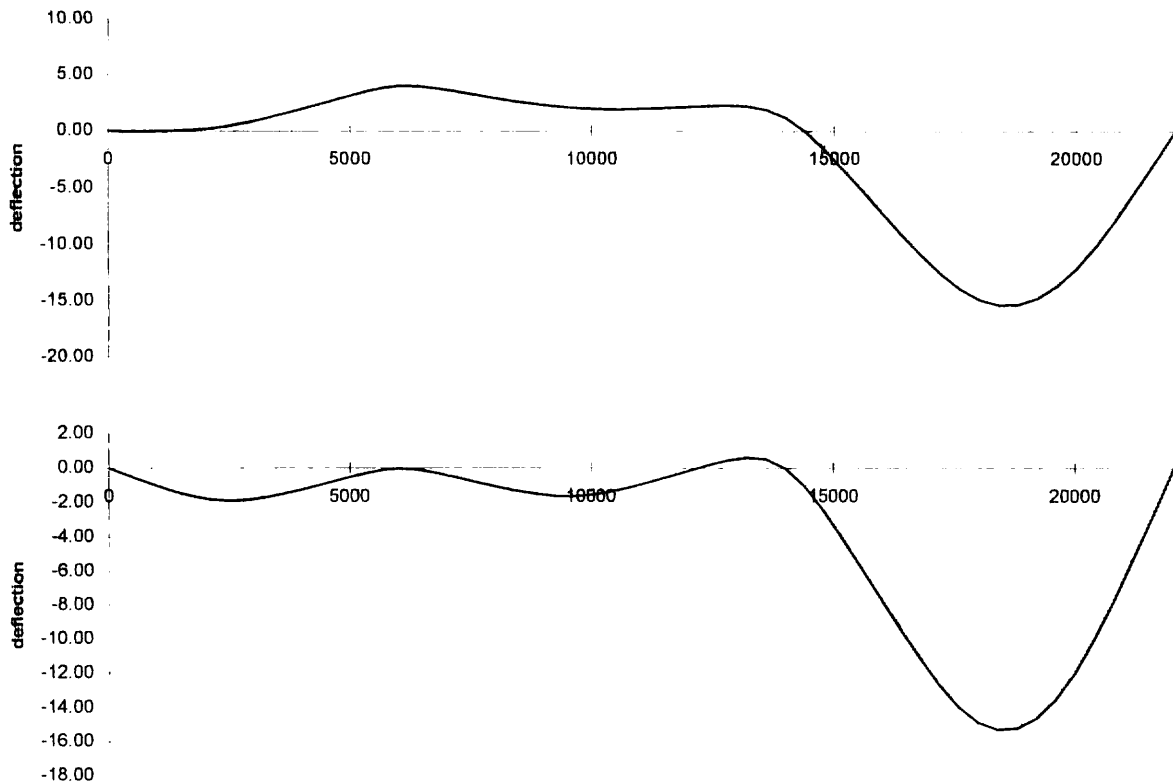
Fig. 4.3-19: Continuous beam example.

In making the correction for the boundary conditions, the spreadsheet only applies a linear transformation to the whole deflected shape so that the deflection at the end supports is zero. The resulting deflected shape is shown in Figure 4.3-19(a). It will be seen that the deflections at the inner supports are not zero, as they should be. This occurs because the elastic bending moment distribution from which the deflections were calculated is incorrect. The true distribution will be influenced by the changes in stiffness from point to point along the beam due to variations in reinforcement quantities and, more importantly, due to the variable development of cracking. For the deflections to be estimated correctly, it is necessary to start from a bending moment diagram obtained from a rigorous non-linear analysis of the structure. In fact, the spreadsheet may be used to obtain this. It is simply necessary to redistribute the support moments by trial and error until the calculated deflection becomes zero at the inner supports. It is not difficult to develop a systematic method of carrying out this trial and error adjustment. An approach is to make a unit adjustment to the moment at each support in turn and note the change in deflection at each of the inner supports. If δ_{aa} and δ_{ab} are the change in deflection at supports a and b respectively caused by a unit change in support moment at a and, similarly, δ_{ba} and δ_{bb} are the change in deflection at supports a and b respectively caused by a unit change in support moment at b, then an estimate of the change in moment necessary at a and b to give zero deflection can be obtained by solving the equations given below for ΔM_a and ΔM_b.

$$a_a = \Delta M_a \delta_{aa} + \Delta M_b \delta_{ab}$$
$$a_b = \Delta M_a \delta_{ba} + \Delta M_b \delta_{bb}$$

where:

a_a and a_b deflection at supports a and b respectively

ΔM_a and ΔM_b adjustment to the moment necessary at supports
    a and b respectively to reduce the deflection to zero.

span of beam (m)	=	8				
overall section depth (mm)	=	500				
effective depth (mm)	=	450				
section breadth (mm)	=	300		load	=	12.4
depth to top steel (mm)	=	50		concrete grade	=	30
area of bottom steel (mm²)	=	2000				
area of top steel (mm²)	=	500				

modular ratio, α =	5.961154		elastic modulus (kN/mm²)	=	33.55055
			tensile strength (N/mm²)	=	2.896468
			cracking moment (kNm)	=	44.83247
cracked n. axis dpth =	148.3848				
cracked I x 10⁻⁶ =	1440.158				
uncracked n depth =	260.8448				
uncracked I x 10⁻⁶ =	3701.721				

1 distance from support (mm)	2 moment (kNm)	3 $(1/r)_1$ x 10^6	4 $(1/r)_2$ x 10^6	5 ζ	6 $(1/r)$ x 10^6	7 first integral x 10^3	8 second integral	9 deflection (mm)
0	0.00	0.00	0.00	0.00	0.00	0	0.00	0.00
400	18.85	0.15	0.39	0.00	0.15	0.03	0.01	-1.67
800	35.71	0.29	0.74	0.00	0.29	0.12	0.04	-3.32
1200	50.59	0.41	1.05	0.21	0.54	0.28	0.12	-4.91
1600	63.49	0.51	1.31	0.50	0.91	0.58	0.29	-6.42
2000	74.40	0.60	1.54	0.64	1.20	1.00	0.60	-7.78
2400	83.33	0.67	1.72	0.71	1.42	1.52	1.11	-8.95
2800	90.27	0.73	1.87	0.75	1.59	2.12	1.84	-9.90
3200	95.23	0.77	1.97	0.78	1.70	2.78	2.82	-10.59
3600	98.21	0.79	2.03	0.79	1.77	3.48	4.07	-11.02
4000	99.20	0.80	2.05	0.80	1.80	4.19	5.60	-11.16
4400	98.21	0.79	2.03	0.79	1.77	4.91	7.42	-11.02
4800	95.23	0.77	1.97	0.78	1.70	5.60	9.52	-10.59
5200	90.27	0.73	1.87	0.75	1.59	6.26	11.90	-9.90
5600	83.33	0.67	1.72	0.71	1.42	6.86	14.52	-8.95
6000	74.40	0.60	1.54	0.64	1.20	7.38	17.37	-7.78
6400	63.49	0.51	1.31	0.50	0.91	7.81	20.41	-6.42
6800	50.59	0.41	1.05	0.21	0.54	8.10	23.59	-4.91
7200	35.71	0.29	0.74	0.00	0.29	8.26	26.86	-3.32
7600	18.85	0.15	0.39	0.00	0.15	8.35	30.18	-1.67
8000	0.00	0.00	0.00	0.00	0.00	8.38	33.53	0.00
					maximum deflection (mm) =			11.16

Fig. 4.3-16(b): Calculation of the short term deflection of a simply supported beam.

The resulting corrections to the support moments will not be exact due to the non-linearity of the problem but it will be found that very few cycles of iteration will be necessary to obtain convergence. In this case it was found that a change of the moment at the left-hand inner support (a) from -68 to -60.4 and at the right-hand inner support moment from -103 to -105.8 results in a deflected shape which satisfies the boundary conditions. The resulting deflected shape is shown in Figure 4.3-19(b). The adjusted bending moment diagram is not the correct diagrams taking account of the variations in stiffness from section to section along the beam.

The CEB MC90 states that the curvature at time t under the permanent and variable load may be obtained from Equation (3.6-5) of MC90, repeated below.

$$(1/r)_{(g+q)} = (1/r)_g + (1/r)_{0(g+q)} - (1/r)_{0g} \qquad\qquad (4.3-31)$$

where:

$(1/r)_{(g+q)}$ curvature at time t due to g + q including the effects of creep, loss of tension stiffening and shrinkage

$(1/r)_g$ curvature at time t due to g including the effects of creep, loss of tension stiffening and shrinkage

$(1/r)_{0(g+q)}$ instantaneous curvature at time t due to g+q

$(1/r)_{0g}$ instantaneous curvature at time t due to g

The effect of creep may simply be allowed for by using an effective modulus of elasticity in calculating the curvatures and the long term tension stiffening is calculated by using β = 0.5 instead of 0.8.

(6) Long term deflections

The Model Code does not appear to give a method for the calculation of the curvature due to shrinkage, however Eurocode 2 does give a formula which, for uncracked sections can be derived from first principles. This derivation is as follows:
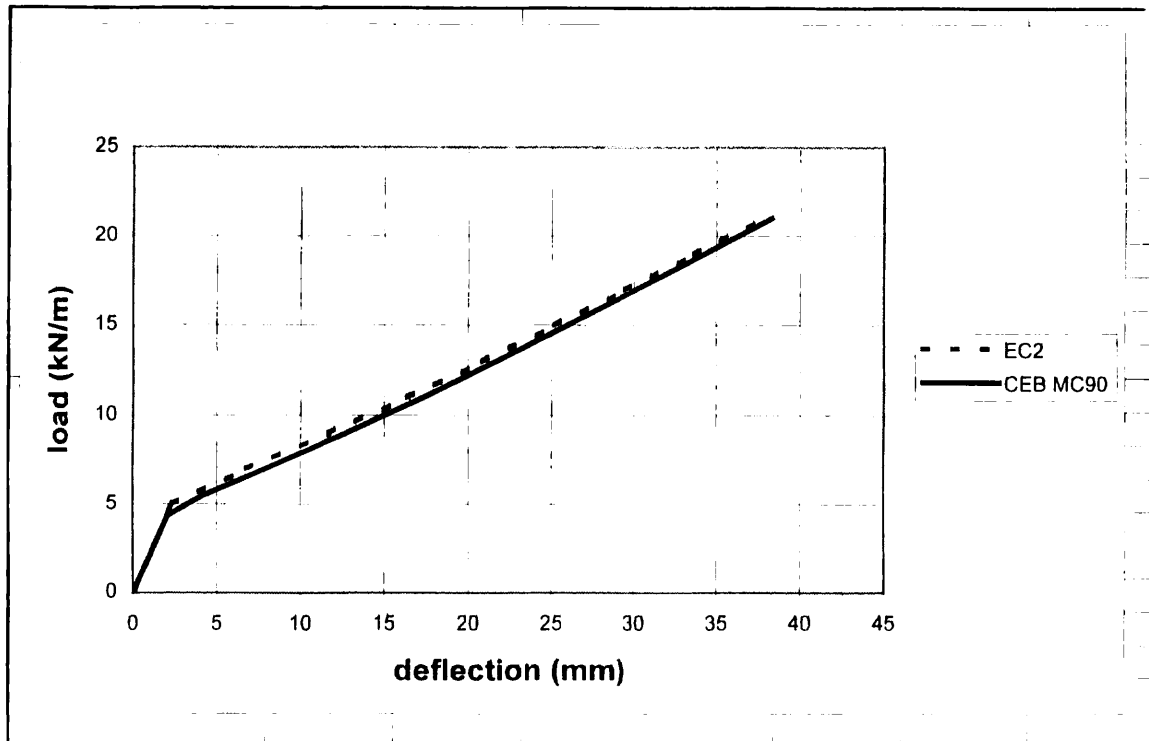
Fig. 4.3-17: Calculated load-deflection response.

Consider the beam shown in Figure 4.3-20. If this beam is constrained to shorten by an amount equal to the free shrinkage, then the stress developed in the concrete will be zero while a stress equal to $\varepsilon_{cs}E_s$ will develop in the reinforcement, since this doesn't shrink. If the beam is released, the force in the reinforcement will be applied to the concrete and the section

will deform. The effective force applied to the section is given by $\varepsilon_{cs}E_s\,A_{s,tot}$ and this acts at the centroid of the reinforcement (both top and bottom steel). A moment is therefore applied to the section equal to the first moment of area of the reinforcement about the centroid of the concrete section multiplied by the stress in the steel $= \varepsilon_{cs}E_s\,S$. The curvature is thus given by:

$$(1/r)_{cs} = \varepsilon_{cs}E_s\,S/E_cI_1 = \alpha\varepsilon_{cs}S/I_1 \qquad\qquad (4.3\text{-}32)$$

where:

$(1/r)_{cs}$ curvature due to shrinkage

ε_{cs} free shrinkage strain

S first moment of area of the reinforcement about the centroid of the concrete section

I_1 second moment of area of the uncracked section

α modular ratio $= E_s/E_c$

1. Initial state

2. Constrained to shorten by an amount equal to the free shrinkage

3. System released
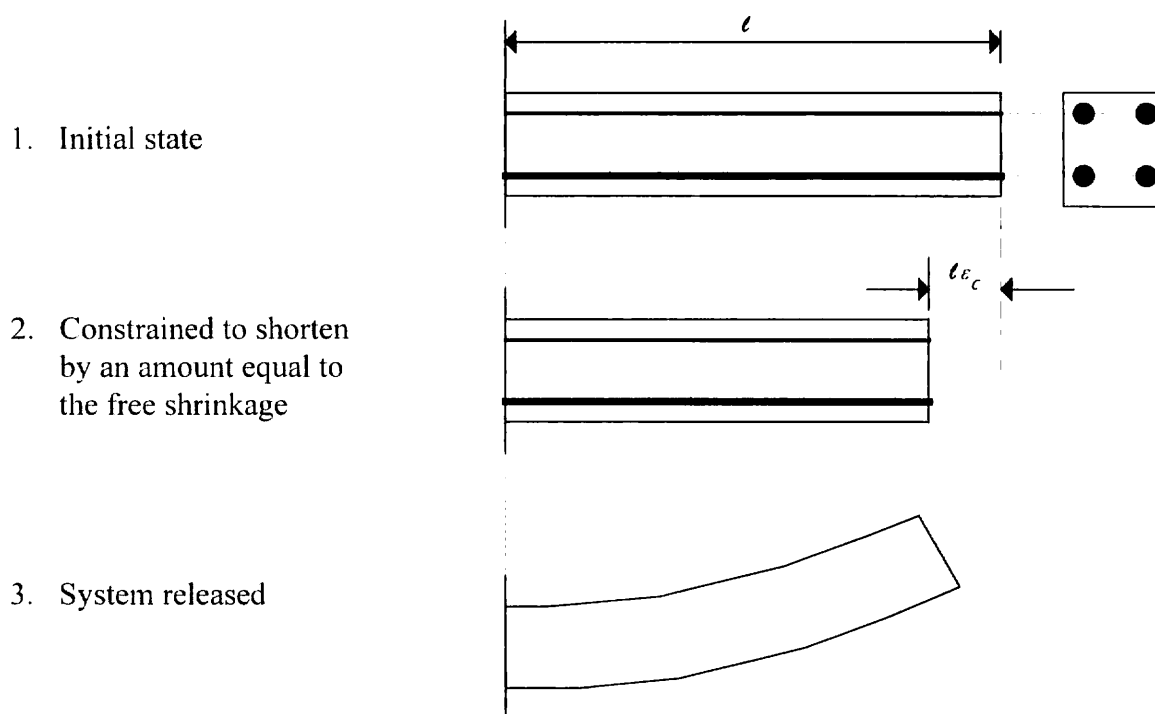
Fig. 4.3-20: Model for the calculation of shrinkage deformations.

It is not so clear how a cracked section would deform under the action of shrinkage but Eurocode 2 assumes that this can be calculated simply by taking S as the first moment of area of the reinforcement about the centroid of the cracked section and using I_2 to calculate the curvature. The curvature under any particular state of cracking is then calculated using the relation:

$$(1/r)_{cs} = \zeta(1/r)_{cs2} + (1 - \zeta)(1/r)_{cs1} \qquad\qquad (4.3\text{-}33)$$

where:

$(1/r)_{cs}$ curvature due to shrinkage

$(1/r)_{cs2}$ curvature due to shrinkage calculated on the basis of an uncracked section

$(1/r)_{cs1}$ curvature due to shrinkage calculated on the basis of a fully cracked section.

ζ distribution coefficient $= (1 - \beta(M_r/M)^2)$

Since the curvatures under the long term load can now be calculated, the numerical integration procedure presented above may be used to calculate the deflection. The easiest way to do this is probably to recast Equation (3.6-5) of MC90 in terms of deflections as:

$$a_{(g+q)} = a_g + a_{0(g+q)} - a_{0g}$$

Each of the deflections may be calculated separately using the spreadsheet given in Figure 4.3-16(a). Except that, for the long term deflections, β will have to be changed and the shrinkage curvature will need to be added. This has been done in Figure 4.3-16(c). The shrinkage curvatures in the uncracked and the fully cracked states are the same at all sections since the reinforcement is uniform in this spreadsheet. They have therefore been calculated only once and are then added into Columns 3 and 4. The Eurocode 2 formulation has been used since this is necessary for the calculation of the shrinkage curvature and, for bending, the EC2 and CEB approaches are identical. For this example, a creep coefficient of 2 and a free shrinkage strain of 200 x 10-6 have been assumed. If the permanent load is 12.4 kN/m and the total load (g+q) is 16 kN/m, spreadsheet 4.3-16 (a) and (c) may be used to calculate the various deflections as follows:

$$a_{0g} = 11.62 \text{ mm}$$
$$a_g = 21.01 \text{ mm}$$
$$a_{0(g+q)} = 15.98 \text{ mm}$$

hence the deflection is $21.01 + 15.98 - 11.62 = 25.37$ mm

(7)   Accuracy of deflection calculations

No method of calculation, for whatever aspect of behaviour, is perfect and all introduce a degree of uncertainty into the result. There are many sources of uncertainty which should be borne in mind when considering calculations and what trust to accord to the result. In considering the accuracy of deflection calculations, one can identify the following possible sources of uncertainty:

- Uncertainty about the level of loading and the load history.
- Uncertainty about the properties of the concrete in the actual structure (E - value, tensile strength, creep, shrinkage)
- Uncertainty about the accuracy of the modeling of behaviour by the formulae
- Uncertainty about the geometry of the member (sizes, cover, span etc.)

Most of these are no more important for deflection than for any other mode of behaviour, however, one source of uncertainty is worth considering in more detail. This is uncertainty about the tensile strength of the concrete in the structure as built. What we know about the concrete at the design stage is the specified characteristic compressive strength. The relation between this and the tensile strength is very uncertain. For some idea of the scatter in the relationship between compressive and tensile strength, see Jaccoud, Farra and Leclercq (1995). There is also uncertainty about the exact compressive strength of the concrete in the actual structure and its relation to the specified characteristic value. To gain some idea of the variability in tensile strength,

    Table 4.3-5 in CEB MC90 suggests that the scatter in the tensile strength for a given compressive strength is about ± 1/3. This figure will be used to investigate the effect of uncertainties in tensile strength on the calculated result. Figure 4.3-21 shows the load - deflection response for a beam with 0.4% of tension reinforcement calculated using the spreadsheet in Figure 4.3-16(a) with the maximum, mean and minimum tensile strengths given in CEB MC90 for the concrete grade chosen. If, as an example, the deflections for a load of 5 kN/m are taken, it will be found that the deflection calculated using the maximum tensile strength is 43% below that calculated with the average strength while the deflection calculated using the minimum tensile strength is 121% greater than that calculated using the mean strength. At a higher load (say 7 kN/m) the errors are somewhat smaller (± 37%). More extensive studies will show that the errors decrease with increasing reinforcement ratio and increasing load above the cracking moment. Clearly, the errors from this cause alone can be very large; particularly where the service load is close to the cracking load. Since there is no way by which the tensile strength can be known with precision at the design stage, substantial uncertainties about the calculated deflection cannot be avoided in many cases. For a more detailed study of this problem, Deak, Hamza and Visnovitz (1997).
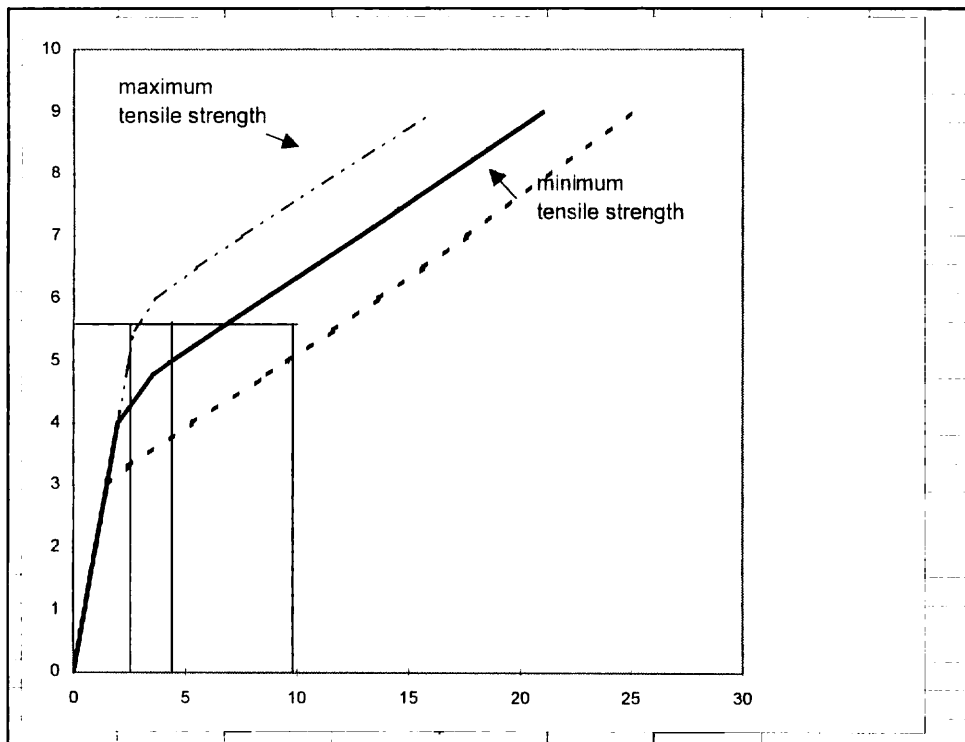
Fig. 4.3-21: *Effect on calculated deflection of variation in tensile strength.*

    This uncertainty reduces the value of calculated deflections in practice and leads to the conclusion that much more approximate methods of calculation could be used without any significant further reduction in the reliability of the result.

(8) **Simplifications to the calculation of deflections**

It would be inconvenient to have to carry out the calculation of the deflection by numerical integration in all circumstances and, generally, simplified methods will give sufficient accuracy. A number of possibilities will be considered here.

(8.1) Assuming that the distribution of curvature is proportional to the distribution of the moment.

This is true for an elastic beam and leads to Equation 4.3-25 given earlier. It is not true for partially cracked beams but, as will be shown, the error is commonly not large. The procedure is to calculate the curvature at mid-span using the MC90 method and then applying the relation:

$$a_{max} = \eta_m L^2 (1/r)$$

where η_m may be obtained from Table 4.3-4.

As an example, the deflection at the centre of the beam for which the calculations by numerical integration are presented in Figure 4.3-16(a) may be calculated as follows.

For a uniformly loaded simply supported beam, η_m is given in Table 4.3-4 as 0.104. From Table 4.3-8(a) the curvature at mid span is 1.85×10^{-6}. The span is 8 m. Hence, the deflection is given by:

$$a_{max} = 0.104 \cdot 8^2 \cdot 10^6 \cdot 1.85 \cdot 10^{-6} = 12.31 \text{ mm}$$

The numerical integration procedure gave a deflection of 11.62 mm. Thus, in this case, the approximate approach overestimates the deflection by 6%. This is an acceptable error. In fact the errors may be larger than this in many practical situations but the error is always on the safe side.

The rigorous calculation of the deflected shape of a continuous beam has been considered in (7). In practice, this approach could only be attempted in special circumstances. For normal calculations, a simpler approach which is not dependent on the establishment of the 'true' bending moment diagram is needed. A commonly used approach is to assume that the curvature diagram follows the elastically obtained bending moment diagram for the continuous beam and then apply the method suggested above. This introduces the further source of inaccuracy over the calculation for a simply supported beam given above that not only the shape of the curvature diagram relative to the bending moment diagram is approximated but also the bending moment diagram. There is also the additional source of inaccuracy introduced by the different amounts of reinforcement used at the supports and in the span. There are two ways of dealing with this: firstly, the problem can be ignored and the deflection calculated on the basis of the area of reinforcement at mid-span or, secondly, an effective area of reinforcement may be used which aims to adjust for the varying areas along the beam. The CEB MC90 method set out below gives a formula for the estimation of an effective percentage of

reinforcement, ρ_m. These two approaches may be tried out on the continuous beam example considered in (7) above.

Considering the simplest approach first, the elastic mid-span moment in the left-hand span is 68.5 kNm and the support moment is -103 kNm At mid-span, the top steel area is 400 mm^2 and the bottom steel area is 600 mm^2. If the modulus of elasticity of the concrete is 33.6 kN/mm^2 and the tensile strength of the concrete is 2.9 N/mm^2 then the section properties can be calculated as follows:

From Equation 4.3-26, the uncracked neutral axis depth is 252 mm and from Equation 4.3-27 the uncracked second moment of area is 3363 mm^4 x 10^6. This gives the cracking moment (Equation 4.3-30) as 39.2 kNm. Similarly, for the fully cracked section properties, Equation 4.3-28 gives the cracked neutral axis depth as 89.3 mm and the cracked second moment of area as 540 mm^4.

The uncracked and fully cracked curvatures may now be calculated as:

$(1/r)_1 = 68.5 \cdot 10^6/(33.6 \cdot 10^3 \cdot 3363 \cdot 10^6) = 0.606 \cdot 10^{-6}$

$(1/r)_2 = 68.5 \cdot 10^6/(33.6 \cdot 10^3 \cdot 540 \cdot 10^6) = 3.78 \cdot 10^{-6}$

The tension stiffening correction, $(1/r)_{ts}$ is now given by:

$(1/r)_{ts} = 0.8M_r/E_c(1/I_2 - 1/I_1)(M_r/M)$
$= 0.8 \cdot 39.2/33.6 \cdot 10^3 (1/540 - 1/3363) (39.2/68.5) = 0.83 \cdot 10^{-6}$

Hence, the curvature $= (37.8 - 8.3) \cdot 10^{-6} = 2.95 \cdot 10^{-6}$

The coefficient η may be obtained from Table 4.3-4 where it gives the relation:

$\eta = 0.104(1 - (M_a + M_b)/10M_c)$
$= 0.104(1 - (103 + 0)/(68.5 \cdot 10)) = 0.085$
The deflection is now given by:

$a = \eta L^2(1/r) = 0.085 \cdot 82 \cdot 10^6 \cdot 2.95 \cdot 10^{-6} = 16.0$ mm

This compares reasonably with the exact deflection of 14.0 mm. A slightly improved result will be achieved by using the average reinforcement areas.

(8.2) Simplified method given in CEB MC90

A bilinear relationship is assumed between load and deflection which is defined as follows:

For $M < M_r$
$a = (1 + \phi)a_c$

For $M \geq M_r$
$a = (h/d)^3\eta_\rho(1 - 20\rho_{cm})a_c$

where:

a   calculated deflection

a_c deflection calculated using the rigidity $E_c I_c$ of the cross section
(neglecting the effect of the reinforcement)

ρ_{cm} geometrical mean compression reinforcement ratio

η_ρ coefficient which depends on the geometrical mean percentage
of tension reinforcement ρ_{tm}

ϕ creep coefficient

It should be noted that CEB MC90 defines ρ_{cm} as a percentage however, the equation only appears to make sense if it is included as a ratio.

In continuous beams, the mean percentage of reinforcement (compression or tension) is calculated from the expression:

$$\rho_m = \rho_a L_a / L + \rho L_o / L + \rho_b L_b / L$$

where:

ρ_a and ρ_b are respectively the percentages of reinforcement at the
left and right hand supports

ρ percentage of reinforcement at the section of maximum sagging moment

L_a and L_b are respectively the distances from the left and right hand
supports to the point of contraflexure

$$L_o = L - L_a - L_b$$

The coefficient η may be obtained by interpolation from the table below:

ρ_{tm}	0.15	0.2	0.3	0.5	0.75	1.0	1.5
η_ρ	10	8	6	4	3	2.5	2

Table 4.3-5: Coefficient for simplified MC90 method.

Taking the example of an 8 m span uniformly loaded simply supported beam with a 300 x 500 mm deep rectangular section with an effective depth of 450 mm supporting a load of 12.4 kN/m and assuming that the tensile strength of the concrete is 2.9 N/mm² and E_c is 33.6 kN/mm², we can calculate the deflection as follows.

The second moment of area, $I_c = bh^3/12 = 300 \cdot 500^3/12 = 3125 \cdot 10^6 \, mm^4$
The cracking moment, $M_r = f_{ctm} bh^2/6 = 2.9 \cdot 300 \cdot 500^2/6 = 36.25 \, kNm$

Since the beam is simply supported, there is no reinforcement at the supports and hence the average percentages are the percentages at mid span. These are:

$100 A_s/bd = 2000/(300 \cdot 450) \cdot 100 = 1.48\%$
$100 A'_s/bd = 500/(300 \cdot 450) = 0.0037\%$

The mid-span moment $= qL^2/8 = 12.4 \cdot 8^2/8 = 99.2 \, kNm$

This is greater than M_r and hence the second equation applies.

The deflection calculated on the basis of the uncracked section is given by:

$$a_c = \frac{5qL^4}{384E_cI_c} = \frac{5 \cdot 12.4 \cdot 8000^4}{384 \cdot 33.6 \cdot 10^3 \cdot 3125 \cdot 10^6} = 6.3\,mm$$

From the table, $\eta_p = 2$ and hence the deflection is given by:

$$a = (500/450)^3 \cdot 2 \cdot (1 - 20 \cdot 0.37/100) \cdot 6.3 = 16\,mm$$

This is slightly less than the long term deflection calculated using the spreadsheet in Figure 4.3-16(c). The difference may well be due to the inclusion of the effect of shrinkage in 4.3-16(c).

It can be seen that the calculation is basically very simple to carry out and probably adequately accurate.

(9) Span/depth ratios

The basic method of controlling deflections given in most design codes is the use of span/overall depth or span/effective depth ratios. A ratio is given for members with particular support conditions. The check for adequacy consists simply in ensuring that the span/depth ratio of the member being designed is less than the appropriate limiting value specified in the code. Since this method is so universally used, some discussion of the rationale behind it is necessary.

To understand the basic idea, consider a beam made of an elastic material where the adequacy of the strength is checked simply by ensuring that the stress, calculated on the basis of elastic theory, does not exceed some specified permissible value, f_{lim} under service loads. This concept formed the basis of the great majority of design methods at one time and it is only over the last 40 years that ultimate strength approaches have superceded the old elastic methods of section design. The moment capacity calculated on this basis for a member subjected to flexure is given by:

$$M = f_{lim}\alpha_1 bh^2$$

where

α_1 constant
b   breadth of the section
h   overall depth of the section

The deflection, as discussed earlier (Equation 4.3-24) is given as:

$$a = kL^2M/EI$$

where

L   span
I   second moment of area which can be expressed as $\alpha_2 bh^3$
Substituting for M and I now gives:

$$a = \frac{k\alpha_1 bh^2 f_{lim} L^2}{\alpha_2 bh^3 E}$$

As discussed in 4.3.3.2, limiting deflections are often defined as a fraction of the span and thus, in the limit:

$$a_{lim} = \alpha_3 L$$

hence: $$\alpha_3 L \geq \frac{k\alpha_1 bh^2 f_{lim} L_2}{\alpha_2 bh^3 E}$$

For a given shape of section, support conditions and material, $\alpha1$, $\alpha2$, $\alpha3$, K, E and f_{lim} are all constant and hence the above equation can be written as:

$$\alpha_4 \geq L/h$$

where $$\alpha_4 = \frac{\alpha_2 \alpha_3 E}{k\alpha_1 f_{lim}}$$

Hence, specifying a permissible value for and ensuring that L/h is less than this will ensure that the deflections do not exceed the required limit when the member is carrying its maximum service load. This approach is valid as long as the material considered is elastic and the limiting deflection can be expressed as a fraction of the span. Reinforced concrete does not truly obey these requirements. Even though reinforcement and concrete are reasonably elastic under service conditions, cracking means that the second moment of area of the section depends upon the amount of reinforcement in the section hence α_2 is not constant; also, the second moment of area is more a function of the effective depth, d, than the overall depth, h. Nevertheless, the method worked reasonably well where α_4 was effectively defined from practical experience rather than theory. The reason for this was probably that, in the earlier days of reinforced concrete design, high safety factors and low steel strengths were sufficiently low that slabs, which are the most critical members from the point of view of deflection control, were generally not cracked in service and were therefore close to elastic. With more modern materials and lower safety factors, this has ceased to be true and simple span/depth ratios have largely become untenable as a reliable design aid. However, the simplicity of the method compared with the actual calculation of deflections makes it an ideal approach and various adjustments to the basic method have been made to make it continue to work. A parameter study can be carried out using the spreadsheet program presented in Figure 4.3-16 which will indicate the nature of the adjustments that are necessary. What we need to do is to calculate the deflections under service loads of a series of beams or slabs which are so designed that they just contain the amount of reinforcement required for the ultimate limit state. For convenience, the same cross section will be used as was used for the earlier examples. For a given area of tension reinforcement, the ultimate moment may be calculated and the permanent load may be taken as some fraction of this. For the purposes of this study, a permanent load equal to half the ultimate load will be assumed and this will be used to compute the long term deflection under the permanent load using the spreadsheet in Figure 4.3-16(c).

span of beam (m)	=	8				
overall section depth (mm)	=	500				
effective depth (mm)	=	450				
section breadth (mm)	=	300	load	=		12.4
depth to top steel (mm)	=	50	concrete grade	=		30
area of bottom steel (mm²)	=	2000	creep coefficient	=		2
area of top steel (mm²)	=	500	free shrink age strain x10⁶	=		200

modular ratio, α =	17.88346		elastic modulus (kN/mm²) =	11.18352
			tensile strength (N/mm²) =	2.896468
			cracking moment (kNm) =	62.05182
cracked n. axis dpth =	214.9642			
cracked I x 10^{-6} =	3212.504		$(1/r)_{cs1}$	0.344247
uncracked n depth =	277.5542		$(1/r)_{cs2}$	0.650037
uncracked I x 10^{-6} =	4765.517			

1	2	3	4	5	6	7	8	9
distance from support (mm)	moment (kNm)	$(1/r)_1$ x 10^6	$(1/r)_2$ x 10^6	ζ	$(1/r)$ x 10^6	first integral x 10^3	second integral	deflection (mm)
0	0.00	0.34	0.65	0.00	0.34	0	0.00	0.00
400	18.85	0.70	1.17	0.00	0.70	0.21	0.04	-3.33
800	35.71	1.01	1.64	0.00	1.01	0.55	0.19	-6.56
1200	50.59	1.29	2.06	0.25	1.48	1.05	0.51	-9.62
1600	63.49	1.54	2.42	0.52	2.00	1.75	1.07	-12.43
2000	74.40	1.74	2.72	0.65	2.38	2.62	1.95	-14.94
2400	83.33	1.91	2.97	0.72	2.68	3.63	3.20	-17.06
2800	90.27	2.04	3.16	0.76	2.90	4.75	4.87	-18.76
3200	95.23	2.13	3.30	0.79	3.05	5.94	7.01	-20.00
3600	98.21	2.19	3.38	0.80	3.14	7.18	9.63	-20.76
4000	99.20	2.21	3.41	0.80	3.18	8.44	12.76	-21.01
4400	98.21	2.19	3.38	0.80	3.14	9.70	16.38	-20.76
4800	95.23	2.13	3.30	0.79	3.05	10.94	20.51	-20.01
5200	90.27	2.04	3.16	0.76	2.90	12.13	25.13	-18.77
5600	83.33	1.91	2.97	0.72	2.68	13.25	30.21	-17.07
6000	74.40	1.74	2.72	0.65	2.38	14.26	35.71	-14.94
6400	63.49	1.54	2.42	0.52	2.00	15.13	41.59	-12.44
6800	50.59	1.29	2.06	0.25	1.48	15.83	47.78	-9.62
7200	35.71	1.01	1.64	0.00	1.01	16.33	54.21	-6.57
7600	18.85	0.70	1.17	0.00	0.70	16.67	60.81	-3.35
8000	0.00	0.34	0.65	0.00	0.65	16.94	67.53	0.00
					maximum deflection (mm) =			21.01

Fig. 4.3-16(c): Calculation of the long term deflection of a simply supported beam using the curvature calculation given in EC2 Appendix A.

Figure 4.3-22(a) shows the resulting calculated deflections plotted against the reinforcement percentage ($100A_s/bd$). It will be seen that the deflection increases as the reinforcement percentage increases. If the member was a slab, which would be likely to have a reinforcement percentage in the 0.4 to 0.6% range, then the deflection could be expected to be about 15 - 25 mm. If it was a beam which commonly have significantly higher reinforcement percentages then the deflection would be likely to exceed 30 mm. All the members in the study had the same effective depth.

Figure 10 Deflections under permanent load as a function of reinforcement ratio
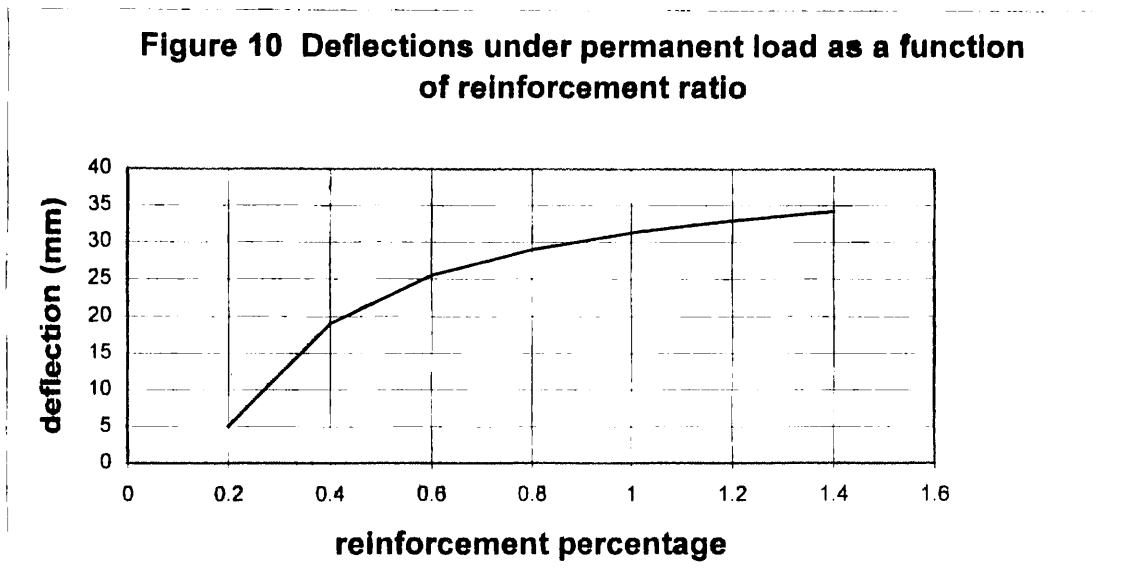
Fig. 4.3-22(a): Deflections under permanent load as a function of reinforcement percentage.

span/effective depth ratios to give deflection of span/250
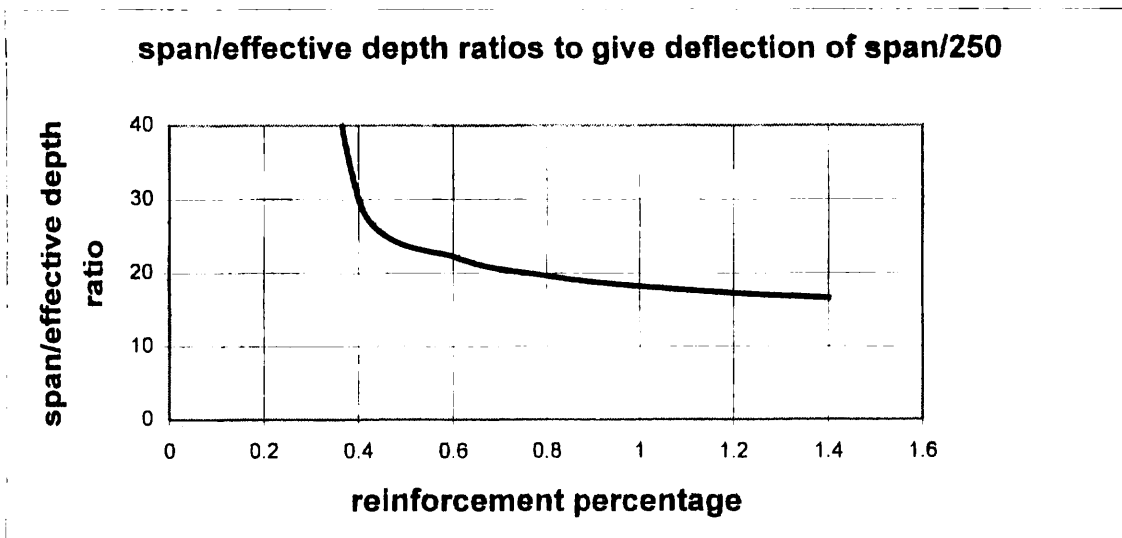
Fig. 4.3-22(b): *Span/effective depth ratios calculated to give a deflection of span/250.*

A common limiting deflection is span/250 which, for the 8 m span members considered, is equivalent to a deflection of 32 mm. We can estimate from the results presented in Figure 4.3-22(a) the depth of a member which will just give this deflection. If the reinforcement percentage is constant then the factor will remain constant and hence, for a given span, the service load deflection will be inversely proportional to the effective depth. Hence, the effective depth required to give a deflection of 32 mm for a given reinforcement ratio and span will be obtained by multiplying the effective depth used in the study of 450 mm by the ratio of the actual deflection to the required deflection. This may now be taken a step further by calculating the corresponding span/effective depth ratio. Figure 4.3-22(b) shows the span/effective depth ratios calculated in this way from the parameter study plotted against the reinforcement percentage. It will be seen how the allowable ratio decreases with increasing reinforcement percentage. The precise line obtained will depend on the ratio of the

permanent load to the ultimate load, the reinforcement strength, the values chosen for the creep coefficient and the free shrinkage, the ratio of the overall depth to the effective depth, the amount of compression reinforcement and the concrete strength. It is clearly possible to carry out much more extensive parameter studies to assess the effect of these variables and from this develop a series of correction factors which would permit the continued use of the span/depth ratio method for modern reinforced concrete construction. This has been done and some design codes include very sophisticated systems. An example is BS8110 British Standards Institution (1997) which contains a set of basic factors for flexural members with different support conditions. These factors then have to be multiplied by factors to take account of the tension and compression reinforcement ratios and the stress in the reinforcement. There is also a factor for correcting for flanged sections. Eurocode 2 and CEB MC90 adopt a simpler approach by effectively picking two points on the curve shown in Figure 4.3-22(b); a ratio for about 0.5% of reinforcement and another for 1.5% reinforcement. For simply supported beams the values given are, respectively, 25 and 18 which can be seen to correspond closely to the values for these percentages in Figure 4.3-22(b). It may be assumed that the higher figure will apply to slabs and the lower to beams or, if the reinforcement ratio is known, then linear interpolation between these values is permitted.

Because of the high level of uncertainty involved in the calculation of deflections, the use of span/effective depth ratios is generally considered to be as accurate a method as is necessary in most normal practical situations.

(10)   Deformations and stresses due to temperature change

Almost all structures are subjected to a regime of varying temperatures. This can lead to overall movements of members and also the development of stresses within members. The overall expansion or contraction of a member may lead to problems in other members, unless expansion joints of adequate size are provided. Non-uniform changes in temperature of a member can lead to deflections or the development of non-linear distributions of stress. All these problems may need consideration in design.

There are two major ways in which temperature changes arise in concrete structures. These are:

(i)   Temperature changes due to hydration of cement. This is a once-only effect. As the concrete sets and hardens, heat is released which causes the temperature to rise and then drop back to ambient. The problems arise in practice because the temperature rise commonly occurs while the concrete is relatively plastic but the cooling occurs after it has hardened. If the resulting movement is restrained, tensile stresses develop which may lead to the formation of cracks.

(ii) Temperature variations due to environmental conditions in service. This is the question discussed here.

(10.1)   Temperature variations in service

An area where this question has been studied in some detail is in bridges. Extensive experimental work has been carried out in many countries to monitor temperature variations and these have been incorporated into design standards. Figure 4.3-23 gives, as an example, the requirements from the UK Bridge Code, BS 5400 British Standards Institution (1998), for a slab bridge deck 1000 mm thick. The temperatures are the design daily temperature changes; not absolute temperatures. The increases in temperature apply to situations where, due to solar gain, there may be major heating of the top of the slab during the day. The temperature decreases apply to situations where a particularly cold night may lead to cooling of the exposed surfaces. Other values are given for the changes in average temperature between summer and winter.
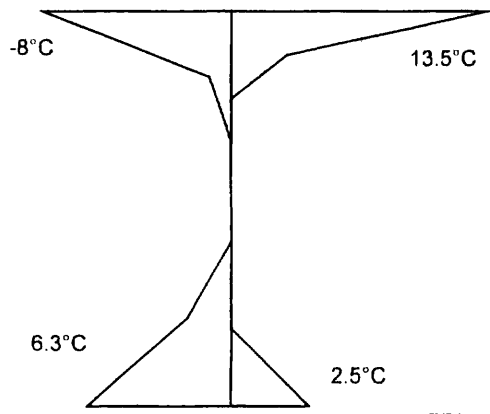
Fig. 4.3-23: Positive and negative temperature.

(10.2)   Calculation of stresses and strains

The coefficient of expansion of concrete, α_t varies somewhat depending on the aggregate type and moisture conditions. The UK code for structural concrete design, BS 8110 provides the following table of values:

Aggregate type (see BS 812)	Typical coefficient of expansion $(1 \times 10^{-6}/°C)$	
	Aggregate	Concrete
Flint, quartzite	11	12
Granite, basalt	7	10
Limestone	6	8

Table 4.3-6: Thermal expansion of rock group and related concrete.

Where the properties of the concrete are not accurately known at the design stage, it is common to assume a coefficient of expansion of $10 \times 10^{-6}/°C$ for concrete and the same for reinforcement.

Having established the temperature history in a member, the next step is to use this information to predict the stresses and strains that will be induced in structural members.

This can be achieved by complex mathematical methods such as finite element analysis but such methods should only be necessary for particularly complex problems. An adequate picture of the structural effects of temperature change can be obtained by much simpler and more easily understood methods.
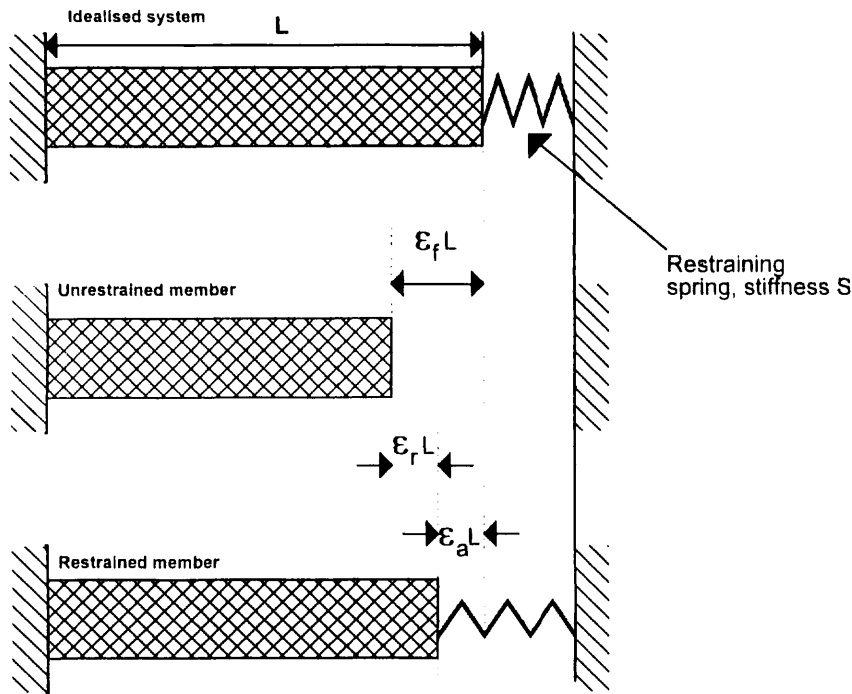
Fig. 4.3-24: Effects of temperature change on a restrained member.

The basic concepts necessary to understand the possible influences of temperature change can be seen by reference to Figure 4.3-24. If an element changes its temperature, then, if the element is unrestrained, its length will change by $\alpha_t L \Delta T$ where L is its length and ΔT is the temperature change. No stresses will be induced in the element unless this change in length is restrained. Figure 4.3-24 shows an element where its shortening due to temperature drop is restrained by a spring of stiffness S N/mm. If the spring was removed, the member would shorten by $\alpha_t L \Delta T$ For simplicity and generality, it is convenient to write $\alpha_t \Delta t$ as ε_f, the free strain. With the spring in place, the movement will be restrained to some extent and will actually only be ε_a L (ε_a = actual strain). The element will be subjected to tension since, effectively, it has been stretched by $(\varepsilon_f - \varepsilon_a)$ L. The stress in the element will be E $(\varepsilon_f - \varepsilon_a)$, or if $(\varepsilon - \varepsilon_a) = \varepsilon_r$ where ε_r is the restrained strain, then the induced stress, $f_r = E \varepsilon_r$.

While it is obvious, it is worth noting that restrained thermal effects are different to normal load effects in one very important way. When an elastic element is loaded and the deformations measured, the forces in the element are proportional to the deformation (i.e. $f = E \varepsilon_a$). When the same element is stressed by restraint of a temperature moment, the forces in the element are not proportional to the measured deformations but to the difference between the free deformation and the measured deformation.

So far, only elements subject to uniform temperatures have been considered. What about non-uniform distributions?
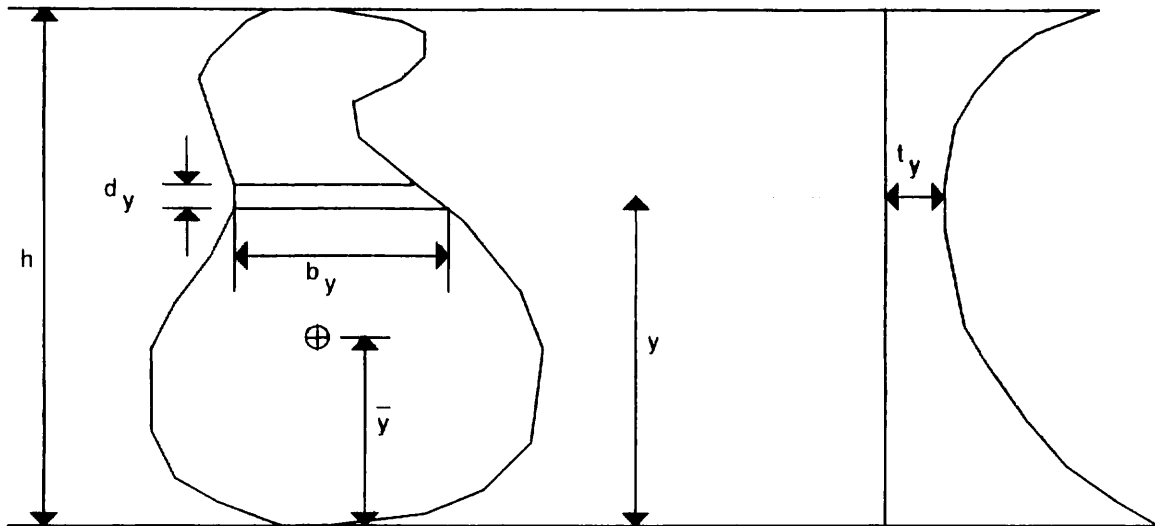
Fig. 4.3-25: Notation for the calculation of temperature effects.
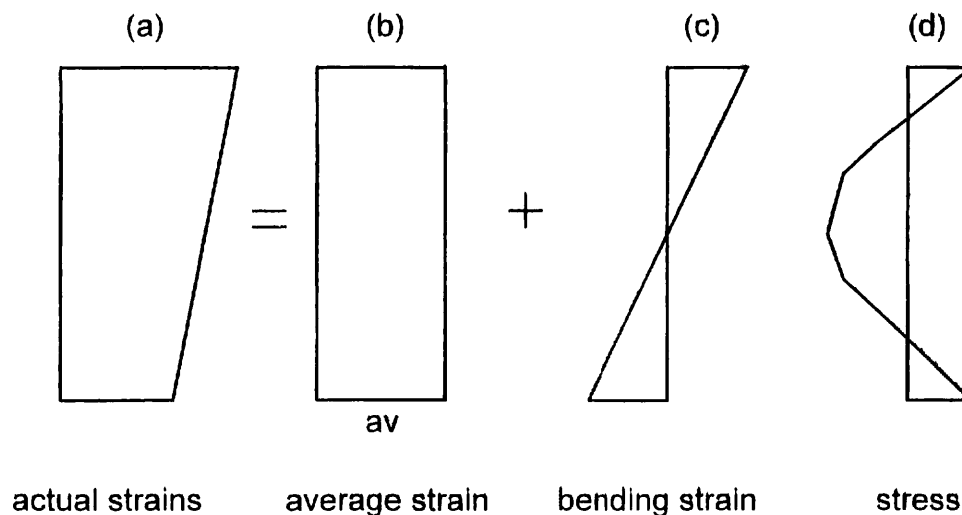
Fig. 4.3-26: Distributions of stress and strain due to non-linear temperature distribution

The derivation of appropriate equations for this more general situation is as follows. The notation etc can be seen from Figure 4.3-25. The final stress distribution could be as shown in Figure 4.3-26(a). This can be considered to be made up of the three components shown in Figure 4.3-26(b), (c) and (d).

From the relationships derived earlier, the stress at any level, y is given by:

$$\sigma_y = E (\varepsilon_{fy} - \varepsilon_{ay}) = E (\alpha T_y - \varepsilon_{ay})$$

From Figures 4.3-26 (b) and (c), this can be written as:

$$\sigma_y = E (\alpha T_y - \varepsilon_{av} - \frac{1}{r} (y - \bar{y})) \qquad (4.3-34)$$

The total force, for member without external restraint must be zero. Hence,

$$F = E \int b \, (\alpha T_y - \varepsilon_{av} - \frac{1}{r} (y - \bar{y}) \, dy = 0$$

or

$$0 = \int b \, \alpha T_y \, dy - \varepsilon_{av} \int b \, dy - \int \frac{1}{r} (y - \bar{y}) \, dy$$

$\int (y - \bar{y}) \, dy$ is the first moment of area of the section about its centroid which, by definition, $= 0$ hence,

$$\int b \, \alpha T_y \, dy = \varepsilon_{av} \int b \, dy$$

$$\int b \, dy = A = \text{Area of section}$$

Hence:

$$\frac{\alpha}{A} \int b \, T_y \, dy = \varepsilon_{av} \tag{4.3-35}$$

For no moment restraint at the ends, to moment at any section must be zero.
Hence,
$$M = \int b \, T_y \, (y - \bar{y}) \, dy = \varepsilon_{av}$$
or

$$O = \int b \, (y - \bar{y})(\alpha T_y - \varepsilon_{av} - \frac{1}{r} (y - \bar{y})) \, dy$$

$$= \alpha \int b(y - \bar{y}) \, dy - \varepsilon_{av} \int b \, (y - \bar{y}) \, dy - \frac{1}{r} \int b \, (y - \bar{y})^2 \, dy$$

As before, $\int b \, (y - \bar{y}) \, dy = 0$.

Also, $\int b \, (y - \bar{y})^2 \, dy$ is the second moment of area of the section about its centroid $= 0$, hence:

$$\alpha \int b \, T_y \, (y - \bar{y}) \, dy = \frac{I}{r}$$
or
$$\frac{1}{r} = \frac{\alpha}{I} \int b \, T_y \, (y - \bar{y}) \, dy \tag{4.3-36}$$

The residual strain, which will result in stress, is now given by the relation:

$$\varepsilon_{ry} = \alpha \, T_y - \varepsilon_{ay} \tag{4.3-37}$$

and the stress by:

$$\sigma_y = E \, \varepsilon_{ry} \tag{4.3-38}$$

While this may look very complicated, the equations can quite easily be solved. Clearly, since the temperature profiles are not going to fit any convenient mathematical function, numerical methods of integration will be needed. In what follows, Simpson's Rule will be used.
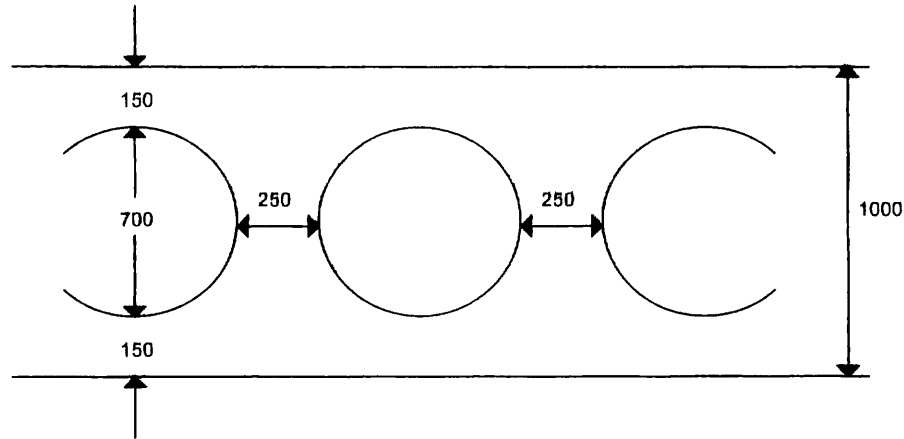
Fig. 4.3-27: Bridge deck slab used in example.

The procedure can conveniently be carried out in a tabular form as indicated below. It will immediately be seen that this procedure can be very easily carried out with the aid of a Spread Sheet programme. Figure 4.3-27 and Figure 4.3-28 give an example of a spread sheet calculation. This is slightly more general than set out above in that the spread sheet and Simpson's Rule is also used to compute the cross-sectional area of the section, the depth to the centroid and the second moment of area.

Section	Depth to section	Breadth	Temp. change	Simpsons coefficient	U	V
1.	0	b_1	T_1	1	$U_1 = b_1 T_1$	$V_1 = U_1 y$
2.	Δh	b_2	T_2	4	$U_2 = 4b_2 T_2$	$V_2 = U_2 (y - \Delta h)$
3.	$2\Delta h$	b_3	T_3	2	$U_3 = 2b_3 T_3$	$V_3 = U_3 (y - 2\Delta h)$
4.	$3\Delta h$	b_4	T_4	4	$U_4 = 4b_4 T_4$	$V_4 = U_4 (y - 3\Delta h)$
					ΣU	ΣV

Table 4.3-7   Summary of Procedure.

$$\varepsilon_{av} = \frac{\alpha \Sigma U \Delta h}{3A} \qquad \frac{1}{r} = \frac{\alpha \Sigma V \Delta h}{3I}$$

(10.3)   Example

Calculate the stresses induced in the slab shown in Figure 4.3-27 due to the positive temperature changes specified in BS5400 for this depth of slab. The coefficient of expansion may be taken as $10 \times 10^{-6}/°C$ and the elastic modulus as $28 \times 10^3 N/mm^2$.

It is convenient to use a spacing of sections of 100mm in the integration. This is probably more than are strictly necessary, but in a spreadsheet, there is no difficulty in using a substantial number of sections.

Figure 4.3-20 in BS5400 Part 2 (reproduced here as Figure 4.3-23) gives a maximum top temperature of 13.5°C and a bottom temperature of 2.5. The table in the figure permits intermediate values to be interpolated. The resulting spreadsheet output is shown in Figure 4.3-28.

Coefficient of expansion x 10^6 10

Modulus of elasticity (kN/mm^2 28

section	1 depth mm Y	2 breadth mm B	3 temp difference T	4 simpson coeff S	5 s x B	6 S x B x Y	7 SB(Y-Y$_b$)^2	8 S x B x T	9 SBT(Y-Y$_b$) x α
1	0	950	13.5	1	950	0	237.50	12825	-64.13
2	100	950	6.5	4	3800	380000	608.00	24700	-98.80
3	200	590	2	2	1180	236000	106.20	2360	-7.08
4	300	376	0	4	1504	451200	60.16	0	0.00
5	400	279	0	2	558	223200	5.58	0	0.00
6	500	250	0	4	1000	500000	0.00	0	0.00
7	600	279	0	2	558	334800	5.58	0	0.00
8	700	376	0	4	1504	1052800	60.16	0	0.00
9	800	590	0.8	2	1180	944000	106.20	944	2.83
10	900	950	1.7	4	3800	3420000	608.00	6460	25.84
11	1000	950	2.5	1	950	950000	237.50	2375	11.88

                       sum   16984   8492000   2034.88   49664   -129.46

area mm^2	Y$_b$ mm	I mm^4 x 10^{-6}	ε$_{av}$ x 10^6	(1/r) x 10^9
566133	500.00	67829.33	29.24	-0.0636

section	10 average strain x 10^6	11 bending strain x 10^6	12 total strain x 10^6	13 restrained strain x 10^6	14 stress (N/mm^2)
1	29.24	31.81	61.05	73.95	2.07
2	29.24	25.45	54.69	10.31	0.29
3	29.24	19.09	48.33	-28.33	-0.79
4	29.24	12.72	41.97	-41.97	-1.18
5	29.24	6.36	35.60	-35.60	-1.00
6	29.24	0.00	29.24	-29.24	-0.82
7	29.24	-6.36	22.88	-22.88	-0.64
8	29.24	-12.72	16.52	-16.52	-0.46
9	29.24	-19.09	10.16	-2.16	-0.06
10	29.24	-25.45	3.79	13.21	0.37
11	29.24	-31.81	-2.57	27.57	0.77

Sign convention: Compression positive; Tension negative.

Figure 4.3-28 Spreadsheet for calculating temperature stresses

Notes to solution to example:

Column

(1) - (4)   Basic data

(5)   Calculation of section area $= \int b \, dy$
            Area is (column sum) $\cdot$ 100/3 $= A$

(6)   Calculation of location of centroid of section ($\bar{y} =$ Yb).
            $\underline{\bar{Y}}$ =(sum of column) $\cdot$ 100/3A

(7)   Calculation of second moment of area of section ($= \int (y - \bar{y})dy$)
            I = (sum of column) $\cdot$ 100/3

(8)   Calculation of average strain ε_{av} = (sum of column) $\cdot$ 100 $\cdot$ $\alpha/3A$

(9)   Calculation of curvature. $(\frac{1}{r})$ = (sum of column) $\cdot$ 100 $\cdot$ $\alpha/3I$

(10)   Average strain from column (8)

(11)   Bending strain $= (\frac{1}{r}) (y - \bar{y})$

(12)   Total actual strain = column (10) + column (11)

(13)   Restrained strain, ε_r $= \alpha\Delta T - \varepsilon_a$
                              $= \alpha \cdot$ column (3) - column (12)

(14)   Stress = column (13) $\cdot$ E

The overall change in length may now be calculated from the average strain times the length of the bridge deck. Assuming this to be 20 m gives a length change of 0.6 mm.

The deflection may be calculated from the curvature multiplied by the span squared and the appropriate coefficient from Table 4.3-4. Assuming uniform conditions over the whole span, the appropriate coefficient is 0.125, giving a deflection of 3.2 mm.

So far the discussion has been concerned with statically determinate members. This is very commonly the case with prestressed beams. The treatment of indeterminate structures is more complex as it is necessary to account for the effect of other members in the structure and the boundary conditions. It is not intended to pursue this problem here.

References

1. Mayer, H and Rusch, H. R. Bauschaden als folge der Durchbiegung von Stahlbeton-bauteilen. Deutscher Ausschuss fur Stahlbeton, heft 193, 1967.

2. Kidder, F. E., Architects and Builders Pocket Book. John Wiley and Sons Inc. 1984

3. Odeen, K., Trends and developments of building materials. Proceedings of IABSE Symposium on Selection of Structural Form. London 1981.

4. Rowe et al. Handbook on the Unified Code for Structural Concrete (CP110: 1972). Cement and Concrete Association, 1972.

5. Jaccoud, J-P., Farra, B., Leclercq, A. Tensile strength - Modulus of elasticity - Bond - Tension stiffening - Limit state of Cracking. Report to the Joint CEB/FIP Working Group on HSC/HPC. IBAP, EFPL Lausanne, March 1995.

6. Deak, G., Hamza, I. and Visnovitz, G. Variability of deflections and crack widths in reinforced and prestressed concrete elements. CEB Bulletin d'Information 235: Serviceability Models. April 1997.

7. British Standards Institution. BS8110:Part1:1997: Structural Use of Concrete. BSI 1997.

8. British Standards Institution. BS5400:Part 1:1978. (loads on bridges).

4.4   Ultimate Limit State Principles

4.4.1   Basic design for moment, shear and torsion

by Paul Regan

(1)   Purpose and place of ultimate limit state design

The objective of design for the Ultimate Limit State is to provide a satisfactory margin of safety against structural failure. The diagram below indicates its place in the overall framework of design for ordinary reinforced concrete. The sequence is shown as being linear but, if reasons for changes emerge at any stage, it may be necessary to revise the work of previous steps. For example, if there are difficulties in the design for the ultimate limit state the sizes of members may need to be revised and the structure may have to be analysed again.

Another reason for revision can arise with a progressive refinement of the design. The initial structural analysis is likely to be based on the uncracked stiffnesses of the concrete sections, but it may be desirable for the final analysis to take account of cracking and of the areas of reinforcement. This can only be done once an initial ultimate limit state design has been made.

> **CONCEPTUAL DESIGN**
> (type of structure, arrangement of members)

> **SIZING OF MEMBERS**
> (from experience, span/depth/ratios, etc)

> **IDEALISATION FOR STRUCTURAL ANALYSIS**

> **STRUCTURAL ANALYSIS**
> (giving moments, shears, axial forces)

> **ULTIMATE LIMIT STATE DESIGN**
> (dimensioning of reinforcement, verification of concrete resistances)

> **SERVICEABILITY LIMIT STATE DESIGN**
> (checks of deflections and vibrations, details to control cracking)

> **DETAILING OF REINFORCEMENT**

The ultimate limit state may be reached in a number of ways. One limit is that of the static equilibrium of the structure, with respect to overturning or sliding.

More commonly the limit is that of material resistance in relation to static or fatigue loading. Static loading is treated in parts (3) to (7) of this Section and fatigue is the subject of Section 4.4.3.

Instability is another form of ultimate limit and may relate to the structure as a whole or to individual elements. Elastic buckling is improbable in concrete members and the effects normally needing consideration are those of additional moments arising from axial loads and lateral displacements. They finally produce a limit state in relation to material resistance. The moments may be assessed as part of a non-linear overall analysis, but they can be treated separately and means of doing this are described in Section 4.4.2.

(2)   Structural modelling

The approach to ultimate limit state design is described by MC90's statement. "The determination of resistance should be based on physical models of the internal forces and external reactions of the structure. The models should represent continuous systems of internal forces in equilibrium under design ultimate conditions and should, at least approximately, consider compatibility of deformations."

This makes it clear that it is the designer's responsibility to formulate valid paths by which loads can be transmitted from their points of application to the foundations. The actions involved must be defined, at least in a simplified manner, using models which should, so far as possible, provide the mathematical basis for the verifications of resistance. It is also clear that the necessary resistance should be verified in all parts of the load paths and this calls for special attention to be paid to the connections of members.

The output of a structural analysis is a distribution of moments and forces in the members of a structure. Where the reinforcement is bonded to the surrounding concrete, the concept of a 'member' is clear and includes the reinforcement, which undergoes the same local deformations as the surrounding concrete, when the member is loaded. If the reinforcement is unbonded the equality of deformations between the reinforcement and concrete applies only to average movements over the lengths between anchorages. In this case the unbonded reinforcement should be regarded as a separate member and the forces in it should be determined from the structural analysis rather than the ultimate limit state design in the sense of this text.

In practice unbonded reinforcement is pre-stressed and as a conservative simplification the tension in it may be assumed to remain at its level in the unbonded structure and to act on the member as an external force.

The approach of treating pre-stressing forces as external actions can also be applied where tendons are bonded, but in this case the changes of tendon forces during loading are obtained by treating the pre-stressing steel as a part of the member when determining its response to load.

The ultimate limit state design and verifications are made in terms of internal forces and the areas of material resisting them. The areas may be those of internal 'members', i.e. the struts and ties of a model, or unit areas where the design is in terms of force resultants (n_x, n_y, n_{xy}) per unit width. Either case requires knowledge of the distribution of actions (forces) and limits for material stresses.

Truss or strut-and-tie modelling is a simple method of representing the principal actions in a member or connection. The compression members or struts represent uniaxial compression stress fields. They are generally of concrete but can include compression reinforcement. Occasionally there may be struts of compression steel alone. The tension members, or ties, are generally of steel and must coincide geometrically with the centre-lines of bars or groups of bars. The struts and ties are connected at nodes where forces are transferred between them.

In the drawings of this Chapter, struts are shown as heavy broken lines and ties as heavy full lines, while nodes are depicted as black circles. It should be noted that the lines are drawn at the centres of struts and ties and that reinforcement is normally required to extend beyond the node at the end of a tie. This is because its action is needed over the full widths of the struts with which it interacts - see Fig.4.4-1.

The modelling of a given structural situation may be more or less complex depending largely on the scale of the member being designed. Fig.4.4-2 shows two deep beams, one small and one large. In the small beam the only reinforcement would be the main bars at the bottom, and the model consists of just the main tie and two inclined struts. In the large beam there would be distributed reinforcement and extra members are included in the model to represent it.

The justification for such a system of modelling lies in the lower bound theorem of plasticity. According to the theorem, a system of loads and reactions will not produce failure so long as a system of internal actions can be found which is in equilibrium and does not cause the yield strengths of the materials to be exceeded.

For the theorem to be applicable in any given case, the deformations required for the internal actions to be realised must not be greater than the plastic limits of the materials. Steel reinforcement is ductile but concrete has only limited deformability in compression and very little in tension. In some cases, such as simple bending, the strains of the concrete can be calculated and the limited strain capacity can be treated explicitly. Where this is not possible the modelling must still take account of the concrete's limited plasticity and does so by:

1. not relying on concrete in tension except where plasticity is not required;

2. using force systems close to those from (uncracked) elastic analyses except where there is adequate experimental evidence to justify the deviation.

This approach has the advantage of not only ensuring safety at the ultimate limit state but also tending to produce good behaviour in service by avoiding high stresses in the reinforcement at the SLS.
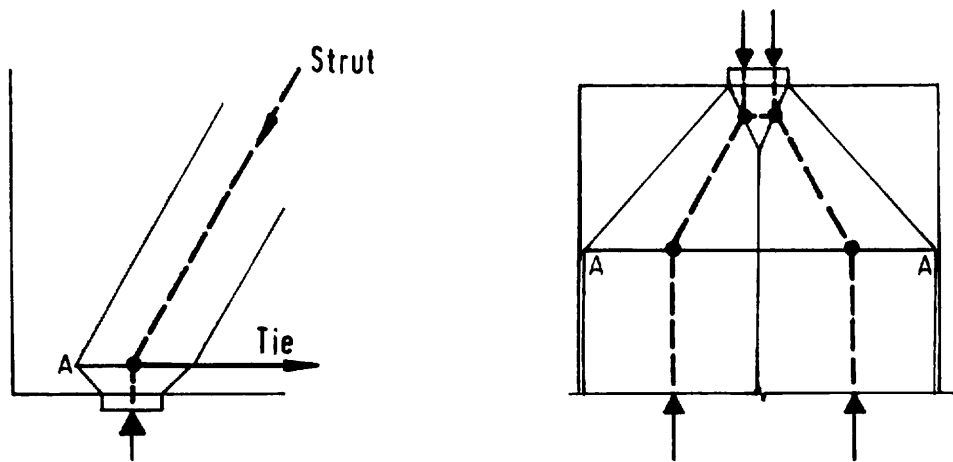
NODES ARE DRAWN AT INTERSECTIONS OF STRUTS AND TIES REPRESENTED
BY LINES AT THEIR CENTRES. TIES MUST EXTEND BEYOND NODES TO COVER
THE FULL WIDTHS OF STRUTS ie EXTEND TO POINTS 'A' ABOVE

Fig. 4.4-1:   *Depiction of strut and tie systems*
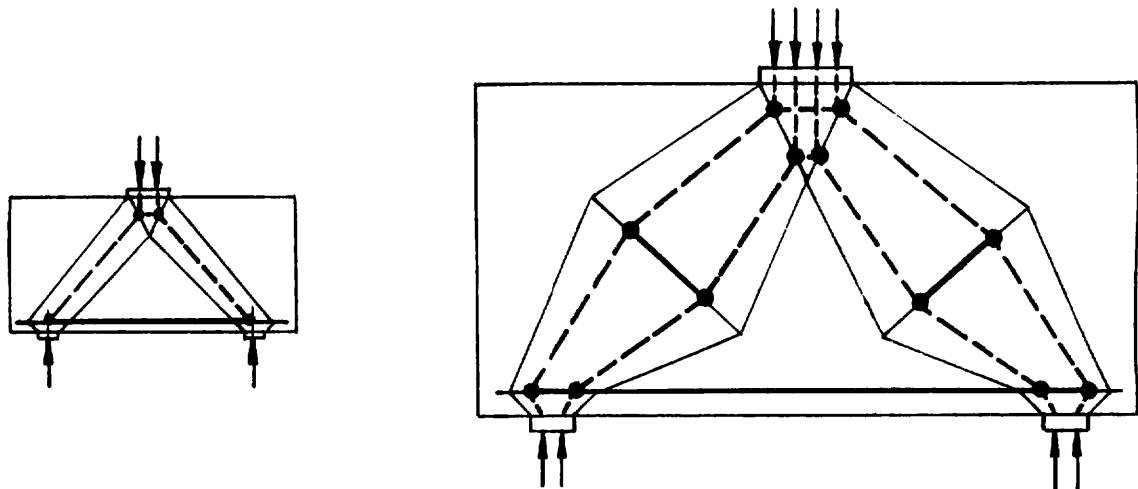
THE DEGREE TO WHICH A MODEL SHOULD BE SIMPLIFIED IS A FUNCTION OF THE SIZE
AND IMPORTANCE OF THE MEMBER IN QUESTION

Fig. 4.4-2:   *Complexity of strut and tie models*

(3)   Limiting stresses for static design

(3.1)   Reinforcement

For steel reinforcement the limit stress in either tension or compression is the design value of the yield stress, $f_{yd} = f_{yk}/\gamma_m$. To be treated as compression reinforcement bars must be prevented from buckling by the provision of adequate cover and links.

The attainment of yield is dependent on the strain at the ultimate limit state and on the stress-strain characteristics of the reinforcement, which may be assumed to be as in Fig.4.4-3, although more correct diagrams may be used if the characteristics of the particular steel are known at the design stage.

The assessment of ultimate limit state strains is practicable in some but not all cases. Where it is impractical the design relies on the modelling process to ensure that bars are in positions and directions such that they will be able to reach the assumed stresses. In some instances, e.g. shear reinforcement in slabs, this may require a limitation of the useful yield stress.

(3.2)   Concrete - generalities

For concrete the situation is more complex. The basic mechanical properties of concrete are described in Chapter 3 and reference should be made there for guidance on special cases. For general use the characteristics require some interpretation and simplification.

There are differences between both the material and its behaviour in standard tests and in structures.

Concrete in a structure is neither compacted not cured in the same way as that in a control cylinder. One significant difference is that, where a considerable depth of concrete is cast in one pour, there is a tendency for water and fine material to rise, while the larger aggregate tends to sink. The result is that the material near the top is weaker. This is specifically accounted for in the treatment of bond, where lower limiting stresses are used for top bars. It is also a reason to be somewhat prudent in the choice of limiting compression stresses for columns.

In standard control tests, concrete is loaded to failure in a few minutes. In structures the loading is normally much slower. There is no requirement for a structure to be able to resist its ultimate limit state design loading indefinitely and the situation normally envisaged is one in which service loading is carried for a long period and then overloading occurs in a matter of hours.

Slow or maintained loading produces creep in concrete and tends to transfer forces from it to compression reinforcement. It leads to a lower peak stress, higher strains and a more ductile stress-strain characteristic. The effects tend to cancel one another at least in flexural compression zones, where slower loading produces lower maximum stresses but higher ratios of average to maximum stress.

The limiting stresses adopted for design are not the results of exact scientific derivations but are reasonable values taking account of the above and of the inevitable variations which

arise from the use of different aggregates and from the variety of environmental conditions to which structures are subject.

The basic need in design is to be able to verify that the resistances of compression zones or struts are sufficient for the forces produced in them by the ultimate limit state design loading. It is necessary that the limits adopted reflect the most important characteristics of the concrete – its uniaxial strength and its ductility. They must also account for the difference in behaviour between uncracked and cracked zones, for example the flexural compression zones and the webs of beams.

(3.3)   Uncracked concrete in compression

The flexural compression zones of beams and columns are the major examples of uncracked struts resisting essentially uniaxial compression. Their behaviour is well understood, but even so the definition of limiting stresses and strains is not totally straightforward.

For a singly reinforced rectangular beam subjected to pure bending

$$M = k_1 k_3 f_c b x (d - k_2 x)$$

where

f_c	is the cylinder strength of the concrete
$k_3 f_c$	is the maximum stress in the compression zone
$k_1 k_3 f_c$	is the average stress in the compression zone
b	is the breadth of the beam
x	is the depth of the compression zone
$k_2 x$	is the depth to the centre of the compression zone

Fig. 4.4-4 shows the variations with extreme fibre strain of:

-	the maximum compressive stress	$k_3 f_c$
-	the average stress	$k_1 k_3 f_c$
-	the compressive force	$F = k_1 k_3 f_c b x$
-	the moment	M

all drawn for a particular beam, using Sargin's stress-strain curve for the concrete (which is used in MC90) and with the tension reinforcement not yielding.

The attainment of a limiting maximum stress ($k_3 f_c = f_c$) is clearly not a suitable definition of the ultimate limit state of a member, which should ideally be defined by the maximum value of M. The problem with treating M or F directly is that their maxima are reached at different extreme fibre strains and average ($k_1 k_3 f_c$) stresses in different members. For practicality the ultimate limit state limit is expressed in terms of the average stress and the extreme fibre strain.

The limits used correspond to the highest average stress in a flexural compression zone and the corresponding extreme fibre strain. They may be expressed either very simply in terms of just these two parameters or in terms of a limit strain and a simplified stress-strain relationship.

ORDINARY REINFORCEMENT
$f_{yd} = f'_{yd} = f_{yk}/1.15$

PRESTRESSING REINFORCEMENT
$f_{pyd} = 0.9\, f_{ptk}/1.15$
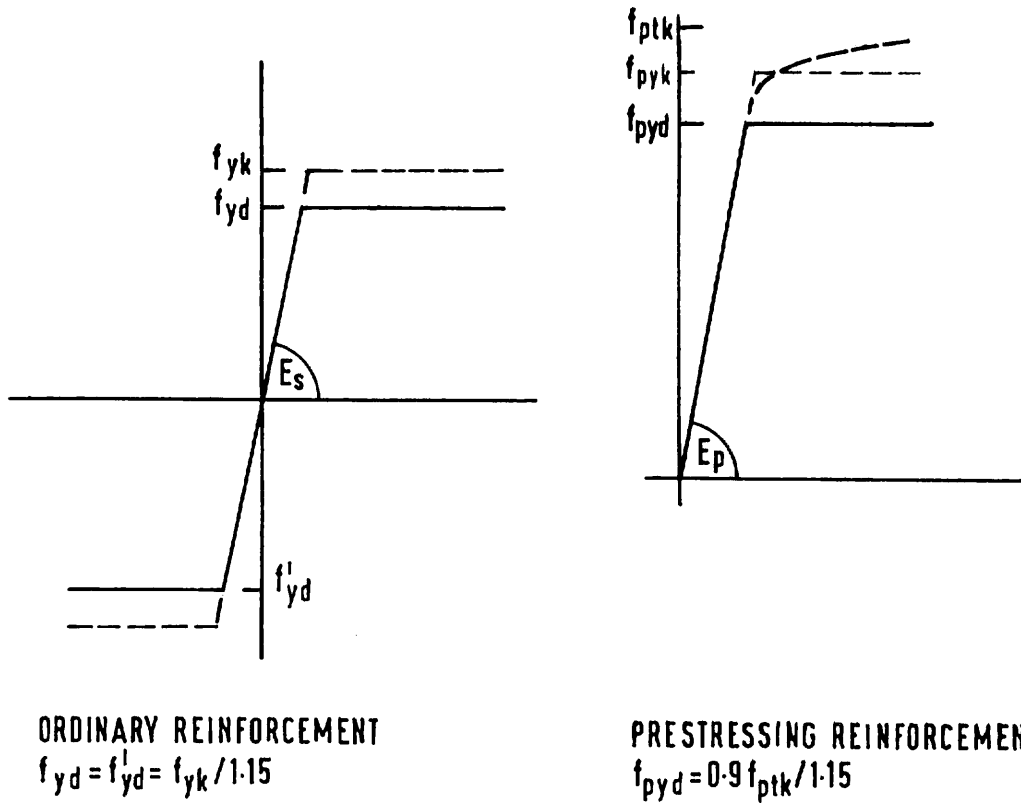
Fig. 4.4-3:   *Stress-strain characteristics of reinforcement for ULS design*

$f_c = 30\,MPa$

$\rho = 0.04$

$F = k_1 k_3\, f_c\, b\,x$
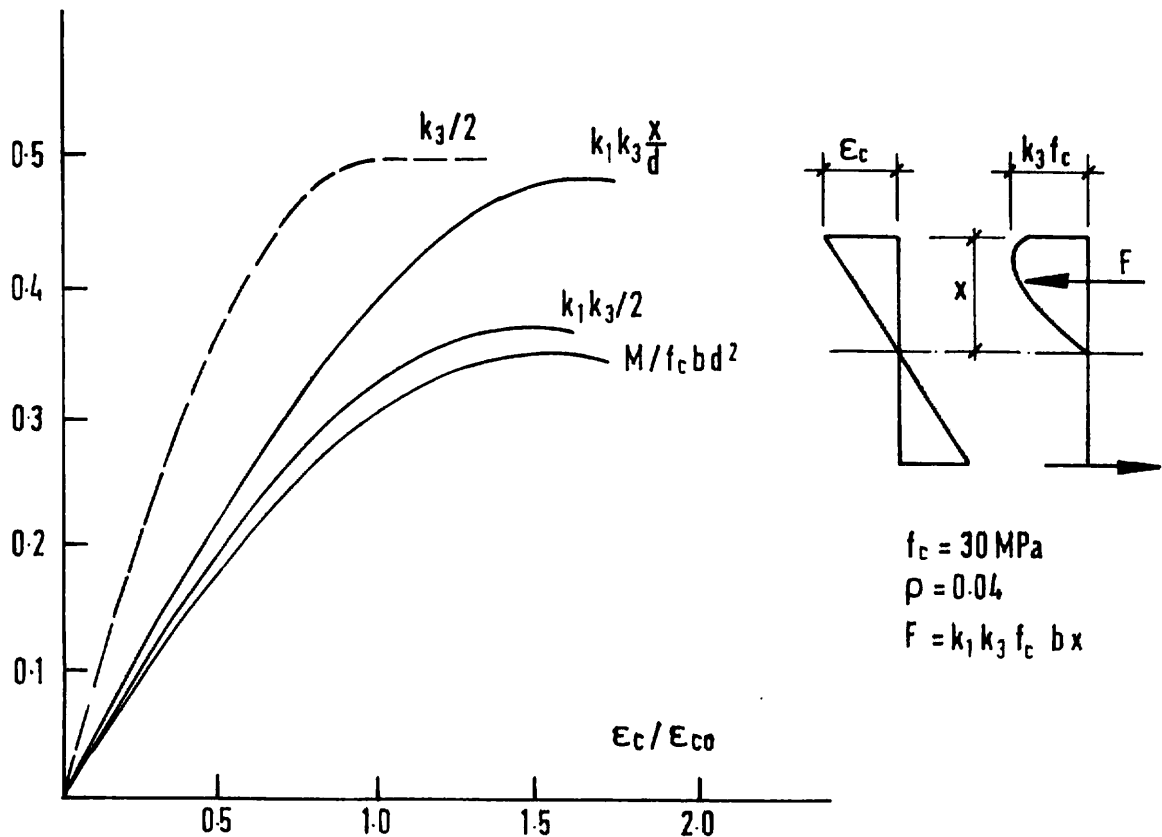
Fig. 4.4-4:   *Variations of stress block functions with extreme fibre strain*

For flexural compression zones the results from either type of expression are practically identical. For compression zones with compressive strains at both edges, for example in columns, the results diverge to some extent. If the same average stress is used as for flexure it is clearly below the peak stress and the maximum strain is greater than the strain at peak stress. This introduces an element of conservatism, which may be desirable in view of the critical function of columns and of the tendency for the strength of concrete to vary over the height of a column. It also allows for the use of higher yield stresses in reinforcement.

The simplified stress-strain relationship allows the use of a higher average stress as the section comes closer to uniform compression but in MC90 the ultimate limit state strain is then limited to that at peak stress.

The expressions for design stresses and strains used in the MC90 are as follows:

For a parabolic-rectangular diagram:

$$\sigma_{cd} = 0.85 f_{cd}\left[2\left(\frac{\varepsilon_c}{\varepsilon_{c0}}\right) - \left(\frac{\varepsilon_c}{\varepsilon_{c0}}\right)^2\right] \quad \text{for } \varepsilon_c < \varepsilon_{c0}$$

$$\sigma_{cd} = 0.85 f_{cd} \qquad\qquad\qquad \text{for } \varepsilon_{c0} \leq \varepsilon_c \leq \varepsilon_{cu} \qquad\qquad (4.4\text{-}1)$$

$$\sigma_{cd} = 0 \qquad\qquad\qquad\qquad \text{for } \varepsilon_{cu} < \varepsilon_c$$

where

$$\varepsilon_{c0} = 0.002$$

For flexure:

$$\varepsilon_{cu} = 0.0035 \qquad\qquad\qquad \text{for } f_{ck} \leq 50\text{MPa}$$

$$\qquad\qquad\qquad\qquad\qquad\qquad\qquad\qquad\qquad\qquad (4.4\text{-}2)$$

$$\varepsilon_{cu} = 0.0035\left(\frac{50}{f_{ck}}\right) \qquad \text{for } 50\text{MPa} < f_{ck} \leq 80\text{MPa}$$

For axial compression:

$$\varepsilon_{cu} = 0.002 \qquad\qquad\qquad\qquad\qquad\qquad\qquad\qquad\qquad (4.4\text{-}3)$$

With a rectangular stress block for both flexure and axial compression

$$f_{cd1} = 0.85\left[1 - \frac{f_{ck}}{250}\right] f_{cd} \qquad\qquad\qquad\qquad\qquad (4.4\text{-}4)$$

$$\varepsilon_{cu} = 0.004 - 0.002\frac{f_{ck}}{100} \qquad\qquad\qquad\qquad\qquad (4.4\text{-}5)$$

where

f_{ck} is in MPa and

ε_{cu} is the maximum extreme fibre strain.

A constant ε_{cu} of 0.0035 could be used in place of equation (4.4-5) above without creating any major problems.

In conditions of biaxial or triaxial compression the stress limit may be considerably higher than f_{cd1} (or f_{cd}).

These expressions were originally derived for concretes with characteristic strengths f_{ck} up to 50 MPa. They are not altogether realistic for higher grades of material as the strain at peak stress (ε_{c0}) rises above 0.002 while the drop of stress at strains beyond ε_{c0} is very rapid.

(3.4)   Cracked concrete in compression

In regions such as the webs of beams containing inclined cracks, compression stress fields act on concrete which is cracked in directions not necessarily parallel to the compression and is also subjected to transverse stresses due to its bond with the stirrups which are in tension.

The need to transmit forces across cracks and the existence of transverse tension (even if this is neglected in the modelling) reduce the compression capacity of the concrete. This reduction has been the subject of much recent research. Collins and his co-researchers in Toronto have treated the concrete and its reinforcement as a single composite material and have derived stress-strain relationships for the principal compression which are functions of the transverse tensile strain. In particular cases these can be approximated by relationships dependent on the angles between the web compression and the main steel of the beam. This work is expressed in terms of overall strains but it can well be argued that the widths of individual cracks must be relevant.

A recent review of research on cracked panels of concrete by Zhang (1997) illustrates the very considerable differences between the various theories and the apparent divergencies in test results.

Given the present state of knowledge only a rather simple approach seems justified for design and MC90 gives a single stress limit:

$$f_{cd2} = 0.6 \left[1 - \frac{f_{ck}}{250} \right] f_{cd} = 0.7 f_{cd1} \tag{4.4-6}$$

The type of failure associated with this limit varies. In regions with high ratios of transverse reinforcement the concrete suffers overall compression failure but where the transverse steel is lighter the failure is by local movements at cracks and associated spalling of the adjacent concrete. The resistance to the first type of failure can readily be calibrated against the results of panel tests and of beam tests analysed on the basis of truss models.

Resistance to the second type is more difficult to verify as test strengths depend primarily on the reinforcement and are relatively insensitive to the concrete's limit stress. In a sense this is convenient as any errors in f_{cd2} have little effect on the results of design.

Equation (4.4-6) has been derived from tests of panels and webs under approximately uniform stresses and with cracking generally not parallel to the final compression. There are instances of compression in cracked concrete where conditions are more favourable. One example is where the cracks are parallel to the final compression. Another more important one is where a compression strut is surrounded by less strained material, which can provide some confinement. In such cases it may be possible to use limit stresses higher than f_{cd2}.

(3.5)   Concrete in tension

Concrete tensile strength is not normally used explicitly in ultimate limit state design. So far as the main longitudinal tensile forces are concerned it is indeed generally not sensible to place reliance on the tensile capacity of concrete as it may be reduced to zero by the effects of settlements or of restrained shrinkage or temperature movements. Such effects are however unlikely to cause longitudinal cracking or to give rise to inclined cracking except in wall like construction.

Tensile resistance is relied upon implicitly in relation to bond and in the shear resistance of members without shear reinforcement, for which limits are imposed on rather nominal bond and shear stresses. These are expressed as functions of the concrete's compression strength, partly because concrete in usually specified in terms of compression strength but also because the complex nature of the phenomena involved make it extremely difficult to define the tension due to loading.

(4)   Axial load and flexure

(4.1)   Basic assumptions

It can be assumed that:

(i)   sections plane in the unloaded state remain plane during loading;

(ii)   bonded reinforcement undergoes the same strain increments as the adjacent concrete;

(iii)   at the ultimate limit state the maximum strain of the concrete is equal to ε_{cu};

(iv)   tension in the concrete can be neglected.

The modelling of internal forces resisting pure axial load and flexure is trivial as it involves only longitudinal struts and ties.

(4.2)   Pure bending of ordinary reinforced concrete

For a simply supported rectangular section in bending, the ultimate limit state situation is as illustrated in either Fig.4.4-5 a) or b) where rectangular stress blocks have been used to represent the concrete compression.

In case (a) the reinforcement has yielded and the condition of longitudinal equilibrium gives:

$$x = \frac{A_s f_{yd}}{b f_{cd1}}$$

(4.4-7)

Taking moments about the centre of compression the design resistance moment

$$M_{Rd} = A_s f_{yd} \left[d - \frac{A_s f_{yd}}{2 b f_{cd1}} \right]$$

(4.4-8)

or writing $A_s/bd = \rho$.

$$\frac{M_{Rd}}{f_{cd1} bd^2} = \frac{\rho f_{yd}}{f_{cd1}} \left[1 - \frac{\rho f_{yd}}{2 f_{cd1}} \right]$$

(4.4-9)

In case (b), which should not normally arise in design, the reinforcement has not yielded and longitudinal equilibrium requires

$$b x f_{cd1} = A_s E_s \varepsilon_{cu} \left(\frac{d-x}{x} \right)$$

(4.4-10)

With $A_s/bd = \rho$ and $E_s \varepsilon_{cu}/f_{cd1} = \lambda$

$$\frac{x}{d} = \frac{1}{2} \left[\sqrt{(\rho\lambda)^2 + 4(\rho\lambda)} - \rho\lambda \right]$$

(4.4-11)

and

$$\frac{M_{Rd}}{f_{cd1} bd^2} = \frac{x}{d} \left[1 - \frac{x}{2d} \right]$$

(4.4-12)

To avoid the situation of over-reinforcement in which the concrete fails in compression before the main steel yields, it is common practice to limit (x/d) to 0.5. Then, if the design moment M_{sd} exceeds $0.375 \, f_{cd1} bd^2$, compression reinforcement is added to resist the excess moment. So long as the compression steel yields:

$$A'_s f_{ycd} = \frac{M_{Sd} - 0.375 f_{cd1} bd^2}{d - d'}$$

(4.4-13)
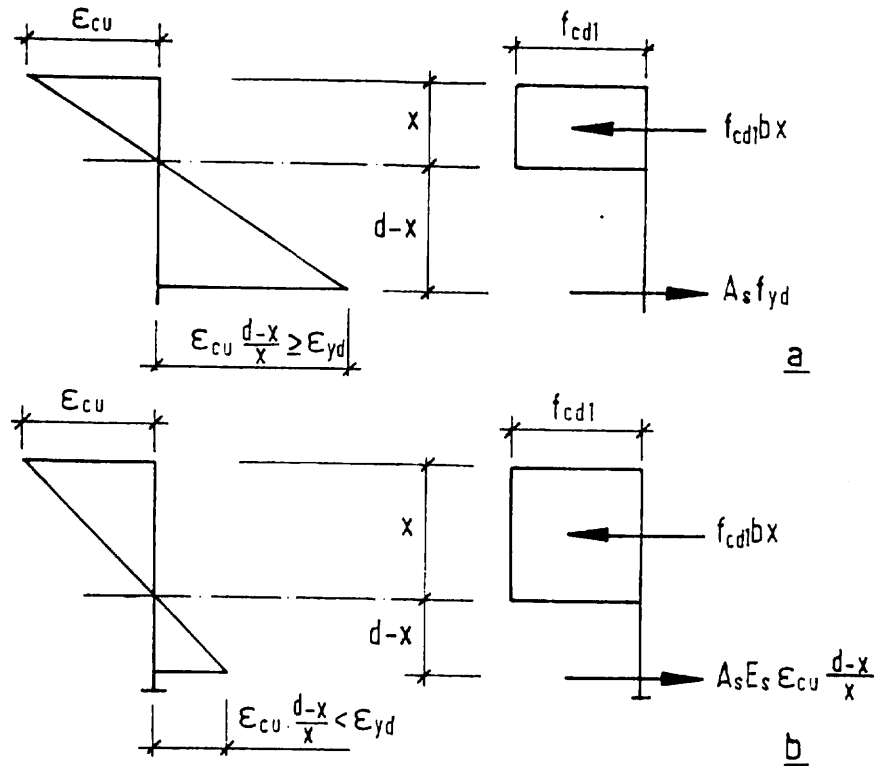
Fig. 4.4-5:   *ULS strains and stresses for sections in pure bending*
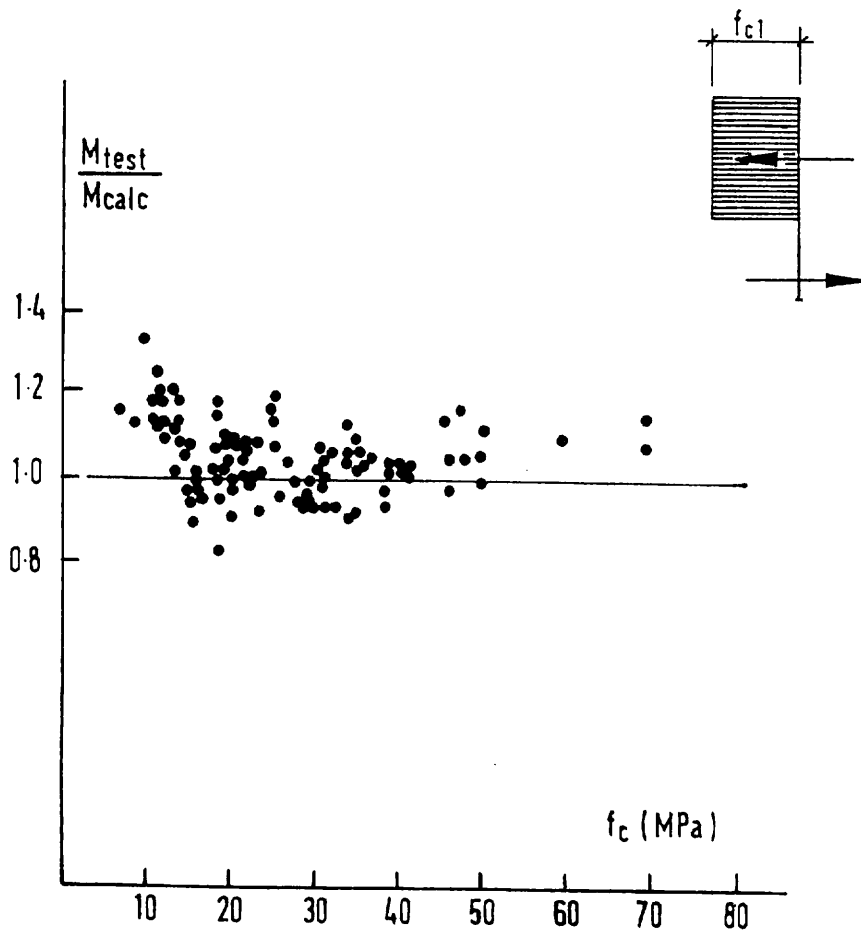

Fig. 4.4-6:   *Comparisons of experimental and calculated ultimate moments for over-reinforced beams*

$$A_s f_{yd} = 0.5 f_{cd1} bd + A_s' \frac{f_{ycd}}{f_{yd}}$$ (4.4-14)

It is necessary to check that the compression steel will yield and for this the condition is:

$$\varepsilon_{cu} \frac{x - d'}{x} \geq \frac{f_{ycd}}{E_s}$$ (4.4-15)

If this condition is not met the stress in the compression steel will be $f_{sc} = \varepsilon_{cu} E_s \left(\dfrac{x - d'}{x} \right)$ and an iterative solution will be required for x.

The limitation of x to 0.5d is slightly more severe than the 0.6d referred to in MC90. 0.6d is adequate for the development of the design yield stress (435 MPa) of a grade 500 steel, but is insufficient for developing the actual yield stress even where ε_{cu} is not reduced below 0.0035.

The expressions above apply to flanged beams so long as $h_f \geq x$.

Although over-reinforced cross-sections are normally undesirable in design, test results from them do provide a valuable check on the appropriateness of values for f_{cd1} and ε_{cu} since their ultimate moments are much more dependent on the behaviour of the concrete than is the case for under-reinforced members.

Over-reinforcement will be the normal situation in members where fibre reinforced plastics are used as main reinforcement, since these materials have high yield stresses and low elastic moduli.

Fig.4.4-6 presents a comparison of test data from Granholm (1965) and others with predictions based on equations (4.4-11 and 12) using mean experimental cylinder strengths in place of f_{cd} and f_{ck} in the MC90 stress limits. The ratios of experimental and calculated moments can be seen to be substantially independent of f_c. There is a scatter in the ratios, but this can probably be attributed to tolerances in effective depths (many of the specimens were small) and to the use of reinforcement with somewhat non-linear behaviour before yield.

(4.3)   Combined axial load and bending

For members subjected to flexure and axial load the range of possible ultimate limit state situations in regard to strains is large, with various permutations of yielding and elastic behaviour in at least two sets of reinforcement - see Fig.4.4-7.

With ε_{cu} known, a value for x can be assumed and the corresponding forces and moments for uniaxial bending can be calculated straightforwardly. This is the basis of the many design charts available for use with limit state design codes.

The case of axial loading on short columns is another one, which, while rare in practice, provides a check on the limit stresses and strains for concrete. If the limit strains were not
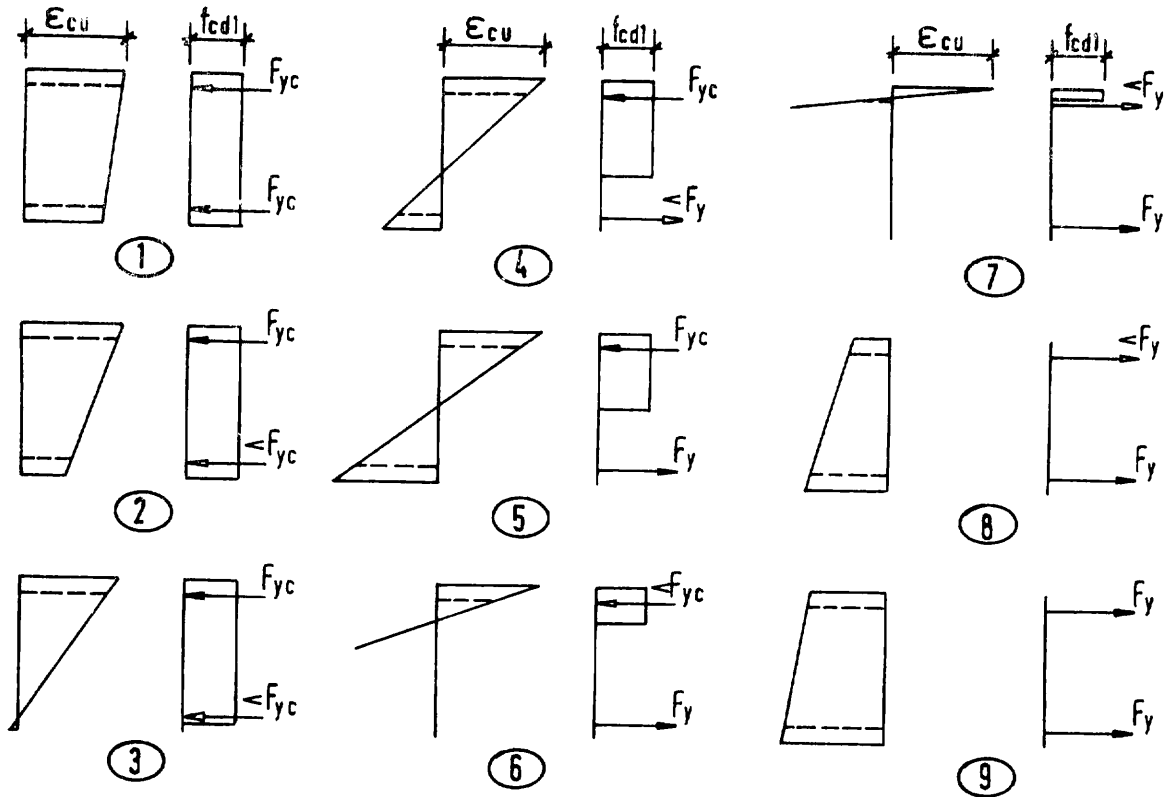
Fig. 4.4-7:   ULS strains and stresses/forces for a member subjected to axial load and bending

PARABOLIC RECTANGULAR DIAGRAM
Max. stress = 0.85 f$_c$ Max. strain = 0.002

RECTANGULAR DIAGRAM
Max. stress = 0.85 f$_c$ [1 – f$_c$ / 250]
Max. strain = 0.004 – 0.002 f$_c$ /100
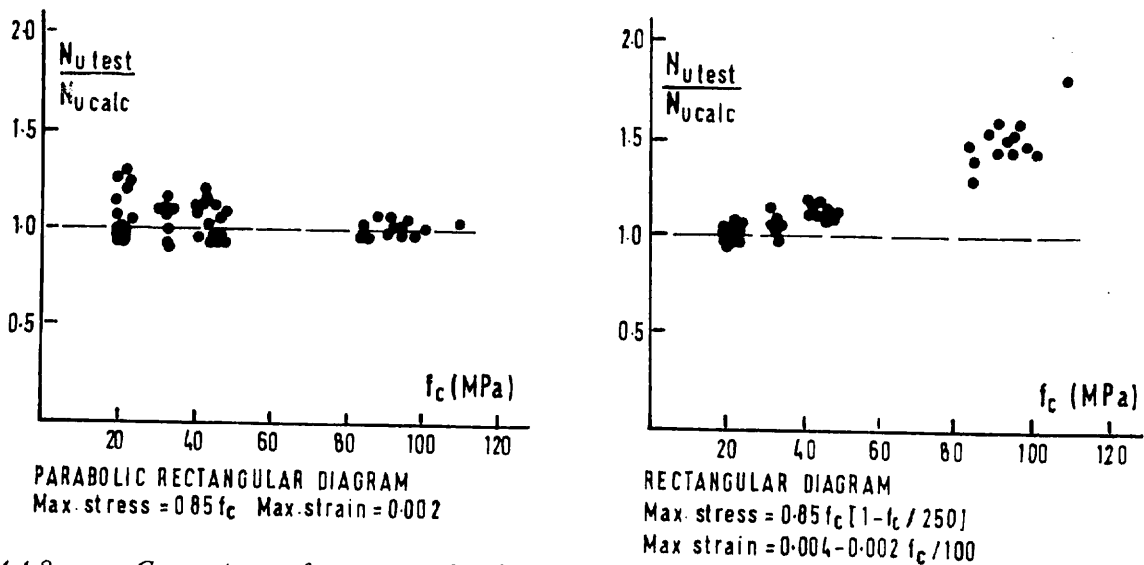
Fig. 4.4-8:   Comparisons of experimental and calculated strengths of axially loaded columns
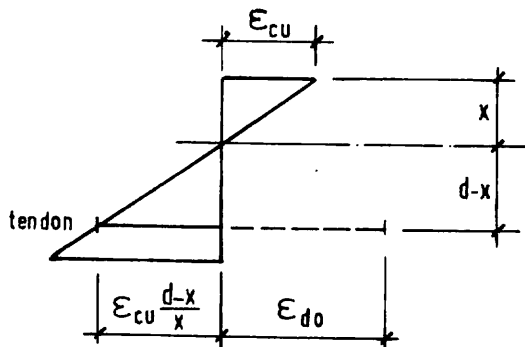

Fig. 4.4-9:   ULS strains in a prestressed section

reasonable problems could arise in columns reinforced with high strength steels due to failures to predict when the reinforcement would or would not yield.

There is also the apparent problem that the use of the rectangular stress block, or simple average stress, limits the concrete's resistance to a value lower than the peak ($0.85 \, f_{cd}$) of the parabolic rectangular diagram.

Fig.4.4-8 shows the results of a comparison of test results by Søpler (1978), Hoff (1979) and Al-Hussaini (1993) with predictions made using both of MC90's sets of limiting stresses and strains, again with the mean strength f_c replacing both f_{cd} and f_{ck}.

The parabolic-rectangular diagram can be seen to give good results in most cases, while the simple average stress method is a little conservative for high strength concretes.

(4.4)   Bending of prestressed concrete

In MC90, the design value (P_{do}) of the prestressing force in a tendon is defined as the force, after losses, and when the stress in the surrounding concrete is zero.

Since a bonded tendon undergoes the same changes of strain as the surrounding concrete, the strains at the ultimate limit state of a section are as shown in Fig.4.4-9.

The total strain of the tendon is

$$\varepsilon_p = \varepsilon_{do} + \varepsilon_{cu} \frac{d - x}{x} \tag{4.4-16}$$

where

ε_{do} is the strain corresponding to P_{do}.

If the simple stress-strain diagram of Fig.4.4-3 is used, the tendon force can be calculated as

$$A_p E_p \varepsilon_p \leq A_p f_{pyd} \tag{4.4-17}$$

The position of the neutral axis can be calculated much as for ordinary reinforced concrete. If the tendon and any supplementary non-prestressed reinforcement yield in a singly reinforced beam

$$x = \frac{A_p f_{pyd} + A_s f_{yd}}{b f_{cd1}} \tag{4.4-18}$$

where

b is the (uniform) breadth of the compression zone.

If there are bonded tendons within the ultimate limit state compression zone, the forces in them will be decreased because of the shortening of the concrete and will become

$$A_p E_p \left(\varepsilon_{do} - \frac{x - d'}{x} \right) \not< A_p E_p (\varepsilon_{do} - 0.0015) \qquad\qquad (4.4\text{-}19)$$

The limit of 0.0015 for the reduction of strain is imposed because the maximum strains in the concrete may exist only over a short length and the bond-slip characteristics of grouted tendons are such that the tendon strain may not follow a local peak of concrete deformation. The restriction seems to be unnecessary for pretensioned members.

(5)   Combined shear and flexure

(5.1)   Shear cracking

All practical beams and slabs develop flexural cracks before flexural failure. Some also develop shear cracks and the onset of shear cracking is an important stage. For most members without shear reinforcement it is the cause of immediate failure, while in members with shear steel it marks the transition from beam to truss action.

In the absence of flexural cracking shear is resisted by tensile and compressive stresses in the concrete and shear, or inclined, cracking occurs when the tension in the web reaches the resistance of the concrete.

In practice there is little interest in the shear cracking resistance of uncracked sections of ordinary reinforced concrete, but it is of importance in prestressed members and members subjected to high axial compression and is treated in Section (5.4). For ordinary reinforced concrete, the important shear cracking resistance is that of sections cracked in flexure.

Fig.4.4-10 a shows a part of a beam containing flexural cracks. At the sections of the cracks, the shear is resisted by three actions - shear stresses in intact concrete above the cracks, shear transfer between the crack faces and dowel action by the main reinforcement.

If the presence of flexural cracks did not result in local reductions of shear stiffness, the distributions of stresses would be as in Fig.4.4-10 b and shear cracking would be expected to occur when the shear stress $\tau = V/bz$ reached the tensile strength of the concrete. At the opposite extreme, if no shear were transmitted across cracks, the "teeth" of concrete between the cracks would have to behave as cantilevers, fixed in the compression zone and loaded by bond forces at the level of the main steel, as in Fig.4.4-10 c. In this case the resistance of the system would be limited by the flexural strengths of the cantilevers.

Reality lies between these two extremes. The cracks are relatively narrow and their surfaces are not smooth planes. They have overall roughness and aggregate particles project from the fracture surfaces. As a result, any vertical movement at a crack gives rise to shear across the crack. Such vertical movements are produced by even limited flexure of the teeth and by any curvature of cracks. Vertical movements at cracks also produce dowel forces in the main bars.

The exact mechanism of shear cracking is uncertain, but it involves the widening of flexural cracks leading to a reduction in the stiffness of the transfer of shear across them, inclined

shear in uncracked
compression zone

shear transferred
across cracks

dowel force

bond force from
main bars
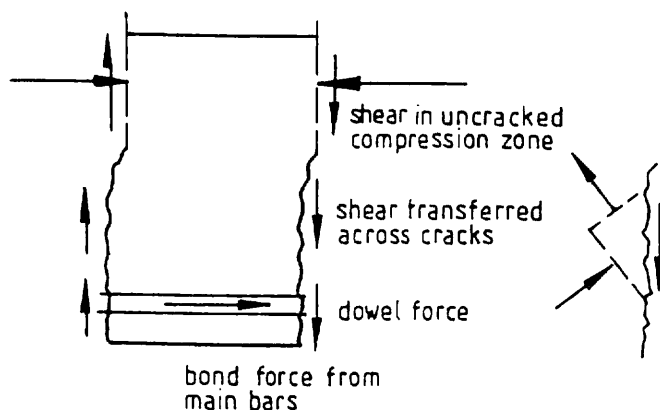
**actions resisting shear in a beam with
flexural cracks**   a)

$$\tau = \frac{V}{bz}$$ b)   c)
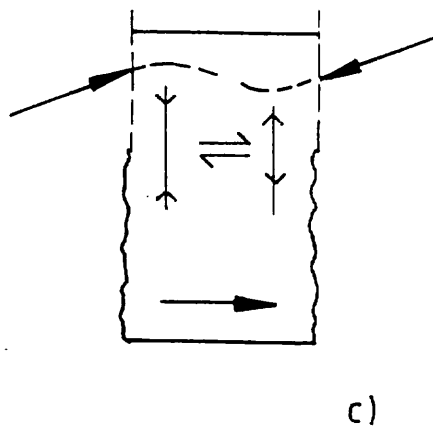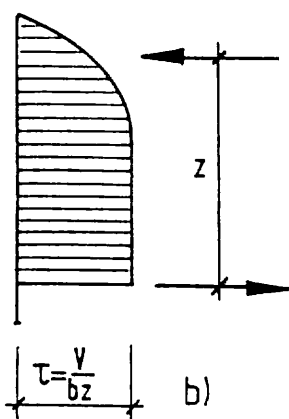
**extreme possibities of behaviour
b) no loss of shear transfer at cracks
c) complete loss of shear transfer at cracks**

Fig. 4.4-10:   *Shear resistance of beams with flexural cracks*

tension resulting from the combination of shear and vertical tension near the crack tips and vertical tension at the level of the main bars resulting from dowel action.

Various somewhat divergent analyses of shear cracking have been proposed, but the main factors determining shear cracking loads for rectangular, I and T sections are fairly well established as:

- the dimensions of the section, b_w and d
- the properties of the concrete
- the ratio of flexural tensile reinforcement based on the web breadth, $A_s/b_w d$
- the effective depth of the section.

The ratio of moment to shear at the section considered (M/Vd) has a lesser influence, which is commonly neglected in design formulae. This neglect is reasonable provided that the formulae relate to the greatest value of (M/Vd) at which shear cracking can precede flexural failure.

The design resistance to shear cracking at sections already cracked in flexure is given in MC90 as:

$$V_{Rd} = 0.12\xi \sqrt[3]{\left(\frac{100A_s}{b_w d}f_{ck}\right)}b_w d \qquad (4.4\text{-}20)$$

where

$\xi = 1 + \sqrt{200/d}$ with d in mm.

This expression is applicable for members of concretes made with normal dense aggregates and having strengths f_c up to 50 MPa.

If lightweight aggregates are used, or if the concrete strength is very high, the flexural tensile cracks may go through rather than around aggregate particles thus reducing the stiffness of the action transferring shear across the bending cracks. The resulting loss of shear transfer at the cracks can mean that there is no increase in shear resistance with further increases of concrete compression strength. There are even examples of reductions of shear cracking resistances as concrete strengths increase.

The problem is particularly severe in deep members, where the reduction in the roughness of crack surfaces combines with increasing crack widths. Equation (4.4-20) implicitly assumes that the influence of longitudinal reinforcement can be expressed simply in terms of the ratio ρ. This is true for its control on the heights of flexural cracks and thence the area of the uncracked compression zone and the spans of the partially cantilevering teeth. It is less true for the dowel action that depends largely on the diameter of the main bars, which tends to be a smaller fraction of 'd' in large members. It is also not universally true for the control of crack widths. If a member is very deep, satisfactory control over the widths of flexural cracks in the web requires the use of additional horizontal bars above the level of the main steel - see Section 4.3 (2).
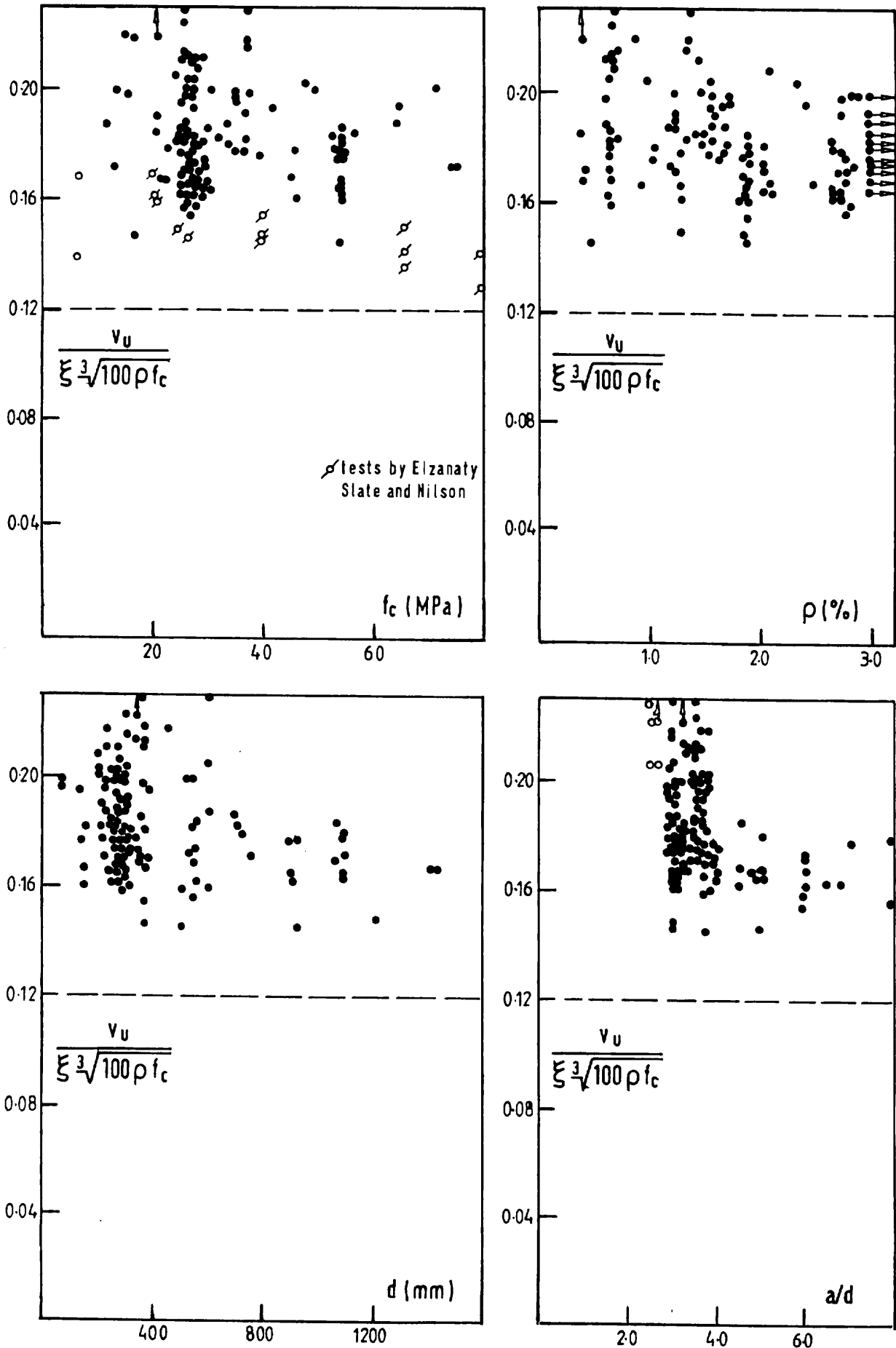
Fig.4.4-11 compares equation (4.4-20) with results from tests of rectangular beams without shear reinforcement. The data comes from Aster and Koch (1974), Bhal (1968), Kani (1967), Kim and Park (1994), Leonhardt and Walther (1962), Morrow and Viest (1957), Mphonde and Frantz (1984), Petersson (1983) and Regan (1998). Most results are repeated in all parts of the figure and are plotted as solid symbols. A few results from these sources for very low concrete strengths and low shear span/effective depth ratios are plotted only in relation to these parameters and are indicated by open symbols, as are data from Elzanaty, Nilson and Slate (1986), shown only in Fig.4.4-11 a.

In overall terms, the results show a characteristic strength level consistent with equation (4.4-20) with the constant 0.12 replaced by 0.16, implying a partial safety factor of 1.33. This is below the 1.5, which might perhaps be expected, but higher than the 1.14 obtained if γ_m is applied to f_{ck} in the expression.

Fig.4.4-11 a shows that the cube root relationship is generally a satisfactory expression of the influence of the concrete compression strength over a wide range of f_c, but the results from Elzanaty show practically no increase of shear resistance for concrete strengths above 50 MPa. This illustrates the reason for limiting the applicability of equation (4.4.20) to $f_{ck} > 50$ MPa unless information on the particular concrete is available.

Fig.4.4-11 d shows that for a/d < 3.0 the shear resistance of beams, loaded from above and supported from below, increases significantly as a/d decreases. For short shear spans, shear resistance should be treated by strut and tie modelling - see Section 4.4 (4).

(5.2)   Beams with shear reinforcement

The behaviour of a beam containing shear cracks can be represented by truss models such as those of Figs.4.4-12 a and b, in which each model stirrup represents a number of actual stirrups. The truss of Fig.4.4-12 a is statically determinate, whereas the model in Fig.4.4-12 b, which may appear more realistic, is strictly speaking indeterminate. This is however primarily a matter of representation, as determinacy can be restored by assuming the stirrup forces in the latter truss to be equal, in which case the stirrup force per unit length of beam is the same in either system. Figs.4.4-12 c and d show alternative more detailed models of the region near the support. They both give the same resultant web force at the support as the original system of part a.

The angle θ between the horizontal and the web compression is not fixed to any particular value, since even if cracks may exist at a given inclination shear can be transferred across them. It has a lower limit of about 18.4° (cot θ = 3) imposed by the difficulty of force transfer across cracks at very low inclinations.

Considering vertical equilibrium at section AA of Fig.4.4-13

$$V = A_{sw}\sigma_{sw}(z\cot\theta)/s \qquad\qquad (4.4\text{-}21)$$
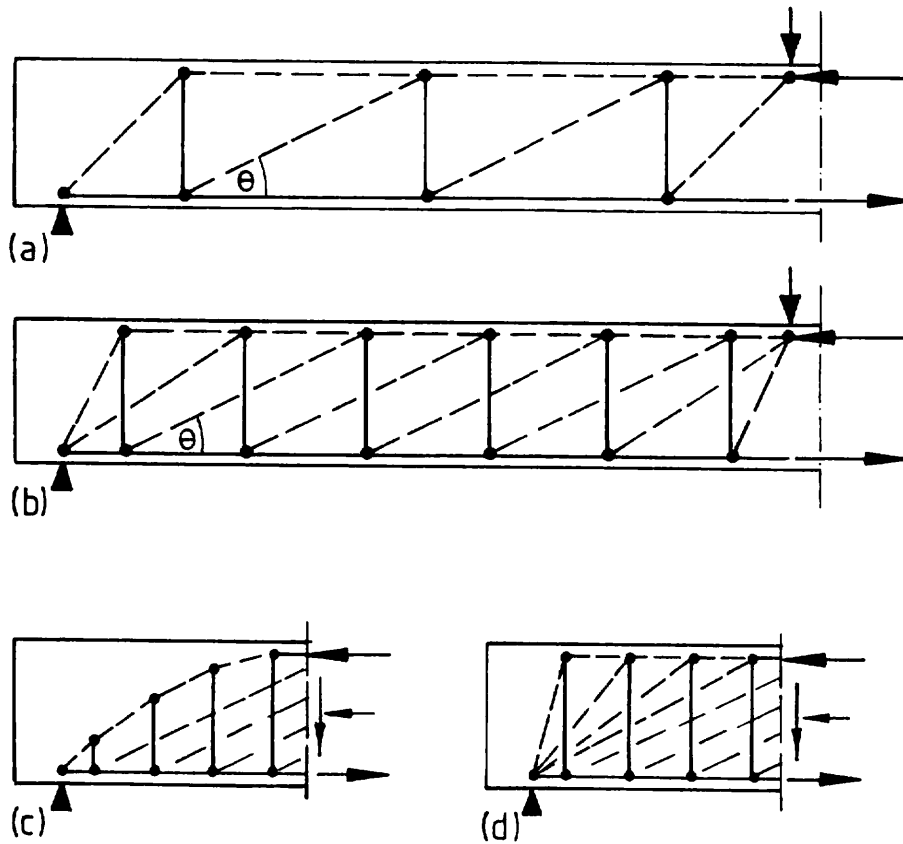
Fig.4.4.12:   Truss modelling

Fig.4.4-13:   Equilibrium conditions in a truss model

(a) DIRECT LOADING   (b) INDIRECT LOADING [if suspension steel
                                          is not provided]
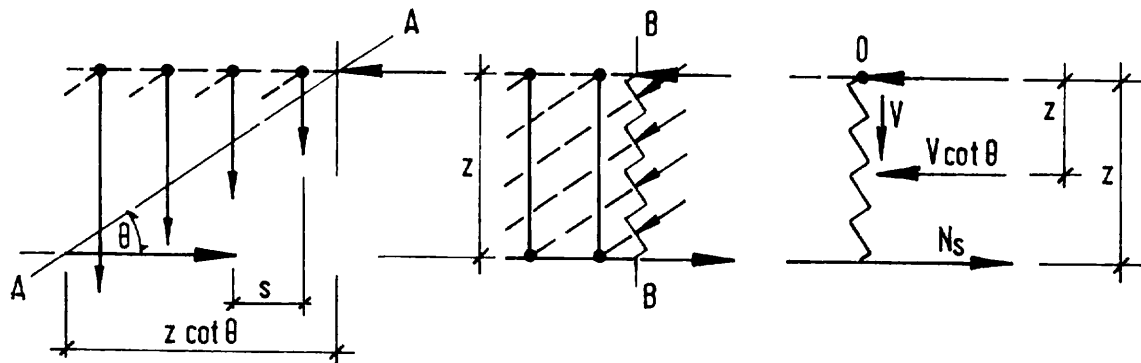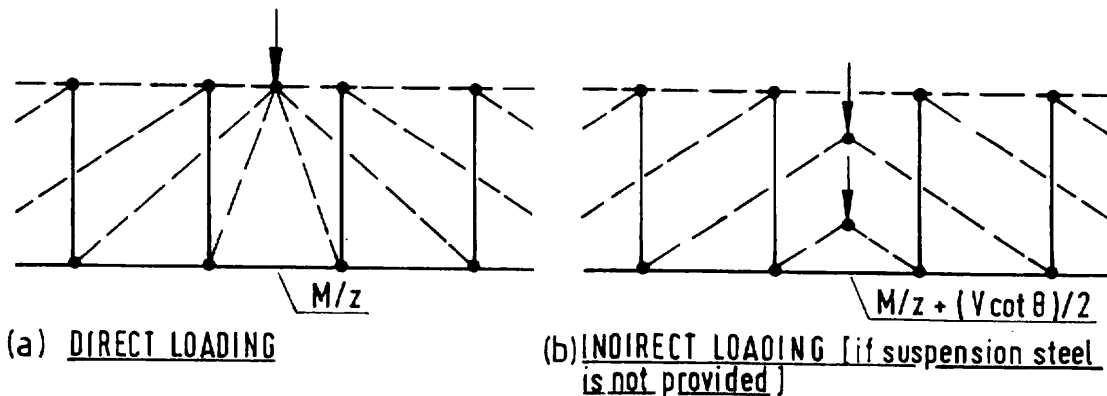
Fig.4.4-14:   Forces in main steel at sections of maximum moment

where

A_{sw} is the area of one stirrup,

σ_{sw} is the stirrup stress, and

s   is the spacing of the stirrups

z   is the internal lever arm and can be taken to be constant throughout a length over which the moment retains the same sign. Its value can be taken as the ultimate limit state value for flexure at the section of maximum moment.

Considering vertical equilibrium at section BB of Fig.4.4-13 and assuming the stirrups are sufficiently closely spaced (s/d≤ 0.75) for the concrete to be taken to be uniformly stressed

$$V = \sigma_{cw} b_w z \sin\theta\cos\theta$$

(4.4-22)

where

σ_{cw} is the compressive stress in the web concrete.

Finally considering equilibrium of moments about 0 in Fig.4.4-13.

$$M = N_s z - \frac{1}{2} V z \cot\theta$$

(4.4-23)

Equations (4.4-21 to 23) are sufficient for design and allow the designer to choose an angle θ, so that the web concrete is not overstressed

$$\sigma_{cw} = \frac{V_{Sd}}{b_w z \sin\theta\cos\theta} \leq f_{cd}$$

(4.4-24)

the stirrups are sufficient

$$\sigma_{sw} = \frac{V_{Sd}s}{A_{sw} z \cot\theta} \leq f_y$$

(4.4-25)

and the resistance of the tension chord is satisfactory

$$N_{sRd} \geq \frac{M_{Sd}}{z} + \frac{V_{Sd}\cot\theta}{2}$$

(4.4-26)

If all the main steel is within the breadth of the web, N_{sRd} is equal to the force that can be developed by the main bars at the section in question. If some of the steel is in the outer parts of a tension flange N_{sRd} is reduced by the presence of inclined compressions in the flange as explained in Section (5.3).

Where loads act directly on the top surface of a member, the value of N_s in a zone with moments of a given sign is never greater than M_{max}/z, as the web force V cot θ is not present at the section of maximum moment, Fig.4.4-14 a. However, where the loading is indirect or the

beam frames into a diaphragm, equation (4.4-26) may still be applicable - see Fig.4.4-14 b - depending on the detailing of the junction.

If the shear resistance of a beam is controlled by the stirrups and web concrete alone, i.e. if condition (4.4-26) is not critical, it can be assumed that the stirrups will yield, so long as it is favourable for them to do so, and that the web concrete will reach its limiting compression. Then in design terms, from equation (4.4-21)

$$V_{Rd} = A_{sw}f_{yd}(z\cot\theta)/s \tag{4.4-27}$$

and from equation (4.4-22)

$$V_{Rd} = f_{cd2}b_w z \frac{\cot\theta}{1+\cot^2\theta} \tag{4.4-28}$$

Setting these two equal and writing $\rho_w = A_{sw}/b_w s$

$$\cot\theta = \sqrt{\left(\frac{f_{cd2}}{\rho_w f_{yd}} - 1\right)} \tag{4.4-29}$$

$$\frac{V_{Rd}}{b_w z f_{cd2}} = \sqrt{\frac{\rho_w f_{yd}}{f_{cd2}}} \sqrt{1 - \frac{\rho_w f_{yd}}{f_{cd2}}} \le \frac{3\rho_w f_{yd}}{f_{cd2}} \le 0.5 \tag{4.4-30}$$

The first of these limits corresponds to the limiting truss angle of 18.4° and the second to $\theta = 45°$; the value above which vertical stirrups will not yield.

The relationship between $V_{Rd}/b_w z f_{cd2}$ and $\rho_w f_{yd}/f_{cd2}$ is show in Fig.4.4-15 and compared there with test results from Hamadi and Regan (1980), Placas and Regan (1971), Regan and Rezai-Jorabi (1987), Regan (1980) and Watanabe and Kabeyasawa (1997).

A minimum amount of stirrups is required to ensure that failure does not occur immediately upon shear cracking and that a truss action is developed. The minimum defined in MC90 is equivalent to

$$(\rho_w f_{yd})\min \ge 0.06(f_{ck})^{2/3} \tag{4.4-31}$$

f_{ck} (MPa)	15	20	30	40	50	60	70	80
$(\rho_w f_{yd})_{min}$ MPa	0.32	0.39	0.50	0.61	0.71	0.80	0.89	0.97

Table 4.4-1:   Minimum shear reinforcement ratio

As with shear cracking this method of design relies upon the concrete's ability to transfer forces across cracks. With web reinforcement present the problem of excessive crack widths is reduced and available experimental evidence suggests that the method can be used safely with values of f_{ck} up to 80 MPa.
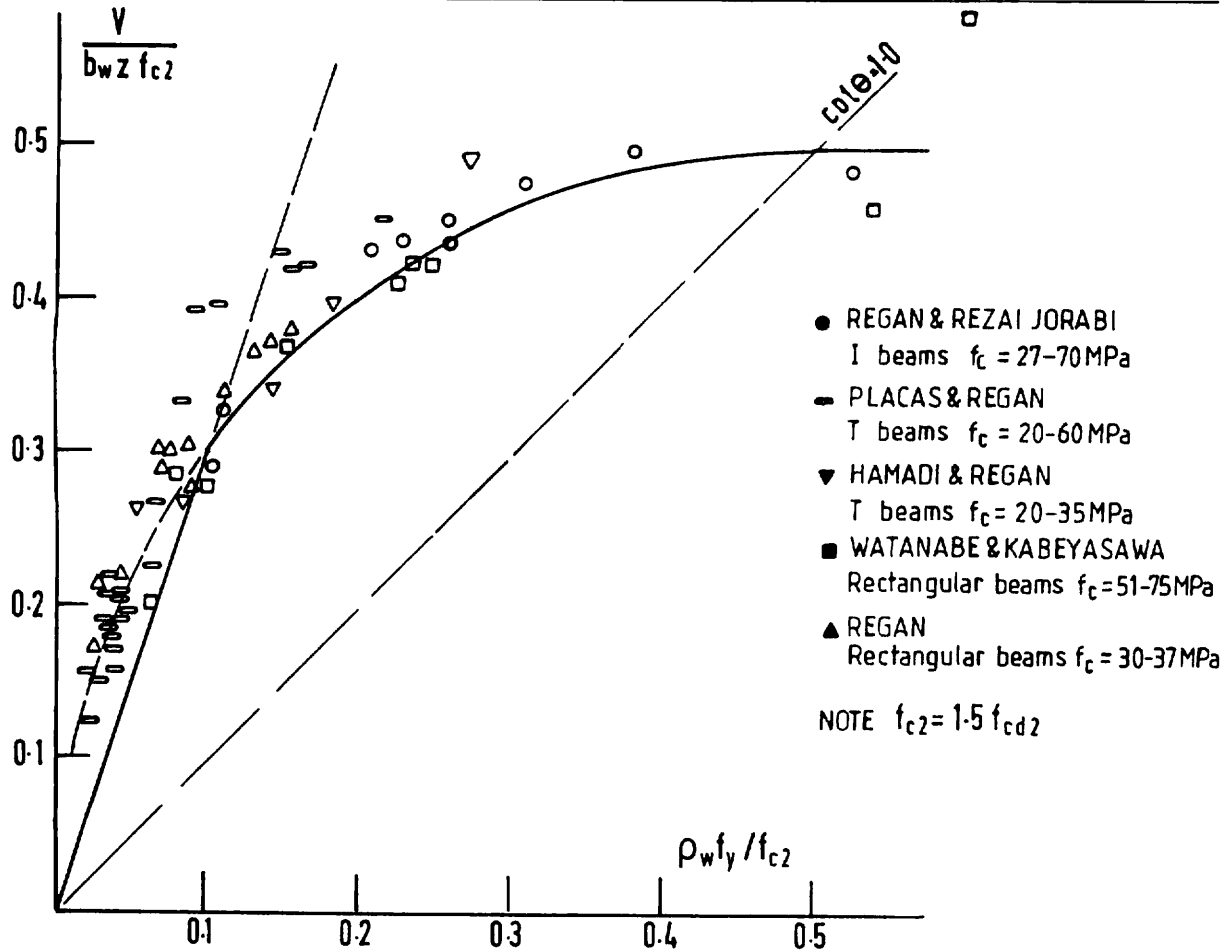
Fig.4.4-15: *Beams with vertical stirrups - relationship between shear strength and stirrup reinforcement*
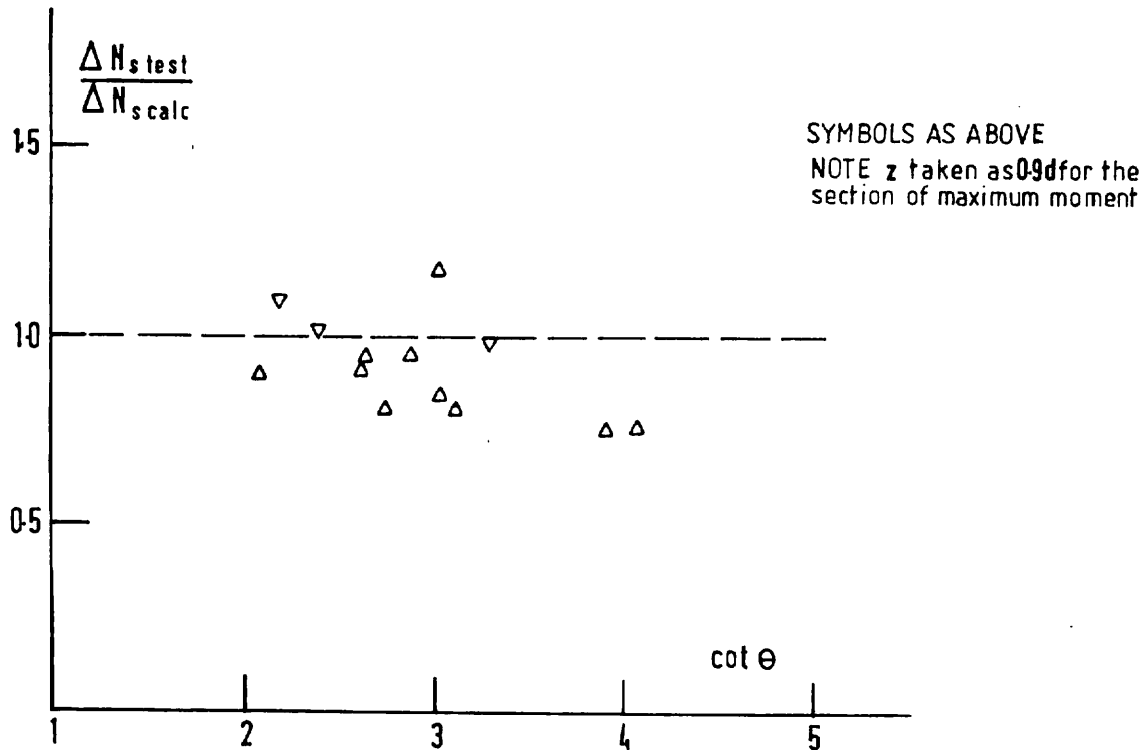

Fig.4.4-16: *Forces in main steel at supports of beams failing in shear - comparison with test results*

As a design method it may be convenient to determine the maximum possible value for cot θ from equation (4.4-28)

$$\cot\theta = \sqrt{\frac{1}{1-\left(V_{Sd}/f_{cd2}b_w z\right)^2}} \not> 3.0 \tag{4.4-32}$$

The design can be based on this cot θ, but a smaller value may be preferable if it is desired to curtail main steel or if there would be a problem in providing an end anchorage for the reinforcement at a simple support, for the force ½V cot θ. A design example is given at the end of Section (5.3).

A very important feature of truss modelling as compared with more empirical design methods is that it allows the distribution of force along the main steel to be rationally assessed, and this is very necessary if the curtailment of main bars is to be treated properly. Its assessments are relatively accurate as is shown by the test results presented in Fig.4.4-16. The values of ΔN_s, i.e. N_s - M/z, from the experiments have been determined from measured strains ignoring any tension stiffening by the concrete, while the theoretical ones have been derived from known ultimate loads taking cot $\theta = V_u/b_w z \rho_w f_y$.

The simple method of truss modelling can readily be applied to continuous beams (Fig.4.4-17 a), beams with uniformly distributed loads (Fig.4.4-17 b), tapered beams (Fig.4.4-17 c), and beams subjected to axial tension in addition to bending and shear (Fig.4.4-17 d).

In the case of continuous beams it should be noted that there is tension in both the top and bottom steel at sections of contraflexure and excessive curtailment can lead to failure at a diagonal crack in such a region. This was the main cause of a collapse in a USAF base in the 1950's [Elstner and Hognestad (1957)]. At the time the failure was attributed to the effect of axial tension, but this is unlikely to have been a real problem for the shear strength as can be seen from Fig.4.4-18.

For tapered beams the basic equations must be slightly extended to allow for the chord forces having both vertical and horizontal components. There is also a slight degree of approximation in assuming the inclined compression in the web concrete to be uniform over a vertical section. Rather than using the equations it may be preferable to make design calculations directly from the model truss. In this case it should be observed that the load acting at any node must be concentric with the node.

If the shear reinforcement is inclined rather than vertical, the basic equilibrium conditions become (see Fig.4.4-19).

At a vertical section

$$V = A_{sw}\sigma_{sw} \sin\alpha \frac{z\cot\alpha}{s} + \sigma_{cw}b_w z \sin\theta\cos\theta \tag{4.4-33}$$

At a section parallel to the web compression

a) Continuous beam

b) Uniformly loaded beam

shear force
shear reinforcement required

c) Tapered beam

d) Beam subjected to axial tension

$$\frac{M}{z} - \frac{V\cot\theta}{2} - \frac{N}{2}$$

$$\frac{M}{z} + \frac{V\cot\theta}{2} + \frac{N}{2}$$
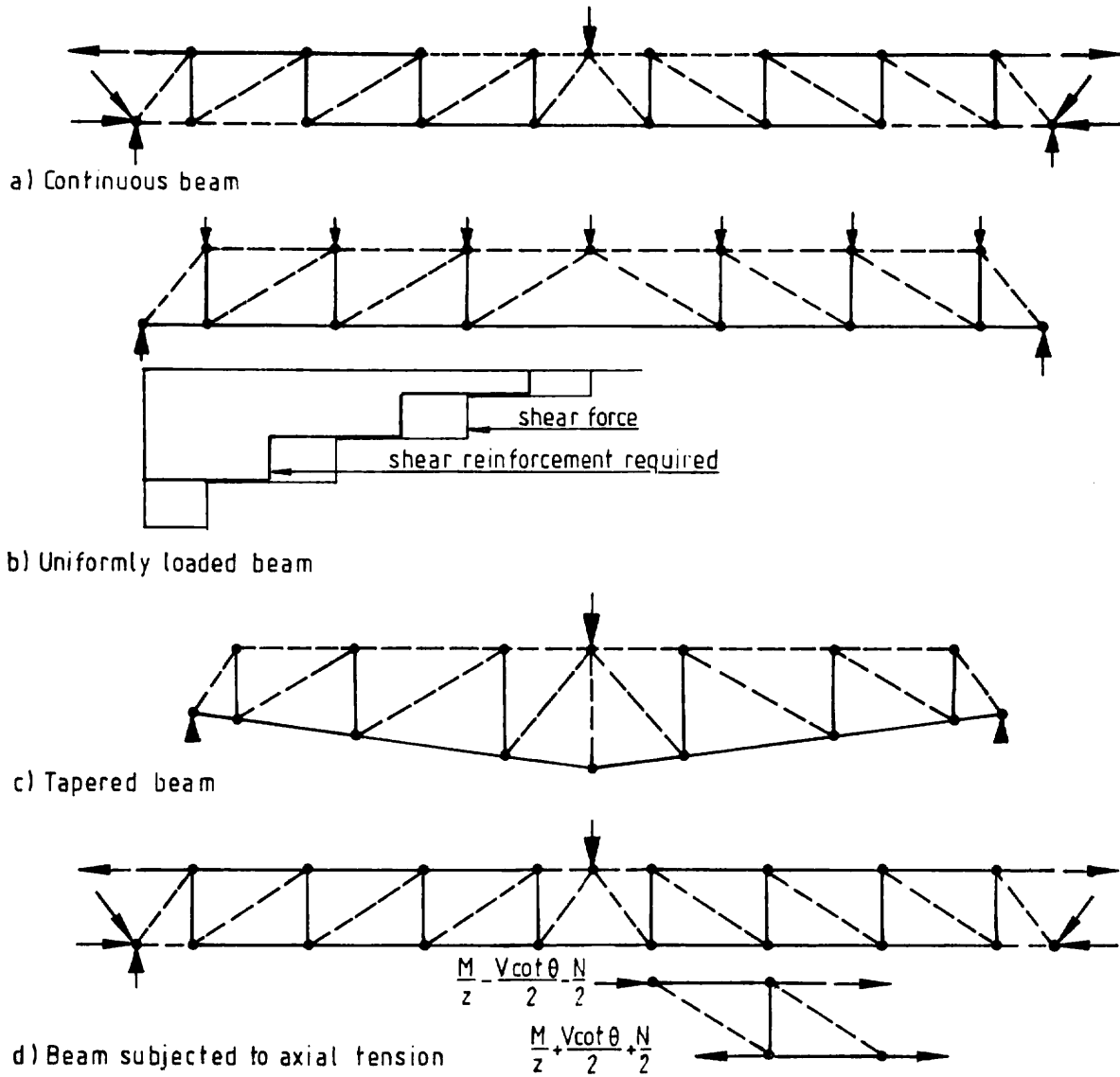
Fig. 4.4.17:   *Examples of truss models for beams subjected to bending and shear*

$\frac{V_u}{bd}$ [MPa]

2·0

Truss $\cot\theta = 3$

$0.16 \, \xi \sqrt[3]{f_c \, 100 A_s/bd}$

1·0

$\frac{N_u}{bd}$ [MPa]

1·0   2·0   3·0   4·0

2·8d   2·8d   2·8d   2·8d

b = 152 mm   d = 272 mm $100 A_s/bd = 1\,46$
$f_c = 30-37$ MPa
o beams without stirrups
● beams with stirrups $A_{sw} \, f_{yw}/b \, s = 0\,58$ MPa
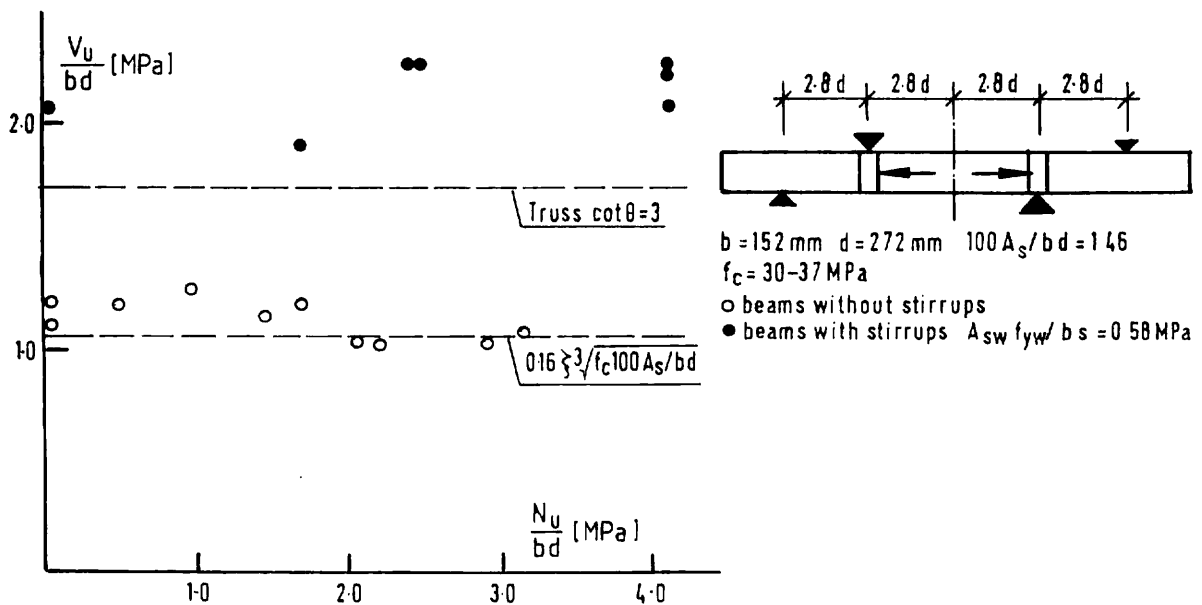
Fig. 4.4.18:   *Results of tests of beams subjected to axial tension, bending and shear and failing in shear*

$$V = A_{sw}\sigma_{sw} \sin\alpha \frac{z(\cot\alpha + \cot\theta)}{s} \qquad (4.4\text{-}34)$$

If limit values are substituted for σ_{sw} and σ_{cw}, simultaneous solution of these equations gives

$$\sin^2\theta = \frac{A_{sw}f_{yd}\sin\alpha}{f_{cd2}b_w s} \qquad (4.4\text{-}35)$$

Writing $\rho_w = A_{sw}/b_w s\sin\alpha$, which makes ρ_w equal for equal amounts of shear steel irrespective of α

$$\sin^2\theta = \frac{\rho_w f_{yd}}{f_{cd2}}\sin^2\alpha \qquad (4.4\text{-}36)$$

and

$$\cot\theta = \sqrt{\left(\left[1 - \frac{\rho_w f_{yd}\sin^2\alpha}{f_{cd2}}\right] \middle/ \left[\frac{\rho_w f_{yd}\sin^2\alpha}{f_{cd2}}\right]\right)} \qquad (4.4\text{-}37)$$

whence from equation (4.4-33)

$$\frac{V_{Rd}}{b_w z f_{cd2}} = \frac{\rho_w f_{yd}\sin^2\alpha}{f_{cd2}}\left[\cot\alpha \sqrt{\frac{1 - \dfrac{\rho_w f_{yd}\sin^2\alpha}{f_{cd2}}}{\dfrac{\rho_w f_{yd}\sin^2\alpha}{f_{cd2}}}}\,\right] \qquad (4.4\text{-}38)$$

Fig.4.4-20 compares the variations of $\cot\theta$ and $V_{Rd}/b_w z f_{cd2}$ with $\rho_w f_{yd}/f_{cd2}$ for vertical and 45° stirrups.

The most important feature of inclined shear reinforcement is that it reduces the forces on the web concrete and increases the maximum shear for which a beam of given dimensions b_w and z and a given concrete strength can be designed.

Another advantage of inclined reinforcement is that its presence reduces the force in the tension chord

$$N_{Sd} = \frac{M}{z} + \frac{V}{z}\cot\theta - \frac{F_{ywd}}{2}(\cos\alpha + \cot\theta) \qquad (4.4\text{-}39)$$

where

F_{ywd} is the force in the inclined shear reinforcement intersecting the vertical section in question.
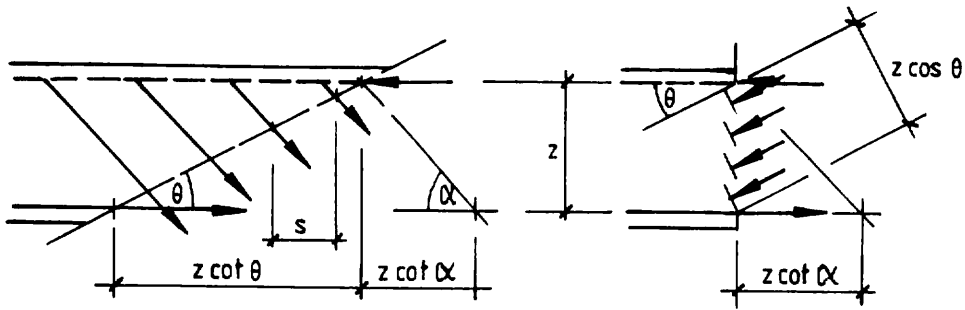
*Fig. 4.4.19:*   Equilibrium conditions in a truss model of a beam with inclined stirrups
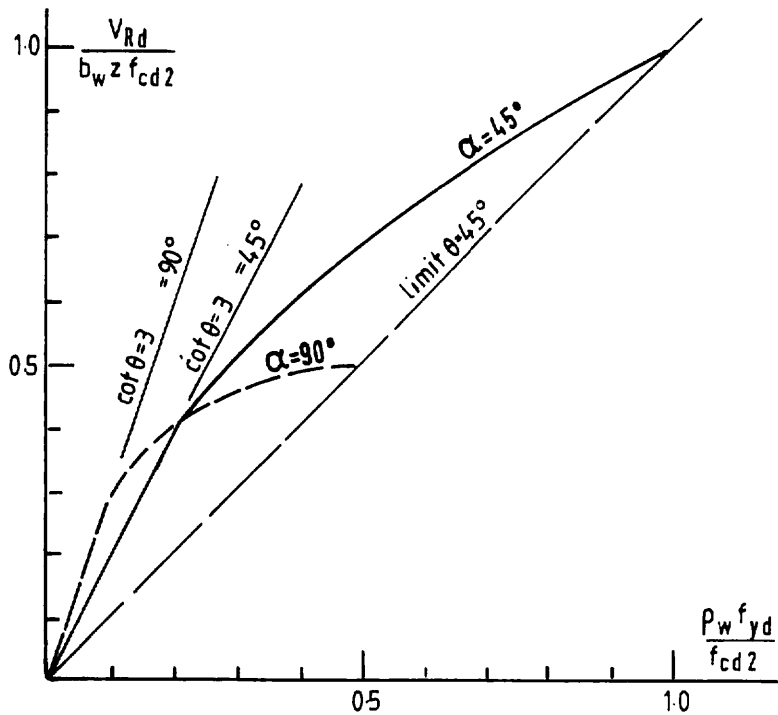
Fig. 4.4-20:   Comparison of 45° and 90° stirrups
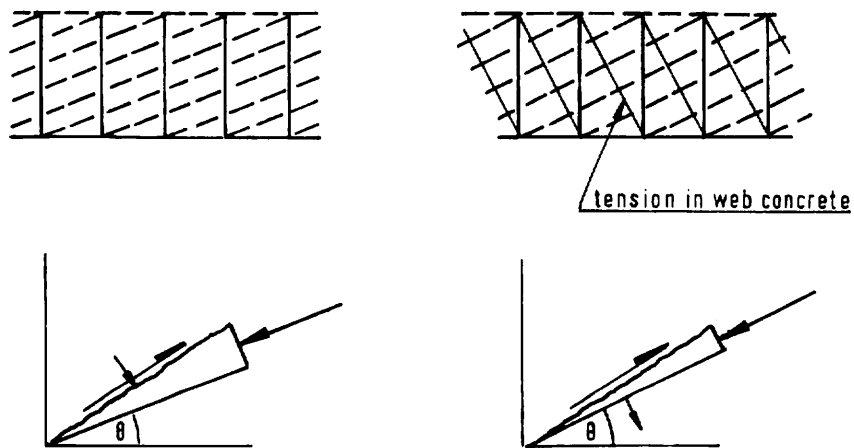

Fig. 4.4-21:   Cracked webs - models without and with tension in the concrete

The system of modelling described above, in which the only actions considered in the web are tension in the shear reinforcement and uniaxial compression in the concrete is the simplest available. More complex models exist in which the web concrete is taken to resist some overall tension beyond the local stresses induced by the bond of the shear reinforcement.

Fig.4.4-21 contrasts the simple model with one involving a principal tension in the concrete acting at right angles to the principal compression. The two models produce similar results if the web compression is assumed to be at a slightly lower inclination in the simple version. The forces in the cracks implied in the two representations are a little different and the more complex model predicts a slightly reduced addition to the main steel force.

(5.3)   Longitudinal shear in flanges

For the outstanding parts of flanges to contribute to resistance at sections of maximum moment, forces must be introduced to them by shears at, their junctions with webs. The situation of an uncracked compression flange is shown in Fig.4.4-22 a and can be seen to involve both the shear referred to above and transverse tension near the section of maximum moment.

It would be possible to assess the resistance of a flange to cracking due to these effects, but it is more practical to design all flanges as potentially being cracked at their junctions with webs.

Fig.4.4-22 b shows simple models for the design of both a compression and a tension flange for the effects of longitudinal shear.

Considering the compression flange first, the shear from the web in a typical length $\delta\ell$, is $V\delta\ell/z$. This divides into three parts, one $(\eta V\delta\ell/z)$ remaining within the web breadth and the other two going out to the flange outstands. The transverse tensile resistance required per unit length of flange to the high moment side of the length δl is thus:

$$n_{Rd} = \frac{(1-\eta)}{2}\frac{V}{z}\tan\theta_f$$ (4.4-40)

where

θ_f is the angle, on plan, between the inclined compression in the flange and the longitudinal axis of the beam.

The shear resistance of the junction has an upper limit per unit length

$$\frac{(1-\eta)}{2}\frac{V}{z} \not> f_{cd2}h_f \sin\theta_f \cos\theta_f$$ (4.4-41)

the angle θ_f recommended in MC90 is arc cot 2.
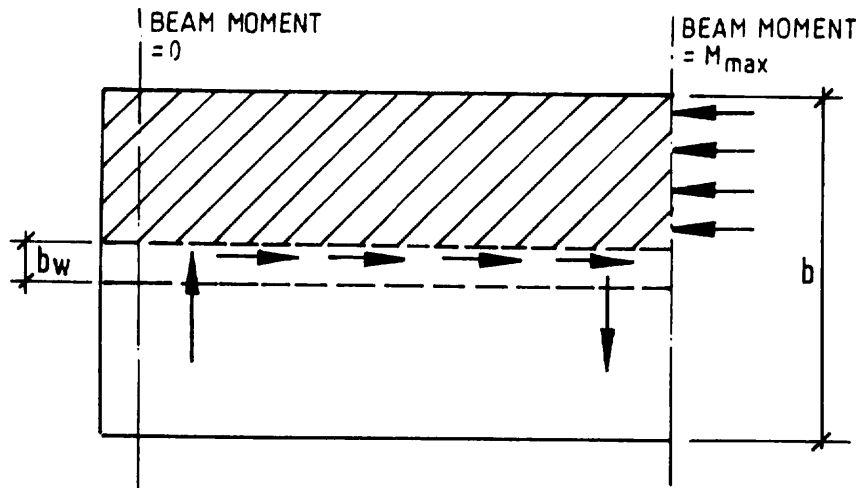
a) OVERALL EQUILIBRIUM OF AN OUTSTAND OF A
   COMPRESSION FLANGE
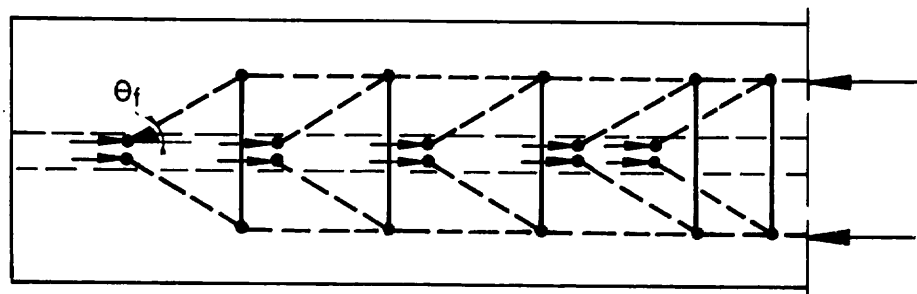

PLAN OF COMPRESSION FLANGE
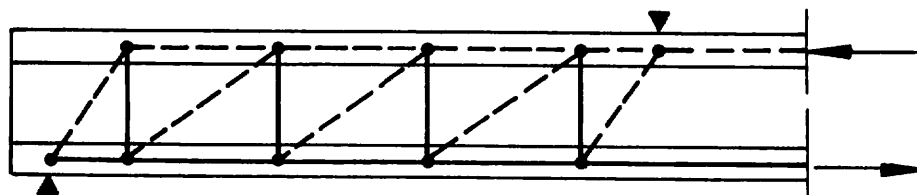
ELEVATION OF WEB
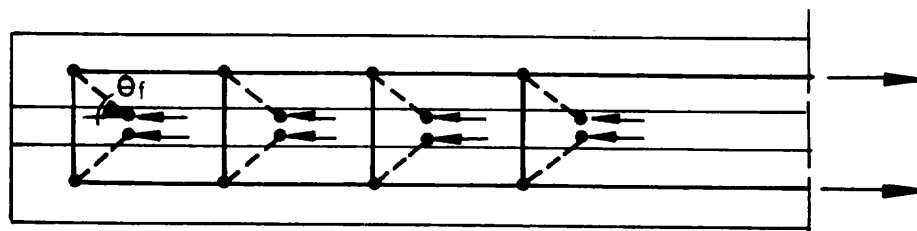
PLAN OF TENSION FLANGE

NOTE FORCES REMAINING WITHIN BREADTH OF WEB ARE NOT SHOWN ON PLANS

b) SIMPLE TRUSS MODELS TREATING LONGITUDINAL SHEAR

Fig. 4.4-22:   Longitudinal shear in flanges

The definition of the proportion (η) of the force which remains within the web merits some consideration. An obvious value could be $\eta = b_w/b$, but it may be worthwhile to use other values.

If the beam carries a major concentrated load in a high moment region, the force coming into the flange from the local 'fan' in the web may be high in relation to $b_w h_f f_{cd1}$ and the part of the flange with a breadth b_w may not be able to resist it, if already stressed by compression built up along the shear span. In such a case it may be that η should be taken as zero for most of the span.

A more common situation is that in which the full effective flange breadth is not required for flexural resistance. In this case, the use of $\eta = b_w/b$ may lead to unnecessary demands for flange steel. Here the force within the web breadth at the section of maximum moment can be taken as $b_w h_f f_{cd1}$ leaving only $\frac{1}{2}[(M_{Sd}/z) - b_w h_f f_{cd1}]$ to be transmitted to each outstand. This can produce a considerable saving of reinforcement and is very unlikely to cause any problems at the serviceability limit.

The paragraphs above define the transverse tensile resistance required in a flange to provide resistance to longitudinal shear. If such shear acts alone the reinforcement can be detailed with the steel divided equally between the top and bottom of the flange. If, as is more usual, the longitudinal shear acts together with transverse bending, the flange adjacent to the web can be designed for the two actions using the method given in Section (7.3) and sketched in Fig.4.4-23.

The major source of transverse bending is the flexure of the flange acting as a slab spanning between webs, but it should be realised that curvature of a flanged beam is itself the cause of second order moments produced by the effects shown in Fig.4.4-24 and these affect both tension and compression flanges.

For a tension flange the proportion of the force from the webs which remains within the web breadth, is a function of the detailing of the longitudinal reinforcement.

At simple supports there is normally very little chance of mobilising bars at any significant distance outside the web. The bars within, or very close to, the web, should thus be able to resist the longitudinal component of the force from the web fan at the support, i.e.

$$N_s = \frac{V \cot \theta}{2}$$

In narrow flanges the longitudinal reinforcement outside the web can reasonably be treated as two units - one in each flange outstand - but in wide flanges a more detailed model may be desirable and Fig.4.4-25 shows a possible method of detailing. The model is clearly a simplification and some reduction of forces is to be expected in the bars near the web within the high moment region and at least a minimum transverse reinforcement should be provided throughout the flange. The simple model does however lead to a sensible pattern of curtailment for the main steel and does make it clear that the decrease of main steel forces with decreasing moment is far slower than implied by the simplistic (M/z).

UPPER PART OF FLANGE

m/z_f

tension per unit length

$$= \frac{v \tan \theta}{2} + \frac{m}{z_f}$$

LOWER PART OF FLANGE

m/z_f

tension per unit length

$$= \frac{v \tan \theta}{2} - \frac{m}{z_f}$$

z_f
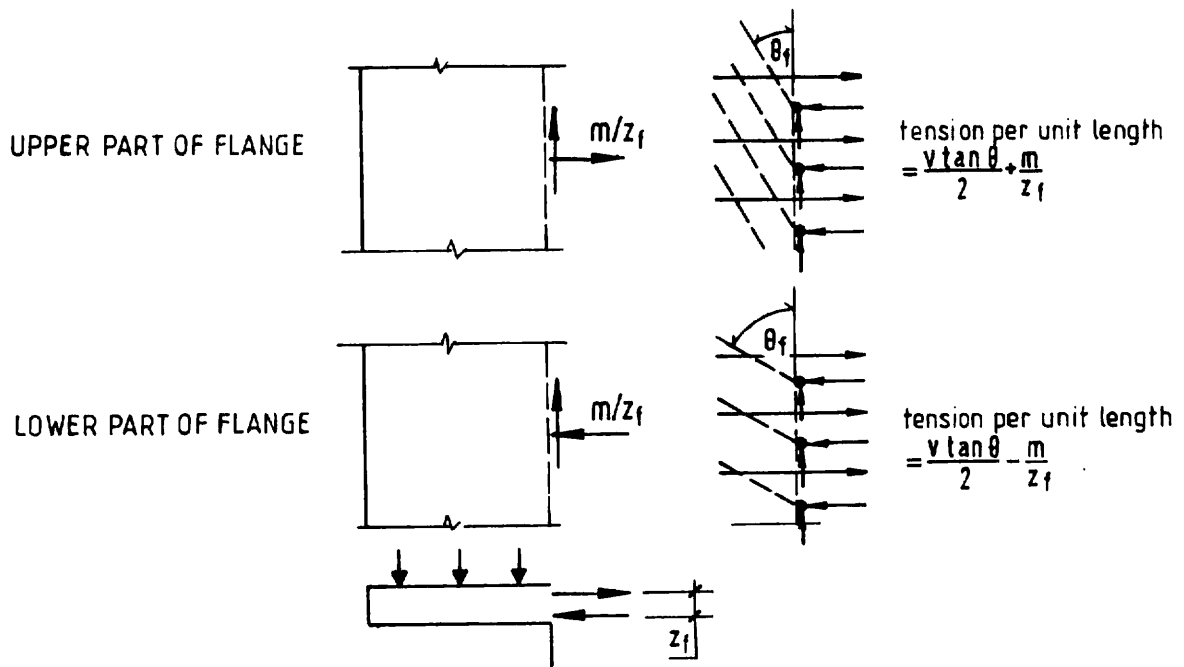
Fig. 4.4-23:　　*Combined effects of longitudinal shear and transverse bending*

$F \sin \varphi$

φ

F

$F \sin \varphi$

interface with web

φ

F

$\frac{b - b_w}{4}$

$M = 2F \sin \varphi \frac{b - b_w}{4}$

$2F \sin \varphi$
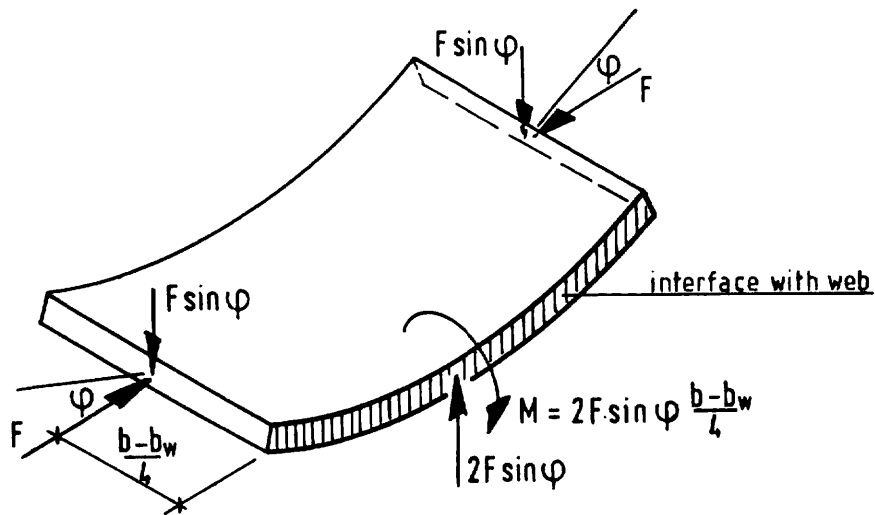
Fig. 4.4-24:　　*Transverse flexure of a compression flange due to longitudinal curvature*
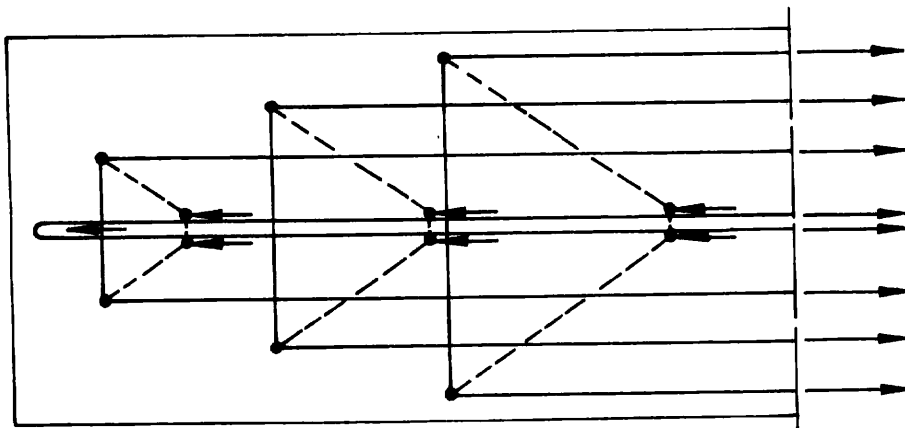
Fig. 4.4-25:　　*A more detailed model of a tension flange*

The steel force required at a vertical section, where the applied moment is M is increased over (M/z) by:

$$\delta N = \frac{V \cot \theta}{2} + \frac{(1-\eta)V}{z}\left(\frac{b - b_w}{2}\right)\cot \theta_f$$

(4.4-42)

MC90 recommends a value of 1.25 for $\cot \theta_f$.

Example

The span shown in Fig.4.4-26 is to be designed for a uniformly distributed ULS design load of 160 kN/m. The concrete is to have a characteristic strength f_{ck} = 30 MPa and the reinforcement is to be of deformed bars with f_{yk} = 460 MPa.

The design resistances of the concrete and steel are:

f_{cd} = 30/1.5 = 20 MPa

f_{cd1} = 0.85 x 20 [1 - 30/250] = 15.0 MPa

f_{cd2} = 0.6 x 20 [1 - 30/250] = 10.6 MPa

f_{yd} = 460/1.15 = 400 MPa

The flexural design requirements at the sections of maximum moments are met using $6\phi32$ in the span with d = 820 mm and $6\phi20$ at the right end support with d = 860 mm.

In the span $A_s f_{yd}$ = 1930 kN and x = $A_s f_{yd}/b\ f_{cd1}$ = 129 mm, which is less than h_f, and the internal lever arm z = 820 - 65 = 755 mm.

At the support $A_s f_{yd}$ = 754 kN and x = $A_s f_{yd}/b_w f_{cd1}$ = 201 mm. Here the lever arm is 860 - 101 = 759 mm.

For convenience in the construction of a truss model, z is taken as 750 mm throughout.

In the region where the inclination of the web compression is constant, the maximum shear is 540 kN, making $V_{Sd}/b_w z$ = 2.88 MPa.

$V_{Sd}/b_w z \sin \theta \cos \theta$ must be less than f_{cd2}, thus $\sin \theta \cos \theta$ > 2.88/10.6 = 0.27

At the support where V_{Sd} = 780 kN the web compression is at an inclination 2θ and $\sin 2\theta \cos 2\theta$ > 4.16/10.6 = 0.39

These conditions would be satisfied by θ = arc cot 3, but a value of arc cot 2 is used here to avoid problems with the anchorage of the main steel.

The resulting truss model is shown in Fig.4.4-26 c, although in daily design there is no need to construct such a model and equations (4.4-26) and (4.4-27) can be used directly.

distributed load 160 kN/m

540kNm

9000

B

V=660

1361.25

540

V=780kN

a BENDING MOMENTS [kNm]

1000

900

820

6Ø32

Midspan

3x2Ø20

150

860

250 Support B

b CROSS SECTIONS

c TRUSS MODEL OF WEB [forces in kN]

240 240 240 240 240 240

660 1500 1740 1140 60 720

420 180 60 300 540 750

660 1500 1860 1740 1140 60 720

1500 1500 1500 750

3Ø32

4Ø32

5Ø32

Stepped diagram from truss

Smooth diagram for distributed stirrups

d DISTRIBUTION OF FORCE ALONG BOTTOM STEEL

Transverse tensile forces

165 154 150 164 192

330 618 338 240 240

660 616 638 600 676 480 240

(660) (840) (240) (600) (1080) (780) 240

224 464 464 60 240

Forces within web breadth

On the plan the forces given above arrows are those dispersed to the flange outstands. The figures in parenthesis are the total forces from the web model.

e TRUSS MODEL OF FLANGE [forces in kN]

6Ø20

Ø10 %c 225   Ø8 %c300   Ø10 %c 175

6Ø32

f REINFORCEMENT

Fig. 4.4-26: *Example - design of a web and flange for shear*

The model stirrup forces correspond to stirrup requirements as follows:

540 kN or 360 kN/m needs 900 mm²/m, e.g. ϕ10 $^c/_c$ 175

420 kN or 280 kN/m needs 700 mm²/m, e.g. ϕ10 $^c/_c$ 225

300 kN or 200 kN/m needs 500 mm²/m, e.g. ϕ10 $^c/_c$ 300

Minimum shear reinforcement ($\rho_w f_{yd}$ = 0.5 MPa for f_{ck} = 30 MPa) corresponds to ϕ10 $^c/_c$ 500 or ϕ8 $^c/_c$ 300.

Fig.4.4-26 d shows the distribution of force along the main bottom steel both as a stepped diagram direct from the truss model and in a smoothed form corresponding to distributed shear reinforcement. The same diagram includes the resistances of different numbers of 32 mm bars and their intersections with the force diagram define the points at which bars are theoretically no longer needed. Actual curtailments can be made beyond these points (see 4.5.3(1.2)).

At the simply supported end the main steel force to be anchored at the support is 660 kN. Taking three bars to the support this force can be anchored (see Section 4.4.5) with a 385 mm length and a 90° bend. Two bars would be sufficient for the tensile force but the anchorage would be difficult.

Fig.4.4-26 e shows the model of the flange and indicates the forces coming from the web (see part c of the figure), the longitudinal components of the forces distributed to the flange outstands and the build-up of force within the web breadth. The transverse tensile forces are fairly uniform and the maximum is 192/1.5 = 128 kN/m.

Fig.4.4-26 f shows the details of the main steel and web stirrups.

(5.4)   Prestressed beams

(5.4.1)   Shear cracking

Prestressing or axial compressive loading increases shear cracking loads by retarding flexural cracking. At sections not cracked in bending shear cracks develop when the principal tension in the web reaches the tensile strength of the concrete, i.e. when

$$\sigma_1 = \sqrt{\left(\tau^2 + \frac{\sigma^2}{4}\right)} - \frac{\sigma}{2} = f_{ct} \qquad (4.4\text{-}43)$$

where

σ_1 is the principal tensile stress

τ is the shear stress

σ is the longitudinal compressive stress

Although both τ and σ vary over the depth of the section the principal tension responsible for shear cracking in rectangular and T-sections with webs of uniform breadth can usually be assessed sufficiently accurately taking:

$$\tau = \frac{3V_{ef}}{2b_{red}h} \quad \text{and} \quad \sigma = \sigma_{cp}$$ (4.4-44)

where

V_{ef}	is the shear acting on the concrete, that is the applied shear minus the vertical component of the prestress at the section considered
b_{red}	is the web breadth minus the sum of the diameters of tendon ducts at any level in it
h	is the overall depth of the section
σ_{cp}	is the longitudinal compression at the centroid of the section due to prestress

If the centroid of the section is within the compression flange the critical stresses are those at the underside of the flange and

$$\tau = \frac{V_{ef}Ay}{b_w I}$$ (4.4-45)

where

|	
A	is the area of the part of the section further from the centroidal axis than the level considered
y	is the distance from the centroid of A to the centroidal axis
I	is the second moment of area of the whole section about the centroidal axis

Equation (4.4-45) and the longitudinal prestress at the relevant height should also be used in the calculation of the critical value of σ_I, if the web does not have parallel sides and its minimum width occurs at a level other than that of the centroid.

For pretensioned members in which the transmission length extends into the span, account must he taken of the lesser prestress. If the section is symmetrical about its x-axis the calculations can be made for a section at a distance h/2 from the inner face of the support.

Where flexural cracking occurs the distributions of longitudinal stresses are as shown in Fig.4.4-27 a and the prestress can be seen to have two effects. One of these is for any inclined component of the prestressing force to directly resist a part of the transverse loading, the other is to create an arching action within the concrete which can resist a further part of the load. The shear resistance equivalent to that in an ordinary reinforced concrete beam is required only to resist the residue of the applied shear.

Looked at in a different way, the shear cracking of ordinary reinforced concrete beams is the product of the bond force from the main reinforcement. In prestressed beams, whether pre- or post-tensioned, a large part of the total tension does not require bond stresses acting on a flexurally cracked web for its development.

line of thrust in concrete

tendon profile

uniformly distributed load

concentrated load at midspan
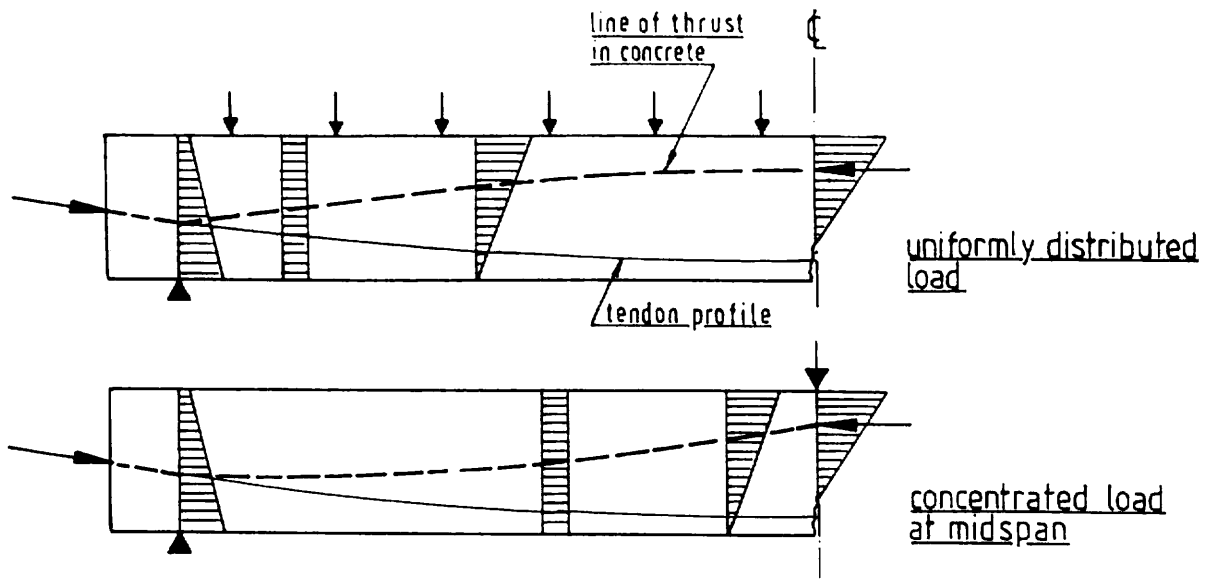
a) STRESS PROFILES AFTER CRACKING OF PRESTRESSED BEAMS

distributed load $= P_{do}\,8z/l^2$

P_{do}

z

1 horizontal tendon

$l/2$

P_{do}

β

y

$z-y$

z

2 parabolic tendon
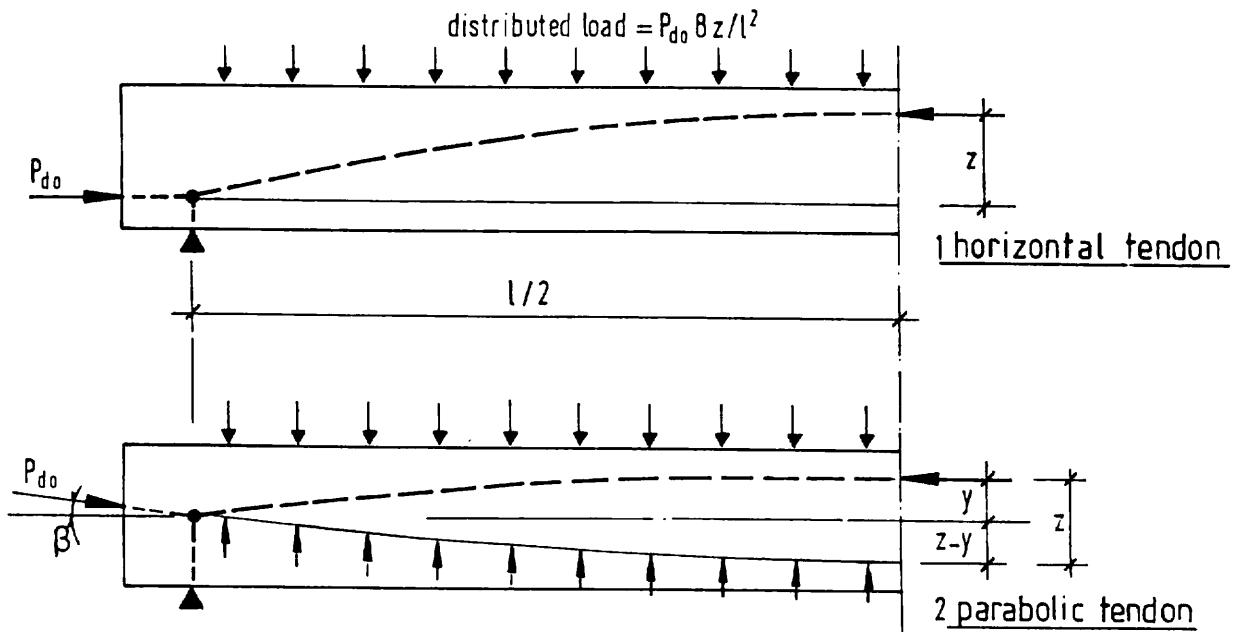
load carried by funicular [arch] $= P_{do}\cos\beta \cdot 8y/l^2$

load carried by uplift from tendon $= P_{do}\cos\beta \cdot 8(z-y)/l^2$

total load carried by system shown $= P_{do}\cos\beta \cdot 8z/l^2$

note $\cos\beta \approx 1\cdot0$

b) ARCHING AND TENDON CURVATURE EFFECTS RELIEVING SHEAR FORCES

Fig. 4.4-27:   *Effects of prestress on shear resistance*

The ordinary shear cracking formula of equation (4.4-20) remains applicable, but the transverse forces carried by the tendons acting at P_{do} and the corresponding forces resisted by funicular (arch) action can be deducted from the applied shear.

Thus for the uniformly loaded simply supported beam of Fig.4.4-27 b1 with straight tendons the loading to be considered in equation (4.4-44) is

$$q_{Sd} - 8P_{do}\left(\frac{z}{\ell^2}\right) \text{ per unit length}$$

where

z   is the lever arm at the section of maximum moment.

With tendons draped as in Fig.4.4-27 b2, the loading system which can be deducted from the external loading is as shown.

(5.4.2)   Simple design of shear reinforcement

Once shear cracks form, prestressed members need shear reinforcement, and a simple model for a post-tensioned beam with a bonded horizontal tendon is shown in Fig.4.4-28. In effect it is the same model as for an ordinary reinforced concrete beam, but with forces due to prestress applied at the ends of the chords. The bottom chord is in compression near the supports. Where the prestress is overcome, the chord force becomes tensile and the equilibrium at the lower edge of the web lattice relies upon the bond of the tendon and of any supplementary non-prestressed reinforcement. The maximum force that can be developed in the tendon by bond is $A_p f_{pyd}$ - P_{do}.

In the more usual case of a curved bonded tendon, a part of the external load is resisted by the upward forces due to tendon curvature. For a parabolic tendon with a rise in a span ℓ the uplift is $8P_{do}r/\ell^2$ per unit length, and this can be subtracted from the external loading when designing shear reinforcement. The truss model for the design of shear reinforcement can be any of the three variants shown in Fig.4.4-29 and the angle of the web compression can be chosen freely in the range $1 \le \cot \theta \le 3$ subject to the limit:

$$\frac{V_{ef}}{b_{red} z} \not> f_{cd2}$$

where

V_{ef} is the shear from a loading system comprising the downward effects of the applied loads and the upward forces due to the curvature of the tendon

b_{red} is b_w minus the sum of the diameters of the ducts at any level in the web if they are ungrouted or b_w minus half the sum if they are grouted

In pretensioned members it has to be assumed that the bond stresses of the wires or strands within the transmission length cannot increase with the applied load. Thus the main chord forces that have to be developed close to supports should be provided by supplementary
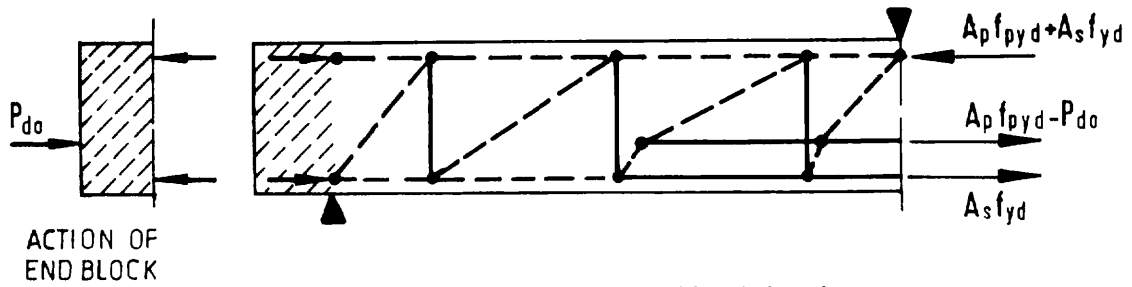
Fig.4.4-28:   *Simple truss model for a beam with a horizontal bonded tendon*
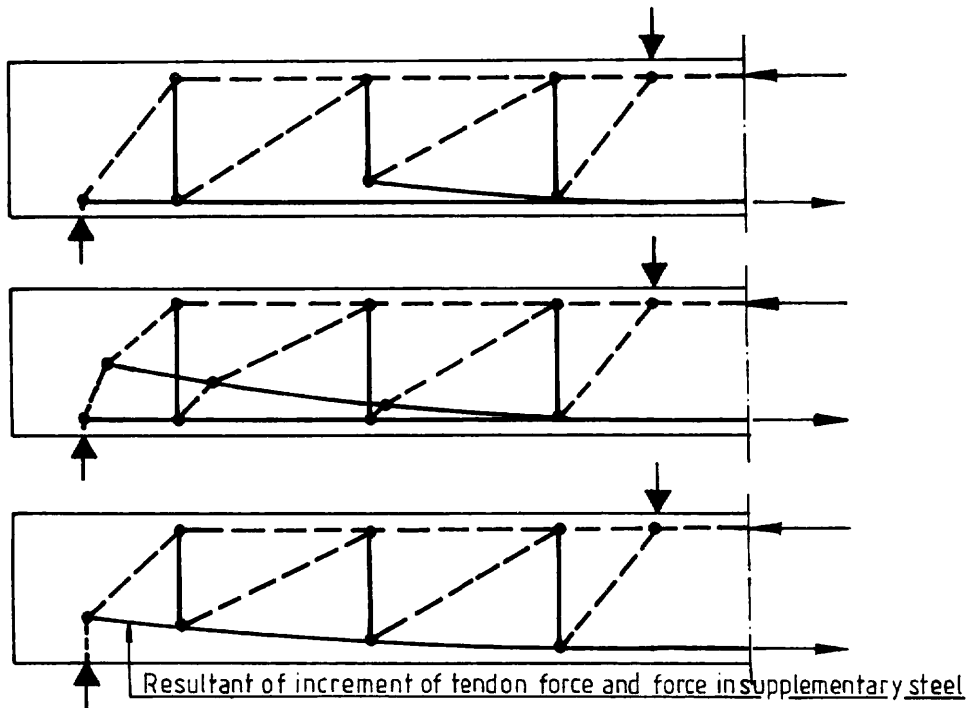

Fig.4.4-29:   *Variants of truss modelling for prestressed beams treating the action of the increment of tendon force above P_{do} and the action of supplementary steel*
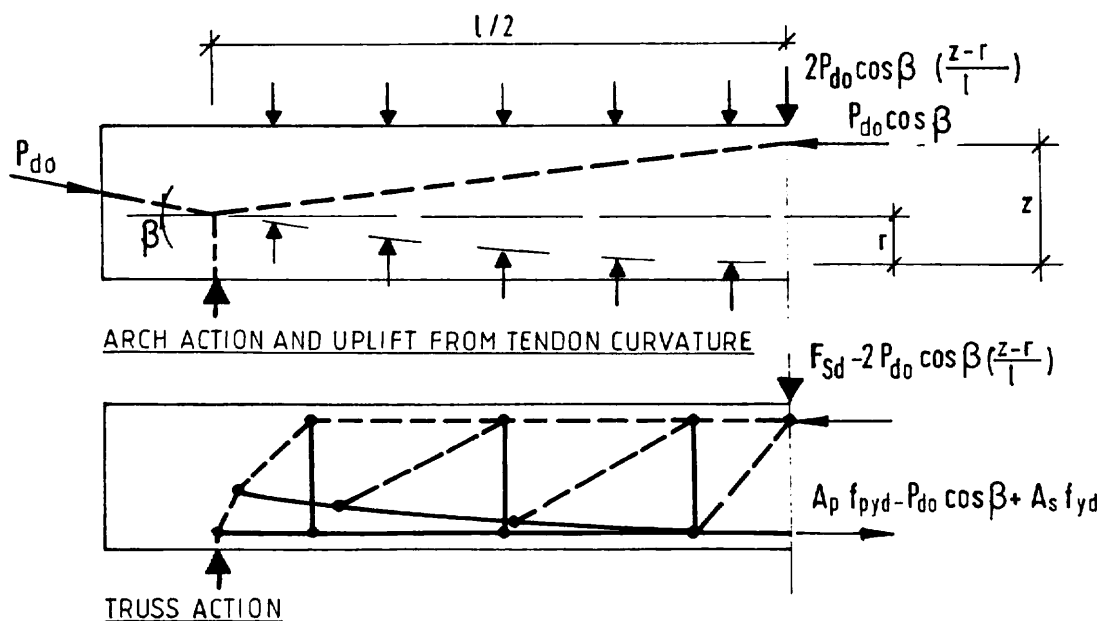

Fig.4.4-30:   *Models to be superimposed in design incorporating arch action*

reinforcement. If this steel is not required at the section of maximum moment it can be lapped with the tendon in the span. The assumption of no additional bond in the transmission lengths is somewhat conservative as the presence of transverse pressure from the supports can increase bond resistance.

(5.4.3)   Design of shear reinforcement incorporating arch action

The above approach to design is always safe but can be over-conservative, particularly in beams with relatively thick webs. For such cases there is an alternative which makes use of the ability of a beam to function partly by arch action, when the tie to the arch is as positive as in the case of end-anchored prestress.

The overall equilibrium system is arrived at by the superposition of two models. The first accounts for some or all of the effects of prestress and those of a part of the applied loading, while the second includes the shear reinforcement, the increases of tendon forces beyond prestress, any supplementary non-prestressed main steel and the remainder of the loading.

Fig.4.4-30 shows an example of this type of modelling applied to a simple span carrying a uniformly distributed load and a concentrated load. The parabolic tendon has a shallow profile chosen so that the uplift from the tendon balances the uniform load. The arch thrust or funicular with a horizontal component equal to $P_{do}\cos\beta$ rises from the level of the tendon at the supports to the ultimate limit state centre of compression at the concentrated load, thus supporting a vertical force equal to $2P_{do}\cos\beta(z-r)\ell$, where r is the rise of the tendon. In the second system a conventional truss action carries the remainder of the concentrated load, i.e. $F_{Sd} - 2P_{do}\cos\beta(z-r)/\ell$.

For verification of stresses:

- In the compression zone at midspan, the actions of the two systems are directly additive and the necessary check is simply

$$\frac{M_{Sd}}{z} \leq bxf_{cd1}$$

(4.4-46)

- In the tension zone at midspan, the actions are again additive and

$$\frac{M_{Sd}}{z} \leq A_p f_{pyd} + A_s f_{yd}$$

(4.4-47)

- For the stirrups which act only in the second system

$$F_{Sd} - 2P_{do}\cos\beta(z-r)/\ell \leq A_{Sw}f_{yd}z\frac{\cot\theta}{s}$$

(4.4-48)

The vertical component of the increment of prestress during loading can be subtracted, but it is small and depending on the details of the truss system may not act along the whole shear span. In the example shown, in order to maximise $z \cot \theta$ in the support region the increase of tendon force has been concentrated to the high moment area.

- For the web concrete there are compression stresses from both systems. They act at different angles and this could be taken into account in determining the maximum stress, but, as the difference of inclination is unlikely to be large, it is reasonable (and conservative) to use a direct addition.

The stress in the truss system is

$$\sigma_{cw2} = [F_{Sd} - 2P_{do} \cos\beta(z - r)/\ell]/b_{red}z \sin\theta\cos\theta \tag{4.4-49}$$

That from the funicular system is difficult to determine precisely and a simple approximate expression can be used

$$\sigma_{cw1} = P_{do}/0.96b_{red}h \tag{4.4-50}$$

Verification of resistance then requires

$$\sigma_{cw1} + \sigma_{cw2} \le f_{cd2} \tag{4.4-51}$$

A practical approach in design is to calculate σ_{cw1} and thence the web stress ($f_{cd2} - \sigma_{cw1}$) available for the truss model. The inclination of the web struts in the truss can then be found from equation (4.4-49) and the stirrups can be determined.

Solutions in which θ values are close to 45° may well lead to designs which are less economic than the results from simple truss models. In such cases the design can be based entirely on a simple model (including the effects of tendon curvature). Alternatively the value of P_{do} used in the funicular system can be reduced to reduce σ_{cw1}. The difference in prestress should then be included in the truss model.

In general any tendons which rise high in the sections near the supports should be treated in the truss system and not with the funicular as the arching resistance developed by them is small, because (z-r) is small, and yet they increase σ_{cw1}. In very simple terms, very flat arches are poor structural systems.

<u>Example</u>

A post-tensioned beam, with the cross-section shown in Fig.4.4-31 is to span 12 m carrying a design ultimate load of 95 kN/m. Its concrete is to have a characteristic strength f_{ck} of 50 MPa.

The prestressing reinforcement comprises three tendons, two of which run horizontally in the bottom flange while the third has a parabolic profile. The tendons are grouted in metal duct tubes.

Data for the prestressed reinforcement, which has been designed for conditions at transfer and in service are as follows:

$A_p = 396$ mm^2/tendon

a) **MIDSPAN CROSS SECTION**

b) **ULS STRAINS AT MIDSPAN**

c) **SHEAR RESISTANCE ASSOCIATED WITH PRESTRESS**

d) **SHEAR RESISTANCE BY TRUSS ACTION** [to carry 56.3 kN/m]
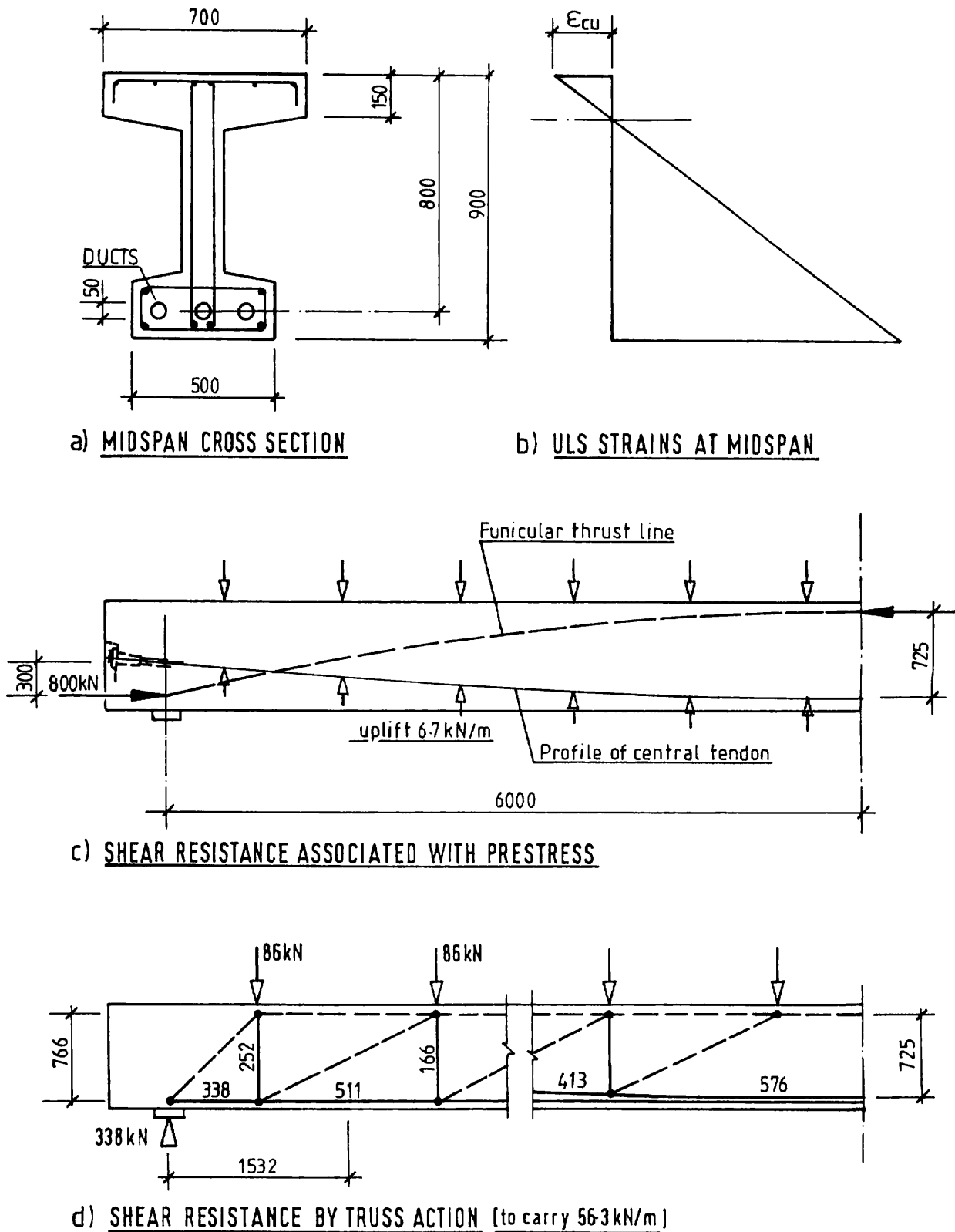
Fig. 4.4-31:   Example - design for shear in a prestressed beam

P_{do} = 400 kN/tendon, cos β = approximately 1.0, $A_p f_{pyd}$ = 576 kN
Non-prestressed reinforcement will have a yield stress of 500 MPa (f_{yd} = 435 MPa).

The maximum moment is M_{Sd} = 95 x $12^2/8$ = 1710 kNm

Assuming the neutral axis depth to be 150 mm, the midspan strain profile at the ULS is as shown and it is obvious that the tendons and any bars in the bottom flange will yield.

The moment resistance from the tendons is thus

$M_{Rd,p}$ = 3 x 576 x 0.725 = 1253 kNm

Ordinary reinforcement is then required for 1710 - 1253 = 457 kNm.

If the centres of the lower bars are 40 mm and those of the upper bars 160 mm above the underside of the beam, the corresponding lower arms are 785 and 665 mm. With 4 no. ϕ20 at the bottom and 2 no. ϕ12 higher up in the bottom flange, the resistance moment from the bars is

M_{Rds} = (547 x 0.785) + (98 x 0.665) = 495 kNm (> 457 kNm)

With this reinforcement, the total tension force at midspan is 2373 kN.

The average stress in the 700 x 150 mm (area = 105 x 10^3 mm^2) compression zone is 2373/105 = 22.6 MPa.

f_{cd1} = 0.85 x 33.33 (1 - 50/250) = 22.7 MPa

The assumed neutral axis depth is thus appropriate.

In regard to shear resistance, the parabolic cable has a rise of 0.3 m in 6 m. With y = kx^2, k = 0.0083 and d^{2}y/dx^2 = 2k = 0.0167, giving an uplift of 0.0167 x 400 = 6.67 kN/m due to the curvature of the tendon.

As the parabolic tendon rises fairly high at the supports its contribution to a funicular shear resisting action would not be very efficient. The web compression would be relatively large for only a small load capacity. The two straight tendons can provide a useful funicular. The rise of the thrust line in Fig.4.4-31 c) is 0.725 m, making k = 0.02 and the load carried 2 x 0.02 x 800 = 32 kN/m.

With one grouted tendon in the web, the effective web breadth is

b_{red} = b_w - ½ϕ_{duct} = 125 mm

The web compression in the funicular system is 800 x 103/0.9 x 125 x 900 = 7.9 MPa while f_{cd2} = 16 MPa. A resistance of 8.1 MPa is thus available for the truss system which will carry the remainder of the load (95 - 6.7 - 32 = 56.3 kN/m).

With a truss action as in Fig.4.4-31 d), the maximum shear, where the angle of web compression θ = arc cot 2, is 338 - 86 = 252 kN/m.

With θ = arc cot 2, $V/b_w z \sin\theta \cos\theta$ = 252 x 10^3/125 x 725 x 0.4 = 6.95 MPa, which is below the residual capacity of 8.1 MPa.

The model stirrup force of 252 MPa corresponds to 164.5 kN/m and could be provided by $\phi8$ $^c/_c$ 250. This is not very much above the minimum stirrup requirement and could be continued throughout the span.

(5.5)   Columns

An approach similar to that for prestressed beams can be applied to take account of the potential beneficial effects of axial loads in columns. If the axial load is high enough to suppress all cracking, the shear resistance can be calculated in terms of the principal stresses at the centroid of the section. For lesser axial loads the compression in the concrete (not including the reinforcement) can be taken as the equivalent of a prestressing force and the funicular line runs between the centres of compression at the upper and lower ends of the storey in question.

(6)   Torsion

(6.1)   Introduction

There are two types of torsion - circulatory (or St Venant) torsion and warping torsion. In the former the torque is resisted by a flow of shear around the cross-section, while in the latter components of the section act in bending in opposite directions - see Fig.4.4-32.

The types of section which are efficient in resisting torques are solid circles, rectangles, etc. and especially boxes. These act primarily in circulatory torsion and it is this mode of action which is considered here.

In most building frames, beams are subjected to some torsion but it is only a secondary action arising from the requirement of compatibility of deformations and is not necessary for the equilibrium of the structure. Since the response of a member with minimum reinforcement for torsion is extremely ductile at the stage of torsion cracking, such "compatibility torsion" can normally be neglected in design so long as minimum closed stirrups are provided.

(6.2)   Torsion cracking

Distribution of shear stresses due to circulatory torsion of uncracked sections can be determined by elastic theory and a number of standard results and approximations are given in Table 4.4-2.

For pure torsion loading of ordinary reinforced concrete members, torsion cracking can be predicted from

circulatory torsion   warping torsion
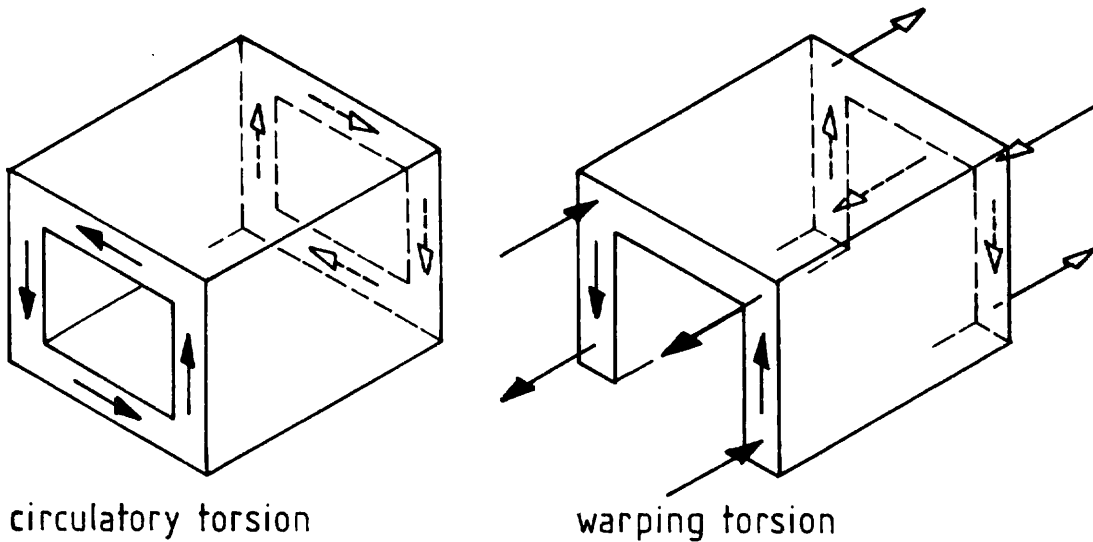
Fig. 4.4-32:   *Circulatory and warping torsion*

a) <u>CIRCULAR SECTIONS</u>
external diameter D, internal diameter d
Maximum shear stress (at the outer surface)

$$\tau_{max} = T \Big/ \frac{\pi[D^4 - d^4]}{16D}$$

b) <u>SOLID RECTANGULAR SECTIONS</u>
smaller dimension b_x, larger dimension b_y
Maximum shear stress (at centres of longer sides)

$$\tau_{max} = T / K\, b_x^2\, b_y$$

Shear stress at centres of shorter sides

$$\tau = T / K'\, b_x^2\, b_y$$

b_y/b_x	1.0	1.5	2.0	3.0	4.0	6.0	∞
K	0.21	0.23	0.25	0.27	0.28	0.30	0.33
K'	0.21	0.27	0.31	0.33	0.37	0.40	—

c) <u>T SECTIONS</u>

Torsion in any component rectangle

$$T_i \simeq \frac{b_{xi}^3\, b_{yi}}{\Sigma\, b_x^3 b_y}$$

Then τ_{max} can be calculated
for each component rectangle
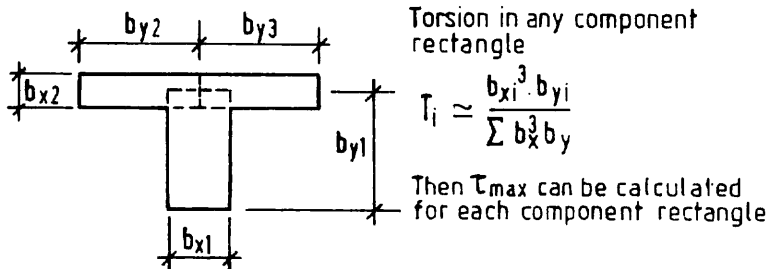
Table 4.4-2:   *Torsion constants (elastic theory)*

$$\tau_{max\,Sd} = f_{ct} \tag{4.4-52}$$

The prediction tends to be slightly conservative since concrete is not absolutely brittle in tension.

Where torsion is combined with bending, shear stresses are carried across the flexural cracks and equation (4.4-52) is still a reasonable predictor of inclined cracking, although there may be a size effect in larger members with wider cracks.

If torsion acts in combination with shear, the interaction obtained depends on whether or not the maximum stresses from the two actions act on the same part of the section. For a rectangle, with the larger dimension 'b$_y$' parallel to the shear force, if the section is not cracked in flexure

$$\frac{3}{2}\frac{V}{b_x b_y} + \frac{T}{Kb_x^2 b_y} = f_{ct} \tag{4.4-53}$$

If the section is cracked in flexure

$$\frac{V}{1.5V_{Rd1}} + \frac{T}{Kb_x^2 b_y f_{ct}} = 1 \tag{4.4-54}$$

If the larger dimension of the section is perpendicular to the direction of the shear the critical condition may occur on the longer or shorter side.

For the longer side

$$\frac{T}{Kb_x^2 b_y} = f_{ct} \tag{4.4-55}$$

and for the shorter one

$$\frac{3}{2}\frac{V}{b_x b_y} + \frac{T}{K'b_x^2 b_y} = f_{ct} \tag{4.4-56}$$

or

$$\frac{V}{1.5V_{Rd1}} + \frac{T}{K'b_x^2 b_y f_{ct}} = 1.0 \tag{4.4-57}$$

All of these equations have been given without safety factors since torsion cracking is not likely to define the ultimate limit state. If factored versions are wanted f$_{ct}$ should be substituted by f$_{ctd}$ and 1.5V$_{Rd1}$ by V$_{Rd1}$.

(6.3)   Beams in pure torsion

The post-cracking behaviour of both solid and hollow sections can be analysed by considering the torsional shear flow to be concentrated to a hollow 'shell' around the periphery. So long as the actual wall thickness of a hollow section is not less than the shell for a solid section, the two are directly equivalent as can be seen from the results of comparative tests by Lampert and Thürlimann (1968 & 1969) and Leonhardt and Schelling (1974), which are reproduced in Fig.4.4-33.

The model of torsional resistance is then as in Fig.4.4-34. The torque produces shear stresses in a 'shell' and these are resisted by inclined compression in the concrete. Considering a polygonal section, the shell comprises a number of walls, of dimensions z_i and the longitudinal and transverse forces in any wall are

$$F_l = \sigma_{cw} tz\cos^2 \theta \qquad\qquad (4.4\text{-}58)$$

$$F_t = \sigma_{cw} tz\sin \theta\cos\theta \qquad\qquad (4.4\text{-}59)$$

where

σ_{cw} is the inclined compression in the concrete
t is the thickness of the wall and
θ is the angle between the compression and the longitudinal axis

While σ_{cw} and t can vary from wall to wall, the product $\sigma_{cw}t$ is the same for all the walls.

Taking moments about the longitudinal axis of the beam, the torsion due to the force in the wall is:

$$T_i = F_{ti}y_i = \sigma_{cw} tz_iy_i \sin \theta\cos\theta \qquad\qquad (4.4\text{-}60)$$

where

y_i is the distance from the line of action of F_{ti} to the centre of the beam section.

Summation of these elemental torques from the individual walls gives

$$T = 2\sigma_{cw} tA_{ef} \sin \theta\cos\theta \qquad\qquad (4.4\text{-}61)$$

where

A_{ef} is the area enclosed by the centrelines of the walls.

In reality the torsional resistance is generally below this. One reason for the discrepancy is that the shear flow cannot turn abruptly at the junctions of the walls, with the result that A_{ef} is reduced for all but circular sections.

LAMPERT & THÜRLIMANN			Reinforcement	Test Results	
				T_u [kNm]	M_u [kNm]
T1/T4		80 — 500	longitudinal steel 16Ø12 stirrups Ø12 110	129/129	— / —
T84/T81		80 — 500	longitudinal steel 16Ø12 stirrups Ø12 110	114/115	146/134
LEONHARDT & SCHELLING				T_{cr} [kNm]	T_u [kNm]
VQ1/VH1		80 — 324	longitudinal steel 12Ø6 stirrups Ø6 100	13/12	21/21
VQ4/VH2		80 — 324	longitudinal steel 24Ø6 stirrups Ø6 50	11/12	31/34

Fig.4.4-33:   *Torsional resistances of solid and hollow sections*
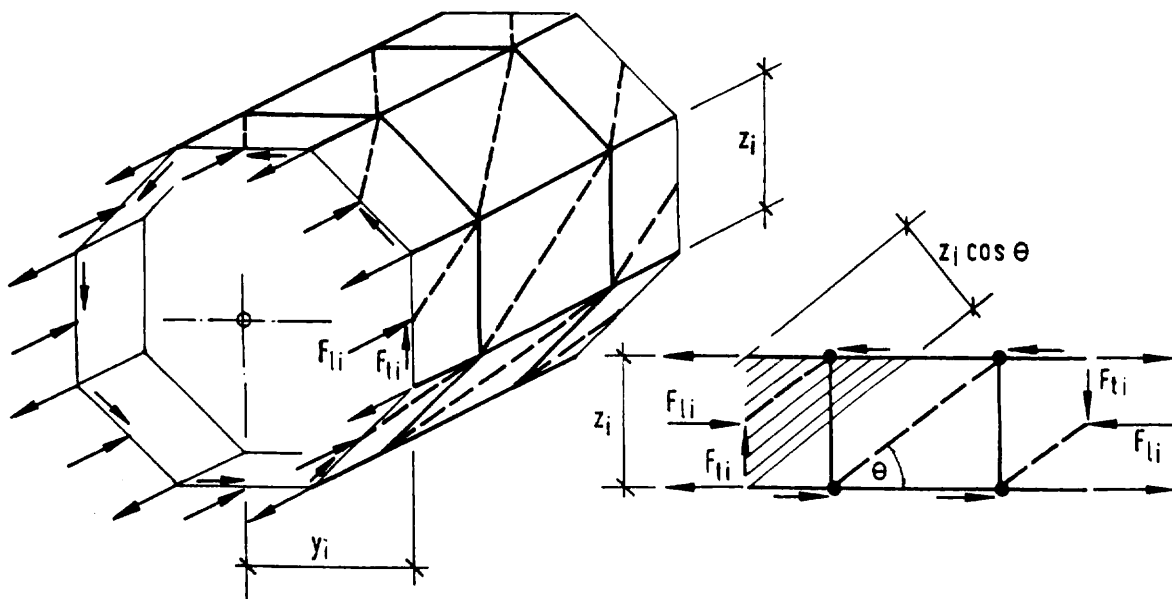
Fig.4.4-34:   *Truss modelling of a polygonal section resisting torsion*

For design this is treated by enhancing the internal forces due to the applied torque, and this can be done by designing for an enhanced effective torsion

$$T_{Sd,ef} = T_{Sd} / \delta \qquad\qquad (4.4\text{-}62)$$

where

δ = 1.0 - 0.25 bx/by for a rectangular section with bx < by and δ = 1.0 for a circular section. These values can also be used for hollow sections.

Thus, equation (4.4-61) becomes

$$T_{Sd,ef} = 2\sigma_{cw} t A_{ef} \sin\theta\cos\theta \qquad\qquad (4.4\text{-}63)$$

The shear force in any one wall is then

$$F_{ti} = \frac{T_{Sd,ef} z_i}{2A_{ef}} \qquad\qquad (4.4\text{-}64)$$

and the transverse reinforcement required, which is the same for all the walls, is:

$$\frac{A_{sh} f_y}{s} \geq \frac{F_{ti}}{z_i \cot\theta} = \frac{T_{Sd,ef}}{2A_{ef}\cot\theta} \qquad\qquad (4.4\text{-}65)$$

Where the suffix 'h' for hoop refers to one leg of a single stirrup going around the whole section, or to two legs if each wall contains two legs.

The longitudinal reinforcement for one wall, needed to balance F_{ℓ} is:

$$A_{s\ell} f_{yd} \geq \frac{T_{Sd,ef} z_i}{2A_{ef}} \cot\theta \qquad\qquad (4.4\text{-}66)$$

This steel should normally be distributed over the dimension z_i, but in small beams, the longitudinal steel can be concentrated to the intersections of the walls. If this is done each intersection requires the sum of ($A_{s\ell} f_{yd} / 2$) from the two walls.

At least one bar must always be provided at the intersections of walls and should have a diameter at least equal to $s_h/8$, while the spacing s_h of the hoops should not exceed $u_{ef}/8$, where u_{ef} is the length of the perimeter of A_{ef}.

The need to control the compression in the concrete requires:

$$t\sin\theta\cos\theta \geq \frac{T_{Sd,ef}}{2A_{ef} f_{cd2}} \qquad\qquad (4.4\text{-}67)$$

For a hollow section, the wall thickness can normally be taken as the actual thickness. For a solid section a reasonable estimate is

$$t = \frac{A}{u}$$

(4.4-68)

where

A   is the area bounded by the perimeter of the section and u is the length of the perimeter.

This estimate can be adjusted upward if condition (4.4-67) is critical, or downward if the concrete stress is low. The thickness should never be taken as less than twice the distance from the outside of the section to the inside of the outer hoops, since the hoop tension must 'turn' the concrete forces at the corners.

In design, θ can be chosen freely in the range $1.0 \leq \cot \theta \leq 3.0$. In a given beam, the longitudinal and transverse reinforcement will both yield so long as condition (4.4-67) is not violated. Then equating torques from (4.4-65) and (4.4-66):

$$\cot \theta = \sqrt{\left[\frac{\sum A_{s\ell} f_y}{u_{ef}} \Big/ \frac{A_{sh} f_y}{s_h} \right]}$$

(4.4-69)

and

$$T_{Rd} = 2 A_{ef} \sqrt{\frac{A_{sh} f_y}{s_h}} \sqrt{\frac{\sum A_{s\ell} f_y}{u_{ef}}}$$

(4.4-70)

For design $T_{Rd} \geq T_{Sd,ef}$

For T-sections, the torque to be resisted by any one component rectangle can be determined as in Table 4.4-2 and each rectangle can be designed as above.

(6.4)   Torsion combined with shear and bending

The use of a 'shell' or 'wall' model allows the applied loading to be resolved into actions on the individual walls, as shown in Fig.4.4-35 a for a hollow rectangular section.

The side walls resist only shear forces, and the total shear in a wall is:

$$V_{Sdi} = \frac{V_{Sd}}{2} \pm \frac{T_{Sd,ef} (h - t)}{2 A_{ef}}$$

(4.4-71)

The bottom wall resists tension from flexure and shear from torsion:

torsion   bending
              &shear
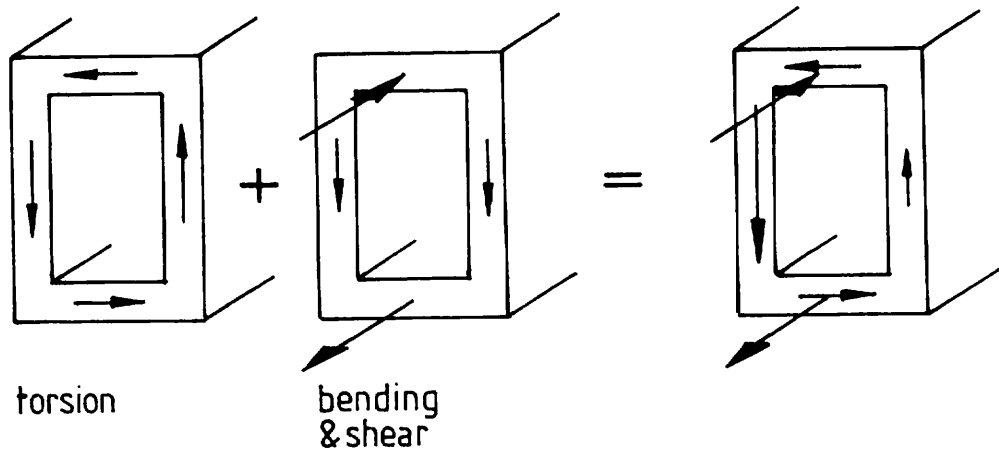
a) <u>COMBINATION OF LOAD EFFECTS IN A HOLLOW SECTION</u>
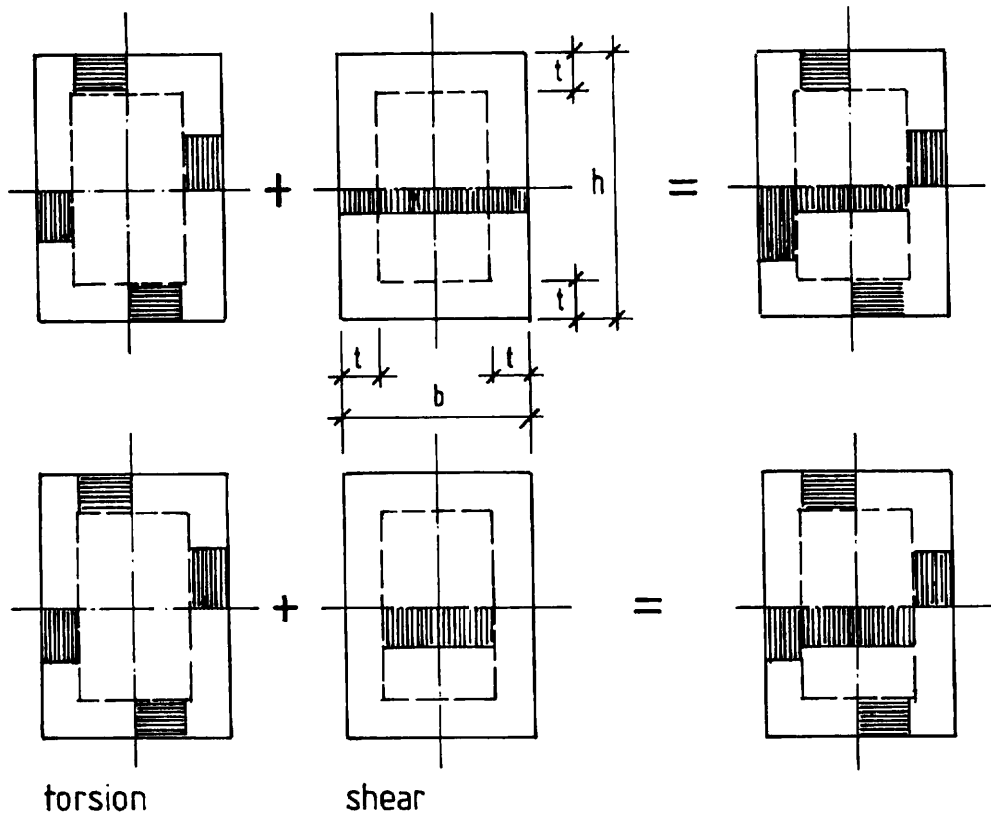
torsion   shear

b) <u>ALTERNATIVE COMBINATIONS OF SHEAR STRESSES IN A
SOLID RECTANGULAR SECTION</u>

Fig. 4.4-35:   *Combined shear, torsion and bending*

$$N_{Sdi} = \frac{M_{Sd}}{z}$$
(4.4-72)

$$V_{Sdi} = \frac{T_{sd,ef}(b-t)}{2A_{ef}}$$
(4.4-73)

The top wall carries compression from flexure and shear from torsion.
In the side and bottom walls the resulting internal forces requiring reinforcement are

$$F_{\ell i} = N_{Sdi} = V_{Sdi}\cot\theta \qquad \leq A_{S\ell i}f_{yd}$$
(4.4-74)

$$F_{ti} = V_{Sdi} \qquad\qquad \leq A_{shi}f_{yd}z_i\cot\theta$$
(4.4-75)

The limitation of the concrete stresses requires:

$$V_{Sdi} \leq f_{cd2}t\sin\theta\cos\theta$$
(4.4-76)

The top wall may be cracked, in which case equations (4.4-74) to (4.4-76) are applicable, but it may be uncracked. Its condition can be determined by calculating the longitudinal and shear stresses

$$\sigma = \frac{N_{Sdi}}{tb} \qquad\qquad \tau = \frac{V_{Sdi}}{t(b-t)}$$

and from them the principal tension

$$\sigma_I = \sqrt{\left[\tau^2 + \frac{\sigma^2}{4}\right]} - \frac{\sigma}{2}$$

The wall may be considered to be uncracked if $\sigma_I \leq f_{ctd}$.

For a solid section there is an additional shear in the core of width (b - 2t) and the shears in the vertical walls may be determined from either of the two summations illustrated by Fig.4.4-35 b). The first of these is perhaps the more natural, but it produces higher stresses in the concrete. The second is the simpler in practice as the thickness of the outer wall can be determined solely with reference to the torsion. The thickness of the top wall is influenced by considerations of both bending and torsion. Where the moment is high the principal compression

$$\sigma_{II} = \sqrt{\left[\tau^2 + \frac{\sigma^2}{4}\right]} + \frac{\sigma}{2}$$

should not exceed f_{cd1}.

<u>Example</u>

A section of a solid 600 mm square reinforced concrete beam is to be designed for the following ULS actions: $M_{Sd} = 800$ kNm, $V_{Sd} = 500$ kN, $T_{Sd} = 180$ kNm. The concrete is to have a characteristic strength $f_{ck} = 40$ MPa ($f_{cd} = 26.7$ MPa) and the reinforcement is to be of steel with $f_{yk} = 500$ MPa ($f_{yd} = 435$ MPa).

$f_{cd1} = 19.0$ MPa $f_{cd2} = 13.4$ MPa

The actions to be used in calculations are M_{Sd} and V_{Sd} as above and $T_{Sd.ef} = T_{Sd}/\delta$. With $\delta = 0.75$ for a square section $T_{Sd.ef} = 240$ kNm.

The internal actions resisting the torsion will be concentrated to an outer shell, and an estimate of the thickness of the shell walls is

$t = A/u = 600^2/4 \times 600 = 150$ mm

The shear forces due to torsion are equal in the four walls

$F_t = 240 \times 0.45/2 \times 0.45^2 = 267$ kN

Longitudinal forces due to flexure are $M_{Sd}/z = 800/0.45 = 1778$ kN. Here z is taken equal to (h - t) as an approximation, but the exact depths to the centres of compression and tension are not necessarily the same as those to the centres of the torsion-carrying walls.

The shear due to V_{Sd} can be allotted to the core of width (b - 2t).

The shear stresses in the walls and core are then $\tau = 267 \times 10^3/450 \times 150 = 3.96$ MPa and $\tau = 500 \times 10^3/450 \times 300 = 3.70$ MPa. The minimum acceptable value for sin θ cos θ is $\tau/f_{cd2} = 3.96/13.4 = 0.3$, and this would allow the use of a truss model with cot $\theta = 3$. However, the amount of longitudinal steel required in such a model would be large and cot θ is chosen to be 2.

The reinforcement requirements for shear and torsion for the outer walls are then:

- transverse reinforcement for $267/2 \times 0.45 = 297$ kN/m
- longitudinal reinforcement for $2 \times 267 = 534$ kN

For the core the corresponding results are

- transverse reinforcement for $500/2 \times 0.45 = 556$ kN/m
- longitudinal reinforcement for $2 \times 500 = 1000$ kN

The longitudinal forces may be taken by steel distributed over the height of the walls/core or may be divided between the top and bottom. As it is simpler to have distributed longitudinal bars at the outside of the section rather than in its centre, such steel will be provided in the side walls, requiring $534/0.435 = 1228$ mm^2 per wall. The core force will be distributed as 500 kN to each of the top and bottom walls.

CROSS-SECTION   (a)

LEFT SIDE   CORE   RIGHT SIDE

BOTTOM
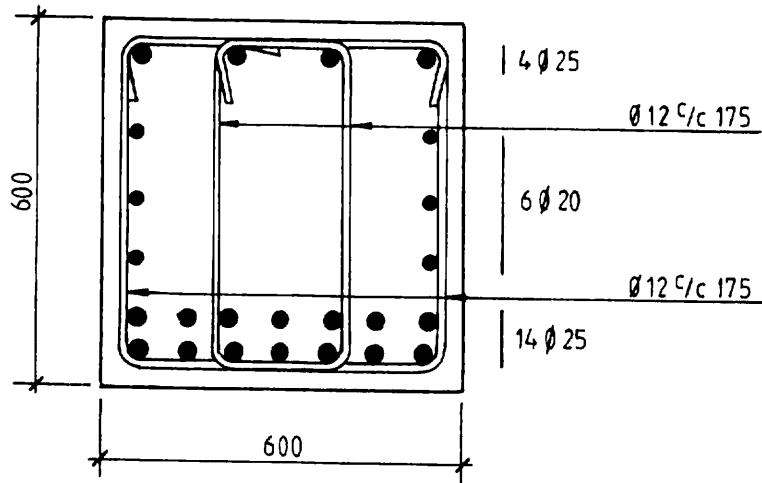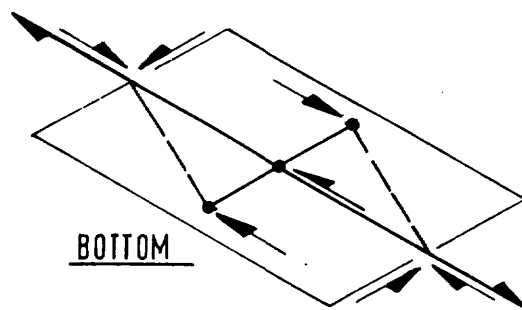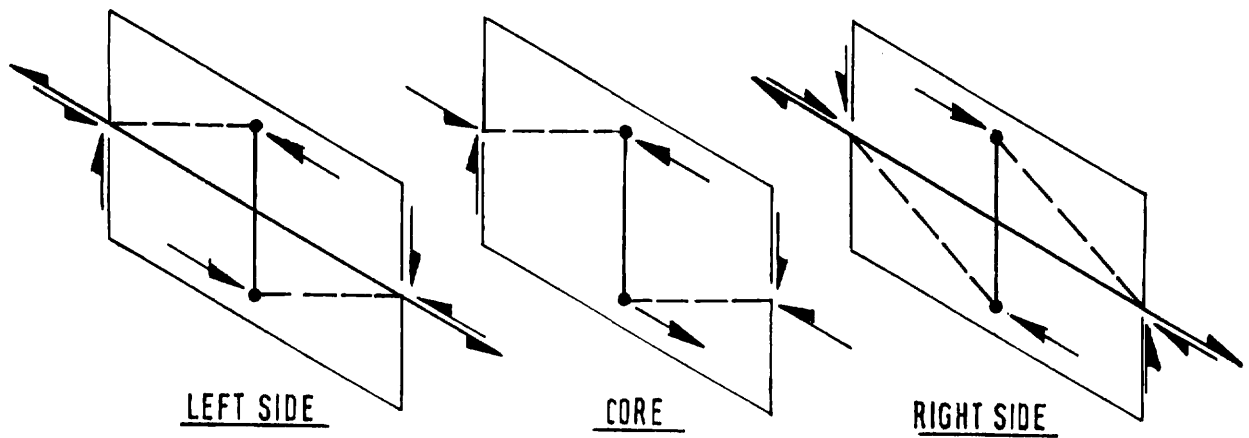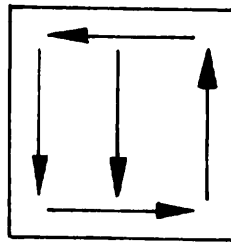
b) LOCAL TRUSS MODEL

Fig.4.4-36:   Example - design for shear, torsion and bending

The transverse steel needed is 683 mm^2/m in each wall and 1278 mm^2/m in the core. This can be provided by outer hoops (closed stirrups) $\phi 12\,^c/_c\,175$ and inner stirrups $\phi 12\,^c/_c\,175$.

In the bottom, the total requirement of longitudinal steel is for a force of 1778 kN for flexure and 534 kN for torsion plus 500 kN for the effect of shear in the core. The 2812 kN requires 6464 mm^2. $14\phi 25$ give 6873 mm^2 thus leaving 205 mm^2 as a contribution to the longitudinal reinforcement of each side wall.

The remaining requirement for longitudinal steel in each side wall is for 1228 - 205 = 1023 mm^2, which will be provided by $3\phi 20$, with an extra contribution from the corner top bars, similar to that from the bottom steel. These corner bars will be $\phi 25$ to satisfy the requirement $\phi \geq s_h/8$.

The actions in the top wall are a shear of 267 kN and a longitudinal compression of 1778 = 500 kN, the 500 kN being the tension for the core. The average stresses are then:

- longitudinal compression $\sigma = 1278 \times 10^3/600 \times 150 = 14.2$ MPa
- shear $\tau = 267 \times 10^3/450 \times 150 = 3.96$ MPa

The principal stresses are $\sqrt{3.96^2 + 7.1^2} \pm 7.1$, i.e. a compression of 15.2 MPa and a tension of 1.03 MPa. The compression is less than f_{cd1} and the tension is sufficiently low that the top would probably be uncracked.

The final detailing of the section is shown in Fig.4.4-36 a, while the actions involved are illustrated by part b) of the same figure.

(7) Plates and slabs

(7.1) Introduction

Plate systems include shear walls loaded in-plane, slabs loaded out of plane and folded plates and walls of bunkers, silos, etc., which are subjected to both in-plane and out-of-plane loading. They are commonly analysed by means such as the finite element method, which give distributions of stress resultants varying continuously over the areas, which it may be inappropriate to simplify to global strut and tie models. In such cases the ultimate limit state design is made at a local level by considering systems of concrete compression and steel tension which respect the stress limits of Section (3) above and comply with local requirements of equilibrium at a chosen number of points.

(7.2) Plates Loaded In-Plane

Fig.4.4-37 a shows a plate element of unit plan dimensions, subjected to normal (n_x, n_y) and shear (n_{xy}) forces per unit width. The normal forces are viewed as positive if tensile.

Fig.4.4-37 b shows the boundary forces corresponding to a uniaxial concrete compression (n_c per unit width) at an angle θ to the x-axis and Fig.4.4-37 c shows the boundary forces from the reinforcement (n_{sx} and n_{sy} per unit width).

For equilibrium between the applied actions of Fig.4.4-37 a and the internal ones of Figs.4.4-37 b and 4.4-37 c

$$n_{xy} = n_c \sin\theta\cos\theta \tag{4.4-77}$$

$$n_x = n_{sx} - n_c \cos^2\theta \tag{4.4-78}$$

$$n_y = n_{sy} - n_c \sin^2\theta \tag{4.4-79}$$

Eliminating n_c from these equations:

$$n_{sx} = n_x + n_{xy}\cot\theta \tag{4.4-80}$$

$$n_{sy} = n_y + n_{xy}\tan\theta \tag{4.4-81}$$

These expressions allow reinforcement to be designed for any chosen value of θ, subject to the condition

$$n_{xy} \not> f_{cd2}t\sin\theta\cos\theta \tag{4.4-82}$$

or

$$\frac{n_{xy}}{f_{cd2}t} \not> \frac{\cot\theta}{1+\cot^2\theta} \tag{4.4-83}$$

where

f_{cd2} is the design compression resistance of the cracked concrete, and
t is the thickness of the plate.

The minimum total amount of reinforcement is obtained with $\theta = 45°$ and $\tan\theta = \cot\theta = 1$, which also permits the highest possible value of n_{xy} (= $0.5\ f_{cd2}t$).

It should be noted that no sign convention has been used explicitly for the shear n_{xy}. If the direction of the shear is changed from that of Fig.4.4-37 the effect is not to reduce the reinforcement required according to equations (4.4-80) and (4.4-81), but to change the direction of the compression in the concrete so that $\theta > 90°$ and both $\tan\theta$ and $\cot\theta$ are negative.

If the applied loading is such that n_{sx}, according to equation (4.4-80) is zero, then no x-direction steel, beyond minimum reinforcement, is required. This arises where n_x is a sufficiently large compression. With $n_{sx} = 0$
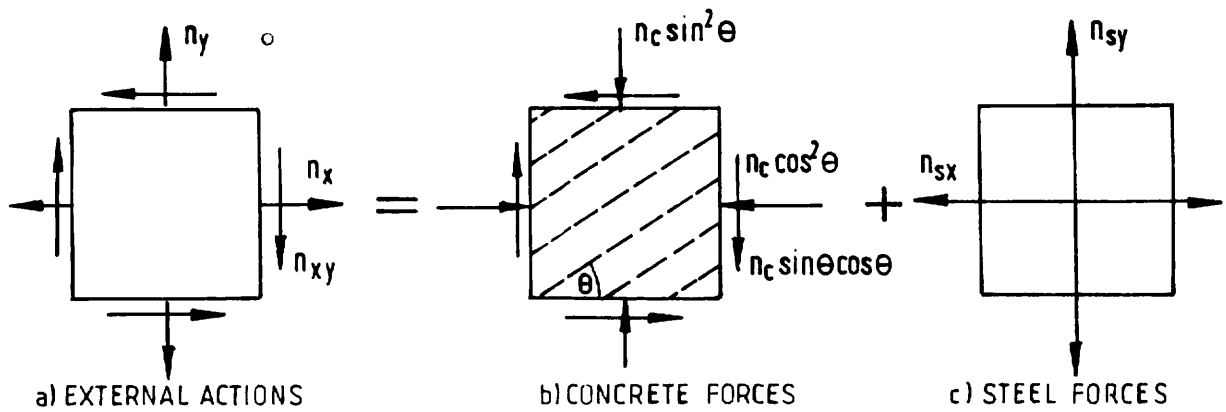
Fig. 4.4-37:   External and internal actions on a unit plate element

a) EXTERNAL ACTIONS   b) CONCRETE FORCES   c) STEEL FORCES
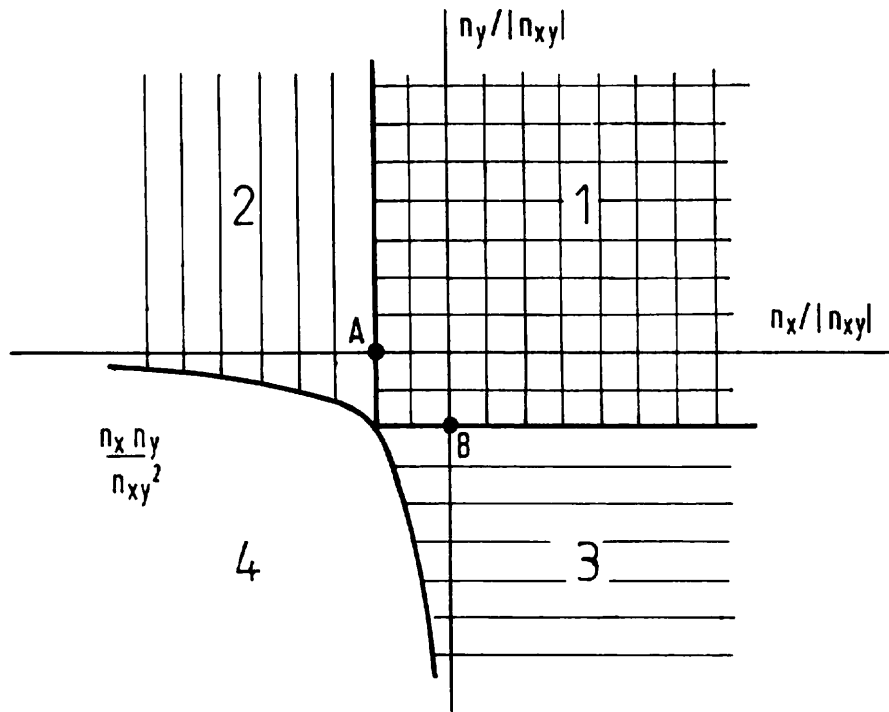
COORDINATES OF A AND B ARE (-1,0) AND (0,-1) IF θ=45°

CASE 1 Reinforcement required in x and y directions
CASE 2 Reinforcement required only in y direction
CASE 3 Reinforcement required only in x direction
CASE 4 No reinforcement required

Fig. 4.4-38:   Boundaries between loading cases requiring different arrangements of reinforcement

$$n_x = -n_c \cos^2 \theta \tag{4.4-84}$$

$$n_y = n_{sy} - n_c \sin^2 \theta \tag{4.4-85}$$

$$n_{xy} = n_c \sin \theta \cos \theta \tag{4.4-86}$$

From (4.4-84) and (4.4-86)

$$\cot \theta = \frac{-n_x}{n_{xy}} \tag{4.4-87}$$

While from (4.4-85)

$$n_{sy} = n_y + \frac{n_{xy}^2}{|n_x|} \tag{4.4-88}$$

The concrete stress limit remains that of equations (4.4-82) and (4.4-83), but it should be observed that θ is now determined by the loading and cannot be freely chosen.

The corresponding expressions when $n_{sy} = 0$ are:

$$\tan \theta = \frac{-n_y}{n_{xy}} \tag{4.4-89}$$

$$n_{sx} = n_x + \frac{n_{xy}^2}{|n_y|} \tag{4.4-90}$$

If both n_x and n_y are sufficiently large compressions, the plate is in biaxial compression, with principal forces per unit width:

$$n_I, n_{II} = \frac{n_x + n_y}{2} \pm \sqrt{\left[\frac{(n_x - n_y)^2}{4} + n^2_{xy} \right]} \tag{4.4-91}$$

which requires $n_x n_y \geq n^2_{xy}$.

The design limit for the larger compression can reasonably be taken as f_{cd1}, although a somewhat higher value could be justified in view of the biaxial compression.

Fig.4.4-38 shows the boundaries between the four design cases. Cases 2 and 3, covered by equations (4.4-87) to (4.4-90) are the same as for beam webs carrying shear.

The case of pure shear loading of a plate is one which offers opportunities for verification of the above by comparison with test data. If the reinforcement is equal in the x and y directions, equations (4.4-80) and (4.4-81) give

$$n_{xy} = n_{sx} = n_{sy}$$

with yield values applying for the steel forces at failure, subject to the upper limit of resistance from equation (4.4-82). Thus

$$\left(n_{xy}\right)_u = \left(n_{sx}\right)_y = \left(n_{sy}\right)_y \leq 0.5f_{c2}t$$

where the suffices u and y outside the brackets denote 'ultimate' and 'yield' and f_{c2} is the unfactored resistance to compression in cracked concrete

$$f_{c2} = 0.6f_c\left(1 - f_c / 250\right)$$

If one set of reinforcement has a lower resistance than the other, failure may occur after its yield but without the yielding of the second set, i.e. by compression of the concrete while the direction of the compression is adjusting to the value required for both sets of reinforcement to yield.

Taking the x-direction steel to have the lesser resistance, equation (4.4-78) gives

$$n_x = 0 = \left(n_{sx}\right)_y - n_c \cos^2\theta \text{ or } n_c = \left(n_{sx}\right)_y / \cos^2\theta$$

then from equation (4.4-77)

$$\left(n_{xy}\right)_u = n_c \sin\theta\cos\theta = \left(n_{sx}\right)_y \tan\theta$$

with $n_c = f_{c2}t$, $\cos\theta = \sqrt{[(n_{sx})y / f_{c2}t]}$

Finally

$$\left(n_{xy}\right)_u = f_{c2}t\sqrt{\frac{(n_{sx})_y}{f_{c2}t}}\sqrt{\left[1 - \frac{(n_{sx})_y}{f_{c2}t}\right]}$$

which is the same as the ultimate shear in a web failing with stirrups yielding and concrete crushing.

If both sets of steel yield, equations (4.4-78) and (4.4-79) give

$$\sin\theta = \sqrt{[(n_{sy})_y / n_c]} \text{ and } \cos\theta = \sqrt{[(n_{sx})_y / n_c]}$$

whence $\left(n_{xy}\right)_u = \sqrt{[(n_{sx})_y(n_{sy})_y]}$

The effects of axial loading in addition to shear can be treated by the basic equations. In the particular case of equal biaxial forces ($n_x = n_y = \lambda n_{xy}$, with λ positive for tension), if both sets of reinforcement yield:

$$\left(1-\lambda^2\right)\left(\frac{n_{xy}}{f_{c2}t}\right)^2+\lambda\left(\frac{n_{sx,y}+n_{sy,y}}{f_{c2}t}\right)\left(\frac{n_{xy}}{f_{c2}t}\right)-\frac{n_{sx,y}}{f_{c2}t}\frac{n_{sy,y}}{f_{c2}t}=0$$

If only the x-direction reinforcement yields:

$$\left(1+\lambda^2\right)\left(\frac{n_{xy}}{f_{c2}t}\right)^2+\lambda\left(1-\frac{n_{sx,y}}{f_{c2}t}\right)\left(\frac{n_{xy}}{f_{c2}t}\right)-\left(\frac{n_{sx,y}}{f_{c2}t}\right)\left(1-\frac{n_{sx,y}}{f_{c2}t}\right)=0$$

Fig.4.4-39 shows a comparison between predictions made as above and results of tests by Vecchio and Collins (1982), Vecchio, Collins and Aspiotis (1994) and Pang and Hsu (1995). The data covers concrete strengths from 11.6 to 68.5 N/mm², ratios of y-direction to x-direction reinforcement up to 9:1 and cases of loading in pure shear, shear plus biaxial tension and shear plus biaxial compression. The only results not plotted are those for a few specimens reinforced in only one direction, secondary failures at the loading points and three specimens from the first reference subject to axial compression and shear, with the compression high enough to prevent a fully cracked state.

(7.3)   Combined in-plane and out-of-plane loading

The effects of out-of-plane loading acting alone or in combination with in-plane loading can be treated by viewing the slab or plate as a sandwich in which the outer layers resist in-plane forces while the core carries transverse shear.

If the outer layers are assumed to be of equal thickness and a single value (z) is assumed for all the lever arms, the actions on the outer layers are as illustrated in Fig.4.4-40, from which it should be noted that the effects of in-plane shear and torsion from the out-of-plane loading are always additive in one layer and subtractive in the other.

As a first approximation the outer layers can be taken to have thicknesses equal to $^1/_3$ of the plate thickness t and z can be taken as 2t/3.

The outer layers can then be designed as plates loaded in-plane and subjected to the actions of Fig.4.4-40. If necessary the lever arms can be adjusted once the initial calculations have been made, the stresses in the concrete have been examined and the depths to reinforcement can be assessed.

In selecting values for the angles θ it should be noted that a local minimum for the total amount of reinforcement required is always obtained for $\theta = 45°$. However other values may be preferred to keep the principal compressions in directions close to those in an uncracked plate or because of the practicalities of arranging reinforcement. As a general rule $15° \le \theta \le 75°$ is a prudent range in order to avoid problems of compatibility which arise if the compression is too nearly coincident with reinforcement intended to yield in tension.

The core of the sandwich resists the out-of-plane shear accompanying changes in m_x, m_y or m_{xy}. For equilibrium of a layer such as that in Fig.4.4-41

Solid symbols $f_c > 40\,MPa$
Open symbols $f_c < 30\,MPa$

● ○ No yield of steel

▼ ▽ Yield of steel in one direction

▲ △ Yield of steel in both directions
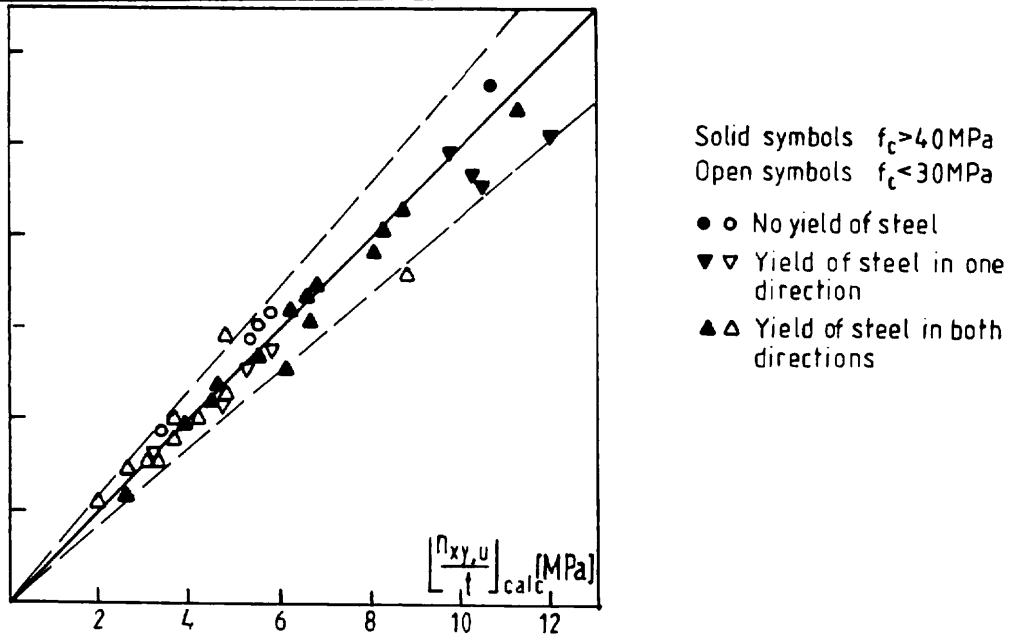
*Fig.4.4-39:*   Comparison of theoretical and experimental shear strengths of plate elements

a) external actions   b) top layer   c) bottom layer
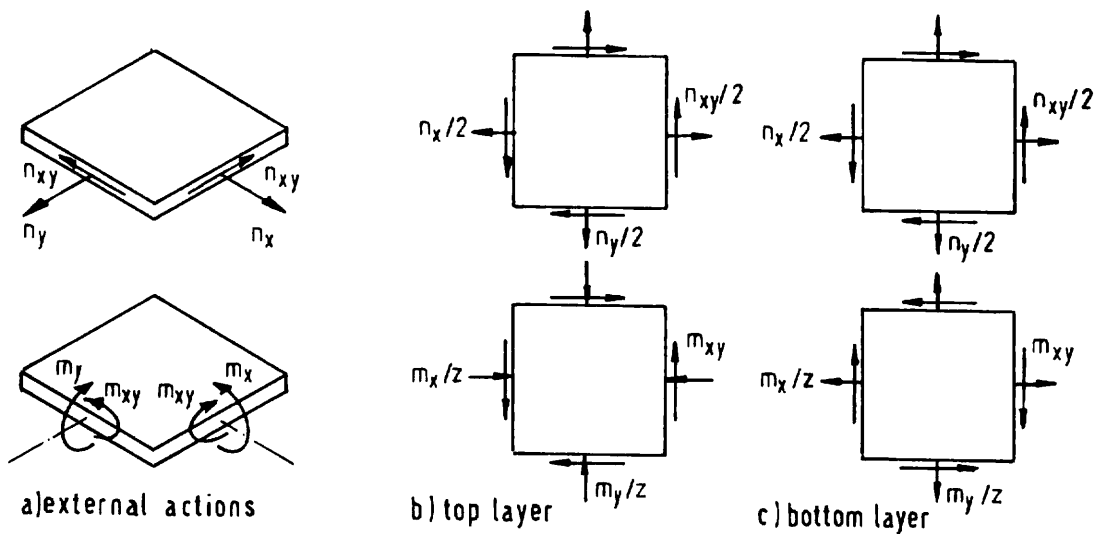
Fig.4.4-40:   Actions on the top and bottom
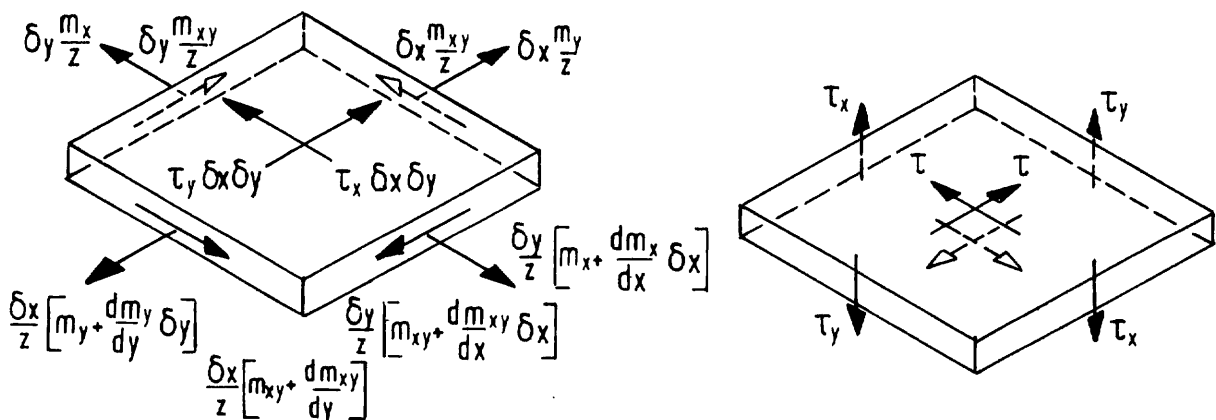
Fig.4.4-41:   Transverse shear in two-way slabs

$$\tau_x = \frac{1}{z}\left[\frac{\partial m_x}{\partial x} + \frac{\partial m_{xy}}{\partial y}\right]$$

$$\tau_y = \frac{1}{z}\left[\frac{\partial m_y}{\partial y} + \frac{\partial m_{xy}}{\partial x}\right]$$

The resultant shear on an element $\partial_x\,\partial_y$

$$V = \partial x \partial y \sqrt{\tau_x^2 + \tau_y^2}$$

giving a unit shear stress

$$\tau = \sqrt{\tau_x^2 + \tau_y^2}$$

This is the equivalent of V/bz for a one-way spanning element, and the shear resistance of the two-way element is affected by cracking due to moments in the same way as that of a one-way member. Thus for design the check needed is that of equation (4.4-20), requiring

$$\sqrt{v_x^2 + v_y^2} \le 0.12\xi\sqrt[3]{\frac{100 A_s}{bd} f_{ck}}$$

where

v_x, v_y are shear forces per unit width.

The evaluation of $100A_s/bd$ in such cases is somewhat uncertain but a reasonable expression is

$$\frac{100 A_s}{bd} = \frac{v^2{}_x(100 A_s/bd)_x + v^2{}_y(100 A_s/bd)_y}{v_x^2 + v_y^2}$$

(7.4)   Punching

Punching is the action by which a truncated cone of concrete is forced out of a slab. It arises at columns in flat slabs and raft foundations and at concentrated loads on slabs. The following is written principally in terms of conditions at columns in flat slabs but is generally equally applicable to the other cases.

(7.4.1)   Symmetrical punching at interior columns

The type of cracking observed from well before failure on the top surface of a flat slab in the vicinity of an internal column is illustrated by Fig.4.4-42. There is a crack around the column and a dominant pattern of radial cracks dividing the slab into segments which rotate as

practically rigid bodies about axes close to the column. At higher loads a few circumferential cracks appear at short distances from the column but do not materially affect the rigid body rotation. At about $\frac{2}{3}$ of the eventual punching load there is a sharp increase of vertical strain in the slab at around 0.5d from the column, marking the formation of internal inclined cracks.

If failure is by punching, it occurs at a surface, such as that shown in Fig.4.4-43, which has a trumpet-like shape between the face of the column at the underside of the slab and its intersection with the main steel at a distance which is typically about 2d from the column. This distance can vary and tends to be reduced if the slab is lightly reinforced. If deformation continues after the peak load, the failure surface extends horizontally at the level of the main bars.

The primary actions resisting punching are inclined compression in the concrete between the crack tip and the bottom of the slab and forces transferred across the inclined cracks.

The classical theory of punching by Kinnunen and Nylander (1960) - see also Kinnunen (1963) and Nylander and Kinnunen (1976) - concentrates on the former action, while more recent work, e.g. Menétrey (1997), points to the importance of the forces in the cracks. Both actions are strongly influenced by the main steel in a considerable area around the column as it controls both the depth and width of the cracking.

Most practical design methods are phrased in terms of nominal applied stresses - the load divided by an area. The plan area of an assumed failure surface at 45° has been used for checking the pull-out resistances of embedments in concrete, which is a problem having much in common with punching. The inclined surface area can be used and can be associated with a failure criterion in which the ultimate stress is related to the angle between the surface and the motion at failure. This allows resistances to be verified for different surfaces and can be useful when the applied load is a function of the inclination of the surface, e.g. in foundations where soil pressure reduces the punching force, and also in slabs with shear reinforcement.

Codes of practice define their nominal shear stresses as the load divided by the product of the slab's effective depth and the lengths of control perimeters constructed at specified distances from the column. In older codes the distance was generally d/2, but recent recommendations use much larger distances such as 1.5d in EC2 and 2d in MC90. There are two main reasons for the change. Firstly it makes the limiting shear stress much more uniform for different column sizes. Secondly, it allows the limiting stresses to be made the same as for other forms of shear in slabs. Thus in MC90, for concentric loading (no transfer of moment to the column), the applied shear is

$$\tau_{Sd} = \frac{F_{Sd}}{u_1 d} \tag{4.4-92}$$

where

|	
F_{Sd}	is the applied punching load and
u_1	is the length of the perimeter illustrated by Fig.4.4-44
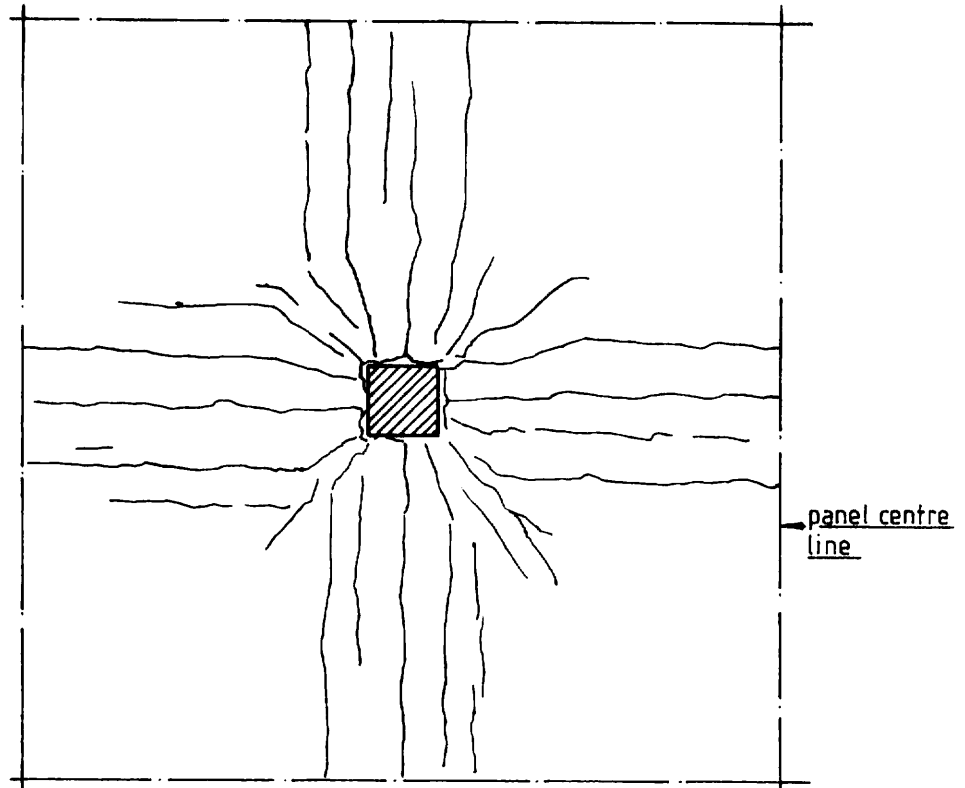
*Fig.4.4-42:*   Typical cracking of the top surface of a flat slab
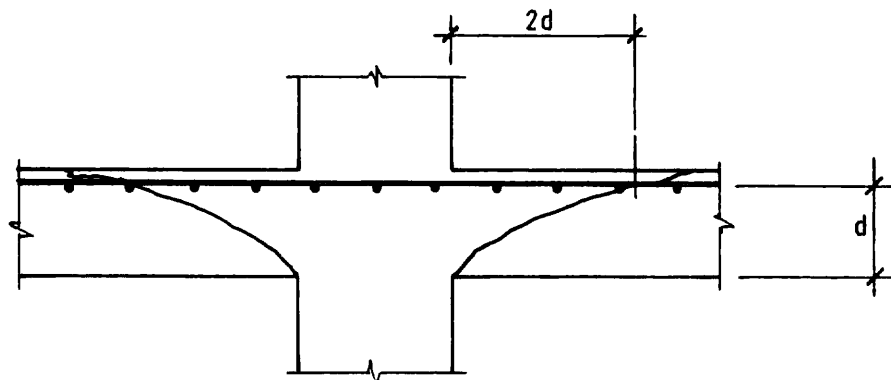

Fig.4.4-43:   Typical form of punching failure
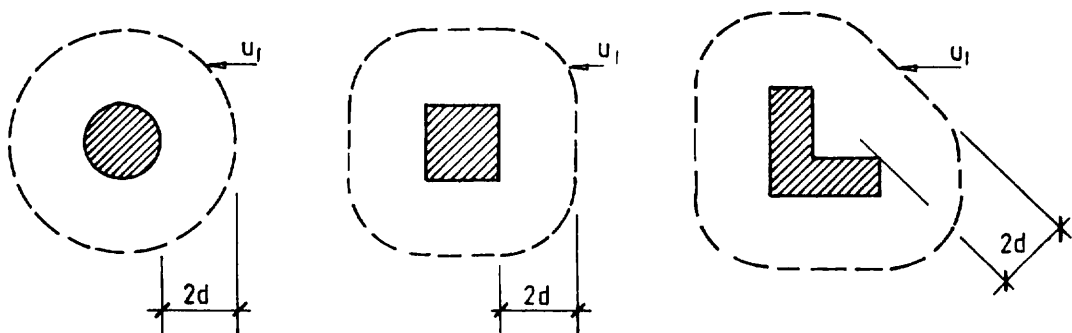
Fig.4.4-44:   Control perimeters u_1 according to MC90

The corresponding resistance is

$$\tau_{Rd} = 0.12\xi(100\rho f_{ck})^{1/3}$$ (4.4-93)

with

ξ $= 1 + \sqrt{200/d}$ with d in mm

ρ $= \sqrt{\rho_x\rho_y}$, are ρ_x and ρ_y are the reinforcement ratios in orthogonal directions, calculated for widths equal to the side dimensions of the column plus 3d to either side of it

d $= (d_x + d_y)/2$

The MC90 approach to punching is largely empirical so it is relevant to consider its accuracy and Fig.4.4-45 compares predictions from the code with test results for punching failures due to concentric loading at interior locations in slabs without shear reinforcement.

The data used is taken from Hallgren (1996), Kinnunen and Nylander (1960), Kinnunen, Nylander and Tolf (1980), Marzouk and Hussein (1991), Moe (1961), Ramdane (1996), Regan (1986) and Regan (1997).

Most results are plotted in all four parts of the figure and are shown as solid symbols. A few results are shown as open symbols and appear in only one part. These are for Regan's (1986) two slabs with extremely low concrete strengths in Fig.4.4-45 a and one slab by Hallgren and one by Marzouk and Hussein with low ratios of reinforcement which potentially failed in flexure in Fig.4.4-45 b and some slabs by Regan with very small loaded areas plotted only in Fig.4.4-45 d.

As with the MC90 expression for the shear resistances of beams without shear reinforcement, the objective characteristic strength level corresponds to a partial safety factor of 1.33, i.e. $\tau_{Rk} = 0.16\ \xi\ (100\rho\ f_{ck})^{1/3}$. Thus equation (4.4-93) does not have a factor of 1.5 applied to τ itself, but does have a factor greater than 1.5 applied to f_{ck}.

Fig.4.4-45 a to c show no systematic trends to error with variations of f_c, ρ or d. Fig.4.4-45 d shows that the combination of equations (4.4-92) and (4.4-93) should not be used where the loaded area is very small - equivalent diameter B less than about 0.75d. This is the reason for MC90's upper limit on punching resistance.

$$F_{Sd} \not> 0.5\ f_{cd2}\ u_o\ d$$

where

u_o is the length of the periphery of the column or loaded area.

(7.4.2)   Eccentric punching

If the load applied to a column is eccentric, the moment is transferred by a combination of bending, torsion and uneven shear. Elastic analysis - Mast (1970) - shows that the distribution

$$\frac{V_u}{\xi\sqrt[3]{100\rho f_c}}$$

f_c (MPa)

(a)

$$\frac{V_u}{\xi\sqrt[3]{100\rho f_c}}$$

ρ (%)

(b)

$$\frac{V_u}{\xi\sqrt[3]{100\rho f_c}}$$

d (mm)

(c)

$$\frac{V_u}{\xi\sqrt[3]{100\rho f_c}}$$

B/d

(d)
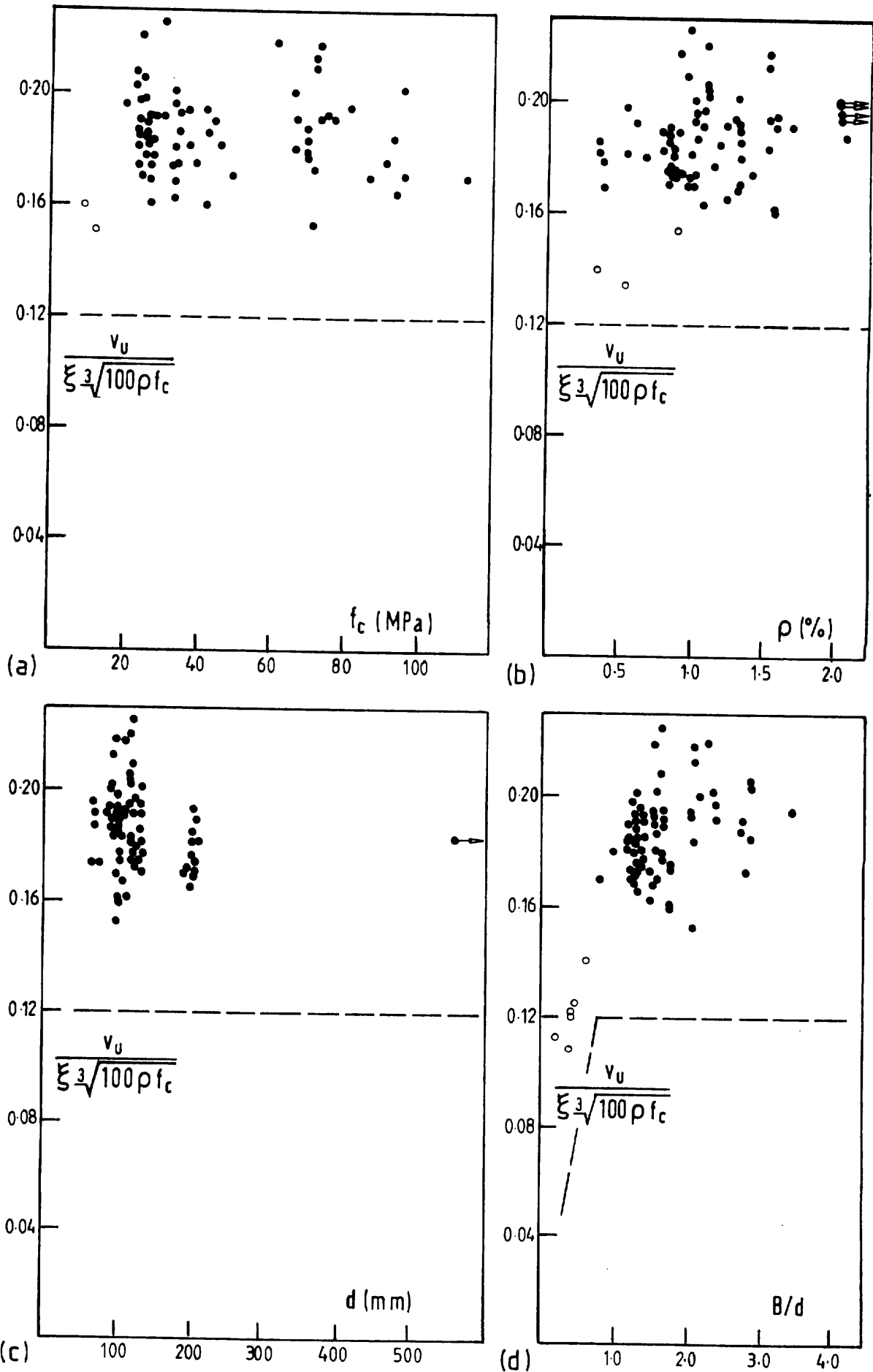
Fig. 4.4-45:   Punching strengths of slabs without shear reinforcement – comparisons of test results with groups of fib.

of shear due to a moment acting between a slab and a column is close to the rectangular form of Fig.4.4-46.

Combining the effects of the vertical loading and part of the transferred moment

$$\tau_{Sd} = \frac{F_{Sd}}{u_1 d} + \frac{KM_{Sd}}{W_1 d}$$

(4.4-94)

where

M_{Sd}	is the transferred moment
KM_{Sd}	is the part transmitted by uneven shear, with K depending primarily on the ratio of the column dimensions parallel and perpendicular to the eccentricity of the load, and
W_1	$= \int_0^{u_1} / e / d\ell$, where $d\ell$ is an elementary length of the perimeter u_1 and e is its distance from the axis about which the moment acts

For an interior rectangular column

$$W_1 = \frac{c_1^2}{2} + c_1 c_2 + 4c_2 d + 16d^2 + 2\pi d c_1$$

if the perimeter u_1 is that of MC90, 2d from the column.

The values of K given in MC90 are as below

c_1/c_2	0.5	1.0	2.0	3.0
K	0.45	0.60	0.70	0.80

Table 4.4-3:   *Ratio of moment transferred to the column*

where

c_1	is the column dimension parallel to the load eccentricity and
c_2	is the dimension perpendicular to the eccentricity

At interior columns, if the moment is high, and in the extreme, if the slab/column connection is subjected to a pure moment, the failure takes the form of asymmetric punching. This is because the flexural resistance is high, even for low ratios of reinforcement, thanks to the capacity of the action illustrated in Fig4.4-47.

For design purposes it can be convenient to work in terms of an "effective" concentric load

$$F_{Sd,ef} = F_{Sd}\left[1 + K \frac{M_{Sd}}{F_{Sd}} \frac{u_1}{W_1}\right]$$
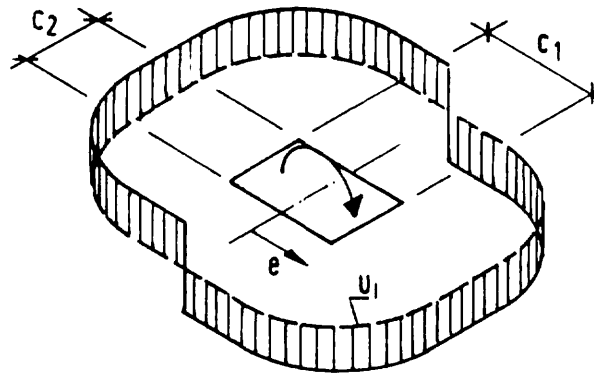
Fig. 4.4-46:   *Distribution of shear stresses in a slab due to transfer of a moment from a column*
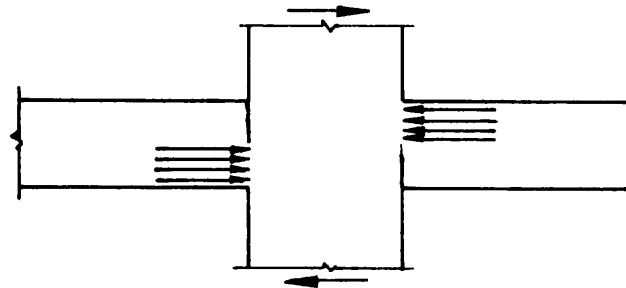

*Fig. 4.4-47:*   *Transfer of moment between slab and column by opposite compression zones*
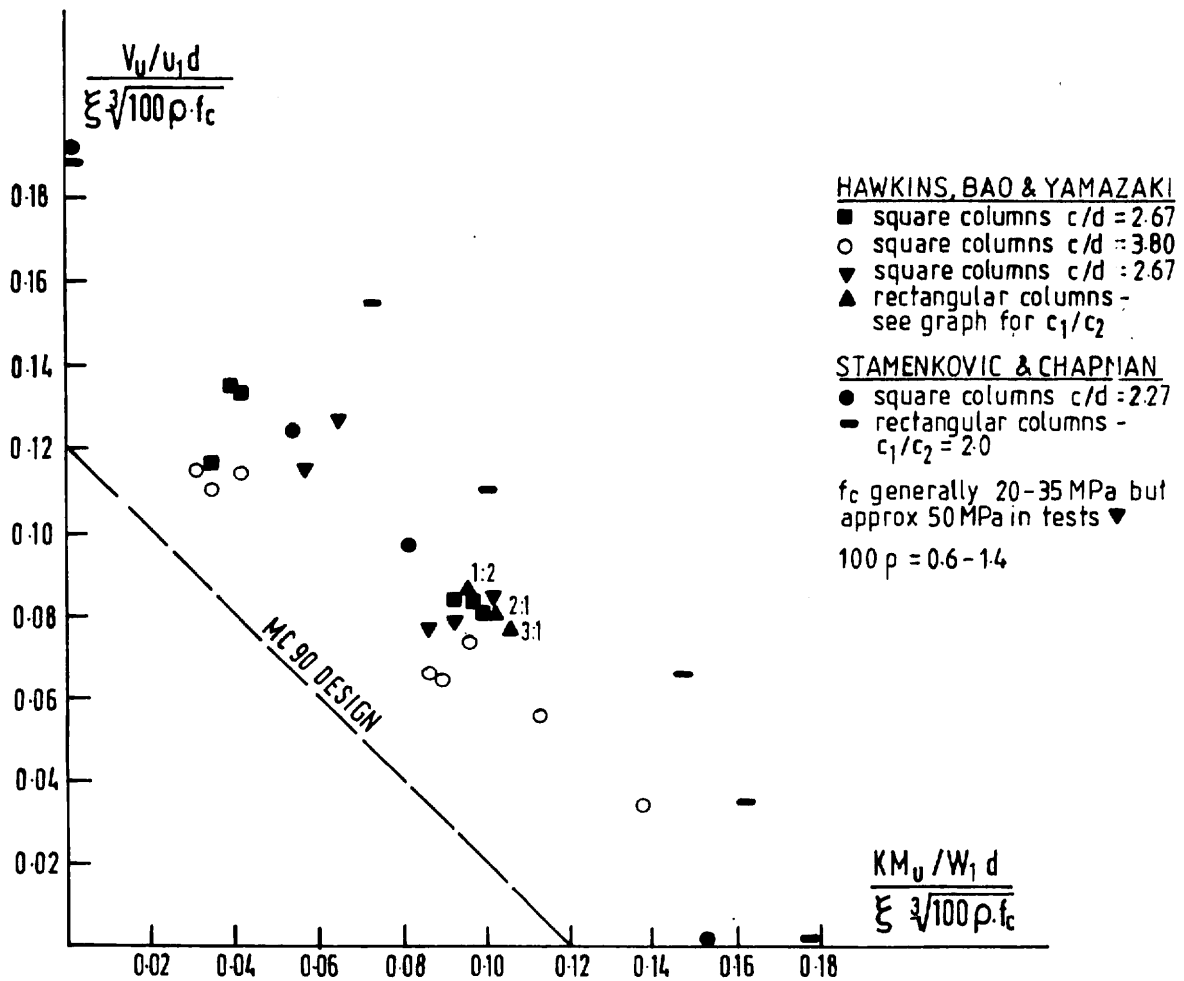
Fig. 4.4-48:   *Results of tests of eccentrically loaded slab-interior column connections*

and an upper limit

$$F_{Sd,ef} \not> 0.5 \, f_{cd2} \, u_o \, d$$

Fig.4.4-48 compares equations (4.4-93) and (4.4.94) with test results from Stamenkovic and Chapman (1974) and Hawkins, Bao and Yamazaki (1989) and demonstrates that the linear interaction implied by equation (4.4-94) is appropriate.

The effect on an edge column connection of a moment about an axis perpendicular to a slab edge is similar to that of eccentric loading at an interior connection, but the action of Fig.4.4-47 is not possible in relation to a moment about an axis parallel to the slab edge, or to any moment at a corner column.

In the normal case, where the latter type of moment dominates, any punching failure is generally preceded by torsional cracking at the edge of the slab (Fig.4.4-49) and yielding of the main bars perpendicular to the slab edge and within the width of the column. The full interaction between the moment and the shear is of the form shown in Fig.4.4-50. Point A corresponds to uniform shear at the column faces in contact with the slab and negligible forces in the flexural reinforcement of the slab. Point B corresponds to shear on a reduced perimeter at the column and the full use of the flexural steel, while point C represents pure moment loading. The moment at point B is greater than that at C because of the eccentricity of the shear.

The moment that can be resisted by the slab's top steel can be assessed on the basis of the reinforcement within the width of the column and $0.5c_2$ to either side of it. This formulation represents the reinforcement effectively anchored beyond the crack lines marked a-a in Fig.4.4-49. The width within which reinforcement is effective can be increased somewhat by the provision of stirrups for torsion at the slab edge and possibly by the use of extra steel parallel to the edge, but the use of an effective width $(c_1 + c_2)$ for both the steel and the concrete contributions to flexure is generally reasonable.

Although the results from tests of isolated columns by Stamenkovic and Chapman, plotted in Fig.4.4-50, demonstrate the existence of the full interaction described, tests of statically indeterminate systems representing flat slab floors show that, in practical terms, the ultimate limit state usually corresponds to complete or nearly complete development of the flexural capacity. Design for punching can thus normally be based on point B of Fig.4.4-50 with the shear resistance taken as the product of τ_{Rd} from equation (4.4-93), the mean effective depth and the length of the reduced perimeter shown in Fig.4.4-51.

This approach is compared with test results in Fig.4.4-52 and can be seen to give reasonable, though not precise results. The main problem is that the estimation of the flexural capacity derived from the reinforcement is sometimes conservative. It is however difficult to make improvements in this in view of the very short anchorage lengths of bars crossing the critical cracks.
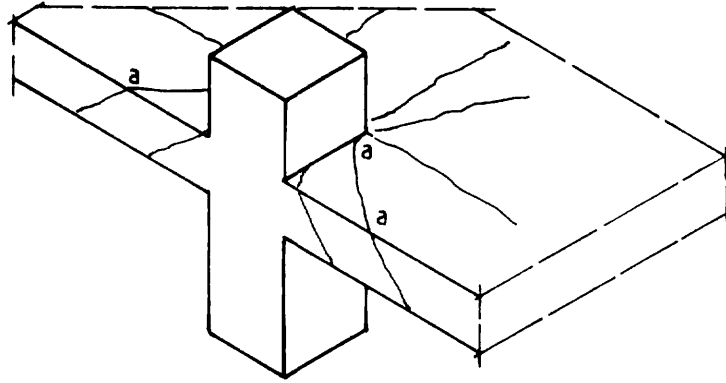
Fig.4.4-49:   Torsional cracking of a slab at an edge column

F_u(kN)

80   A

60   B

40

20

C   M(kNm)

2·5   5·0   7·5   10·0

A   Shear concentric with total column perimeter

B   Shear concentric with effective perimeter. Flexural reinforcement fully utilized.

C   Zero shear. Flexural reinforcement fully utilized.
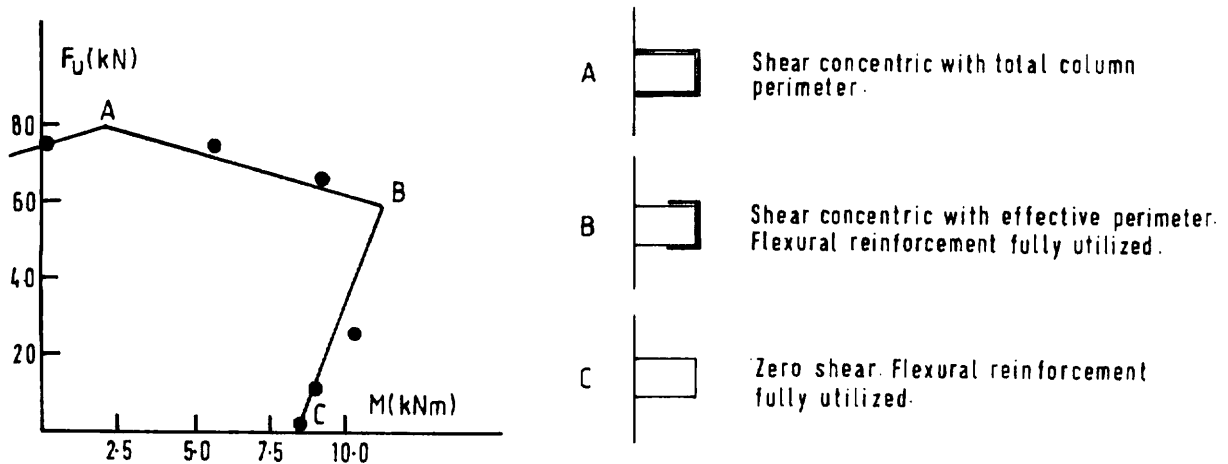
Fig.4.4-50:   Tests by Stamenkovic and Chapman (1974) of isolated column specimens

c_1 2d

0·5c_1

c_2

0·5c_1

width for reinforcement transfering moments

lesser of 1·5d and 0·5c_1

c

0·5c

width for reinforcement transfering moments

2d

lesser of 1·5d and 0·5c

$\frac{F_{u\,test}}{F_{u\,calc}}$

Note Partial safety factors have been removed in the calculation of $F_{u\,calc}$ and $M_{u\,calc}$. Points on the y axis are from tests with columns free to rotate

1·4

1·2

1·0

0·8

0·6

0·4

0·2

$M_{u\,test}/M_{u\,calc}$

0·2   0·4   0·6   0·8   1·0   1·2   1·4

Regan
▼ h = 200   ◯ h = 125
■ h = 104
Kinnunen
▲ h = 130

Fig.4.4-51:   Effective control perimeters and locations of reinforcement for moment transfer at exterior columns
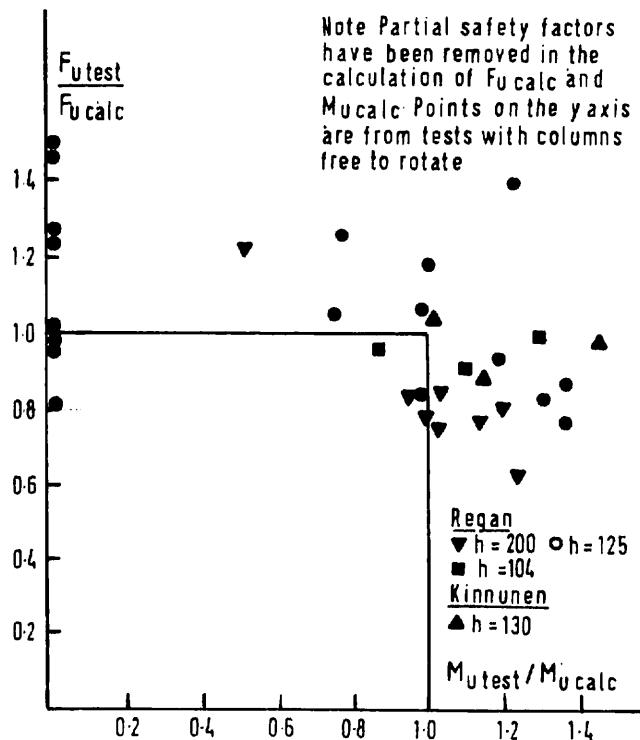
Fig.4.4-52:   Results of tests of connections between slabs and edge columns

(7.4.3)   Slabs with shear reinforcement

The use of shear reinforcement in slabs has grown considerably in recent years and there are many systems available. In general terms they can be divided into two main types:

- Shearheads (Fig.4.4-53) which are structural steelwork assemblies and effectively increase the size of the column. They are generally designed to carry the full punching force. Recommendations on the design of some types can be found in the ACI code.

- Shear Reinforcement (Fig.4.4-54) which works in tension in conjunction with inclined compression in the concrete.

The following paragraphs relate to 'Shear Reinforcement'.

The most obvious difficulty in providing effective shear reinforcement in relatively shallow members is that of giving it satisfactory anchorages to both sides of potential cracks. In the following it is assumed that the forces able to be developed by the shear steel are known.

Lower-bound models for slabs with shear reinforcement are not well developed and behaviour is, at least for the present, better described in upper-bound terms of potential failure mechanisms. Fig.4.4-55 shows a range of possible punching surfaces for an interior slab-column connection.

The area of the slab in which shear reinforcement is required is defined from consideration of the surface outside the reinforced zone. Conditions here are not identical to those around a column in a slab without shear reinforcement, but they are similar, and the design requirement can be expressed as

$$u_n \geq \frac{F_{Sd}}{\tau_{Rd} d} \tag{4.4-95}$$

where

u_n is the length of a perimeter constructed treating the perimeter of the outermost shear reinforcement as being equivalent to that of the column in the determination of u_1 - see Fig.4.4-56.

To ensure that the shear per unit length of perimeter is reasonably uniform around u_n the circumferential spacing of the shear reinforcement should be limited to about 2d.

The intensity of shear reinforcement required within the zone defined as above can be found by considering the resistances of possible failure surfaces such as those in Fig.4.4-55. The surfaces are drawn so as to just miss successive layers of shear reinforcement because most current types of shear steel are unlikely to be highly stressed by the dowel action of the main bars.

At each of the potential failure surfaces crossed by shear reinforcement the resistance has two components - one from the concrete and the other from the shear steel:
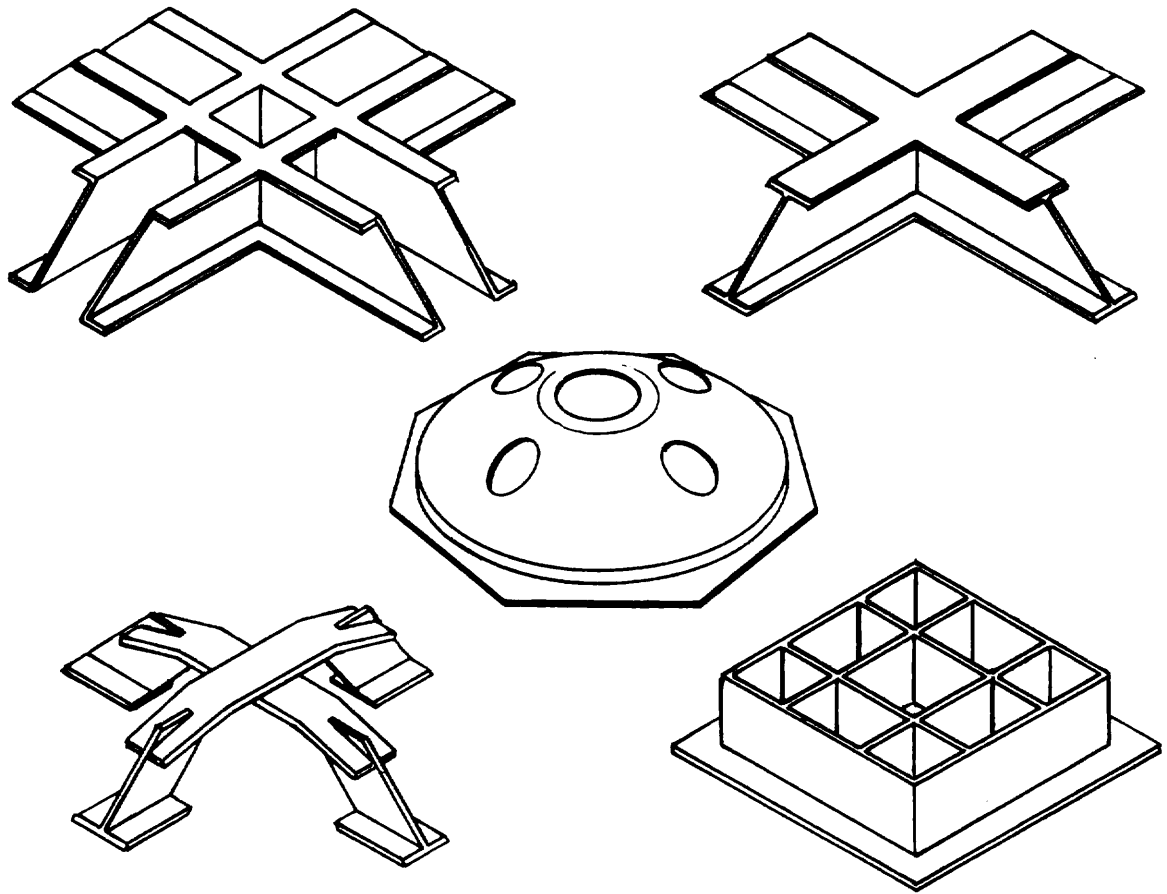
*Fig.4.4-53:*   **Examples of shearheads**
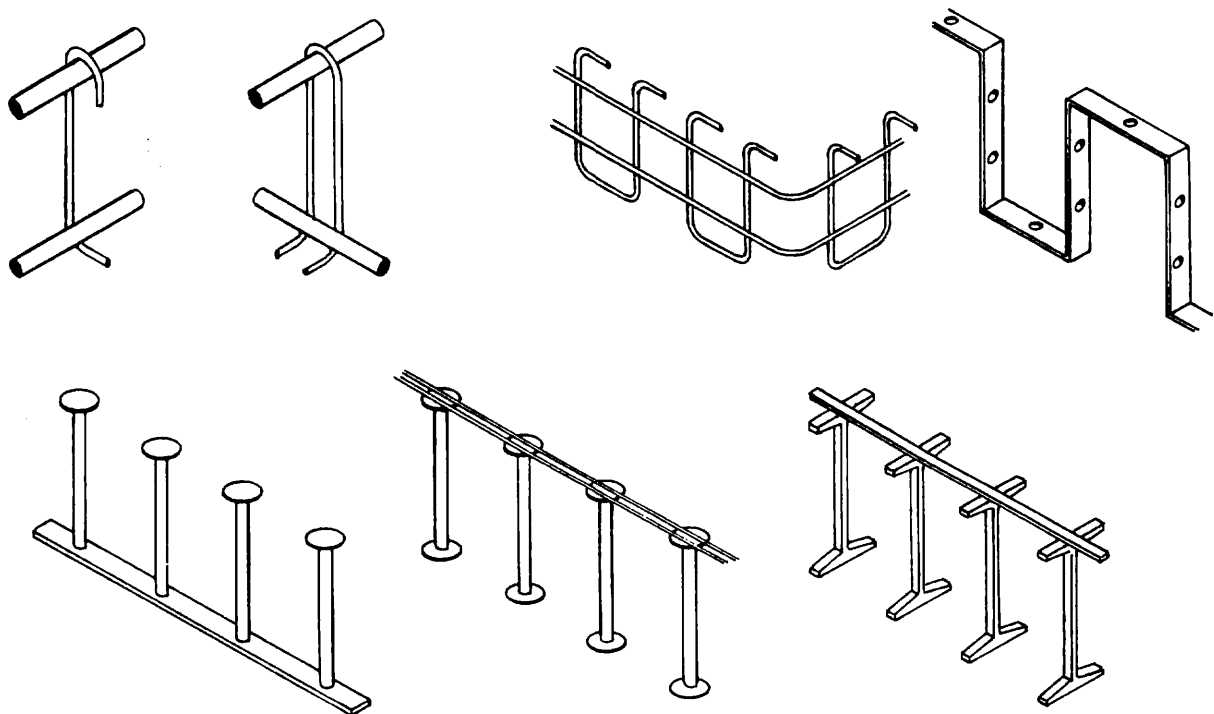
Fig.4.4-54:   **Examples of shear reinforcement for flat slabs**
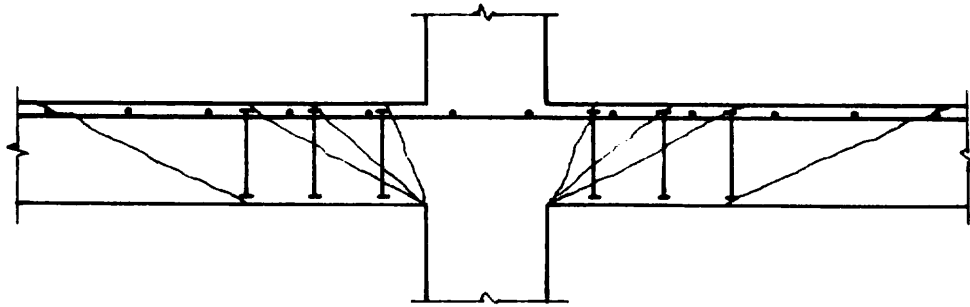
Fig. 4.4-55:   *Potential failure surfaces in a slab with shear reinforcement*
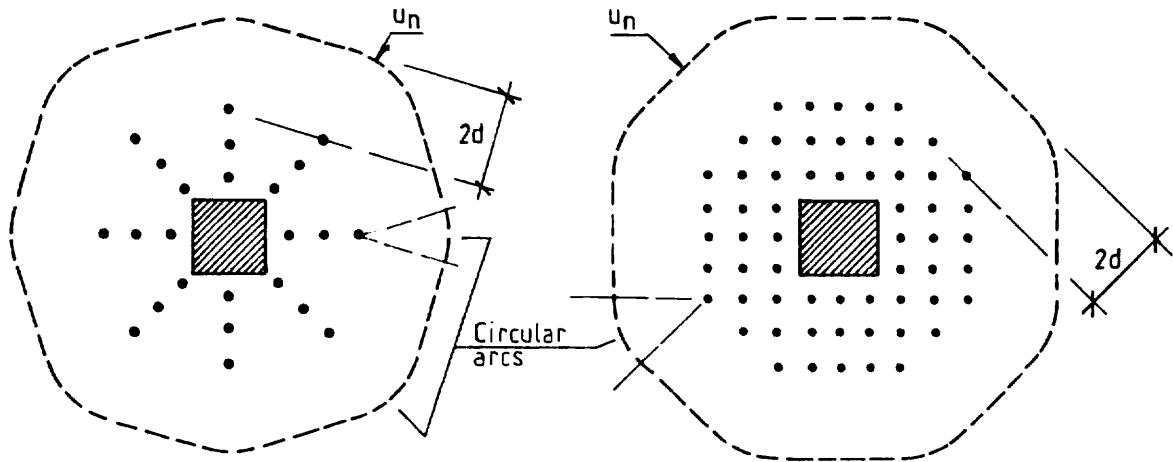

Fig. 4.4-56:   *Control perimeters for calculations of resistances outside regions with shear reinforcement*
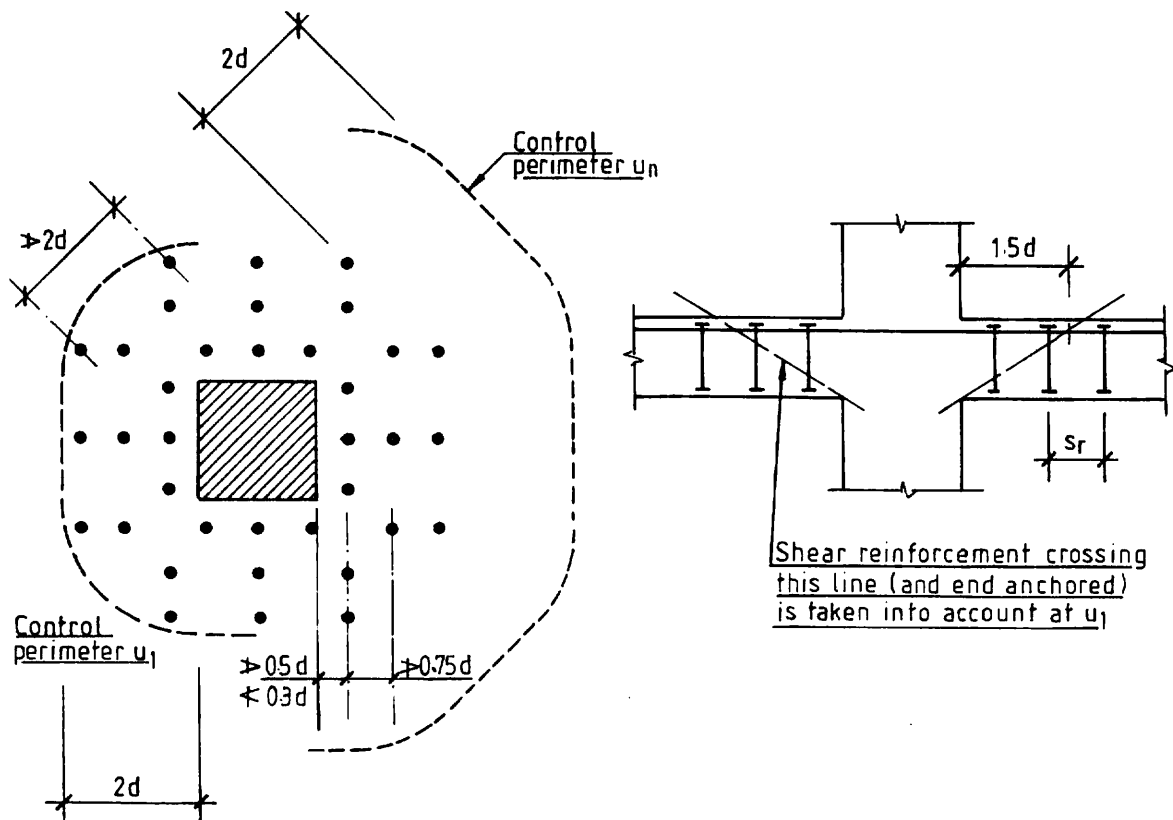

Fig. 4.4-57:   *MC90 approach to shear reinforcement in flat slabs*

$$F_{Rd} = F_{Rd,c} + F_{Rd,s}$$ (4.4-96)

As the angle θ of the failure surface decreases, more layers of shear reinforcement become active, increasing $F_{Rd,s}$, but the ability of the concrete to carry forces across the crack reduces, thus decreasing $F_{Rd,c}$.

As the loading increases beyond the original shear cracking load, stresses are developed in the steel. Up to a certain point, when the deformations are similar to those at the ultimate limit state of a slab without shear steel, the concrete resistance also increases, but the greater crack opening required to produce yield of the reinforcement is likely to lead to a reduction of the concrete component.

The variation of F_{Rd} with θ is not too rapid and MC90 in effect treats just two failure surfaces. At the first the failure is between the column and the innermost shear steel and the design resistance is the maximum:

$$F_{Rd} = 0.5 f_{cd2} u_o d$$ (4.4-97)

The distance from the column to the inner shear reinforcement should be no greater than 0,5d. It should not be less than 0,3d since steel closer than this will not be well anchored in the compression zone if crossed by cracks at lower inclinations.

At the second surface cot θ is about 2.0 and the steel contribution comes from the shear reinforcement crossing a surface at arc cot 1.5 to ensure some anchorage at the upper end. The concrete component of resistance is taken to be 75% of the design strength of a slab without shear reinforcement.

$$F_{Rd} = 0.09\xi(100\rho f_{ck})^{1/3} u_1 d + 1.5\frac{d}{s_r} A_{sw} f_{yd}$$ (4.4-98)

where

s_r is the radial spacing of layers of shear reinforcement each of area A_{sw} and
             $s_r \not> 0.75d$

The shear reinforcement is required to be anchored at the level of the mean plane of the tension steel and at the level of the centre of the compression zone and $f_{yd} \not> 300$ MPa.

If the shear reinforcement is not arranged in circumferential layers, the second term of equation (4.4-98) can be replaced by the sum of the resistances of the elements crossing the surface at arc cot 1.5, provided that the radial distribution is relatively uniform. If too much steel is placed near the outer edge of the zone, failure occurs at a steeper surface.

Fig.4.4-58 shows the results obtained with the above approach compared to tests by Gomes and Andrade (1995) and Gomes and Regan (1999). The types of punching (inside and outside the region with shear reinforcement) are correctly predicted in all cases. So far as these particular types of shear reinforcement are concerned the limit on f_y appears to be somewhat restrictive, while the limit on the spacing of the outer shear steel is seen to be
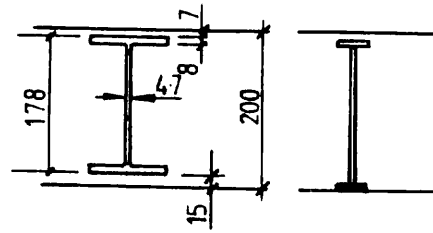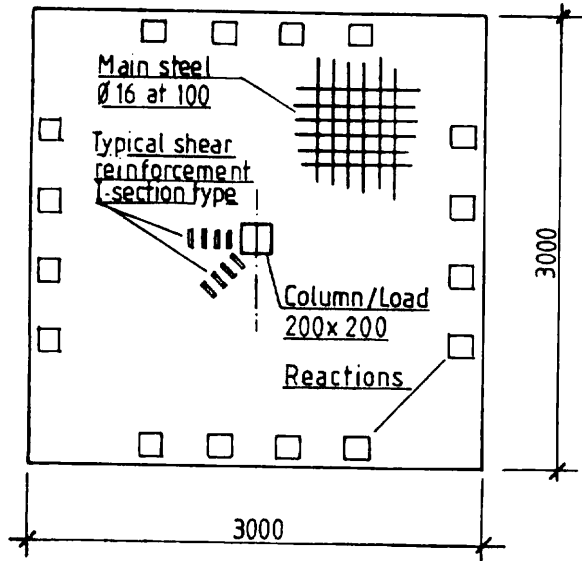
I SECTIONS [9 tests]   STUDS [1 test]
TYPICAL SHEAR REINFORCEMENT

F_u = Experimental ultimate load

F_c Calculated (unfactored) strength of a slab without shear reinforcement

F_s Calculated (unfactored) shear resistance due to shear reinforcement

Note Steel forces calculated using actual f_y (= 430 MPa)

● O u_n = full perimeter 1·5d beyond outer shear steel

├──   shows result of using reduced perimeter shown above
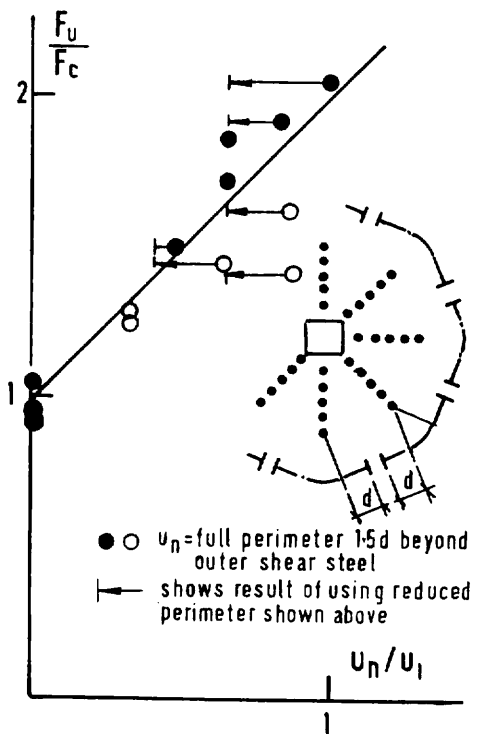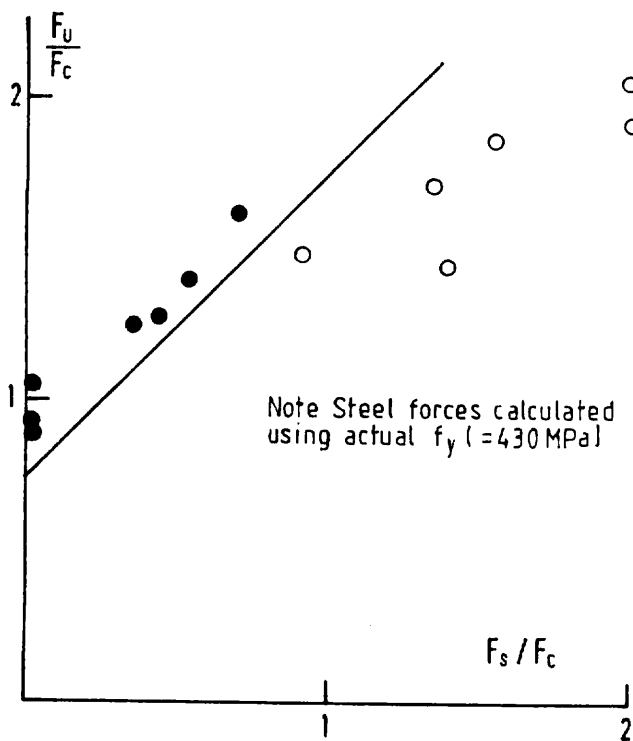
FULL SYMBOLS RELATE TO THE CRITICAL RESISTANCES. OPEN SYMBOLS RELATE TO NON-CRITICAL RESISTANCES. EACH TEST APPEARS IN BOTH GRAPHS ~ ONCE AS CRITICAL, ONCE AS NON-CRITICAL

Fig. 4.4-58:   *Punching of slabs with shear reinforcement - comparisons of calculated strengths with results of tests by Gomes (1991, 1995)*

necessary but perhaps a little too severe. Some care is needed to be confident that a type of shear reinforcement to be used is actually able to develop the intended stresses in a slab of the relevant thickness.

If shear reinforcement is required at eccentrically loaded interior slab-column connections or at edge columns, it can be designed with reference to the maximum shear per unit length of perimeter. The reinforcement so determined should be provided around the whole of the perimeter.

(7.4.4)   Punching of prestressed slabs

The design of prestressed slabs with respect to punching is beyond the scope of this book. Guidance on it can be found in the FIP Recommendations.

Example

Design of a column-slab connection

A column with a 400 x 300 mm cross-section is to support a reinforced concrete flat plate with an effective depth of 250 mm. The slab concrete is to have a characteristic strength f_{ck} = 30 MPa and the ratio of flexural reinforcement in the critical zone is to be 0.84%.

The ULS design loading for the connection is a shear F_{Sd} = 900 kN and a transferred moment M_{Sd} = 200 kNm, with the eccentricity of loading parallel to the longer dimension of the column, i.e. c_1 = 400 mm and c_2 = 300 mm.

The control perimeter at a distance 2d from the column has the following properties:

$$u_1 = 2(300 + 400) + 4\pi \times 250 = 4542 \text{ mm}$$

$$K = 0.63$$

$$W_1 = 400^2 + (400 \times 300) + (4 \times 300 \times 250) + (16 \times 250^2) + (2\pi \times 250 \times 450) = 2128 \times 10^3 \text{ mm}^2$$

Rather than calculating the nominal shear stresses separately from the shear and the moment it is practically convenient to work in terms of an effective concentric shear load

$$F_{Sd,ef} = F_{Sd}\left[1 + K\frac{M_{Sd}}{F_{Sd}}\frac{u_1}{W_1}\right] = 1.3F_{Sd} = 1170 \text{kN}$$

The nominal shear stress due to the design loading is then

$$\frac{F_{Sd,ef}}{u_1 d} = \frac{1170 \times 10^3 4542 \times 250}{4542 \times 250} = 1.03 \text{MPa}$$

The design resistance of a slab without shear reinforcement is

$$\tau_{Rd} = 0.12\xi(100\rho f_{ck})^{1/3} = 0.12\left(1+\sqrt{\frac{200}{250}}\right)(0.84\times30)^{1/3} = 0.67\,\text{MPa}$$

Since $\tau_{Rd} < F_{Sd,ef}/u_1 d$ the slab requires shear reinforcement.

The upper limit of the design shear is given by

$$F_{Sd,ef} / u_o d \leq 0.5 f_{cd2}$$

in which the value of $F_{Sd,ef}$ can be taken as for the perimeter u_1,
u_o is the length of the periphery of the column = 1400 mm

$$f_{cd2} = 0.6\, f_{cd}\left[1 - \frac{f_{ck}}{250}\right] = 10.56\,MPa$$

$$F_{Sd,ef} / u_o d = 1170\times10^3 / 140\times250 = 3.34\,\text{MPa}$$

$$0.5\, f_{cd2} = 5.28\ \text{MPa}$$

and the loading is comfortably within the upper limit.

At the perimeter u_1 the design resistance of a slab with vertical shear reinforcement is

$$F_{Rd1} = 0.75\tau_{Rd}u_1 d + 1.5\frac{d}{s_r}A_{sw}f_{yd}$$

or

$$F_{Rd1} = 0.5\times4.542\times250\,\text{kN} + 1.5\frac{d}{s_r}A_{sw}f_{yd} = 568\,\text{kN} + 1.5\frac{d}{s_r}A_{sw}f_{yd}$$

The shear reinforcement required is thus defined by

$$1.5\frac{d}{s_r}A_{sw}f_{yd} = 1170 - 568 = 602\,\text{kN}$$

where

A_{sw} is the area of shear reinforcement in one layer, the layers having a radial spacing s_r.

With $s_r = 0.75d$ and $f_{yd} = 300$ MPa (the upper limit in MC90)

$$A_{sw} = \frac{602}{2\times0.3} = 1003\,\text{mm}^2$$

Fig. 4.4-59:   *Example - design of a slab-interior column connection*

This could be provided in various forms (stirrups, studs, etc.). Using 12 mm diameter studs, the number required per layer is 8.9 or in practical terms 9.

At least two layers of shear reinforcement are required to provide the above 602 kN resistance. More layers may be required in order to limit the nominal shear stress in the outer unreinforced slab zone to τ_{Rd}.

If only two layers are provided and are detailed as in Fig.4.4-59, the length u_n of the control perimeter outside them is

$$u_n = [2(550 + 650) + 4(265)] + 4\pi \times 250 = 3460 + 3142 = 6602\,mm$$

The ratio $F_{s.ef}/F_s$ for this perimeter could be taken conservatively as being the same as for the perimeter u_1, but MC90 allows 'W' to be calculated for the larger perimeter. For the purpose of calculating W the actual outline of the second layer of shear reinforcement can be approximated to a rectangle having the same length (3460 mm), i.e. by a rectangle 915 x 815 mm.

Treating these dimensions as the equivalents of c_1 and c_2 in the expression for W_1

$$W_n = 4.416 \times 10^6$$

and

$$F_{Sd.ef} = F_{Sd}\left[1 + 0.63\frac{200}{900}\frac{6.602}{4.416}\right] = 1.21F_{Sd} = 1089\,kN$$

$$\frac{F_{Sd.ef}}{u_n d} = \frac{1089}{6.602 \times 250} = 0.66\,MPa$$

which is just below $\tau_{Rd} = 0.067$ MPa, so that the two layers provide a just sufficient region of shear reinforcement.

The final detailing, respecting the limit of 2d on circumferential spacing, is shown in Fig.4.4-59.

REFERENCES

Al-Hussaini, A., Regan, P.E., Xue, H.-Y. & Ramdane, K.-E. (1993), 'The behaviour of HSC columns under axial load', Symposium on Utilization of High Strength Concrete, Lillehammer, June 1993, Norwegian Concrete Association, Proceedings Vol 1, pp.83-90

Aster, H. & Koch, R. (1974), 'Schubtragfähigkeit dicker Stahlbetonplatten', *Beton- und Stahlbetonbau*, 69, (1974) H11, pp.266-270

Bhal, N.S. (1968), 'Über den Einfluss der Balkenhöhe auf die Schubtragfähigkeit von einfeldrigen Stahlbetonbalken mit und ohne Schubbewehrung'. Dr Ing thesis, Universität Stuttgart

Elstner, R.C. & Hognestad, E. (1957), 'Laboratory investigation of rigid frame failure' *ACI Journal*, V. 53 No 1, Jan 1957, pp.637-668

Elzanaty, A.H., Nilson, A.H. and Slate, F.O. (1986), 'Shear capacity of reinforced concrete beams using high strength concrete', *ACI Journal*, V.83, No.2, Mar-Apr, pp.290-296

FIP (1997), 'Recommendations for the design of post-tensioned slabs and foundation rafts', Federation Internationale de la Précontrainte

Gomes, R.B. & Andrade, M.A.S. (1995), 'Punching in reinforced concrete flat slabs with holes', *Developments in Computer Aided design and Modelling for Structural Engineering*, Civil-Comp Press, Edinburgh, pp.185-193

Gomes, R. & Regan, P., (1999), 'Punching strength of slabs reinforced with offcuts of rolled steel I-section beams', *Magazine of Concrete Research*, Vol.51, No.2, Apr, pp.121-129

Granholm, H. (1965), 'A general flexural theory of reinforced concrete', Almqvist and Wiksell, Stockholm

Hallgren, M. (1996), 'Punching shear capacity of reinforced high strength concrete slabs', *TRITA-BKN Bulletin 23*, Department of Structural Engineering, KTH, Stockholm

Hamadi, Y.D. & Regan, P.E. (1980), 'Behaviour of normal and lightweight concrete beams with cracks', *The Structural Engineer*, Vol 58B No 4, Dec 1980, pp.71-79

Hawkins, N.M., Bao, A. & Yamazaki, J. (1989), 'Moment transfer from concrete slabs to columns', *ACI Structural Journal*, V 86, No.6, Nov-Dec 1989, pp.705-716

Hoff, A. (1979), Bruk av høyverdig kamstål (KS60) i betongkonstruksjoner - Søyleforsøk', *SINTEF Rapport STF65-A79053*, Forskningsinstituttet for Cement og Betong, NTH, Trondheim

Kani, G.N.J. (1967), 'How safe are our large concrete beams?', *ACI Journal*, V 64, No.3, Mar 1967, pp.128-141

Kim, J.-K. & Park Y.-D. (1994), 'Shear strength of reinforced high strength concrete beams without web reinforcement', *Magazine of Concrete Research*, Vol.46, No.166, Mar 1994, pp.7-16

Kinnunen, S. & Nylander, H. (1960), 'Punching of concrete slabs without shear reinforcement', *Transaction*, Nr.158, KTH, Stockholm

Kinnunen, S. (1963), 'Punching of concrete slabs with two-way reinforcement', *Transaction*, Nr.198, KTH, Stockholm

Kinnunen, S. (1971), 'Försök med betongplattor understödda av pelare vid fri kant', *Rapport R2*, 1971, Statens Institut för Byggnadsforskning, Stockholm

Kinnunen, S., Nylander, H. & Tolf, P. (1980), 'Plattjocklekens inverkan på betongplattors hållfasthet vid genomstansning', Försök med rektangulära plattor, *Meddelande*, Nr.137, Institutionen för Byggnadsstatik, KTH, Stockholm

Lampert, P. & Thürlimann, B. (1968), 'Torsionsversuche an Stahlbetonbalken', *Bericht*, Nr.6506-2, Institut für Baustatik, ETH, Zürich

Lampert, P. & Thürlimann, B. (1969), 'Torsions-Beige-Versuche an Stahlbetonbalken *Bericht*, Nr.6506-3, Institut für Baustatik, ETH, Zürich

Leonhardt, F. & Walther, R. (1962), 'The Stuttgart shear tests 1961', Translation III, Cement and Concrete Association Library, London

Leonhardt, F. & Schelling, G. (1974), 'Torsionsversuche an Stahlbetonbalken', *Deutscher Ausschuss für Stahlbeton*, Heft 239

Marzouk, M. & Hussein, A. (1991), 'Experimental investigation on the behaviour of high strength concrete slabs', *ACI Structural Journal*, V 88, No.6, Nov-Dec 1991, pp.701-713

Mast, P.E. (1970), 'Stresses in flat plates near columns', *ACI Structural Journal*, V 67, No.10, Oct 1970, pp.761-768

Menétrey, P., Walther, R., Zimmermann, T., Willam, K.J. & Regan, P.E. (1997), 'Simulation of punching failure in reinforced concrete structures', *ASCE Journal of Structural Engineering*, Vol.123, No.5, May 1997, pp.652-659

Moe, J. (1961), 'Shearing strength of reinforced concrete slabs and footings under concentrated loads, *Bulletin D47*, Research and Development Laboratories, Portland Cement Association, Skokie, Illinois

Morrow, J. & Viest, I.M. (1957), 'Shear strength of reinforced concrete frame members without web reinforcement', *ACI Journal*, V 53, No.9, Mar 1957, pp.833-870

Mphonde, A.G. & Frantz, G.C. (1984), 'Shear tests of high- and low-strength concrete beams without stirrups', *ACI Structural Journal*, V 81, No.4, Jul-Aug 1984, pp.350-357

Nylander, H. & Kinnunen, S. (1976), 'Genomstansning an betongplatta vid innerpelare - brottstadieberäkning, *Meddelande*, Nr.118, Institutionen för Byggnadsstatik, KTH, Stockholm

Pang, X.-B. & Hsu, T. T.-C. (1995), 'Behaviour of reinforced concrete membrane panels in shear', *ACI Structural Journal*, V 92, No.6, Nov-Dec 1995, pp.665-679

Petersson, T. (1983), 'Balkhöjdens inverkan på betongbalkars skjuvhållfashet', *Meddelande*, 2/83, Institutionen för Brobyggnad, KTH, Stockholm

Placas, A. & Regan, P.E. (1971), 'Shear failure of reinforced concrete beams', *ACI Structural Journal*, V 68, No.10, Oct 1971, pp.763-773

Ramdane, K.-E. (1996), 'Punching shear of high performance concrete', 4th International Symposium on Utilization of High Strength/High Performance Concrete, Paris

Regan, P.E. (1972), 'Shear in reinforced concrete - an experimental study', *Technical Note 45*, Construction Industry Research and Information Association, London

Regan, P.E. (1980), 'Shear tests of rectangular reinforced concrete beams', Polytechnic of Central London

Regan, P.E. (1981), 'Behaviour of reinforced concrete flat slabs', *Report 89*, Construction Industry Research and Information Association, London

Regan, P.E. (1986), 'Symmetric punching of reinforced concrete slabs', *Magazine of Concrete Research*, Vol 38 No 136, Sept 1986, pp 115-128.

Regan, P.E. & Rezai-Jorabi, H. (1987), 'The shear resistance of reinforced concrete I-beams', *Studi e Ricerche*, No 9, Politecnico di Milano.

Regan, P.E. (1993), 'Tests of connections between flat slabs and edge columns', School of Architecture and Engineering, University of Westminster.

Regan, P.E. (1997), 'Punching resistances of reinforced concrete slabs loaded over small areas', School of Architecture and Engineering, University of Westminster.

Regan, P.E. (1998), 'Factors affecting the diagonal tension strength of reinforced concrete', School of the Built Environment, University of Westminster.

Stamenkovic, A. & Chapman, J.C. (1974), 'Local strength at column heads in flat slabs subjected to a combined vertical and horizontal loading', *Proceedings*, Institution of Civil Engineers, Pt 2, 57, June 1974, pp 205-232.

Søpler, B. (1978), 'Bruk av høyverdig kamstål (KS 60) i betongkonstruksjoner', *Delrapport 1, Søyleforsøk*, SINTEF Rapport STF 65 A78002, Forskningsinstituttet for Cement og Betong, NTH, Trondheim.

Tolf, P. (1988), 'Plattjocklekens inverkan på betongplattors hållfasthet vid genomstansning - Försök med circulära plattor', *Meddelande*, Nr 146, Institutionen för Byggnadsstatik, KTH Stockholm.

Vecchio, F., Collins, M.P. & Aspiotis, J. (1982), 'The response of reinforced concrete to in-plane shear and normal stresses', *Publication No 82-03*, Department of Civil Engineering, University of Toronto.

Vecchio, F. and Collins, M.P. (1994), 'High strength concrete elements subjected to shear', *ACI Structural Journal*, V 91 No 4, July-Aug 1994, pp 423-433.

Watanabe, F. & Kabeyasawa, T. (1997), 'Shear strength of RC members with high strength concrete', Kyoto University.

Zhang, J.-P. (1997), 'Strength of cracked concrete, Part 3, Load carrying capacity of panels subjected to in-plane stress', *Report R18*, Department of Structural Engineering and Materials, Technical University of Denmark, Lyngby.

4.4.2   ULS of buckling

by Marco Menegotto

(1)   Introduction

Vertical bearing structural members, such as columns or walls, are made to sustain axial loads and they may be geometrically "slender", i.e. long and thin, rather flexible. Their own deformation may induce additional eccentricities of the axial forces and modify the state of stress, compared with that of a "short" member, where it would depend only on the properties of the cross-sections.

The phenomenon is called in many ways, namely: geometric non linearity (non linear effects related to displacements of the applied forces); second order effects (alteration of eccentricities, after the deflections); instability of deformation (no deformed shape in equilibrium can be found, independently of materials' strength); buckling (uncontrolled effects of finite actions).

The latter term "buckling" is somehow misleading in this context, as it recalls the idea of sudden instability of centrically compressed members, typical mainly of steel trusses but not common in concrete structures.

In fact, the actual phenomenon, that may affect concrete members, is a progressive non proportional increase of the deformations, due to yet initially eccentric axial loads. When the member is slender, its deformation, although small, modifies sensibly the load eccentricity along all cross-sections; whence the second order effects arise, in terms of additional bending moments (Fig. 4.4-60).

Concrete has been viewed in its beginnings to make rather massive structures, not subject to slenderness problems. However, the increase of concrete strength - coupled with need of saving material, reducing self weight and gaining pay space - have given rise to thinner columns, walls and piers, that may show sensible second order effects, which cannot be compensated by greater mechanical stiffness, because concrete modulus does not increase as much as its strength, unfortunately.

Nonlinear analysis of structures is concerned by different sources of nonlinearity in their behavior. One of them is geometric, that is pointed out here but cannot be dealt with separately, given the interactions with other ones, such as constitutive laws, bond relationships, cracking patterns, time-dependant effects, etc. Thus, this chapter, dealing with "buckling", may be seen as an enlargement on a particular item of nonlinear behavior.

The CEB-FIP Model Code for concrete structures 1990 (MC90), in chapter 6.6 "Ultimate Limit State of Buckling", deals mainly with columns. Some observations will follow here, on various features involved in the behavior of slender columns, as well as comments on the verification means given by MC90.

(2)   Reduction of capacity

Great flexural deformability of compressed members leads to reduction of their capacity, both in terms of strength and of ductility.


a) Geometric nonlinearity   b) Mechanic nonlinearity
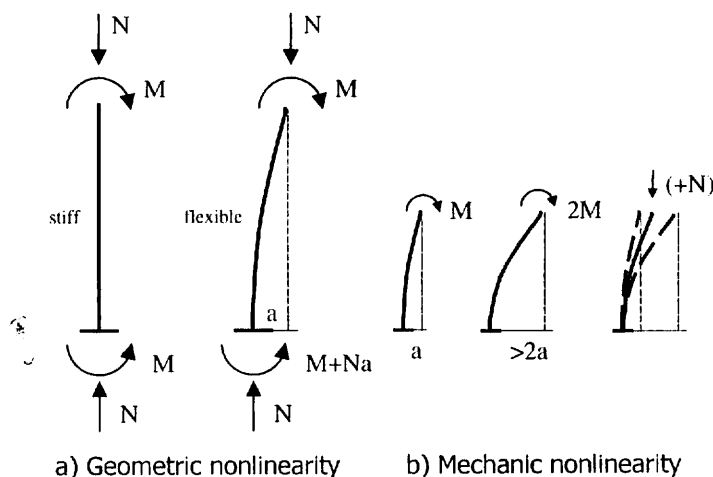
Fig. 4.4-60: "Geometric" and "Mechanic" nonlinearities

Several "mechanical" parameters control the deformation of a column having given geometry and loading. Namely, concrete's stress-strain curve in compression, its tensile strength, the reinforcement and, possibly, the loading time and duration. The σ–ε curve is governed by the initial E_c modulus, which may increase with the compressive strength f_c, but not proportionally; the same happens to the second (f_{ct}), which seems upper bounded and it is not fully reliable; the third (E_s) is independent of steel strength; as for time, long term strains depend on application and duration of loads and roughly on E_c, too.

Moreover, the deformability of the cross sections varies along a member, following the local state of stress, thus depending partly on the second order effects themselves. This means an *interaction* of (a) mechanical (materials') and (b) geometric (2nd order effects') nonlinearities (Fig. 4.4-60), in affecting the structural behavior. Due to the first (a) in a flexible column the deflection a increases the bending moment by $N \cdot a$; for the second (b), the deflection a is not proportional to the applied moment, whereas the addition of a normal force may increase or decrease it.

Service limit states are not sensibly affected by second order effects, being all stresses still in the linear range over the whole column.

Instead, under ultimate conditions, high strains induce large concentrated deformations in critical regions, while the stiffness decreases as well all along the structure, due to both softening E_c in compressed parts and cracking in tensile ones. Thus, second order bending moments develop. The bearing capacity of the column gets reduced: in fact, additional bending moments are in any case unfavorable to the *resistance capacity* of any concrete cross section.

Yet another relevant structural requirement is the *ductility capacity*, i.e., the ability of undergoing relevant "plastic" deformations with more or less constant moment response to bending actions, while dissipating energy.

Ductility, too, is affected by the interacting nonlinearities: (i) normal forces anticipate concrete crushing before the elongation of tensile reinforcement, thus reducing the extension of plastic rotations; (ii) plastic rotations increase much the columns deflection: the available moment response, largely absorbed by second order moments, drops sharply as for the external actions.

Fig. 4.4-61 sketches a comparison of diagrams of the lateral force H vs. the deflection a of a short wrt. a long column with the same cross section and axial force. The 2nd order effects lower the entire curve, reducing not only the resistance R but also the dissipated energy D. This impairs the ductility, in terms of possible moments' redistribution and of plastic damping of dynamic actions.
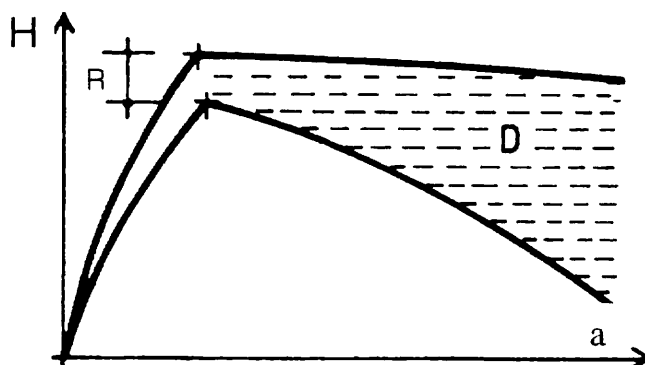
Fig. 4.4-61: Reduction of strength (R) and energy dissipation (D) due to 2nd order effects in a slender column (upper diagram) compared with a short one (lower diagram)

That is a reason why, in design of seismic structures, ductility demand is assigned to non compressed members, such as beams or bracing walls, rather than to columns or bearing walls, especially if slender.

(3)   Effects of prestressing

Prestressing may be a means of improving the bearing capacity of axially loaded slender columns. In fact, it influences the deflections, by modifying the stiffness of the cross-sections.

When applied to columns, prestress is generally symmetric, if external bending actions do not have a preferred sign.

The influence is twofold: on one hand it is unfavorable, as the increase of average compressive stress tends to reduce the stiffness; on the other hand, it tends to increase the stiffness, by delaying the formation and the deepening of cracks. If the external axial force is very low, centric prestressing may even improve the cross-section flexural strength.

Fig. 4.4-62 sketches Moment M vs. deflection *a* diagrams of three similar slender columns, axially prestressed: fully (1), partially (½) and non prestressed (0), respectively. The higher the prestress, the lower is the initial stiffness, following the mean stress level; but when bending rise, cracking points (C) are delayed, and the stiffness comparison reverses. The final capacity of fully prestressed structure may be greater or not, according to the calibration of the prestress level.
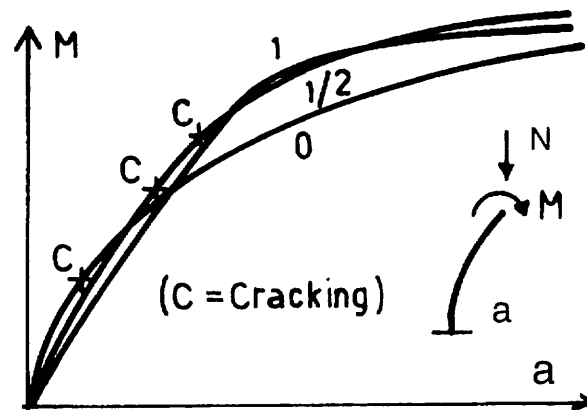

Fig. 4.4-62: Typical behavior of slender prestressed members:

      (1) Fully prestressed; (½) Partially prestressed; (0) Non prestressed

Contrary to an external axial force, internal prestressing does not produce itself second order effects, as it follows the structure's displacements. Also the ductility reduction is less than that of an external axial force.

Prestressing force should be well calibrated in compressed members, to be helpful (the more accurately the more the member is slender). Partial prestressing is advisable.

Economy governs the "if and how much" to prestress. In the balance, prestress may give an additional advantage to precast columns, helping in transient loading conditions during handling and erecting.

Unbonded external tendons are not fitted for the purpose, as they do induce second order effects, unless they are linked to the structure all along. However, their 2nd order effects are theoretically less then those of real external axial forces, because eccentric though symmetric tendons strain favorably and oppose to members' rotations.

On the contrary, bonded tendons would also have the favorable effect of contributing flexural cross-section reinforcement.

(4)   Effects of restraints

The actual restraint acted on by the supports of the columns, as well as by beams or floors, must be known. The restraint stiffness may vary, following the current forces applied, both in statically determinate and indeterminate cases. In fact, second order effects render all structures statically indeterminate.

The stiffness of the restraint determines in particular the "effective length" l_0 between virtual points of contraflexure in the buckling mode (which have nothing to do with the contraflexure points as related to the applied actions).

Even in the simplest case of an isolated cantilever clamped at the base (as in Fig. 4.4-60), in principle, account should be made both for the rotation of the foundation, when evaluating l_0, and for the second order moment, when verifying the foundation resistance.

Often, columns are part of frames, where the beams form the restraints. Theoretically, their stiffness should be evaluated at a state of stress corresponding to the ULS of the columns; this comes out automatically in a full nonlinear analysis of the frame but requires some judgment if the column is picked out of its frame and analyzed as "isolated".

A major point is whether the joints (beam/columns intersections) of a frame may or may not displace, which is meant by "sway" vs. "non sway" frames. As far as buckling problems are concerned, this distinction refers to the positive presence of a rigid structure bracing the whole frame, i.e. providing it a fixed restraint to lateral displacements of all joints (Fig. 4.4-63 a).

A frame, whose joints do not displace under a certain loading condition but it is not itself positively braced, cannot be considered as non sway, if second order effects are expected. For it, either a full nonlinear analysis is to be performed, incorporating some forces exciting lateral displacements, or criteria for evaluating the overall slenderness are needed.

The overall non linear analysis of a sway frame is sufficient for verifications, if the columns of every storey are regular, i.e. uniform in dimensions and loads. Otherwise, it must be integrated with the check of the most slender columns in their own isolated buckling mode.

The effective length of a column belonging to a non sway frame is lower than the interstorey height L_i; i.e. $L_i/2 < l_0 < L_i$. Whereas in a sway frame it is always greater than L_i and does not have an upper limit, unless any restraints are perfectly rigid, i.e. $L_i < l_0 < \infty$.
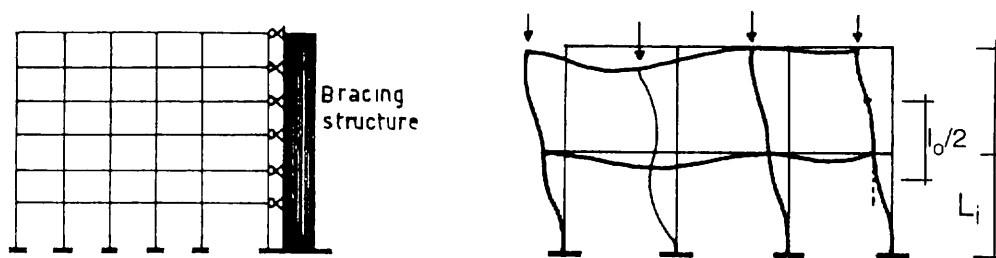
Fig. 4.4-63: a) Non sway frame, braced by an external rigid structure
b) Sway frame, with a column of lower stiffness (l<<)

Fig. 4.4-63 a sketches a non sway frame (positively braced), where $l_0/2 < L_i/2$. Fig. 4.4-63 b shows a slender frame, which would not sway for its loads but sways for 2nd order effects: the typical column has $l_0/2 > L_i/2$ and the very weakest (l<<) has its own buckling form. In fact, columns much more slender than the nearest become soft elements, which "refuse" increments of loading from the structure, thus altering the force pattern in the beams. It is matter of proper design to avoid such situations.

The above considerations on sway frames are theoretical. In practice, slender sway frames would not be recommended for buildings, anyhow.

(5)   Slenderness limits

The analysis of second order effects in a concrete structure implies more or less complex calculations, due to the seen interaction of geometric and mechanic nonlinearity. Even with the simplified methods and design aids, it represents a computational cost.

Theoretically, all members, when subject to external compressive forces, show an increase of internal bending moments. Practically, the majority of compressed members might not need 2nd order analysis. Therefore, it is useful to asses limits, up to whom second order effects may be disregarded.

(5.1)   Uniaxial bending

The parameter used in past codes, as for instance in CEB-FIP Model Code 78, is the "slenderness ratio" $\lambda = l_0 / i$ between the effective length and the radius of gyration of the solid concrete cross section, in the plane of bending.

This ratio λ is merely geometric and, deriving from elastic theory, it is used in the verifications of steel structures, combined with the well known coefficient ω for fictitiously increasing the applied load. But even there, the lower limit of λ varies according to the different steel grades, although the elastic modulus is the same for all. Thus, it reveals insufficient as such for being a limit of sensitivity to 2nd order effects.

In concrete structures, where the interaction of normal force (N) and bending (M) is more complex, due to varying σ/ε ratio, cracking, etc, and ω is not valuable, the slenderness ratio λ alone is quite a poor parameter, not able to represent a significant boundary for the rise of second order effects.

In fact, in former CEB Recommendations 1970, the adopted lower bound was $\lambda = 50$. As it was realized that also some columns having $\lambda < 50$ might show important second order moments, subsequent MC 78 adopted the limit value $\lambda = 25$; but the same drawback appeared. The newest MC90 uses a different approach, as well as the Eurocode EC2.

In fact, even short columns, with λ tending to zero, may be affected by 2nd order effects, if loaded with a very high axial force. On the opposite, even extremely slender columns, with negligible axial forces, are not affected by them. Thus, a better parameter was worked out.

The new parameter, formulated as $\lambda\sqrt{\nu}$, incorporates, throughout the specific normal force $\nu = N / f_c A_c$, the average compression and indirectly the stiffness, which are the other essential factors. It showed to detect with much greater precision the bound where second order effects start rising sensibly.

For fixing a limit value of that parameter, it was assumed that second order effects are not negligible when the total moment exceeds by 10% the first order one, i.e., when μ (ratio between total and first order moment) = 1.1. The new parameter was checked in numerical tests and its corresponding limit value appeared to be around $\lambda\sqrt{\nu} \approx 20$.

The same parameter may be used also for defining an upper limit, above which the column would be too slender whatsoever and should not be so made. This was assumed corresponding to the ratio μ being 2.0 (increase of moment due to second order = 100%) and the limit value resulted $\lambda\sqrt{\nu} \approx 70$.

Of course the above values are averaging most cases, and do not give the actual μ for a specific case, which needs the analysis. But the use of $\lambda\sqrt{\nu}$ as indicative limiting parameter represents a substantial improvement with respect to λ alone, though not more complex: Fig. 4.4-64 shows how the results of the analyzed cases are much less scattered as function of the new parameter, than of the previous one.
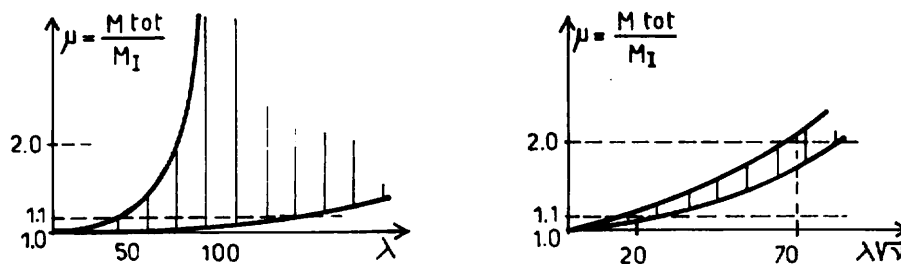
Fig. 4.4-64: As function of $\lambda\sqrt{\nu}$ instead of λ, slenderness effects are better identified

Limits of slenderness corrected with the ratio of load eccentricities at the ends of the column e_{01}/e_{02}, adopted in some rules (see MC90, 6.6.3.3.1), must be handled with care - especially when both eccentricities are small - because they could rely upon favorable moment distributions that may not influence really the buckling mode, and allow for easily doubling the lower limit, with no physical justification and unsafe result.

(5.2)   Biaxial bending

When the slenderness lower limit in one principal direction is exceeded, biaxial check would be necessary - applying at least the minimum eccentricities stated by codes - especially if the design forces act only in the other principal direction.

Indeed, the interaction of first order moments about two principal axes of a cross-section is low, when the combined eccentricity is close to one axis. But this may be not true for the second order moments, when slenderness ratios about both axes are much different. In fact, the reduced (due to second order effects) moment capacity about the stronger axis has two distinct values, whether accounting or not for side buckling, as shown in the reduced interaction diagram sketched in Fig. 4.4-67.

A criterion for avoiding biaxial check (when the loading condition lays in a principal plane) is yet to be found, stating almost equal column slenderness about both principal directions.

(5.3)   Frames

Slenderness limits for entire non braced frames have been sought for. The problem is finding an equivalent slenderness for the storey, to be associated with an average specific normal force, in order to enter in the criterion under item (5.1). If the frame is "regular", an average effective length of columns in lateral buckling mode may be easily estimated and assumed for the scope (Fig. 4.4-63).

Simplified formulae have been proposed for a rough check of the storey slenderness, e.g.: $\lambda=\sqrt{(12 \cdot a_c \cdot A/ L_i)}$, where A is the sum of concrete areas of columns, L_i the interstorey height and a_c a conventionally calculated displacement.

(6)   Analysis

(6.1)   General methods

It is called "general method" any analytical procedure able to solve with sharp approximation the stress-strain state all over the structure.

The difficulties in these procedures are the correct modelization and the computational work. The strain state must be determined all over the structure, to work out the deformation, accounting for mechanical and geometrical nonlinearities. It is well known that, by discretization, it is rather simpler to work out the internal forces over a section, given the strains, than vice-versa. However, the latter are needed in iterative procedures, when searching for the deformations under the current tentative action effects along the structure.

There exist now several methods and algorithms for performing a global analysis of a concrete column or frame, based on various criteria of linearization. Among others, a criterion has been elaborated for building up the correct stiffness matrix of the most generic concrete structure, subject to axial force and biaxial bending, and responding to any given materials $\sigma-\epsilon$ relationship, which is of particular help in case of biaxial bending.

The criterion is based on the linearization, in every point of a cross-section, of the local stress strain path on the constitutive law of the point's material during a given loading step, during an iterative procedure. All the linearized step paths represent fictitious linear materials (changing at every step), each with a different modulus of elasticity E_i, making up a conventional cross-section, that can be treated, by a suitable transformation into one having a common modulus E_0 as a homogeneous elastic section.

Its ellipse of inertia can be drawn, which figures the relationships between forces and deformations under biaxial bending and compression (Fig. 4.4-65) and solves the problem. Any phenomenon, like cracking, tension stiffening, bond, non elasticity, etc., may be incorporated for each material, provided it can be fit into a stress-strain curve.
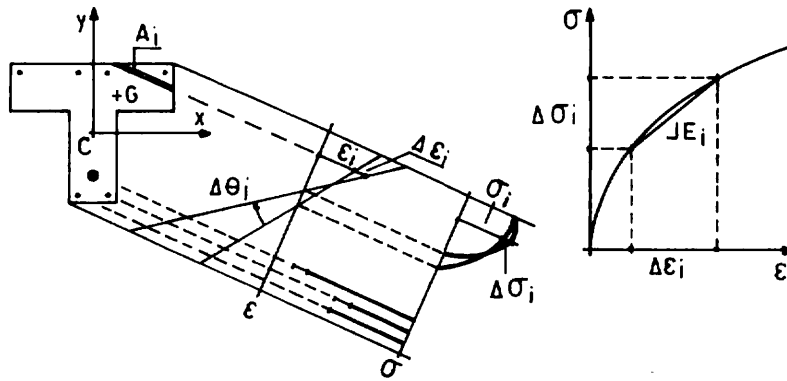
Fig. 4.4-65: Transformation of a non linearly stressed cross-section by means of fictitious local secant moduli E_i

The above relationships must be found anew at every iteration of the analysis of the structure, as the stresses change and with them the fictitious elastic section. However, they are the most effective ones in driving the iterations toward convergence.

(6.2)   Approximated methods

(6.2.1)   Uniaxial bending

For a simple cantilever column, loaded only at the top (as in Fig. 4.4-60), the integration of deformations is solved approximately in the "model column method", the most used tool in concrete columns buckling problems, as the results obtained for this simple case may be extended, with further easy approximations, to columns with various loadings or pertaining to a frame.

The method consists in assigning the column a (sinusoidal) shape function, whose amplitude is determined by the compatibility of the curvature of the axis line ($1/r$) and of the strain diagram in only one cross section (the critical one at the column base). The assumption permits to derive easily the 2nd order moment M_{II} in the critical section:

$$M_{II} = N \cdot a = N \cdot (1/r) \cdot l_0^2/\pi^2 \cong N \ (1/r) \ 0.4(l_0/2)^2$$

Thus, M_{II} is represented by a straight line on the Moment vs. Curvature (M vs. $1/r$, given N) diagram of the critical section. Being M the total moment available, a column may be acted on only by a 1st order moment M_I given by he difference M - M_{II} (Fig. 4.4-66). The maximum 1st order moment M_{Imax} does not coincide necessarily with the ULS of the critical section while it represents the ULS of the column.

From that, it is easy to work out the so-called "reduced interaction diagram", by plotting the resulting moments M_{Imax} for all the values of N. This diagram refers to the structure, not merely to the section, M_{Imax} being a means of representing the applied forces net of 2nd order effects. Such diagrams are also prepared in non dimensional form as design aids. Obviously, they may be built-up using exact methods, too.
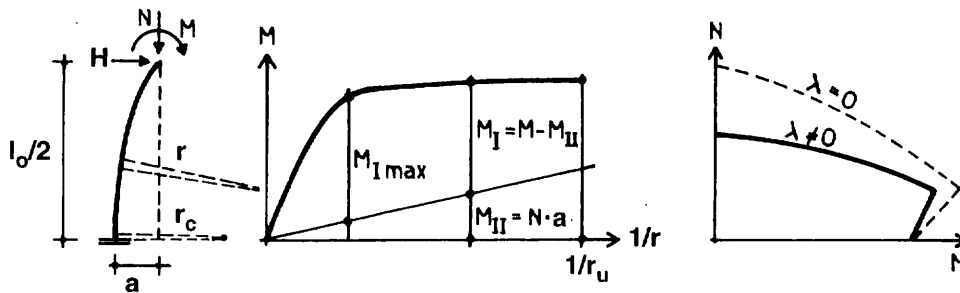
Fig. 4.4-66: Model Column and "Reduced" Interaction Diagram (M, N / λ)

(6.2.2) Biaxial bending

The model column might be used in case of biaxial actions, too. But the approximation is worst, as it disregards that the deflection is non plane (Fig. 4.4-68) and it changes direction, when loads increase, even if the actions are plane. In fact, due to 2nd order effects, internal forces vary along the structure and, with them, the angle of skew.

Nevertheless, reduced interaction diagrams may be still worked out, by more refined means. The actions being triaxial (N, M_x, M_y) it is worth to plot them in M_x, M_y planes, for various intensities of N (Fig. 4.4-67).

It has to be noted that the reduced diagram ($\lambda \neq 0$) has two points on the axis of greater stiffness M_x. One is M_{Ix}, which corresponds to the available 1st order moment calculated accounting for 2nd order effects in uniaxial bending but not for a skewed deflection; the other is the point, where the diagram meets the M_x axis, which actually accounts for the skewed deflection even with an external bending action contained only in the y,z plane.

This shows why a linearized reduced diagram between M_{Ix} and M_{Iy} (calculated in their respective uniaxial modes) may be unsafe in the region close to M_x, that needs to be covered by a minimum unintentional eccentricity e_{xu} (see also 5.2 and 7.1).
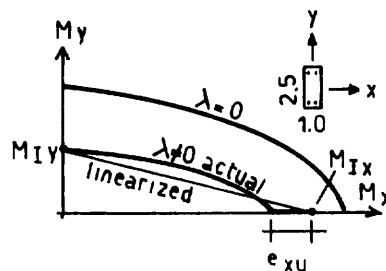
Fig. 4.4-67: Reduced Interaction Diagram. M_x, M_y for a given axial force N
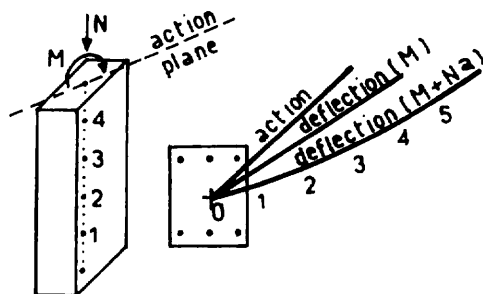
Fig. 4.4-68: Non-plane deflection in biaxial bending due to variable skewed M_{II}

Due to the complexity of biaxial verification with general methods, a roughly simplified verification criterion for the most general case was also proposed, as follows.

A column - with any possible kind of section, restraint, loading - is first analyzed in uniaxial bending on both principal directions x and y, with any appropriate method, accounting for second order effects. Design bending loads on directions x and y are given multipliers α_x, α_y, respectively, and both "critical multipliers" α^*_x and α^*_y, i.e., those producing ULS in their direction, are found. Finally, an interaction diagram is drawn, bounded by a straight line between both critical values α^*_x and α^*_y (Fig. 4.4-69).
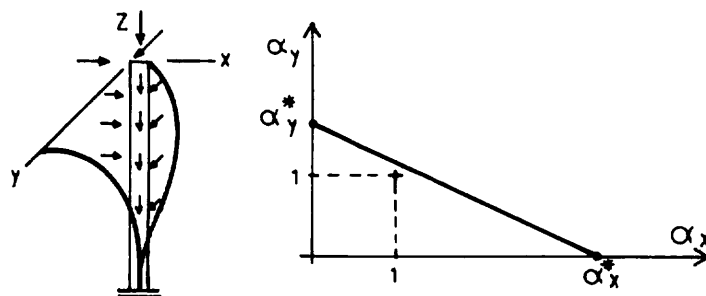
Fig. 4.4-69: Reduced Interaction Diagram referred to all actions on a structure

The verification is satisfied if the point ($\alpha_x=1$, $\alpha_y=1$), representing the design load combination considered, is contained in the safe part of the diagram.

Note that the diagram is referred directly to the overall actions (through the multipliers α_x, α_y) and not to the action effects on one section, because critical sections may be more than one.

The criterion is generally conservative, except for a small region, close to the axis of the greater α^*, in cases of much different slenderness about both directions, as it was shown in Fig. 4.4-67. However, this leak must be covered by assigning minimum eccentricities.

(6.2.3)   Frames

A traditional approximated method for overall check of sway frames is the so-called "N-a (formerly P-δ) method". It consists of an iterative analysis of the frame, acted on by lateral

forces at the storey levels, "equivalent" to the local second order effect ($H \cdot L_i = N \cdot a$), H being the lateral resultant, N the vertical one, L_i the height and a the deflection, all referred to the storey.

At each iteration the equivalence is checked with the obtained a, until convergence is reached. The difficulty, determining the degree of approximation, is assigning correct stiffness to columns and beams, consistent with the ULS.

(6.2.4)   Walls

Walls are bi-dimensional plane structural elements, subject to complex in-plane and out-plane forces.

Bearing concrete walls are usually slender out of their plane. They might be analyzed accurately as plates, by means of appropriate non linear methods. However, in building practical design, they are treated with approximated criteria, reducing the problem to that of an equivalent one-dimensional element, i.e., a column.

As well as for columns restrained at the ends in a frame, nomograms are given, for estimating the reduction of the effective buckling length, as function of the type of restraints on the four wall edges and of their respective distance.

Codes give guidance for estimating conventional and additional eccentricities. Accordingly, the checks are then performed on the critical vertical strips of the wall, acted on by their resultant normal forces, derived from the overall analysis of the structure (see MC90, 14.5.2).
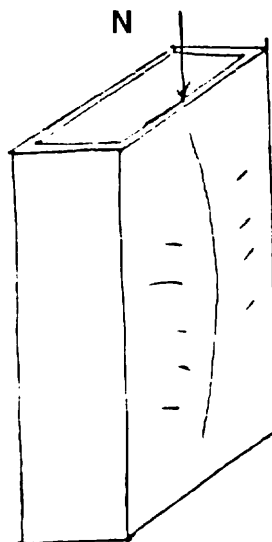
Fig. 4.4-70: Buckling of a wall as a plate

A particular case is represented by non reinforced concrete walls. For them, the slenderness limits cannot be based on the criterion of 10% increase of the moment due to the

second order effects – see (5.1) - because the moment capacity depends almost totally on the normal force actually present, and the eccentricity becomes the critical parameter.

Graphs and coefficients are given for the reduction of capacity of wall strips, accounting for the multiple parameters involved, including safety elements. Some reliance is made both on tension stiffening and on tensile strength of concrete, justified by the redundancy of the bi-dimensional behavior.

Short (horizontally) walls, unrestrained along vertical edges, actually become "non reinforced columns". Such seldom concrete elements should not rely upon tensile strength and should be designed thick enough, in order not to be sensitive to second order effects.

(6.2.5) Beams

Similarly to walls, also beams may be seen as plates, with the compressed flange restrained against buckling by web and tensile flange and / or by the slabs supported by the beam itself.

Therefore, lateral buckling of beams over the whole length is influenced by many variables, like the loading pattern and the points (not only the sections) of application of the loads and of the restraints.

This does not regard possible local buckling of flange portions – normally not the case in concrete beams - whose nearing should be avoided anyhow.
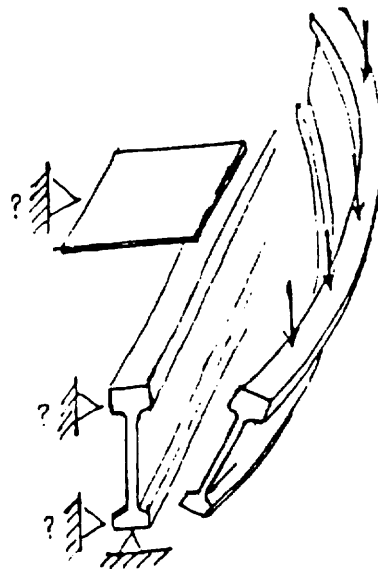
Fig. 4.4-71: Lateral buckling of a slender beam: points of application of loads and restraints are relevant

The need is felt of specific rules for simply idealizing the most frequent cases. The models should involve the stiffness under various stress conditions, type of loading, safety elements and also slenderness limits.

In absence of such tools, for daily cases one may refer to the well developed elastic theory, but cautiously accounting for unfavorable effects of concrete non linearities in estimating the stiffness under the combined action effects. MC90, under 6.6.3.3.4, gives a criterion for avoiding interaction with torsional cracking, by limiting a conventional elastic rotation about the axis line.

(6.2.6)   Arches

Methods for estimating buckling of concrete arches are not available, neither. As for the above cases, reference may be made to the elastic theory, assigning reduced conventional stiffnesses related to the state of stress of the relevant cross sections at ULS.

(7)   Safety

(7.1)   Code provisions

According to Level I approach, characteristic values of the relevant variables involved in a limit state are to be given partial safety factors, to obtain the "design values": generally, actions are amplified, strengths are reduced and possibly the model uncertainty is covered by special factors. The corresponding "state" of the structure must be within the given limit.

General hints related to design format, safety criteria, load combinations and materials' properties are given in Chapters 4.1.4 and 4.2.

However, contrary to all other cases, ULS of "buckling" has the peculiarity of being affected also by the deflection of the structure, which otherwise represents only a SLS. Therefore, also the relevant variables controlling deflections should be safely modified into design values, for verifications. This is done by the following conventional additional means:

i   an initial unintentional inclination is induced, or an equivalent eccentricity
ii   creep deformations due to sustained loads are summed up to deflections
iii   possible deformations of restraints are accounted for
iiii   the parameters of materials deformability are factored

The first item (i) accounts for unavoidable geometrical imperfections, that in slender structures may raise or amplify the deflections. Standard specified inclinations are quite severe, between 1/150 and 1/200, but some reductions are allowed, depending on site controls. Inclination could even be neglected, when many mutually connected columns act in parallel (see MC90, 6.6.3.2). For walls and beams, other eccentricities or rotations are given, respectively.

Item (ii), creep deflection, is generally calculated under the unintentional inclination and the quasi-permanent load combination (how factored is also matter of discussion – see iiii). For sake of simplicity, the creep deflection may be calculated separately, then added as a further initial to the unintentional one (i), while the analysis is performed considering all design loads considered as short-time actions.

Item (iii) covers an obvious extension of the safety criteria to the connected bodies involved in the deformation. The deformability of restraints (foundations, connected members) should be referred to the action effects intervening at the ULS of the column.

Item (iiii) implies that γ_c factor be applied not only to the strength, but to the whole σ - ε curve, reducing the initial modulus E_c, too. Indeed, it is the same model used for checking the cross-section resistance; but here it assumes the particular meaning of reducing also the "design stiffness" of the structure for ULS. However, the initial part of the curve is much relevant for calculating the deflection, and it should be modeled more realistic than the conventional parabola, in order to better match E_c.

The question is under discussion whether the same γ_c should apply to f_c and E_c: in fact, by factoring both E modulus and loads, the deformation is factored twice.

Also the stiffening effect of concrete in tension is to be judged: whereas, for small size isostatic columns, it must be surely neglected (consistently with the local effect governing the whole behavior), for larger cross sections like those of walls or towers, or for highly redundant frames, it would be really too conservative not to account for it.

The initial stiffness of steel, E_s is commonly not factored. The elastic limit is automatically lowered by factoring the strength, thus influencing the ultimate curvature and deflection.

Partial factors on prestressing force are not mentioned by codes in this context. In fact, it seems reasonable to factor steel curves as for ordinary steel (i.e., only beyond the yielding point) and to consider the nominal tensioning strain unfactored in the analysis.

(7.2)   Safety analyses

Numerical checks of MC 78 provisions, applied to a large set of different columns, were performed in a research project within CEB, by means of a Level II method , in order to assess the consistency of its design rules for buckling.

Some indicative conclusione were drawn, so summarized:

- partial factors γ_F on variable axial forces should be increased, compared with those on dead loads;
- the special γ_F on permanent loads, for calculating the creep deflection (assumed = 1.1), should be increased
- the minimum reinforcement, assumed $A_{s, min} = 0.8\%$ A_c, should be increased in slender members (as function of concrete grade or of design axial force).

(8)   Detailing

Few remarks may came out on detailing of columns themselves:

- longitudinal reinforcement: minimum value, expressed as % of concrete area as in MC 78 (see above) should be increased for slender columns, as function of design axial

force, and in general, for columns with higher concrete grades, to provide bending capacities proportional to the implicit higher axial force capacities;

-   confinement: overall confinement of axially loaded slender columns does not increase their bearing capacity, as ULS is governed by bending.

The above provisions refer to the so-called B-regions. Of course, D-regions features may be present in columns, namely at the ends or in splice joints of precast units; confining reinforcement placed in the end sections of framed columns, it increases their ductility capacity but it does not play a direct role in buckling problems.

Walls generally carry lesser average nominal stress than columns and may need a lesser minimum vertical reinforcement. Instead, significant horizontal reinforcement is needed, to help the plate action. In "non reinforced" walls, minor reinforcements (bars or meshes) are placed for taking over local tensile stresses. Care should be taken to prevent the low diameter vertical bars from buckling and spalling concrete out.

4.4.3   Fatigue

by Gert König

(1)   Problem

It is well known that a structure built to resist a certain static load may fail under a cyclic load (Fig. 4.4-72) even if the latter stresses the material much less than the static load. Cyclic loads might occur e.g. due to trucks on bridges or due to crane loads on crane runways.
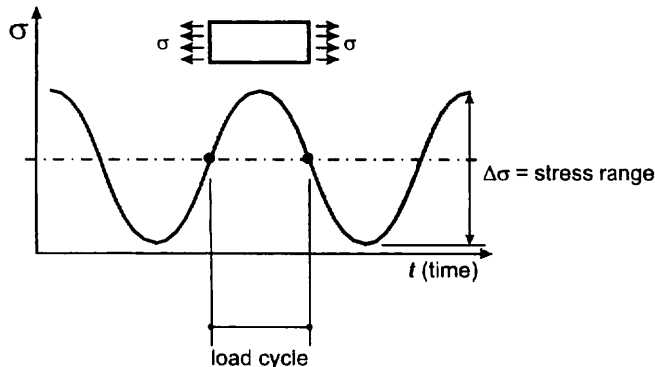
Fig. 4.4-72 Periodically applied stresses

In the design and use of steel structures allowance is made for this phenomenon, known as fatigue failure, by requiring fatigue assessment as standard.

The number of load cycles up to failure is limited. In the middle of the last century August Wöhler already observed this phenomenon. He counted the number of stress ranges up to failure and observed a dependency of the shaping of the test specimens. Thus the fatigue resistance is not only a material property. It was also found that under laboratory conditions some test specimens survived if the applied stress ranges remained under a certain limit – the so called endurance limit – whereas others did not survive and showed a time dependent strength (Fig. 4.4-73).
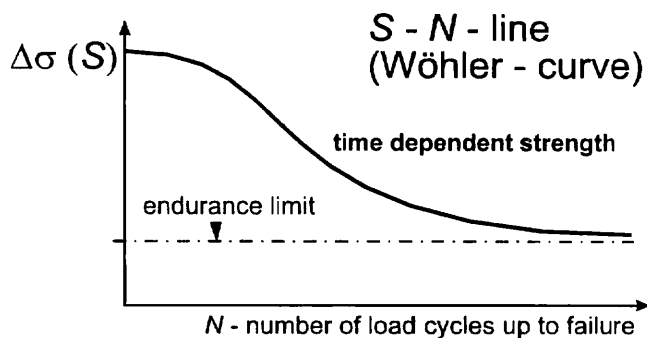
Fig. 4.4-73 S-N-line (Wöhler-curve)

Under real conditions at a site this endurance limit does not exist, because other influences as e.g. corrosion contribute also negatively to the fatigue resistance. The fatigue failure starts from a local defect, e.g. a pit due to corrosion. Around this defect a crack starts to progress

until the remaining area of the specimen is not able to bear the load. A rupture takes place (Fig. 4.4-74).
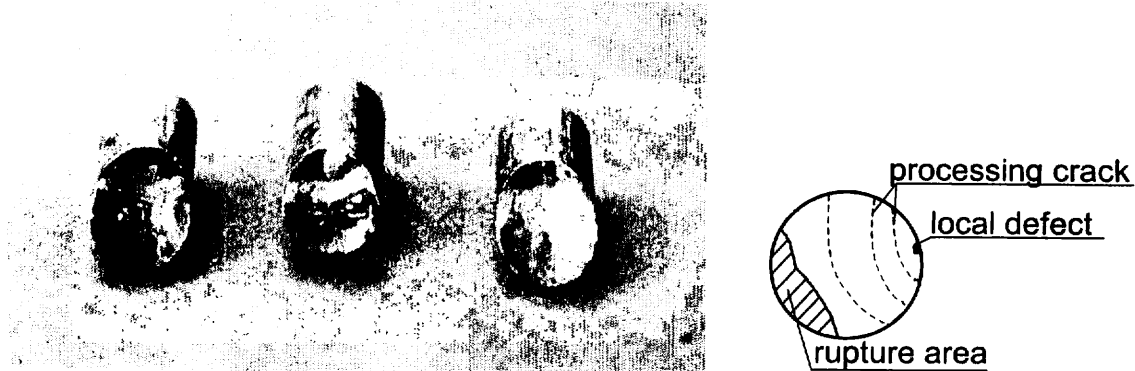
Fig. 4.4-74 Progressing crack up to the fatigue failure

It was also detected that for steel the *S-N*-curve behaves linearly if a double logarithmic scale for *S* and *N* is chosen (Fig. 4.4-75).
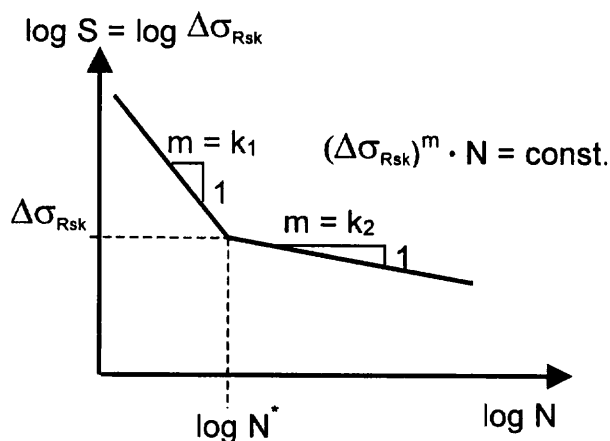
$$\log S = \log \Delta\sigma_{Rsk} = \log \Delta\sigma_{Rsk,d} + 1/m \cdot \log(N^*/N)$$

Fig. 4.4-75 S-N-curve for steel with a descending branch also beyond N* (endurance limit does not exist)

Fatigue failure is also a risk in R.C. structures which are becoming more slender, requiring closer studies of fatigue behaviour in view of the trend toward better material utilization. In most of the observed failures, where the fatigue behaviour of R.C. structures might have contributed to a major part, it was firstly observed, that the behaviour under service conditions was progressively injured. Failures were early indicated by increased deflections and crack widths (Fig. 4.4-76).
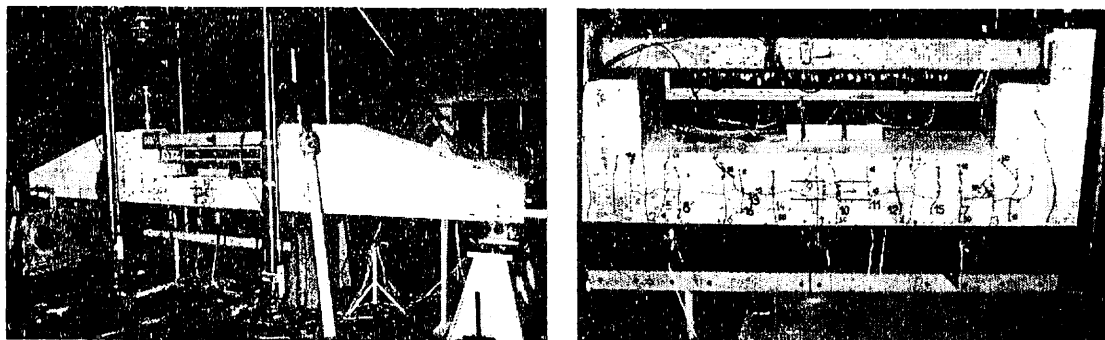
Fig. 4.4-76 Announced fatigue failure of a test-beam

Therefore unannounced fatigue failures are up to now not known. In many cases not only fatigue contributed to the failure, a combination with corrosion endangered the R.C. structures much more (Fig. 4.4-77).

Fig. 4.4-77 Getting corrosion as crack initiator for a fatigue failure

The necessity of a special verification of sufficient safety to fatigue failure can be derived from the fact, that the failure mode under static and cyclic loads might differ. A well known example is the railway sleeve, which fail under static load due to shear failure, bending compression failure and/or bond failure of the prestressing wires, but under cyclic load because of fatigue failure of the prestressing wires.

Therefore the existing European standards and those under preparation attach greater attention to avoid fatigue failure in the design of concrete structures.

The regulations of the MC90 are now being discussed and practically applied to fatigue designs for Eurocode 2, part 1. The new design rules already form part of the standard for bridges, Eurocode 2, part 2. They may be tested now by European experts. On the other hand, European regulations do not exist e.g. for crane runways, up to now.

(2)   Fatigue verification in Model Code 1990

In general the fatigue verification must be carried out by means **of limiting the damage** D_d **of the structure caused by cyclic loads**. The purpose is to ensure

$$D_d < D_{lim} = 1. \tag{4.4-99}$$
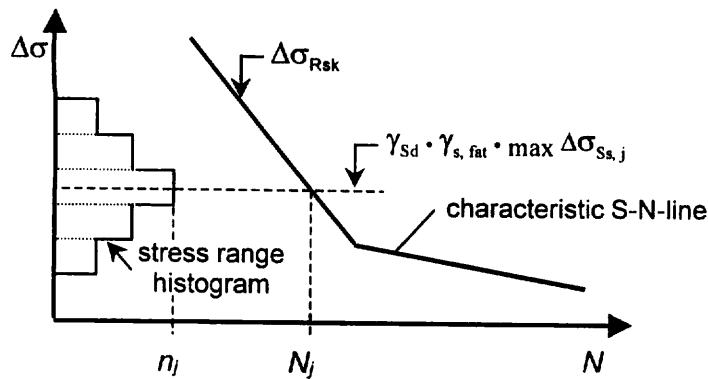
Fig. 4.4-78 γ_{Sd} - $\gamma_{s,fat}$ multiplied stress-range-histogram caused by cyclic loads and the characteristic S-N-line

The design value $d_{d,j}$ of damage contribution of class j to the total damage D_d consists of

$$d_{d,j} = \frac{n_j}{N_j(\Delta\sigma_{Ss,j} \cdot \gamma_{Sd} \cdot \gamma_{s,fat})} \tag{4.4-100}$$

with

$N_j(\Delta\sigma_{Ss,j} \cdot \gamma_{Sd} \cdot \gamma_{s,fat})$	= number of cycles to fatigue failure under the stress range $\Delta\sigma_{Ss,j} \cdot \gamma_{Sd} \cdot \gamma_{s,fat}$;
n_j	= number of repetitions (occurrences) of stress range $\Delta\sigma_{Ss,j}$;
$\Delta\sigma_{Ss,j}$	= stress range of class j;
γ_{Sd}	= partial safety factor, which takes into account the model uncertainties in determining the applied stress ranges. $\gamma_{Sd} = 1$ might be allowed if the models are chosen on the safe side, otherwise $\gamma_{Sd} = 1,1$;
$\gamma_{s,fat} = 1,15$	= partial safety factor for fatigue resistance of steel reinforcement, if the S-N-line is defined as 5 %-fractile (90 % level of confidence).

The total damage of the given stress range spectrum follows applying the Palmgren-Miner-Hypothesis

$$D_d = \sum_{j=1}^{m} \frac{n_j}{N(\Delta\sigma_{Ss,j} \cdot \gamma_{Sd} \cdot \gamma_{s,fat})} \tag{4.4-101}$$

Simplified verification procedures are:

a)   **Limiting the maximum acting stress range to a value below endurance limit**

if such an endurance limit does not exist to stress range of *S-N*-line associated to $N = 10^8$ cycles to fatigue failure. Nevertheless, the endurance limit is usable from the technical point of view at load cycles < 10^8 over the operating life.
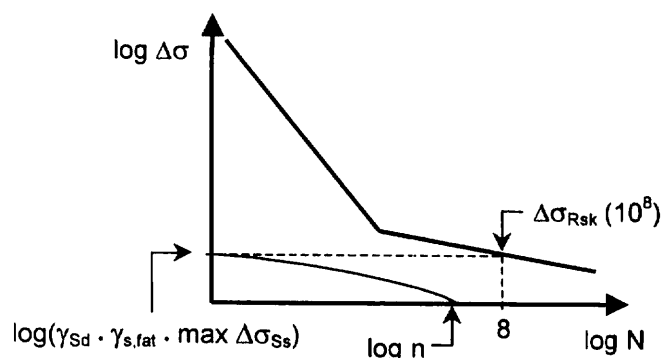
Fig. 4.4-79 Simplified verification by limiting the maximum stress range to a value below endurance limit or below $\Delta\sigma_{Rsk}$ (N = 10^8)

It must be verified

$$\gamma_{Sd} \cdot \max \Delta\sigma_{Ss} \leq \sigma_{Rsk}/\gamma_{s,fat} \qquad\qquad (4.4\text{-}102)$$

where $\Delta\sigma_{Rsk}$ is the characteristic fatigue strength at 10^8 cycles.

b)   **Limiting the actual acting stress ranges**

taking into account the number of repetitions n expected in the whole service life of a structure.

It leads to the following verification (Fig. 4.4-80):

$$\gamma_{Sd} \cdot \max \Delta\sigma_{Ss} \leq \sigma_{Rsk}(n)/\gamma_{s,fat}. \qquad\qquad (4.4\text{-}103)$$
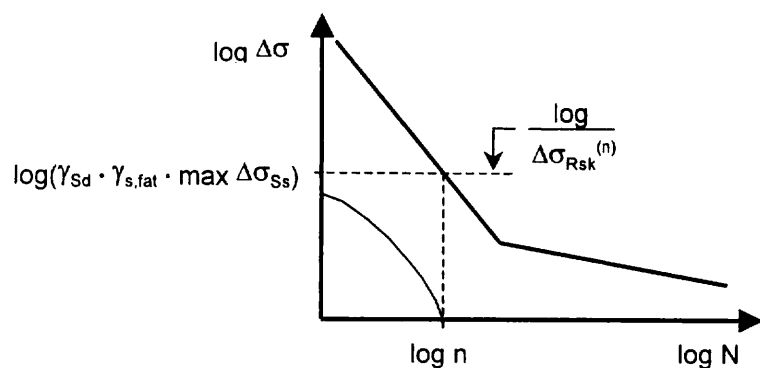
Fig. 4.4-80 Simplified verification by limiting the actual acting stresses taking into account the number of repetitions n expected in the service life

c)   **Limiting the damage equivalent stress ranges**

From the comparison of the design value D_d of the total damage of a given stress range spectrum with the damage at failure $D_{lim} = 1$ can be derived so called damage equivalent stress ranges $\Delta\sigma_{s,equ}$. These stress ranges must be compared with values of the S-N-line $\Delta\sigma_{Rsk}(N^*)$ at a defined number of cycles e.g. N^*.

$$\gamma_{Sd} \cdot \Delta\sigma_{s,equ} \leq \frac{\Delta\sigma_{Rsk}(N^*)}{\gamma_{s,fat}} \tag{4.4-104}$$

The latter method is widely used where load spectra are known (see e.g. EC2, Part 2).

To realize the verification some rules have to be given to determine the stress ranges or stresses in the R.C. structure as well as the fatigue resistance of steel and concrete.

(3) Stress calculations under cyclic loads

The stress calculation may be performed basing on linear elastic behaviour of steel and concrete; by way of simplification, the ratio of the elastic moduli for steel and concrete may be assumed as $\alpha_e = 10$.

Steel stress in R.C. structures is calculated usually assuming cracked concrete cross sections, for prestressed components only if the decisive fatigue load generates tensile stresses in the checked cross section. The calculations of the steel stresses shall be made without considering the tensile strength of the concrete. In the proof of steel stress, allowance must be made for the different bond properties of reinforcing and prestressing steels. Where no detailed analysis is made, the steel stresses of the reinforcing steel calculated under the assumption that the cross section remains plane must be increased by a factor η_s.
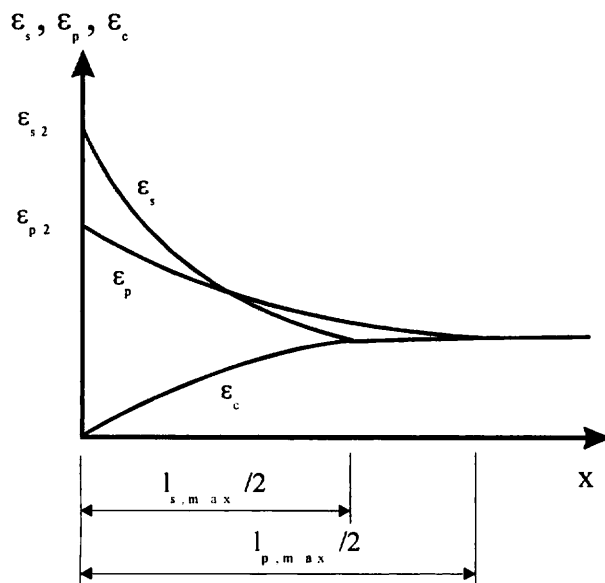
Fig. 4.4-81 Single crack strains of concrete (ε_c), reinforcing bars (ε_s) and prestressed wires (ε_p) in the vicinity of a single crack (l_{smax}, l_{pmax} length over which slip between steel and concrete occurs)

The equivalent steel stress in the reinforcing steel, calculated on the basis of different bond characteristics for reinforcing bars and prestressing tendons, can be taken from chapter 4.3.2 (7.3):

$$\sigma_{s2} = \frac{\Delta F_{s+p}}{A_s + \sqrt{\xi_I} \cdot A_p} \qquad \text{where} \qquad \xi_I = \frac{\tau_{bp,k}}{\tau_{bs,k}} \frac{\varnothing}{\varnothing_p}$$

A_p = prestressing steel area

A_s = reinforcing steel area

$\varnothing$ = smallest reinforcing steel diameter

$\varnothing_p$ = prestressing steel diameter   for 7 wire strands = 1,75 $\varnothing_{wire}$
                                                for 3 wire strands = 1,2 $\varnothing_{wire}$

                                                for bundles = $1,6\sqrt{A_p}$

$\dfrac{\tau_{bp,k}}{\tau_{bs,k}}$ see chapter 4.3.2 (7.3)

η_s can be derived as follows:

$$\eta_s = \frac{\sigma_{s2}}{\frac{\Delta F_{s+p}}{A_s + A_p}} = \frac{A_s + A_p}{A_s + \sqrt{\xi_I} \cdot A_p} \qquad (4.4\text{-}105)$$

(4)   Fatigue resistance of steel and concrete

(4.1)   Fatigue resistance of steel

The S-N-curves given in the MC90 reflect the experimentally estimated fatigue strengths of reinforcing and prestressing steel.

The S-N-curves of reinforcing and prestressing steel are expressed by eq. (4.4-106)

$$N \cdot \Delta\sigma^k = C \qquad (4.4\text{-}106)$$

where

k = stress exponent (inverse of the slope coefficient of the *S-N*-curve in double logarithmic scale);

N = number of cycles to failure;

$\Delta\sigma$ = stress range.

The change of slope of the S-N-curve is assumed to take place at $N^* = 10^6$ cycles for straight and bent bars, for prestressing steel, and at $N^* = 10^7$ cycles for welded bars and steel

under marine environment. The slopes of the S-N-curves are called k_1 for $N < N^*$ and k_2 for $N > N^*$.
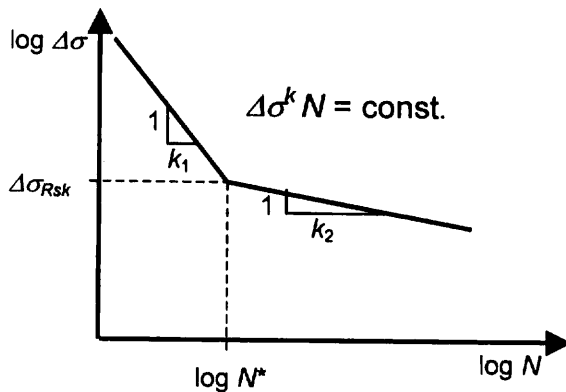
Fig. 4.4-82 Qualitative representation of the S-N-curve for steel

The characteristic fatigue strength of steel embedded in concrete is 40 to 70 % lower than its material fatigue strength. This reduction of fatigue strength is mainly caused by fretting corrosion effects. The S-N-curves in Table 4.4-4 a and b take this effect into account.

The 95 % fractile of survival that was obtained at a 90 % level of confidence from test results has to be considered as a characteristic value of the fatigue strength. The scatter of fatigue strength in the test series is considerable. Furthermore, even for straight reinforced bar samples the test results vary widely depending on product and country of origin. For example, the test results indicate a higher fatigue strength for German reinforced steel (ribbed bars) than for British ones. In both mentioned cases, and the case where one S-N-curve represents the fatigue strength of a whole group of different structural elements (for example mechanical connections), the S-N-curves have to be interpreted as worst case lines. Often there is not enough data available to carry out a proper statistical analysis (for example on the fatigue strength of curved steel tendons and on splice devices). In this case the S-N-curve is to be seen as an engineering judgement considering the scatter of the test results. The curve is expected to be a safe assumption. Hence, a design using the S-N-curves in Table 4.4-4 might lead to conservative results. The user of the standards is at liberty to apply higher values of fatigue strength than shown in Table 4.4-4, insofar these higher values are determined by testing.

	N^*	Stress exponent		$\Delta\sigma_{Rsk}$(MPa)[e]	
		k_1	k_2	at N^* cycles	at 10^8 cycles
Straight and bent bars $D \geq 25\ \emptyset$					
$\emptyset \leq 16$mm	10^6	5	9	210	125
$\emptyset > 16$ mm[a]	10^6	5	9	160	95
Bent bars $D < 25\ \emptyset$ [b]	10^6	5	9	_[c]	_[c]
Welded bars[b] including tack welding and butt joints mechanical connectors	10^7	3	5	50	30
Marine environment[b],[d]	10^7	3	5	65	40

Table 4.4-4 a: Parameters of S-N curves for reinforcing steel (embedded in concrete)

[a] The values given in this line represent the S-N curve of a 40 mm bar; for diameters between 16 and 40 mm interpolation between the values of this line and those of the line above is permitted.

[b] Most of these S-N curves intersect the curve of the corresponding straight bar. In such cases the fatigue strength of the straight bar is valid for a cycle number less than that of the intersection point.

[c] Values are those of the according straight bar multiplied by a reduction factor ξ depending on the ratio of the diameter of mandrel D and bar diameter $\emptyset$: $\xi = 0.35 + 0.026\ D/\emptyset$.

[d] Valid for all rations $D/\emptyset$ and diameters $\emptyset$.

[e] In cases where $\Delta\sigma_{Rsk}$-values calculated from the S-N curve exceed the stress range $f_{yd} - \sigma_{min}$, the value $f_{yd} - \sigma_{min}$ is valid.

Prestressing steel	N^*	Stress exponent		$\Delta\sigma_{Rsk}$(MPa)[e]	
		k_1	k_2	at N^* cycles	at 10^8 cycles
Pretensioning Straight Steels	10^6	5	9	160	95
Post-tensioning Curved tendons[a]	10^6	3	7	120	65
Straight tendons	10^6	5	9	160	95
Mechanical connectors	10^6	3	5	80	30

Table 4.4-4 b: Parameters of S-N curves for prestressing steel (embedded in concrete or mortar)

[a] In cases where the *S-N* curve intersects that of the straight bar, the fatigue strength of the straight bar is valid.
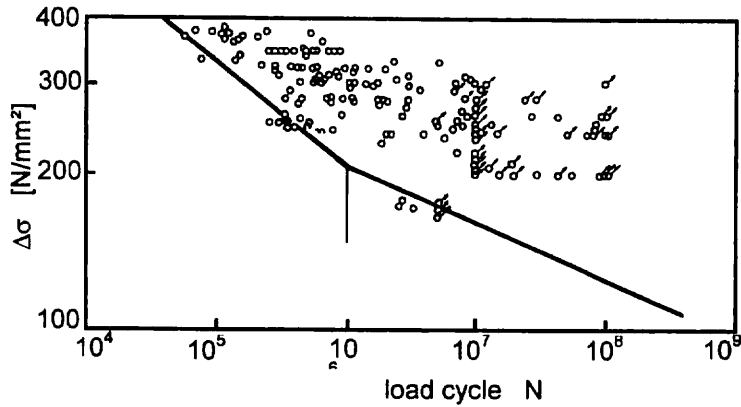
Fig. 4.4-83 Fatigue performance of 6 to 16 mm diameter continuous bars [Tilly and Moss (1982)] and S-N-line for Ø ≤ 16 mm bars according to MC90 [Comité Euro-International du Béton d'Information No 188 (1988)]
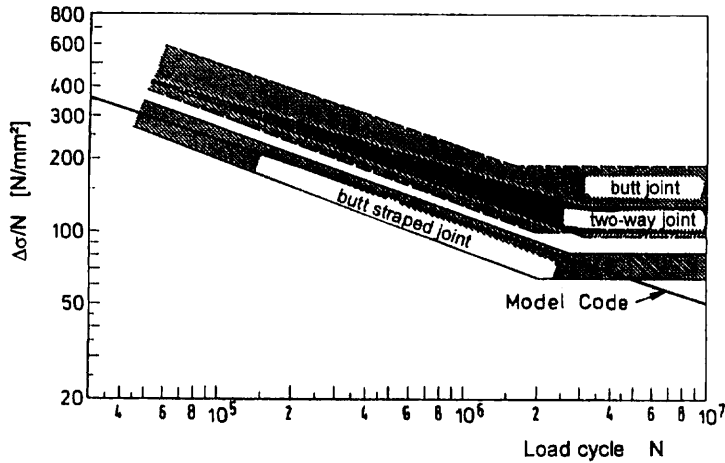

Fig. 4.4-84 Scatter of the fatigue strength of tack-, lap- and butt-welded bars [Rehm, Harre and Rußwurm (1981)] and S-N-line according to MC90
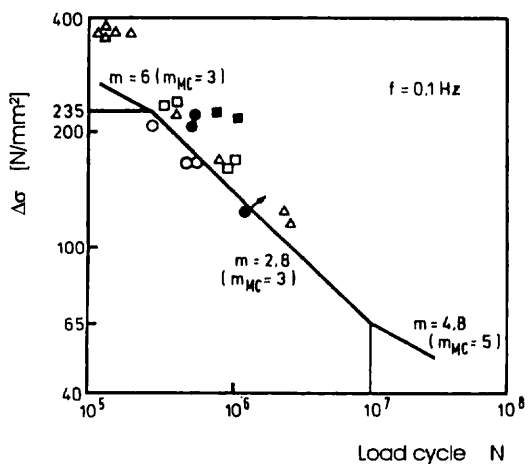

Fig. 4.4-85 Characteristic S-N-line for straight bars in the splash zone [Booth, Leeming, Paterson and Hodgkiess (1986)] and parameter of S-N-line according to MC90
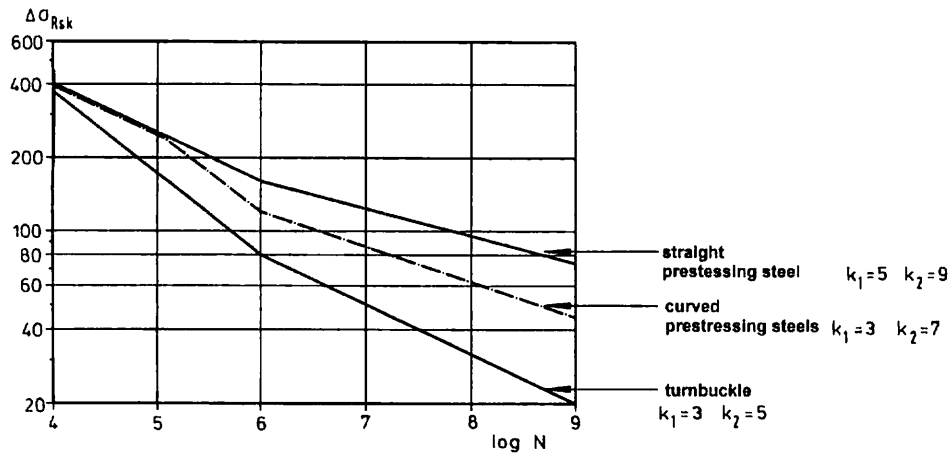
Fig. 4.4-86 S-N-line for prestressing steel according to MC90
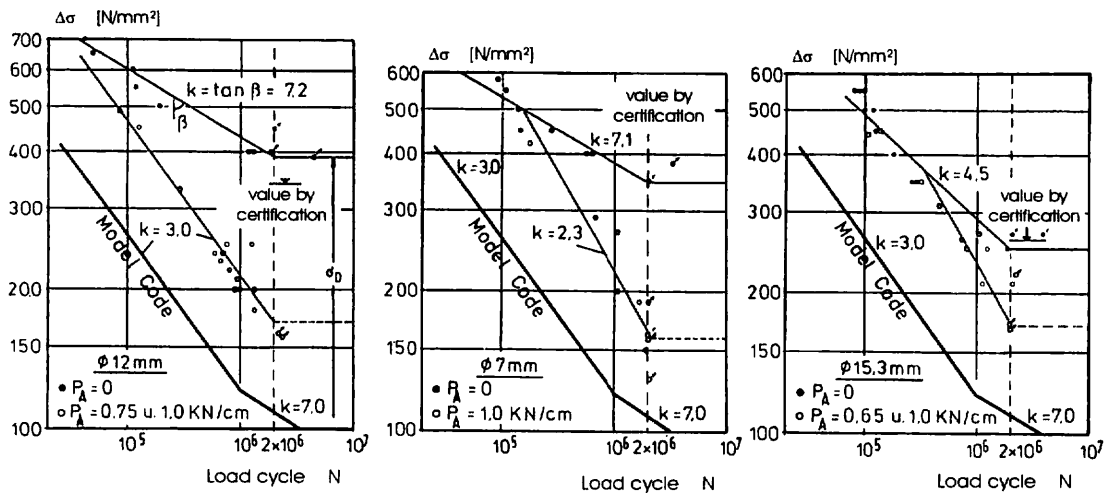
Fig. 4.4-87 S-N-lines for cold drawn prestressing steel ∅7 mm, strands ∅15,3 mm, heat-treated smooth
prestressing steel ∅12,2 mm [Cordes (1986)] and S-N-line for post-tensioned, curved tendons according to MC90
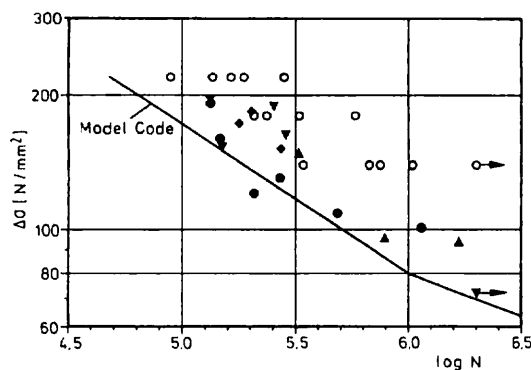
Fig. 4.4-88 Fatigue performance of splicing devices [Kordina and Günther (1982)], [König and Sturm (1991)]
and characteristic S-N-line for mechanical connectors according to MC90
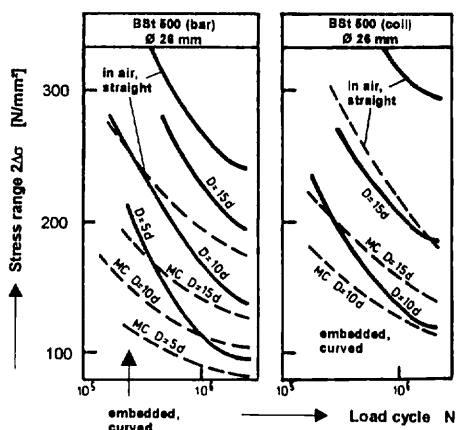
Fig. 4.4-89 Influence of the bending curvature on fatigue strength; S-N-lines according to [Soretz (1965)], [Spitzner (1971)] and MC90

Diameter of mandrel [-]	Reduction of the fatigue strength by [Nürnberger (1982)] [%]	Coefficient ζ [-]	Reduction of the fatigue strength by MC90 $(1-\zeta) \cdot 100$ [%]
5Ø	52 – 68	0,48	52
10Ø	22 – 41	0,61	39
15Ø	16 – 22	0,74	26

Table 4.4-5 Fatigue strength of bonded reinforcing steel

(4.2)   Fatigue resistance of concrete and verification procedure

The experimental results concerning fatigue resistance of concrete under compression are within the MC90 described by the following set of equations

for $0 < S_{cd,min} < 0,8$

$$\log N_1 = (12 + 16 \cdot S_{cd,min} + 8 \cdot S_{cd,min}^2) \cdot (1 - S_{cd,max})$$

$$\log N_2 = 0,2 \cdot \log N_1 \cdot (\log N_1 - 1)$$

$$\log N_3 = \log N_2 \cdot (0,3 - \tfrac{3}{8} S_{cd,min}) / \Delta S_{cd}$$

if $\log N_1 \leq 6$,   then $\log N = \log N_1$

if $\log N_1 > 6$ and $\Delta S_{cd} \geq 0,3 - 3 S_{cd,min} / 8$,   then $\log N = \log N_2$

if $\log N_1 > 6$ and $\Delta S_{cd} < 0,3 - 3 S_{cd,min} / 8$,   then $\log N = \log N_3$ (4.4-107)

with

$$S_{cd,max} = |\gamma_{Sd} \cdot \sigma_{c,max}| / f_{cd,fat} \, ,$$

$$S_{cd,min} = |\gamma_{Sd} \cdot \sigma_{c,min}| / f_{cd,fat} ,$$

$$\Delta S_{cd} = S_{cd,max} - S_{cd,min} ,$$

$$f_{cd,fat} = 0.85 \cdot \beta_{cc}(t) \cdot \left[f_{ck}\left(1 - \frac{f_{ck}}{25 f_{ck0}}\right)\right] / \gamma_c ,$$

$\gamma_c \quad = \quad 1.5,$

$\beta_{cc}(t) =$ coefficient which depends on the age of concrete t in days when fatigue loading starts (see MC90)

$f_{ck0} \quad = \quad 10$ MPa (reference strength)

in which the safety considerations are already incorporated (see also Fig. 4.4-90).
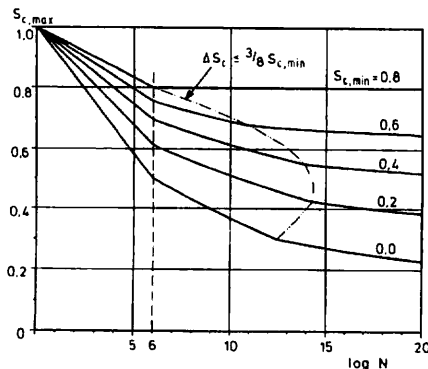
Fig. 4.4-90 S-N-lines for concrete in compression according to MC90

The S-N-line for concrete behaves more or less polygonal in a half logarithmic scale.

The fatigue load is seldom applied directly after the erection phase. This can be taken into consideration by the knowledge of the coefficient $\beta_{cc}(t)$, which takes into account the development of strength with time.

The verification methods can be simplified following the same procedure as for steel.

No further verification is necessary, if

$$\sigma_{cd,max} \leq 0.45 f_{ct,fat} \tag{4.4-108}$$

which is based on Eq. (4.4-107) with $N = 10^8$ cycles.

Otherwise it must be shown, that fatigue safety requirements are met by inserting the required lifetime (expressed by the number of load cycles) and comparing it with the number of cycles to failure

$$n \leq N. \tag{4.4-109}$$

N should be calculated by Eq. (4.4-107).

If the Eq. (4.4-109) doesn't apply, the verification by means of spectrum of load levels can be used. In this case the actual stress levels for concrete can be calculated by Eq. (4.4-107) and (4.4-101).

(5)   Application example

Given is a reinforced crane girder for crane runways according to the German DIN 15018 [König and Gerhardt (1982)]. The stress spectrum S2 is defined according to Fig. 4.4-91. The expected lifetime is expressed with $n = 10^7$ load cycles.
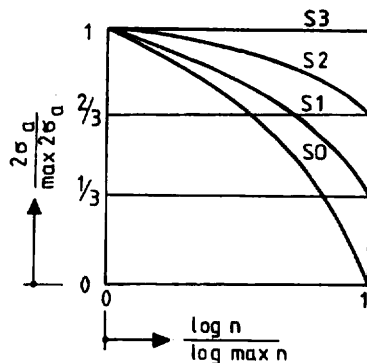

Fig. 4.4-91 Stress spectra for crane runways according to DIN 15018

System and section are given in Fig. 4.4-92.
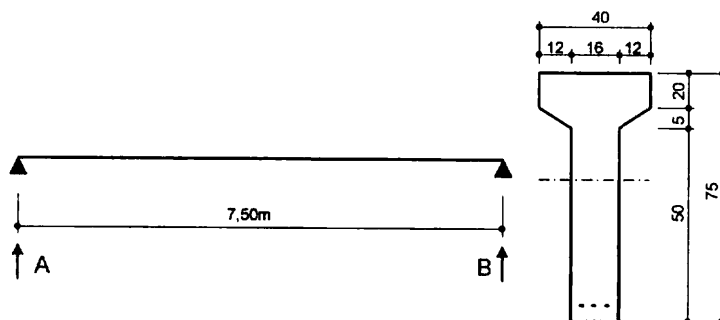
Fig. 4.4-92 Crane girder

The static calculation of loads leads to the following values:

reactions:

$$A_g = 18 \text{ kN}$$
$$+ \quad \max A_p = 84 \text{ kN}$$
$$\overline{\max A = 102 \text{ kN}}$$

moments:

$$\max M_g = 36{,}6 \text{ kNm}$$
$$+ \quad \max M_p = 144{,}0 \text{ kNm}$$
$$\overline{\max M = 180{,}6 \text{ kNm}}$$

To met the ultimate load condition for bending a longitudinal reinforcement of 3 ∅ 22 with $A_s = 11,4$ cm³ is chosen.

The fatigue verification is performed for a damage equivalent stress level according Eq. (4.4-104).

Firstly, the height of compression zone x and the inner lever arm z have to be determined.

$$x = \frac{n \cdot A_s}{b} \left\{ -1 + \sqrt{\frac{2 \cdot b \cdot d}{\alpha_e \cdot A_s} + 1} \right\}$$

$$x = \frac{10 \cdot 11,4}{40} \left\{ -1 + \sqrt{\frac{2 \cdot 40 \cdot 70}{10 \cdot 11,4} + 1} \right\}$$

$$= 17,3 \text{ cm} < 20 \text{ cm}$$

$$z = d - \frac{x}{3} = 70 - \frac{17,3}{3} = 64,2 \text{ cm}$$

These values lead to the maximum stress range in the longitudinal reinforcement.

$$\min \sigma_s = \frac{M_d}{z \cdot A_s} = \frac{0,0366}{0,642 \cdot 11,4} \cdot 10^4 = 50 \text{ MN/m}^2$$

$$\max \sigma_s = 50 \cdot \frac{180,6}{36,6} = 247 \text{ MN/m}^2$$

$$\max \Delta \sigma_s = 247 - 50 = 200 \text{ MN/m}^2$$

The relation between damage equivalent stress range for the stress spectrum S2 according to Fig. 4.4-91 and the given $n = 10^7$ and the maximum stress range can be taken from [König and Gerhardt (1982)] with

$$\alpha_p = \frac{\Delta \sigma_{s,equ}}{\max \Delta \sigma_s} = 1,1$$

related to $N^* = 2 \cdot 10^6$ load cycles.

$$\Delta \sigma_{Rsk} (N = 2 \cdot 10^6) = 160 \cdot \sqrt[9]{\frac{1}{2}} = 148 \text{ N/mm}^2$$

with Eq. (4.4-104) and $\gamma_{Sd} = 1$

$$\gamma_{s,fat} \cdot \Delta \sigma_{s,equ} = 1,15 \cdot 1,1 \cdot 200 = 253 \text{ N/mm}^2 > 148 \text{ N/mm}^2$$

chosen 4 ∅ 28 ($A_s = 24,6$ cm²) for fatigue requirement leads to

$$x = 23,8 \text{ cm} \approx 20 \text{ cm}$$

$$z = 62 \text{ cm}$$

thus $\alpha_p \cdot \max \Delta \sigma_s \cdot \gamma_{s,fat} = 1,1 \cdot 253 \cdot \frac{11,4}{24,6} \cdot \frac{64,2}{62} \cdot 1,15 = 154 \text{ N/mm}^2 \approx 148 \text{ N/mm}^2$

References

Booth E. D., Leeming M. B., Paterson W. S., Hodgkiess T. (1986): "Fatigue of reinforced concrete in marine condition", Marine Concrete 86 – International Conference on Concrete in the Marine Environment, The Concrete Society London

Comité Euro-International du Béton d'Information No 188 (1988):"Fatigue of concrete structures", State of the Art Report

CEB-FIP Model Code 1990 (1993)

Cordes H. (1986):"Dauerhaftigkeit von Spanngliedern unter zyklischen Beanspruchungen", Deutscher Ausschuß für Stahlbeton, Heft 370

Kordina K., Günther J. (1982):"Dauerschwellversuche an Koppelankern unter praxisähnlichen Bedingungen", Bauingenieur, No 57

König G., Gerhardt H.-Chr. (1982):"Nachweis der Betriebsfestigkeit gemäß DIN 4212 "Kranbahnen aus Stahlbeton und Spannbeton, Berechnung und Ausführung", Beton- und Stahlbetonbau, Heft 1, S. 12-19

König G., Sturm R. (1991):"Wöhlerlinien für einbetonierte Spanngliedkopplungen", Institut für Massivbau der TH Darmstadt, Forschungsbericht AIF-Nr. 6956, DBV-Nr. 118

Kurylla A. (1976):"Versuche über das Verhalten auf Biegung beanspruchter Stahlbeton-Bauteile unter häufig wiederholter Belastung", Beton- und Stahlbetonbau, 4

Müller H. H. (1985):"Prüfverfahren für die Dauerfestigkeit von Spannstählen", Lehrstuhl für Massivbau, TU München, Bericht Nr. 1111

Nürnberger U. (1982):"Fatigue resistance of reinforcing steel", IABSE Colloquium, "Fatigue of Steel and Concrete Structures", IABSE Report Vol. 37

Rehm G., Harre W., Beul W. (1986):"Schwingfestigkeitsverhalten von Betonstählen unter wirklichkeitsnahen Beanspruchungs- und Umgebungsbedingungen", Deutscher Ausschuß für Stahlbeton, Heft 374

Rehm G., Harre W., Rußwurm D. (1981): "Untersuchungen über die Schwingfestigkeit geschweißter Betonstahlverbindungen", Deutscher Ausschuß für Stahlbeton, Heft 317

Soretz S. (1965):"Ermüdungseinfluß im Stahlbeton", Zement und Beton

Spitzner J. (1971):"Zur Prüfung von Betonrippenstahl unter schwingender Beanspruchung im freien und einbetonierten Zustand", Dissertation TH Darmstadt

Tilly G.P., Moss D.S. (1982):"Long endurance fatigue of steel reinforcement", IABSE Colloquium, "Fatigue of steel and concrete structures", IABSE Report, Vol. 37

4.4.4 Nodes

by Kurt Schäfer

(1) Introduction to the design of nodes

(1.1) Location and significance of nodes

Checks for a reinforced concrete member are not complete without special consideration of node regions, where stress concentrations occur in the concrete.

A node region is defined as a volume of concrete in which forces acting in different directions meet and balance (Fig. 4.4-93 a). Such forces normally appear as

- compression forces from concrete stress-fields, represented by concrete struts,
- tensile (or compressive) forces from reinforcement, which is anchored or bent in the node region, and
- external forces applied at the node, such as support reactions or concentrated loads.

In some cases also concrete tensile stress-fields contribute to the equilibrium of nodes, but they shall be disregarded in practice.
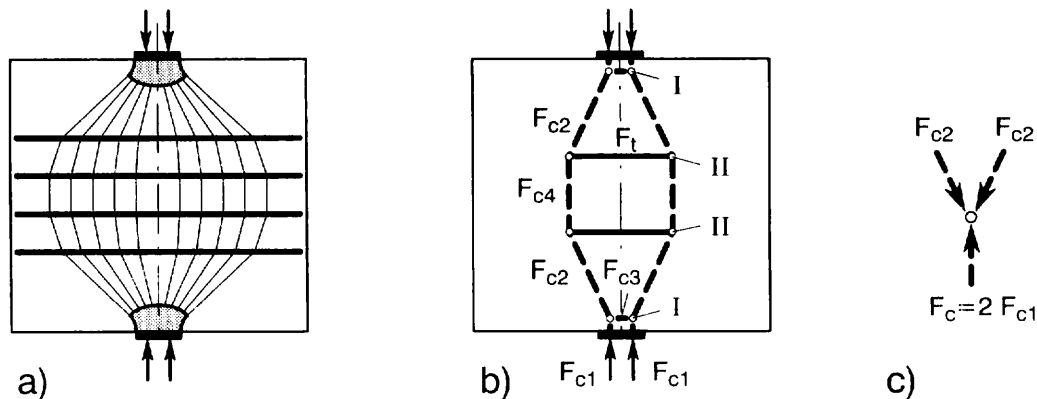
Fig. 4.4-93: *"Singular nodes" (I) and "smeared nodes" (II) in a discontinuity-region:*
  a) Stress field and distributed transverse tensile reinforcement.
  b) Strut-and-tie model (F_c: compression forces, dashed lines; F_t: tensile forces, full lines).
  c) Simplified scheme of compression node (I).

In strut-and-tie models of the structure the nodes are intersection points of struts and ties (Fig 4.4-93 b). In reality, the nodes are regions where stresses are deviated over a certain length and width. Most of the nodes in strut-and-tie models represent "smeared" or "continuous" nodes, where wide concrete stress-fields balance each other or are deflected by many closely spaced reinforcing bars (for example nodes II in Fig. 4.4-93 b). These nodes are not critical. It is sufficient to secure safe anchorage of the reinforcing bars in the smeared node area and to catch the outermost fibers of the deviated compression field with reinforcement (Fig. 4.4-93 a).

On the other hand, where stress concentrations occur in the concrete, the deviation or anchorage of forces is locally concentrated in "singular" or "concentrated" nodes (for example node I in Fig. 4.4-93 b). These are the bottlenecks of the stresses and therefore very often govern the design and dimensions of structural elements. Poor detailing of singular node regions is the most frequent cause for insufficient bearing capacity of reinforced concrete members.

Stress concentration as an indication for a singular node is evident at supports, at bearings under concentrated loads and below anchor plates. These singular nodes are a result of concentrated forces (e.g. support reactions, loads, prestressing forces), which act externally on the node region. In other cases, singular nodes are due to discontinuity of cross-section or other change of the member geometry, as for example in frame corners and near openings in beams or deep beams. Such geometrical discontinuity may provoke an abrupt change of direction of large internal compression forces in the structure. For example, re-entrant corners funnel compression stresses flowing around the corner and make it a singular node. Accordingly, the deviation of large tensile forces at the bends of reinforcing bars may constitute a singular node. Furthermore, anchorage of concentrated reinforcement is always an indication for a singular node.

(1.2)   Mechanism of singular nodes

Although numerous cases of different nodes and detailing of node regions exist, in all cases their forces will ultimately balance each other in the node region essentially through direct compressive stresses. This is quite obvious for pure "compression nodes," where only compression struts meet, as for nodes I in Fig. 4.4-93. It is true also for "compression-tension nodes," where tensile forces from reinforcement equilibrate the compression struts in the concrete, or deviate them (Fig. 4.4-94). The ideal tie anchor (with a plate) transfers its tie force "from behind," causing compression in the node concrete (Fig. 4.4-94 a). Likewise the anchorage by bond is essentially a load transfer by way of concrete compressive stresses, that are supported by the ribs of the steel bar (Fig. 4.4-94 b) or by radial pressure from bent bars (Fig. 4.4-94 c).

Anchorage by bond begins where the compression stress trajectories meet the anchored bar and are deviated by the bond stresses. Above a support, for instance, anchorage begins at the front face of the support (Fig. 4.4-94 b-d). The reinforcement bars must extend to the other end of the support, as a minimum requirement, to catch the deviated stress field completely.

However, it is also permissible to locate part of the anchorage "behind" the support or node area, as indicated in Fig. 4.4-94 d. In this case, a concrete compression field will transfer the corresponding part of the anchor force back to the actual node region. The concrete compression field and the tensile force in the reinforcement behind the node constitute a self-equilibrating stress state which is similar to that of the brake cable of a bicycle. This stress state is normally not reflected in the strut-and tie model or the structural analysis. The corresponding concrete stresses, which superimpose the stresses from sectional effects, are therefore often overlooked.

Strut-and-tie models drawn in a horizontal plane of the node region disclose some transverse tensile forces. Their locus and magnitude depend on the layout of reinforcing bars within the width of the beam or deep beam (Fig. 4.4-95 a). The corresponding "transverse"
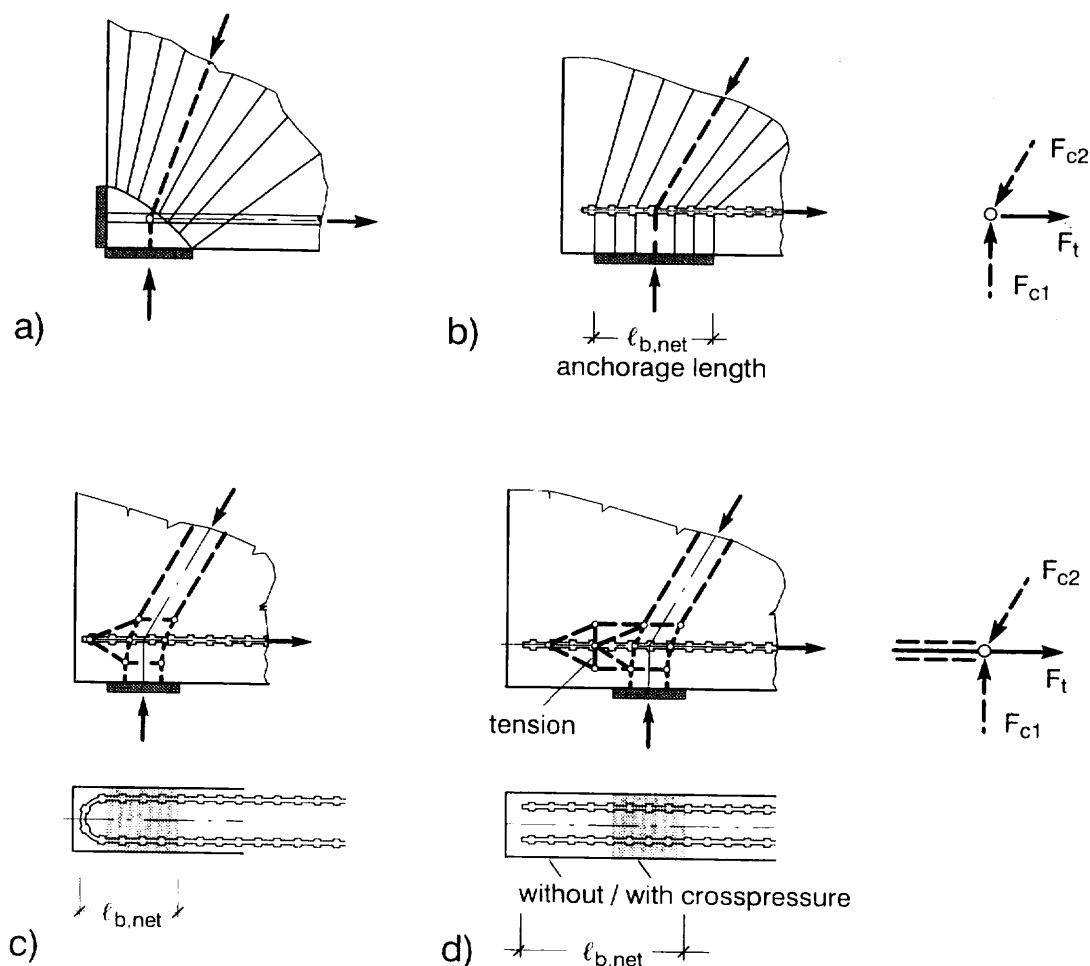
Fig. 4.4-94: Different possibilities for reinforcement anchorage in a compression-tension node
(end support of a beam or deep beam).
a) Anchorage by means of anchor plate behind the node.
b) Anchorage by bond within the node; scheme of the forces acting on the node.
c) Anchorage by radial pressure and bond.
d) Anchorage by bond within and "behind" the node; scheme of forces showing the self-equilibrating forces behind the node.

stresses result from the stress flow of the compression fields onto the reinforcing bars' surface. At least the horizontal component of the main compression strut must go there, to balance the main tie force by bond. Furthermore, the vertical stresses must concentrate at the surface of the reinforcing bars, if there is no anchorage length behind the node, as in Fig. 4.4-94 b. When detailing a node region, the designer should be aware of these stress concentrations, which are necessary for equilibrium and therefore cannot disappear due to plastic behaviour or creep of concrete.

The example above shows, that node regions should be considered also in the "third direction", and that their behaviour depends on the detailing of reinforcement. Normally the transverse tensile stresses are low and need not be analysed numerically. However, the transverse tensile stresses have a considerable influence on the node's bearing capacity, if transverse reinforcement in the node region (or behind it) is inadequate. Strut-and-tie models can explain the flow of forces even in these cases and indicate any tension that is necessary for equilibrium. They are suitable also for a quantitative analysis of major transverse tensile forces, as in the case of nodes with "partially loaded surface" (Section (3.3)).
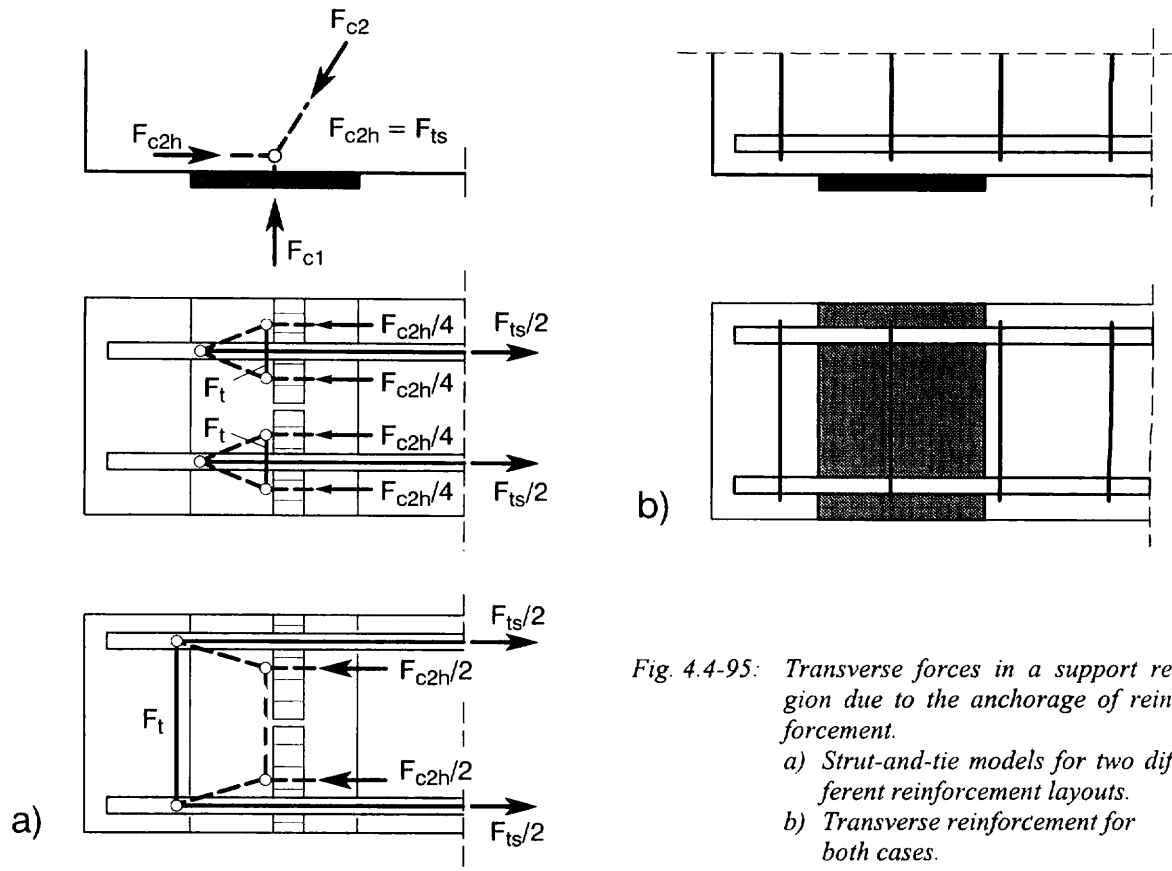
Fig. 4.4-95: Transverse forces in a support region due to the anchorage of reinforcement.
a) Strut-and-tie models for two different reinforcement layouts.
b) Transverse reinforcement for both cases.

(2) Principles for the verification of singular nodes and anchorage

(2.1) General

The three-dimensional stress distribution in singular nodes with their steep stress gradients is normally so complicated, that it cannot be analysed individually with bearable expenditure. Given the high stresses prevailing in the nodal zone, considerable plastic stress redistribution will always take place before actual failure occurs. This justifies the approach of checking average stresses in a defined node region against a representative strength value, instead of comparing the concrete stresses at individual points with the corresponding triaxial strength values. Only stresses required for equilibrium of the node region are checked. Compatibility is approximately observed by orienting the model from which node forces are derived at the elastic behaviour.

Two kinds of stresses are considered in the nodes:

• Average principal stresses in the node region or at the node boundary, as explained in Section (2.3) below.

• Average bond stresses at the anchored reinforcement surface. The bond stresses are controlled by rules about the anchorage length of reinforcing bars, as explained in Chapters 3 and 4.5.3.

Before checking principal concrete stresses in the nodes, it is necessary,

• to determine the forces acting on a node (Section (2.2) below),

• to define a node region (Section (3) below), and

• to judge applicable representative strength values for the given case (Section (2.3) below).

A great variety of nodes and many possibilities of detailing each node exist. However, experience shows, that some types of node and detail are recurring again and again in quite different structures and can be designed safely by simplified rules. Four very common but essentially different types of nodes are termed as "standard cases of nodes" in the MC90. Proposals for the formal delimitation of their node regions and the associated check-ups are given in Clause 6.9.2 of the MC90 and in Section (3) below. Almost all the other nodes are more or less variations or combinations of these standard types; they can therefore be designed following the same principles.

Unless otherwise stated, it will be assumed thereafter, that the node regions are part of a beam or deep beam with constant stresses over its width and that no external forces are applied in the third direction (plane stress problem).

(2.2)   Forces for the check of nodes

Concentrated loads or support reactions, causing the singular node considered, are always taken from the structural analysis of the whole structure or structural member. Like struts, they act as compression forces on part of the node region's boundary. Accordingly, for the check of nodes they can be represented by struts.

The strut and tie forces acting on a node are most conveniently and reliably derived from a strut-and-tie model of the discontinuity-region, to which the node belongs [Schlaich/Schäfer (1998); Schlaich/Schäfer/Jennewein (1987)]. The strut-and-tie model defines also the angles under which struts and ties meet in the node.

In many cases the forces necessary for the check of singular nodes can be derived without developing a complete strut-and-tie model. For example, for the typical end-support node in Fig. 4.4-94 or 99, the resulting strut force F_{c2} and its inclination θ follow from equilibrium with the support reaction F_{c1} and the anchored tie force F_t. The tie force, however, must be derived for cracked concrete behaviour. This implies, for example, to apply the shift rule for beam reinforcement, or to fully anchor the maximum tie force of a deep beam at its support.

Compression forces in singular nodes of beams or columns can frequently be derived from a standard analysis of the cross-section for bending moment and axial force (Section 4.4.1 (4)).

(2.3)   Representative strength values for nodes

The concrete strength in nodes depends to a large extent on the multiaxial stress state and disturbances from cracks and reinforcements. The MC90 permits in Clause 6.2.2.2 to determine the design resistance of a zone under essentially uniaxial compression by means of a stress block over the full area of this zone if appropriately selected. The average design strength values f_{cd1} for uncracked and f_{cd2} for cracked concrete, as specified in the same clause, are referred to also for the design of nodes in Clause 6.9.2.1 of MC90 (see also Sections 4.4.1 (3.3) and (3.4)):

- $f_{cd1} = 0.85 \left[1 - f_{ck}/250 \right] f_{cd}$ (4.4-110)

    for **compression nodes** with only compression struts, furthermore for compression-tension nodes with favourable parameters according to Section (3.2.2).

- $f_{cd2} = 0.6 \ [1 - f_{ck}/250] \ f_{cd}$ (4.4-111)
  $= 0.7 \ f_{cdi}$

  for **compression-tension nodes**, where main tensile bars are anchored
  and an allowance in strength must be made for tensile strains and local
  pressures due to bond action.

- $f_{cd3} = 0.7 \ [1 - f_{ck}/250] \ f_{cd}$ (4.4-112)

  for compression-tension **nodes with ties in one direction only**
  (CCT-nodes, Section (3.3.2). Unlike the strength specifications f_{cd1}
  and f_{cd2} the intermediate value f_{cd3} is not explicitly stated in the
  MC90, but can be justified for normal cases of such nodes as a
  reasonable compromise between the wide limits given in the
  Code. A similar, slightly less conservative limit is proposed by
  Schlaich/Schäfer in several papers and included for example in the
  Canadian Code [CSA Standard A23.3-94].

- For **nodes with secured triaxial compression**, e.g. due to local compression or due to
  lateral confinement by reinforcement, the increased strength values for local compres-
  sion (Chapter (3.3)) or for multiaxial states of stress (Chapters 3.1 and 3.3.5) may be
  applied to individual node surfaces, e.g. at bearings [MC90, Clause 6.9.2.1]. As a pre-
  requisite, all tensile forces in the node region and in adjacent struts must be carried by
  reinforcement.

The designer should choose an adequate value of the design strength considering also the
following background information:

(a) The compression strength decreases essentially with transverse tensile strains and
cracks, in particular if the cracks are not parallel to the principal compression
[Collins/Mitchell (1995), Collins/Vecchio (1982)]. Transverse tensile strains tend to be
higher in regions with (skew) tensile reinforcement in two (orthogonal) directions, as
compared with tensile reinforcement in only one direction. Transverse tension in both
orthogonal directions, including the "third direction" in plane structural elements, are
relevant in this respect.

(b) In plane compression nodes with approximately uniform stress distribution, the biaxial
compressive strength justifies an increase of the design resistance by 10 or 15 % com-
pared to the uniaxial design resistance.

(c) Node forces and node regions should be derived from a strut-and-tie model, which is
oriented at elastic behaviour. Small angles between struts and ties in CCT-nodes (Sec-
tion (3.2.2)) indicate poor modelling and may cause compatibility problems in the node
region. Angles less than $45°$ between major struts and ties in CCT-nodes must be
avoided.

(d) The strength of nodes is endangered by wide cracks in nearby tensile chords, which
eventually penetrate into the node region. Tensile forces in the adjacent stress fields
must be carried by reinforcement and crack distribution reinforcement provided also in
adjacent zones with low tensile strains.

(e) The widths of stress blocks in the node and the widths of the struts at the node boundaries, over which the node stresses are averaged, should not include areas of relatively low compressive stresses. Accordingly, the strut widths of a beam's compression chord acting on a node should be chosen not more than 80 % of the depth of the beam's compression zone.

(f) The reinforcement in node regions with high compressive stresses should be detailed very carefully: The main reinforcement should be distributed over the width of the node, in which it is anchored. Heavy reinforcement should be placed in several layers to avoid congestion and improve the shape of the node region (Section (3.2.2)). The radius of curvature for thick reinforcing bars should be chosen as large as feasible for the node region. Transverse reinforcement should be provided by stirrups or U-bars. The whole reinforcement layout should be chosen with due consideration of placing and compacting the concrete in the node region.

(g) The effective concrete strength in apparently plane stress node regions is also increased by the restraint of lateral deformations due to friction in supports or bearings. A similar effect is due to the restraint of large lateral expansions in the highly compressed node region by the adjacent concrete [Weischede (1983)]. These effects, together with the restraint due to confining reinforcement, may explain, why the bearing capacity of singular nodes in tests and in practice is often much higher than expected. On the other hand, the detrimental effect of transverse tensile forces introduced into node regions that are supported on soft bearings or rubber bearings has to be taken into account.

(h) The effective strength of compression-tension nodes is increased, if the tie force or an essential part of it is applied to the node region "from behind" via compression (Fig. 4.4-94 a, c and d).

Higher design strengths for singular nodes, e.g.. the application of f_{cd1} of Eq. (4.4-110) for compression-tension nodes as mentioned in MC90 and commented in Section (3.2.2), may be justified for individual cases if the above provisions are carefully observed. On the other hand, the design value f_{cd2} from Eq. (4.4-111) should not be exceeded in node regions with essential tensile strains in two directions (Section (3.2.3) and (3.2.4)) or if the above provisions are not reasonably observed.

(2.4) Verification of nodes and anchorage

The verification of nodes and anchorage is well explained in Section 6.9 of the MC90. Referring to it and to the preceding explanations, the practical check of singular nodes can be summarised in three interdependent steps, namely:

- *Tuning the geometry of the node region* to conform with the model and the forces applied.

The geometry of the node region and the arrangement of reinforcement in it should be consistent with the model on which the design of the structure is based, and with the applied forces. Therefore, the node region and the model geometry have to be tuned in such a way, that struts and ties act at the centroid of the node faces, on which constant stresses are assumed. It is not necessary that they act at right angles (see Section (3)). Reinforcement an-

chored in the node should be distributed over a certain height and width with due regard to the widths of the oncoming stress fields and the magnitude of their forces.

- *Checking average compressive stresses* in the node region or at the node boundaries.

 Average compressive stresses (principal stresses) shall not exceed (see Section (2.3))
 f_{cd1} in compression nodes,
 f_{cd2} in compression-tension-nodes,
 f_{cd3} in compression-tension-nodes with ties in one direction only (see Section (2.3)).

 These checks should be performed for relevant faces or sections of the node, as explained in Section (3).

- Checking the reinforcement in the node for safe anchorage. This includes:

 Check of anchorage length to conform with the Code specifications (MC90, Clauses 4.5.3 and 6.9.3 - 6.9.5). The anchorage length is defined in Section (1.2) and in the figures of Section (3).

 Check of mandrel diameter in case of reinforcement bends (MC90, Clause 9.1.1.2).

 Accommodation of transverse tensile forces, including those in the third direction, by means of transverse reinforcement, unless experience has shown that the tensile strength of the concrete will safely resist them.

(3)   Typical nodes

 The following standard details contain proposals for the formal delineation of very frequently occurring nodes and the associated checks of the concrete compression. It is emphasized that the dimensions, stresses and strength values specified therein do not reflect the true picture, but should rather be understood as an indirect means for confirming the satisfactory performance of the node. The proposed method of node design also spotlights the structural requirements to be observed in the detailing of the nodes and permits a comparison and assessment of different design versions. The method may be analogously adopted for other cases.

(3.1)   Plane compression nodes

 Plane compression nodes typically occur under concentrated loads and over intermediate supports of beams and deep beams, as well as in the compressed re-entrant corners of frames, corbels and at openings.

 To simplify their analytical check, it is proposed to idealise the boundaries of the node regions by plane faces. The node region of a compression node in a deep beam similar to node I in Fig 4.4-93 b will then assume a triangular shape, as shown in Fig 4.4-96 a. The state of stress in the whole node region is constant.
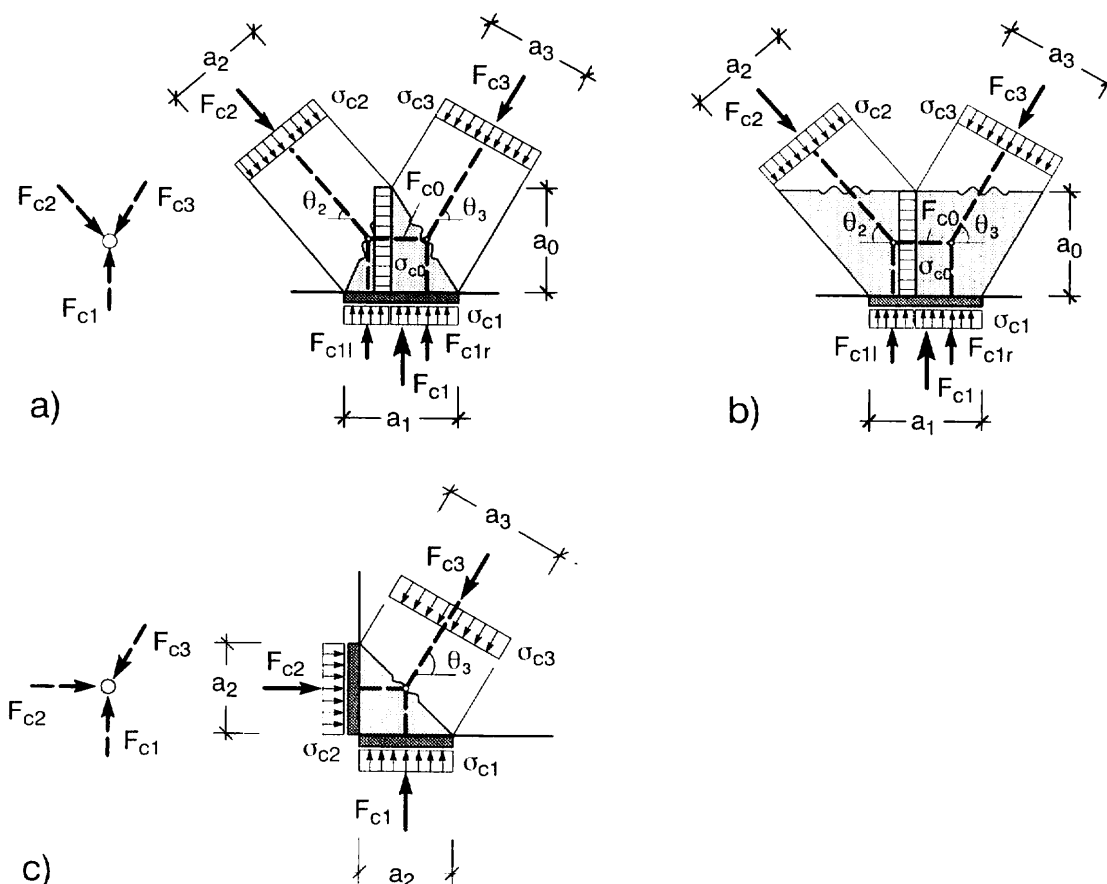
Fig. 4.4-96:   Standard compression nodes with three struts.

    a) General triangular node region with bearing pressure.

    b) Alternative trapezoidal node region for the same node.

    c) Right triangular node region.

If the three faces of the above node region were chosen normal to the compression struts (including the support reaction) then the stresses in all three node faces and within the node region would be constant and equal in all directions (plane hydrostatic pressure). In this case only one stress needs to be checked against f_{cd1} from Eq. 4.4-12, which is most conveniently performed for the bearing pressure σ_{c1}.

As drawn in the figure, the struts may also be assumed inclined at skew angles with respect to the node faces. If one of the struts remains orthogonal, like the bearing pressure σ_{c1} in Fig. 4.4-96 a, then this pressure constitutes one of the two principal stresses in the node region.

The other principal stress σ_{c0} normal to this face and all stresses in the other node faces are smaller than σ_{c1}, if the node height a_0 is chosen larger than that of the hydrostatic node with the same basis a_1. This is true for the shape of node region as drawn, which has the advantage of modelling the real behaviour of the structure more realistically. Again it is sufficient to check only the stress σ_{c1} at the bearing.

However, if for any reason the height a_0 of the node triangle is less than that of the corresponding hydrostatic node, the principal stress σ_{c0} will become the critical one and needs to be checked against f_{cd1}. This applies e.g. to nodes with a restricted height due to cracks in between the diagonal struts.

Sometimes it is helpful to split the triangular node into two rectangular triangles as indicated in Fig. 4.4-96 a. The model for the two parts of F_{cl} (which are equal to the vertical components of F_{c2} and F_{c3}, respectively) also explains the horizontal force F_{c0} in the node region.

An alternative trapezoidal layout for the same node with three compression struts is shown in Fig. 4.4-96 b. The two triangular parts added to the node region in Fig. 4.4-96 a are uni-axially stressed, which is a (safe) idealisation, since stress trajectories in reality are curved and always create biaxial compression near the loaded area. The same checks apply for σ_{cl} and σ_{c0}, and the same results are obtained as for the triangular node shape of Fig. 4.4-96 a.

The right triangular node region in Fig. 4.4-96 c is applicable for example to end supports of prestressed beams and to compressed re-entrant corners of structures (Fig. 4.4-97). In general, both (principal) stresses σ_{cl} and σ_{c2} in the orthogonal node faces have to be checked against f_{cd1}. The stress intensity in the diagonal node face is in between those stresses.

In compressed re-entrant corners of frames (Fig. 4.4-97 b) and in similar situations, the two node stresses can be verified using standard methods for beams (Section 4.4.1 (4)).

a)   b)
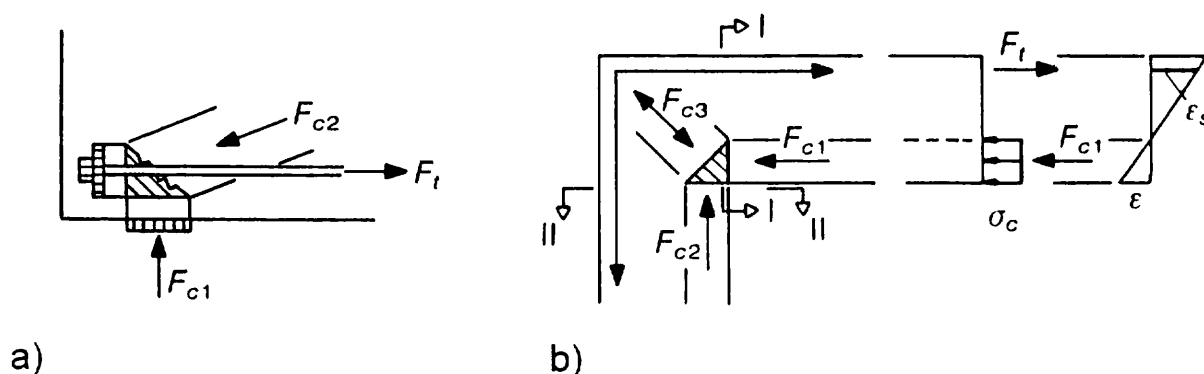
Fig. 4.4-97: Applications of the right triangular compression node region [MC90, Fig.6.9.2].
  a) Node over end support of prestressed beam.
  b) Node in compressed re-entrant corner with simplified check of node pressures in sections I and II assuming linear strain distribution

A trapezoidal node region similar to that in Fig. 4.4-96 b is suitable also for nodes with five struts (Fig.4.4-98). This standard node occurs for example over the inner supports of beams or deep beams and under concentrated loads applied to such members. The three triangular parts of the node region are subject to different biaxial compression stresses, with the highest stresses occurring in the inner triangle. Therefore, the nesessary checks of compression stresses σ_{c1} and σ_{c0} are the same as for the compression nodes above.

Looking at compression nodes in linear members, one principal compression stress is usually checked automatically as the bending compression zone of a cross-section. The second principal stress normally is the bearing pressure.

If more than five struts meet in a singular node, the node area can be adjusted by just adding one or more triangular parts to it, keeping the whole node area convex (without re-entrant corners). Alternatively, two adjacent struts can be combined and their resultant force applied to a simpler standard node area. Considering that node regions with rounded borderlines may

be checked in the same manner [Baumann (1988)], the proposed plane boundaries are suitable for all types of nodes and all types of adjoining compression fields (including fan-shaped stress fields).
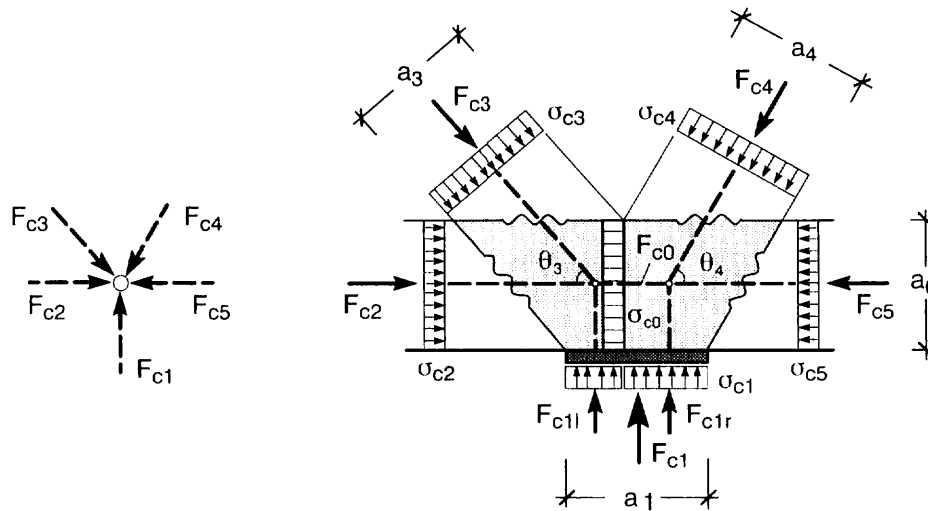

Fig. 4.4-98:   *Standard compression node with five struts over an intermediate support of continuous beam*

(3.2)   Plane compression-tension nodes

(3.2.1)   General

The characteristic feature of all compression-tension nodes is that principal reinforcement is anchored or deviated in the node region. The state of stresses and strains in the interior of the node region is much more complicated than in compression nodes and cannot be checked likewise (see Section (1.2)). Instead, the bond stresses of anchored reinforcement are limited by code rules, and mean stresses of struts acting on the node surfaces are compared with representative resistance values f_{cd2} or f_{cd3}, as explained in Section (2.4).

The mean concrete stresses in the node boundaries are analyzed in the direction of the axis of the corresponding compression strut F_c from $\sigma_c = F_c / A_c$ where the cross section A_c is defined perpendicular to the strut axis. As indicated in Fig. 4.4-99 b for the strut F_{c2}, we may imagine the node boundaries to be serrated sections in which only the serrated areas that stand perpendicular to the strut axis are loaded with σ_c.

In the following three subsections three standard types of tension-compression nodes are described. The first one, a "CCT node", is essentially different from the other two insofar as just one main tensile force F_t acting at the node is balanced by two compression struts F_{c1} and F_{c2}, whilst the other two standard nodes are "CTT nodes" with two tie forces acting in different directions. In CTT nodes with tensile strains imposed on the node concrete by main reinforcement in two directions, the concrete compression strength in general will be less than for CCT nodes (Section (2.3)). Therefore the lower value f_{cd2} from Eq. 4.4-111 should be applied.

(3.2.2)   Standard node with anchorage of parallel bars only
             (end support node, CCT-node)

This type of tension-compression node is typical for corners of structural elements with external concentrated forces applied there. Most common is the node at end supports of beams and deep beams, and we may therefore shortly refer to it as "end support node". It is also normally found under the bearing plates of corbels or under columns resting on the corners of walls. Somehow hidden, this type of node occurs further in frame corners with opening moments and in dapped ends (half-joints) of beams (Chapter 7.3).

For an analysis of the structure's main loadbearing plane, it is convenient to imagine the reinforcement replaced by a layer that continues through the entire thickness b of the component and has an effective height u, across which the compression fields are deviated (Fig. 4.4-99 a). The node region can then be idealised as shown in Fig. 4.4-99 b. A node region thus bounded will normally cover the overlap regions of the incoming compression fields (including the bearing pressure) and reinforcement ties. As suggested by Baumann (1988) the effective height u of the node, can be assumed as given below:
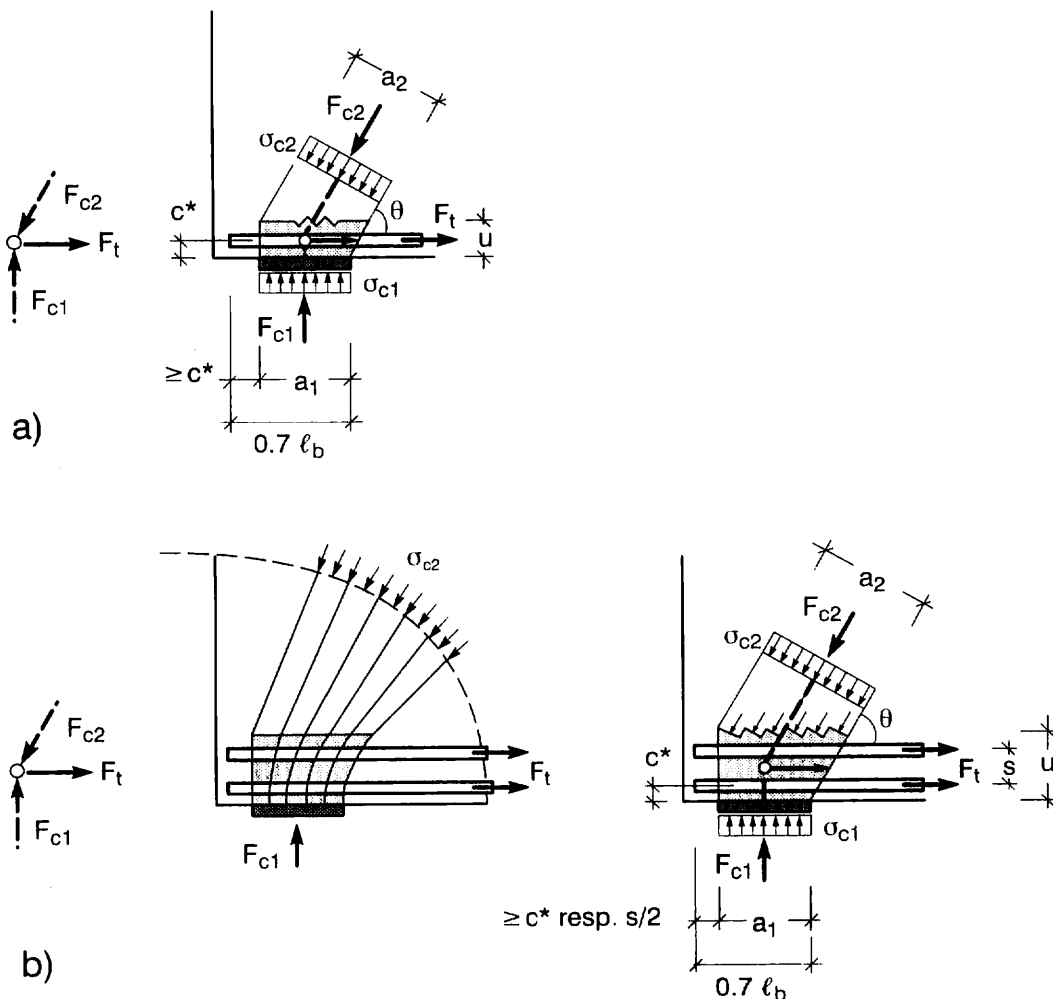
Fig. 4.4-99: Standard end support node.

     a) Idealized node region for one-layer reinforcement with excess length.

     b) Flow of forces for multi-layer reinforcement with excess length and corresponding idealised node region.

$u = 0$	for one-layer of reinforcement not extending beyond the deviated compression field (Fig. 4.4-94 b)	(4.4-113 a)
$u = 2 c^*$	for one-layer of reinforcement with a minimum length c^* in excess of the deviated compression field (Fig. 4.4-99 a)	(4.4-113 b)
$u = 2 c^* + (n-1) s$	for n layers of reinforcement with a distance s between layers and an excess length of at least c^* or $s/2$ (Fig. 4.4-99 b).	(4.4-113 c)

Where the node geometry is to some extent known (support width a_1, angle θ of strut, effective height u), the widths a_2 of the diagonal compression field is determined by

$$a_2 = a_1 \sin\theta + u \cos \theta \tag{4.4-114}$$

The necessary checks for the node are

- Compression stress in the node surface (bearing stress) due to F_{c1}

$$\sigma_{c1} = F_{c1} / a_1 b \leq f_{cd3} \tag{4.4-115}$$

- Compression stress in the node surface due to strut F_{c2}

$$\sigma_{c2} = F_{c2} / a_2 b \leq f_{cd3} \tag{4.4-116}$$

- Anchorage length not less than $l_{b,net}$ according to the relevant code, including a reduction factor $\alpha_5 = 0.7$ for the beneficial effect of the transverse pressure provided by F_{c1} and F_{c2}. (Chapter 4.5.3).

- Transverse reinforcement arranged according to the relevant code or good practice.

In the above equations b denotes the thickness of the member or node, normal to the plane of the figures.

It is obvious from the figures and the formulae that in most practical cases the stresses σ_{c2} in the diagonal strut are higher than σ_{c1} in the support area, a fact that is frequently overlooked. The stresses σ_{c2} increase with decreasing strut angle θ, whereby an angle below 55° should be avoided in CCT-nodes with high stress level, unless the principal tie is prestressed. On the other hand, an arrangement of the main reinforcement in several layers or additional reinforcement (for example loops) placed above the main reinforcement layer increase the effective height u of the node region and the width a_2 of the oncoming diagonal strut, thereby reducing the stresses σ_{c2} on that strut.

As pointed out in Section (2.3), the above dimensioning rules apply if the internal forces and reactions are derived from reasonable models and if crack widths are controlled in the usual way. Considering the reliability of his assumptions and analysis, the designer may have to reduce the proposed strength value to f_{cd2}. On the other hand he may justify the higher value f_{cd1} for the check of node stresses, if in addition to the above mentioned requirements one or several of the following parameters apply (see Section (2.3) f , g and h):

- The main reinforcement is anchored to a considerable part behind the node.

- The bearing or support provides lateral restraint for the supported node region by reliable friction, and it can carry itself the transverse tensile force associated with the friction.

- The reinforcement in the node area is very well detailed and provides some lateral restraint.

If the bearing extends to the very edge of the structural element as drawn in Figure 4.4-100, the main reinforcement cannot have an anchorage length beyond the bearing. Instead, the bars must end inside the node region at a distance from the node boundary, which is necessary for the concrete cover (in reality, considering practical tolerances of bar cutting and construction, the distance from the node end may be more than that). The same type of node region, turned around by 90^0, is found at the edges of structural elements, where a concentrated internal tie force is directed orthogonal to the edge and has to be anchored there in a deviated compression field or a compression chord. This applies in particular to suspending forces in dapped ends and at openings in beams or deep beams (Chapter 7.3).
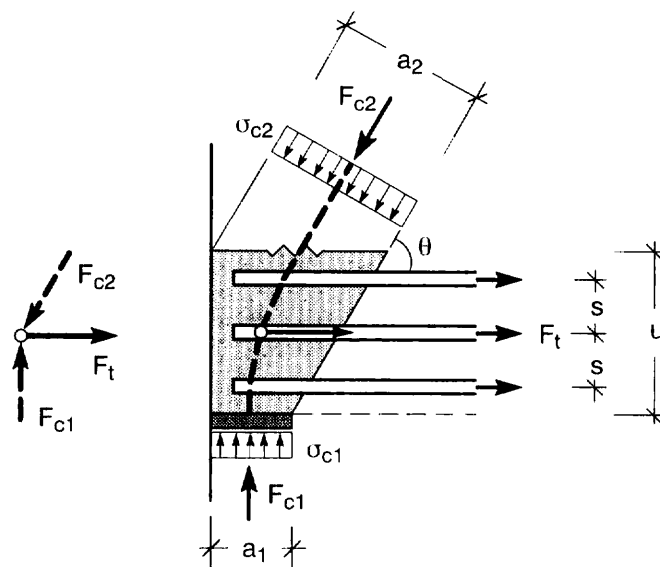
Fig. 4.4-100: Compression-tension node for reinforcement ending in the node region

In such cases, the concrete cover behind the bar ends has to accomplish the deviation of a considerable part of the compression field by its tensile strength. To avoid spalling of the concrete cover and reduce bond stresses on the reinforcing bars, the reinforcement shall be distributed over a not too small effective height (resp. length) u. Stirrups or relatively thin hairpin-shaped bars bent in the plane orthogonal to the compression are preferable. Such reinforcement is also recommended as a supplementary reinforcement for the anchorage of thick straight bars. Following MC90, Clause 6.9.2.1, it is sufficient without further check of anchorage length to transfer 2/3 of the tie force to such additional parallel bars. The transverse tie force due to the lap requires additional transverse reinforcement for approximately $F_t/4$, unless this force is compensated by compression.

(3.2.3)   Compression-tension node with bent bars

Such nodes occur where a strut force is balanced mainly by the radial pressure of bent bars, such as bent-up reinforcement in beams or main reinforcement bent around a frame corner.

Since concrete stresses are not acting at right angles to the bar surface, there is always some bond action involved, in particular if the forces in the reinforcement are different at both ends of the bend.

The node region may be idealised according to Fig. 4.4-101, with a strut width

$$a = d_m \sin \theta \qquad (4.4\text{-}117)$$

where θ denotes the smaller angle θ_1 or θ_2 between the reinforcement legs and the strut. Based on this width, the representative strut stresses in the node can be checked for any angle α of reinforcement bend with the general formula

$$\sigma_c = \frac{F_c}{a\,b} \leq f_{cd2} \qquad (4.4\text{-}118)$$

For nodes with orthogonal ties ($\alpha = 90^\circ$), the concrete stress can be derived directly from

$$\sigma_c = \frac{\max F_t}{b\,d_m \sin\theta \cos\theta} \leq f_{cd2} \qquad (4.4\text{-}119)$$

where $\max F_t$ is the larger of the two tie forces and θ is any of the angles between the strut and the ties.
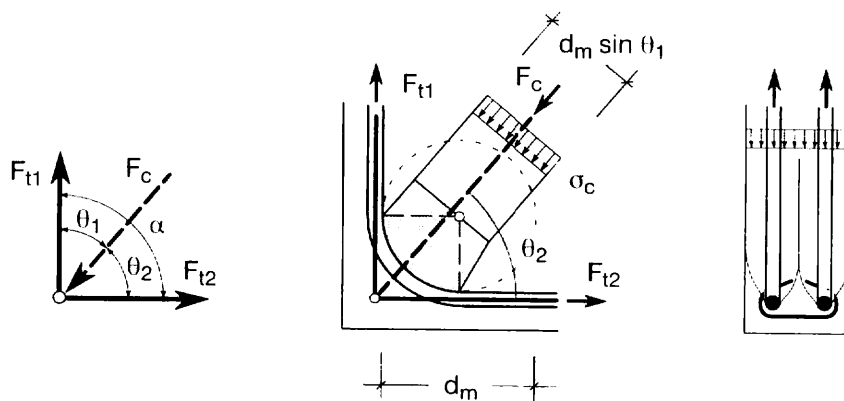
Fig. 4.4-101: Node with bent bars. Scheme of forces, standard node region and cross-section

Radii of curvature or mandrel diameters have to conform with the relevant code (e.g.. MC90 Clause 9.1.1.2). The respective rules are mainly intended to avoid bursting or splitting of the concrete due to individual bent bars (Chapter 4.5.2). However, observing these rules is not enough to prevent inadmissible strut stresses in nodes with closely spaced bent bars or several layers of bent reinforcement. The radii of curvature should be chosen as large as structurally feasible. Concrete corners outside the curved bars can be secured from splitting by additional loops of thin bars.

Regarding the transverse tensile stresses, the main reinforcement should be distributed uniformly across the thickness of the component and transverse reinforcement (stirrups, loops or equivalent) should be provided according to good practise. Bars bent around a rectangular corner tend to anchor the diagonal strut partly ahead of the bend by bond similar to the node described in the next Section (3.2.4). Therefore transverse ties should be arranged also imme-

diately before and after the bend. These reinforcements effectively widen the node area and thereby reduce the stresses in the bent bar and the strut.

(3.2.4)　　Standard nodes with ties in orthogonal directions

This type of node is most typical for beams, but appears also in any other member where main reinforcement is anchored along an unsupported edge or surface. The anchorage is essentially performed by diagonal concrete compressive stresses in combination with transverse reinforcement like stirrups (Fig. 4.4-102 a). Considering that the anchorage of the transverse reinforcement must be achieved within the thickness of the tension chord, only small diameter bars with hooks or angles (bent around the chord reinforcement) are appropriate.

If such thin bars are distributed over a great length of the main reinforcement, as is normally the case in beams, the node is of the "smeared" type and needs not be checked in detail. However, with closely spaced stirrups or loops it is possible and sometimes necessary to anchor large chord forces within a relatively short length, associated with high diagonal concrete stresses. Examples are nodes due to vertical suspension forces in half joints and in beams with large openings.

The corresponding node in the corner of a member (Fig. 4.4-102 b) can also be used as an alternative to the node with (thick) bars bent around the corner of a structure. It occurs in the corners of structural elements without direct support (Chapter 7.3).
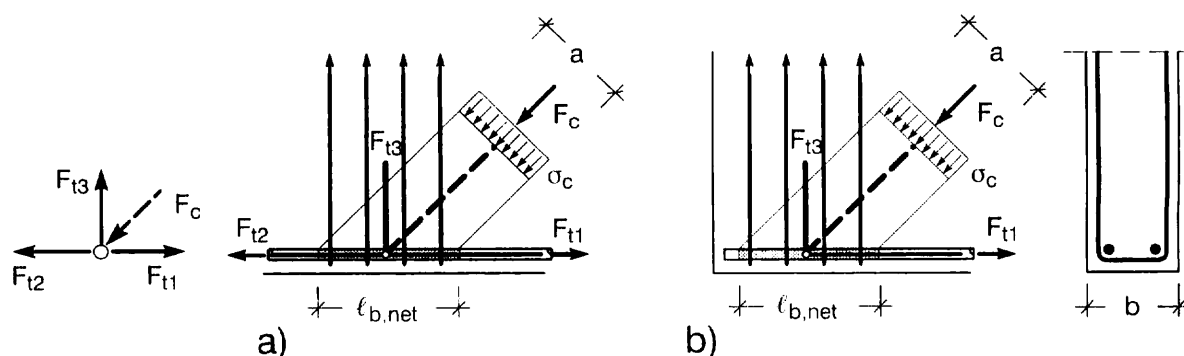
Fig. 4.4-102: Standard nodes with ties in orthogonal directions:
a) Anchorage of reinforcing bars near an unloaded concrete surface,
b) anchorage of reinforcing bars near an unloaded corner (special case of a)

In undisturbed regions of beams (B-regions) the diagonal concrete stresses from the anchorage are identical with the web compression stresses and checked against f_{cd2} from Eq. (4.4-111), applying the standard design for shear forces (see also Chapter 4.4.1 (5) and MC90 Clause 6.3.3.2). The concrete compression in singular nodes of this type can be checked accordingly, but will be critical only where heavy and closely spaced reinforcement is used. In those cases the following checks are proposed:

• Diagonal compression stress

$$\sigma_c = \frac{F_c}{a\,b} \leq f_{cd2} \qquad (4.4-118)$$

- Anchorage of main reinforcement for the differential force F_{t1}-F_{t2} according to Fig. 4.4-102 a or for F_{t1} in the case of a corner node (Fig. 4.4-102 b). The available anchorage length can be increased if additional orthogonal reinforcement in both directions is arranged next to the reinforcements, which are necessary for carrying the forces.

- Anchorage of the reinforcement for F_{t3}. Where thin bars are adequately spaced along the anchorage length, bond requirements can be satisfied by means of loops or hooks (stirrups in beams).

- Transverse reinforcement in the third direction according to good practise (horizontal legs of stirrups or loops).

(3.3)   Nodes with reduced support width and other tree-dimensional nodes

The recommended procedure is to deal with the main loadbearing plane first as for plane nodes and then consider the load effects in the third direction. However, it should be kept in mind, that the flow of forces in the different planes is interdependent.

Fig. 4.4-103 illustrates, as an example, a node which in its main loadbearing plane is similar to the node drawn in Fig. 4.4-99 b. In the third direction, the compression field is constricted by the reduced support widths $b_1 < b$. As a result, the concrete immediately above the bearing plate is under triaxial compression, and transverse tensile stresses develop farther up. Therefore, the increased strength values for local compression or multiaxial states of stress may be applied to the bearing area, provided that all tensile forces in the node region and adjacent struts are carried by reinforcement.

Following MC90, Clause 6.9.2, for nodes with local compression as shown in Fig. 4.4-103 c the design bearing pressure can be increased by a factor

$$\beta = min \ (b/b_1 \ or \ a/a_1) \ \leq 4$$ (4.4-120)

with notations as defined in Fig. 4.4-103 c. Remember, that no increase is justified, if the loaded area lies at an edge of the structure!

In the same section of MC90 the following formula for the transverse tension force F_{t1} is given, which can be derived from the strut-and-tie model in Fig. 4.4-102 b, if the internal lever arm of the tie force with the transverse compression force is assumed to be $b/2$:

The reinforcement ties for F_{t1} in the thickness direction of the member should be distributed over a height which is approximately equal to the member thickness b.

The check of concrete stresses from the strut is the same as for plane nodes (Section (3.2.2)). However, different from plane nodes, the anchorage length for the main reinforcement F_t should not be assumed to begin above the inner edge of the support, but rather in the centreline of the support to account for the fact that the support reaction is initially not deviated by the reinforcement but by concrete pressure. As the detailed model in Fig. 4.4-103 a shows, the node 1, which represents the centre of anchorage length, is shifted behind the bearing plate.

a)

b) c)
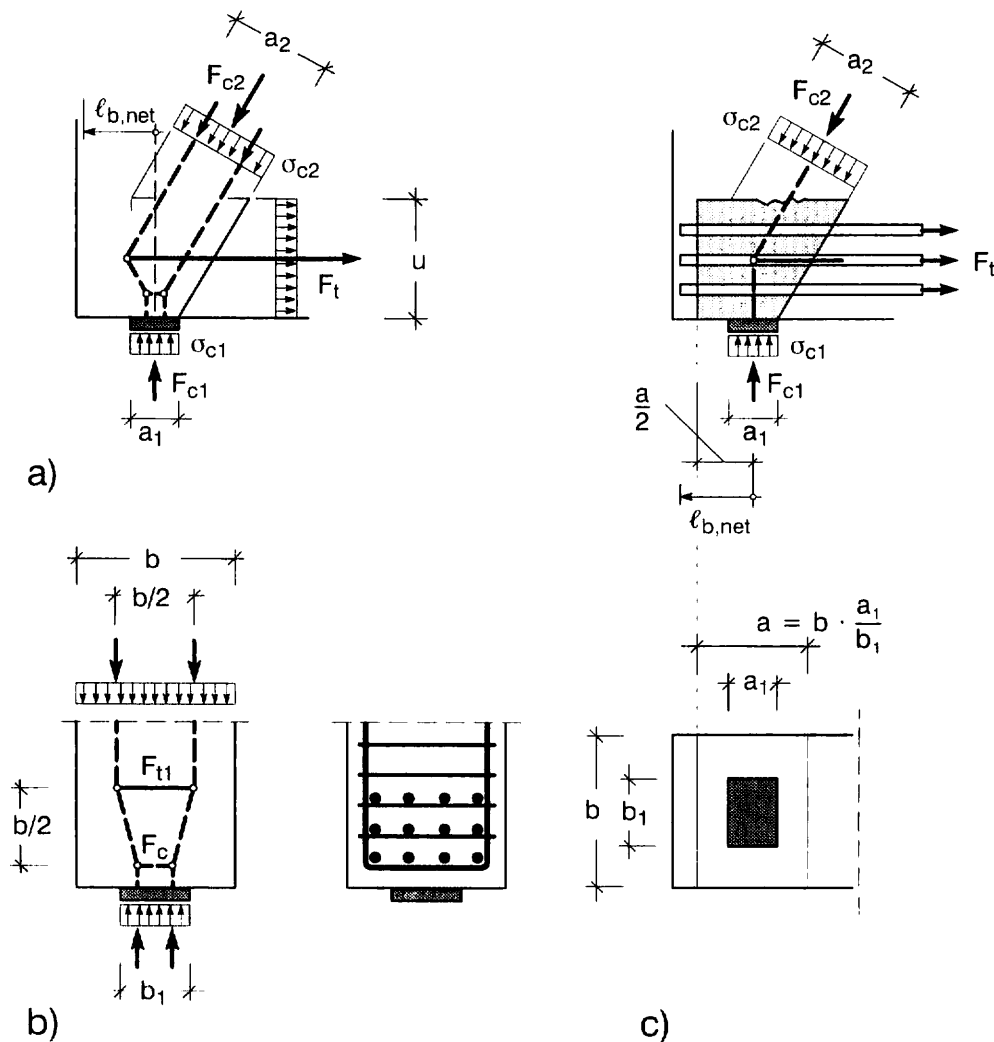
Fig. 4.4-103: Node over a support with local compression.
a) Longitudinal section of the node region with refined strut-and-tie model and corresponding reinforcement.
b) Cross section with model and corresponding reinforcement.
c) Support area and geometrically similar area in plan

$$F_{t1} = \frac{b - b_1}{4b} F_{c1}$$

(4.4-121)

A modification of the above node occurs frequently at the other end of the orthogonal reinforcement (stirrups), where this reinforcement is anchored in a compression chord parallel to the tension chord. This type of node is less critical, because the node area has tensile strains only in the (vertical) direction of the transverse reinforcement and compression in the direction of the chord. Accordingly f_{cd3} would apply for the check of the node stresses from the struts. However, the compression chords of beams are usually checked against αf_{cd} (Chapter 4.4.1), disregarding the transverse strains, which are very small near the surface.

(4)   References and indication of numerical examples

As a general introduction to the application of plastic methods on reinforced concrete the book from Muttoni/Schwartz/Thürlimann (1997) is recommended. Some more variations of standard nodes are discussed in the papers of Schlaich/Schäfer referenced below. Sundermann/Schäfer (1997) investigated the bearing capacity of some singular nodes using a refined strut-and-tie model and carried out tests with micro-concrete for comparison.

Numerical examples are included in particular in the two workshop reports from Schlaich et al (1993) and Schäfer et al (1996), which are almost identical. Some numerical examples for the check of nodes and the corresponding reinforcement will be included in Chapter 7.3 of this textbook.

References

Baumann, P. (1988): Die Druckfelder bei der Stahlbetonbemessung mit Stabwerkmodellen. Diss. Inst. f. Massivbau, Univ. Stuttgart 1988

Collins, M. P.; Vecchio, F.: (1982): The response of reinforced concrete to inplane shear and normal stresses. Publ. No. 82-03, Univ. of Toronto, March 1982

Collins, M. P.; Mitchell, D. (1995): Shear and torsion. Chapter 4 of the Concrete Design Handbook. Canadian Portland Cement Association 1995

Muttoni, A.; Schwarz, J.; Thuerlimann, B. (1997): Bemessung von Stahlbetontragwerken mit Spannungsfeldern. Birkhaeuser Basel/Boston/Berlin 1997

Schäfer, K. et al.(1996): Strut-and-tie models for the design of structural concrete. Workshop National Cheng Kung University Tainan, Taiwan 1996

Schlaich, J. et al (1993): The design of structural concrete. IABSE Workshop New Delhi, India, 1993.

Schlaich, J.; Schäfer, K. (1998): Konstruieren im Stahlbetonbau. Betonkalender 1998, Vol. 2, pp. 721-895. Ernst & Sohn Berlin 1998

Schlaich, J.; Schäfer, K. (1991): Design and detailing of structural concrete using strut-and-tie models. Structural Engineer, Vol. 69; No. 6, March 1991

Schlaich, J.; Schäfer, K.; Jennewein, M. (1987): Towards a consistent design of structural concrete. PCI-Journal Vol. 32, No. 3, May/June 1987, pp. 74-150

Sundermann, W.; Schäfer, K. (1997): Tragfähigkeit von Druckstreben und Knoten in D-Bereichen. DAfStb.-Heft 478, Beuth Berlin, 1997

Weischede, D. (1983): Untersuchungen zum methodischen Konstruieren im Stahlbetonbau. Diss. Inst. f. Massivbau, Univ. Stuttgart 1983

4.5 Anchorage and Detailing Principles

by Rolf Eligehausen and Agnieszka Bigaj-van Vliet

4.5.1 Reasons and background for detailing rules

Structures shall be designed, constructed and operated in such a way that, under the expected environmental influences, they maintain their safety, serviceability and acceptable appearance during an explicit or implicit period of time, without requiring unforeseen high costs for maintenance and repair. The quality of the structure depends significantly on the quality of detailing of the reinforcement. Failures are often caused by poor detailing and rarely by incorrect structural analysis. The detailing principles intend to ensure a sufficient low probability of failure and an adequate behaviour under service load. To that end both strength and durability aspects are considered. Last but not least it should be remembered that detailing of the reinforcement may considerably influence the cost of the assembled reinforcement and the construction time.

Following a description of bond behaviour, given in Chapter 3, in this Chapter the reasoning is given that supports the detailing rules provided by the CEB-FIP Model Code 1990 (MC90). In general, the MC90 intends to maintain a close connection between the general models describing the mechanical behaviour of reinforced concrete and the operational models used for member design. This intention is at present only *partially* fulfilled. In particular with respect to the bond model and the provisions on anchorages and splices there is a clear discrepancy: while the bond stress-slip relationship is a close to the reality non-linear approach, the analysis of anchorages and splices is based on the concept of evenly distributed bond stresses, which are not directly derived from the non-linear bond stress-slip relationship. This conservative approach has an advantage of being more simple, yet sufficiently accurate. Here the general tendency for simplification and unification of detailing rules (e.g. for different anchorages) also plays a role.

It should be stressed that, similar to the bond model given in MC90, the detailing rules apply only to the reinforcing steel that fulfils the requirement of current standards with respect to bar/strand geometry and surface characteristics. Furthermore, the detailing rules are valid for the usual safety level at present time, referred especially to the safety factors. A reduction of so called hidden reserves with a better fitting of loads and/or calculation methods to realistic ones would need higher requirements on detailing of reinforcement and a revision of the detailing rules.

4.5.2 Arrangement of reinforcement

(1) Minimum concrete cover

Concrete cover on the reinforcement is one of the most important factors with regard to the durability of reinforced concrete structures. For that reasons an appropriate quality of concrete in the outer layer of the structural elements shall be secured and an adequate thickness of concrete cover should be provided. Moreover, adequate detailing should ensure the integrity of critical surfaces or corners and edges in order to avoid any unforeseen concentration of aggressive influences. Since chlorides penetrate to the interior of concrete at a lower rate than given by a square-root time function, the critical state for incipient danger of

corrosion is reached more than four times faster if concrete cover is halved. To secure the corrosion protection of the reinforcement the minimum cover c_{min} of any bar, stirrup, tendon or sheathing should be not less than 10, 25 and 40 mm (plus tolerance) for exposure classes 1, 2 and 3-4, respectively (for exposure class 5 minimum thickness of the concrete cover depends on the individual type of environment encountered).

Other reasons, such as ensuring bond strength, fire protection and execution requirements, may warrant larger covers. To ensure that bond forces are safely transmitted and to prevent spalling of the concrete, the minimum cover c_{min} of any reinforcing unit of diameter $\emptyset$ should be at least equal to $1\emptyset$ (supplementary rules are given for high bond bars of $\emptyset > 32$ mm and for bundled bars). Special attention should be given to prevent bursting in the region of bar curvature (e.g. for hooks, bents and loops). In such cases the required concrete cover perpendicular to the curvature should be enlarged, if necessary. A too small concrete cover can be increased by directing the plain of curvature towards the inner concrete parts. Finally, from the execution requirements (concreting) it follows that the minimum thickness of the concrete cover c_{min} should not be less than two times the largest aggregate size. The tolerance value, Δc depends on the distance of spacers, however it can be taken as 10 mm unless in the individual case it can be demonstrated that a lower value (yet not less than 5 mm) is obtainable.

(2)   Spacers

Spacers are components fixed to reinforcement which provide cover between the reinforcement and the formwork. Spacers shall be designed according to nominal values of minimum concrete cover, c_{min} (usually in dimensions which are multiplies of 5 mm) and the spacing of spacers shall be adequate to ensure the required cover. Recommendations for spacing are aimed at achieving the specified cover between the steel reinforcement and the formwork and maintaining the reinforcement in its correct position during concreting.

In slabs (including foundations) bar reinforcement in the bottom of slabs should have spacers at maximum centres of 50 times size of bar (with a maximum of 1000 mm) and should be staggered. Welded fabrics should have spacers at 500 mm maximum spacing in two directions at right angles. Where line spacers are used they should not exceed 350 mm in length and they should be staggered. Top reinforcement should be supported either by continuous chairs, spaced at maximum centres of 50 times size of bar and resting on line spacers at a maximum of 500 mm centres, or by individual chairs with plastic tips, spaced at centres of 50 times size of bar with a maximum of 500 mm in two directions at right angles. Where cover at the edges of slabs is important (e.g. exposed edges or edges subject to condensation) end spacers should be located at 50 times size of bar or at 1000 mm maximum centres.

In beams and columns spacers are required in sets at centres not exceeding 1000 mm for beams, and 50 times size of main bar for columns with at least three sets along the length of the member, and a maximum spacing of 2000 mm. At least one spacer is required at the middle of the link on each cover face. Note that where the face exceeds 50 times size of link bar at least two spacers are required on that face. Double links require at least 3 spacers on the cover faces where they overlap. At exposed end faces of beams a suitable end spacer should be specified to each bar.

In walls cover should be provided by spacers at 50 times size of bar or 500 mm maximum centres, whichever is the greater, and staggered. Spacers on opposite faces should be coincident in elevation. Two layers of the reinforcement should be separated by vertical continuous chairs at not more than 1000 mm centres. Note that walls cast in a horizontal position should be treated as slabs, while slabs cast in a vertical position should be treated as walls as far as requirements for spacing are concerned. For more details the reader is referred to *CEB Bulletin d'Information No.201 - Recommendations for spacers, chairs and tying of steel reinforcement (1990).*

(3) Single bar spacing

The clear spacing of parallel reinforcing bars should be big enough to ensure that all of the bars will be surrounded by dense concrete and that enough concrete area is available for transmission of forces from concrete to steel or vice versa. The horizontal or vertical intermediate free space between parallel single bars or horizontal layers of parallel bars should therefore be at least equal to the largest bar diameter but not less than 20 mm. In contrary to this rule twin bars of welded wire meshes are allowed to touch each other. Special rules are valid for bundles of bars, see Section 4.5.1-(4). Bars spliced by lapping might be in contact along the lap length, while the spacing between splices should be not less than $2\emptyset$ and at least 20 mm to avoid splitting of the cover. The maximum size of the aggregate should be chosen such that adequate compacting of the concrete is permitted.

(4) Bundled bars spacing

Compared to the arrangement of reinforcement in the section using single bars, the use of bundles of bars has an advantage of leaving larger place for compacting concrete or allowing for the higher amount of reinforcement in the same section. This is illustrated with an example of a beam in Fig. 4.5-1.
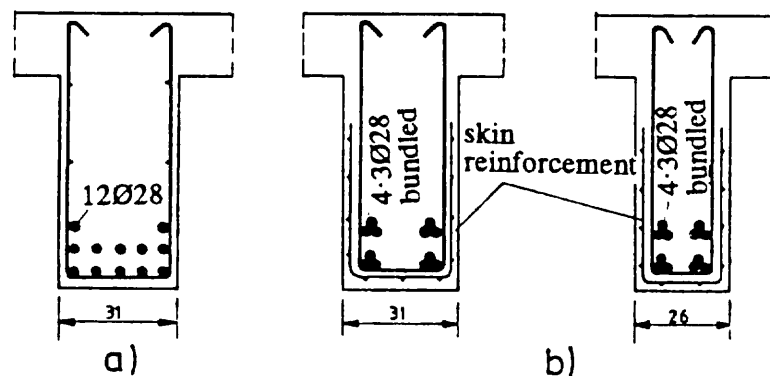
Fig. 4.5-1: Arrangement of reinforcement in the section: a) single bars, b) bundled bars, after Rehm et al (1978)

Due to the concentration of concrete casting of concrete is much simpler while embedding of reinforcing bars in concrete is still ensured. Furthermore, large diameter bars can be substituted with bundles of bars, which additionally contributes to the simplification of reinforcing work and storekeeping, hence to a rationalisation with a simultaneous increase in quality compared to the densely arranged single bars. However, the use of bundled bars does have some disadvantages as well. The concrete that surrounds the bundles is subjected to

higher stresses due to the concentration of reinforcement and forces, respectively, compared to the case of single reinforcing bars (considering otherwise equal conditions). This aspects are taken into account when elaborating the regulations, otherwise large cracks widths and premature longitudinal cracks would be induced in tensile members.

The number of bundled bars, n, is limited to 4 for vertical bars in compression and for lapped splices otherwise to 3 for all other cases. For design purposes, bundles of bars containing n bars of the same diameter are replaced by a single equivalent bar having the same centroid: $\phi_n = \phi \sqrt{n} < 55$ mm. In order to limit the concrete stresses around the bundles as to single bars, spacing and concrete cover for bundles must be fulfilled at least for the equivalent bar diameter. Hence, ϕ_n is taken into account in evaluating the minimum cover to avoid splitting and in defining horizontal and vertical free distances. Using this method, the cover provided should be measured from the actual outside contour of the bundle. Note that anchoring, splicing and application of stirrups in case of bundled bars require special attention.

(5)   Skin reinforcement for crack width control for thick and bundled bars

Concentration of reinforcement together with the increased concrete cover may produce worse cracking behaviour in case of thick and bundled bars. In these cases an additional skin reinforcement might be needed to keep the crack widths within acceptable limits and protect the concrete cover against bursting, see Fig. 4.5-2.
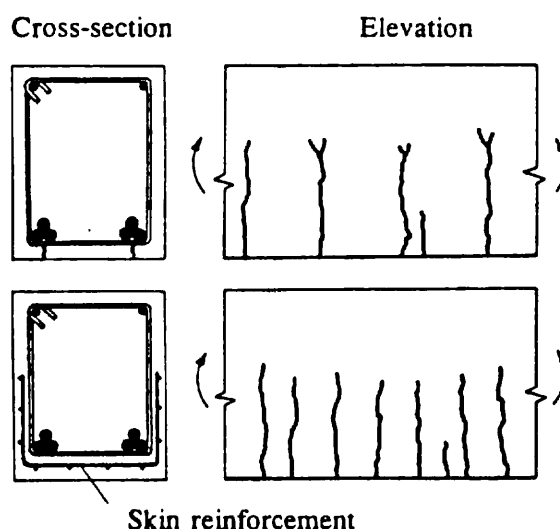
Fig. 4.5-2: Crack patterns for bundled bars with and without skin reinforcement, after Rehm et al (1978)

Although the required area of skin reinforcement parallel to the tensile reinforcement increases with decreasing steel ratio, with decreasing allowable crack width and with increasing steel stress, for the seek of simplicity it is assumed that the area of the skin reinforcement related to the cross-section of the outer layer of the concrete zone in tension should not be less than 0.01 in perpendicular direction to the large diameter bars and 0.02 parallel to those bars. Skin reinforcement is most effective if placed as close to the surface as allowed by the regulations on concrete cover. The additional skin reinforcement can be taken into account in design provided that it meets the requirements for detailing and anchorage.

(6)   Allowable mandrel diameter

The minimum value of mandrel diameter is controlled either by the bending capability of steel or by the concrete pressure in the region of curvature. Because of the limited plastic elongation of the steel under flexural conditions and taking into account rate effects and temperature effects, for hooks of longitudinal bars the minimum mandrel diameter should not be less than $5\emptyset$ in any circumstances. To avoid bursting of the concrete cover or splitting of the concrete cross-section caused by the high pressure occurring inside the bend should not be to small, see Fig. 4.5-3. The values of permissible radii of bends depend in this case on the concrete cover/distance between bars, steel stress to be anchored, anchorage scheme (hairpin, hook, stirrup angle), transverse reinforcement, concrete strength, etc. Attention should be given to the cases where several bars are bent in one place (as in frame corners) due to the possible negative influence of the overlapping splitting forces. In usual cases, the limit values given in the standard can be used as an indication (in the absence of transverse reinforcement for 90° bends that anchor 60% of the yield strength of a deformed bar with the diameter $\emptyset$ the minimum mandrel diameter varies from $10\emptyset$ to $25\emptyset$ for the value of min[*cover thickness, half bar spacing*] equal to $7\emptyset$ and to the minimum allowable value of $1\emptyset$, respectively).
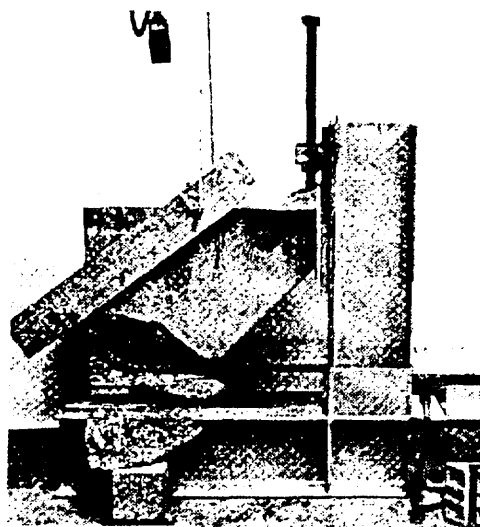
Fig. 4.5-3: Bursting of concrete cover in the region of a hook, after CUR

In general welding in the bent portion of a rebar is permitted and there are no additional restrictions for minimum mandrel diameter if after bending the reinforcement is to be welded. On the contrary bending on welded joints or within the heat affected zone (i.e. within $3\emptyset$ to $4\emptyset$ of the weld) is not permitted owing to the structural changes of steel and increased notch effects produced by the welding. However, it is not always possible to follow this principle. Therefore for welded reinforcement which is bent after welding the same minimum mandrel diameter values as for reinforcing bars can be used, provided that the distance between the point of welding and the beginning of the curvature is big enough to avoid tensile or compressive strains in the region of welding, i.e. is not less than $4\emptyset$.

(7)   Minimum reinforcement ratio

Requirements of limit state of cracking guarantee that, with an adequate probability, cracks will not impair the durability and serviceability of the structure. Of major importance

for durability of concrete structures is the provision of a minimum amount of reinforcement to avoid extremely wide cracks (i.e. for reinforced concrete members $w > 0.4$ mm). Moreover a minimum amount of reinforcement must be provided in order to satisfy the specific appearance and function requirements with respect to cracking. The rules given for crack control should rather be understood as an advice for an appropriate choice of the reinforcement. In MC90 one finds the following limitation for minimum amount of reinforcement:

$$\min\rho = f_{ct,max} / f_{yk}$$ (4.5-1)

where:

ρ	reinforcement ratio, related to the concrete tension zone just before the formation of cracks (non-linear stress distribution considered)
$f_{ct,max}$	upper fractile of the concrete tensile strength at the moment when the first crack is expected
f_{yk}	characteristic value of steel yield strength

The minimum required reinforcement area may be reduced or even dispensed with altogether in the members where the imposed deformations are unlikely to cause cracking or in prestressed members and reinforced members subjected to compressive normal force (due to the influence of the increased flexural stiffness of the compression zone and due to the effect of prestress or compressive normal force on crack width limitation).

4.5.3   Anchorage regions

(1)   Anchorage of reinforcing steel

(1.1)   Behaviour of anchorage for straight ends, hooks, bends, loops and welded cross bars

The shape of the anchored bar influences its anchorage capacity very much. In Fig. 4.5-4 steel stress and slip distribution over the anchorage length are compared considering a straight-end or bent bar as well as a straight-end bar with a welded crossbar. For the derivation of the design bond stress values a displacement at the beginning of the anchorage in the case of combined anchorages was not permitted to be considerably larger than in the case of pure bond anchorages neither in SLS nor in ULS, and it was required that a slip at the unloaded end of the bar in the case of pure bond anchorages was 0 under the service load and less than 0.10 mm under ultimate load. Hence, calculations were performed for identical steel stress and approximately identical slip at the beginning of the anchorage. It shows that, if an adequate confinement is provided and if the bursting of concrete cover in the region of curvature is avoided, a shorter length is required to develop the same steel stress in the second and third cases compared to the first one. The conditions for anchorages of straight-end bars are discussed in Chapter 3. The slip behaviour does not differ considerably for hooks, bends or loops using the same mandrel diameter. In order to have simple and uniform provisions for all types of anchorages, the slip at the beginning of the anchorage is chosen as a design criterion. It is required that the slip at the beginning of anchorage should be approximately equal for all anchorage types of deformed bars to that of a straight-end bar both in serviceability and in ultimate limit states. This condition can be satisfied with a proportional reduction of the straight anchorage length. Based on the above mentioned reasons, favourable effects of hooks or bends on compressed bars should not be considered.
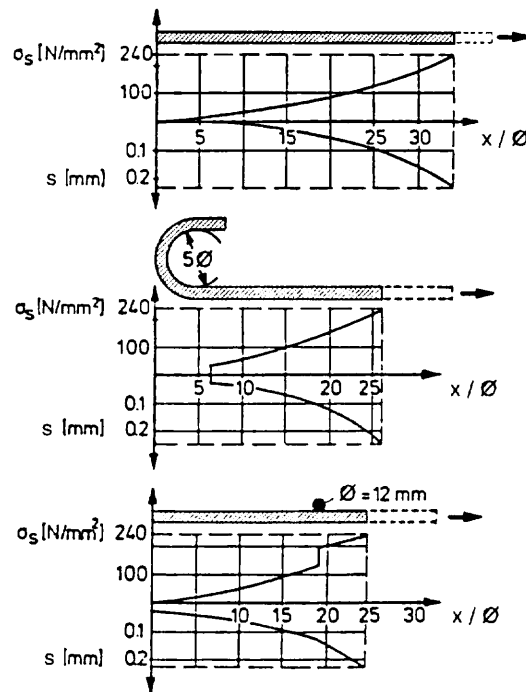
Fig. 4.5-4: Steel stress and slip distribution along various anchorages, after Schießl (1975)

Bond of plain and slightly deformed bars is mainly based on adhesion between concrete and steel and on friction after relative displacement takes place. Both effects deteriorate considerably under long term and cyclic loads. Straight anchorages or anchorages with bends are therefore not allowed for plain bars in tension. Hence, it is compulsory to apply hooks, loops or similar equivalent anchorages (such as anchorage plates or welded bars) at the end of these bars. Bends can also by applied for shortening of the anchorage length of deformed bars, since the better bond due to the ribs produces the favourable influence of curvature already at a 90° bending. However, hooks and bends are to be avoided on compressed bars since because the increase of eccentricity in front of the hooks may produce a loss of stability of the reinforcing bar.

Different confining effects influence anchorage capacity to a high extend. The increase of bond capacity due to pressure transverse to the anchored bar is in more detail discussed in Chapter 3. Considering the slip of loop, hook or bent, the high transverse pressure in the anchorage zone works advantageously, together with the increased mandrel diameter.

(1.2)   Required anchorage length

The various forms of anchorages of reinforcing bars are allowed in any part of the element. However, they are not allowed to negatively influence the behaviour of the element neither for ultimate nor for service loads. The given provisions consider these points of view. They ensure a sufficient safety against bond failure by pull-out or splitting as well as a satisfactory cracking and slip behaviour in the anchorage zone in SLS (i.e. the anchorage length long enough to control crack width at its loaded-end section under service load conditions). An overall safety factor of 2.1 is applied in ULS against the 5% fractile of test results. The factor 2.1 is the product of the material safety factor of concrete being 1.5 and the weighted average of safety factors to dead load (1.35) and live load (1.5) giving 1.4. The consideration of partial safety factors for different combinations of dead load and live load

would unnecessarily complicate the calculations. The anchorage lengths, given by the MC90 were evaluated from test results of specimens where bond failure was caused by pull-out of the bar accompanied by splitting of the concrete cover. However, the pre-assumption that failure is caused by pull-out and not by splitting may be questioned in some applications.

The discussion above clarifies why the basic anchorage length, determined as discussed in Chapter 3, may be reduced considering the beneficial effects of a bent or loop (α_1), of welded transverse bars (α_2), of confinement by concrete (α_3) or by not welded transverse reinforcement (α_4), of pressure p transverse to the plane of splitting (α_5) and the difference in the required ($A_{s,cal}$) and the provided ($A_{s,ef}$) amount of reinforcement. The obtained length considering these effects is called design anchorage length:

$$l_{b,net} = \alpha_1\, \alpha_2\, \alpha_3\, \alpha_4\, \alpha_5\, l_b\, A_{s,cal} / A_{s,ef} \geq l_{b,min} \tag{4.5-2}$$

where:

l_b	basic anchorage length (see Chapter 3.3.2 (3.2.5) and eq. (3.3-40)
α_1	bar shape factor (i.e. 1.0 for all anchorages in compression and for straight bars in tension, 0,7 for bents and loops with sufficient cover in tension)
α_2	welded transverse bar factor (0.7 for all anchorages if transverse bar is welded)
α_3	concrete confinement factor (1.0 for all anchorages in compression, from 0.7 to 1.0 for anchorages in tension - concrete cover dependent)
α_4	not-welded transverse bar factor (1.0 for all anchorages in compression - confining reinforcement dependent)
α_5	transverse pressure factor (from 0.7 to 1.0 for anchorages in tension - pressure dependent)

The product of $\alpha_3\, \alpha_4\, \alpha_5$ is limited to 0.7 for high bond bars and to 1.0 for plain or indented bars or wires which practically means that the reduction factors by confinement are applicable only to ribbed bars.

Limitations on the design anchorage length, $l_{b,min}$, ensure a minimum available anchorage length and take account of tolerances (e.g. inaccuracies in placing):

$l_{b,min} < \max[0.3\, l_b, 10\varnothing, 100\text{ mm}]$ for bars in tension
$l_{b,min} < \max[0.6\, l_b, 10\varnothing, 100\text{ mm}]$ for bars in compression

(1.3)   Transverse reinforcement

Transverse tensile stresses are introduced in the anchorage zone of reinforcing bars due to splitting forces. They have to be balanced by transverse reinforcement unless structural measures (such as relatively thick concrete cover, large spacing, low forces to anchor) or other advantageous influences (e.g. confining pressure) exclude splitting of the concrete cover. Therefore transverse reinforcement should be provided for anchorages in tension if compression is not available transverse to the plane of splitting (for example due to support reaction), and for all anchorages in compression. It is to be designed for approximately 25% of the force to be anchored in the largest bar. This means that the splitting forces perpendicular to the concrete cover are at most only partly taken up by the transverse reinforcement but must be resisted by the concrete tensile capacity. However, the amount of

transverse reinforcement provided in the anchorage zone is enough to avoid longitudinal cracking under the effect of transverse tensile stresses and to guarantee the safety against bursting of the concrete cover, due to contact pressure exerted at the end section of a compressed bar. For bars in compression, the transverse reinforcement should surround the bars, being concentrated at the end of the anchorage and extended beyond it to a distance of at least 4Ø.

(1.4)   Anchorage of bundled bars

In order to avoid unfavourable cracking behaviour and excessive local concrete stresses due to a sharp change in the stiffness, bundles of bars are allowed to be anchored using straight anchorages with staggering. The staggering should be 1.2, 1.3 or 1.4 times the anchorage length of the individual bars for bundles of respectively 2, 3 or 4 bars. Hereby the unfavourable bond behaviour in a bundle compared to an anchorage of a single bar is taken into account. In this respect it must be reminded that casting of concrete is to be carried out here very carefully in order to ensure adequate density of concrete surrounding the bundle.

(2)   Anchorage of prestressing reinforcement

(2.1)   Required anchorage length of pretensioned prestressing reinforcement

While in case of post-tensioned tendons the force transfer from the tendon relies on the bearing capacity of the anchorage device, in case of pretensioned tendons it is the anchorage length of the tendon that has to guarantee the transmission of the design strength of the tendon to the concrete. The anchorage of pretensioned prestressing reinforcement is a basic question from the beginning of the application of pretensioned concrete elements. A point of discussion was the existence of a no-bond transfer zone at the unloaded end of the transmission length. The previous version of the Model Code (MC78) included such kind of length without bond stress, but MC90 omitted it since there is no real evidence for a bond deterioration that would cause such a bond free zone. There is always an uncertainty of the test results in the close vicinity of the end face of the element owing to the difficulties adjusting the points of measurements. If the concrete cover is not splitted along the tendon, the bond stress increases towards the end face due to the slip increase. This is supported by the slight increase of the tendon diameter (Hoyer effect). It provides the maximum bond stress at the end face giving there the highest slope of the tendon stress distribution. Shrinkage and creep of concrete produce an asymptotic decrease of bond stresses but they do not deteriorate to zero. A possible loss of bond might be caused by splitting of the concrete cover due to high circumferential tensile stresses. Spitting is to be prevented by means of adequate detailing (concrete cover, spacing of tendons, confining reinforcement).

The MC90 provisions on prestress transfer are based on the concept of evenly distributed bond stresses. For evaluation of the design value of the bond strength for pretensioned prestressing tendon, f_{bpd}, of the basic anchorage length of an individual pretensioned tendon, l_{bp}, and of the transmission length of a pretensioned tendon, l_{bpt}, the reader is referred to Chapter 3. The design anchorage length, l_{bpd}, is found assuming that along the transfer length the present steel stress (prestress after losses) can be anchored and that beyond the transfer length the design bond stress is available:

$$l_{bpd} = l_{bpt} + l_{bp} \, (\sigma_{pd} - \sigma_{pcs}) \, / f_{pd} \qquad \qquad (4.5\text{-}3)$$

where:

l_{bp} basic anchorage length of an individual pretensioned tendon (see eq. (3.3-41)

l_{bpt} characteristic upper bound value of transfer length (see 3.3.2 (3.2.5) and eq. (3.3-42)

σ_{pd} tendon stress under design load

σ_{pcs} tendon stress due to prestress after all losses

f_{pd} design strength of tendon

The development length equals:

$$l_p = \sqrt{h^2 + (0.6 l_{bpt})^2} > l_{bpt} \qquad\qquad (4.5\text{-}4)$$

where:

h total depth of concrete cross-section

The present MC90 provisions on the anchorage of pretensioned prestressing reinforcement do not take into account the confinement as considered by α_3, α_4 and α_5 for the anchorage of reinforcing bars. However, there is experimental evidence that e.g. close stirrups or spiral reinforcement reduce the transmission length.

(2.2)   Local reinforcement in load anchorage zone

A zone close to any anchorage is a discontinuity region. It extends on both sides of the anchorage and in all directions. In case of prestressing reinforcement the main part of the stress field in the discontinuity region in the load anchorage zone consists of the spreading of the prestressing force by compression from the anchorage up to the end of the discontinuity region. The spreading of the prestressing force in a field of compressive stresses results in tensile splitting, spalling and bursting stresses perpendicular to the compressive stresses, see Fig. 4.5-5.
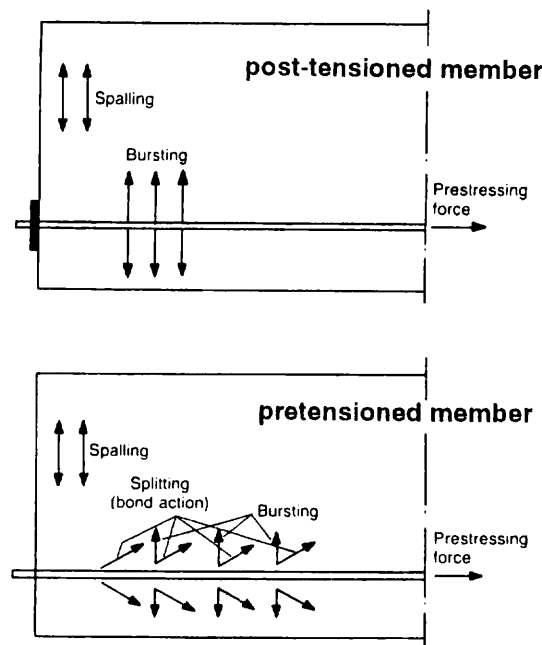
Fig. 4.5-5: Transverse tensile stresses in the anchorage zone of prestressed tendons, after MC90

Additionally, in the case of T-beams shear stress between web and flange results. The resultants of these stress fields shall be superimposed on the shear and axial action effects in order to establish a complete truss model to be used for the verification of the resistance of the region (ULS). Due to the local compression deformation, cracking develops in the discontinuity region in the load anchorage zone. In cases where several anchorages are considered in the same region specific schemes of cracks due to the effects of theses anchorages may result in ultimate failure, if crack widths are not controlled. Yet, the anchorage region should be dimensioned so that all forces are anchored and balanced safely. The bursting action shall be determined both in the vertical and in the horizontal direction. The required confining or net reinforcement shall be distributed within a prescribed region, close to the end face of the member. Also the spalling force resisting reinforcement shall be put parallel to the end face in its close vicinity. Splitting stresses due to bond of pretensioned tendons are assumed to be sufficiently accounted for when the transverse reinforcement required for bursting and spalling confines the tendons or by enlarged concrete cover. Sufficient reinforcement (in no case less than the minimum tensile reinforcement area, see Section 4.5.2 (7)) is necessary for crack control in all parts of the discontinuity region where it is envisaged that tensile stresses may occur. Bearing pressure should be controlled in both orthogonal faces of the node.

(3)   Anchoring devices

Instead of anchoring the reinforcing bars by bond, the tensile force can be transferred by means of anchoring devices mainly in those cases where short anchorage lengths are required. Fig. 4.5-6 presents some examples of anchoring devices The load bearing capacity of anchoring devices and their connection to the reinforcing bar can always be shown by tests and, if possible, by calculations. Also the anchorage of reinforcing bars with welded cross bars of small spacing that work as anchoring devices should be tested. The slip between bar and concrete at the loaded end must not exceed the given limits. To keep sufficient safety margin, the design value of the anchorage resistance should not be taken larger than 50% of the ultimate force of the anchorage, when fatigue loads are negligible and not more than 70% of the experimental fatigue strength of the anchorage.
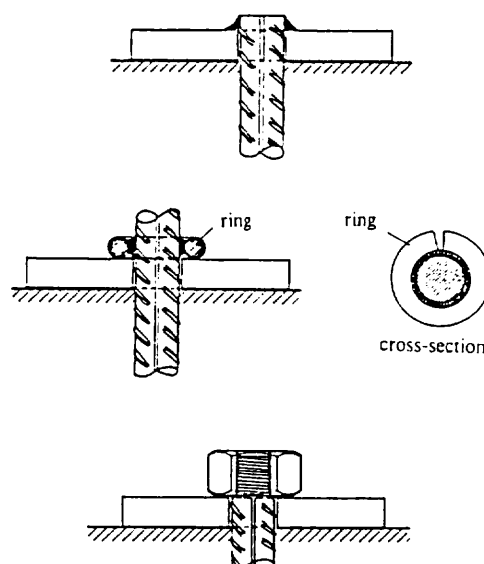
Fig. 4.5-6: Examples of anchoring devices

4.5.4   Detailing of tensile bending reinforcement

(1)   **Envelope line of the tensile force and the load balancing mechanism in members subjected to bending and shear**

The load balancing mechanism of reinforced concrete elements subjected to bending moments and shear forces can be discussed by strut-and-tie models (see also Chapter 7). As a consequence, the tensile force to be balanced by reinforcement is not calculated directly from the inner forces (bending moment and shear force) but a horizontal displacement of the tensile force envelop line is to be considered as well. Among other factors, this depends on the inclination of compressed struts in the concrete and the inclination of the shear reinforcement to the longitudinal axis of the element (see ch. 4.4.1 (5.2) eq. 4.4-26 and 4.4-39). The bars out of the envelop are allowed to be bent-up or cut-off if the envelop of tensile forces is covered. It should be considered that in reality the force in the anchored bar increases continuously. As a first approach a linear increase can be assumed, which corresponds to a constant bond stress. If this realistic tensile force distribution is intended to be considered by covering the tensile force diagram, it is to be shown for each section that the line of resisting tensile force which is variable along the anchorage length does not intersect the line of tensile force. Hereby also other regulations must be met (e.g. minimum section above the support, arrangement and spacing of inclined bars etc.).

Particular attention should be given to envelope line in case of design for moment redistribution. As discussed in Chapter 3.2 on Reinforcement, there may be a considerable effect of steel overstrength e.g. higher yield strength of the reinforcement used in a structure than the nominal value assumed in design. Moreover, it is possible that sections of a structure contain a greater amount of reinforcement than required from the design (overreinforcement). When considering equilibrium conditions overreinforcement leads to an equal result as steel overstrength, namely that the real moment capacity exceeds the design moment. Note that while the force distribution along the member is calculated under the assumption of a nominal or design plastic moment in the most stressed section, due to overstength or overreinforcement the real flexural capacity in the plastic hinge is significantly higher than assumed, causing a different distribution of forces at the ultimate limit state than assumed in the design. This can lead to the overestimation of the anchorage capacity of staggered bars and in the consequence to a bond failure before reaching the design load. With increasing steel overstrength the length of the zone with negative moments increases, reducing the anchorage length of staggered reinforcement. For that reason *Eligehausen and Fabritius (1995)* proposed that in order to avoid a brittle bond failure, staggered reinforcement should be anchoraged with the basic anchorage length $l_b \geq d$, instead of $l_{b,net}$ as allowed by MC90.

(2)   **Anchorage out of support**

Bars can be anchored by bent-up bars or as cut-off bars. The anchorage length of cut-off bars is measured from the theoretical cut-off point of the envelope line of acting tensile force. As discussed above the envelop line for the acting tensile forces can differ from the calculated distribution and its covering will be shown generally approximately. In addition to, the actually available anchorage length can be shorter than the calculated value owing to inaccuracies in placing the reinforcement. For this reasons the reinforcement can be curtailed with an anchorage length of $l_{b,net}$ + 100 mm beyond the section, where it is no longer required to carry the full force. The anchorage length of bent-up bars which end in the region of concrete compressive stresses can be measured from the neutral axis.

(3)   Anchorage over support

The support edge is the line of reference for the beginning of the anchorage over the support. In fact the actual beginning of the anchorage is unknown, however, it will be effective from the edge of the support owing to the transverse pressure. Otherwise, cracks which negatively influence the anchorage are generally not produced there. The favourable influence of the transverse reinforcement by welded fabric is allowed to be considered if they are within the anchorage length, i.e., behind the edge of the support.

Note that the minimum anchorage length at direct end support may be reduced to 2/3 of the value $l_{b,min}$ given in Section 4.5.3 - (1.2) due to the favourable influence of uniaxial transverse pressure at direct supports. Sufficiently high level of transverse pressure (approximately 5 N/mm^2) is generally available in beams, especially in those cases where the anchorage length should be short. Though the transverse pressure in plates is often lower, a crack generally will not appear just at the support edge - as assumed in the calculations - but at a distance from it due to the low shear force. In this way the available anchorage length is longer and the force above the support is smaller compared to its value considered in the calculations.

(4)   Distribution of the reinforcement in the cross-section of box girders or T-beams

The appropriate detailing of bending reinforcement must satisfy the conditions considering the distribution of inner forces (staggering), detailing of reinforcement in ribbed plates or in box sections and anchorages above the supports or in the span. In particular the detailing of tensile bending reinforcement in the plate of box girders or T-beams requires special attention. Test results justify to distribute the tensile bending reinforcement only in the part of the calculated effective width, since extended distribution unfavourably influences a constant distribution of stresses in the bars and the crack widths. On the other hand, a concentration of bars in the region of the web can not provide crack control in the plate region. If the main part of tensile bending reinforcement is placed beside the web as discussed above, the cracking behaviour is favourable. In addition to, the lever arm of inner forces is higher, the anchorage length can be shorter, being often in so-called good bond condition and creating more space for vibration during casting. The portion of bars to place into the web is not quantitatively defined, yet it should be excluded that the entire tensile bending reinforcement is placed into the plate. The requirement is generally fulfilled if the tensile reinforcement is approximately evenly distributed above the web and the half of the effective width in the overhanging flanges.

4.5.5   Splices in structural members

(1)   Lap splices in tension

(1.1)   Behaviour of lap splices for straight bars, hooks, bents and loops

Splices are applied whenever the transportation length of bars is too short, construction joints are required or the prefabricated reinforcement is produced in pieces. In general splices can be created by overlapping the bars, by welding or by mechanical methods such as threaded or compressed sleeves. In addition, the contact pressure at the end faces can be used for transferring the force of compressed bars.

Fig. 4.5-7: Bond cracks by a lap splice, after Goto (1965)

In case of lap splices the force transfer between the spliced bars is provided by the concrete. The bond forces act on compressed struts between the spliced bars that are developed inclined to the axis (Fig. 4.5-7). The radial components of the force in the struts produce tension in the concrete cover and may produce splitting in ultimate limit state over the lap length. Since the splitting forces considerably increase towards the splice ends (Fig. 4.5-8), the failure usually initiates there.
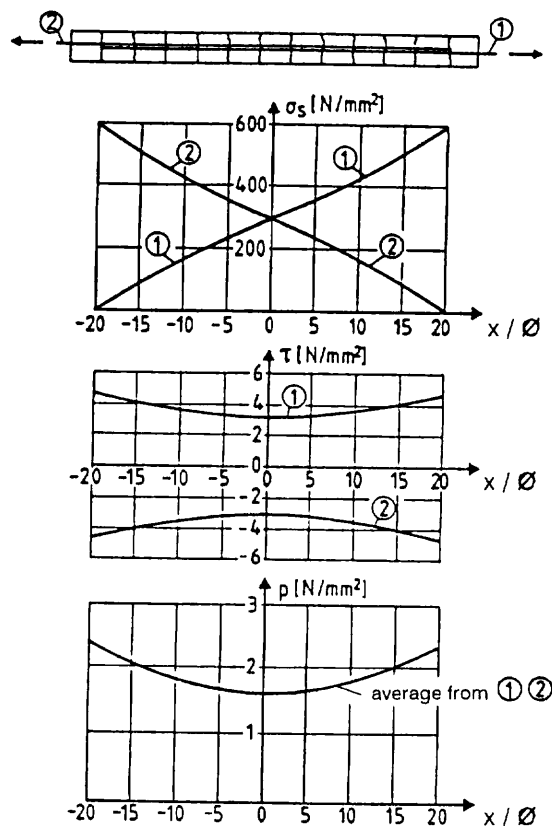
Fig. 4.5-8: Steel stress, bond stress and splitting pressure distribution over the splice length after Eligehausen (1979)

Experiments have shown that under general conditions lap splices fail mostly by splitting. The possible splitting crack patterns are presented in Fig. 4.5-9, where failure is to occur with bursting of the cover either on the entire surface or funnel-shaped depending on the spacing of splices. Splices with no transverse reinforcement or transverse reinforcement inside subjected

to bending fail by bursting of the concrete cover due to straightening of bars (Fig. 4.5-10), which means the sudden and total loss of bearing capacity of the member. Whenever the bending reinforcement is enclosed by stirrups failure is less brittle and a part of the load bearing capacity is maintained. In case of lap splices for bars with hooks, bents or loops similar conditions exist for splitting effects in the curved region as for anchorages with curved bars.

Failure mode A

$$c_s \leq 0.85\ c_b$$

Failure mode B

$$c_s \begin{array}{l} > 0.85\ c_b \\ \leq 4.0\ c_b \end{array}$$

Failure mode C

$$\begin{array}{l} c_s > 4.0\ c_b \\ e > 8.0\ c_b \end{array}$$

① crack prior to failure
② failure crack
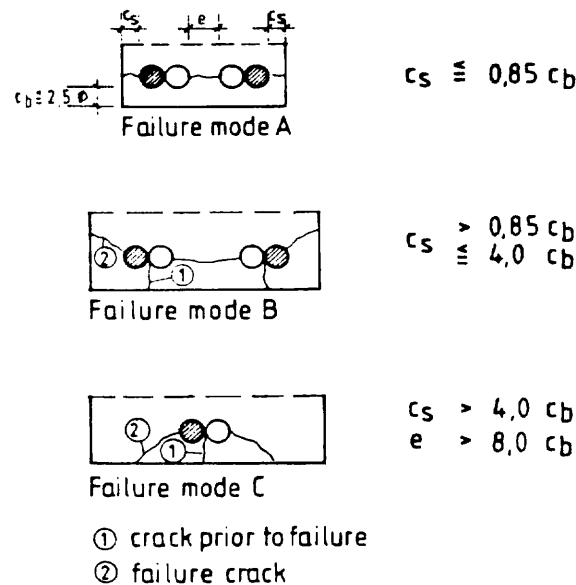
Fig. 4.5-9: Failure patterns of lap splices in beams, after Eligehausen (1979)
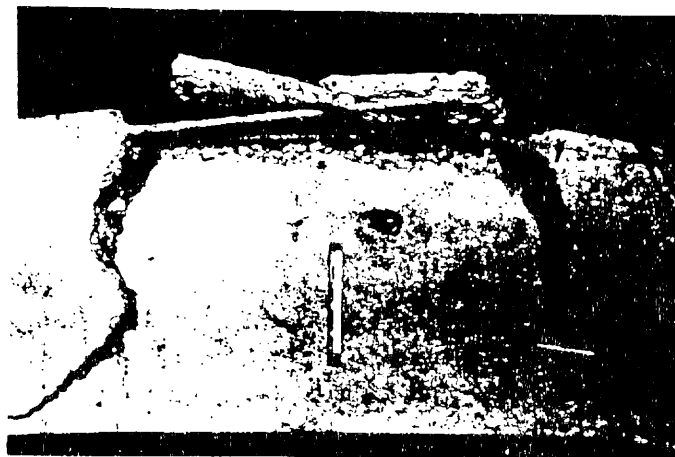
Fig. 4.5-10: Cover failure caused by bar stiffness of an element in bending, after Eligehausen (1979)

The splice strength mainly depends on the lap length, the diameter and spacing of the wires and the concrete strength. The influence of the lap length on the strength of splices made of welded fabric of ribbed wires is shown in Fig. 4.5-11. It can be seen that the splice strength does not increase proportionally to the lap length, which confirms that the splitting forces are not evenly distributed along the splice length. Tests and analytical studies indicated that steel stress, concrete strength, side and bottom cover, bar spacing, amount of transverse reinforcement and bond conditions have a principle effect on the splice length required to transmit certain force. Fig. 4.5-12 shows the influence of the clear spacing between splices on

the splice length required to transmit equal force (results given in relation to the lap length obtained assuming the minimum spacing allowed by MC90). According to the test results, the necessary splice length decreases considerably with increasing spacing.
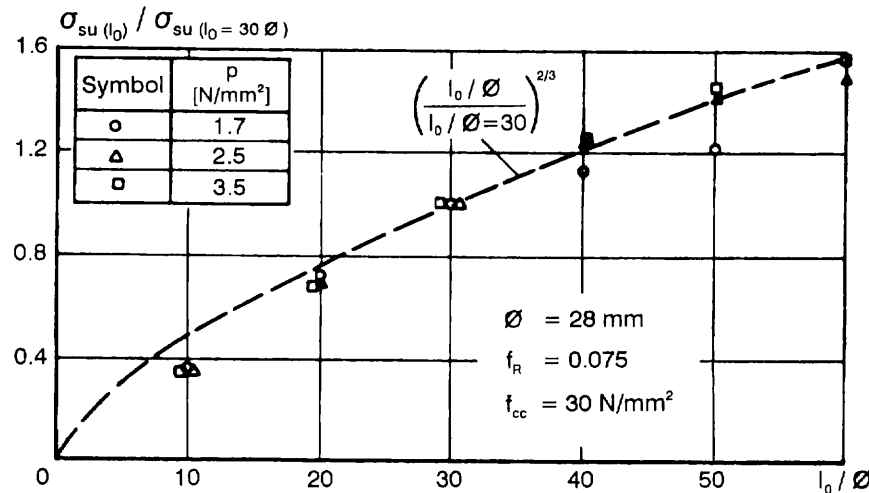
Fig. 4.5-11 : Influence of splice length on the splice strength, after Eligehausen (1979)
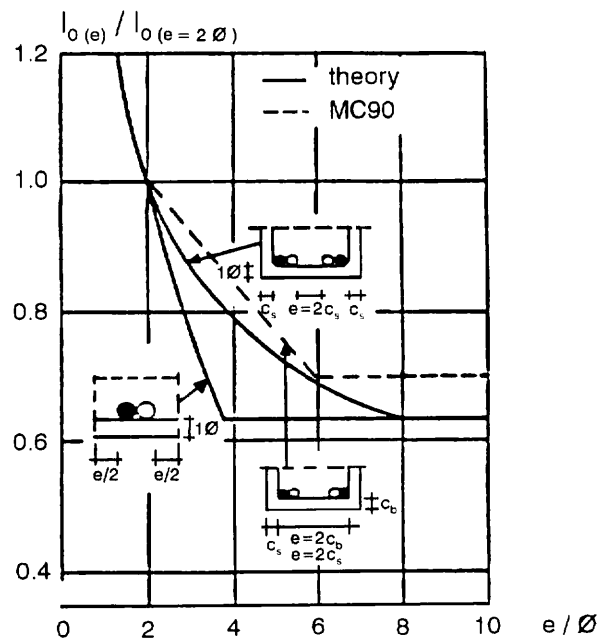
Fig. 4.5-12: Influence of the spacing of spliced bars on the splice length, after Eligehausen (1979)

In Fig. 4.5-13 the lap length is plotted as a function of the area of transverse reinforcement in the splice region. According to the test results, the necessary lap length decreases with increasing amount of stirrups. However, straight bars as transverse reinforcement (commonly used for splices in walls and slabs), have almost no effect on the necessary lap length. MC90 requires a minimum area of transverse reinforcement to avoid large longitudinal cracks. This area of transverse reinforcement was taken into account for the evaluation of the design provisions. In Fig. 4.5-14 the necessary lap length is plotted as a function of the ratio of the required ($A_{s,cal}$) and the provided ($A_{s,ef}$) amount of reinforcement. This figure is valid for splices in beams and slabs meeting the requirements for cover, spacing and transverse reinforcement.
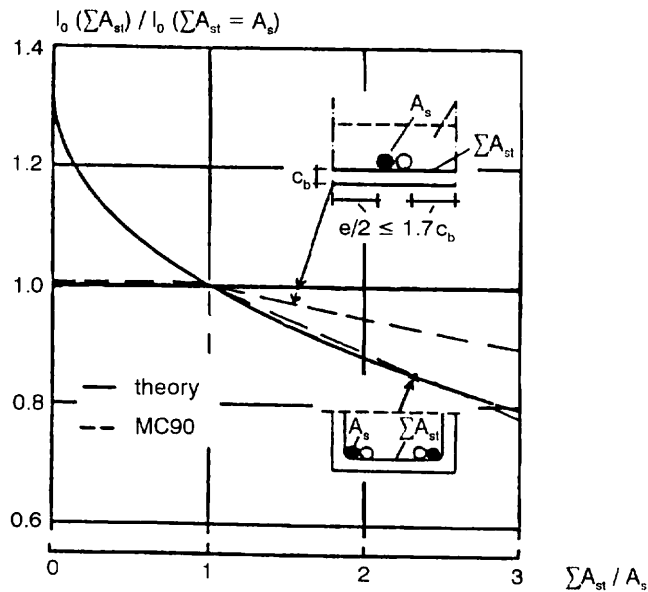
Fig. 4.5-13: Influence of transverse reinforcement on the splice length, after Eligehausen (1979)
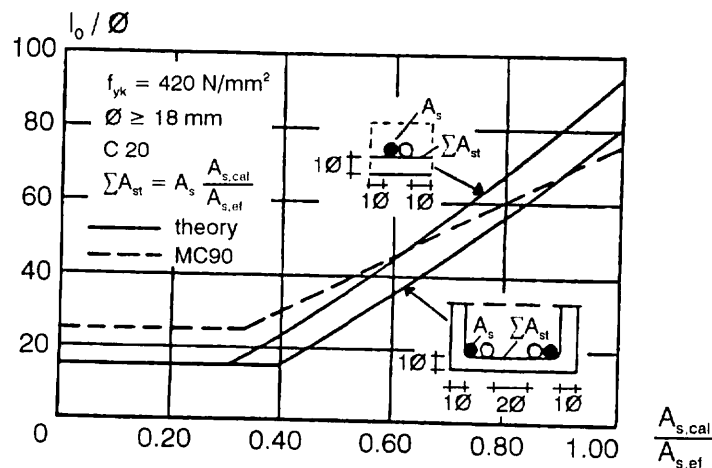
Fig. 4.5-14: Lap length as a function of calculated to provided steel amount, after Eligehausen (1979)

(1.2)   Required lap length of tensioned bars

The connection of bars is not allowed to influence the behaviour of the element negatively neither in serviceability nor in ultimate limit states compared to the behaviour of the element with continuous reinforcement. The width of bending cracks at the splice ends in serviceability limit states should not be (considerably) more than that out of the splice region, and longitudinal cracks are not allowed to appear. To guarantee that the eventual failure of a splice is due to yielding of the steel bar and not to failure of the surrounding concrete, an overall safety factor of 2.1 is required against the 5% fractile of test results.

Following the discussed above principle the definition of required lap length ensures that in general the bursting of concrete cover is excluded. For the bursting phenomenon practically the same effects as the anchorage length are of importance. Therefore MC90 includes a similar formulation for the design lap length, l_0, as for the design anchorage length, $l_{b,net}$:

$$l_0 = \alpha_1 \, \alpha_3 \, \alpha_4 \, \alpha_5 \, \alpha_6 \, l_b \, A_{s,cal} \, / \, A_{s,ef} \geq l_{0,min}$$ (4.5-5)

where:

l_b	basic anchorage length (see Chapter 3)
α_1	bar shape factor (see Section 4.5.3)
α_3	concrete confinement factor (see Section 4.5.3)
α_4	not-welded transverse bar factor (see Section 4.5.3)
α_5	transverse pressure factor (see Section 4.5.3)
α_6	overlapping percentage factor (from 1.2 to 2.0 - dependent on the percentage of lapped bars within a distance $1.3l_0$ measured from the centre of lap length)
$l_{0,min}$	required minimum lap length

and

$$l_{0,min} = \max[0.3 \, \alpha_6 \, l_b, \, 15\varnothing, \, 200 \text{ mm}]$$ (4.5-6)

It should be noted that the lap lengths are determined for the smallest allowable concrete cover and transverse reinforcement. Shorter lap lengths are often possible by an increase in concrete cover thickness and/or an increase in the amount of the transverse reinforcement.

(1.3)   Staggering and transverse spacing of tensioned bars in the splice region

Application of splices always includes a higher risk compared to the application of continuous bars. Therefore they should be avoided if possible or be placed into the region of low stresses. Moreover, staggering of splices in longitudinal direction and/or large enough spacing between them in transverse direction can limit or even eliminate stress concentration due to the mutual influence of neighbouring splices (see Fig. 4.5-15).
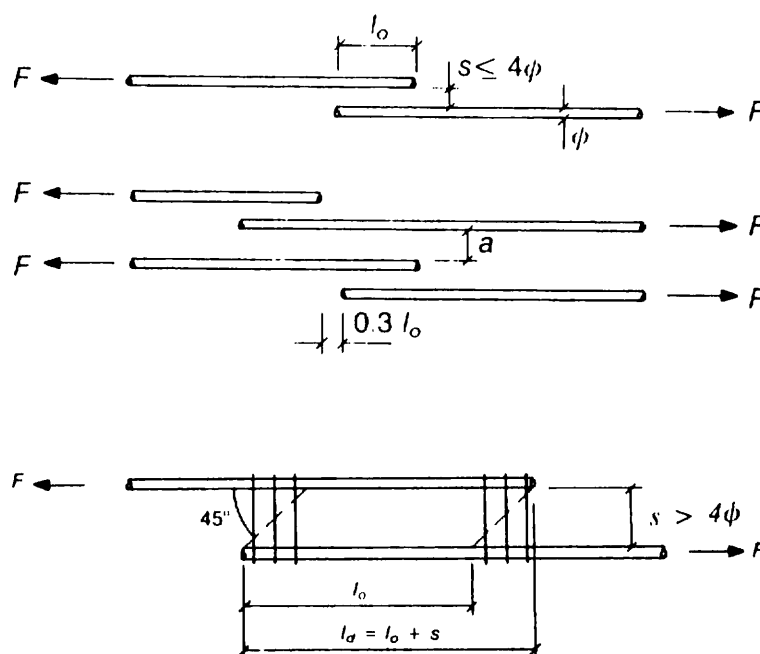
Fig. 4.5-15: Staggering and transverse reinforcement for a splice, after MC90

Staggered splices have no influence to each other when the distance between the middle points of them exceeds 1.3 times the lap length. The clear transverse spacing of neighbouring splices should be not less than $2\emptyset$ and at least 20 mm to avoid splitting of the cover (this spacing is assumed for the determination of required splice lengths). If bars are spliced with a clear spacing larger than $4\emptyset$, the splice length should be increased with the spacing of bars because a system of struts is forming between them. The transverse reinforcement may be calculated using the strut and tie model. The permissible percentage of spliced reinforcement depends basically on the type of bars and on the loads effects. For lapped bars in tension it varies from 100% for high bond bars both under static and repeated loads to 25% e.g. for plain bars under repeated loads. If the joint is arranged in more than a single layer the permissible percentage of lapped bars in tension in a section is to be reduced with 50% with respect to joints with single layer of laps. This limitation is necessary because the concrete receives higher stresses and over a longer length in case of 100% splice of several layers compared to one layer. For transverse distribution reinforcement all bars can be lapped in one section. Lapped splices in a section should preferably be arranged symmetrically otherwise parallel to the outer face of the element.

(1.4)   Required transverse reinforcement

The transverse reinforcement restricts the splitting forces and the widths of the potential longitudinal cracks. Transverse reinforcement is therefore always compulsory in the splice region. Available reinforcement can be considered. The transverse reinforcement of spliced bars should be placed along the two external ⅓ of the splice length. If spliced bar diameter is less than 16 mm, the minimum transverse reinforcement provided for other reasons (e.g. shear reinforcement, distribution bars) is sufficient. If the spliced bar diameter is not less than 16 mm, the total area of transverse reinforcement (one leg) should not be less than the area of one spliced bar. While for beams or columns transverse reinforcement should consist of stirrups or spirals, for plates and shells it is allowed to rely on the tensile strength of concrete and straight bars can be used as transverse reinforcement in these cases.

Fire produces additional tensile stresses in the splice region increasing the danger for bursting of the concrete cover. If the required fire resistance of the member is high, splicing of bars with overlapping should be avoided. If lap splices can not be avoided, an effective tensile reinforcement in form of stirrups has to be used.

(2)   **Lap splices in compression**

(2.1)   Required lap length of compressed bars

The design lap length of compressive splices should comply with the condition:

$$l_0 > l_b \tag{4.5-7}$$

where:

l_b basic anchorage length (see Chapter 3)

(2.2)   Staggering of compressed bars in splice region

It is allowed to splice 100% of bars in one section independently of the bar diameter and type of load (static, repeated load) also in case when the bars to be spliced are situated in several reinforcement layers.

(2.3)   Required transverse reinforcement

Lap splices of compressed bars always fail by bursting of the concrete cover in the region of splice ends owing to the high pressure in front of the end surfaces of bars (Fig. 4.5-16). To balance this splitting force, one of the stirrups has to be situated just in front of the beginning of the splice (i.e. out of the splice length and within 4Ø of the ends of the lap length).

Fig. 4.5-16: Failure pattern of lap splice of compressed bars, after Leonhardt and Teichen (1972)

(3)   **Lap splices of welded fabrics**

(3.1)   Behaviour of intermeshed and layered fabrics with and without stirrup-like cross bars

Splices of welded fabrics are different from splices of bars in the following:

- the allowable maximum diameter of the wires is 12 mm
- the spacing of the wire is usually 100 or 150 mm
- welded cross wires are present along the splice length
- no reinforcement crosses the plane of failure

Considering the position of main bars, two groups are distinguished for overlapping of welded fabrics: in case of an intermeshed fabric the bars to be spliced lie side by side, while

in case of intermeshed splices they lie above each other. Intermeshed splices are typically made by periodical inclination of the fabrics or by making longer overhanging ends for the spliced bars. For easy placing, normally the splices are made with layered (overlapping) fabrics using fabrics with cross bars and not enclosed with stirrups.
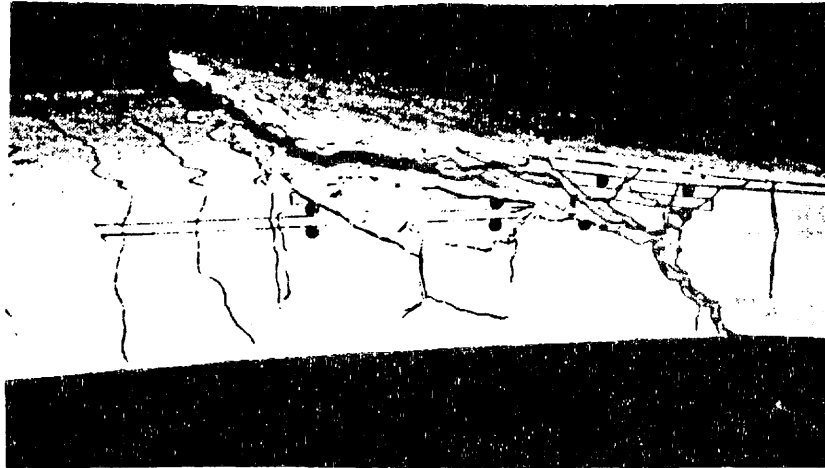
Figure 4.5-17 Typical failure of the lap splice of wire fabric, after Tewes (1982)

The splice failure of layered fabrics usually occurs by bursting of the entire concrete cover, including the fabric nearest to the surface (Fig. 4.5-17). The failure is initiated by forces normal to the cover due to the eccentricity of the spliced fabric and the splitting forces. As well as for splices of bars, the failure load and, hence, the splice strength, mainly depends on the lap length, the diameter and spacing of the wires, anchored force and the concrete strength. The influence of the lap length on the strength of splices made of welded fabric of ribbed wires is shown in Fig. 4.5-18 where each line gives the lower bound (approximately 5% fractile) of 5 to 12 test results.
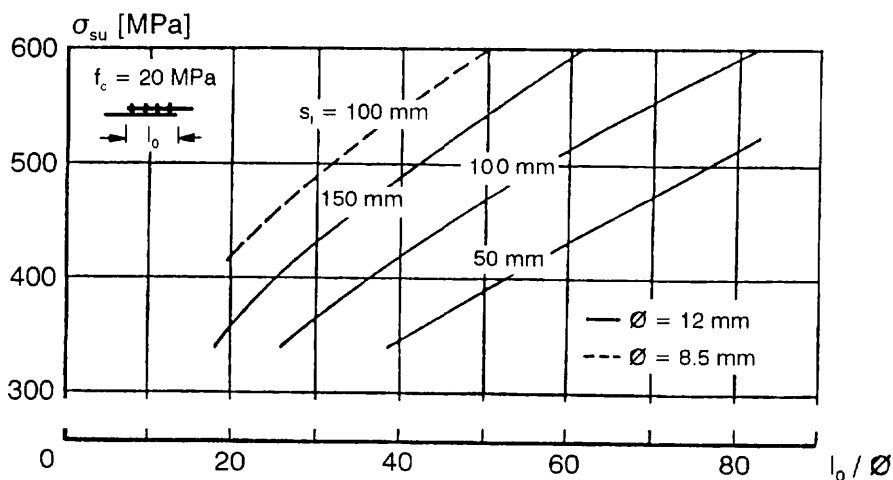
Fig. 4.5-18: Strength of lap splices of welded fabric vs. lap length for different bar diameters ($\emptyset$) and different spacings (s_l) of longitudinal deformed bars, after Tewes (1982)

The influence of welded cross wires on the splice strength is of special interest. In Fig. 4.5-19 the steel stress just outside the splice at splice failure is shown as a function of the number of welded cross wires. The figure is valid for wire mesh made of deformed bars.

Transverse bars are effective as far as they distribute the anchored force on a wider band, hence produce lower tensile stress in the concrete. However, the splice strength does not increase much with increasing number of welded cross wires for small spacing of the longitudinal wires and for a lap length as necessary to provide an appropriate splice strength. Therefore, though MC90 requires a minimum number of transverse wires available along the splice length, it does not allow the lap length to vary with the number of welded cross wires.
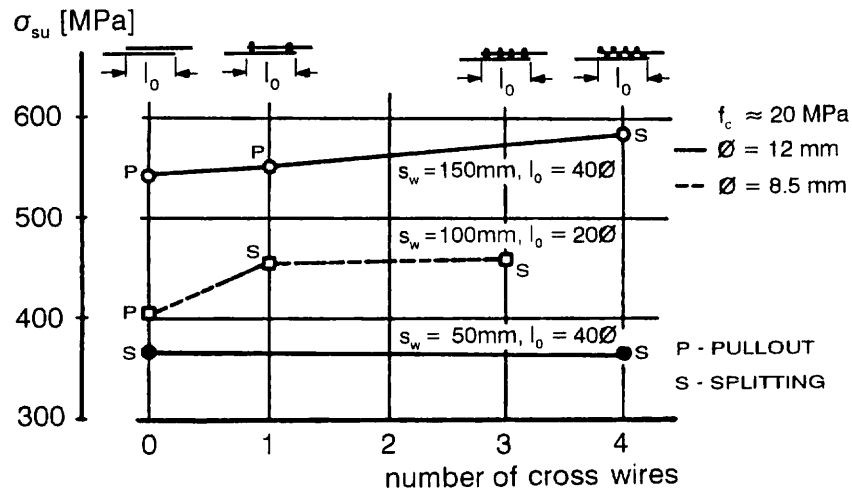
Fig. 4.5-19: Influence of cross wires on the strength of splices made of welded fabric, after Tewes (1982)

(3.2)   Required lap length

The design lap length is expressed similarly to the anchorage length:

-   for intermeshed fabric (as for lap splices of bars):

$$l_0 = \alpha_1 \, \alpha_3 \, \alpha_4 \, \alpha_5 \, \alpha_6 \, l_b \, A_{s,cal} / A_{s,ef} \geq l_{0,min} \qquad (4.5\text{-}8)$$

-   for layered fabric:

$$l_0 = \alpha_7 \, l_b \, A_{s,cal} / A_{s,ef} \geq l_{0,min} \qquad (4.5\text{-}9)$$

where:

l_b basic anchorage length (see Chapter 3.3.2 (3.2.5) and eq. (3.3-40)

$\alpha_1, \alpha_3, \alpha_4, \alpha_5, \alpha_6$ defined as for lap splices of bars, see eq. (4.5-5)

α_7 factor dependent on specific cross-sectional area of the fabric (from 1.0 to 2.0)

$l_{0,min}$ required minimum lap length

and

$$l_{0,min} = \max[0.75 \, l_b, \, 15\phi, \, 200 \text{ mm}] \qquad (4.5\text{-}10)$$

For intermeshed fabric, the lap length should be calculated disregarding the beneficial effects of welded transverse bars and using a welded transverse bar factor $\alpha_2 = 1.0$ when computing $l_{b,net}$.

Considering that bond has no meaningful influence on splices of welded fabrics of plain and slightly deformed bars and aimed to ensure that the failure loads of splices (assuming the same lengths) are independent of the deformation pattern of bars, an adequate number of transverse bars has to be provided over the lap length. The minimum number of welded cross wires over the lap length is: $n = 1$ for fabric made of ribbed wires and $n = 5 \, (A_{s,cal} / A_{s,ef})$ for fabric made of plain or indented wires.

The lap length of welded fabrics in compression is:

$$l_0 > l_b \qquad\qquad\qquad\qquad\qquad\qquad\qquad (4.5\text{-}11)$$

where:

l_b　　　　the basic anchorage length (see Chapter 3.3.2 (3.2.5) and eq. (3.3-40)

(3.3)　　Staggering of welded fabrics

The various possibilities for lapping of welded fabric is presented in Fig. 4.5-20. For layered fabric, the splices of the main reinforcement should generally be situated in zones where the stress in the reinforcement in the ultimate limit state is not more than 80% of the design strength. This requirement is meant to ensure that the crack widths at the end of the splice are not considerably higher than out of the splice region (due to the higher strains of the inner fabrics) and that the acceptable limit values are not exceeded, respectively.

intermeshed fabrics

layered fabrics
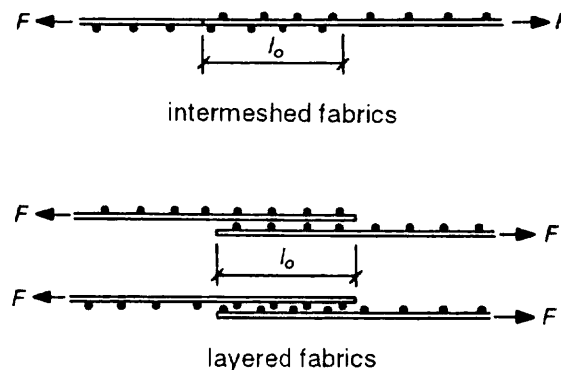
Fig. 4.5-20: Lapping of welded fabrics, after MC90

In structures subjected to fatigue loads splices of welded fabrics are to be provided in the form of intermeshed fabrics. Additional transverse reinforcement is not necessary in the zone of lapping.

(4)　　Splices by welding

In general load bearing joints in axially aligned bars of different diameters are permitted if the difference in diameter is less than 3 mm, however no such restriction is imposed for lap joints. For the common welding methods the conditions of application are defined in relevant Technical Approvals, as discussed in more detail in Chapter 3, Section 3.2.7-(1) on Connections of Reinforcing Steel - Welding. Under static loading all permitted in approvals

welded splices may be used in both tension and compression and similarly to screwed splices, all of the reinforcement is allowed to be spliced in one section. In design load bearing welded splices can be taken into account for calculation purposes by assuming a certain strength of the welded connection.

For full bearing connections under static loading it is required that the ultimate tensile strength of the welded bar is at least equal to 0.95 f_t of the reference bar and uniform elongation of welded splice at maximum load is at least 2.5%. Shear strength of welds shall be at least equal to 0.3 f_y of the anchored bar when tested naked or $0.5f_y$ of the biggest bar when tested in concrete.

(5)   Splices by mechanical devices

On contrary to lap splices, where the force transfer between the spliced bars is provided by the concrete, for splices by mechanical devices concrete is not additionally loaded. Mechanical connections are subdivided according to the force transfer into tension-compression and compression-only splices. The recommendations of appropriate Technical Approvals should be used. The wide variety of mechanical splice devices for reinforcing bars and the general design requirements for splice devices are discussed in Chapter 3.2, Section 3.2.7-(2) on Reinforcement — Mechanical Connections of Reinforcing Bars. Here only the practical details on detailing provisions for splices of reinforcing bars using mechanical connections are treated.

The provisions on the concrete cover and on the clear spacing specified in MC90 are applicable for the connecting elements in the region of splices, in order to avoid corrosion and to allow appropriate casting of the concrete. It is satisfactory to relate the concrete cover and the clear spacing between the sleeves to the spliced bar diameter, e.g. the size of the spliced bar shall be taken as the nominal size. Once the splice device size is known it may be necessary to stagger the splices in accordance with the required clear distances. Staggering may also be necessary depending on the required equipment for carrying out the mechanical splicing. To make sure that the required concrete cover is maintained at the form line, spacing of stirrups should be adjusted at the splice location if the outside diameter of the splice device is substantially larger than that of reinforcing bar.

(5.1)   Tension-compression connections

Tension-compression connections shall be designed for full tension and compression capability and the connection has to meet the requirements regarding elongation and ductility which are given in Chapter 3.2, Section 3.2.7-(2) on Reinforcement — Mechanical Connections of Reinforcing Bars according to CEB *Bulletin d'Information No. 201 - Recommendations for mechanical splices of reinforcing bars (1990)*. In particular, the slip of the sleeve measured at the ends of the sleeve should be low and, hence, the crack widths at the splice ends should not be too large. It is logically required that the sleeve should not be stressed to its yield strength in ultimate limit state, nevertheless, the failure occurs in the spliced bars. Couplers designed for flexural members may be used at one cross-section for all reinforcement, hence - all of the reinforcement is allowed to be spliced by screwed splices in one section.

(5.2)   Compression only splices

Compression-only connections are based on compressive stress transfer by bearing from one bar to the other one. In general it holds that simple end-to-end contact splices shall be used for compressed bars with a diameter not less than 25 mm. Since in columns, a minimum tensile strength is required even where analysis indicates compression only, the maximum amount of reinforcement spliced at one section must be limited if end-bearing splices are used without added splice bars. Some standards (e.g. DIN 1045) advise that at most 50% of the compressed bars are allowed to be spliced by contact splices in one section. There also the requirement is given that, in order to provide a minimum bending capacity to balance unforeseen stresses (e.g. in catastrophic situations), the bars that are not spliced should have at least 0.8% of the statically required concrete section and they have to be evenly distributed over the cross-section. In most compression-only connections, compressive stress is transferred by end bearing of the bars in contact. The centric force introduction into the contact splice is an important condition to the efficiency of the splice. For that reason either care is taken to meet the requirements (e.g. using an installation instrument, sawing the end sections perpendicular to the axis of the bar etc.) or other type of splice should be applied.

(6)   Lap splices of bundled bars

Splices of bundled bars can be made by overlapping, welding or using mechanical devices. Joints can be made on only one bar at a time but at any section. To avoid unfavourable cracking behaviour and too high local concrete stresses owing to a sharp change in the stiffness, the laps of individual bars should be staggered. The staggering varies from 1.2 up to 1.4 times the anchorage length of the individual bar for bundles of 2 up to 4 bars, respectively. Another possibility is to relate the lap length to the anchorage length of the whole of the bundle, determined on the basis of the equivalent bundle diameter. This method may be used for anchorages over supports. In case of screwed splices using sleeved compression joints for bundles, the distance between adjacent sleeves can be reduced to twice the diameter of the sleeve.

4.5.6   Detailing of shear reinforcement

(1)   Efficiency of anchorage of shear reinforcement

The shear reinforcement gives the connection of compressed and tensioned flanges in members subjected to bending. This can only be ensured using a reinforcement which is anchored appropriately both in the compressed and in the tensioned flanges and placed in longitudinal and transverse directions with spacings that are not too large. The anchorage of stirrups and shear assemblies is normally obtained by means of hooks, bends or welded transverse bars. The meaning of sufficient anchorage of shear reinforcement to the overall behaviour of the element is obvious. In addition to, the position of the anchorage should be considered as well. The type of anchorage used should not induce splitting or spalling of the concrete cover. Therefore they should be arranged close to the boundary of section but in every case out of the resultants of bending tensile or compressive forces. The equilibrium of strut-and-tie models can be ensured without concrete tensile stresses only if above conditions are met. To avoid complicated regulations, simplified and practical provisions were developed. The closing of stirrups in the compressed zone can be made by splicing of hooks or bends, or by putting a cap stirrup with short legs on the top of the stirrup etc. The straight

parts at the end of bends must be long enough to ensure that the slip of bends being in a crack in tensioned concrete zone is not very unsatisfactory. To close stirrups in the tension zone of beams, an overlapped splice is to be provided and the stirrup ends must be bent into the inner part of the section to be able to balance dowel forces of the longitudinal reinforcement. In case of improper anchorage, an early shear failure may happen due to bursting of edges of the section, see Fig. 4.5-21.
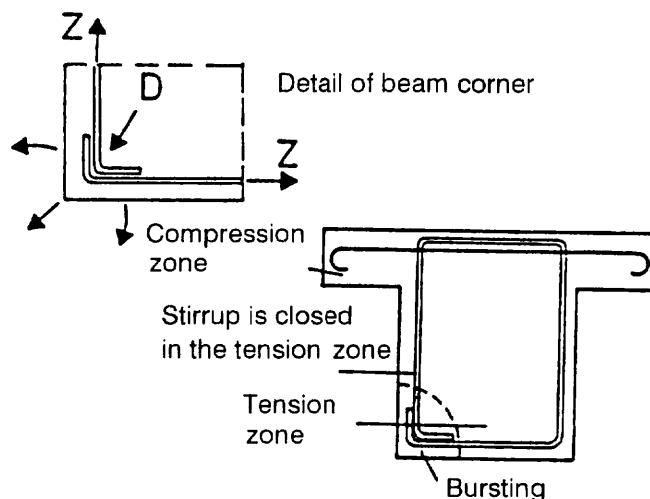

Fig. 4.5-21: Failure mechanism in a beam with stirrups spliced by overlapping of bends, after Rehm and, Neubert (1974)

(2)   Distribution of shear reinforcement

(2.1)   Location and minimum area of stirrups

Stirrups are generally required in beams, T-beams and ribbed plates. Their minimum area should comply with the corresponding section of the MC90. Closed stirrups are required to enclose the tensile reinforcement and the compressed zone in order to ensure ability of rotation, to balance not calculated tension and to provide fire resistance. Stirrups open in the compression zone can be used in structural elements that are hardly subjected to torsion and where the transverse reinforcement allows redistribution of forces in case of local disturbances (e.g. open stirrups occasionally available in plates).

The minimum shear reinforcement is required to ensure that the failure load is higher than the cracking load. Since too large stirrup spacing may lead both to wide shear cracks and to the risk of load bearing of the member, requirements are given for the maximum available stirrup spacing. Furthermore, for the control of shear cracks in SLS it is also required to limit crack width to a given value. The stirrup spacing is not allowed to exceed a given percentage of the depth of the member depending on the level of compression force of web concrete. In this way it is ensured that every shear crack crosses a satisfactory number of stirrups and the required safety against shear is reached. In case of columns stirrup spacing should secure longitudinal compression bars against local buckling and should ensure that stirrup legs intersect at least one possible crack under the most adverse condition. In any case attention must be given to the local damage phenomena (e.g. bursting) and special precautions with respect to the stirrup spacing and diameter should be taken at changes of direction of the longitudinal bars and in zones at column-beam connection.

(2.2)   Distribution of bent-up bars

Bent-up bars are able to carry shear forces only if they cross the shear cracks. To ensure this behaviour, the distance of bent-up bars from the support and between each other should be controlled. The contribution of bent-up bars to balance the shear force must be ensured even in case of unfavourably running shear cracks having an inclination of 45°. It must be remembered that bent-up bars, which are applied only in one region of the element, balance shear forces only over a certain length of the member. To avoid risk of local secondary damage, the minimum mandrel diameter for bend-up bars should comply with corresponding regulations.

4.5.7   Industrialisation of reinforcement

Technical and economic optimisation of a construction refers to all the arrangements resulting in a minimum total cost for the construction, while satisfying as well a number of predefined requirements with respect to structure performance. The industrialisation of reinforcement is a possible way to reduce the cost of labour for preparing and placing the reinforcement. The possible solutions are presented in CEB Bulletins d'Information on Industrialisation of Reinforcement and on Technology of Reinforcement. An example of industrialisation of reinforcement is given in Figure 4.5-22. Here particular attention is given to rationalisation of reinforcement shapes. Simplification consists of using, as far as possible, straight bars which are as long as possible. Reinforcement shapes which are expensive (i.e. due to high degree of bending required) should be avoided, unless an increase in structural quality, greater dimensional strictness or a possible benefit for assembly and fixing can be obtained.
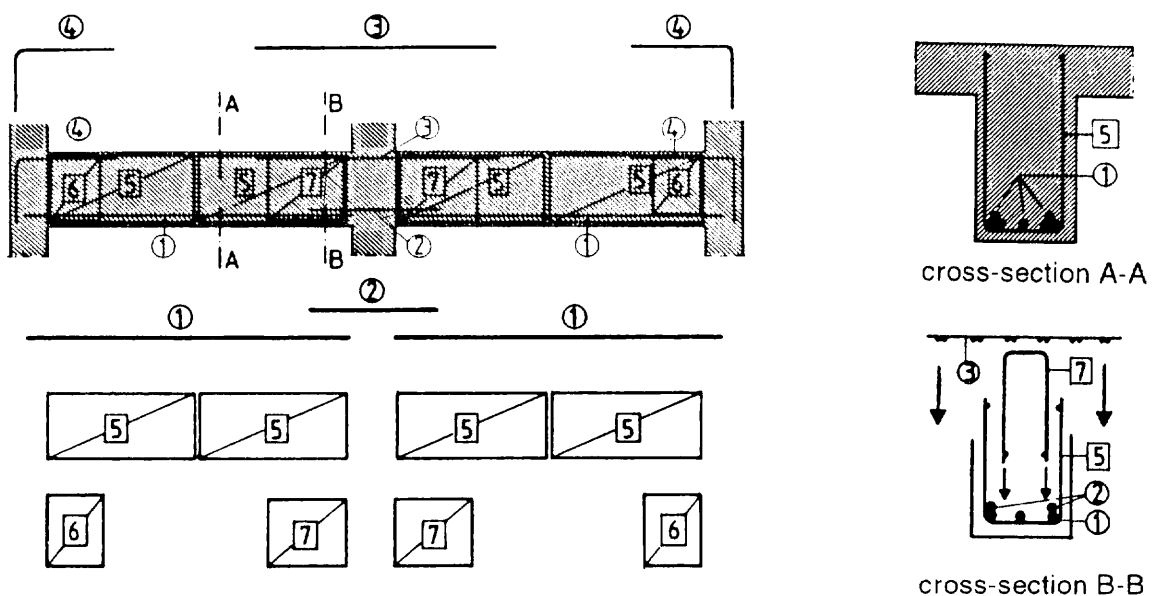
Fig. 4.5-22: Schematic diagram of the reinforcement of a continuous beam using industrialised reinforcement layout, after Rehm et al. (1982)

A good example of the optimum shape is the case of shear reinforcement. Traditionally the shear reinforcement consists of stirrups and bent-up bars. Much more economical is the use of only straight bars as top and bottom reinforcement and as shear reinforcement open

stirrups and supplementary bars, called shear assemblies. The stirrups are closed by the transverse reinforcement of the slab. The prefabricated reinforcement can be easily assembled in the formwork like a meccano system, as shown in the right part of the Fig. 4.5-22. Shear assemblies, which replace bent-up bars, are cage like, ladder-like or garland-like elements made of deformed bars or deformed welded mesh fabrics which do not or only partly enclose the tension reinforcement. Theoretical and experimental studies prove that the modified shear reinforcement described above works as well as the traditional one. Members reinforced with appropriately anchored stirrups and shear assemblies indicate the same behaviour both in SLS and ULS as the conventionally reinforced members.

References

CEB (1981/82), *Manual on Technology of Reinforcement*, CEB Bulletin d´Information No. 140

CEB (1985), *Industrialisation of Reinforcement*, CEB Bulletin d´Information No. 164

CEB (1990), *Recommendations for mechanical splices of reinforcing bars, spacers, chairs and tying of steel reinforcement*, CEB Bulletin d´Information No. 201

CUR (1980), *Strength of lap splices in reinforced concrete*, CUR Report No. 34

Eligehausen, R. (1979), *Tensile lapped-splices of ribbed bars with straight ends*, DAfStb Heft 301

Eligehausen, R.; Fabritius, E. (1995), *Grenzen der Anwendung nichtlinearer Rechenverfahren bei Stabtragwerken und einachsig gespannten Platten, Abschlußbericht zum Forschungsvorhaben*, IV 1-5-584/89, Institut für Werkstoffe im Bauwesen, Universität Stuttgart

Goto, Y. (1965), *Cracks formed in concrete around deformed tension bars*, ACI Journal Vol. 62, No. 1

Kordina, K. (1975), *Detailing of reinforcement in frame corners and frame joints*, Lecture *Betontag 1975*, Deutscher Beton-Verein

Leonhardt, F., Teichen, K.-Th. (1972), *Compression splices of reinforcing bars*, DAfStb Heft 222

Nilson, I. (1973), *Reinforced concrete corners and joints subjected to bending moment*, National Swedish Building Research, Document D7

Rehm, G., Eligehausen, R., Neubert, B. (1978), *Explanation of the New Detailing Rules*, DIN 1045, Sction 18, Edition 12/78, DAfStb Heft 300

Rehm, G., Eligehausen, R., Neubert, B., Lehmann, R. (1982), *Rationalisierung der Bewehrungstechnik – Ein unerschöfliches Foeschungsthema oder eine Möglichkeit zur Kostensenkung und Qualitätssteigerung in Stahlbetonbau*, Bauingenieur

Rehm, G., Neubert, B. (1974), *Allowable load of stirrups of wire meshes in beams*, Report of Institut for Construction Materials, University of Stuttgart

Schießl, P. (1975), *Reevaluation of anchorages with bond laws*, Report of Institut für Betonstahl und Stahlbetonbau (IBS) in Munich

Tewes, R. (1982), *Design of lapped splices of welded wire fabric*, Bond in Concrete (edited by P.Bartos), Applied Science Publishers

Den Uijl J.A. (1992), *Background of the CEB-FIP Model Code 90 clauses on anchorage and transverse tensile actions in the anchorage zone of prestressed concrete members*, CEB Bulletin d'Information No.212

NOTATION LIST

<u>Roman lower case letters:</u>

$1/r$ .... curvature of a section of an element
$1/r_{(g)}$ .... curvature due to g
$1/r_{(g+q)}$ ..... curvature due to g and q
$1/r_{0(g+q)}$ .... instantaneous (initial) curvature due to g and q
$1/r_1$ .... curvature of an uncracked concrete section (state I)
$1/r_{1r}$ .... curvature in state I under cracking moment
$1/r_2$ .... curvature of a cracked concrete section (state II)
$1/r_{2r}$ .... curvature in state II under cracking moment
$1/r_{ts}$ .... tension stiffening correction for curvature
a .... deflection
a_c .... elastic deflection (calculated with rigidity $E_c I_c$)
b .... breadth of compression zone or flange
b_{red} .... reduced breadth of web
b_x .... smaller side dimension of a rectangular section
b_y .... greater side dimension of a rectangular section
b_w .... breadth of web
c .... concrete cover, concentration of a substance in a volume element
c_1 .... column dimension parallel to the eccentricity of the load
c_2 .... column dimension perpendicular to the eccentricity of the load
c_{min} .... minimum concrete cover
c_{nom} .... nominal value of concrete cover ($= c_{min}$ + tolerance)
d .... effective depth to main tension reinforcement
d' .... effective depth to compression reinforcement
d_{max} .... maximum aggregate size
e .... load eccentricity
e_0 .... first order eccentricity ($= M_{Sd} / N_{Sd}$)
e_{01} .... smaller value of the first order eccentricity at one end of the considered element
e_{02} .... greater value of the first order eccentricity at one end of the considered element
e_{tot} .... total eccentricity
f_{bd} .... design value of bond stress
f_c .... cylinder compressive strength of concrete
f_c^* .... cylinder compressive strength of concrete under triaxial loading (confined strength), reduced concrete strength due to transverse tension
f_{cc} .... cylinder compressive strength of concrete under uniaxial stress
f_{cd}^* .... design compressive strength of concrete under triaxial loading (confined strength), reduced design concrete strength due to transverse tension
f_{cd} .... design value of f_c
f_{cd1} .... average design strength value in an uncracked compression zone
f_{cd2} .... average design strength value in a cracked compression zone
$f_{cd.fat}$ .... design fatigue reference strength of concrete under compression
f_{ck} .... characteristic value of f_c
$f_{ck.cf}$ .... value of f_{ck} of confined concrete
$f_{ck.cube}$ ...... characteristic value of cube compressive strength of concrete
$f_{ck.fat}$ .... fatigue reference compressive strength
f_{cm} .... mean value of compressive strength f_c at an age of 28 days

f_{ct} .... axial tensile strength of concrete (determined according to RILEM CPC 7)

f_{ctd} .... design value of f_{ct}

f_{ctk} .... characteristic value of f_{ct}

f_{ctm} .... mean axial tensile strength

$f_{ct,fl}$ .... mean flexural tensile strength (at $T = 20°C$)

$f_{ct,sp}$ .... mean splitting tensile strength

f_d .... design value of strength

$f_{p0,1}$ .... 0,1% proof stress of prestressing reinforcement

$f_{p0,2}$ .... 0,2% proof stress of prestressing reinforcement

$f_{p0,1k}$ .... characteristic 0,1% proof stress

$f_{p0,2k}$ .... characteristic 0,2% proof stress

f_{pt} .... tensile strength of prestressing reinforcement

f_{ptd} .... design tensile strength of prestressing reinforcement

f_{ptk} .... characteristic tensile strength of prestressing reinforcement

f_{py} .... tension yield stress of prestressing reinforcement

f_{pyd} .... design value of tension yield stress of prestressing reinforcement

f_{pyk} .... characteristic value of tension yield stress of prestressing reinforcement

f_R .... relative (or projected) rib area

f_t .... tensile strength of non- prestressing reinforcement

f_{tk} .... characteristic value of tensile strength of non- prestressing reinforcement

f_y .... tension yield stress of non- prestressing reinforcement

f_{yc} .... strength of steel in compression

f_{ycd} .... design strength of steel in compression

f_{yd} .... design value of tension yield stress of non- prestressing reinforcement

f_{yk} .... characteristic value of tension yield stress of non- prestressing reinforcement

g_d .... design value of distributed permanent load

h .... overall depth of member, total height; notional size of a member (2 A_c/u; u: perimeter in contact with the atmosphere)

h_b .... depth of beam

h_f .... depth of flange

Δh_w .... height of water column

i .... radius of gyration

l .... design span, effective span, length of an element, thickness of a penetrated section

Δl .... measured elongation between two measuring points

l_0 .... design lap length, effective length (of columns); distance between measuring points

l_b .... basic anchorage length

l_{bp} .... basic anchorage length of pretensioned reinforcement

l_{bpd} .... design anchorage length of pretensioned reinforcement

l_{bpt} .... transmission length of pretensioned reinforcement

$l_{b,min}$ .... minimum anchorage length

$l_{b,net}$ .... design anchorage length

l_{ch} .... characteristic length (fracture parameter)

l_p .... development length for prestressing reinforcement

l_{pl} .... plastic length (region in which tensile strain is larger than yield strain)

Δl_{pl} .... residual elongation after unloading

$l_{p,max}$ .... length over which the slip between prestressing steel and concrete occurs

$l_{s,max}$ .... length over which the slip between steel and concrete occurs

l_t .... transmission length

m .... moment per unit width (out-of-plane loading); mass of substance flowing; degree of hydration

n .... number of bars, number of load cycles; force per unit width (in-plane-loading)

n_{Ri} .... number of cycles leading to failure at stress levels $S_{i,min}$ and $S_{i,max}$, respectively

n_{Si} .... number of cycles applied at constant minimum and maximum stress levels $S_{i,min}$ and $S_{i,max}$, respectively

p .... local gas pressure

q .... distributed variable load

q_d .... design value of distributed variable load

r .... radius

s .... slip (relative displacement of steel and concrete cross-sections), shear slip (at interfaces); spacing of bars

s_{max} .... maximum bar spacing

s_r .... distance between cracks; radial spacing of layers of shear reinforcement

$s_{r,m}$ .... mean spacing between cracks

t .... time, age, duration; thickness of thin elements

t_0 .... age at loading

t_s .... concrete age at the beginning of shrinkage or swelling

t_T .... effective concrete age

u .... length of a perimeter; component of displacement of a point

u_0 .... length of the periphery of the column or load

u_1 .... length of the control perimeter for punching

u_{ef} .... length of the perimeter of A_{ef}

u_n .... length of the control perimeter for punching outside a slab zone with shear reinforcement

v .... shear force per unit width (out-of-plane loading), component of displacement of a point

w .... crack width; component of displacement of a point

w_c .... crack width for $\sigma_{ct} = 0$

w_k .... calculated characteristic crack width

w_{lim} .... nominal limit value of crack width

x .... depth of compression zone, distance

z .... internal lever arm

Greek lower case letters:

α .... coefficient, reduction factor

α_e .... modular ratio (E_s / E_c)

$\alpha_{e,p}$ .... modular ratio (E_p / E_c)

$\alpha_{e,sec}$ ...... secant modular ratio ($E_{s,sec} / E_{c,sec}$)

α_{sT} .... coefficient of thermal expansion for steel

α_T .... coefficient of thermal expansion in general

β_1 .... coefficient characterizing the bond quality of reinforcing bars

$\beta_c(t,t_0)$ ..... coefficient to describe the development of creep with time after loading

γ .... safety factor

γ_c .... partial safety factor for concrete material properties

$\gamma_{c,fat}$ .... partial safety factor for concrete material properties under fatigue loading

γ_F .... partial safety factor for actions

γ_G .... partial safety factor for permanent actions

γ_Q .... partial safety factor for variable actions

γ_s .... partial safety factor for the material properties of reinforcement and prestressing steel

$\gamma_{s,fat}$ .... partial safety factor for the material properties of reinforcement and prestressing steel under fatigue loading

δ_{ii} .... node displacement

ϵ .... strain

ϵ_c .... concrete compression strain

ϵ_c^* .... concrete compression strain under triaxial stress

ϵ_{cm} .... average concrete strain within $l_{s,max}$

ϵ_{c0} .... concrete strain at peak stress in compression

$\epsilon_{cc}(t)$ .... concrete creep strain at concrete age $t > t_0$

$\epsilon_{ci}(t_0)$ ...... stress dependent initial strain at the time of stress application

$\epsilon_{cn}(t)$ .... total stress independent strain at a concrete age t (=$\epsilon_{cs}(t) + \epsilon_{cT}(t,T)$)

$\epsilon_{cs}(t,t_s)$ ..... total shrinkage or swelling strain at concrete age t (t in days)

$\epsilon_{c\sigma}(t)$ .... total stress dependent strain at a concrete age t (= $\epsilon_{ci}(t_0) + \epsilon_{cc}(t)$)

ϵ_{ct} .... concrete tensile strain

$\epsilon_{cT}(t,T)$ .... thermal strain at a concrete age t

ϵ_{cu} .... ultimate strain of concrete in compression

ϵ_{d0} .... strain of prestressed reinforcement corresponding to P_{d0}

ϵ_{pu} .... total elongation of prestressing reinforcement at maximum load

ϵ_r .... strain at the onset of cracking

ϵ_s .... steel strain

ϵ_{s1} .... steel strain in uncracked concrete

ϵ_{s2} .... steel strain in the crack

ϵ_{sm} .... mean steel strain

$\Delta\epsilon_{sr}$ .... increase of steel strain in cracking state

ϵ_{sr1} .... steel strain at the point of zero slip under cracking forces

ϵ_{sr2} .... steel strain in the crack under cracking forces (σ_{ct} reaching f_{ctm})

ϵ_{sT} .... thermal strain of steel

ϵ_{su} .... strain of non- prestressing reinforcement at maximum load

$\Delta\epsilon_{ts}$ .... increase of strain by the effect of tension stiffening

ϵ_u .... total elongation of reinforcing steel at maximum load

ϵ_{uk} .... characteristic total elongation of reinforcing steel at maximum load

ϵ_{yd} .... design yield strain of non - prestressing reinforcement (= f_{yd} / E_s)

ϵ_v .... transverse contraction

ζ .... ratio of bond strength of prestressing steel and high-bond reinforcing steel

η .... viscosity of gas

θ .... angle between web compression and the axis of a member; rotation

θ_f .... angle between inclined compression in a flange and the axis of the member

λ .... slenderness ratio (= l_0 / i)

μ .... coefficient of friction, relative bending moment

ν .... relative axial force

ν_c .... Poisson's ratio of concrete

ν_s .... Poisson's ratio of steel

ν_{Sd} .... relative design axial force (= $N_{Sd} / A_c f_{cd}$)

ρ .... ratio of (longitudinal) tension reinforcement (= A_s/bd)

$\rho_{s,ef}$ .... effective reinforcement ratio (= $A_s/A_{c,ef}$)

ρ_t .... relaxation after t hours

ρ_w .... ratio of web reinforcement (= $A_{sw}/b_w s \cdot \sin\alpha$)

σ .... stress

$\sigma_1, \sigma_2, \sigma_3$ .. principal stresses

σ_c .... concrete compression stress

σ_{cd} .... design concrete compression stress

σ_{ct} .... concrete tensile stress

$\sigma_{c,cf}$ .... compression stress of confined concrete

$\sigma_{c,max}$ .... maximum compressive stress

$\sigma_{c,min}$ .... minimum compressive stress

$\sigma_{p0}(x)$ ..... initial stress in prestressing reinforcement at a distance x from anchorage device

$\sigma_{p0,max}$ ..... maximum tensile force in prestressing reinforcement at tensioning

σ_{pcs} .... tendon stress due to prestress after all losses (due to creep and shrinkage)

σ_{pd} .... tendon stress under design load

$\Delta\sigma_{Rsk}(n)$ .. stress range relevant to n cycles obtained from a characteristic fatigue strength function

σ_s .... steel stress

σ_{s2} .... steel stress in the crack

σ_{sE} .... steel stress at the point of zero slip

σ_{sr2} .... steel stress in the crack under crack loading (σ_{ct} reaching f_{ctm})

$\Delta\sigma_{Ss}$ .... steel stress range under the acting loads

τ_b .... local bond stress

τ_{bm} .... mean bond stress

$\tau_{fu,d}$ .... ultimate design shear friction capacity

τ_{max} .... maximum value of bond stress

τ_{Rd} .... resistance to shear stress (design value)

τ_{Sd} .... applied shear stress (design value)

$\psi(t,t_0)$ ..... relaxation coefficient

ω .... mechanical reinforcement ratio

ω_{sw} .... mechanical ratio of stirrup reinforcement

ω_v .... volumetric ratio of confining reinforcement

ω_w .... volumetric mechanical ratio of confining reinforcement

ω_{wd} .... design volumetric mechanical ratio of confining reinforcement

Roman capital letters:

A .... total area of a section or part of a section (enclosed within the outer circumference)

A_I .... section area in state I (taking into account the reinforcement)

A_c .... area of concrete cross section or concrete compression chord

$A_{c,ef}$ .... effective area of concrete in tension

A_{core} .... effectively confined area of cross-section in compression

A_{ef} .... area enclosed by the centre-lines of a shell resisting torsion

A_p .... area of prestressing reinforcement

A_s .... area of reinforcement

A_s' .... area of compressed reinforcement

A_{sh} .... area of hoop reinforcement for torsion

A_{sl} .... area of longitudinal reinforcement

A_{st} .... area of transverse reinforcement

A_{sw} .... area of shear reinforcement

$A_{s,cal}$ .... calculated area of reinforcement required by design

$A_{s,ef}$ .... area of reinforcement provided

$A_{s,min}$ .... minimum reinforcement area

D .... fatigue damage, diffusion coefficient

D_{lim} .... limiting fatigue damage

E .... modulus of elasticity

E_c .... reduced modulus of elasticity for concrete

$E_c(t_0)$ .... modulus of elasticity at the time of loading t_0

E_{ci} .... tangent modulus of elasticity at a stress σ_i (at T = 20°C)

$E_{c,sec}$ .... secant modulus of elasticity at failure for uniaxial compression ($E_{c,sec} = f_{cm}/|\varepsilon_{c0}|$)

E_p .... modulus of elasticity of prestressing steel

E_s .... modulus of elasticity of steel

$E_{s,sec}$ .... secant modulus of elasticity of steel

F .... force, applied load or load effect

F_b .... bond force transmitted along the transmission length

F_c .... strut force (compression force)

F_d .... design value of action

F_{pt} .... tensile load of prestressed reinforcement

$F_{p0,1}$ .... characteristic 0,1% proof -load

$F_{Sd,ef}$ .... effective concentric load (punching load enhanced to allow for the effects of moments)

F_t .... tie force (tension force)

F_{ud} .... ultimate dowel force

G .... permanent action

G_F .... fracture energy of concrete

G_{F0} .... base value of fracture energy (depending on maximum aggregate size)

G_{inf} .... favourable part of permanent action

G_{sup} .... unfavourable part of permanent action

H .... horizontal force, horizontal component of a force

I .... second moment of area

I_1 .... second moment of area in state I (including the reinforcement)

I_2 .... second moment of area in state II (including the reinforcement)

I_c .... second moment of area of the uncracked concrete cross-section (state I)

$J(t,t_0)$ .... creep function or creep compliance representing the total stress dependent strain per unit stress

K_g .... coefficient of gas permeability

K_w .... coefficient of water permeability

L .... span, length of an element

M .... bending moment; maturity of concrete

M_r .... cracking moment

M_{Rd} .... design value of resistant moment

M_{Sd} .... design value of applied moment

M_u .... ultimate moment

M_y .... yielding moment

N .... axial force, number of cycles to failure (fatigue loading)

N_r .... axial cracking force

N_{Rd} .... design value of resistance to axial force

N_{Sd} .... design value of applied axial force

P_{d0} .... design value of prestressing force (initial force)

$P_{k,inf}$ .... lower characteristic value of prestressing force

$P_{k,sup}$ .... upper characteristic value of prestressing force

P_m .... mean value of prestressing force

Q .... variable single action; volume of a transported substance (gas or liquid)

R .... resistance (strength); bending radius; universal gas constant

R_d .... design resistance

RH .... ambient relative humidity

RH_0 .... 100% relative humidity

S .... load effect (M, N, V, T); absorption coefficient

ΔS_{cd} .... stress range under fatigue loading

$S_{cd.max}$ ..... design value of maximum compressive stress level (fatigue loading)

$S_{cd,min}$ ..... design value of minimum compressive stress level (fatigue loading)

$S_{c.max}$ ...... maximum compressive stress level (fatigue loading)

$S_{c,min}$ ...... minimum compressive stress level (fatigue loading)

S_d .... design load effect (M, N, V, T)

T .... temperature, torsional moment

ΔT .... temperature change

T_{Rd} .... design value of resistance to torsional moment

T_{Sd} .... design value of applied torsional moment

$T_{Sd,eff}$ ...... effective design value of applied torsional moment

V .... shear force; volume of gas or liquid

V_{Rd} .... design value of resistance to shear force

V_{Sd} .... design value of applied shear force

V_u .... ultimate shear force

W_1 .... section modulus in state I (including the reinforcement)

W_2 .... section modulus in state II (including the reinforcement)

W_c .... section modulus of the uncracked concrete cross-section (state I)

$W_{c,cf}$ .... volume of confined concrete

W_e .... external work

W_i .... internal work

$W_{s,trans}$ ..... volume of closed stirrups or cross-ties

others:

$\emptyset$ .... nominal diameter of steel bar

$\emptyset_n$ .... equivalent diameter of bundles containing n bars

$\emptyset_p$ .... diameter of prestressing steel (for bundles equivalent diameter)

ϕ (t,t_0) ..... creep coefficient

ϕ_0 .... notional creep coefficient

Θ_{pl} .... plastic rotation capacity

ΣU .... total perimeter of rebars

Statistical symbols

<u>Roman lower case letters:</u>

$f_r(r)$.........probability density function (of log-normal distribution)

$f_R(r)$.........probability density function of resistance

$f_S(s)$.........probability density function of action

$f_x(x)$.........probability density function (of normal distribution)

k...............normalised variable or fractile factor

m_R............mean of resistance

m_S............mean of action

m_x............mean (same meaning as $\bar{x}$)

p_f.............failure probability

$\breve{x}$...............median

$\hat{x}$...............modal value

$\bar{x}$..............mean (same meaning as m_x)

x_p...............p-%-fractile

<u>Greek lower case letters:</u>

α.....................sensitivity factor

β.....................reliability index

γ...............(partial) safety factor

σ_R............standard deviation of resistance

σ_S............standard deviation of action

σ_x............standard deviation

σ_x^2.................scattering or variance

<u>Roman capital letters:</u>

$F_r(r)$.........probability distribution function (of log-normal distribution)

$F_x(x)$.........probability distribution function (of normal distribution)

R...............resistance

S...............action

V_x.............coefficient of variation

Z...............safety zone (difference of R and S)

<u>others:</u>

$\Phi(k)$........normalised function

Structural Concrete

Volume 2

Contents

4 Basis